

NASA Contractor Report 195435

IN-20
VOL. 1
49655
P-390

Advanced Small Rocket Chambers Option 3-110 lbf Ir-Re Rocket Volume I

Donald M. Jassowski and Leonard Schoenman
Gen Corp Aerojet
Sacramento, California

February 1995

Prepared for
Lewis Research Center
Under Contract NAS3-25646



National Aeronautics and
Space Administration

(NASA-CR-195435-Vol-1) ADVANCED
SMALL ROCKET CHAMBERS. OPTION 3:
110 lbf Ir-Re Rocket, VOLUME 1
Final Report (GenCorp Aerojet)
390 p

N95-31169

Unclass

G3/20 0049655

Advanced Small Rocket Chambers
110 lbf Ir-Re Flight-Type Thruster

Option 3

Final Report

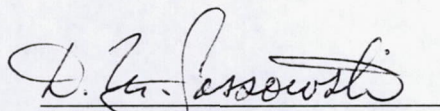
Contract NAS 3-25646

February 1995

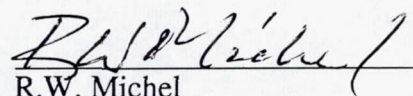
Prepared For:

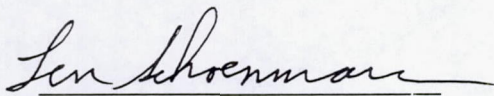
NASA-Lewis Research Center
Cleveland, Ohio 44135

Prepared By:


D.M. Jassowski
Project Engineer

Approved By:


R.W. Michel
Program Manager


Len Schoenman
Manager of Research Projects

Notice: This report incorporated items covered under U.S. Patents
4882904 and 4936091 and German Patent P39 23 948.9-13.

TABLE OF CONTENTS

	<u>Page</u>
1.0 Summary	1
2.0 Introduction	2
2.1 Program Description	2
2.2 Engine Description and Capabilities	6
2.2.1 Envelope	8
2.2.2 Performance and Operating Limits Demonstrated	11
2.2.3 Interfaces	19
2.2.4 Capabilities, Performance, Durability and Thermal Validation	19
2.2.5 Specific Impulse/Operating Box	21
3.0 Conclusions and Recommendations	38
4.0 Thruster Design	39
4.1 Preliminary Design/Optimization	39
4.1.1 Conversion to Flightweight Design	39
4.1.2 Design Optimization	43
4.1.3 Thermal Design Optimization	43
4.1.4 Structural	45
4.1.5 Configuration Design Optimization	45
4.1.6 Layout and Assembly	47
4.2 Component Design/Selection	47
4.2.1 Valve	50
4.2.2 Injector	50
4.2.3 Fuel Cooled Flange	53
4.2.4 Rhenium Chamber	53
4.2.5 Columbium Skirt	53
4.2.6 Tooling	57
5.0 Fabrication	57
5.1 Valve	57
5.2 Injector	57
5.3 Cooled Flange	63
5.4 Rhenium Chamber	63
5.5 Columbium Skirt	68
5.6 Mini Skirts	70
5.7 Engine Assembly	70

TABLE OF CONTENTS (cont.)

	<u>Page</u>
6.0 Testing	79
6.1 Weld Joint Bench Tests	79
6.2 Proof, Leak and Water Flow Tests	88
6.3 Hot Firing (NTO/MMH)	130
6.3.1 Sea Level Tests	130
6.3.2 44:1 Tests	167
6.3.3 Weld Thermal Cycle Tests	208
6.3.4 286:1 Performance Tests	215
6.3.5 47:1 Durability Tests	238
6.3.6 47:1 Endurance Tests	301
6.4 Work Hardening of Rhenium	342
6.5 NTO/AH Tests	349
7.0 References	372

APPENDICES

<u>Appendix</u>		<u>Page</u>
A	Nozzle Contour Optimization	A-1
B	Thermal Analysis	B-1
C	Dynamic Analysis	C-1
D	Valve Acceptance Data From Moog	D-1
E	Ir-Re Chamber Inspection Data	E-1
F	Nozzle Skirt Fabrication and Inspection	F-1
G	I _s Error Analysis	G-1
H	Performance Data	H-1
I	Thermal Data	I-1
J	Test Facility and Instrumentation	J-1
K	Durability Data Listings	K-1
L	Joint Failure Analysis	L-1
M	Post Test Thruster Photos	M-1
N	Rhenium Strainhardening Experiment	N-1

TABLE LIST

<u>Table</u>		<u>Page</u>
2.1-1	Demonstrated Performance	6
2.2-1	Existing Hardware Weights	11
2.2-2	Moog Model 53 X-179 Torque Motor Bipropellant Valve	19
2.2-3	44:1 Performance for Injectors SN 6-1 and SN 6-2 Was Demonstrated to be Identical	25
2.2-4	Isp of AJ10-221 With 286:1 Area Ratio	28
2.2-5	The 110 lbf Iridium/Rhenium Chambers Have Accumulated a Substantial Test History	31
4-1	Environmental Design Requirements	41
4-2	Optimization of Nozzle Contour	46
4-3	High Performance 100 lbf Engine Supply Pressure Envelope and Resulting Operating Parameters	48
4-4	Weight of 100 lbf Thrust Engine Components	49
4-5	Injector Orifice Diameters, in mils	50
5-1	Parts List for 100 lbf Thruster	59
5-2	Weight of Columbium Skirts	68
6.1-1	Metal Joining Study Test Results	86
6.2-1	Injector Water Flow Conditions	94
6.2-2	Water Flow Conditions for SN 5 Injector	100
6.2-3	Injector SN 5 Platelet 3C Status	104
6.2-7	Summary of Leak and Proof Checks	127
6.2-8	Leak Check 47:1 Thruster Assembly Prior to Test -279	128
6.2-9	Results of Post-Test Leak Test of AJ10-221 Engine Assy at Dev Ops Post Test -351	129
6.3-1	Summary of Hot Fire Tests	131
6.3-2	Summary of 100# Testing – Preliminary Data	132
6.3-3	100# Thruster – Bay 2 Sea Level Tests (1.68:1 Area Ratio)	156
6.3.4	100 lb Bay 2 Checkout Instrumentation List – Heat Sink Chamber (@ S.L.)	158
6.3-5	Compatibility Test Data	165
6.3-6	100 lb Bay 2 Instrumentation List – Altitude Tests at 44:1	172

TABLE LIST (cont.)

<u>Table No.</u>		<u>Page</u>
6.3-7	Summary of Test Group C: 44:1 Performance Tests – Ir-Re Radiation-Cooled Chamber With NTO/MMH Propellant	177
6.3-10	Test Summary – Tests 225-244	195
6.3-11	The Miniskirt Test Series Thermally Cycled the Nozzle Weld Joint in Hot-Fire Tests	215
6.3-12	100 lb Bay 2 Instrumentation List – Altitude Tests at 286:1	217
6.3-13	490N Liquid Apogee Engine Final Performance Data – Welded Assembly With 286:1 Area Ratio	223
6.3-14	Maximum Operating Temperatures Ir-Re Welded 286:1 Thruster at Nominal Conditions	235
6.3-15	Performance Data – Durability Test Data – 279-347	255
6.3-17	Endurance Test Instrumentation Locations	318
6.3-18	Endurance Test Data Display Locations	319
6.3-19	Comments on Endurance Test Data Listings	323
6.3-20	Flight Thruster Component Resistance	315
6.3-21	Test Results for 110 lbf Endurance Test	328
6.5-1	Test Results, Runs -245 and -246	352
6.5-2	Sequence of Events for Test -246	361
6.5-3	Post Test Hardware Status	363
6.5-4	Post Test Analysis of Injector SN 1	367

FIGURE LIST

<u>Figure No.</u>		<u>Page</u>
2.1-1	AJ10-221 100 lbf Ir-Re Engine With 286:1 Expansion Nozzle	3
2.1-2	Chamber Exterior at End of Durability Tests	5
2.1-3	Close-Up View of Engine Assembly After Two-Hour Endurance	7
2.2-1	Major Components of the AJ10-221	9
2.2-2	Drawing of Engine Test (286:1)	10
2.2-3	92 Element Splashplate Injector	12
2.2-4	Iridium-Rhenium Chambers With Bimetallic Transition Rings Welded on Both Ends (Left: Stainless Steel to Rhenium; Right: C-103 to Rhenium)	14
2.2-5	Basic Fabrication Steps for Iridium-Coated Rhenium Combustion Chamber	15
2.2-6	286:1 Silicide Coated C-103 Skirt	17
2.2-7	Moog Torque Motor Bipropellant Valve Assembled to AJ10-221 Engine	18
2.2-8	Engine 100 lbf Thrust	20
2.2-9	Demonstrated Operating Envelope	22
2.2-10	The Engine Has Been Tested Over a Wide Range of Operating Conditions	23
2.2-11	Front-End Temperatures Provide Wide Thermal Margin	24
2.2-12	Isp Vac for SN 6-1 and SN 6-2 Injectors at Area Ratio = 44:1 is Identical From MR 1.4 to 1.8	26
2.2-13	SN 6-1 and SN 6-2 Injectors Are Identical at the Design Point	27
2.2-14	AJ10-221 Isp vs Mixture Ratio and Thrust With the 286:1 Nozzle	29
2.2-15	The Chamber Operates 600°F Cooler Than the Demonstrated 15-Hr-Life Temperature	30
2.2-16	The Nozzle Weld Joint Was Demonstrated in Hot Firings Using a Miniskirt (44:1 Nozzle)	32
2.2-17	Rhenium-to-Columbium Joint Temperatures Are Well Below Material Limits	34
2.2-18	Regenerative Fuel Coolant Outlet Temperatures Are Well Below the Design Limit	35
2.2-19	Hot Restarts Have Been Demonstrated for Temperatures Approaching 200°F	36
2.2-20	The AJ10-221 Engine Responds Stably to Gas Bubble Injection	37
4-1	JPL 44:1 Thruster Drawing (Ref. 3)	40
4-2	100# Propellant Tank Operating Range	42
4-3	100 lbf Thrust Engine Drawing	44

FIGURE LIST (cont.)

<u>Figure No.</u>		<u>Page</u>
4-4	100# Final Assy Drawing	49
4-5	Moog Torque Motor Bipropellant Valve	51
4-6	Injector Design, Top Assembly	52
4-7	Fuel Cooled Head End Design and Acceptance Test Conditions	54
4-8	Iridium/Rhenium Chamber	55
4-9	Skirt Design Nozzle	56
4-10	Thruster Leak Check Fixture	58
5-1	Engine Assembly Flow Chart	60
5-2	Diffusion Bonded Platelet Injector SN 6-1 Prior to Welding Film Cooling Ports	61
5-3	Welded Assembly of Injector, Fuel Cooled Adapter, and Rhenium Chamber	62
5-4	Fuel Cooled Mounting Flange	64
5-5	Final Assembly Component of Fuel Cooled Adapter	65
5-6	Iridium-Rhenium Chamber as Delivered by Ultramet	66
5-7	Ir-Re Chamber for 286:1 Thruster SN-1 With Weld Adapter Rings in Place	67
5-8	SN-1 286:1 Cb Nozzle Exterior Before and After Chem Milling	69
5-9	SN-1 Cb Skirt Actual and Print Dimensions During Fabrication	71
5-10	Validation of the Rhenium to Columbium Joining Method	72
5-11	47:1 Area Ratio Coated C-103 Miniskirt	73
5-12	Engine Components and Tooling for Assembly	74
5-13	Weld Ring Photos	75
5-14	Joining of the 304L Cooled Flange to the Rhenium Chamber	76
5-15	Weld Assembly Injector Cooled Flange and Iridium Lined Rhenium Chamber	77
5-16	Columbium Skirt EB Weld	78
6.1-1	General Design for Weld Joint Specimen	81
6.1-2	Re-SS Test Specimen as Fabricated	82
6.1-3	Weld Joint Specimen Test Facility	84
6.1-4	Automatic Joint Thermal Cycling Test Setup in the Cooling Position	85
6.2-1	100 lb Injector Manifold Water Flow Data	89
6.2-2	Oxidizer Inlet Relative to Manifold Orifices	90
6.2-3	Manifold-Only Mixture Ratio	92

FIGURE LIST (cont.)

<u>Figure No.</u>		<u>Page</u>
6.2-4	Manifold + Injector Mixture Ratio	93
6.2-5	Water Flow of 100 lbf – Injector SN 2 – Oxidizer $\Delta P = 64$ psi, Fuel $\Delta P = 96$ psi	95
6.2-6	Water Flow of 100 lbf – Injector SN 4 – Oxidizer $\Delta P = 59$ psi, Fuel $\Delta P = 79$ psi	96
6.2-7	Injector SN 5 Water Flow – Oxidizer Circuit at 111 psi ΔP	97
6.2-8	Injector SN 5 Water Flow – Fuel Circuit at 108 psi ΔP	98
6.2-9	Injector SN 5 Water Flow – Oxidizer and Fuel Circuits at 111 and 108 psi ΔP Respectively	99
6.2-10	100 lb SN 5 in. Kw vs Water Flow	101
6.2-11	Mod B SN 4 Injector Orifice Dimensions	102
6.2-12	Mod C SN 5 Injector Orifice Dimensions	103
6.2-13	Mod B SN 4 Injector Local MR	106
6.2-14	Mod C SN 5 Injector Local Mixture Ratio	107
6.2-15	100# Injector SN 2, 4, and 5 Inner and Outer MR	108
6.2-16	100# Injector Mass Ratio = Outer/Inner	109
6.2-17	Water Flow Pattern Test – SN 6-1	110
6.2-18	Water Flow Pattern Test – SN 6-2	111
6.2-19	Kw vs Water Flow Rate SN 6-1 and 6-2 Oxidizer Circuit Water Flow 11-14-91	112
6.2-20	Kw vs Water Flow Rate SN 6-1 and 6-2 Fuel Circuit Water Flow 11-14-91	113
6.2-21	SN 6-1 and -2: % Inner and Outer Oxid Flow – Outer = Rows 6 and 7; Water	114
6.2-22	SN 6-1 and -2: % Inner and Outer Fuel Flow – Outer = Rows 6 and 7; Water	115
6.2-23	SN 6-1, 6-2, 2, 4 and 5 Inner and Outer MR Outer = Rows 6 and 7; Water Flow	116
6.2-24	Proof, Leak and Flow Test Cooled Adapter	117
6.2-25	Test Setup for Leak Testing Fuel-Cooled Chamber Head Ends	118
6.2-26	Fuel-Cooled Chamber Head End Showing Strain Gage Installation	120
6.2-27	100 lb Cooled Section SN 1 – Proof Test (Gages 0, 1, 2 and 3)	121
6.2-28	100 lb Cooled Section SN 1 – Proof Test (Gages 4, 5, 6 and 7)	122
6.2-29	100 lb Cooled Section SN 2 – Proof Test (Gages 0, 1, 2 and 3)	123
6.2-30	100 lb Cooled Section SN 2 – Proof Test (Gages 4, 5, 6 and 7)	124
6.2-31	100 lb Fuel-Cooled Adapter Kw vs Water Flow Rate	125

FIGURE LIST (cont.)

<u>Figure No.</u>		<u>Page</u>
6.2-32	490 Newton Flight Engine Balance — Available Pressure vs Thrust	126
6.3.1-1	Drawing of Bolt-Up Sea Level Thruster Assembly	135
6.3.1-2	Compatibility/Performance Chamber	136
6.3.1-3	100-lbf Compatibility Chamber Materials	137
6.3.1-4	100-lbf Ir-Re Thruster Injector Characterization Foil After Test	138
6.3-5	100# Rhenium Loss Rate vs I_{svac}	139
6.3-6	100# Thruster POJ vs PFJ – Sea Level Tests -101 thru -161	140
6.3-7	100# Thruster Pc Versus MR – Sea Level Tests -101 thru -161	142
6.3-8	100# Thruster Delta T Regen vs Is – Sea Level Tests -101 thru -161	143
6.3-9	100# Thruster Pc-1/Pc-2 vs Pc-2 – Sea Level Tests -101 thru -161	144
6.3-10	100# I_{svac} Versus Pc-2 – Injector #2, Trip #4 (101-116) Bay 3	145
6.3-11	100# I_{svac} Versus Pc-2 – Injector #4, Trip #2 (117-127) Bay 3	146
6.3-12	100# I_{svac} Versus Pc-2 – Injector #4, Trip #4RW (128-134) Bay 3	147
6.3-13	100# I_{svac} Versus Pc-2 – Injector #2, Trip #4RW (135-147) Bay 3	148
6.3-14	100# I_{svac} Versus Pc-2 – Injector SN 2, Trip 4RW (-148-161) Bay 2	149
6.3-15	View of Bay 2 Test Cell	150
6.3-16	View of Nozzle Exit and Aft End of Bay 2 Stand	151
6.3-17	Side View of Bay 2 Thrust Stand	152
6.3-18	Heat Sink 1.6:1 Chamber in Bay 2 Stand	153
6.3-19	Frames From Sequence Camera Coverage of Bay 2 Sea Level Checkout Test With SN 2 Injector	155
6.3-20	Thrust Bias vs Thrust	157
6.3-21	100# I_{svac} Versus MR – Bay #2 – Injector #2, Trip #4RW (148-161)	160
6.3-22	100# Delta T Regen Versus Pc-2 – Bay #2 – Injector #2, Trip #4RW (148-161)	161
6.3-23	100# Max Trip Temp Versus Pc-2 – Bay #2 – Injector #2, Trip #4RW (148-161)	162
6.3-24	Oxid Kw vs Oxid Mass Flow – Injector #2, Tests -148 – -161	163
6.3-25	Fuel Kw vs Fuel Mass Flow – Injector #2, Tests -148 – -161	164
6.3-26	Mass Loss Rate, GM/HR, Runs -253 to -258, SN 6-1	166
6.3-27	I_{svac} vs Chamber Pressure – Runs -247 to -248, Injector SN 6-1, 1.68:1	168
6.3-28	Measured I_{svac} vs Area Ratio – Ir-Re Thruster, NTO/MMH, MR = 1.65	169
6.3-29	100 lb 44:1 Bolt-Up Thruster Assembly	170

FIGURE LIST (cont.)

<u>Figure No.</u>		<u>Page</u>
6.3-30	JPL 44:1 Ir-Re Chamber in Altitude Facility for Injector Performance Comparison Tests	171
6.3-31	Test Bay A-2 Propellant Feed System	174
6.3-32	Altitude Duct Diffuser Mount and Support in Bay 2	175
6.3-33	6 in. Diffuser Set Up for 44:1 Injector Performance Screening Tests	176
6.3-34	Vacuum Specific Impulse at 44:1 for Injector SN -2, -4 and -5 Versus Chamber Pressure Over Full Test Range	179
6.3-35	Vacuum Specific Impulse at 44:1 for Injectors and SN -2, -4 and -5 Versus Mixture Ratio Over Full Test Range	180
6.3-36	C* vs Pc-1 – Final Data (Cold Throat) – 100# Ir-Re; Injector SN 2, 4, 5	181
6.3-37	C* vs MR – Final Data (Cold Throat) – 100# Ir-Re; Injector SN 2, 4, 5	182
6.3-38	Chamber Temperature vs Pc-1 – Final Data – 100# Ir-Re; Injector 2, 4, 5	183
6.3-39	Chamber Temperature vs MR – Final Data – 100# Ir-Re; Injector SN 2, 4, 5	184
6.3-40	Oxid Line Temp vs Run Number – 100# Ir-Re, e = 44:1; Injector SN 2, 4, 5	185
6.3-41	Fuel Line Temp vs Run Number – 100# Ir-Re, e = 44:1; Injector SN 2, 4, 5	186
6.3-42	Regen Q vs MR – Final Data – 100# Ir-Re; Injector SN 2, 4, 5	187
6.3-43	Regen Q vs Pc – Final Data – 100# Ir-Re; Injector SN 2, 4, 5	189
6.3-44	100# Thruster Internal Regen Temp – Run -170, Hot Start Test	190
6.3-45	100# Thruster Internal Regen Temp – Run -170, Initial Transient	191
6.3-46	100# Thruster Plume Spectral Emission – Test -164 With Helium Ingestion	192
6.3-47	SN 5 Injector After Performance Tests	194
6.3-48	Vacuum Specific Impulse at 44:1 for Injectors SN 6-1 and SN 6-2 Versus Mixture Ratio Over Full Test Range	197
6.3-49	Vacuum Specific Impulse at 44:1 for Injectors SN 6-1 and SN 6-2 Versus Mixture Ratio at Nominal Conditions	198
6.3-50	Vacuum Specific Impulse at 44:1 for Injectors SN 6-1 and SN 6-2 Versus Chamber Pressure Over Full Test Range	199
6.3-51	Vacuum Specific Impulse at 44:1 for Injectors SN 6-1 and SN 6-2 Versus Chamber Pressure at Nominal Conditions	200
6.3-52	Specific Impulse and Percent Theoretical vs MR SN-6 at $\epsilon = 44:1$	201
6.3-53	SN 6-1 and 6-2 Injectors C* vs MR at 44:1; Full Test Range	202

FIGURE LIST (cont.)

<u>Figure No.</u>		<u>Page</u>
6.3-54	SN 6-1 and 6-2 Injector C* vs MR Data at 44:1; At Nominal	203
6.3-55	SN 6-1 and 6-2 Injectors C* vs Pc – Final Performance Data at 44:1	204
6.3-56	SN 6 Injector Oxid Kw vs Flow Rate	205
6.3-57	SN 6 Injector Fuel Kw vs Flow Rate	206
6.3-58	SN 6-1 Injector Fuel Kw vs Time Test -244	207
6.3-59	SN 6-1 and 6-2 Injectors Regen Q vs MR Final Performance Data at 44:1	209
6.3-60	100# Ir-Re SN 6-1 Temperature vs Time – Test -244, 90 Seconds	210
6.3-61	100# Ir-Re SN 6-1 Temperature vs Time – Test -244, 90 Seconds	211
6.3-62	Miniskirt Chamber Prior to Assembly	212
6.3-63	Miniskirt Weld Joint Thermal Cycle Chamber Prior to Test	213
6.3-64	Miniskirt Weld Joint Thermal Cycle Chamber After 15 Cycles	214
6.3-66	Instrumentation Locations on 286:1 Welded Thruster SN-1	220
6.3-67	286:1 Thruster Installed in Altitude Cell	221
6.3-68	Pre-Test Appearance of 286:1 Nozzle Interior	222
6.3-69	Capacity of Oxidizer PDFM	224
6.3-70	Capacity of Fuel PDFM	225
6.3-71	Specific Impulse Error Versus Cell Pressure Error	227
6.3-72	Vac Is at 286:1 Versus Mixture Ratio for Tests -271 to -278	228
6.3-73	Vac Is at 286:1 Versus Pc for Tests -271 to -278	229
6.3-74	Vac Is at 286:1 Versus Mixture Ratio; All Tests	230
6.3-75	Vac Is at 286;1 Versus Pc; All Tests	231
6.3-76	Chamber Wall Temperature Versus Mixture Ratio for Tests -271 to -278	232
6.3-77	Chamber Wall Temperature Versus Pc for Tests -271 to -278	233
6.3-78	Regen Fuel ΔT Versus Mixture Ratio, Tests -271 to -278	234
6.3-79	Bay A-2 Altitude Test Facility and 286:1 Welded Ir Re Thruster, Post Test -278	236
6.3-80	Welded 286:1 Ir-Re Thruster in Altitude Cell, Post Test -278	237
6.3-81	Welded 286:1 Ir-Re Thruster Overall nozzle Interior, post Test -278	239
6.3-82	Welded 286:1 Ir-Re Thruster – Nozzle Interior Downstream of Weld, Post Test -278; Note Injector in Background	240
6.3-83	Welded 286:1 Ir-Re Thruster – Detail of Nozzle Interior From Throat to Weld, Post Test -278	241

FIGURE LIST (cont.)

<u>Figure No.</u>		<u>Page</u>
6.3-84	Detail of Nozzle "Bumper" Ring Installed to Prevent Nozzle Damage When Diffuser Unloads	242
6.3-85	Welded 286:1 Ir-Re Thruster Assembly - Post Test -278	243
6.3-86	Welded 286:1 Ir-Re Thruster – Thermocouple Detail – Post Test -278 at Approximately 330 Degrees	244
6.3-87	Welded 286:1 Ir-Re Thruster - Thermocouple Detail - Post Test -278 at Approximately 120 Degrees	245
6.3-88	Welded 286:1 Ir-Re Thruster - Post Test -278 Detail of Chamber and Nozzle Transition Weld	246
6.3-89	Welded 286:1 Ir-Re Thruster – Post Test -278 Showing Glazed Area From Melted Thermocouple Insulation	247
6.3-90	Drawing of 47:1 Mod 1 Welded Thruster Assembly	248
6.3-91	Welded SN 1, Mod Thruster – 286:1 Cut Back to 47:1, Overall Assembly	249
6.3-92	Welded SN-1, Mod Thruster – 286:1 Cut Back to 47:1, View of Chamber and Interior of Nozzle (Throat Plug In Place)	250
6.3-93	Welded SN-1 Mod Thruster – 286:1 Cut Back to 47:1, Closeup of Nozzle Interior (Throat Plug In Place)	251
6.3-94	Oxid Inlet Pressure vs Fuel Inlet Pressure	253
6.3-95	Instrumentation Locations for 47:1 490N Welded Thruster	254
6.3-96	New Diffuser Inlet Section	258
6.3-97	47:1 Welded Ir-Re Thruster on Stand Post Test -306	259
6.3-98	System Mixture Ratio Sensitivity to Small Pressure Changes	260
6.3-99	System Chamber Pressure Sensitivity to Small Pressure Changes	261
6.3-100	Ir-Re Welded Thruster – Duration vs TVP Durability Tests; 47:1	262
6.3-101	Isp Predictions for 100 lbf Engine	263
6.3-102	Thrust Bias vs Run Number for Durability Tests	265
6.3-103	Temperatures vs Time Test -306; 47:1 Durability	267
6.3-104	Chamber Exterior at End of Performance Tests	268
6.3-105	Chamber Exterior at End of Durability Tests	269
6.3-106	Change in External Dimensions; Durability Tests, -279 thru -347	270
6.3-107	Change in External Dimensions, Percent; Durability Tests, -279 thru -347	271
6.3-108	Throat I.D. Measurements; Durability Test Series	273
6.3-109	Throat I.D. Measurement Change; Durability Test Series	274

FIGURE LIST (cont.)

<u>Figure No.</u>		<u>Page</u>
6.3-110	AJ10-221, High Performance LAE, the Minimum Chamber Pressure Was 102 psia at Mixture Ratio 1.64	275
6.3-111	Ir-Re 490N Thruster-Nominal Box – 20 sec Flow Cals: -291 thru -301	276
6.3-112	Ir-Re 490N Thruster-Nominal Box – 20 sec Flow Cals: -291 thru -301	277
6.3-113	Chamber Wall Temperature vs MR Durability Tests	278
6.3-114	Fuel Regen Temp Rise vs MR and Pc – Durability Tests W/Duration \geq 120 sec	279
6.3-115	Ir-Re Welded Engine-Regen Delta T Effect of Propellant Inlet Temp	280
6.3-116	Fuel Regen Temp Rise vs MR and T_{prop} – Durability Tests – Effect of Prop/Temp	281
6.3-117	Fuel Regen Outlet Temp vs Pc and MR Durability Tests W/Duration \geq 120 sec	282
6.3-118	Ir-Re Welded Engine-Regen Outlet T Effect of Propellant Inlet Temperature	283
6.3-119	MMH V.P. vs Temperature – USAF Prop HDBK 3-70	284
6.3-120	AJ10-221 High Performance – LAE Margin on Fuel Boiling Pressure is Greater Than 150 psi Over the Operating Range	285
6.3-121	Oxid Inlet Pressure vs Fuel Inlet Pressure JPL Operating Box	286
6.3-122	Nozzle Weld and Chamber Wall Temperature vs Time – Test -311, 504.9 sec; 47:1 Durability	287
6.3-123	Engine Temps, vs Time – Test -311, 504.9 sec, 47:1 Durability	288
6.3-124	Fuel In, Out, Mounting Point Temperatures – Test -311; $\theta = 504.9$ sec	289
6.3-125	Engine Temperatures vs Time – Test -311 – MR = 1.65, Pc = 114.2; 504.9 sec; 47:1 Durability	290
6.3-126	Heat Transfer Thru Engine Mount – Test -311, 504.9 sec; 47:1 Durability	292
6.3-127	Facility Temperature and Pressure vs Time – Test -311, 504.9 sec; 47:1 Durability	293
6.3-128	Fuel Delta T, T_{out} , Heat Flux Test -308; 650.1 sec, 47:1 Durability	294
6.3-129	Line and Inlet Pressures vs Time – Test -311, 504.9 sec; 47:1 Durability	295
6.3-130	Cell Pressures vs Time – Test -311, 504.9 sec; 47:1 Durability	296
6.3-131	Hot Restart Temperatures – Pre-Fire, After Heat Soak	297
6.3-132	Pc vs Time – Test -311; 47:1 Durability: Firing	298
6.3-133	Vac Thrust vs Time – Test -311; 47:1 Durability: Firing	299
6.3-134	Pc, Vac Thrust vs Time – Test -311; 47:1 Durability	300

FIGURE LIST (cont.)

<u>Figure No.</u>		<u>Page</u>
6.3-135	Accelerometer Data for Test -308 – 650-sec Test; X-Axis Noise Floor, G^2/Hz	302
6.3-136	Accelerometer Data for Test -308 – 650-sec Test; Y-Axis Noise Floor, G^2/Hz	303
6.3-137	Accelerometer Data for Test -308 – 650-sec Test; Z-Axis Noise Floor, G^2/Hz	304
6.3-138	Accelerometer Data for Test -308 – 650-sec Test; X-Axis, Firing, G^2/Hz	305
6.3-139	Accelerometer Data for Test -308 – 650-sec Test; Y-Axis, Firing, G^2/Hz	306
6.3-140	Accelerometer Data for Test -308 – 650-sec Test; Z-Axis, Firing, G^2/Hz	307
6.3-141	Accelerometer Data for Test -308 – 650-sec Test; X-Axis, Ignition, G 's	308
6.3-142	Accelerometer Data for Test -308 – 650-sec Test; Y-Axis, Ignition, G 's	309
6.3-143	Accelerometer Data for Test -308 – 650-sec Test; Z-Axis, Ignition, G 's	310
6.3-144	Cross Section of J-4 Altitude Cell and Internal Test Cabin	311
6.3-145	Overall View of J-4 Outer Test Cell and Pumping System	312
6.3-146	Test Cabin Inside J-4 Altitude Cell	313
6.3-147	Internal Test Cabin	314
6.3-148	Layout of Inner Test Cabin	316
6.3-149	Endurance Test Instrumentation Locations	317
6.3-150	CORDAX Measurement System	325
6.3-151	AJ10-221 Engine Being Measured With CORDAX System	326
6.3-152	AJ10-221 CORDAX Measurements at 0 and 180 Degrees	327
6.3-153	Engine Pressures and Flows for 1-sec Test	329
6.3-154	Engine Pressures and Flows for 100-sec Test	331
6.3-155	Cell Pressure and Simulated Altitude for 100-sec Test	332
6.3-156	Engine Temperatures, 100-sec Firing and Coast	333
6.3-157	Engine Temperatures, 100-sec Firing and Coast	334
6.3-158	Engine Pressure and Flow Start Transient, 7200-sec Test	335
6.3-159	Engine Pressure and Flows, 7200-sec Test and 1800-sec Coast	336
6.3-160	View of Engine Assembly on Test Stand After Successful Completion of 2-hr Endurance Test	337
6.3-161	Close-up of Engine Assembly After 2-hr Endurance Test	338
6.3-162	Engine Temperatures, 7200-sec Firing and 1800-sec Coast	339
6.3-163	Engine Temperatures, 7200-sec firing and 1800-sec Coast	340
6.3-164	Detail of Skirt Joint After 2-hr Firing Looks Normal	341
6.3-165	Skirt Separated After Installation of Heat Shield	343
6.3-166	Engine With Heat Shield in Place, Ready for Test	344

FIGURE LIST (cont.)

<u>Figure No.</u>		<u>Page</u>
6.3-167	Engine Pressures and Flows During 1200-sec Test	345
6.3-168	Engine Temperatures During 1200-sec Test	346
6.3-169	Engine Temperatures During 1200-sec Test	347
6.3-170	Thruster and Heat Shield After 1200-sec Test	348
6.5-1	View of Injector, Broken Bolts and Chamber Assembly	351
6.5-2	I_s Versus Time for NTO/MMH and NTO/AH	353
6.5-3	Fuel Temperature Rise, NTO/MMH and NTO/AH	354
6.5-4	Fuel Outlet Temperature, NTO/MMH and NTO/AH	355
6.5-5	Regen Tip Temperature, NTO/MMH and NTO/AH	356
6.5-6	Heat Transfer to Fuel, Test -246	357
6.5-7	Propellant Flow Rate and Mixture Ratio, Test -246	358
6.5-8	External Temperature, Test -246	359
6.5-9	Cell Pressure Versus Time, Test -246	360
6.5-10	Ir-Re Chamber After Test -246	365
6.5-11	Injector SN 6-1 After Test -246	366
6.5-12	Schematic of Cooled Adapter Weld	368
6.5-13	Predicted Cooled Adapter Liquid Side Wall Temperature	370
6.5-14	Comparison of Cooled Adapters	371

ACRONYM LIST

A/R	As Required	NBS	National Bureau of Standards
AT	Acceptance Test	NDE	Nondestructive Evaluation
ATP	Authority to Proceed	NTO	Nitrogen Tetroxide
CDRL	Contract Data Requirements List	OMS	Orbital Maneuvering System
CPIA	Chemical Propulsion Information Agency	OMV	Orbital Maneuvering Vehicle
CVD	Chemical Vapor Deposition	PDFM	Positive Displacement Fuel Meter
EB	Electronbeam	PDR	Preliminary Design Review
FDR	Final Design Review	PQR	Post Qualification Review
FMECA	Failure Modes, Effects, and Criticality Analysis	QA	Quality Assurance
Ir	Iridium	R&D	Research and Development
IR&D	Independent Research and Development	Re	Rhenium
JANNAF	Joint Army-Navy NASA Air Force	REA	Rocket Engine Assembly
JPL	Jet Propulsion Laboratory	RFP	Request for Proposal
LAE	Liquid Apogee Engine	SDI	Strategic Defense Initiative
MMH	Monomethylhydrazine	SEM	Scanning Electron Microscope
MP	Mounting Point	SiC	Silicon Carbide
MR	Mixture Ratio	SN	Serial Number
MRB	Material Review Board	SOW	Statement of Work
MRR	Manufacturing Readiness Review	SS	Stainless Steel
NAS	Naval Air Station	TBD	To Be Determined
NASA	National Aeronautics and Space Administration	WBS	Work Breakdown Structure

1.0 SUMMARY

This report describes the activities of Option III of NASA LeRC Contract NAS 3-25646, Advanced Small Rocket Chambers program. In this phase of the program, the AJ10-221, a high performance Ir-Re 110 lbf (490N) welded rocket chamber with 286:1 area ratio nozzle was designed, built, and hot fired for over 6 hours. It demonstrated an I_s of 321.8 sec which is 10 sec higher than conventional 110 lbf silicide coated Cb chambers now in use. Launch vibration simulation tests remain to be done.

The overall objectives of the Advanced Small Rocket Chambers Program are to advance the state-of-the-art of small chemical rocket chambers significantly by (1) examining fundamental combustion processes, (2) evaluating new high temperature materials in relevant environments, and (3) evaluating small rocket concepts by direct hot fire testing.

The activity reported here was conducted under Option III tasks 13, 14, and 15 of the program. The intent of this work was to demonstrate the understanding of the combustion/materials interaction processes studied in the first phase of the program, Ref. 1, by applying them to a flight-type rocket engine with potential application to NASA planetary missions such as CRAF-Cassini. Prior to this demonstration, a 14 lbf (62N) engine was designed, built and tested under Option II of this program (Ref. 2).

The approach used in this portion of the program was to demonstrate the performance improvement that can be made by the elimination of fuel film cooling made possible by the use of a high temperature (4000°F) (2200°C) Ir-Re chamber materials.

Detailed thermal, performance, mechanical, and dynamic design analyses of the full engine were conducted and two Ir-Re chambers were built to the Aerojet design by Ultramet, using the chemical vapor deposition (CVD) process.

Conventional 110 lbf engines use up to ~40% fuel film cooling; this is required to keep the Cb chamber at an acceptable operating temperature of under 2400°F (1300°C). The requirement for a cool boundary layer throughout the chamber and throat implies unmixed, unreacted fuel exiting the nozzle which may produce a performance loss of up to 25 sec and a potential source of spacecraft contamination. Injectors for this engine were designed to eliminate this fuel film cooling. Head end thermal management was accomplished by fuel regenerative cooling. Incorporation of a secondary mixing device or Boundary Layer Trip (BLT) within the regenerative cooling section of the combustion chamber (Aerojet Patents 4882904 and 4936091) results

1.0, Summary (cont.)

in improvement in flow uniformity, and a significant life and performance increase since most combustion is complete before the products leave the stainless steel regeneratively cooled section.

The 110 lbf engine design was verified in bolt-up hardware tests at sea level and altitude. The effects of injector design on performance were studied. Two duplicate injectors were fabricated matching the preferred design and were demonstrated to be interchangeable in operation. One of these units was welded into a flight type thruster which was tested for an accumulated duration of 22,590 sec in 93 firings, one of which was a continuous burn of two hours.

A design deficiency in the C-103 nozzle skirt near the Re-Cb transition joint was discovered, studied and a corrected design has been prepared but not implemented. Workhardening studies have been conducted to investigate methods for increasing the low yield strength of the Re in the annealed condition.

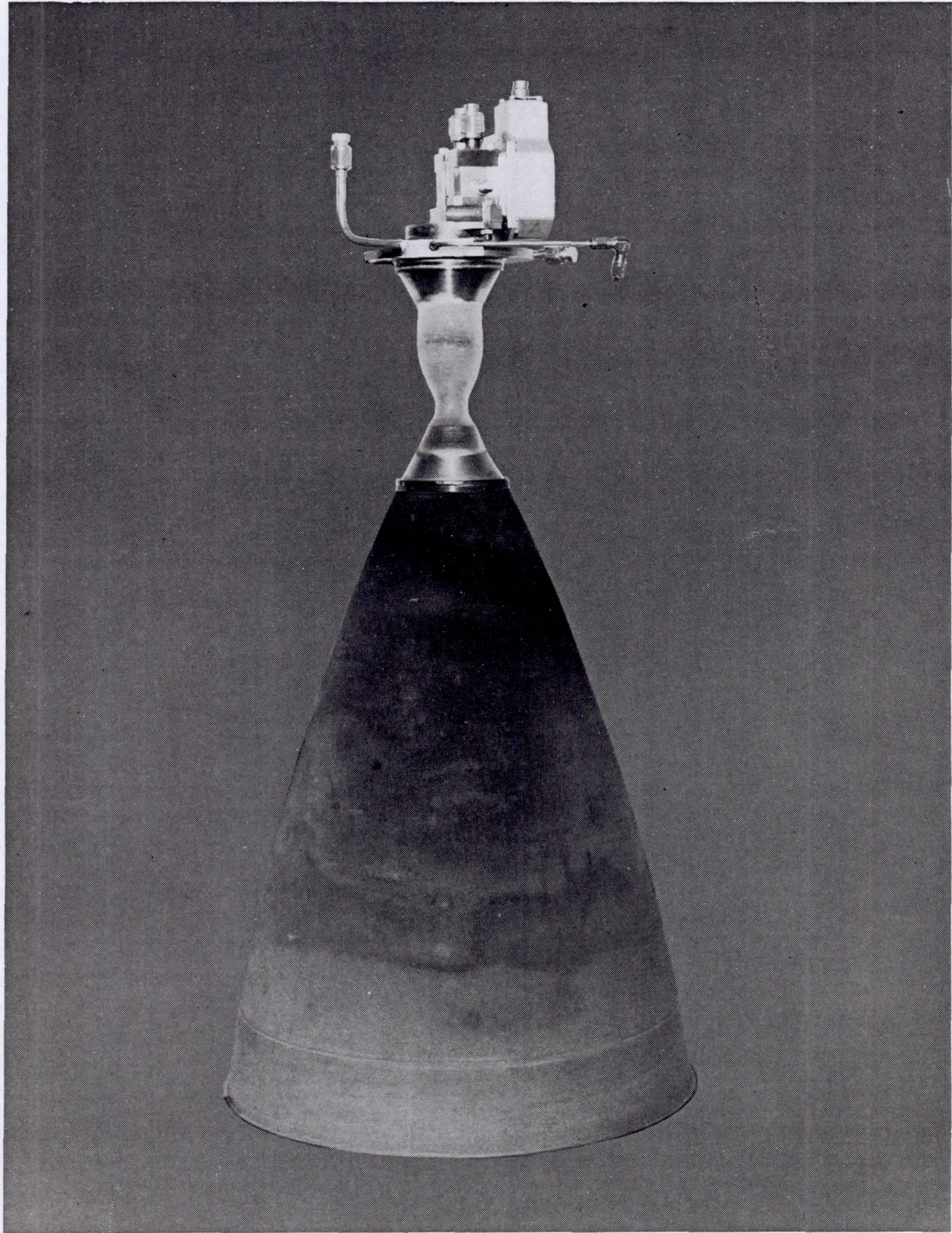
An advanced 490N high performance engine has been demonstrated which, when proven to be capable of withstanding launch vibration, is ready for flight qualification.

2.0 INTRODUCTION

2.1 PROGRAM DESCRIPTION

A high performance, 321.8 sec specific impulse, flight weight prototype 490 N engine (AJ10-221) was designed, fabricated, and hot fire tested for 6.3 hours. This duration was accomplished in 93 tests of which 81 were full thermal cycles. The design of the engine was based on the use of a high temperature iridium-coated rhenium thrust chamber which can operate without fuel film cooling, utilizing a high performance platelet injector, a two stage combustion chamber concept, and a conventional silicide coated columbium nozzle extension to reduce weight.

The flight weight all welded engine assembly was based on component development started under JPL Contract 957882, Ref. 3, using bolt together hardware. This program further optimized the design to maximize the specific impulse and implemented the fabrication technology required to produce the prototype shown in Figure 2.1-1.



C0692 3674

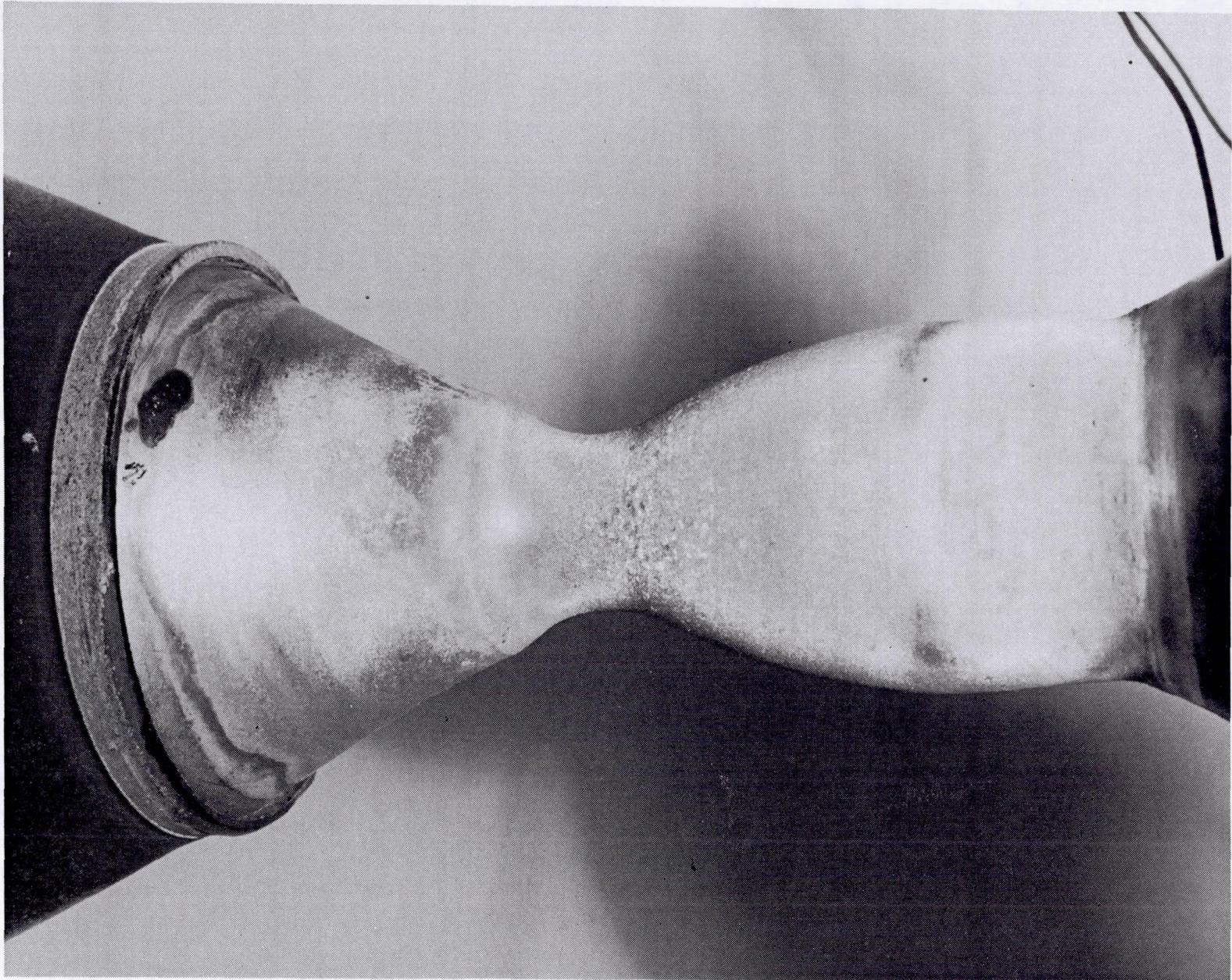
Figure 2.1-1. AJ10-221 100 lbf Ir-Re Engine With 286:1 Expansion Nozzle

2.1, Program Description (cont.)

Hardware for the test article and a full set of spare parts with the exception of the bipropellant torque motor valve were fabricated. The program was completed using only the first set of hardware which was in excellent condition with the exception of the nozzle skirt attachment at the conclusion of testing. The failure of the columbium nozzle attachment occurred during post test handling of the hardware, after 6 hours of firing, in a region of parent metal next to a weld which mated it to the rhenium chamber. An analysis indicated that failure to apply a protective coating over the weld resulted in oxygen embrittlement of the C103 alloy from both the imperfect cell vacuum on the outside and the propellant combustion products on the chamber inside. The rhenium indicated no adverse reaction at this relatively low temperature (2000 F) location.

Testing was accomplished in the following phases: the ability of the iridium/rhenium chamber material to operate safely without fuel film cooling was first demonstrated using bolt together hardware and a unique rhenium foil test method to verify injector compatibility. The injector design was optimized and a duplicate fabricated and tested to verify consistency of the high specific impulse and compatibility. These were identical within the limits of measurement accuracy $< 0.3\%$.

Testing of the all welded prototype was accomplished in three test groups to provide the demonstrated performance data given in Table 2.1-1. The performance characterization testing, consisting of 20 tests, was conducted with a 286:1 nozzle. Testing included surveys of propellant supply and pressure conditions. No limiting conditions were encountered. These tests were followed by 69 durability tests with the nozzle truncated at an area ratio of 47:1 to allow the test duration to be increased from 120 to 600 sec per test. An additional 13,104 seconds were added in the durability testing over a wide range of propellant inlet pressure and temperature. Figure 2.1-2 shows the chamber at the conclusion of this durability test series.



5

Figure 2.1.2. Chamber Exterior at End of Durability Tests

C0792 4646

2.1, Program Description (cont.)

Table 2.1-1. Demonstrated Performance

Parameter	AJ10-221 Demonstrated
Specific Impulse, sec	321.8 ± 1.8 (3σ) (With 286:1 Nozzle)
Life, Hours (Equivalent)	6.275
Full Thermal Cycles	80
Inlet Pressures, psia	
Oxidizer	185 to 265
Fuel	190 to 295
Inlet Temperatures, F	40 to 120
Mixture Ratio, O/F	1.45 to 1.85
Weight, lb	12.8 (With 4.5 lb Over-Dimension 286:1 Nozzle)
Propellants	NTO/MMH

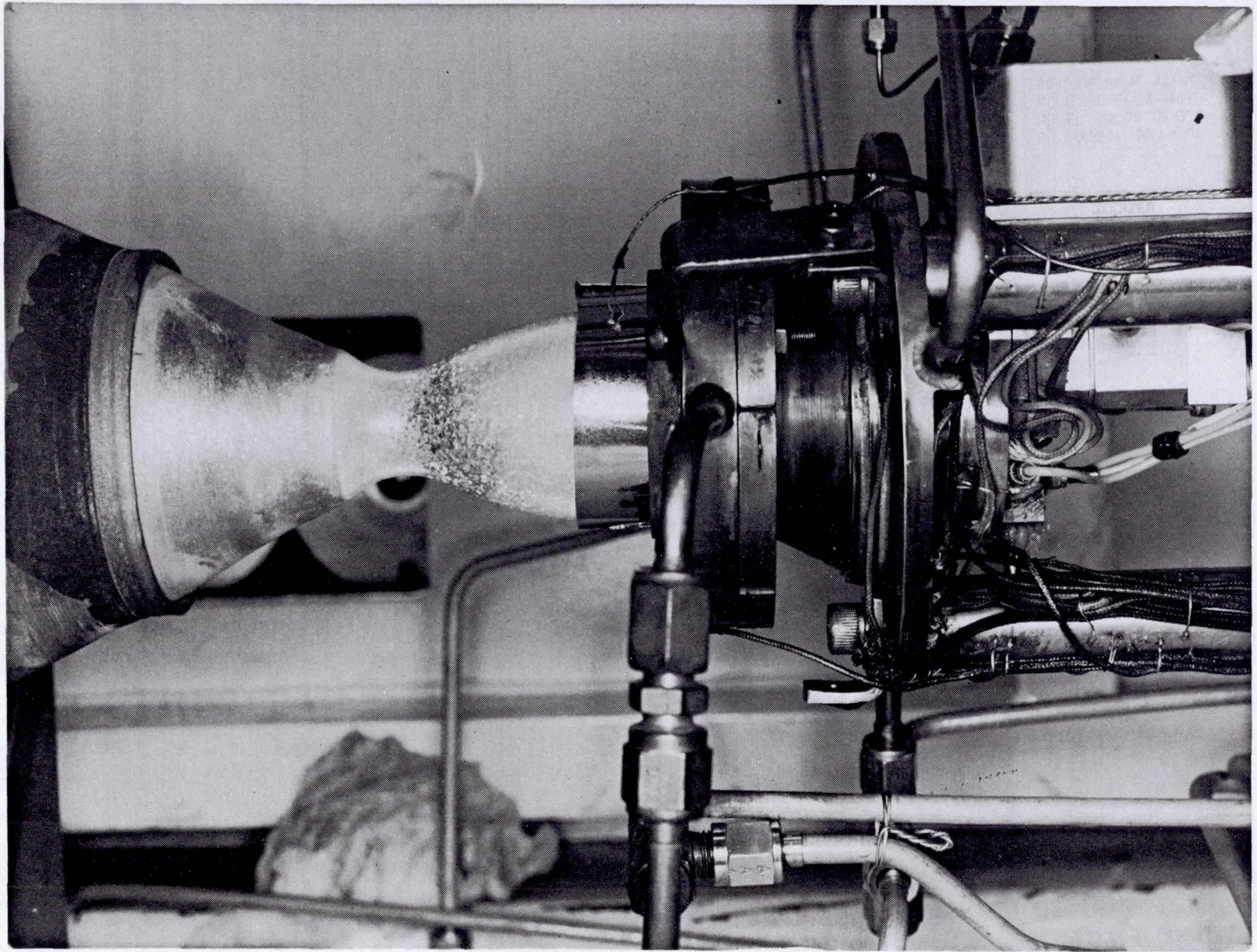
Endurance testing involved four more tests, one of 7200 sec continuous firing and another of 1200 sec with a radiation heat shield which obscured most of the high temperature chamber. No adverse effects or limiting firing/thermal soak conditions were encountered in these tests. Figure 2.1-3 shows the chamber at the conclusion of the two hour endurance test with a total of 6 hours of firing. A total of 6.3 hours of firing was accumulated on the chamber at the conclusion of the test program.

2.2 ENGINE DESCRIPTION AND CAPABILITIES

The AJ-10-221 design, Figure 2.1-1, incorporates the following key features that are essential to the required combination of high performance and long life:

1. Iridium-lined rhenium chamber provides high thermal design margin without need for film cooling.
2. A fuel regeneratively cooled chamber front end with integral boundary layer trip* ensures complete combustion of the oxidizer and results in maximum performance. This also regulates heat soakback to the valve.
3. A ninety-two element splashplate injector provides the highest combustion efficiency (>99%).
4. All-welded construction reduces weight and eliminates less reliable types of hot gas seals.

*U.S. Patents 4882904 and 4936091, and German Patent P39 23 948.9-13, 27 October 1993.



C0293 1207

Figure 2.1-3. Close-up of Engine Assembly After Two Hour Endurance Test

2.2, Engine Description and Capabilities (cont.)

2.2.1 Description

The AJ10-221 is comprised of five major components shown with some duplication in Figure 2.2-1.

The all-welded engine assembly, shown in Figures 2.1-1 and 2.2-2, is radiation cooled and operates without fuel film cooling. The regeneratively fuel-cooled flange and chamber head end minimize heat conduction to the spacecraft and provide the platform to which the high temperature rhenium chamber is attached. The first and second stage of the combustion chamber is contained within this cooled section, which is fabricated from 304L stainless steel to eliminate the low temperature incompatibility between the partially burned propellants and the refractory metals.

Major components of the engine include a Moog Model 53E-179 torque motor bipropellant valve that is fully interchangeable and has parallel redundant coils; a 92-element platelet injector, fabricated from 300 series CRES; 300 series CRES fuel-cooled head end section with mounting flange that minimizes the transfer of heat to the spacecraft via the mounting flange and improves combustion product compatibility; an iridium-lined rhenium chamber that can operate without fuel film cooling for more than 6.3 hour; and an R512E silicide-coated C-103 nozzle extension.

The engine incorporates Aerojet's two-stage combustor design, U.S. Patent Numbers 4882904 and 4936091, German Patent Number P39 23 948.9-13, which simultaneously maximize performance and life.

The engine mass and temperature distribution allow shutdown and restart of any burn/coast combination without risk of overheating the joints, valve, or components.

Table 2.2-1 gives the engine weight distribution by component.



C0891 5947

Figure 2.2-1. Major Components of the AJ10-221

10

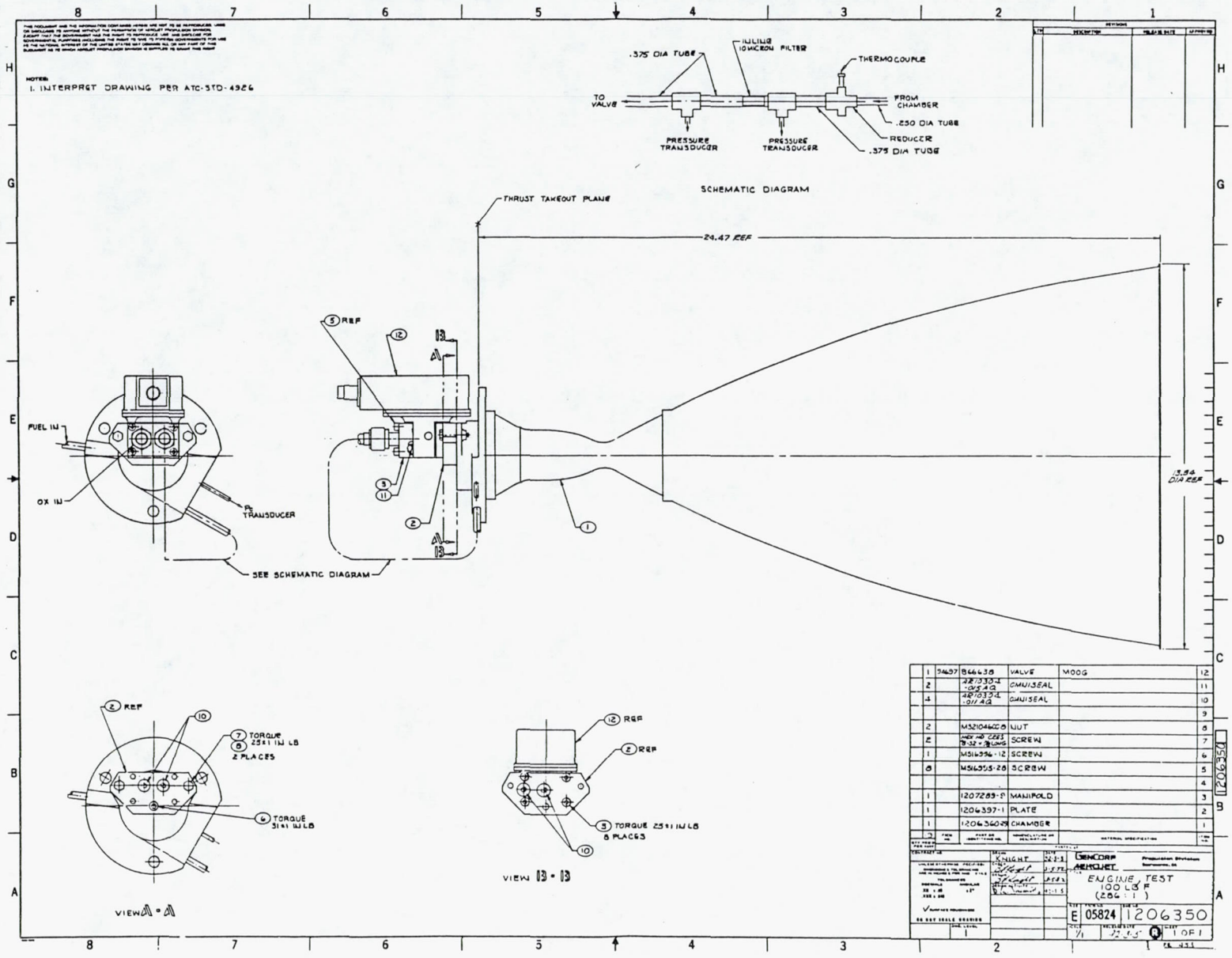


Figure 2.2-2. Drawing of Engine Test (286:1)

2.2, Engine Description and Capabilities (cont.)

Table 2.2-1 Existing Hardware Makes Engine Weight Predictions Low Risk

		AJ10-221 Test Hardware, Weight, lb
B66638	Valve	2.70
1206397-1	Adapter Plate	0.54
1206362-9	Injector	1.00
1206354-9	Chamber Adapter	2.11
1206383-9	Chamber	1.98
1206351-9	Nozzle	<u>4.45</u>
		12.78

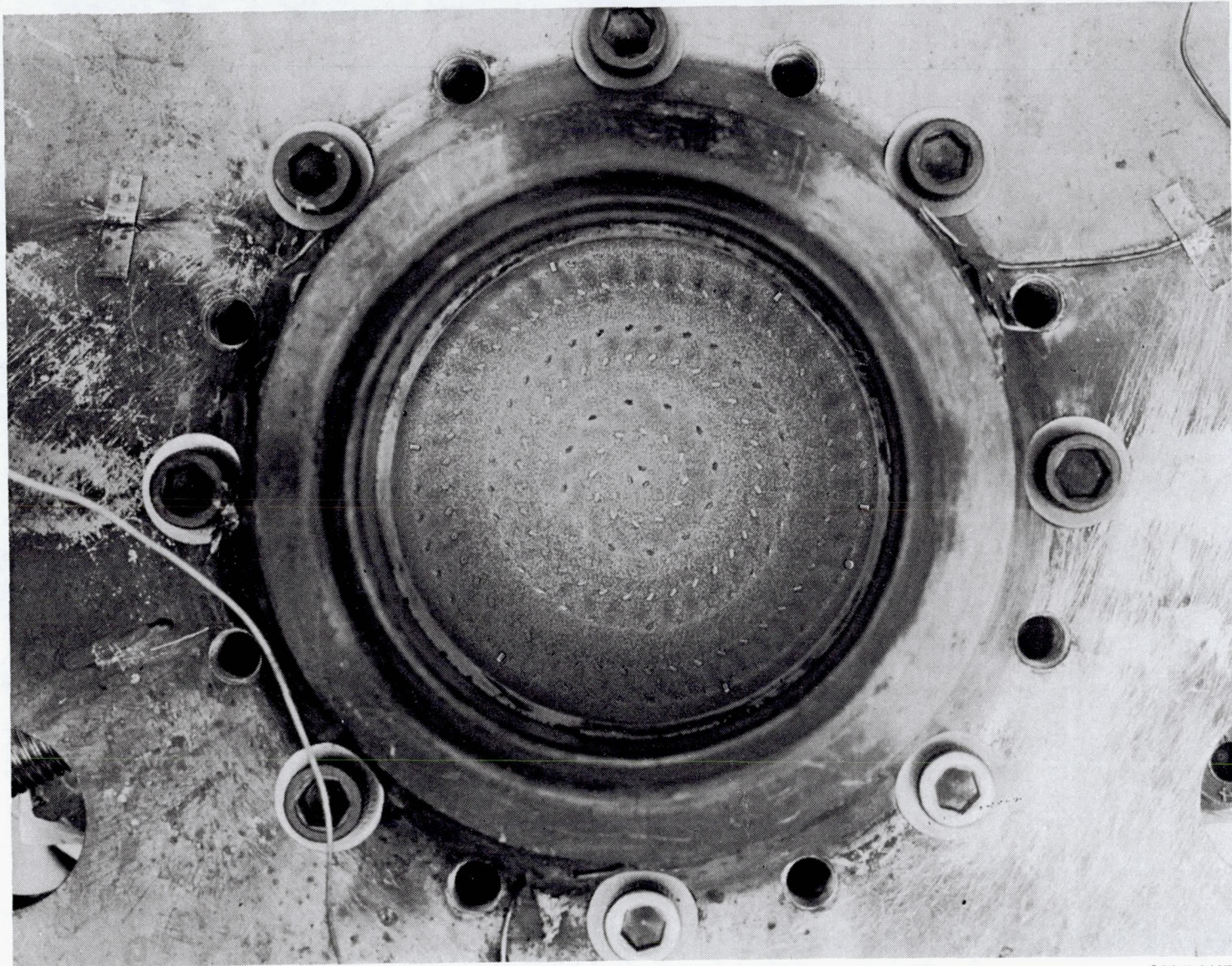
2.2.2 Components

Injector

The injector uses a diffusion bonded platelet design with 92 unlike doublet preatomized splash plate elements, shown in Figure 2.2-3, and is fabricated from CRES 347. In the preatomized design, the propellant leaves each injection orifice in an atomized state. The preatomized element avoids the requirement for perfect alignment/impingement of two small diameter liquid streams for the purpose of propellant atomization. Misalignment of small impinging propellant jets is a major cause of unreproducible engine-to-engine performance, thermal streaking, and poor stability characteristics. The design has demonstrated reproducible performance and compatibility on four injectors. The injector includes an integral filter to prevent flow obstruction. It incorporates an integral, critically damped acoustic resonator cavity as part of the basic design. The combination of a very large number of small length/diameter orifices and the integral acoustic resonator cavity provides a robust, stable design that is insensitive to flow decay, which may result in conventional designs from the presence of ferric salts in the oxidizer.

Fuel-Cooled Chamber Head End

The fuel-cooled chamber head end uses a spiral-flow path for the MMH coolant and is fabricated from CRES 304. Thruster dribble volume is held to a minimum by



C0491 2167

Figure 2.2-3. 92 Element Splashplate Injector



2.2, Engine Description and Capabilities (cont.)

placing this section upstream of the valve. The section was designed to operate at 330 psia and to be a heat sink for the rhenium rocket chamber, both during steady state operation and during shutdown. This section also contains the staged combustion device on the hot gas side to complete combustion of the oxidizer before combustion gases come into contact with the iridium-coated rhenium chamber.

Combustion Chamber

The iridium/rhenium combustion chamber shown with weld rings in Figure 2.2-4 eliminates the need for fuel film cooling. The iridium-lined rhenium combustion chamber fabricated by the chemical vapor disposition process illustrated in Figure 2.2-5 allows operation in a simple radiation-cooled mode, without fuel film cooling. The high temperature portion of the engine is metallurgically joined to the fuel-cooled head end with the joint operating at 365°F during long burns and falling to 270°F immediately after shutdown and then increasing to a maximum of 305°F in postfire coast. The thermal model used to design this engine has been validated by hot-fire testing.

The rhenium structural member is a monolithic construction (no welds).

The 100 lbf design has been proven in extensive hot-fire testing of 4 different chambers fabricated by this process. Rhenium was selected because it provides good low temperature ductility and has a melting point of 5756°F, which exceeds the maximum combustion temperature of the NTO/MMH bipropellant combination by more than 500°F.

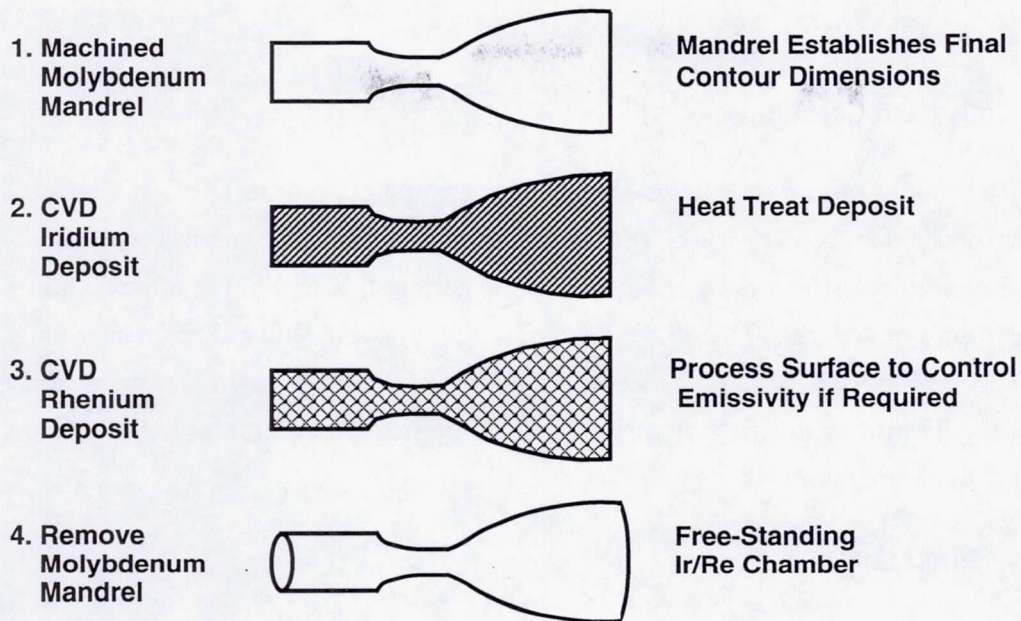
The iridium liner was selected because of its chemical inertness, oxidation and oxygen-diffusion resistance, high melting point of 4449°F, and thermal expansion coefficient that is nearly the same as that of rhenium. The close thermal expansion match of the liner to the substrate eliminates the high temperature-induced thermal cycle life limitations exhibited by disilicide-coated columbium, in which the expansion rates of the two materials differ significantly.

The measured equilibrium operating temperature is 3400°F at a combustion efficiency of 99 percent. This is the highest chamber temperature and occurs when all the propellant is fully burned. An operating life of 15 hour has been demonstrated in subscale (5 lbf)



C0891 5949

Figure 2.2-4. Iridium-Rhenium Chambers With Bimetallic Transition Rings Welded on Both Ends (Left: Stainless Steel to Rhenium; Right: C-103 to Rhenium)



**Chemical Vapor Deposition Processes
Provide the Keys to Chamber Fabrication**

log 922.472A

Figure 2.2-5. Basic Fabrication Steps for Iridium-Coated Rhenium Combustion Chamber

2.2, Engine Description and Capabilities (cont.)

hardware at 4000°F without failure over a wide range of operating conditions (Ref. 4). The anticipated failure mechanism is diffusion of rhenium through the iridium layer and its subsequent oxidation. Laboratory diffusion measurements indicate that this will begin after 40 hours at operating temperature of 4000°F. The 600°F design margin allows using radiation shields, if required by the spacecraft design, without exceeding the engine's demonstrated operating temperature capabilities. Testing with a radiation shield has demonstrated acceptable steady state and post fire heat soak temperatures.

Nozzle Extension

A metallurgically joined disilicide-coated C-103 columbium nozzle extension, Figure 2.2-6, is attached at an area ratio of 16:1 to give the engine a 286:1 expansion ratio. Rhenium and columbium have nearly identical expansion coefficients, thereby avoiding thermally induced fatigue stresses in the joint between the chamber and nozzle. This joint operates conservatively at an experimentally verified temperature of 1900°F. More than 80 deep-thermal-cycle engine firings and a 6-hour thermal simulation at 2150°F validated the durability of this joint design.

The roundness of the exit plane is maintained by a stiffening ring.

Valve

The engine uses a highly reliable Moog bipropellant torque motor valve, Figure 2.2-7, that is free of sliding or rubbing surfaces that can bind, induce wear, or generate contamination. The mechanical linkage ensures simultaneous opening of fuel and oxidizer circuits throughout the valve's life.

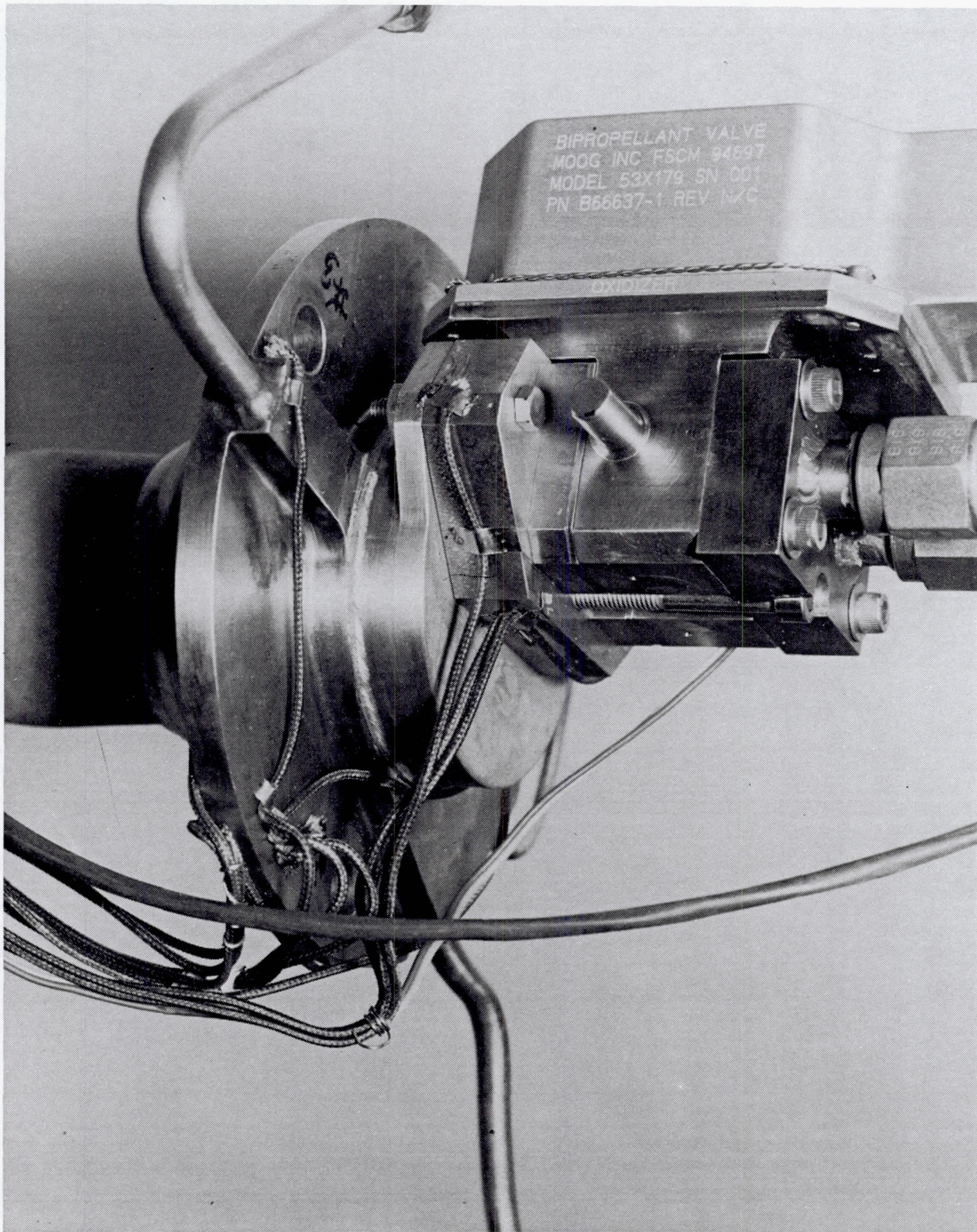
The valve contains an integral 45-micron filter to protect the Teflon seats.

The valve is a mechanically bolted configuration that allows interchangeability between engines. All testing to date has been with Model 53X-179, which is mechanically assembled. Table 2.2-2 gives valve characteristics and responses.



C0891 5758

Figure 2.2-6. 286:1 Silicide Coated C-103 Skirt



C0392 1330

Figure 2.2-7. Moog Torque Motor Bipropellant Valve Assembled to AJ10-221 Engine

2.2, Engine Description and Capabilities (cont.)

Table 2.2-2. Moog Model 53X-179 Torque Motor Bipropellant Valve

Materials	
Body	15-5 PH
Cover	6061-T651
Seats	Teflon
Flexure Tubes	15-5 PH
Response	
Open, msec	<30
Close, msec	<5
Electrical Power Requirements	
Voltage, Vdc	24 to 32
Pull In, Vdc	<18
Drop Out, Vdc	<2
Peak Current, A	1
Continuous Power W	<38

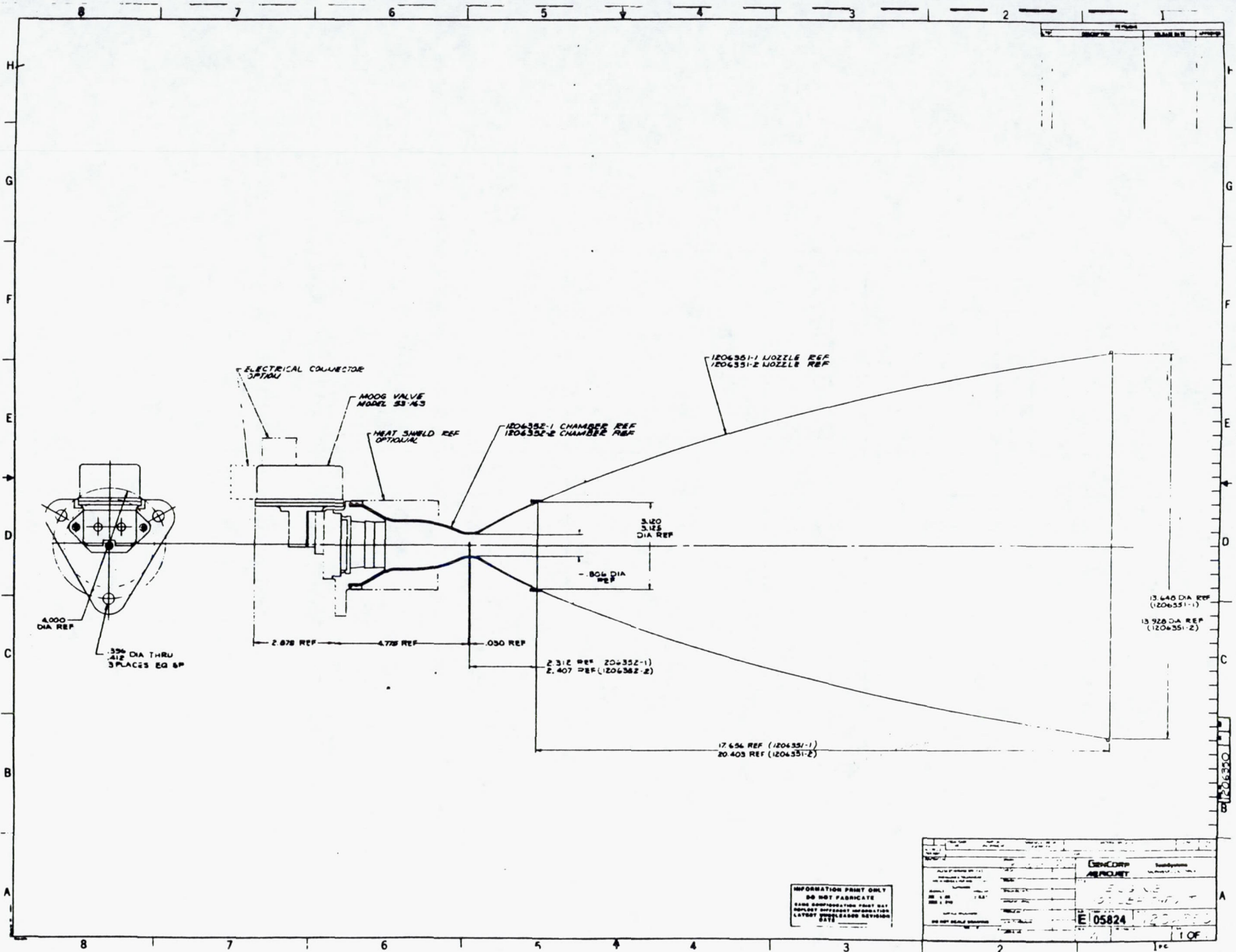
2.2.3 Interfaces

The engine-spacecraft interface consists of the mechanical attachment of the engine to the vehicle thrust mount and the propellant feed lines, which are normally welded. The thrust interface is the flange of the cooled adapter, with three equally spaced mounting holes on a 4.0-in. bolt circle, as shown in Figure 2.2-8.

2.2.4 Capabilities; Performance, Durability and Thermal Validation

The AJ10-221 engine has demonstrated excellent performance, thermal margins, and stability in 93 firings and 6.275 hour of firing as an all-welded lightweight assembly.

20



INFORMATION PRINT ONLY
DO NOT FABRICATE
SAME IDENTIFICATION PART MAY
DISPLAY DIFFERENT INFORMATION
LATEST SUPPLEMENTAL REVISION
DATE

DATE OF ISSUE: 11/11/51 PREPARED BY: [Signature] CHECKED BY: [Signature]		DESIG: 100-1-1 REV: 1 DATE: 11/11/51
AUTHORITY: [Signature] APPROVED: [Signature]		DRAWING NO: E 05824 SHEET NO: 1 OF 1

Figure 2.2-8. Engine 100 lbf Thrust

2.2, Engine Description and Capabilities (cont.)

2.2.5 Specific Impulse/Operating Box

Figure 2.2-9 shows the operating range of the all-welded engine.

The performance and thermal profiles have been experimentally verified as being within safe design margins at mixture ratios of 1.4 to over 2.0, as shown by the operating envelope of Figure 2.2-10 and the steady state and postfire coast data of Figure 2.2-11.

Two identical injectors, SN 6-1 and SN 6-2, were fabricated to reproduce the high performance measured for earlier prototype injectors, SN-1 and SN-2 (Ref. 3). The reproduced designs were identical except for slightly larger orifice diameters in order to increase thrust from 100 to 110 lbf without increasing propellant supply pressures. Table 2.2-3 shows the test data from 20 tests, which verify the reproducibility of the specific impulse performance of the SN 6-1 and 6-2 injectors when hot-fire tested in the 44:1 bolt-together engine. All four injectors, SN-1, SN-2, SN 6-1 and SN 6-2, yielded a specific impulse of 309 to 310 lbf-sec/lbm at the nominal design point. The experimentally determined specific impulse of two injectors of the same design and orifice dimensions, expressed as a function of mixture ratio and chamber pressure, is shown in Figures 2.2-12 and 2.2-13.

Performance Determination

Performance Test Results at Area Ratio of 286:1 – Twenty tests at simulated altitude were conducted in the prototype all-welded configuration. Table 2.2-4 gives test results. Figure 2.2-14 shows the thrust and flow-based specific impulse data from 120-sec duration performance tests as a function of mixture ratio. These were obtained by varying the propellant tank pressures for each test. The measured specific impulse at the nominal operating mixture ratio of 1.65 is 321.8 lbf-sec/lbm (± 0.6 sec 1σ). As noted in these figures, there is little sensitivity to propellant supply pressures. Chamber wall temperature versus mixture ratio is plotted in Figure 2.2-15. The maximum measured temperature for the AJ10-221 was 3400°F without a heat shield. This temperature is 600°F below the 4000°F operation demonstrated for 15 hours in a 5 lbf class material tester chamber (Ref. 4). A thermal margin of 500°F was measured for the Columbiuim skirt.

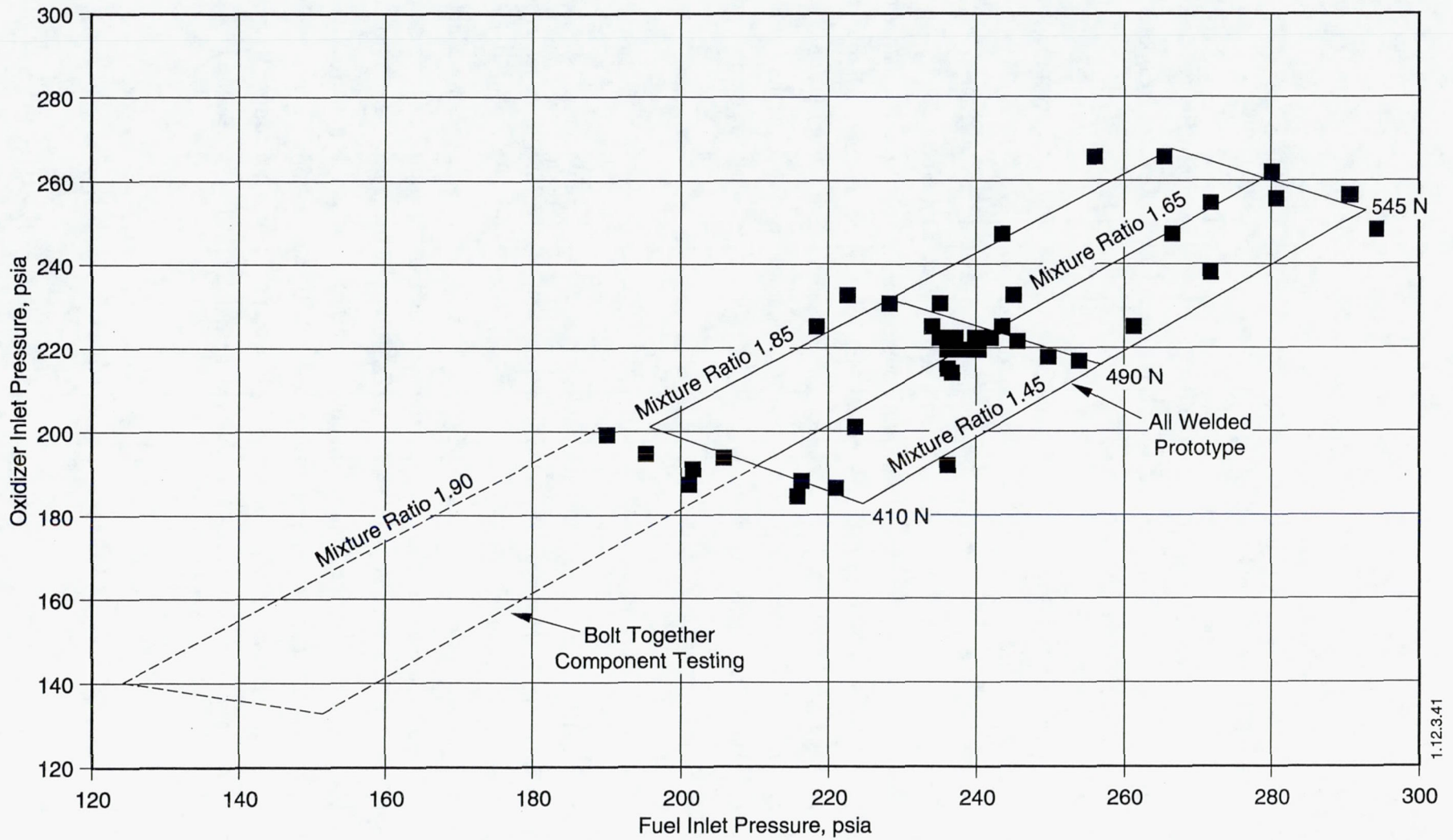


Figure 2.2-9. Demonstrated Operating Envelope

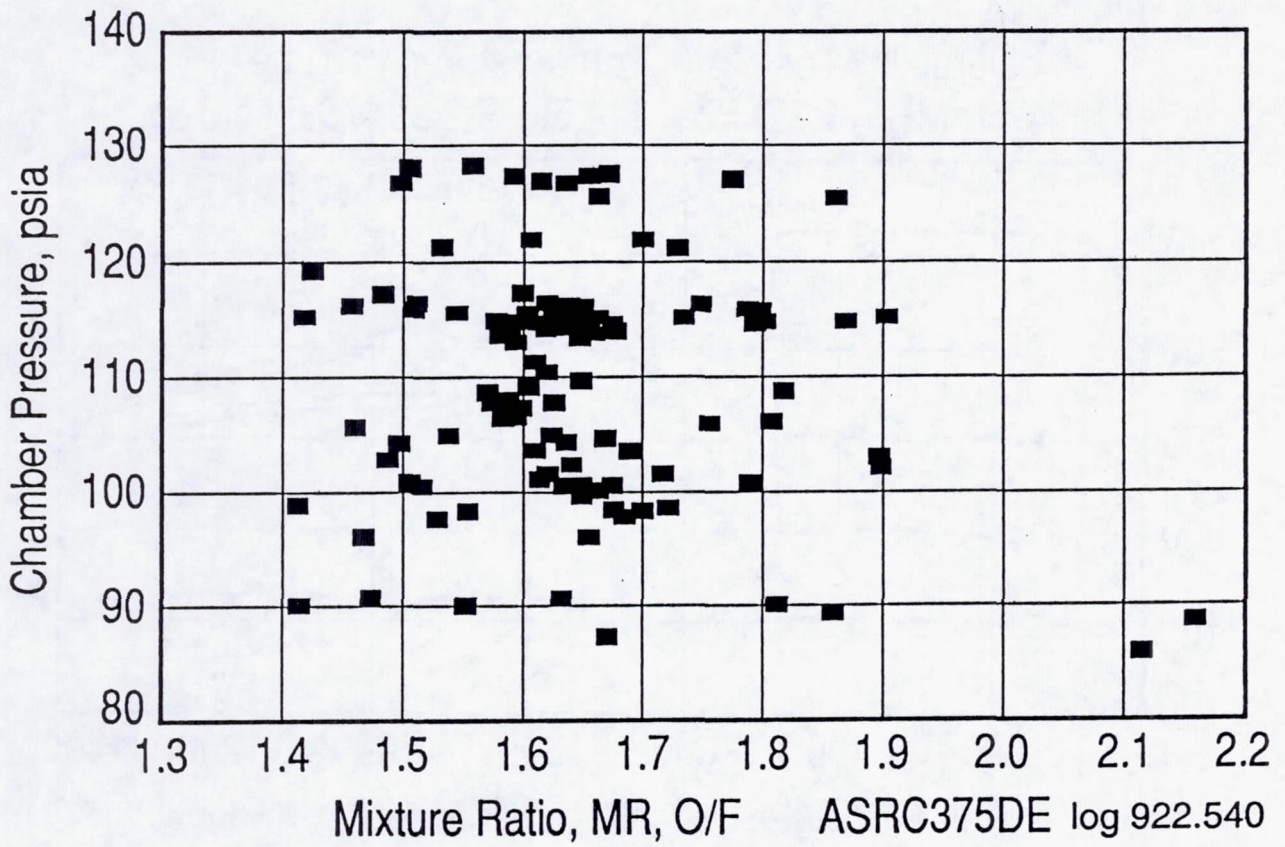


Figure 2.2-10. The Engine Has Been Tested Over a Wide Range of Operating Conditions

Durability Test -306, Temperatures vs Time
 47:1; MR = 1.67, Pc = 114.5, FS-2 at 476.6 sec

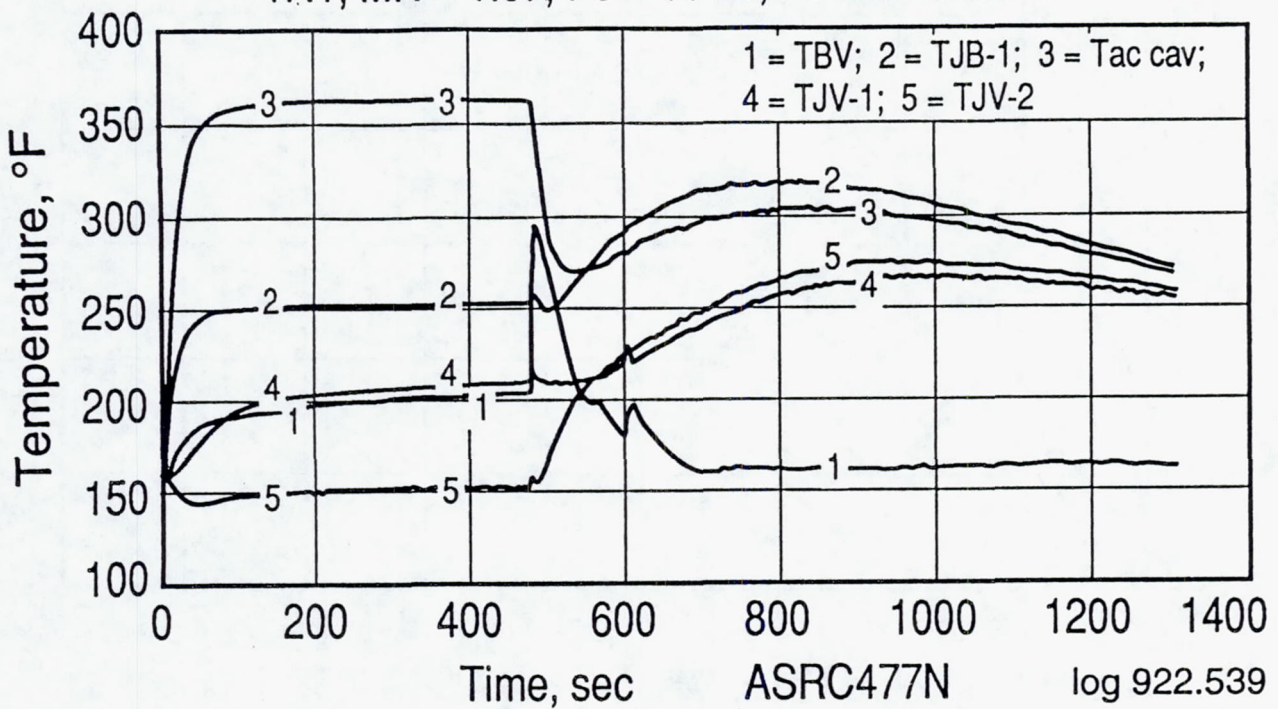


Figure 2.2-11. Front-End Temperatures Provide Wide Thermal Margin

2.2, Engine Description and Capabilities (cont.)

Table 2.2-3. 44:1 Performance for Injectors SN 6-1 and SN 6-2 Was Demonstrated to Be Identical

Run No.	Injector	Firing Time	Pc, psia	MR O/F	Fvac, lbf	Is vac (sec) at 44:1	Regen. Outlet, °F	Regen. Delta T, °F	Regen. Heat Trans., Btu/sec	Chamber Temp., °F
225	SN 6-2	27.0	100.5	1.516	101.3	308.1	166	116	10.8	3514
226	SN 6-2	25.0	100.2	1.662	101.4	309.6	181	132	11.7	3638
227	SN 6-2	25.0	100.2	1.675	101.5	309.7	184	136	12.0	3635
228	SN 6-2	25.0	99.5	1.648	100.7	309.6	180	133	11.8	3631
229	SN 6-2	25.0	110.3	1.620	111.7	308.8	163	116	11.5	3438
230	SN 6-2	25.0	90.5	1.632	91.5	309.7	193	147	12.0	3824
231	SN 6-2	25.0	100.8	1.505	101.5	308.3	166	120	11.4	3487
232	SN 6-2	25.0	100.6	1.788	102.3	310.3	192	146	12.5	3719
233	SN 6-2	25.0	100.5	1.637	101.7	309.8	176	131	11.8	3621
234	SN 6-1	25.0	101.4	1.716	102.8	310.0	188	138	12.1	—
235	SN 6-1	25.0	101.2	1.620	102.3	309.6	190	131	11.9	3704
236	SN 6-1	25.0	100.5	1.647	101.7	309.8	184	135	12.1	3734
237	SN 6-1	25.0	97.4	1.530	98.2	308.6	175	127	11.5	3669
238	SN 6-1	10.5	108.6	1.571	109.6	308.4	159	111	11.0	3204
239	SN 6-1	25.0	107.6	1.576	108.7	308.8	170	122	12.0	3546
240	SN 6-1	25.0	89.6	1.553	90.3	308.6	193	146	12.1	3862
241	SN 6-1	25.0	98.7	1.413	99.1	306.4	163	116	11.2	3510
242	SN 6-1	25.0	98.6	1.720	100.1	310.4	194	147	12.6	3844
243	SN 6-1	10.0	95.8	1.467	96.1	307.0	167	120	11.0	3333
244	SN 6-1	90.0	101.0	1.614	102.3	309.6	179	131	12.0	3668

2.2.6 Component Life and Durability Testing

Life and durability have been verified in full-scale component and engine testing, as indicated in Table 2.1-1.

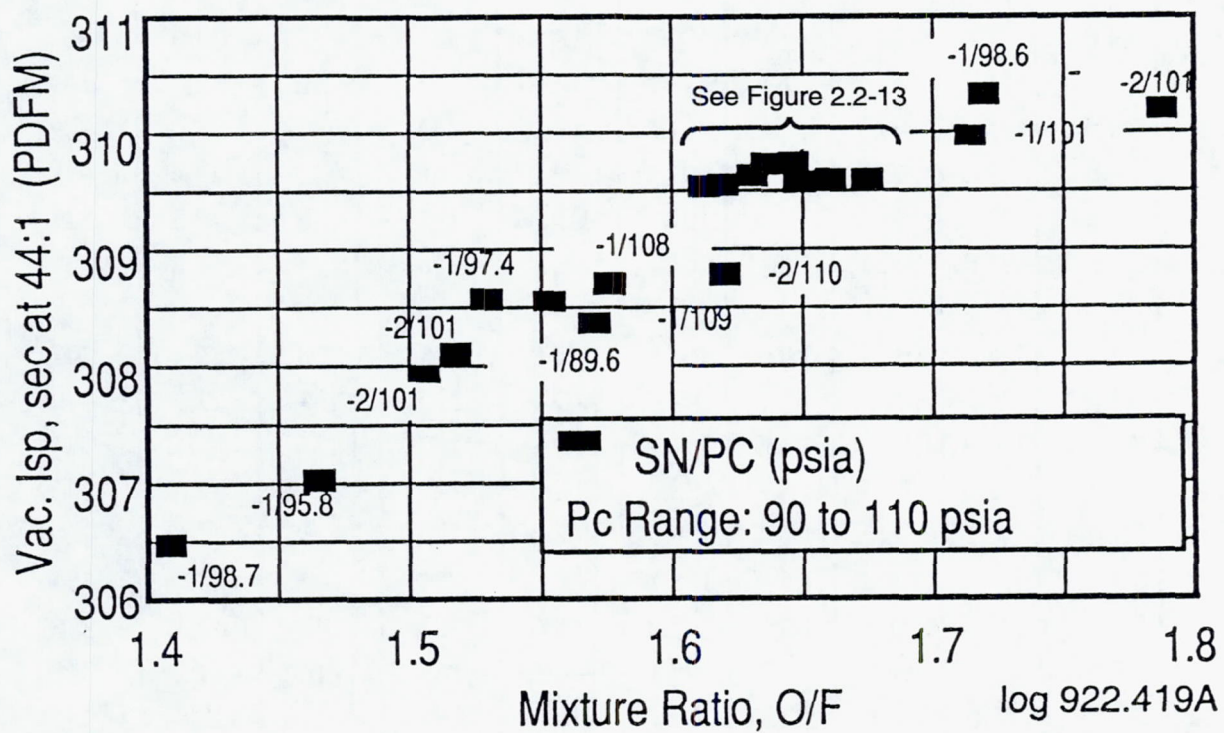


Figure 2.2-12. Isp Vac for SN 6-1 and SN 6-2 Injectors at Area Ratio = 44:1 is Identical From MR 1.4 to 1.8

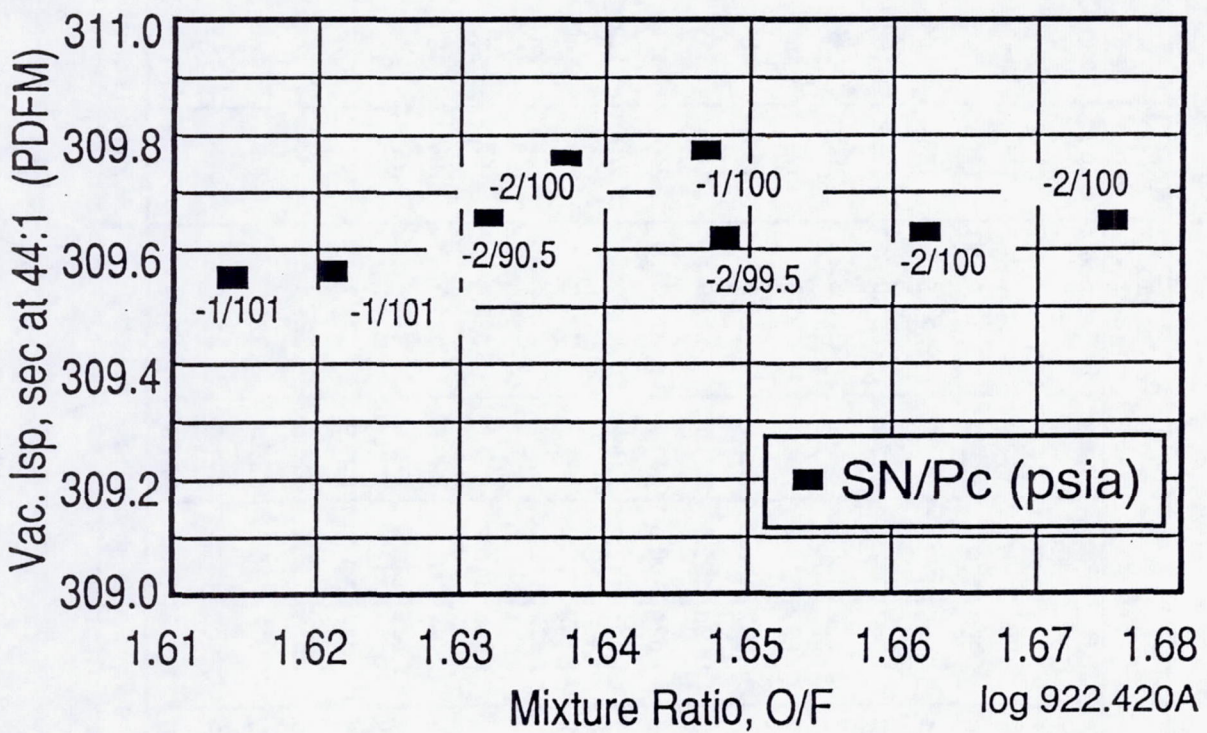


Figure 2.2-13. SN 6-1 and SN 6-2 Injectors Are Identical at the Design Point

Table 2.2-4. Isp of AJ10-221 With 286:1 Area Ratio

Run No.	Firing Time, sec	Pc, psia	MR O/F	Fvac. lbf	Isp vac, sec	Isp vac Normalized [MR=1.650], sec	Regen. Outlet, °F	Regen. Delta T, °F	Regen. Heat Trans., Btu/sec	Chamber Temp., °F*
259	1.0	113.8	1.667	105.6	323.5		119	59		
260	5.0	113.6	1.652	109.0	322.0		179	120	11.0	
261	10.0	116.1	1.639	112.4	323.2	323.3	183	124	11.7	2777
262	10.0	127.4	1.592	112.8	320.2	321.0	168	108	11.6	2707
263	10.0	104.7	1.620	100.3	321.2	321.5	200	142	12.3	2934
264	10.0	117.3	1.599	113.0	321.1	321.8	175	117	11.4	3033
265	25.0	116.1	1.647	112.2	322.2	322.3	193	134	12.8	
266	25.0	126.9	1.636	122.9	321.7	321.9	178	119	12.5	3171
267	23.0	104.8	1.624	100.6	321.3	321.6	210	151	13.1	3381
268	25.0	116.2	1.461	111.0	318.0	322.2	176	118	12.1	3124
269	25.0	115.9	1.789	112.2	321.8	322.0	207	149	13.6	3378
270	5.0	107.8	1.588	102.6	319.3	320.1	178	120	10.8	2626
271	60.0	114.8	1.594	110.7	321.6	322.4	193	133	12.7	3251
272	100.0	113.5	1.581	109.2	320.8	321.8	194	135	12.9	2159
273	120.0	113.7	1.587	109.8	321.8	322.7	195	136	13.0	2163
274	120.0	103.5	1.609	99.5	321.2	321.7	217	157	13.6	3391
275	120.0	116.5	1.514	111.5	318.8	321.4	183	124	12.4	2170
276	120.0	114.8	1.637	110.8	321.5	321.6	200	139	13.2	2188
277	51.7	114.9	1.800	111.2	321.6	322.0	215	153	13.8	3391
278	120.0	127.6	1.672	123.8	321.6	321.4	184	124	12.9	3199
Total	985.7	sec in 20 firings		Average, all tests = 321.8			*With high emissivity surface (e~ = 1.0)			

log 922.421

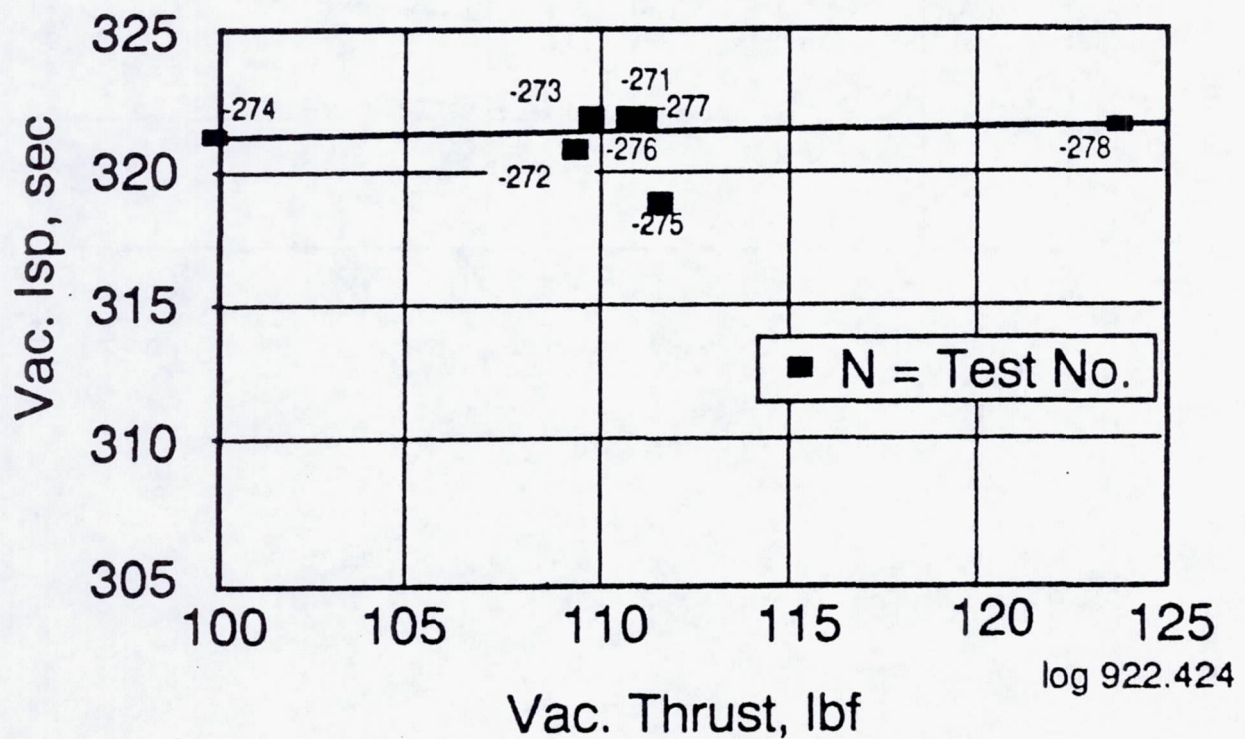
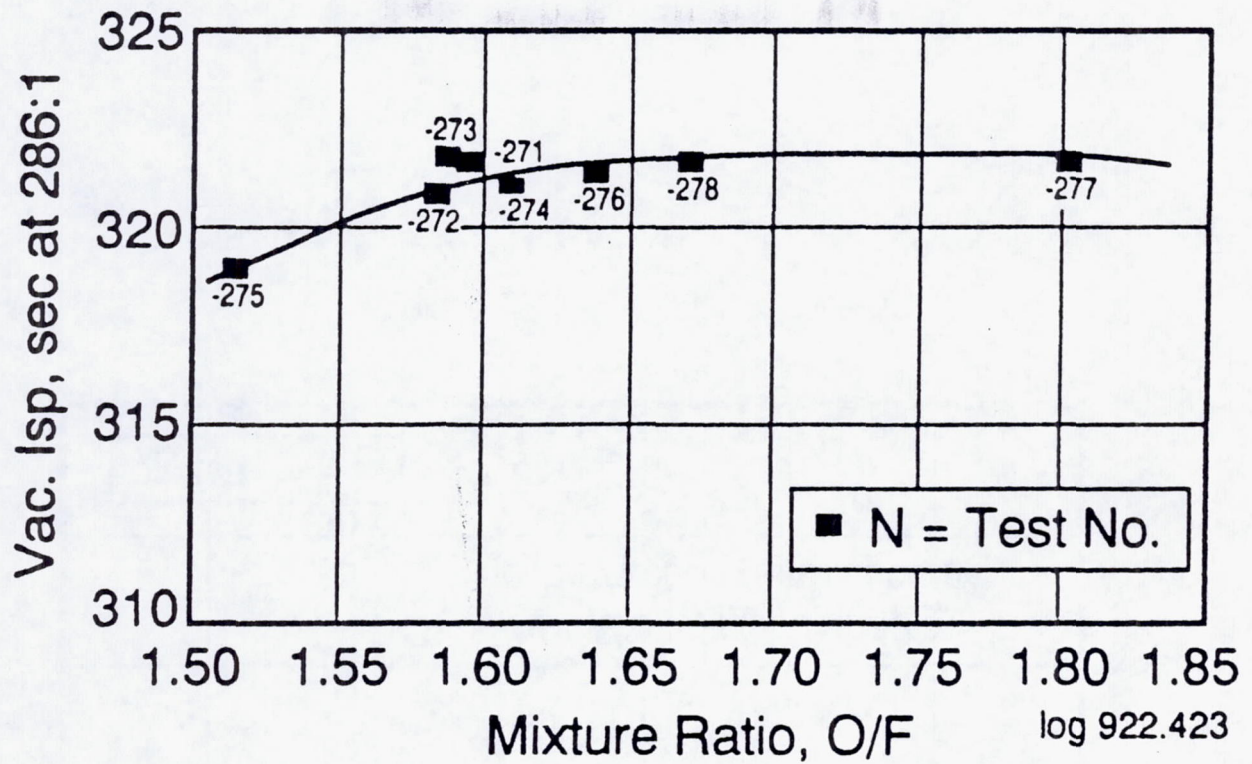


Figure 2.2-14. AJ10-221 Isp vs Mixture Ratio and Thrust With the 286:1 Nozzle

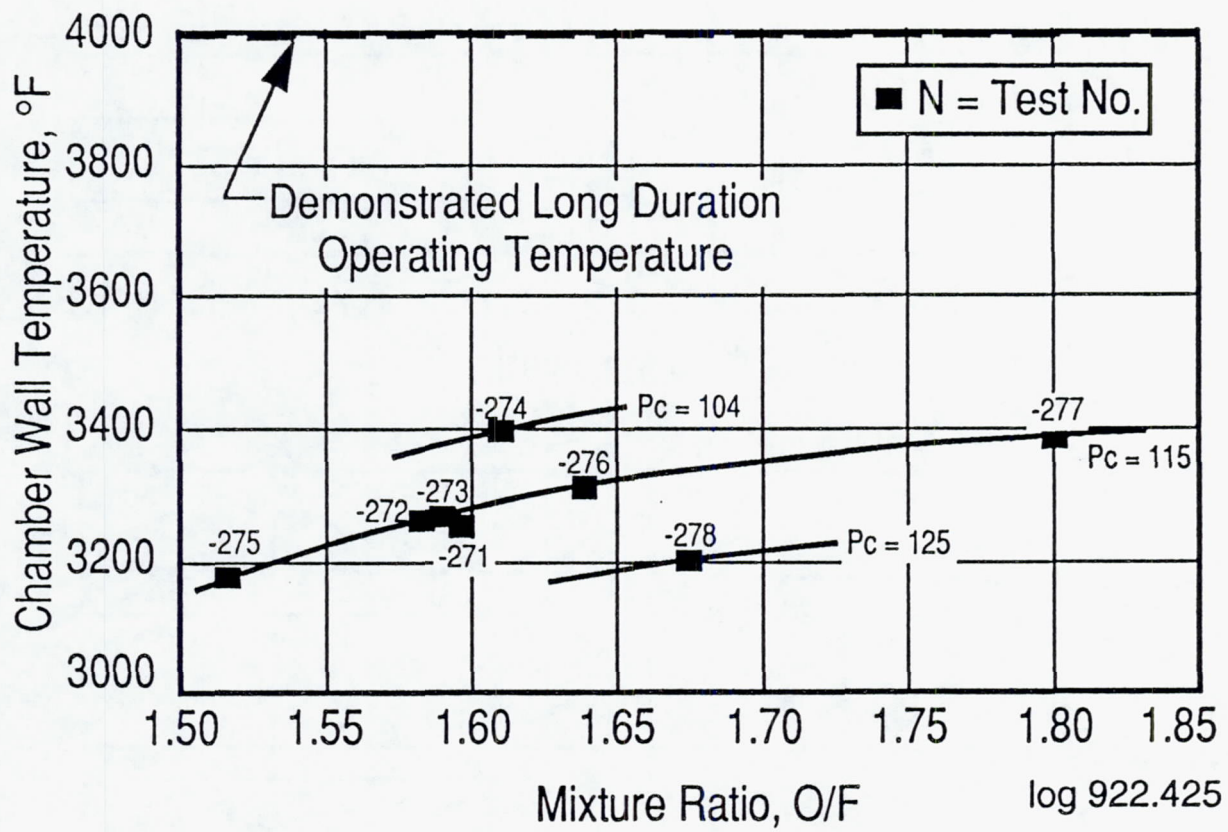


Figure 2.2-15. The Chamber Operates 600°F Cooler Than the Demonstrated 15-Hr-Life Temperature

2.2, Engine Description and Capabilities (cont.)

Iridium/Rhenium Chamber Validation

Four 110-lbf Ir/Re chambers have been built by Ultramet to the Aerojet design standards in lot sizes of two. To date there have been 200 firings at this thrust; of these 182 have been full thermal cycles.

The first two units (Ref. 3) used mechanical joints and accommodate mechanically held nozzle extensions to obtain performance and life data at an expansion ratio of 44:1. The first of the second two units has been assembled metallurgically, including the fuel-cooled stainless steel-to-rhenium joint and the rhenium-to-columbium 286:1 nozzle extension. Table 2.2-5 provides the hot-fire test history of these units.

Table 2.2-5. The 110-lbf Iridium/Rhenium Chambers Have Accumulated a Substantial Test History

Chamber	Burn Time, sec	Thermal Cycles
SN-1	3,885	45
SN-2	16,728	57
SN-3	22,590	80
SN-4	New	

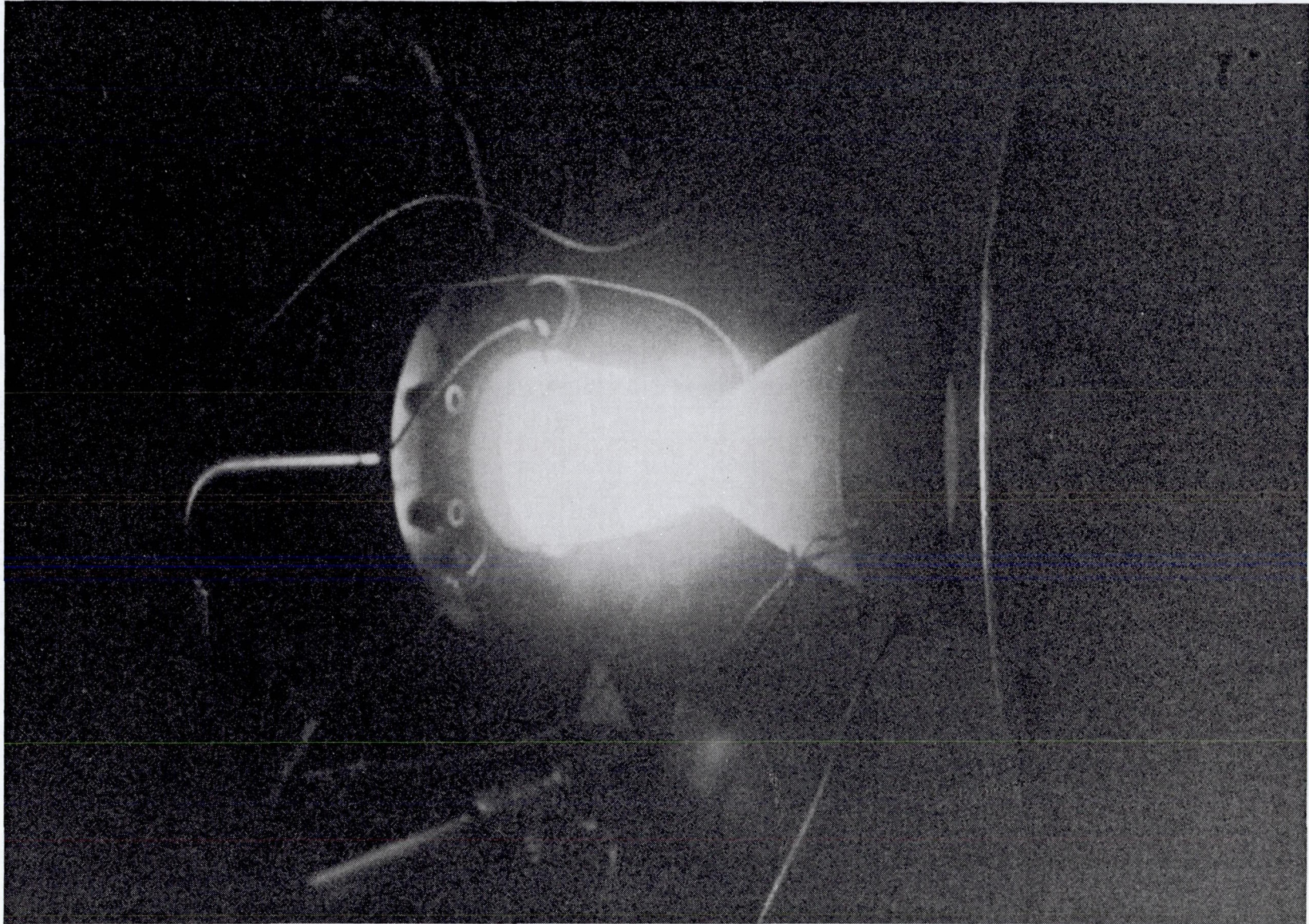
Re-Cb Joint Validation

Engine Test With Miniskirt (44:1 nozzle) – The C-103 columbium-to-rhenium metallurgical joint design was hot-fire engine tested in a miniskirt configuration, shown in Figure 2.2-16, to further validate joint durability.

In this test configuration, the joint was located closer to the throat (area ratio = 12) than in the 286:1 area ratio design to force the cycling temperature to exceed the nominal design values by 200°F. Fifteen full thermal cycles were successfully performed for this evaluation. The joint reached its equilibrium temperature of 2148°F at 30 sec into the first 90-sec test. Subsequent heating and cooling cycles were nominally 30 sec each.

Thermal Performance and Hot Restarts

Thermal performance is measured by the maximum temperature of the chamber, which occurs a short distance upstream of the throat; temperatures at the bimetallic joints; the fuel temperature leaving the regeneratively cooled chamber forward end; and the



C0891 5654

Figure 2.2-16. The Nozzle Weld Joint Was Demonstrated in Hot Firings Using a Miniskirt (44:1 Nozzle)

2.2, Engine Description and Capabilities (cont.)

postfire heat soak temperatures. The engine has demonstrated acceptable post fire soak temperature following a 7200 sec continuous firing. The addition of a heat shield produced no significant changes in thermal design margins.

Figure 2.2-17 shows the measured temperature at the upstream and downstream sides of the rhenium-to-columbium joint as a function of time. Steady state values are noted after 30 sec and show little sensitivity to operating conditions.

The fuel regenerative coolant discharge temperatures, shown in Figure 2.2-18 as a function of mixture ratio, are well below the boiling point of MMH, 375°F at the operating pressure of 200 psi, and below the design limit of 400°F.

The AJ10-221 has demonstrated satisfactory hot restart capability during a test series in which the effects of elevated propellant temperature were also determined. This group of 120-sec tests was conducted with increasing propellant temperatures and with as short a coast time as practical, consistent with reviewing the quick-look test data before retest. Figure 2.2-19 plots measured temperatures of the cooled head end interior, the valve body, and the vehicle mounting points at hot-fire initiation. The figure also shows measured temperatures for test -337, which was one of a group of 20-sec tests with a short coast time preceding it. These tests were satisfactory from a thermal, performance, and stability standpoint. Thermal data for the test with the highest propellant temperature, run -346, which had an initial hardware temperature of over 180°F, show that as soon as the engine fires, the hardware temperatures drop to the lower values typical of the cooled front end. During the coast after firing, they again rise to higher, through acceptable, levels; maximum values are reached by about 1000 sec of coasting.

Gas Ingestion

In the initial facility checkout tests the engine experienced gas ingestion in both the fuel and oxidizer feed lines. The amount of gas is unknown but caused an indicated 1 psi drop in chamber pressure for about 2 seconds before returning to normal. Figure 2.2-20 shows that the ingestion of gas does not cause the engine to go unstable. This test was terminated manually because of continuing evidence of gas bubbles.

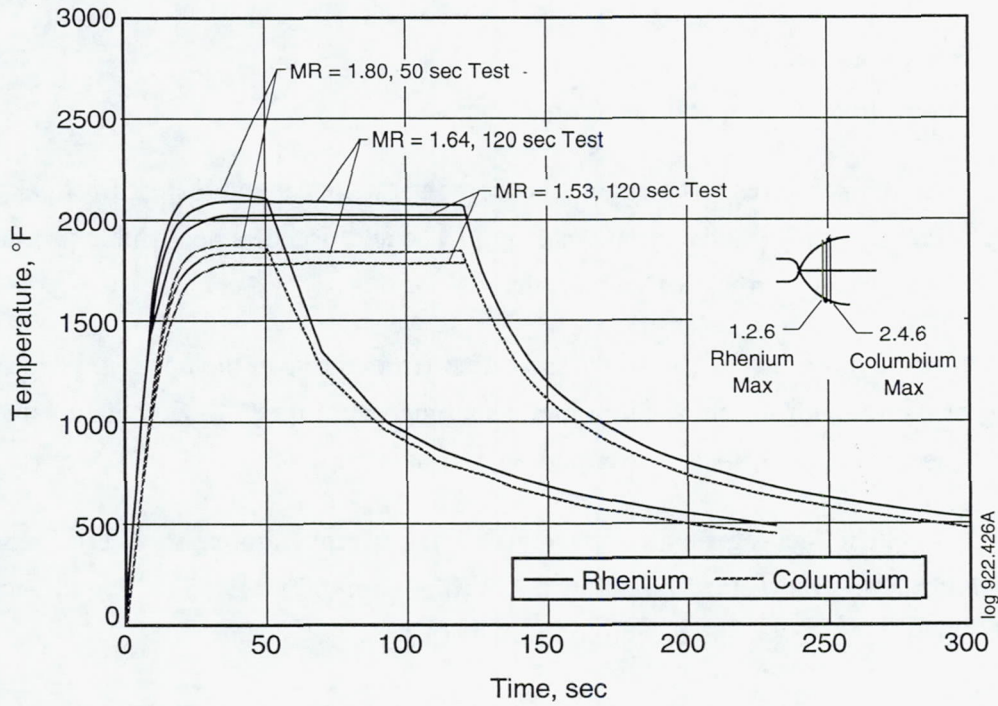


Figure 2.2-17. Rhenium-to-Columbium Joint Temperatures Are Well Below Material Limits

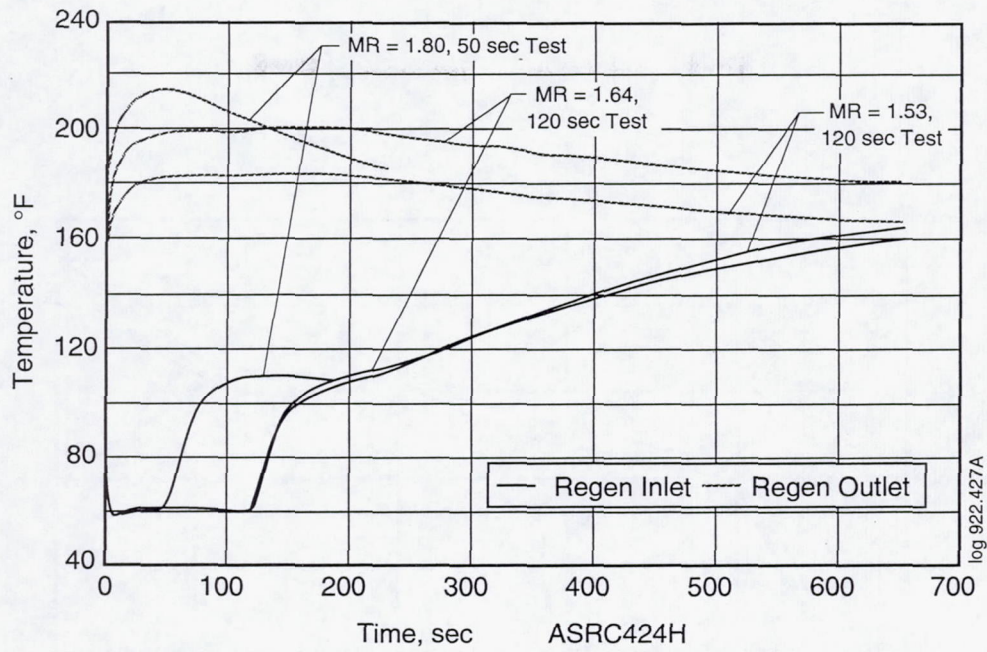


Figure 2.2-18. Regenerative Fuel Coolant Outlet Temperatures Are Well Below the Design Limit

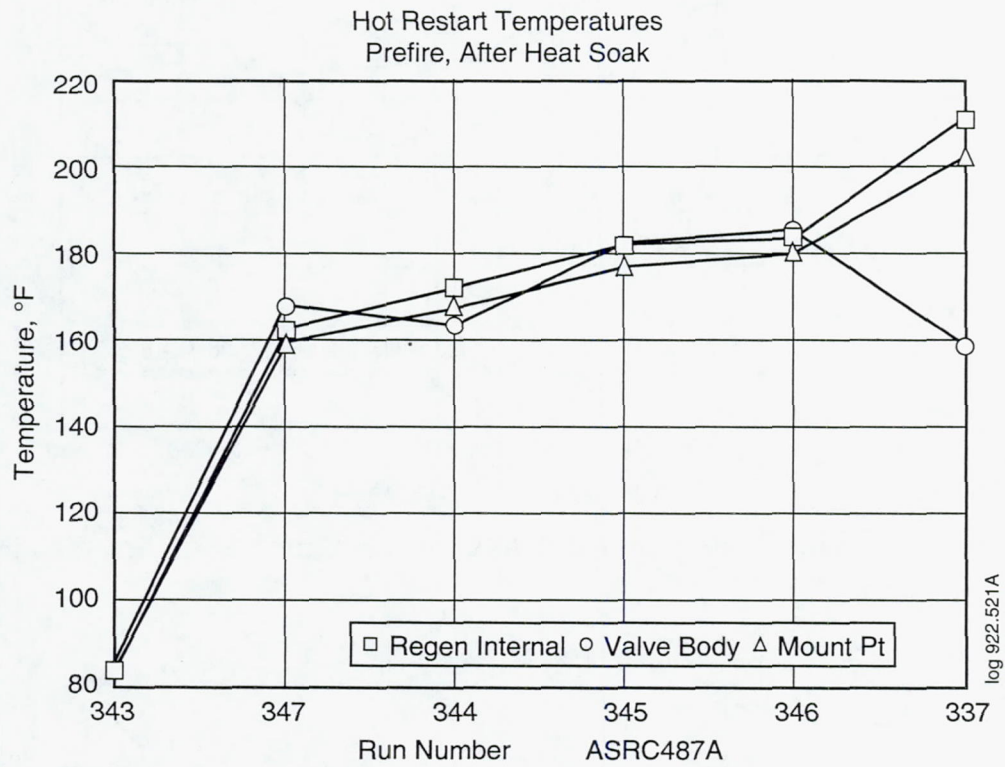


Figure 2.2-19. Hot Restarts Have Been Demonstrated for Temperatures Approaching 200°F

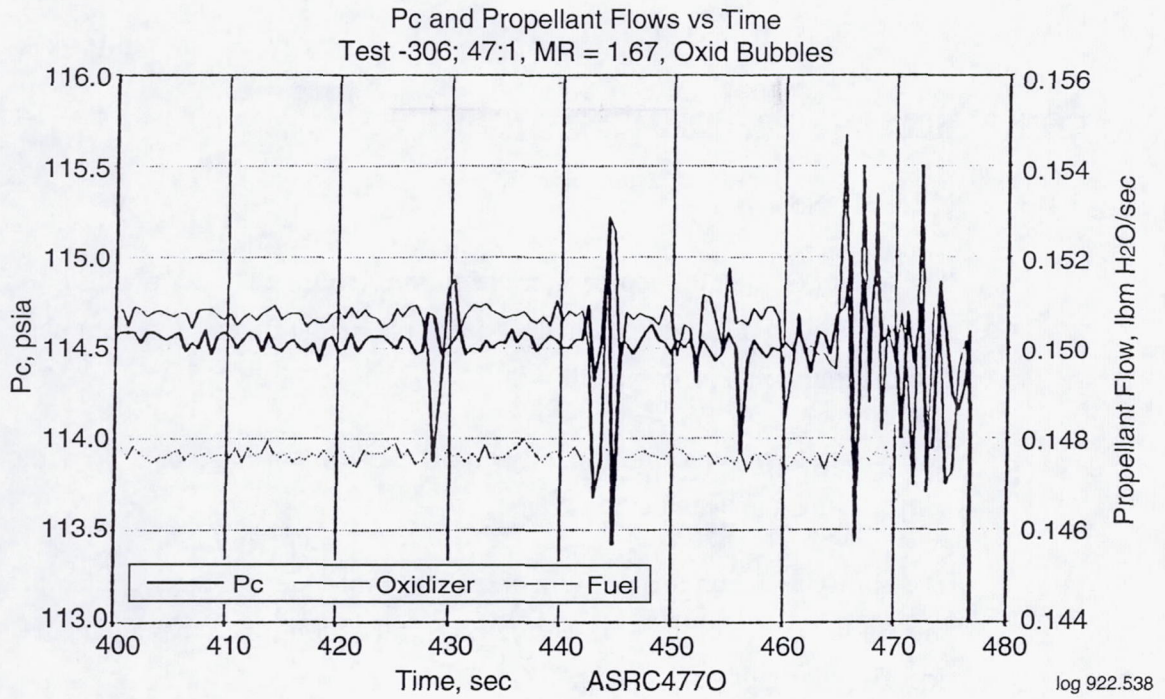


Figure 2.2-20. The AJ10-221 Engine Responds Stably to Gas Bubble Injection

3.0 CONCLUSIONS AND RECOMMENDATIONS

3.1 CONCLUSIONS

- The ability of the high temperature iridium/rhenium chamber material to function successfully in a storable rocket propellant combustion environment has been demonstrated in a prototype design.
- The ability to provide significantly higher performance and operate without fuel film cooling has been demonstrated.
- The ability to attach the rhenium chamber to the stainless steel cooled head end and the hot columbium skirt was demonstrated along with management of the post fire thermal soak.

3.2 RECOMMENDATIONS

The ability of the high area ratio engine assembly to withstand the launch vibration load was not demonstrated for two reasons, funding and the insufficient understanding of the material properties under the dynamic loading conditions. The limited data available indicates the rhenium does not have sufficient strength following the hot fire acceptance test to withstand the expected bending loads. The calculated increase in thickness at the throat to withstand the dynamic loading indicates possible wall thickness requirements of two to four times greater than the 0.060 in. of the present design.

A number of recommendations are appropriate to resolve this situation.

1. A better understanding of the properties of rhenium is required. This includes the influence of the fabrication process and the changes that result when the engine is hot fire acceptance tested and vibration tested.
2. Low cost methods of depositing stronger or locally thicker rhenium are required to improve the dynamic design margin without increasing fabrication cost.
3. The use of a lower weight titanium skirt should be investigated as a means of decreasing the dynamic load on the throat and also the overall engine weight.

4.0 THRUSTER DESIGN

This section discusses the basis for the engine design.

4.1 PRELIMINARY DESIGN AND DESIGN OPTIMIZATION DESIGN REQUIREMENTS

The configuration for the flightweight all metallurgically joined 100 lbf-AJ10-221 engine is based on a high performance engine for the JPL CRAF-Cassini Mission, Ref. 3. The reference program created the design and demonstrated the engine performance and thermal characteristics in a bolt together assembly using a 44:1 area ratio stainless steel nozzle extension as shown in Figure 4-1. In the configuration shown, the engine demonstrated a specific impulse of 309.6 sec which is $\approx 99\%$ of the maximum attainable value in that design. Durability testing at nominal pressure and mixture ratio resulted in four hours of accumulated firing duration without evidence of any life limiting conditions on any of the components, i.e., valve, injector, cooled head end and iridium/rhenium chamber.

The JPL environmental design requirements/goals and tank operating pressure envelope are given in Table 4-1 and Figure 4-2, respectively.

4.1.1 Conversion to Flightweight Design

The objective of this program option was to re-optimize the engine to include a higher area ratio nozzle, (200 to 400:1), modify the interfaces to enable an all metallurgically joined engine with no mechanical hot gas seals, minimize the weight, conform to the CRAF-Cassini stage propellant supply conditions, increase the combustion efficiency and address the launch vibration environment for the selected high area ratio nozzle.

The work conducted in support of the conversion of the bolt together assembly to the flightweight design included the following technical activities:

- (1) Optimize/select the nozzle expansion ratio and contour.
- (2) Reduce the injector pressure drop, (slightly) improve the flow distribution by manifold cold flow and design modification and eliminate all fuel film cooling.
- (3) Refine the thermal management to control the post fire heat soak.

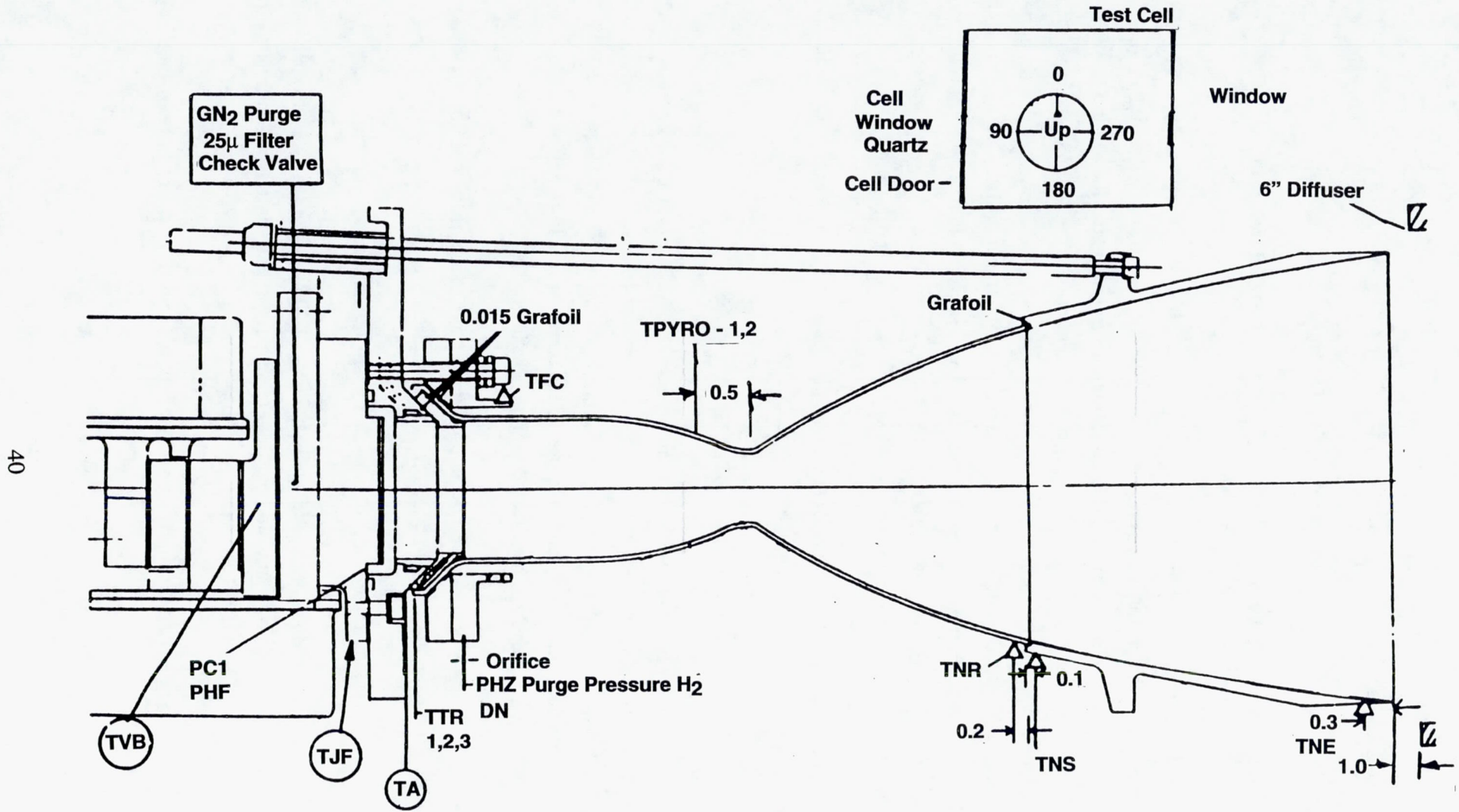


Figure 4-1. JPL 44:1 Thruster Drawing (Ref. 3)

Table 4-1. Environmental Design Requirements

1. Propellant and Engine Temperature: The Rocket Engine Assembly (REA) shall be capable of demonstrating satisfactory and non-detrimental operation within a temperature range of 0°C to 55°C, and a difference in oxidizer and fuel temperature of 15°C.
2. Sinusoidal Vibration: The REA shall be capable of meeting all specified operating requirements after being subjected to the following sine vibration.

Preliminary Requirements

Frequency, Hz	Amplitude
5-25	1.27 cm D.A. displacement
25-100	15.0g peak
100-200	5.0g peak

Sweep Rate = 2 octaves/minute up and down each of 3 axes

D.A. = Double Amplitude

3. Random Vibration: The REA shall be capable of meeting all specified operating requirements after being subjected to the following acceleration power spectral densities and overall RMS level applied separately to each of the three axes of the REA for a duration of 3 minutes per axis (acceptance test levels are TBD):

Frequency, Hz	Accel Spectral Level
20-50	+9 dB/octave
50-500	0.2 g ² /Hz
500-600	-9 dB/octave
600-1000	0.1 g ² /Hz
1000-2000	-12 dB/octave
Overall	13.4g (rms)

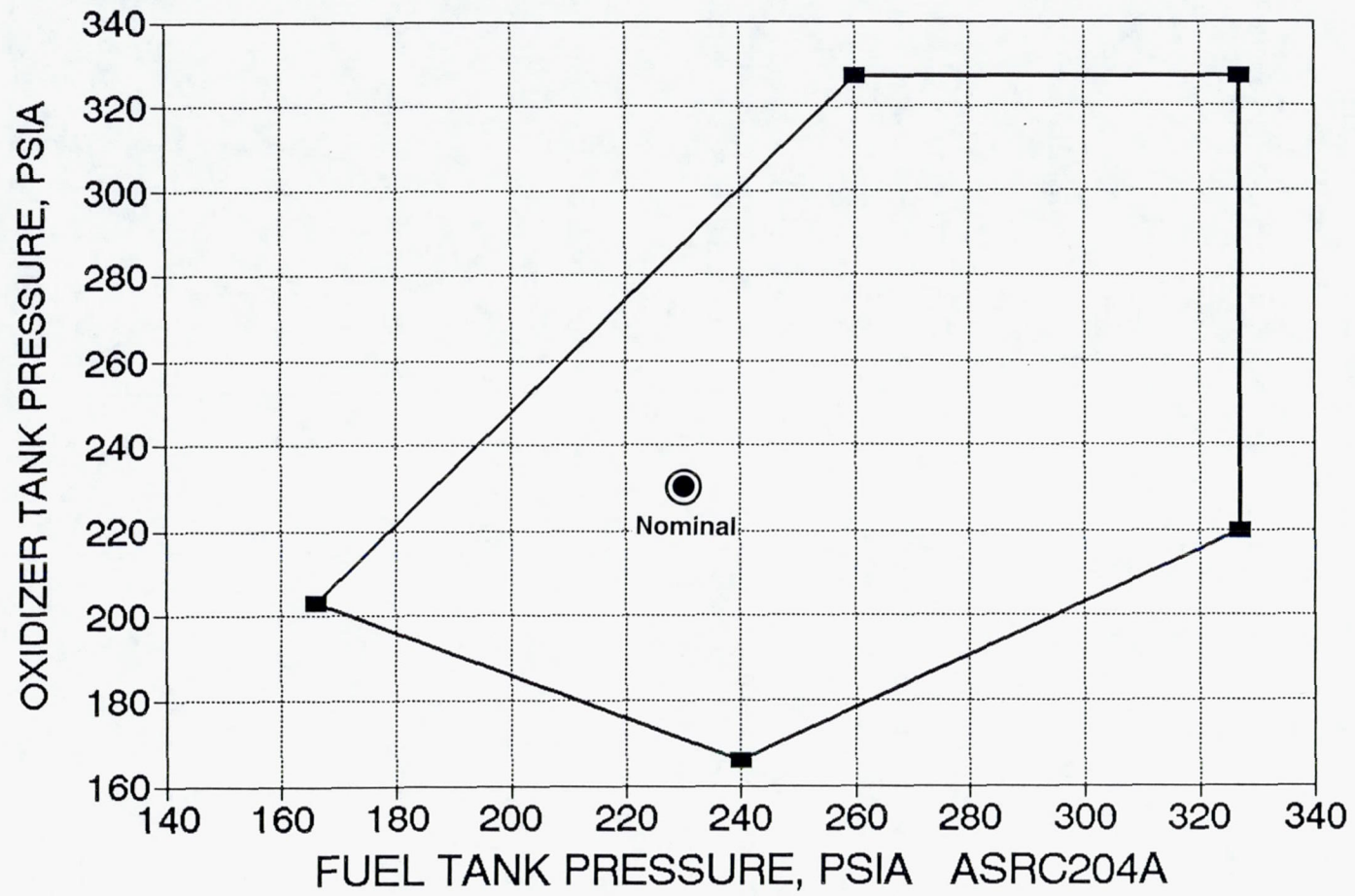


Figure 4-2. 100# Propellant Tank Operating Range

4.1, Preliminary Design and Design Optimization Design Requirements (cont.)

- (4) Investigate the problems caused by the launch vibration environment in combination with the high area ratio nozzle.
- (5) Demonstrate the metallurgically joining of the stainless steel head end to the rhenium chamber and the rhenium chamber to the columbium skirt.

The design and fabrication technology conducted under Item 5 was addressed using Aerojet funding. The optimization of the engine nozzle length, area ratio, and throat diameter is summarized in Appendix A.

4.1.2 Design Optimization

The results of the preliminary design are shown in the layout drawing, Figure 4-3. The differences between this design and the earlier JPL design are summarized as follows:

- (1) The throat area was reduced 10%. Nominal $P_c = 108$ psia vs 100.
- (2) The injector pressure drop was reduced by slight orifice enlargement and provision for fuel film cooling was eliminated.
- (3) An expansion ratio of 250:1 potential flow (286:1 geometric) and a parabolic contour was selected. The design selected was a compromise between maximum I_{sp} , engine length, and acceptable weight.
- (4) The thermal mass and internal cooling channels of the fuel cooled head end were resized and a braze added to enable the joining of the rhenium chamber in a manner that produced acceptable post fire heat soak. The welds were relocated from the original design. The design criteria was to limit the MMH in the cooling channels to a maximum of 400°F.

4.1.3 Thermal Design Optimization

The thermal analysis supporting the selected engine assembly design is provided in Appendix B. The thermal analysis indicates all of the design goals can be achieved with the recommended changes from the original design.

4.1, Preliminary Design and Design Optimization Design Requirements (cont.)

4.1.4 Structural

The structural/vibration analysis is given in Appendix C. No conclusion can be drawn on the ability of the design to meet the launch vibration because the yield strength and fatigue properties of CVD rhenium have not been defined.

The wall thickness of the rhenium chamber was designed based on high temperature creep using the data from Ref. 5 (Westinghouse). The design life was selected as 20 hours minimum at full operating temperature and pressure.

The fuel cooled section was designed with safety factor of 4 (300 psi MOP) 1200 psi proof pressure because this is upstream of the engine valve.

The columbium skirt wall thickness was dictated by fabrication considerations with the primary objective of minimizing weight. The structural loads will allow C-103 wall thickness as low as 0.010 in. with adequate margin. However, fabrication at this thickness could only be considered as a goal. The drawing allowed a range between 0.010 and 0.016 in.

4.1.5 Configuration Design Optimization

The design optimization is based on the nominal operating point of 230 psia in both propellant tanks as given in Figure 4-2. Additional environmental design requirements are defined in Table 4-1.

Additional envelope limitations include a maximum potential flow expansion ratio of 250:1. This corresponds to a 286:1 geometric expansion ratio .

Optimization analyses were conducted to maximize the performance within the prescribed design and operational requirements defined previously. The optimization factors included chamber pressure, chamber length, nozzle % bell and contour as shown in Table 4-2. The contour corresponding to case 14, providing a perfect injector Isp of 326.5 sec was selected because it reduced the engine length by 2.9 in. at the cost of 1 sec of specific impulse.

TABLE 4-2

OPTIMIZATION OF NOZZLE CONTOUR

Case	Pc psia	Type	D _{rad}	e	q	b	L _{Noz} (in.)	Isp _{ODE}	Isp _{ODK}	Kinetic Loss sec	Isp _{TDE}	Noz Eff.	Boundary Layer Loss sec	Isp Perfect Injector sec	
1	100*	Rao	90% BBU	0.5	250:1	37.2/38.2	6.57	21.0	348.95	335.3	(13.66)	346.56	99.31	7.72	325.3
2	100*	Rao	126% BBU	0.5	250:1	32.9/34.9	2.78	29.61	348.95	335.4	(13.59)	348.30	99.81	8.59	326.1
3	100*	Parabolic	L=21"	0.5	250:1	30	7.0	21.0	348.95	335.5	(13.49)	345.75	99.08	7.24	325.1
4	100*	Parabolic	L=24"	0.5	250:1	30	7.0	24.0	348.95	335.5	(13.49)	345.75	99.37	7.34	326.0
5	100*	Parabolic	L=24"	0.5	250:1	30	6.0	24.0	348.95	335.5	(13.49)	346.89	99.41	7.52	325.9
6	100*	Parabolic	L=27"	0.5	250:1	30	6.0	27.0	348.95	335.5	(13.47)	347.35	99.54	7.62	326.3
7	100*	Parabolic	L=21"		250:1	30	7.0	21.0	348.95	336.0					
8	100*	Parabolic	L=21"	2.0	250:1	30	7.0	21.0	348.95	336.0	(12.91)	346.00	99.15	7.35	325.8
9	100*	Rao	120 % Bell	No Solution In Available Length											
10	100*	Parabolic	L=21"	1.0	250:1	30	7.0	21.0	348.95	335.7	(13.28)	345.90	99.13	7.28	325.4
11	100*	Parabolic	L=24"	2.0	250:1	30	7.0	24.0	348.95	336.0	(12.91)	347.12	99.48	7.43	326.9
12	100*	Parabolic	L=18"	2.0	250:1	30	9.0	18.0	348.95	336.0	(12.92)	343.65	98.48	6.89	324.0
13	100*	Parabolic	L=18"	2.0	250:1	30	7.0	18.0	347.23	334.8	(12.48)	343.96	99.05	6.95	324.6
14	110**	Parabolic	L=20"	2.0	250:1	30	7.0	20.0	348.97	336.5	(12.45)	346.02	99.15	7.16	326.5
15	110**	Parabolic	L=22.9"	2.0	250:1	30	7.0	22.9	348.97	336.5	(12.45)	347.15	99.48	7.24	327.5

* r_t = 0.4230

** r_t = 0.4036

$$\epsilon = \frac{A_{\text{exit}} \text{ potential flow}}{A_{\text{Throat}}}$$

4.1, Preliminary Design and Design Optimization Design Requirements (cont.)

Chamber Pressure	110 psia at 100 lbf and 230 psia tank pressures
Chamber L'	4.4 in.
Skirt Designs	Parabolic contour 250:1 potential flow Max divergent angle 30° Length 20.0 in.
Valve	Moog Model 53X-179

This design resulted in the nominal and off design operating characteristics given in Table 4-3.

4.1.6 Layout and Assembly

Figure 4-3 shows the preliminary layout of the full engine for the two skirt options (Cases 14 and 15 of Table 4-2). The shorter skirt length was selected (Case 14). Figure 4-4 (Drawing 1206350-9) shows the final engine assembly as built and tested. Table 4-4 shows the engine component weights and anticipated weight reduction for flight hardware.

Table 4-4. Weight of 100-lbf Thrust Engine Components

Part	Item	Test Hardware Weight, lbm	Flight Hardware Weight, lbm
B66638	Valve	2.70	2.70
1206397-1	Adapter Plate	0.54	0.25
1206362-9	Injector	1.00	0.80
1206354-9	Chamber Adapter	2.11	1.90
1206383-9	Chamber	1.98	1.75
1206351-9	Nozzle	<u>4.45</u>	<u>2.50</u>
	Total Weight =	12.78	9.90

4.2 COMPONENT DESIGN/SELECTION

Detailed discussion and drawings of the valve, injector, cooled head end and flange, iridium/rhenium chamber, and the columbium skirt follows.

Table 4-3. High Performance 100 lbf Engine Supply Pressure Envelope and Resulting Operating Parameters

Inlet Pressure (psia)		C* (ft/sec)	Pc (psia)	Thrust lbf	MR	$\Delta P_{OJ}/P_c$	$\Delta P_{FJ}/P_c$	Tank Pressure Condition
Ox	Fuel							
230	230	5500	108	104	1.65	.77	.71	Nominal
225	330	5200	111	107	1.19	.72	1.27	High Fuel
330	330	5500	134	130	1.64	1.03	.95	High Fuel & Ox
330	265	5500	125	120	2.00	1.12	.69	High Fuel & Ox
205	170	5500	92	88.6	1.98	.84	.52	Low Ox & Fuel
170	240	5200	94	90.5	1.20	.61	1.04	Low Ox
Throat dia 0.807 in cold. Propellant Temperature 70°F								

48

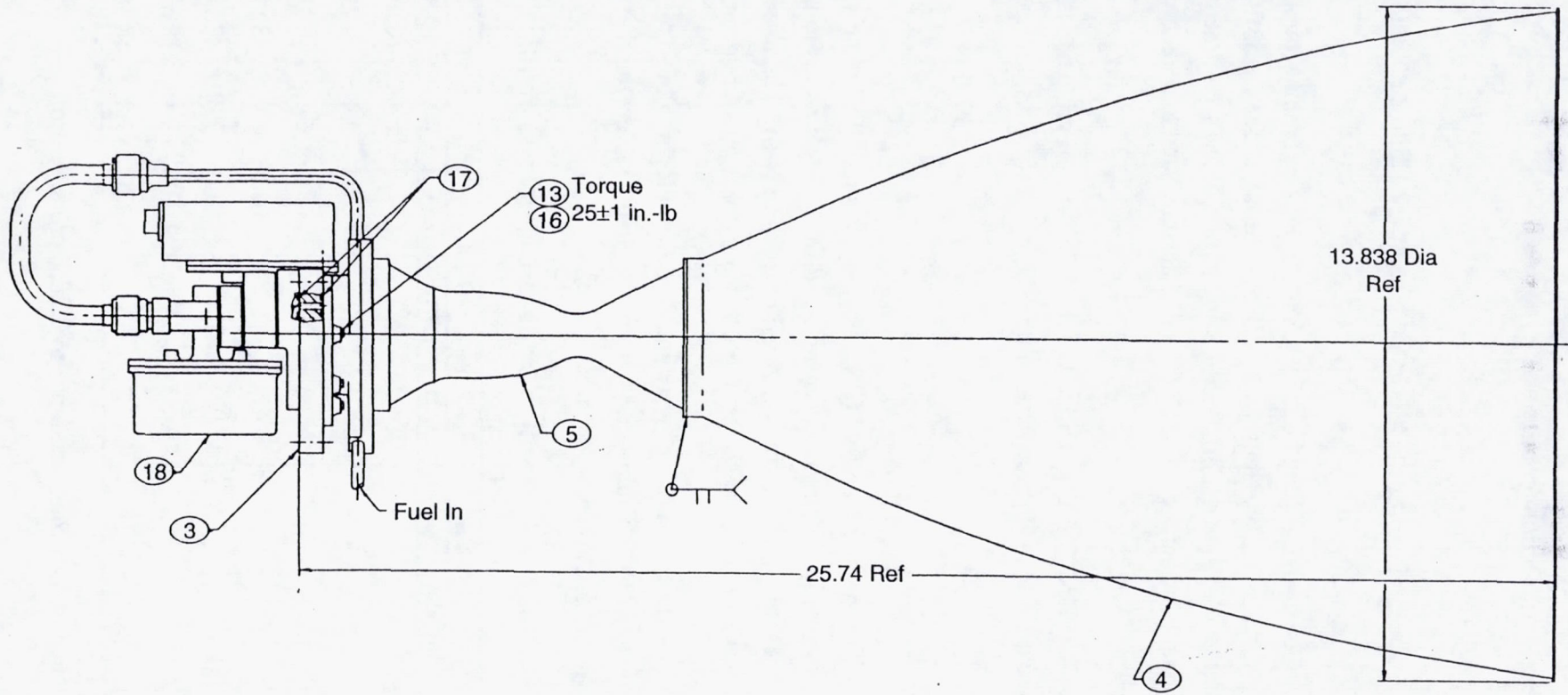


Figure 4-4. Engine 100 lbf Thrust

4.2, Component Design/Selection (cont.)

4.2.1 Valve

The engine uses the Moog Model 53X-179 bipropellant torque motor valve, shown in Figure 4-5.

The design is based on the NASA OMV single shutoff configuration. Four of these derivative valves were previously fabricated by Moog under the 53E-163 designation. They underwent extensive flight qualification testing until the OMV contract was terminated by NASA. In its original configuration, the OMV valve design failed to meet the rigid NASA vibration qualification criteria.

The design was modified by Moog for this program by adding vibration stabilizers to the torque tubes. The modified single shutoff design has now met the NASA qualification criteria.

4.2.2 Injector

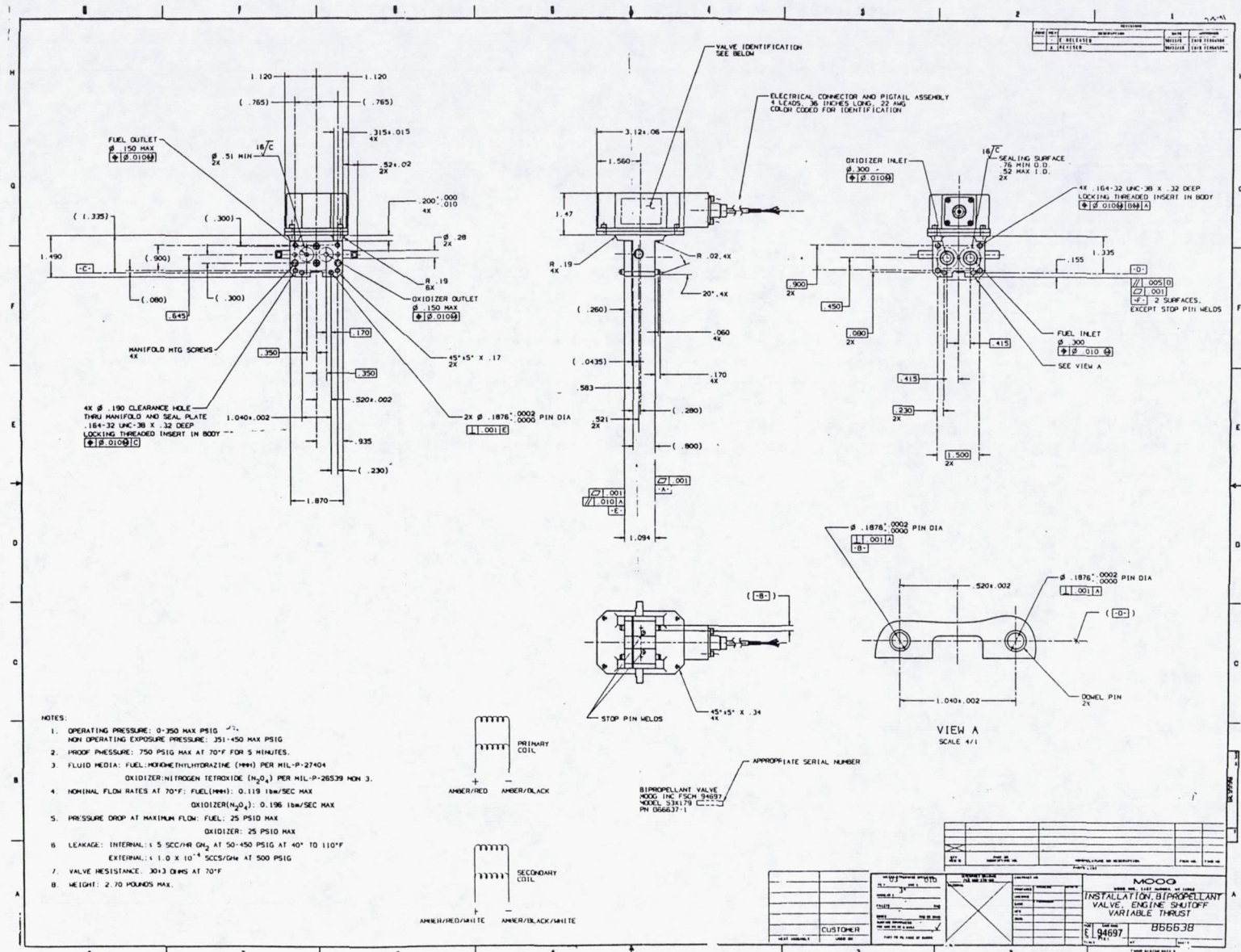
The injector manifold (PN 1195651) was modified from an existing design to improve the flow distribution. This was accomplished by adding a radius to the drilled hole joining the valve discharge port and ring manifold (see Figure 4-6). The injector element design was an iterative process to optimize performance and minimize pressure drop.

The injector orifices were enlarged to conform to the new pressure drop schedule. These are defined in Table 4-5. As indicated in the table a number of changes were made to produce the SN 6-1 and 6-2 injectors.

Table 4-5. Injector Orifices Diameters, in mils

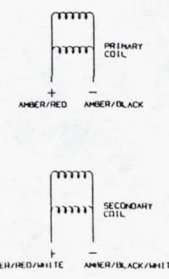
Propellant	Row	Number	JPL	SN-2	SN-4		SN 5		6a	6-1*	6-2*
			Design	(Act)	Design	(Act)	Design	(Act)	Design		
Fuel	1	3	6.4	(6.42)	7.1	(7.32)	6.4	(6.61)	6.4	6.71	6.51
Ox	2	12	8.4	(8.42)	8.9	(9.04)	8.4	(8.73)	8.4	9.17	8.96
Fuel	3	12	6.4	(6.42)	7.1	(8.68)	6.4	(6.47)	6.4	6.70	6.55
Ox	4	32	8.4	(8.42)	8.9	(9.08)	8.4	(8.63)	8.4	9.15	9.01
Fuel	5	32	7.0	(7.02)	7.7	(8.01)	7.0	(7.15)	7.0	7.54	7.47
Ox	6	48	8.4	(8.42)	8.9	(9.09)	8.4	(8.68)	8.4	9.16	9.08
Fuel	7	48	7.8	(7.82)	8.1	(8.43)	7.8	(8.16)	7.8	8.59	8.54

* Orifices were etched to maximum tolerance to reduce pressure drop.



NOTES:

1. OPERATING PRESSURE: 0-250 MAX PSIG
NON OPERATING EXPOSURE PRESSURE: 251-450 MAX PSIG
2. PROOF PRESSURE: 750 PSIG MAX AT 70°F FOR 5 MINUTES.
3. FLUID MEDIA: FUEL: MONOMETHYLHYDRAZINE (MMH) PER MIL-P-27404
OXIDIZER: NITROGEN TETROXIDE (N₂O₄) PER MIL-P-26539 MON 3.
4. NOMINAL FLOW RATES AT 70°F: FUEL(MMH): 0.119 lbm/SEC MAX
OXIDIZER(N₂O₄): 0.196 lbm/SEC MAX
5. PRESSURE DROP AT MAXIMUM FLOW: FUEL: 25 PSIG MAX
OXIDIZER: 25 PSIG MAX
6. LEAKAGE: INTERNAL: 1.5 SEC/HR O₂ AT 50-450 PSIG AT 40° TO 110°F
EXTERNAL: 1.0 X 10⁻⁴ SECS/GM AT 500 PSIG
7. VALVE RESISTANCE: 30-3 OHMS AT 70°F
8. WEIGHT: 2.70 POUNDS MAX.



BIPROPELLANT VALVE
MOOG, INC. P.O. BOX 94697
MODEL 334179
PH 066637-1

MOOG	
INSTALLATION BI-PROPELLANT VALVE, ENGINE SHUTOFF VARIABLE THRUST	94697 856538
CUSTOMER	

4.2, Component Design/Selection (cont.)

4.2.3 Fuel Cooled Flange

The fuel cooled flange PN 1206357-9 shown in Figure 4-7 was a modification of an earlier design, Ref. 3. The changes involved replacing 347 with 304L, adding an extra cooling loop near the rhenium chamber weld attachment, resizing the cooling passages and thinning the gas side wall, and adding a liner-to-housing braze in addition to the electron beam welds to improve the thermal soakout design margin. The trip was retained for improved performance and compatibility even though no film cooling was employed. The configuration was changed to further enhance the efficiency of the secondary mixing chamber. The chamber pressure tap was relocated from the injector body to the cooled flange.

4.2.4 Chamber

The design of the iridium lined rhenium chamber is shown in Figure 4-8. The design includes a 2 mil thick continuous iridium liner, the application of a dentoid high emissivity external coating and thinning of the front end to restrict the heat conduction to the fuel-cooled section based on the results of the thermal analysis, Appendix B. The exit end wall is ground thin to eliminate excess weight. The ends are prepared for weld attachments.

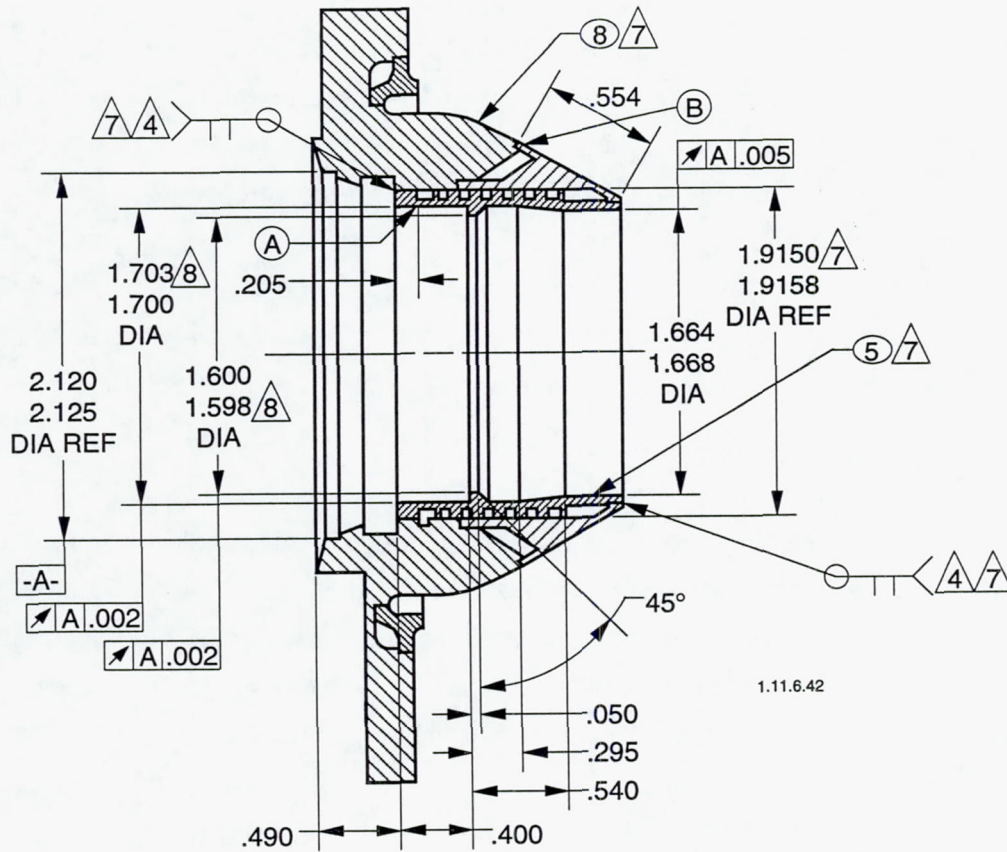
4.2.5 Columbium Skirts

The skirt design is shown in Figure 4-9. The selected skirt material was columbium alloy C-103, with an R-512 E disilicide coating to be applied by the HITEMCO process. The nominal wall thickness required to meet the structural loading is under 0.010 in., however since fabrication of the thin wall was a concern the initial drawing allowed wall thicknesses of up to 0.016 in. before coating.

The thickness of the small end was increased to allow machining of the final dimensions to fit the rhenium chamber and allow liberal weld penetrations. A small flange was added to the large end to keep the exit round and prevent handling damage to the coating.

The R-512 E coating is applied inside and out except for a small region near the final weld area which is shielded from direct exposure to the hot gas but fully exposed on the chamber outside diameter.

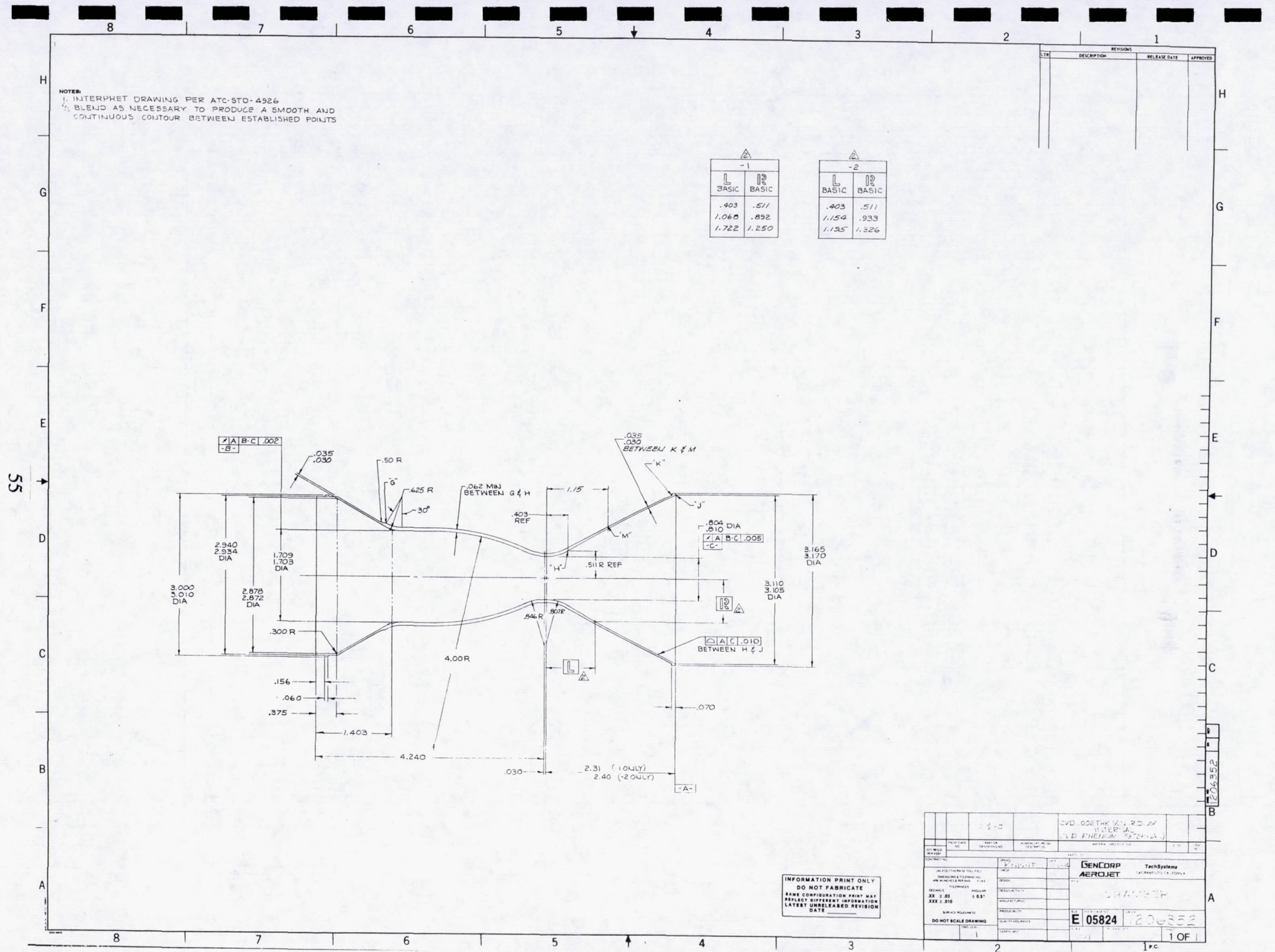
1206354 Adapter, Chamber



Conduct Proof and Leak Tests of Two (2) Adapters

1. Install 2 biaxial strain gages equally spaced at (A) and at (B). Pressurize to 500 PSIG in 5 steps; record strain. (Anticipated strain is low, of the order of 0.05%).
2. Pressurize with GN₂ to 370 PSIG, perform bubble leak check.
3. Flow for K_w (.06 - .20 lb/sec fuel)
~.05 - .175 lb/sec H₂O

Figure 4-7. Fuel Cooled Head End Design and Acceptance Test Conditions Covered by U.S. Patents 4882904 and 4936091 and German Patent P39 23 948.9-13



NOTES:
 1. INTERPHRET DRAWING PER ATC-STD-4926
 2. BLEND AS NECESSARY TO PRODUCE A SMOOTH AND CONTINUOUS CONTOUR BETWEEN ESTABLISHED POINTS

-1		-2	
L	R	L	R
BASIC	BASIC	BASIC	BASIC
.403	.511	.403	.511
1.060	.892	1.154	.933
1.722	1.250	1.195	1.326

REVISIONS			
REV	DESCRIPTION	RELEASE DATE	APPROVED

55

204352

INFORMATION PRINT ONLY
 DO NOT FABRICATE
 SAME CONFIGURATION PRINT MAY
 REFLECT DIFFERENT INFORMATION
 LATEST UNRELEASED REVISION
 DATE

CVD COATING MATERIAL INTERPHRET (D PARTIAL 204352)		PART NO.		REV. NO.	
REVISED	BY	DATE	REVISED	BY	DATE
GENCORP AERJET		TechSystems		SACRAMENTO, CA 95834	
E 05824		204352		1 OF 1	

Figure 4-8. Iridium/Rhenium Chamber

4.2, Component Design/Selection (cont.)

Two other C-103 columbium mini-skirts were designed to allow for fabrication process checkout and test evaluation of the bimetallic joint which is designed to operate at 2000°F. These are reduced length versions of the 286:1 design.

4.2.6 Tooling

Tooling was designed to hold the components in alignment during welding and also to be employed for conducting proof pressure and leak tests at each stage of the assembly. Figure 4-10 shows the tooling Design Drawing 1206381.

5.0 FABRICATION

Table 5-1 and Figure 5-1 define the parts required to assemble AJ10-221 engine and the assembly sequence. The right hand column of the table indicates the quantity of each part fabricated. Two of each major component were fabricated. The availability of two each of the major components from the JPL contract increased the number of test articles to four of each major component. Injectors were reworked to optimize the performance and reduce the pressure drop. Rework consisted machining off the diffusion bonded platelets and bonding on a new set. One full engine was assembled for test.

5.1 VALVE

Two torque motor bipropellant valves were available for the program. The series redundant valve was supplied by Aerojet. The other was a single shut off valve Moog PN B66638 (Figure 4-5) containing the modifications required to sustain the higher vibration test conditions. Appendix D provides the Moog acceptance data for this valve.

5.2 INJECTOR

Two machined and EB welded injector bodies of the improved design (PN 1206359) were subcontracted. Photoetched platelets 1206353 were fabricated and diffusion bonded onto the body at Aerojet. Figure 5-2 shows one of the four injectors fabricated with the flange on for facilitating checkout testing. Figure 5-3 shows the same injector in a later stage of assembly. At this point the flange was machined off and the injector electron beam welded to the cooled flange.

58

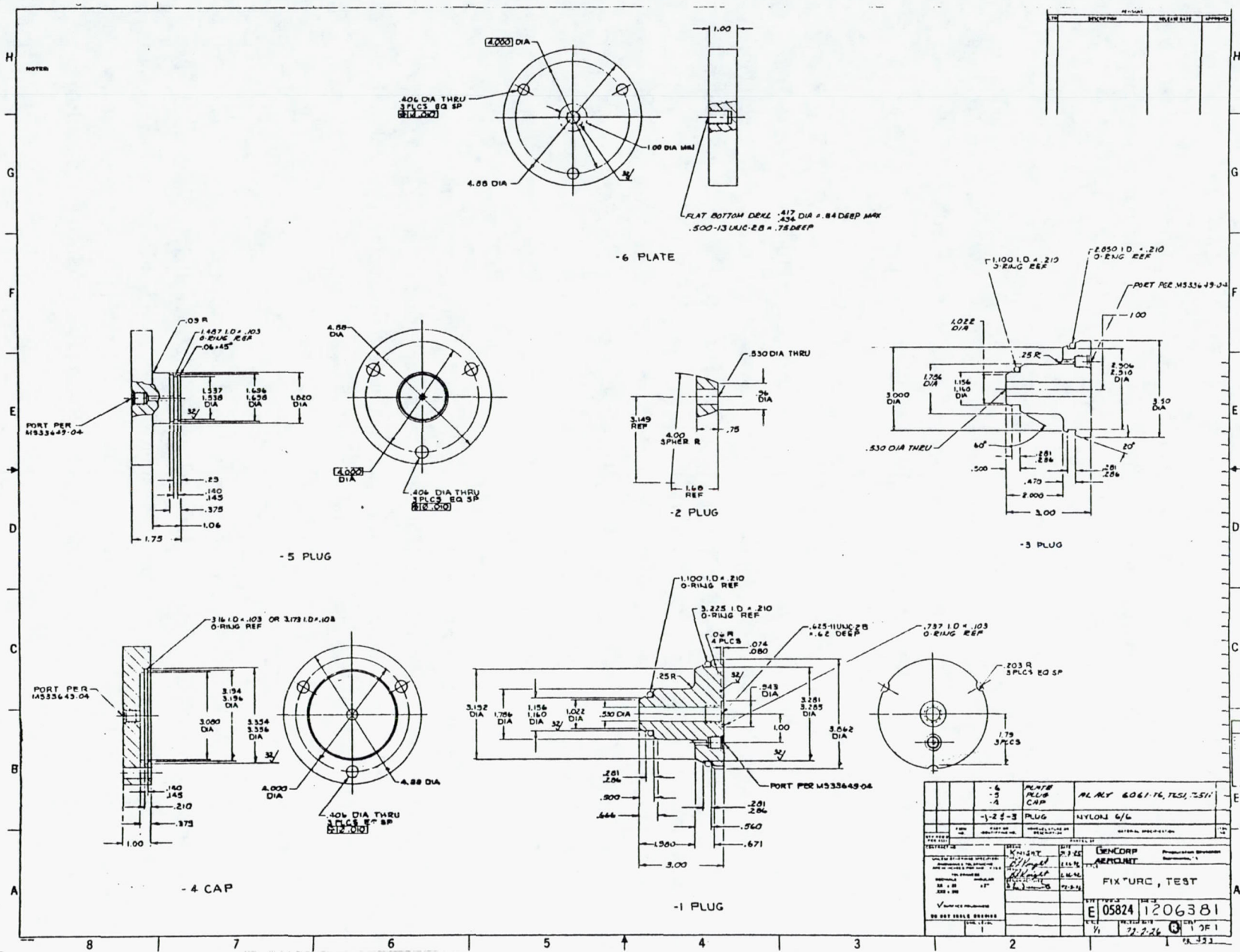


Table 5-1. Parts List for 100 lbf Thruster

APD Number	Item No.	PN	Title	Supplier	Quantity Per Engine	Number Built
1206350	286:1		Fully Assembled AJ10-221 Test Engine			
	1	1206360-29	Chamber Assembly	APD	1	1
	2	1206397-1	Plate	APD	1	
	3	1207289-9	Manifold	APD	1	
	4	-				
	5	MS16995-28	Screw		8	
	6	MS16i996-12	Screw		1	
	7		Screw		2	
	8	MS21046008	Nut		2	
	9	-				
	10	AR10304-011AQ	Omniseal		4	
	11	AR10304	Omniseal		2	
	12	B66638	Valve	Moog	1	
<u>Subassemblies and Components</u>						
120360-29			Chamber Assembly	APD		
	1	-9	Assembly		1	
	2	-19	Assembly		1	
	3	-				
	4	-				
	5	1206351-9	Nozzle	Tecomet	1	2
	6	(1206383-9	Chamber	APD	1	2
		Drawing Calls Next Lower Level in Error)				
	7	1206353-1	Injector	APD	1	2
	8	1206354-9	Adapter	Harris Mach.	1	2
1206383			Chamber Assembly	APD		
	1		Ring	APD	1	
	2		Ring	APD	1	
	3		Ring	APD	1	
	4		Shim	APD	1	
	5					
	6	1206352-1	Chamber	Ultramet	1	2
	7	1206384-9	Ring	APD	1	2
1206353-1			Injector			
	1	Injector	Originally Made from -9 Assy			
	2	1195651-9	Manifold	Harris Mach.	1	2
	3	1195651-7	Platelet	APD	1	4 sets
	4	1195651-6	Platelet	APD	1	4 sets
	5	1195651-5	Platelet	APD	1	4 sets
	6		Platelet	APD	1	4 sets
	7		Platelet	APD	1	4 sets
	8		Platelet	APD	2	4 sets
	9	-				
	10	1195651-1	Platelet	APD	1	4 sets
<u>Transition Joint</u>						
1206384			Ring Assembly			
	1	1206361-1	Ring		1	2
	2	1206361-2	Ring		NR	2
	3	1206392-1	Ring		1	2
	4	Ring			NR	

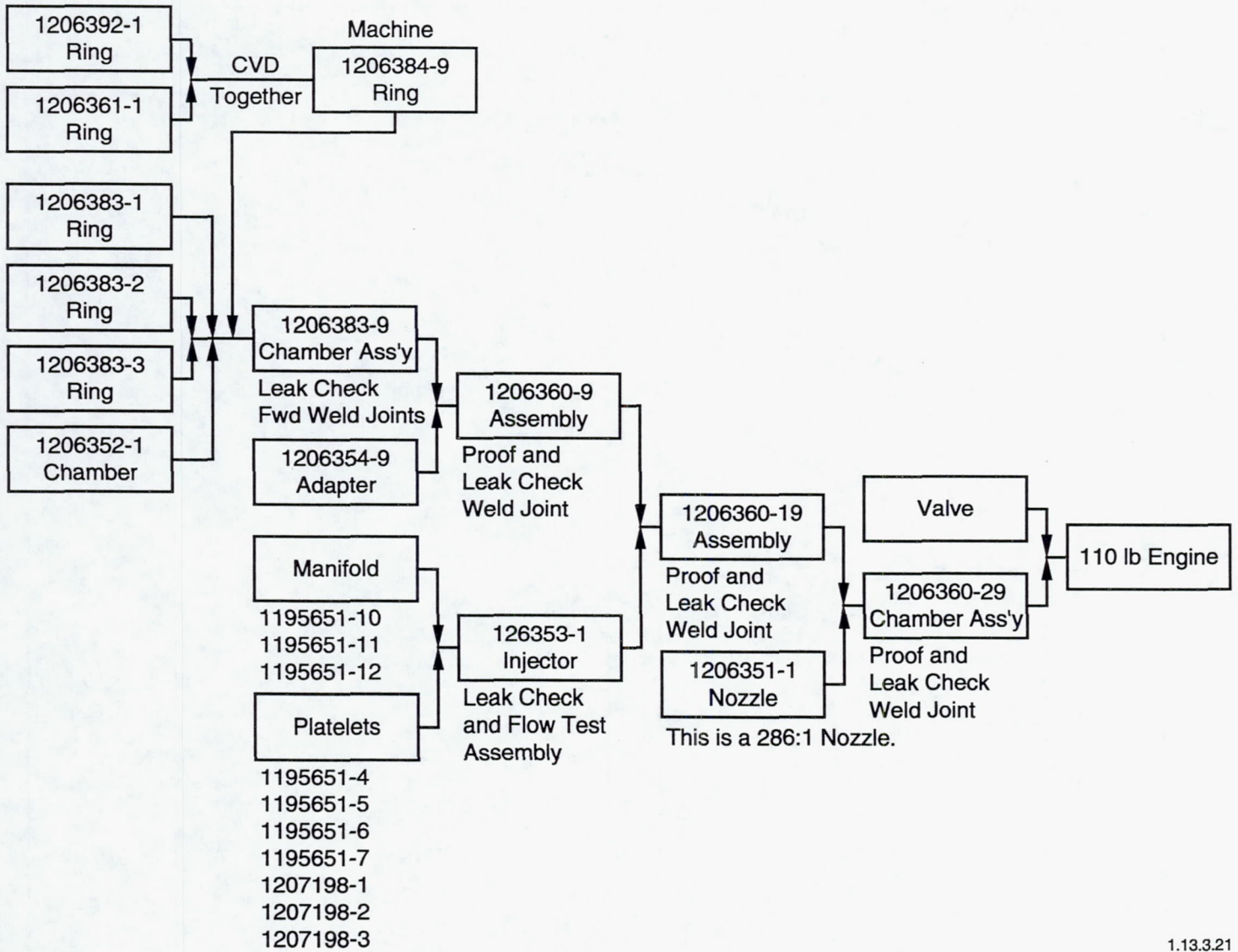
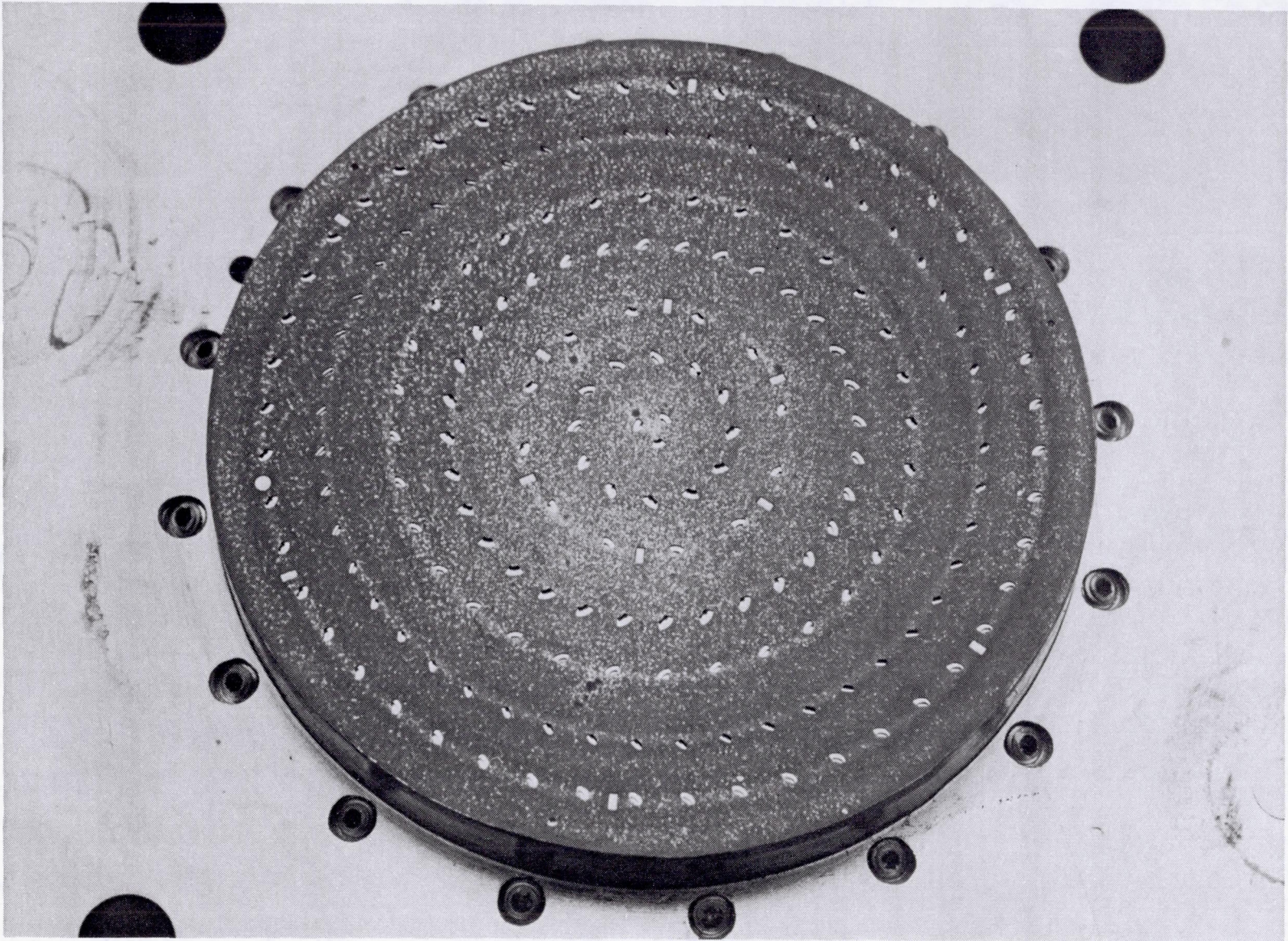


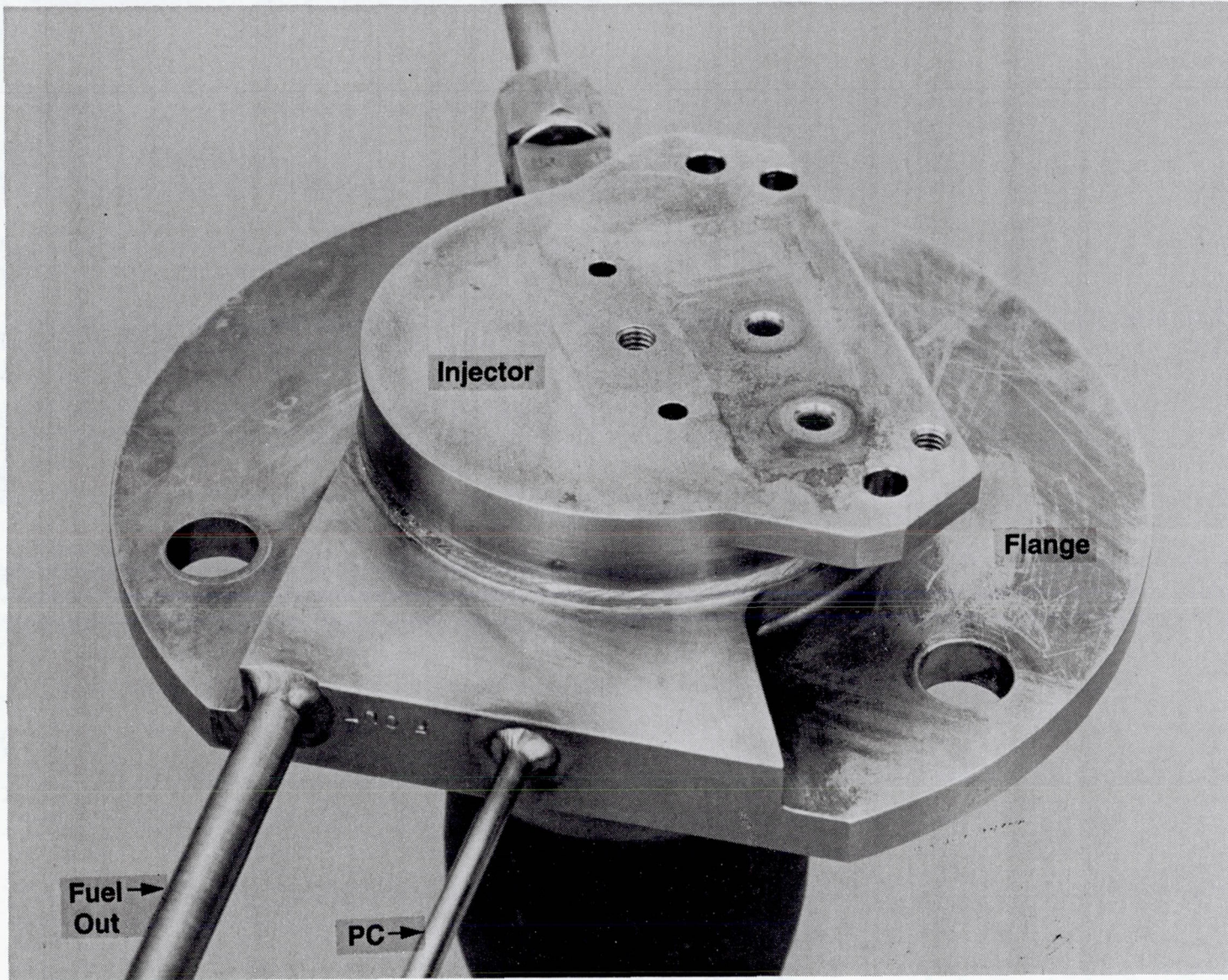
Figure 5-1. Assembly Steps

1.13.3.21



C1191 8099

Figure 5-2. Diffusion Bonded Platelet Injector With Flange



C0292 0621

Figure 5-3. Welded Assembly of Injector, Fuel Cooled Adapter and Rhenium Chamber



5.0, Fabrication (cont.)

5.3 FUEL COOLED FLANGE, PN 1206354-9

This component was fabricated from 304L stainless using conventional machining, brazing, and welding methods. All critical joints are electron beam welded and dye penetrant inspected followed by proof pressure and leak testing. Figure 5-4 shows the two major sub-assemblies. Figure 5-5 shows the component following final assembly. Two identical parts passed all inspections and the 400 psi proof test without need for rework. Strain gages attached to critical areas indicated no yield conditions would occur under the proof pressure loads.

5.4 IRIDIUM LINED RHENIUM CHAMBER, PN 1206352

Two of these chambers were fabricated under a subcontract to the Ultramet Co. using their proprietary inside out CVD processes. A high thermal emissivity rhenium coating was applied to the outside surface as a final CVD operation. The two ends of the chamber were ground to obtain the required wall thickness to conform to the thermal design, reduce weight, and prepare the chamber ends for weld attachments. The final operation was one of removing the mandrel by chemical leaching.

Inspections included close dimensional control of the mandrel before plating, measurement following deposition of the 2 mil iridium layer and inspection of the final assembly before and after grinding the OD. These data are included in Appendix E. The wall thickness in several noncritical areas exceeded the minimum requirements by more than the anticipated values resulting in a somewhat heavier but functional part. No effort was made to correct this on the two delivered parts. Dye pen inspection at Aerojet showed no flaws in the iridium liner after cleanup of the chamber I.D.

A photograph of the Ultramet fabricated chambers is shown in Figure 5-6. The discolorations on the ID are a result of the chemical leaching process employed to remove the mandrels. Figure 5-7 shows the same chamber with the bimetallic weld rings attached, and ready for assembly.

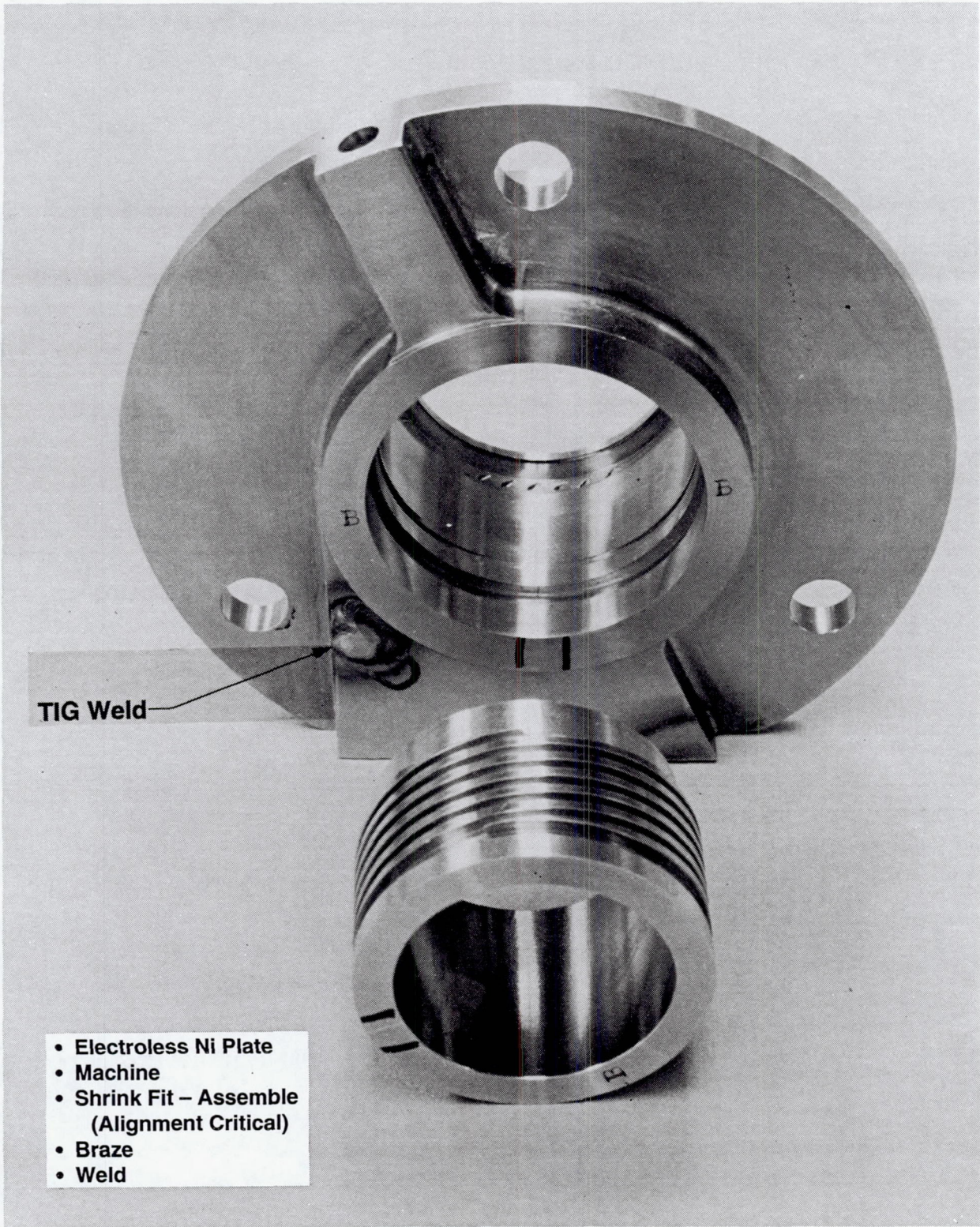
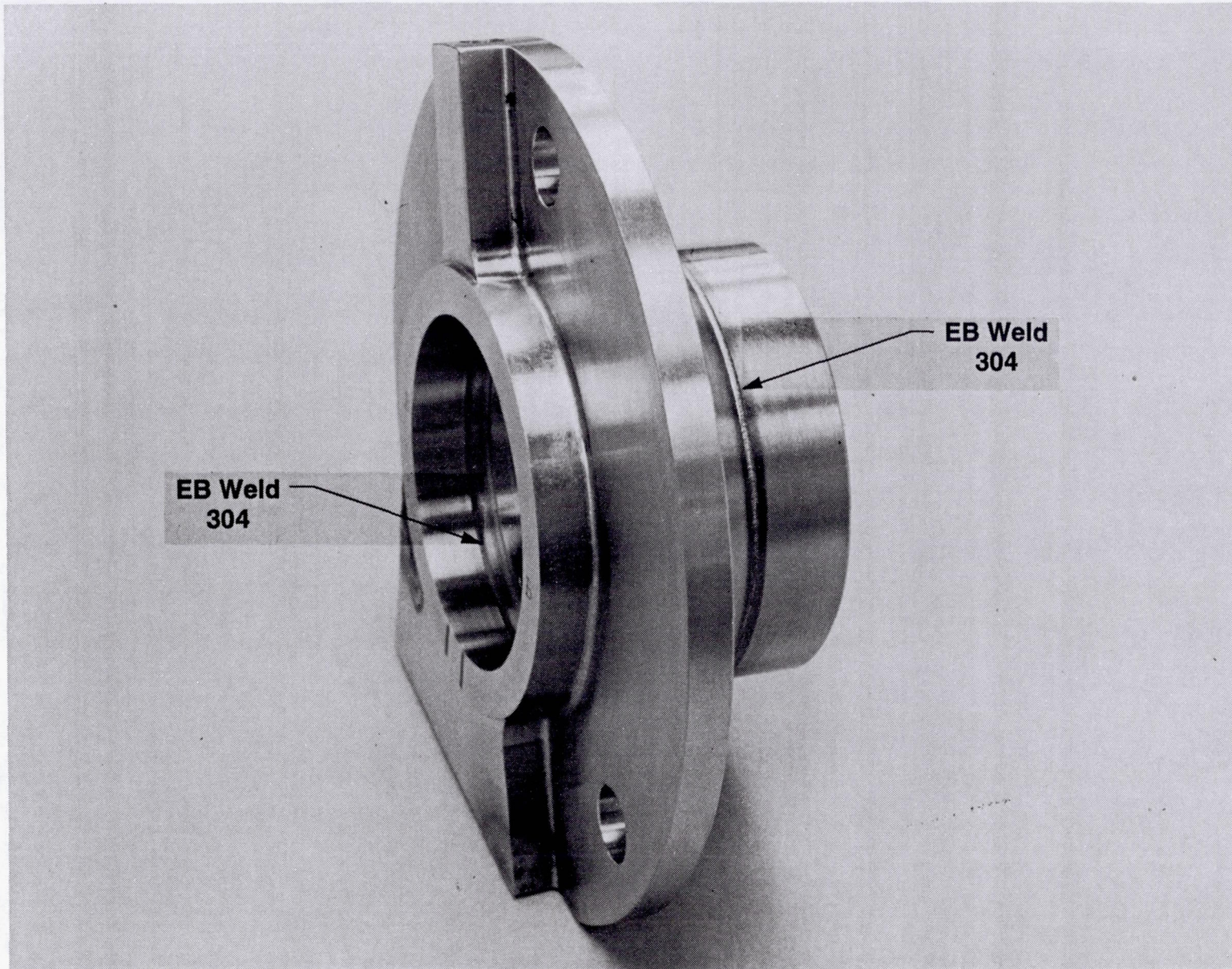
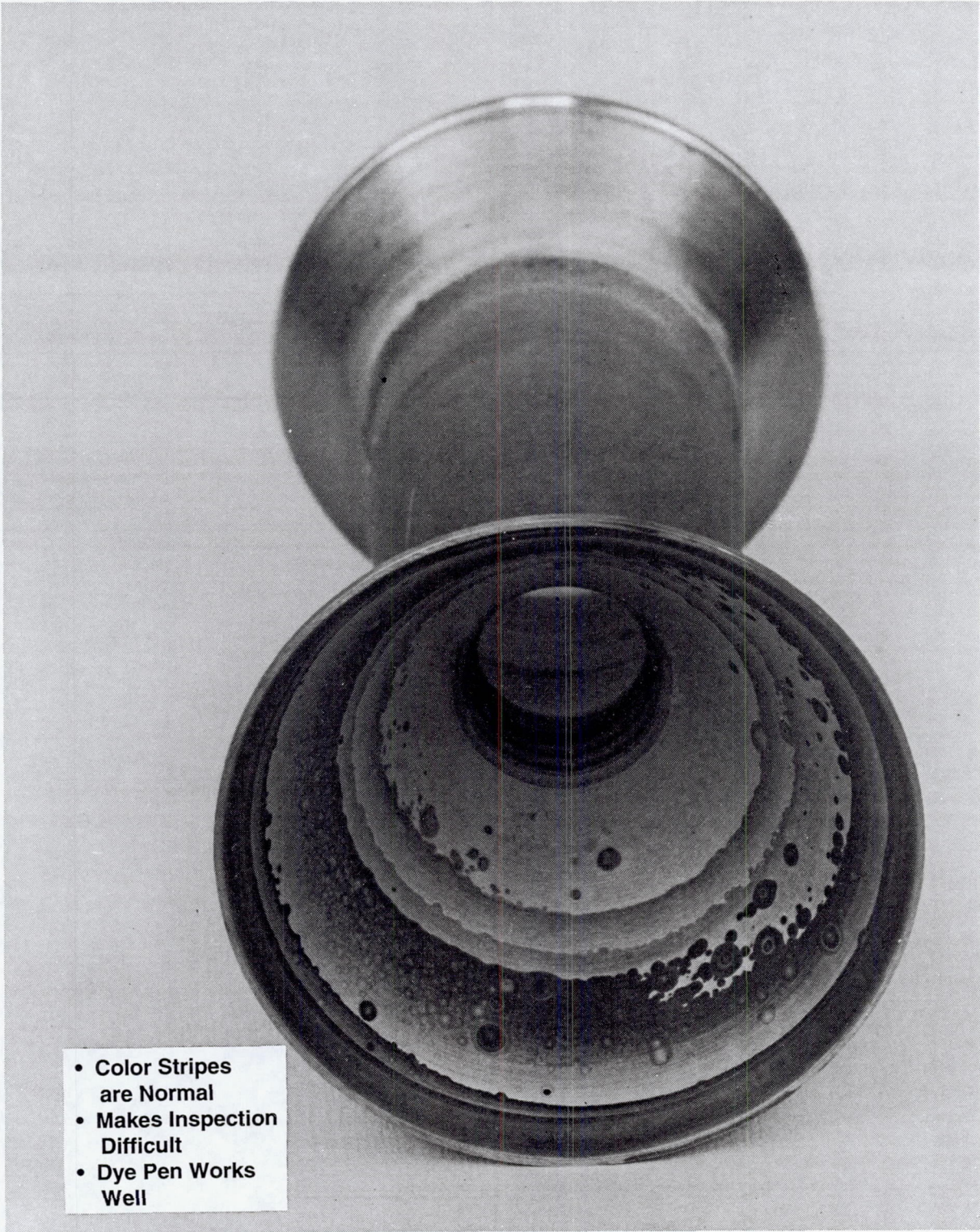


Figure 5-4. Fuel Cooled Mounting Flange



C0491 2371

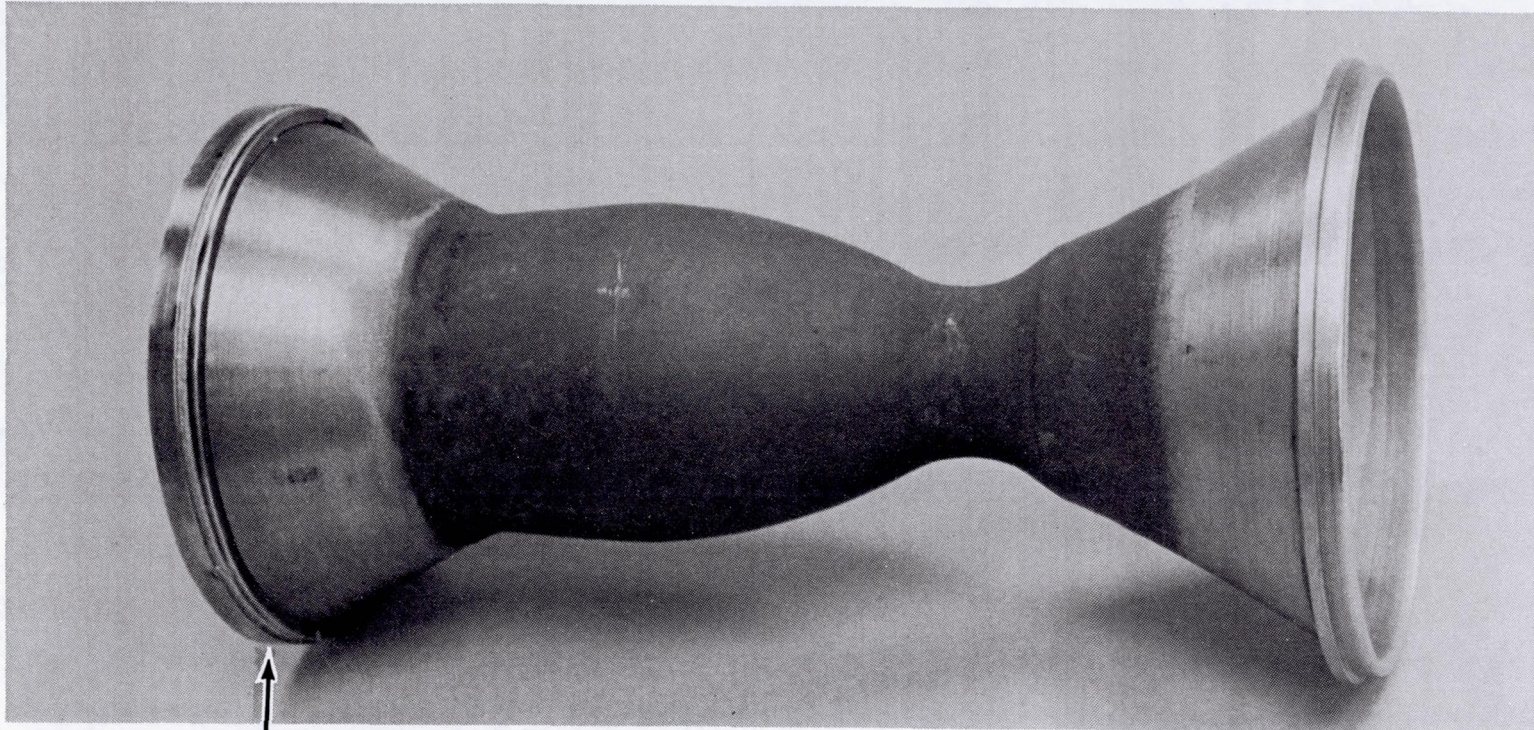
Figure 5-5. Final Assembly Component of Fuel Cooled Adapter



- Color Stripes are Normal
- Makes Inspection Difficult
- Dye Pen Works Well

C0491 2202

Figure 5-6. Iridium-Rhenium Chamber as Delivered by Ultramet



C0891 5949

15-38-23

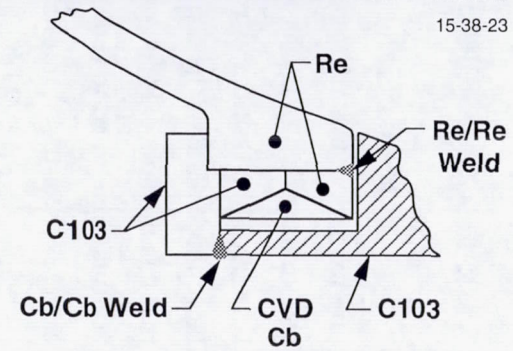
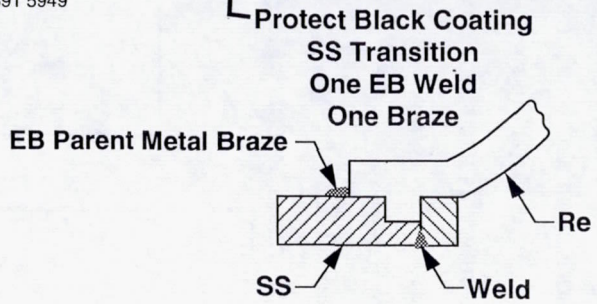


Figure 5-7. Ir-Re Chamber for 286:1 Thruster SN-1 With Weld Adapter Rings in Place

5.0, Fabrication (cont.)

5.5 COLUMBIUM SKIRT, PN 1206351

The skirt is fabricated from columbium alloy C-103 and protected from high temperature oxidation and hydrogen attack at low temperature by the R-512 E disilicide coating. In the preliminary design it was anticipated, based on discussion with sheet metal fabricators, that the skirt could be fabricated as flow formed structure with no welding required. In this process a large thick plate of the C-103 alloy is preformed over a mandrel to provide a thick wall structure that has the approximate nozzle contour. After appropriate stress relief the ID and then the OD are final machined to required dimensions using conventional NC Machining equipment. Several sheet metal fabricators have successfully produced C-103 nozzles using this process at an area ratio of 150:1 with wall thickness in the approximate range of interest. None had demonstrated parts as large as the 286:1 design or with walls as thin as 0.010 in. However, more than one potential fabricator believed it was possible at least with the 0.016 upper limit wall thickness. The task was subcontracted to Tecomet with an order for two nozzles. There were five attempts to fabricate the skirts using the flow turning process in order to advance the fabrication technology. The limited availability of the C-103 material in the proper preform size and thickness and the short schedule required compromises in the fabrication approach which eventually proved unworkable. The final product shown in Figure 5-8 provided an acceptable contour for performance and welding to the rhenium but did exceed the wall thickness and weight requirements. Fabrication and inspection details are provided in Appendix F. These required substantial welding of the C-103 in order to salvage major portions of the original preformed cone. Chemical milling was used to remove excess material up to the point where the minimum wall thickness was as thin as 0.008 in. locally, while other areas remained as thick as 0.027 in. Further reductions were considered to be greater risk. The material removed by chemical milling is defined in Table 5-2 along with the after coated weight. The weight for the two columbium skirts, uncoated and coated compared to the design values are as follows:

Table 5-2. Weight of Columbium Skirts

	Weight in lbs		
	Uncoated		Coated
	As-Spun	After Chem Milling	
Design	2.2	N/A	2.50
SN-1	5.8	4.1	4.45
SN-2	—	—	—



Pre Etch



Post Etch

6-28-91

Figure 5-8. SN-1 286:1 Cb Nozzle Exterior Before and After Chem Milling

5.5, Columbium Skirt, PN 1206351 (cont.)

Measurements of the nozzle contour compared to the required values were acceptable as shown in Figure 5-9.

5.6 MINI SKIRTS

Two mini skirts were fabricated to validate the rhenium to columbium joining process. One was a conical skirt machined from C-103 bar stock as shown in Figure 5-10. The second was a 47:1 skirt salvaged from one of the five rejected flow turned assemblies. This is shown in Figure 5-11.

5.7 ENGINE ASSEMBLY

The components discussed in the previous section were assembled using the flow chart shown in Figure 5-1. Figure 5-12 shows all of the required components and spare parts required for the assembly including the tooling for fixturing, proof pressure and leak testing. Assembly starts with the weld attachment of the columbium/rhenium transition joint on the aft end and the stainless steel rhenium joint on the forward end of the rhenium chamber (Figures 5-7 and 5-13). Leak checks are conducted after each weld.

The cooled flange (Figure 5-14) and the rhenium chamber are electron beam welded next. This is a 304L to 304L stainless steel joint. Following leak check the 304L injector is electron beam welded to the 304L cooled flange as shown in Figure 5-3. This complete weld assembly is shown in Figure 5-15. Leak checking and a 200 psi proof pressure test at this stage of the assembly revealed no detectable leakage based on the use of Leaktec solution.

The final assembly step is the welding of the columbium skirt to the end of the rhenium chamber having the columbium stub from the transition joint. Figure 5-16 shows the skirt weld. A leak check of this joint with 5 psi helium indicated on very small detectable flaw in the final EB weld joint, too small to form measurable bubbles when Leaktec solution is applied. Since the normal gas pressure at this point is only 1 psi no attempt at repair was considered necessary.

The final assembly operation is to bolt on the valve using the valve adapter. This was shown earlier in Figure 2.2-8. The assembled 286:1 engine was shown in Figure 2.1-1.

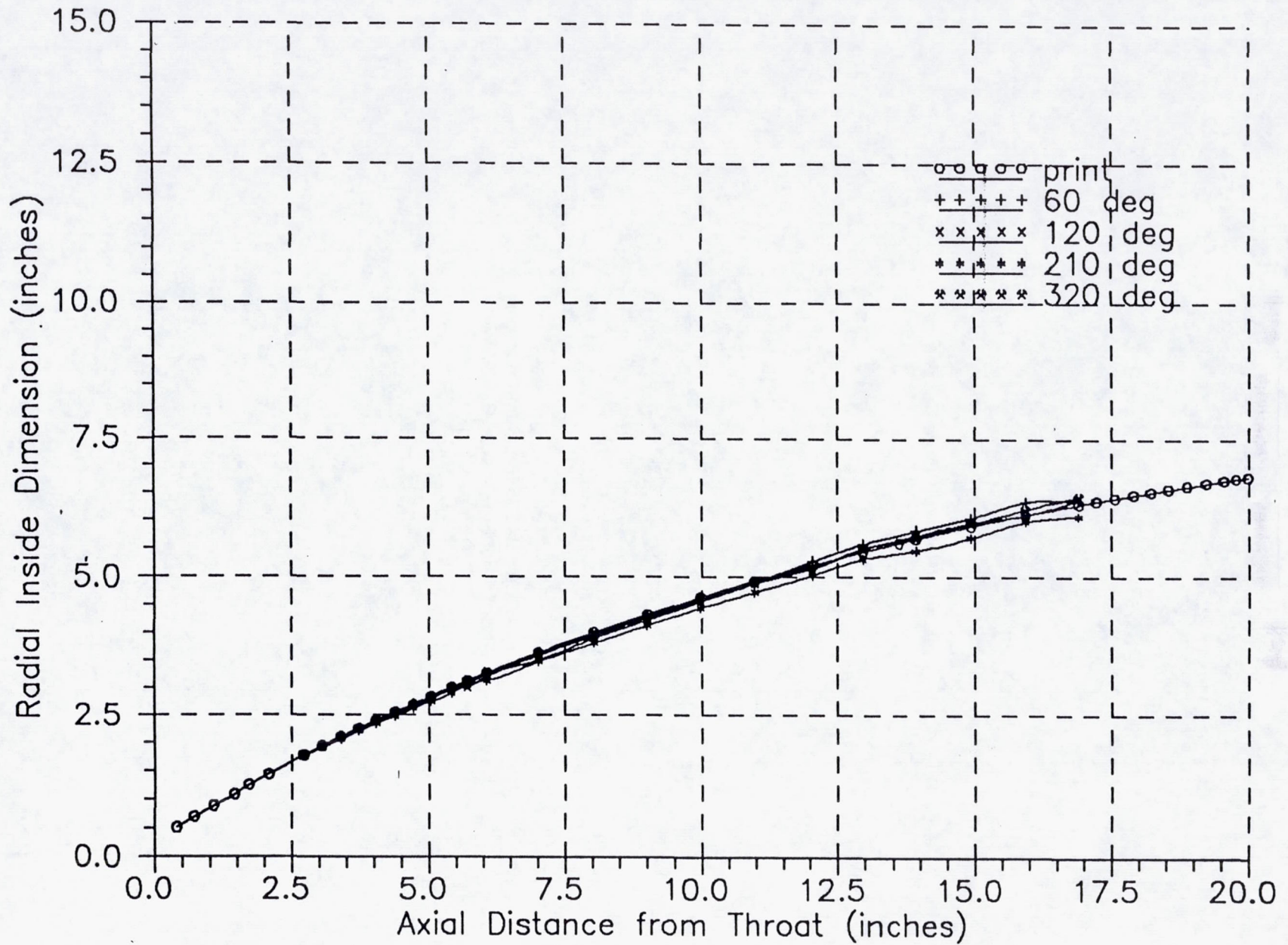
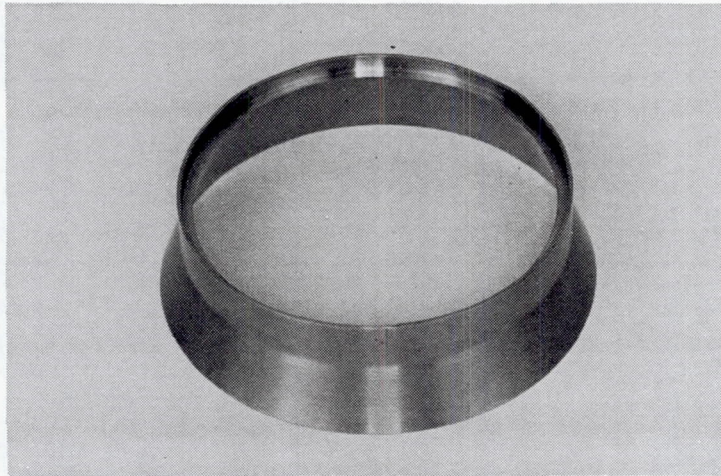


Figure 5-9. SN-1 Cb Skirt Actual and Print Dimensions During Fabrication



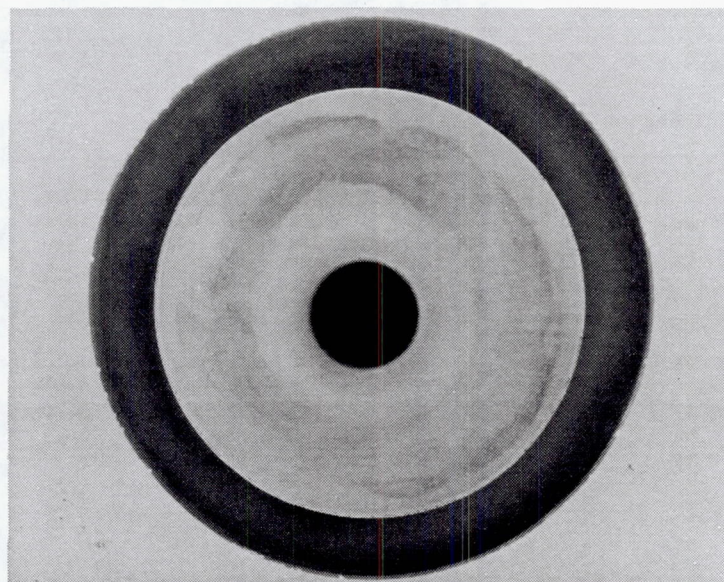
C0491 2207

C-103 Miniskirt Before Coating



C0891 5663

**Miniskirt Welded to Rhenium Chamber
After 15 Hot Fire Tests - Side View**



C0891 5661

Miniskirt - Welded After 15 Hot Fire Tests - End View

15-38-24

Figure 5-10. Validation of the Rhenium to Columbium Joining Method



C0691 4057

Figure 5-11. 47:1 Area Ratio Coated C-103 Miniskirt

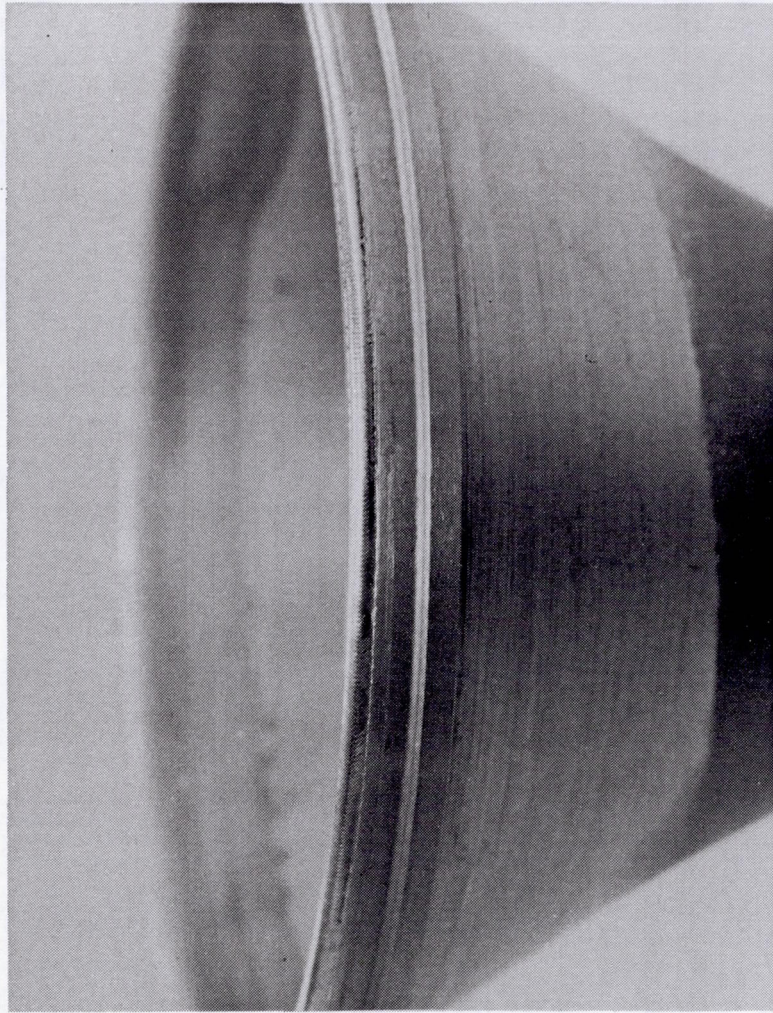


C0891 5947

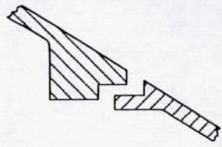
Figure 5-12. Engine Components and Tooling for Assembly



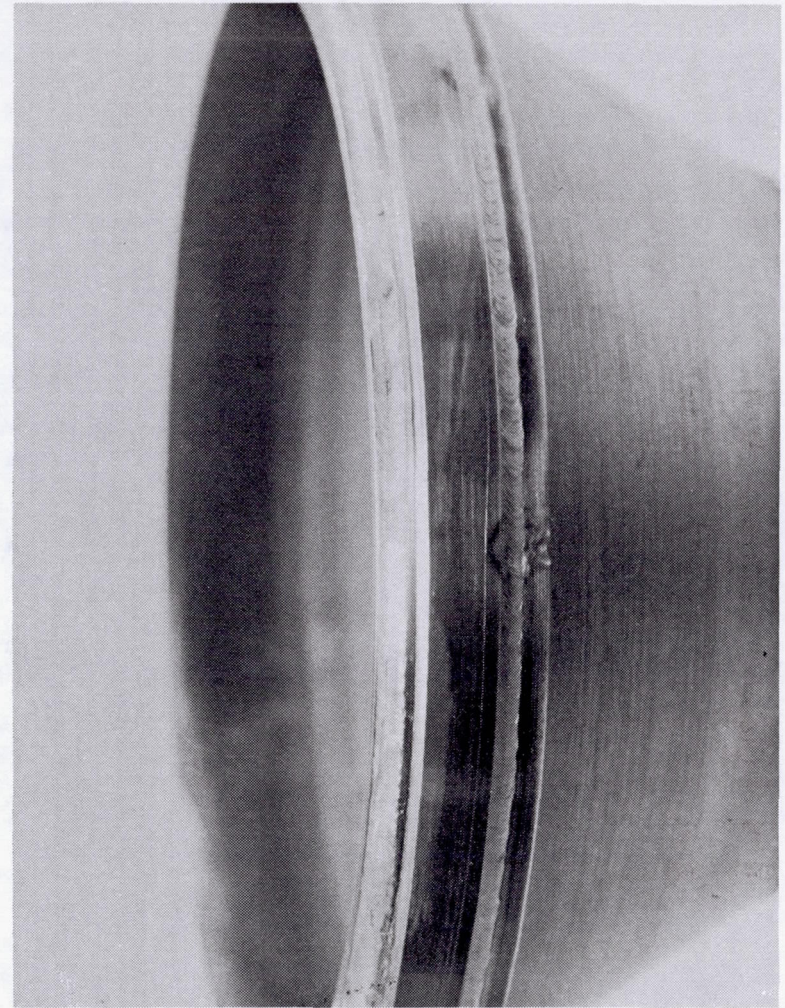
75



C0891 5951



Aft End Ready
for Skirt Weld



C0891 5950

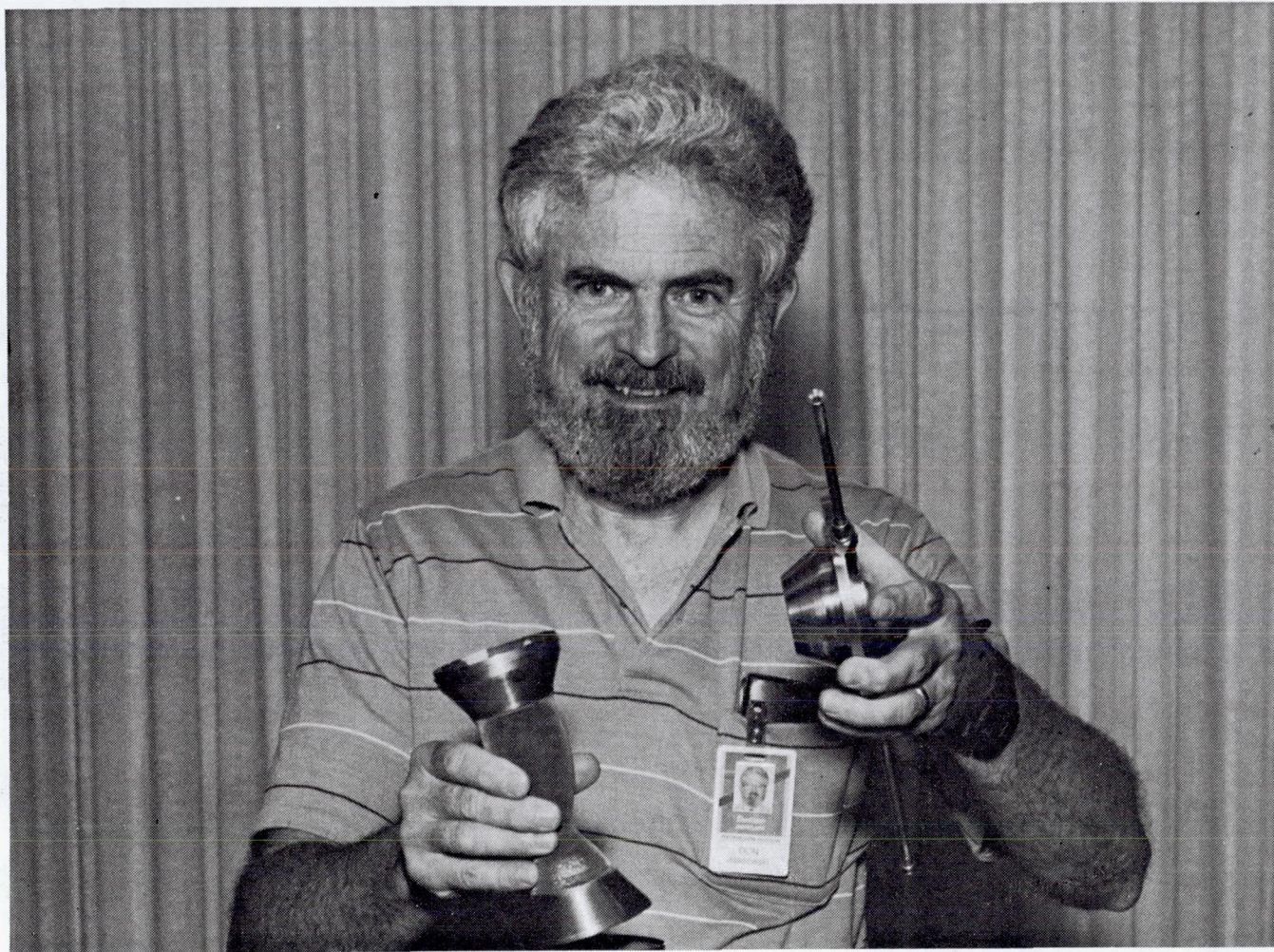
SS-Re Braze Weld
Only Steel Melts
Surface for Next Weld

SS

SS-SS Weld

15-38-25

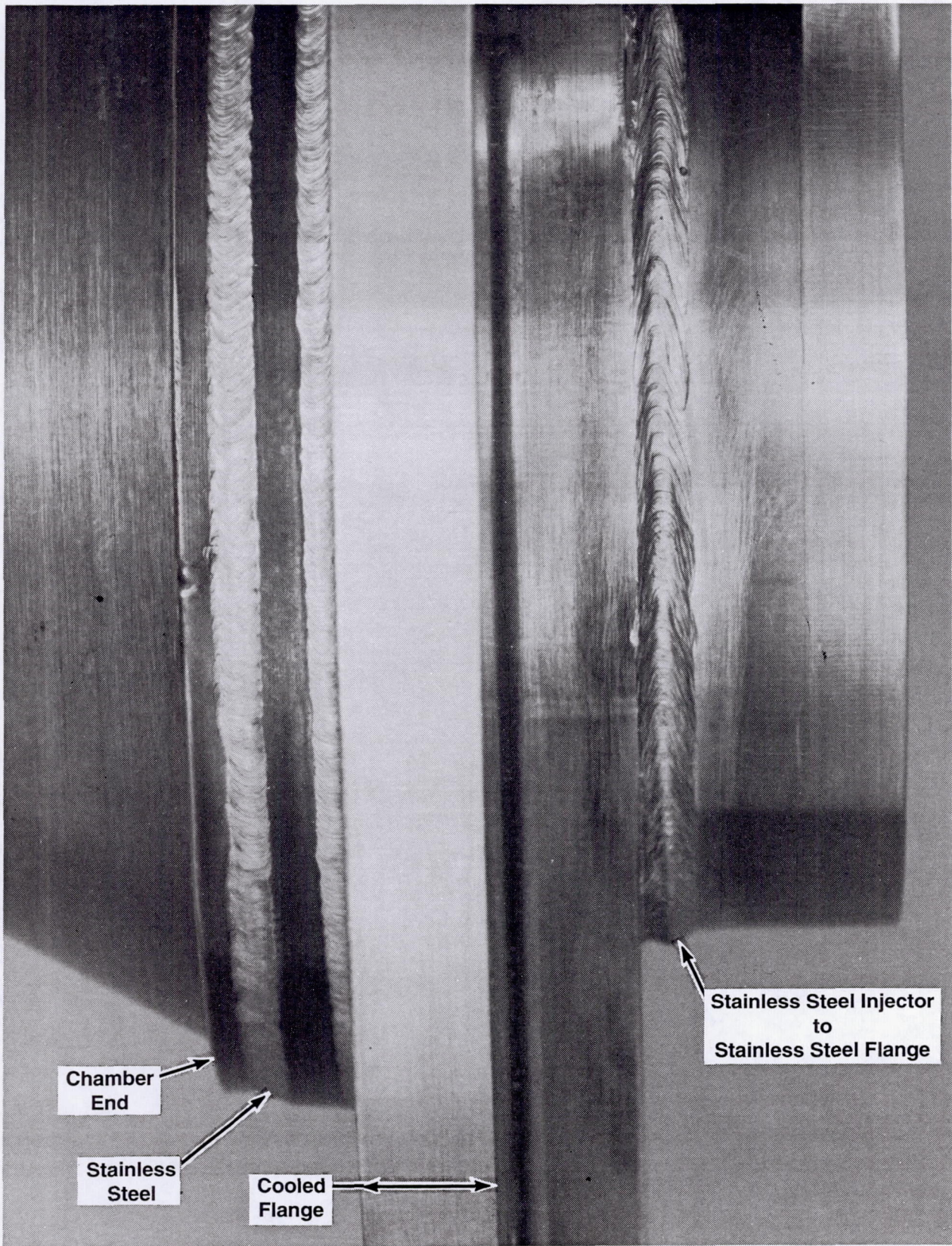
Figure 5-13. Weld Ring Photos



C0891 5754

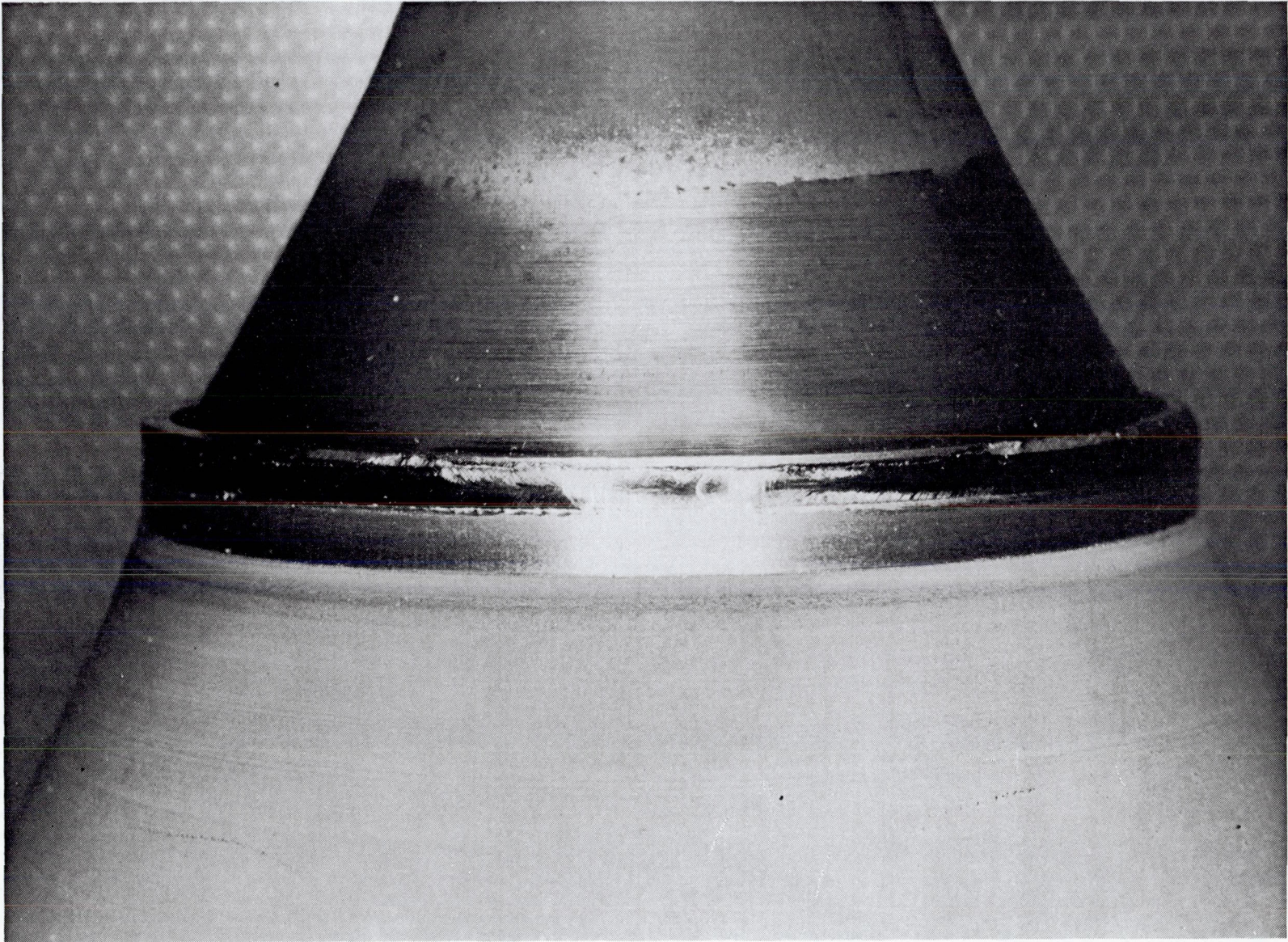
Figure 5-14. Joining of the 304L Cooled Flange to the Rhenium Chamber





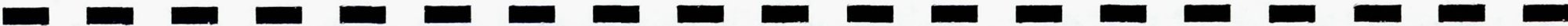
C0292 0616

Figure 5-15. Weld Assembly Injector Cooled Flange and Iridium Lined Rhenium Chamber



C0292 0647

Figure 5-16. Columbium Skirt EB Weld



6.0 TESTING

The 110 lbf Ir-Re radiation-cooled NTO/MMH thruster technology development program relied heavily on two types of experimental data, viz., design development/verification tests and technology demonstration testing. This testing began at subcomponent level, i.e., manufacturing processes such as EB welding, and progressed through hot firing of a prototype flight engine, the AJ10-221. A total of 14 thruster configurations were tested in 248 firings, for a total firing time of 26,169 sec. The flight engine was fired for an accumulated duration of 22,590 sec in 93 firings, one of which was a continuous burn of two hours. Measured specific impulse at nominal conditions of 110 lbf, MR = 1.65 was 321.8 lbf-sec/lbm at an area ratio of 286:1 geometric, demonstrated in a series of 27 altitude performance tests in which thrust was measured directly.

Major test activity areas included design development tests of joining concepts for the dissimilar chamber materials, process development tests to demonstrate reliable, repeatable fabrication of the platelet injector, and proof, leak, flow and hot fire tests of sub-components and assembled hardware.

6.1 WELD JOINT DEVELOPMENT TESTS

The joining processes used for the stainless steel-to-rhenium chamber joint and the rhenium-to-C-103 nozzle skirt joint were investigated under NASA Contract NAS3-24643 (Ref. 4) and were developed as part of Aerojet IR&D programs during 1990 and 1991. This work is reported in Ref. 4, Appendix F, from which some of the following data are taken.

Joint Validation

All the bimetallic joints in this engine are redundant. The steel-to-rhenium and rhenium-to-columbium joints are a parallel combination of mechanical and metallurgical attachments. Either of the two is structurally adequate for safe engine operation.

Laboratory Test

Six subscale stainless steel-to-CVD rhenium EB weld joints were fabricated, leak-tested, and proof pressure-tested to 1000 psi. All samples passed proof and helium leak checks. Two burst-tested joints withstood pressures of 5000 psi. Thermal cycle-induced strains were predicted to be the ultimate failure mode because of the difference in thermal expansion coefficients of these two materials. Four joints were thermally cycled from 150 to 650°F, which is

6.1, Weld Joint Development Tests (cont.)

325°F greater than will be experienced in actual engine operation. The designs exhibited an operational capability of more than 1000 thermal cycles without leakage or degradation.

Six rhenium-to-columbium joints that simulated the chamber nozzle extension interface were fabricated and subjected to 1000 psi proof and helium leak tests. One joint showed a small leak at the point where electron beam fusing started and stopped. This was corrected by modifying the weld parameters. Thermal cycle-induced strains are not a concern at this joint because these materials have nearly identical expansion coefficients. The predicted failure mode for this joint is thermal diffusion because the joint will operate at temperatures up to 2000°F. Two joints were subjected to a 2150°F vacuum thermal diffusion cycle for 6 hours. Posttest evaluation showed no leaks and the ability to withstand the 1000 psi proof pressure testing. Under normal engine operation, the exhaust gas pressure at this joint location is less than 2 psia.

6.1.1 Weld Joint Specimen Design and Test Plan

The object of the Metal Joining Study was to fabricate rhenium-to-various metal weld joint specimen and to evaluate the quality of the weld joints in order to assist the overall design and fabrication of rhenium rocket engines. Figure 6.1-1 shows the design of the weld joint specimen. The specimen is actually fabricated from one rhenium ring and two ring caps of the metal to be joined to rhenium. The three rings are EB welded together with the rhenium ring in the middle to form a cylinder closed at both ends. Thus, each specimen contains two weld joints for evaluation. Finally, the end caps have threaded fittings to allow pressure testing. Figure 6.1-2 is a photograph of the test specimen.

The evaluation test program was as follows:

- 1.0 — Pressure Test at 1000 psig (Helium)
- 2.0 — Leak Test at 500 psig (Helium) and Soapy Water
- 3.0 — Thermal Cycle or Thermal Treatment
- 4.0 — Pressure Test at 1000 psig (Helium)
- 5.0 — Leak Test at 500 psig (Helium) with Soapy Water
- 6.0 — Metallographic Analysis

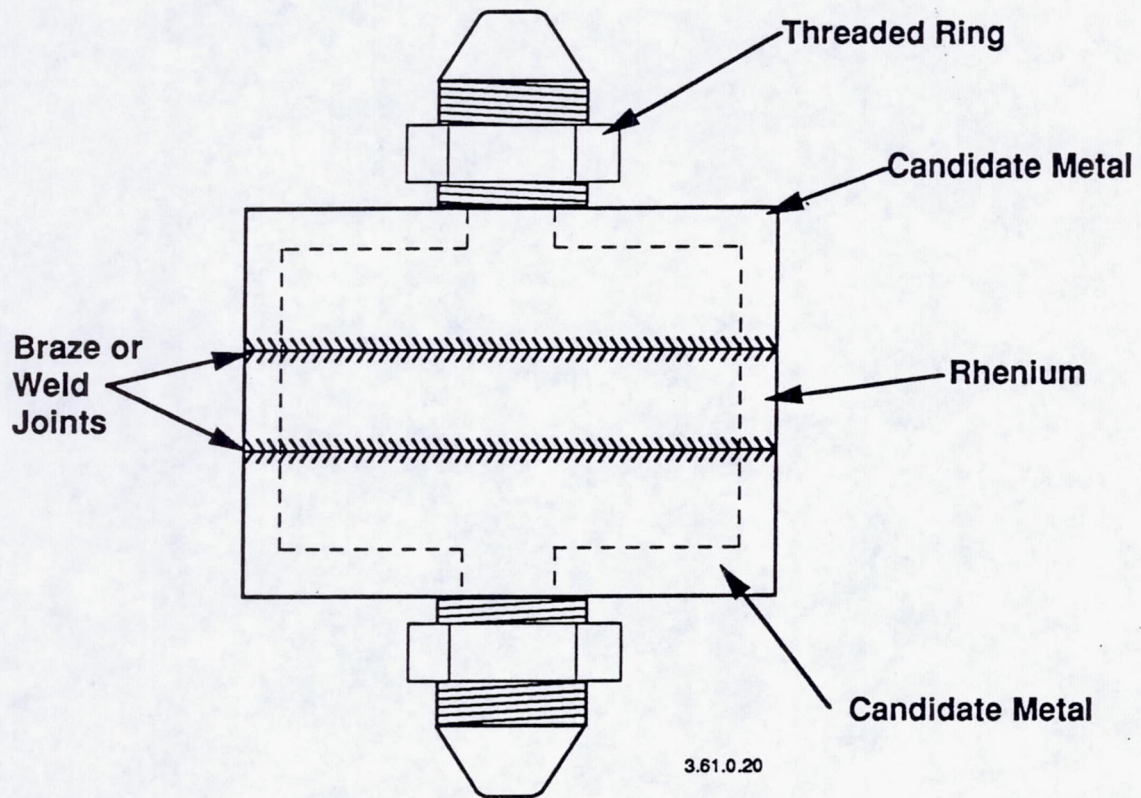


Figure 6.1-1. General Design for Weld Joint Specimen

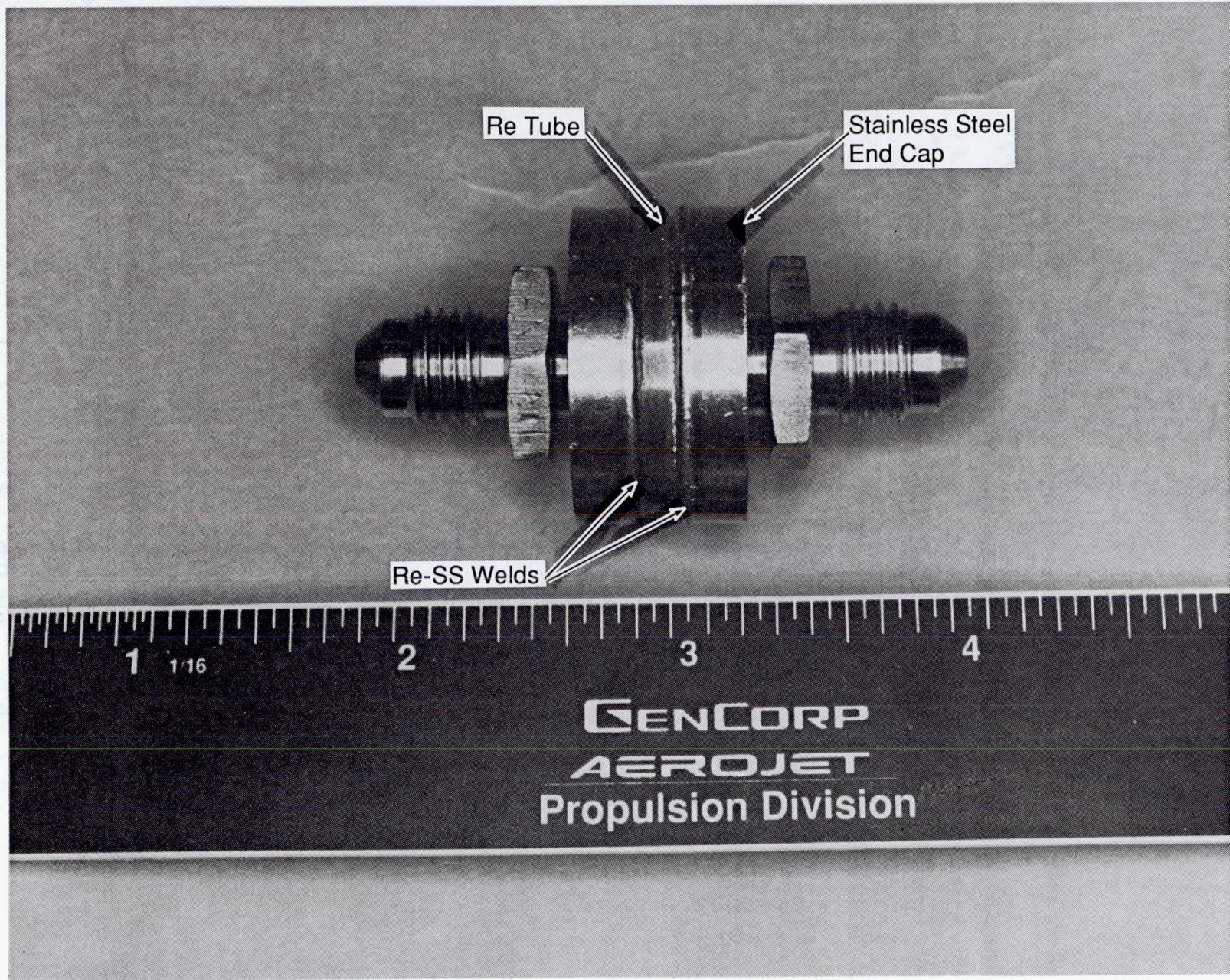


Figure 6.1-2. Re-SS Test Specimen as Fabricated

6.1, Weld Joint Development Tests (cont.)

6.1.2 Thermal Cycle Test Apparatus

A test setup was assembled for automatically thermal cycling the joints under computer control from 150 to 650 F. The setup consists of an electrically heated furnace, GN₂ cooling for the specimen, and a holder for the test specimen which allows the pressurization of the specimen during thermal cycling. This experiment is shown in Figure 6.1-3.

During operation, the test specimen is pressurized with GN₂ and sealed. The specimen is then moved in and out of the hot zone of the furnace and the temperature and pressure of the specimen is monitored. When the specimen is in the down or heating position, the temperature is allowed to climb to 650 F. Then the specimen is removed from the hot zone and GN₂ blown over it for cooling, as shown in Figure 6.1-4. When the temperature drops to 150 F, the specimen is returned to the hot zone and the cycle repeated.

The joint life requirement is 200 thermal cycles. Normal practice is to demonstrate ten times the required life to provide confidence that the joint will not fail due to low cycle life fatigue.

The results of the joint development testing are summarized in Table 6.1-1. These data include the results of vacuum thermal cycle tests.

6.1.3 CVD Columbium to C103 Weld Joint

Since directly welding rhenium to C103 was shown to give poor quality weld joints as shown in Table 6.1-1, the CVD Cb on CVD Re ring was used to fabricate weld joint specimen that effectively joins rhenium to C103 via a surrogate CVD Cb to C103 weld as illustrated by Figure 6.1-1. Three specimen involving a total of six welds were fabricated. All six welds passed the pressure test at 1000 psig, but one weld failed the leak test at 500 psig (Helium) with soapy water. Thus, two specimen were suitable for thermal testing.

A good specimen was put through a thermal treatment by heating to 2100-2200 F for 3 hours under vacuum (0.07 torr). It was then allowed to cool to room temperature at 0.05 torr. The specimen was again heated to 2100-2200 F at about 0.06 torr and held for 4 hours. Finally, the specimen was cooled overnight at 0.05 torr. The surface of the specimen was coated

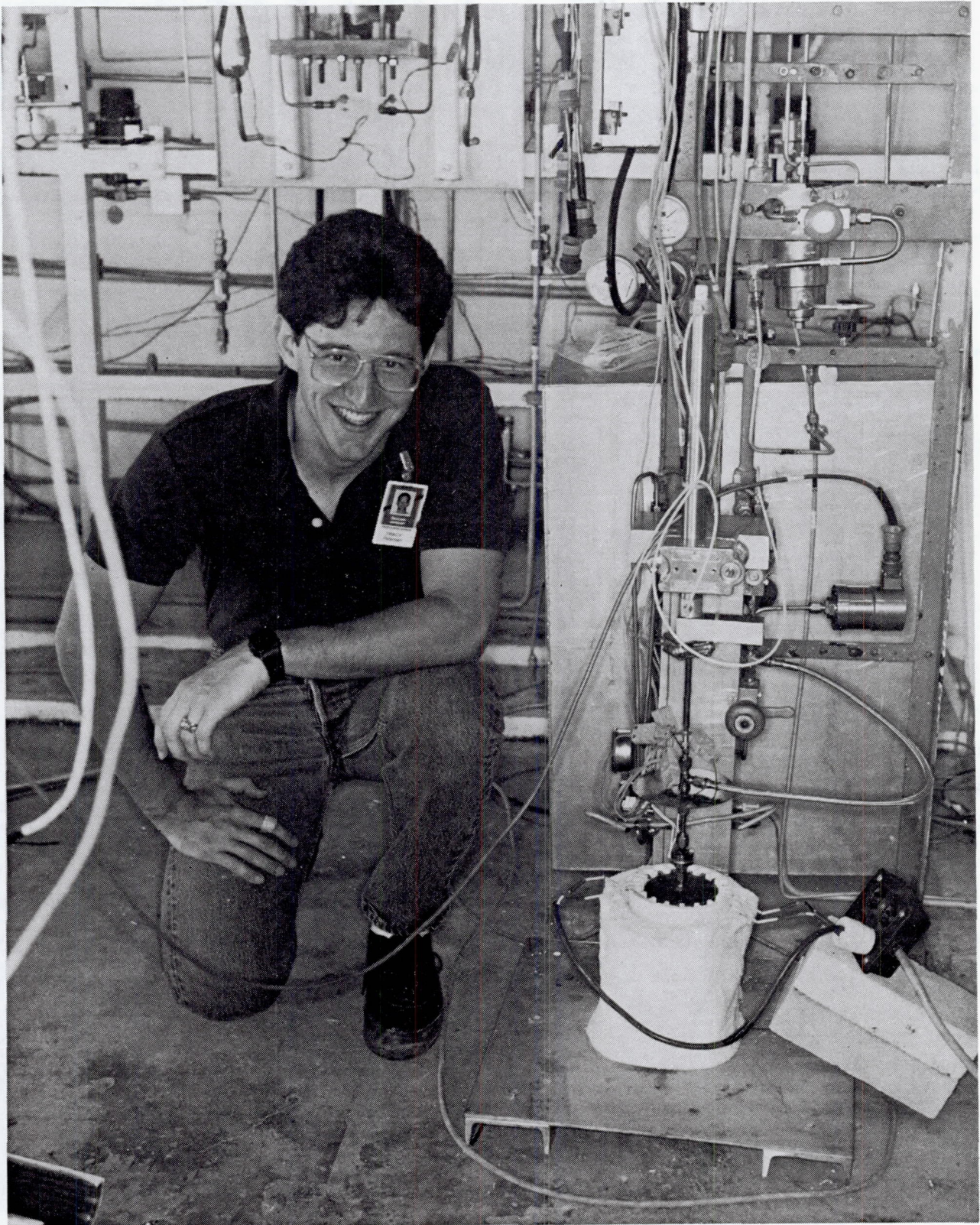


Figure 6.1-3. Weld Joint Specimen Test Facility

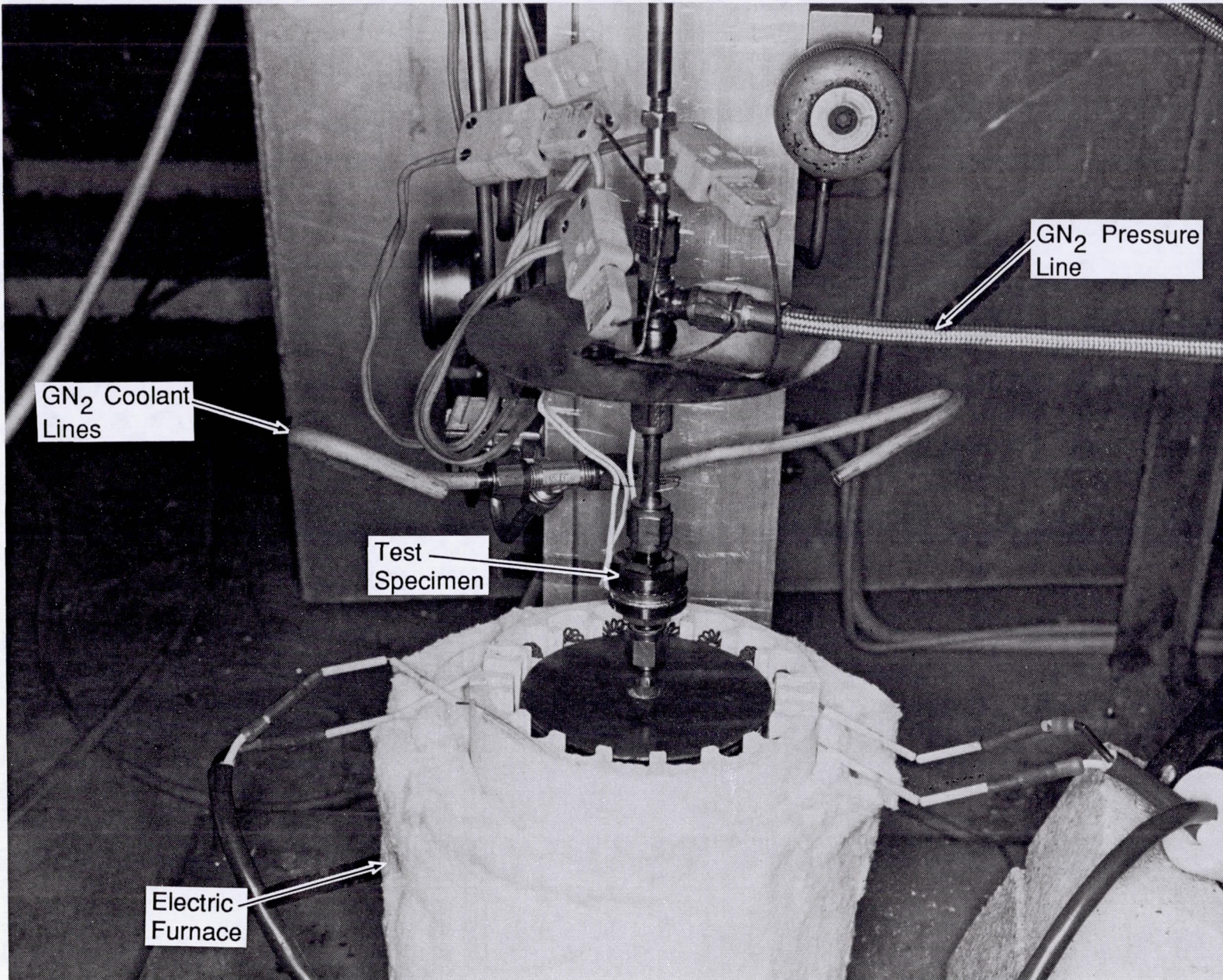


Figure 6.1-4. Automatic Joint Thermal Cycling Test Setup in the Cooling Position

TABLE 6.1-1

METAL JOINING STUDY TEST RESULTS

Metal Joint	Number Joints Fabricated	Fabrication Testing			Thermal Cycle Tests	Post Thermal Cycle Testing		
		Proof Test (1000 psig He)	Leak Test (500 psig He)	Burst Test (psig)		Proof Test (1000 psig He)	Leak Test (500 psig He)	Burst Test (psig)
CVD Re to C103 Columbium Alloy	4	—	All Leaked	—	—	—	—	—
CVD Cb to C103 Columbium Alloy	6	Passed	Leaked	—	—	—	—	—
		Passed	Passed	—	2200 F/0.07 torr/7 hrs	—	—	150 ^a
		Passed	Passed	—	2100 F/10 ⁻⁵ torr/6 hrs	Passed	Passed	—
CVD Re to CRES 304	8	Passed	Passed	5800	—	—	—	—
		Passed	Passed	—	150-650 F/700 cycles	Passed	Leaked ^b	—
		Passed	Passed	—	150-650 F/2000 cycles	Passed	Leaked ^b	—
		Passed	Passed	—	—	—	—	—
CVD Re to Ti (6ALAV)	6	Passed	Passed	2200	—	—	—	—
		Passed	Passed	—	150-800 F/500 Cycles/100% N ₂	Passed	Leaked ^d	—
		Passed	Passed	—	150-800 F/950 Cycles/4% H ₂ in N ₂	Passed	Passed	2800

- a) Specimen broke into two pieces. Severe surface cracking observed under binocular microscopic examination
- b) Leak developed after 516 cycles into the run when test apparatus stuck in heat position and the specimen was exposed to temperatures up to 1100 F for about 30 minutes
- c) Leak did not appear until 1300 cycles
- d) Leak at stop/start weld point

6.1, Weld Joint Development Tests (cont.)

with a thin black scale. The nature and the origin of the scale is unknown, but it may well represent oxidation. Even though oxidation should be slow at 0.05 to 0.07 torr, the total exposure time at 2100-2200 F was 7 hr, which might be long enough to show an effect.

When the specimen was pressure tested, it fractured completely at 150 psig to yield two separate parts. The fracture occurred at the weld joint and binocular microscopic examination showed a brittle failure and extensive micro-cracking in and around the joint including the C103 alloy. Results are summarized in Table 6.1-1.

There is little doubt that the thermal treatment degraded the weld joint. However, two questions required answering before a CVD Cb to C103 weld joint was eliminated from further consideration: (1) was the initial weld completely adequate, and (2) was the thermal treatment test fair. Visual inspection of the weld joint after the failure at 150 psig indicated a fairly thin weld. Although the weld joint did pass the 1000 psig proof test prior to the thermal treatment, it may have been marginal. The more important question deals with the fairness of the thermal treatment test. The failure appears to be due to embrittlement of the weld joint resulting from the thermal treatment. This embrittlement might well have been brought on by exposure to air (oxygen) at 0.05 to 0.07 torr. This is a reasonably low vacuum, but it is not representative of the vacuum encountered during actual use, i.e., low earth orbit and/or inter-planetary firings. Under these conditions the external pressures would run from 10^{-6} torr to 10^{-11} torr or lower. If oxygen embrittlement is responsible for the weld joint failure, then the test was unfair since it is unlikely that this embrittlement mechanism would operate at 10^{-6} to 10^{-11} torr. Considering these uncertainties, the remaining qualified specimen was put through a similar thermal treatment under high vacuum conditions, i.e., about 10^{-6} torr. These specimen exhibited satisfactory performance, as summarized in Table 6.1-1.

6.1.4 CVD Rhenium to SS304 Weld Joint

Four weld joint specimen were fabricated which involved the formation of eight rhenium-to-SS304 welds. All four specimen passed the proof test at 1000 psig and the leak test at 500 psig (helium) with soapy water. One of the specimen was inadvertently over pressurized during proof testing and burst at 5800 psig.

One of the specimen successfully completed 516 thermal cycles from 650 F to 150 F without developing leaks. However, this specimen did develop several small leaks

6.1, Weld Joint Development Tests (cont.)

when the test apparatus stuck in the heat cycle, exposing the specimen to 1100 F. This equipment failure occurred between 600 and 700 cycles.

A second specimen was put through a total of 2000 cycles at 650 F to 150 F. This specimen passed the 1000 psig proof test, but did show three leaks ranging from very small to moderate. Careful examination of the thermal cycle raw data indicates that the leaks first appear after 1300-1500 cycles into the run and gradually grow worse as the thermal cycle continued. This failure mode is a physical process due to the differences in thermal expansion between the two metals. Thus, CVD Re appears to form good weld joints with SS304 capable of withstanding at least 500 thermal cycles at 650 F to 150 F without developing leaks. The test results are summarized in Table 6.1-1.

6.2 PROOF, LEAK, AND WATER FLOW TESTS

Proof, leak and water flow tests of injector and cooled adapter components was conducted to verify their design, fabrication adequacy, and to obtain data for setting subsequent hot fire conditions.

Injector Manifold

Documentation of the existing SN 2 design began with flow testing of a second injector (SN 3) from the JPL program (Ref. 3) which used the same manifold design. To prepare the injector for upgrading to the design for this program, its platelet face was machined away. This permitted flowing the manifold by itself for measuring flow distribution and Kw. The flow distribution proved to be non-uniform, as shown in Figure 6.2-1, which plots fuel and oxidizer flows normalized to their average. The flows at the two downcomers closest to the oxidizer inlet are 1.9 and 1.65 times the average, while the next downcomers are 0.2 and 0.6 times the average. The fuel shows a less pronounced effect; the balance of the flows for both circuits are within 20% of the average.

The nonuniformity is the result of the flow field at the inlet. Two oxidizer ports straddling the inlet are exposed to stagnation conditions and therefore have higher than average flow. The next symmetrical set of ports are in high transverse velocity zones and, therefore, have lower than average flow because of the low static pressures. The oxidizer inlet is slightly offset relative to the first pair of oxidizer downcomers, as illustrated in Figure 6.2-2. The manifold-

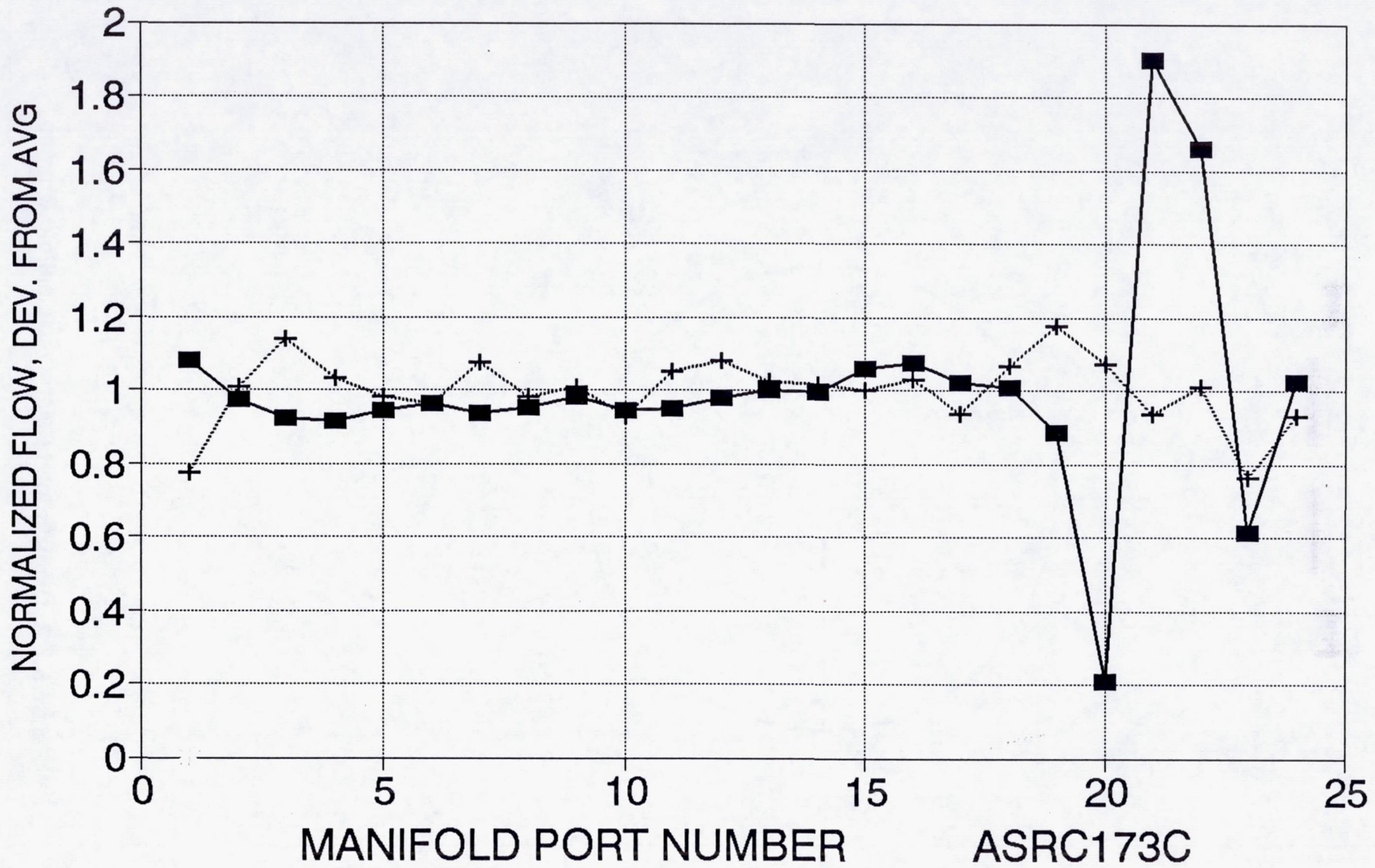


Figure 6.2-1. 100 lb Injector Manifold Water Flow Data

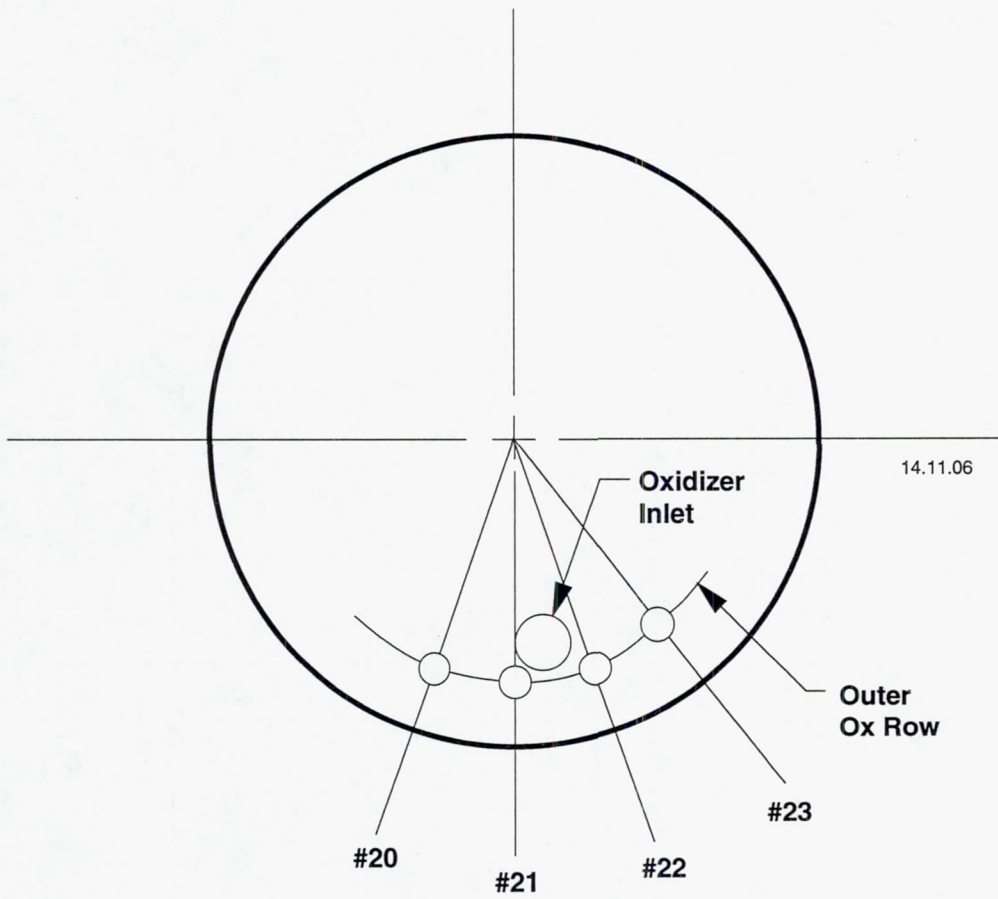


Figure 6.2-2. Oxidizer Inlet Relative to Manifold Orifices

6.2, Proof, Leak, and Water Flow Tests (cont.)

only flow and mixture ratio distribution are plotted in Figure 6.2-3. The inlet off-set is clearly evident, with the highest flow through orifice #21, followed by slightly lower (but still well above average) flow at orifice #22. The flow through orifice #20 is lower than average because the main flow in the manifold passage is not yet well-distributed. Flow through #23 is lower than average but not as low as at #20 because more distribution has taken place, lowering the cross flow velocity. From visual observation, it is apparent that there is also a reduction in flow in oxidizer downcomers located near an injector face diameter through the inlet orifice.

When the hydraulic resistance of the injector faceplate is taken into account, the mixture ratio profile is smoothed markedly, becoming very flat except for one low MR point at orifice #20, as shown in Figure 6.2-4. This plot over predicts nonuniformities in that it does not include further smoothing which will occur because of cross-flow due to interconnections downstream of the manifold. Note that the design of the injector bodies for the welded flight engines was modified to reduce the effects of velocity on distribution by opening up the manifold passage at the inlet; however, the injector body used in the SN 1 flight engine was of the original design.

SN 2 and SN 4 Injectors

Water flow pattern checks were made of the SN 2 and SN 4 injectors under the conditions listed in Table 6.2-1. The flow from the SN 4 injector was symmetrical, while that from SN 2 was slightly off axis. Photographs of the flow under similar operating conditions indicate that SN 2 has a finer droplet pattern than SN 4. Figure 6.2-5 shows water flow of both oxidizer and fuel circuits of injector SN 2 at the nominal operating point. The corresponding condition for injector SN 4 is shown in Figure 6.2-6.

SN 5 Injector

The SN 5 injector was water flow tested; Figures 6.2-7, 6.2-8, and 6.2-9 show the injector during flow testing at nominal flows of oxidizer only, fuel only, and both flows. The range of flow conditions is shown in Table 6.2-2; the resulting oxidizer and fuel circuit Kw is shown in Figure 6.2-10.

Measurements of the critical flow metering platelet oxidizer and fuel orifices for injectors SN 4 and SN 5 are shown in Figures 6.2-11 and 6.2-12 and are summarized in Table 6.2-3. The resulting variation in local mixture ratio for the outer injector elements is shown in

100# INJ MANIFOLD WATER FLOW DATA

1-23-91, (H2O) $W_{ox} = W_{fu} = 0.2/B/SEC$

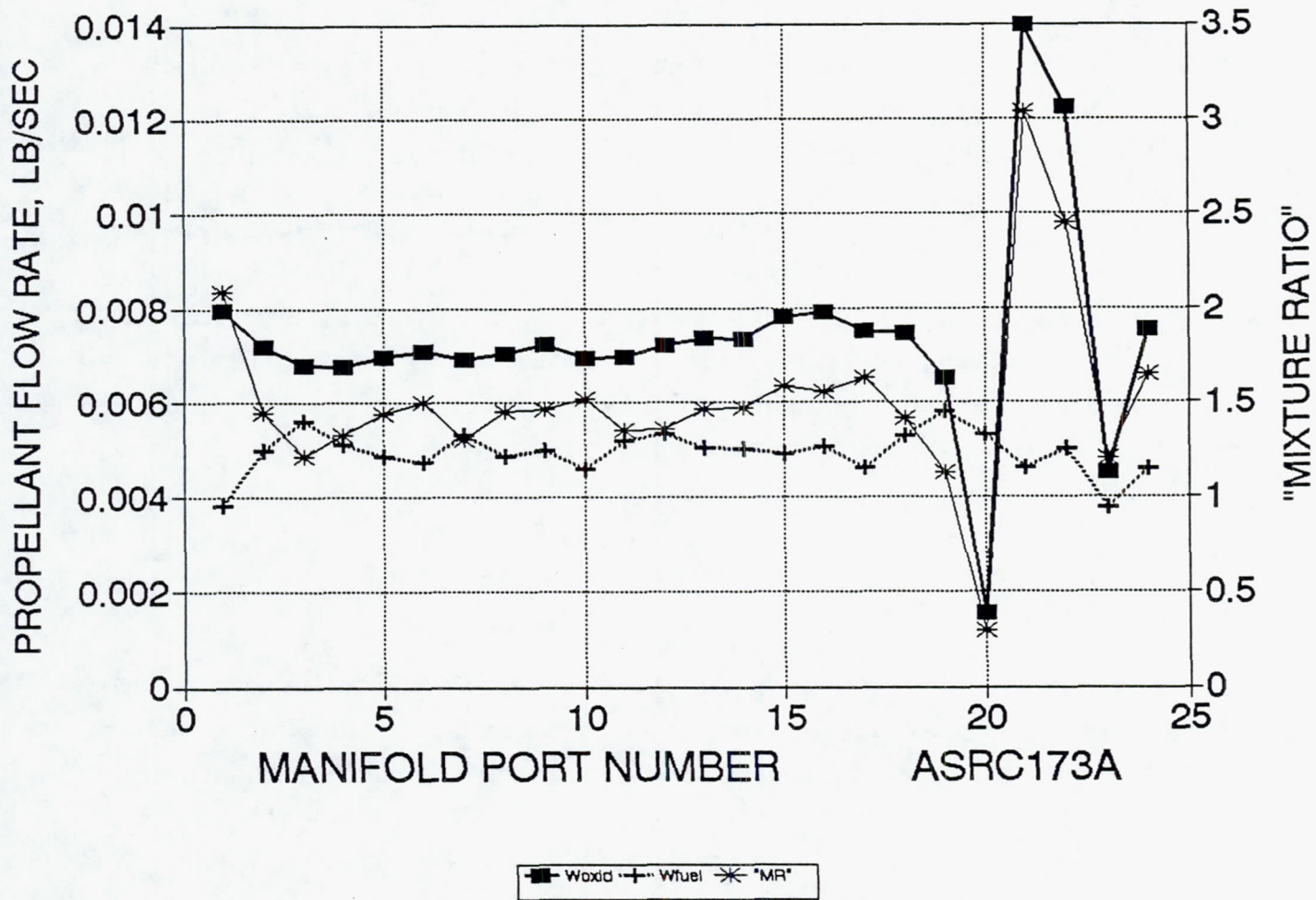


Figure 6.2-3. Manifold-Only Mixture Ratio

100# INJ MANIFOLD CALC FLOW & MR

(H2O) $W_{ox} = W_{fu} = 0.140 \text{ LB/SEC}$; $P_{oj}/P_{fj} = 85/78$

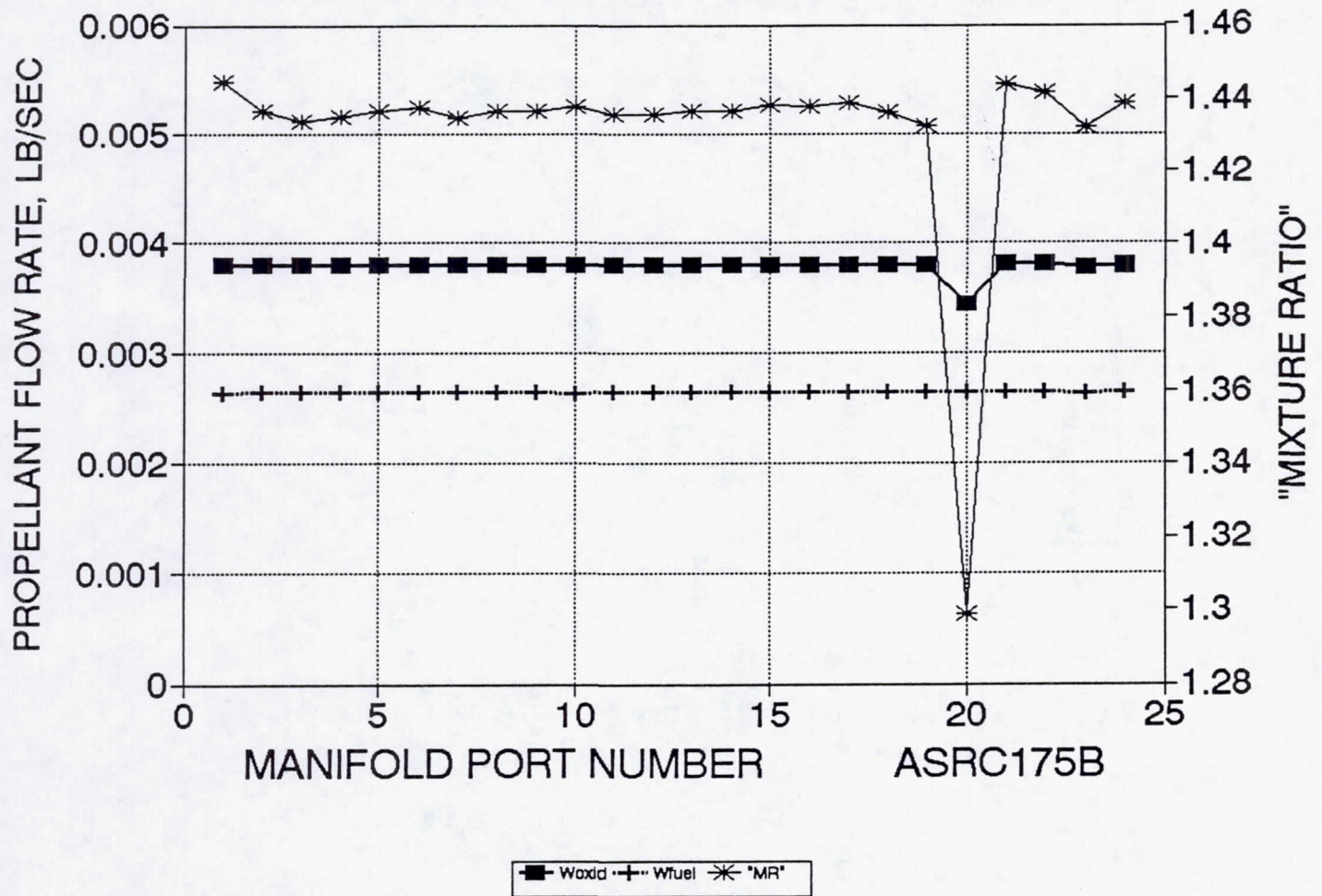


Figure 6.2-4. Manifold + Injector Mixture Ratio

Table 6.2-1. Injector Water Flow Conditions

ASRC237						DELTA P	DELTA P	TO MATCH PROPELLANT	
JPL	INJ.	WOX	WFU	K _{wox}	K _{wfu}	OXID (PROPELLANT)	FUEL (PROPELLANT)	WATER DELTA P	WATER DELTA P
POINT	S/N	lbm/sec	lbm/sec			psi	psi	OXID	FUEL
NOM.	002	0.2073	0.1256	0.018	0.0146	92.1	84.6	64.0	96.7
A		0.1833	0.1576	0.018	0.0146	72.0	133.2	50.0	152.2
B		0.2460	0.1491	0.018	0.0146	129.7	119.2	90.1	136.2
C		0.2512	0.1239	0.018	0.0146	135.2	82.3	93.9	94.1
D		0.1858	0.0914	0.018	0.0146	74.0	44.8	51.4	51.2
E		0.1510	0.1304	0.018	0.0146	48.9	91.2	33.9	104.2
NOM.	004	0.2073	0.1256	0.0188	0.0162	84.4	68.7	58.6	78.5
A		0.1833	0.1576	0.0188	0.0162	66.0	108.2	45.8	123.6
B		0.2460	0.1491	0.0188	0.0162	118.9	96.8	82.6	110.6
C		0.2512	0.1239	0.0188	0.0162	124.0	66.9	86.1	76.4
D		0.1858	0.0914	0.0188	0.0162	67.8	36.4	47.1	41.6
E		0.1510	0.1304	0.0188	0.0162	44.8	74.0	31.1	84.6

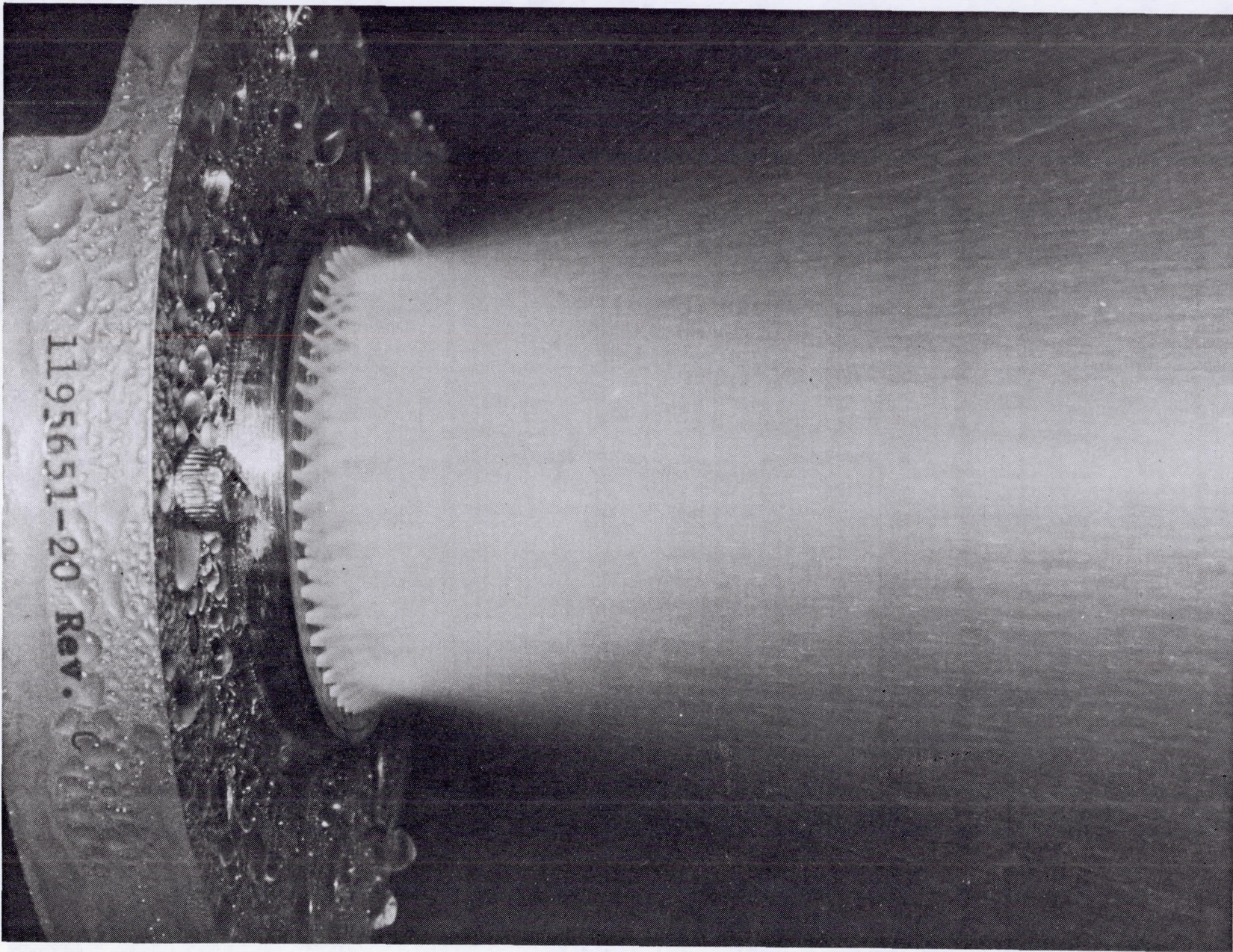


Figure 6.2-5. Water Flow of 100 lbf – Injector SN 2 – Oxidizer $\Delta P = 64$ psi, Fuel $\Delta P = 96$ psi

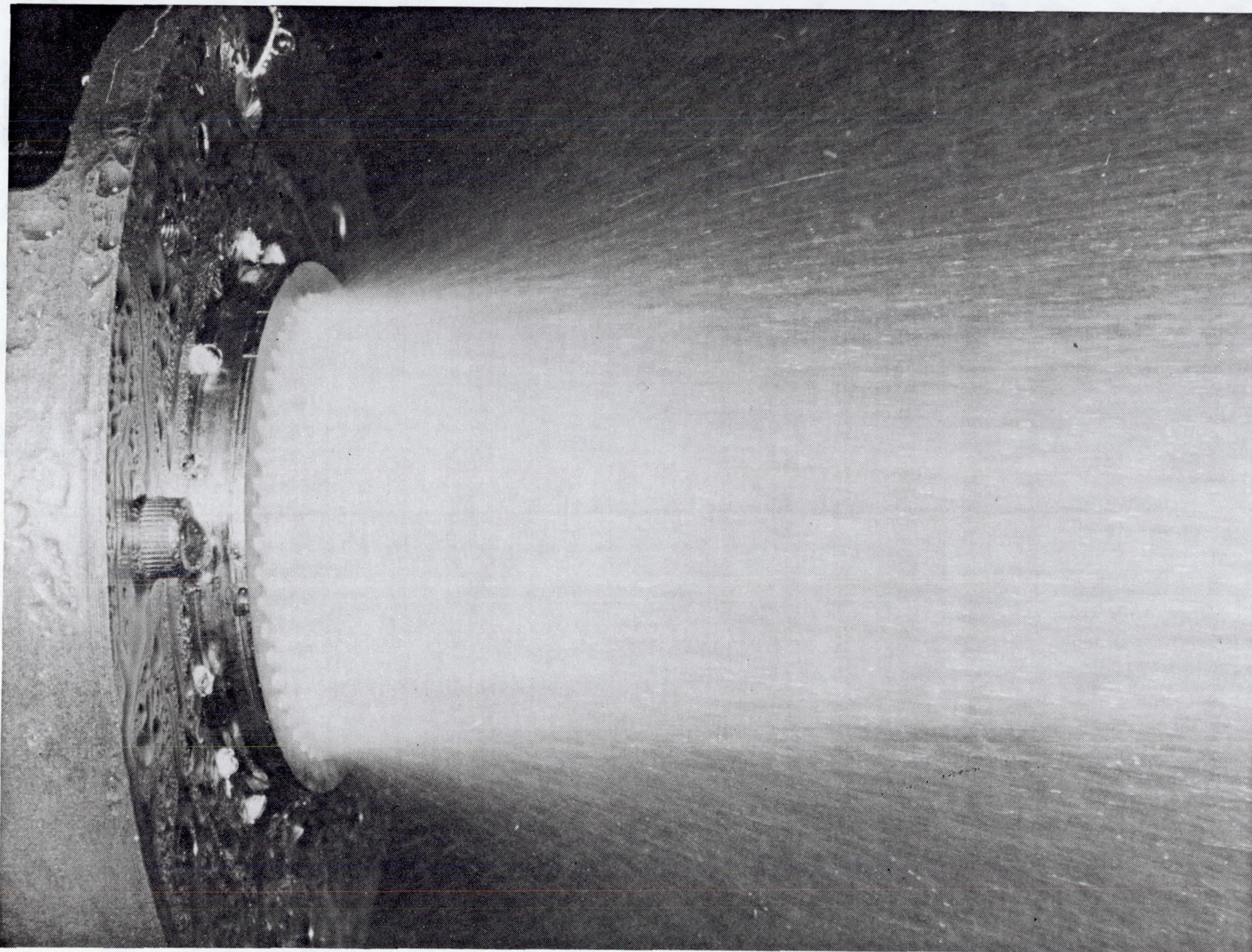


Figure 6.2-6. Water Flow of 100 lbf – Injector SN 4 – Oxidizer $\Delta P = 59$ psi, Fuel $\Delta P = 79$ psi

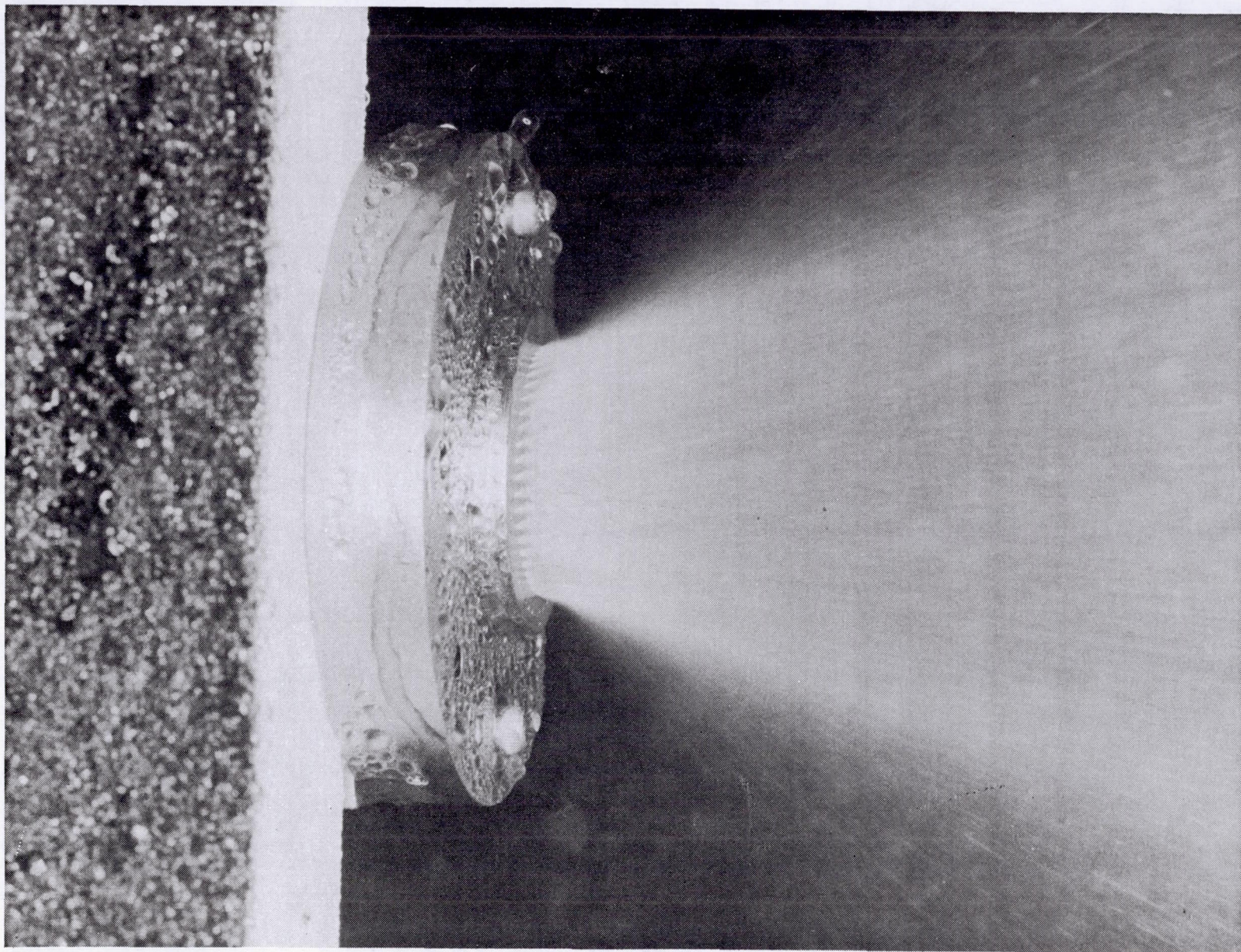


Figure 6.2-7. Injector SN 5 Water Flow – Oxidizer Circuit at 111 psi ΔP

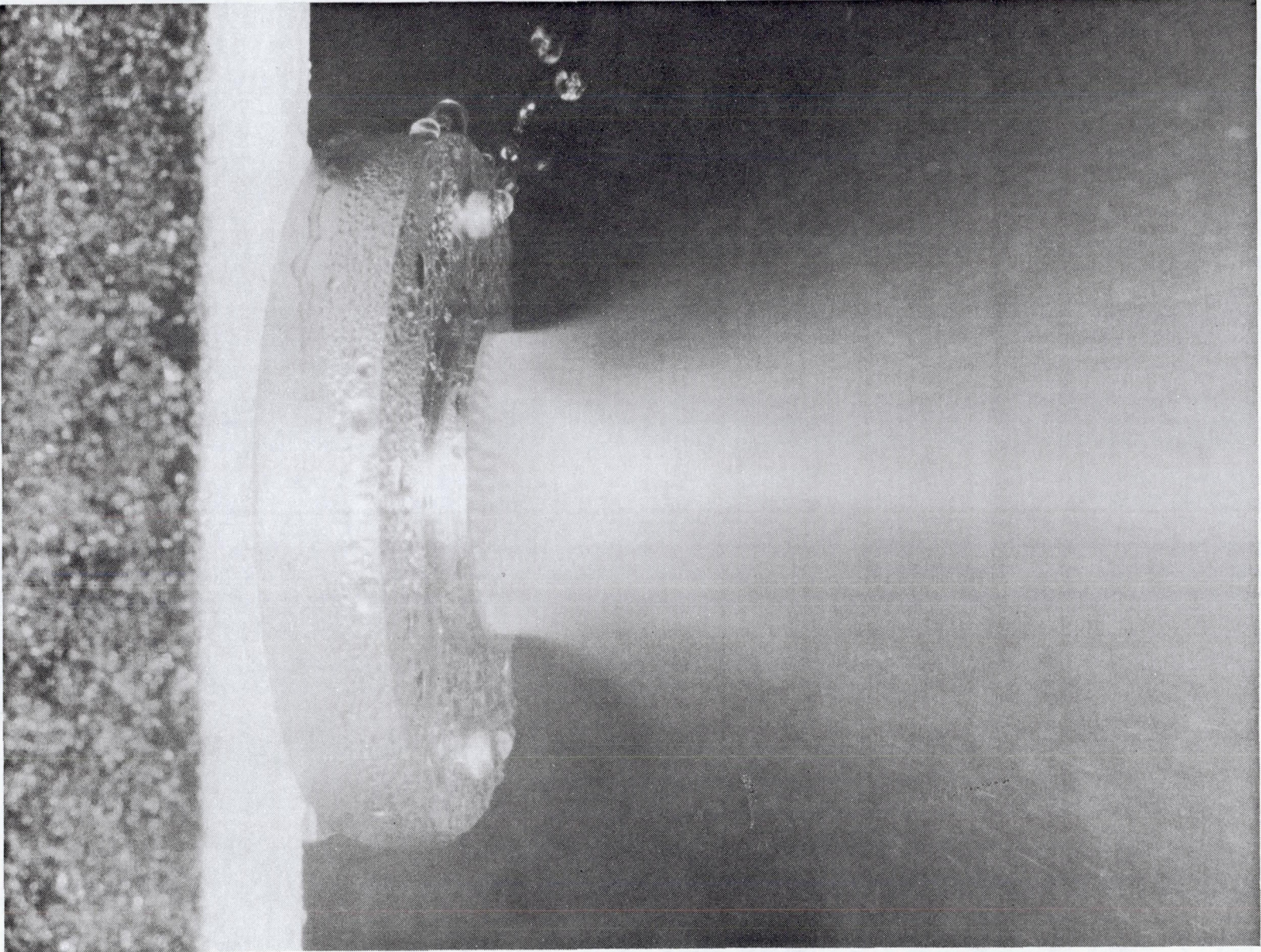


Figure 6.2-8. Injector SN 5 Water Flow – Fuel Circuit at 108 psi ΔP

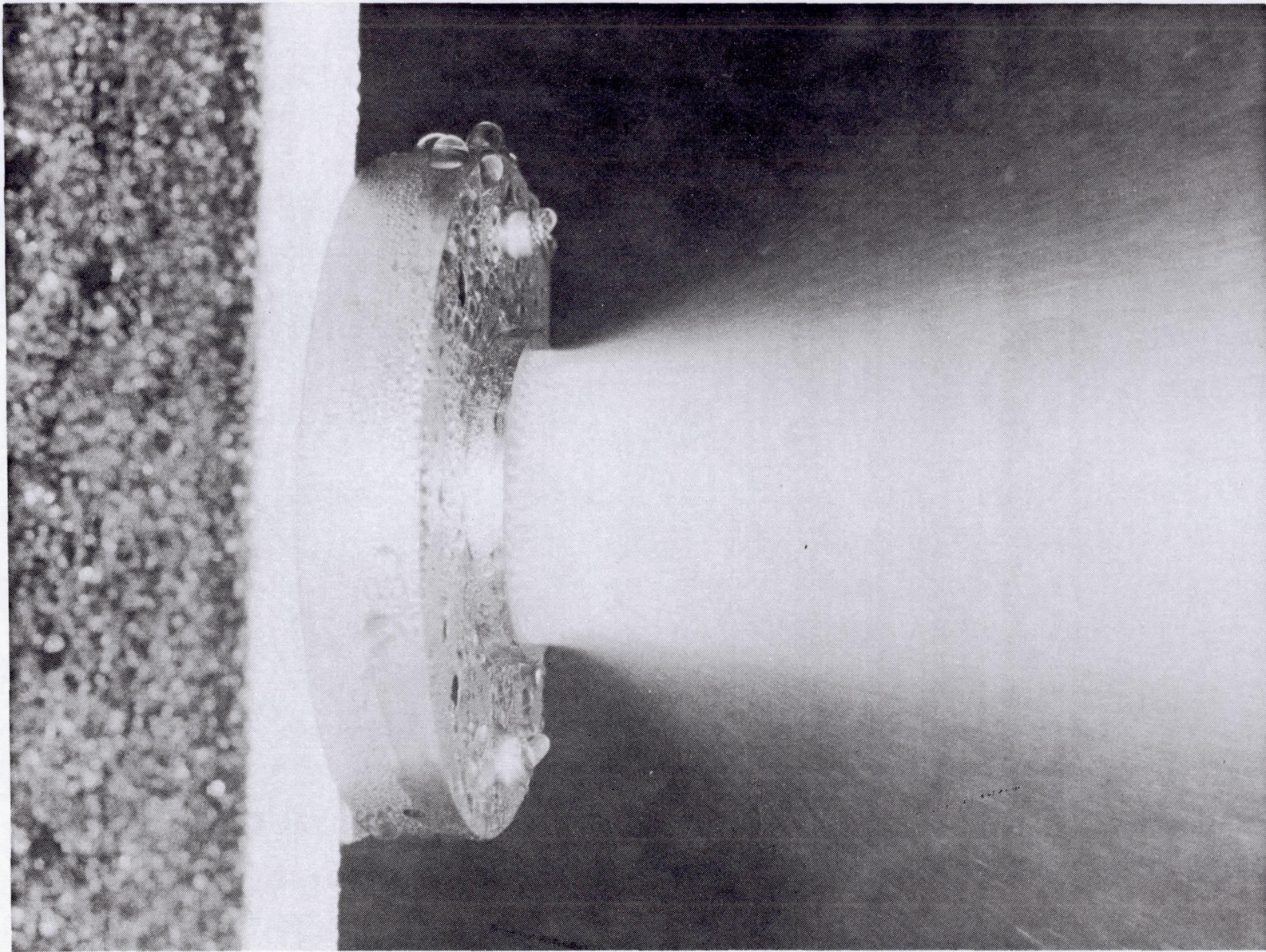


Figure 6.2-9. Injector SN 5 Water Flow – Oxidizer and Fuel Circuits at 111 and 108 psi ΔP Respectively

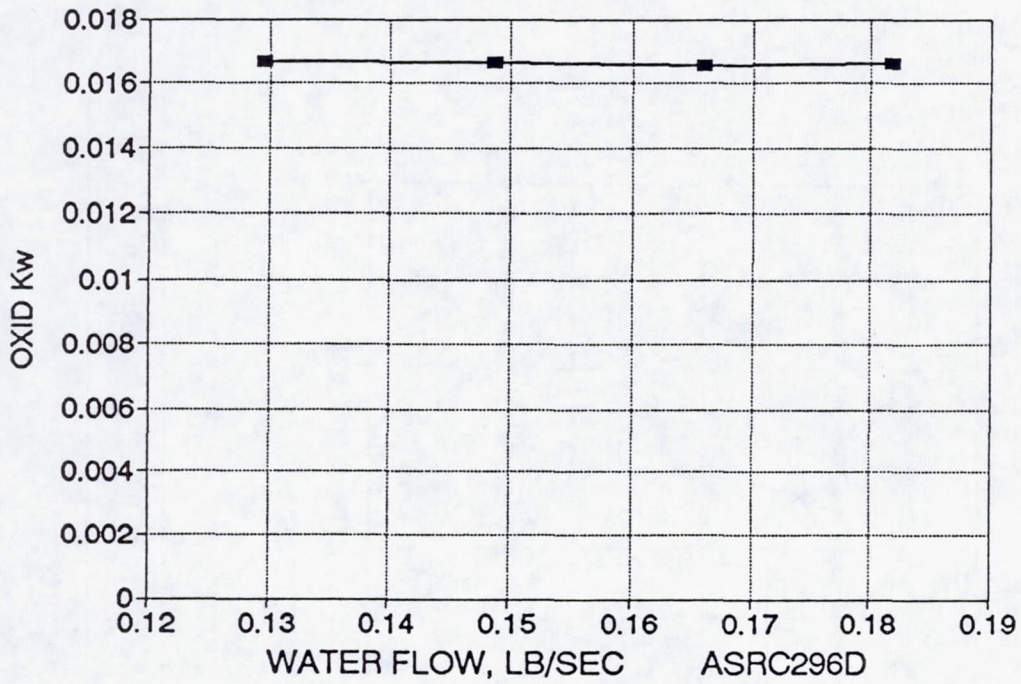
Table 6.2-2. Water Flow Conditions for SN 5 Injector

ASRC297 CONDITION	<u>WATER FLOW S/N 5 INJECTOR FOR PHOTOS</u>					FOR USE WITH LAB'S PSIA GAGES			
	WO	WF	SGO	SGF	DPOX PSIG	DPFU PSIG	DPOX PSIA	DPFU PSIA	
LOW PC, MR=1.65	0.1849	0.1099	1.44	0.83	86.0	80.4	100.7	95.1	
NOM PC,	0.2105	0.1274	1.44	0.83	111.4	108.1	126.1	122.8	
HIGH PC	0.2315	0.1415	1.44	0.83	134.7	133.3	149.4	148.0	

FLOW INDIVIDUAL CIRCUITS AT THE PRESSURES INDICATED (2 CKTS x 3 PRESSURES= 6 PHOT

FLOW OX AND FUEL CKTS COMBINED AT INDICATED PRESSURES=3PHOTOS

100# S/N 5 INJ. Kw VS WATER FLOW
 OXID CKT; 7-29-91



100# S/N 5 INJ. Kw VS WATER FLOW
 FUEL CKT; 7-29-91

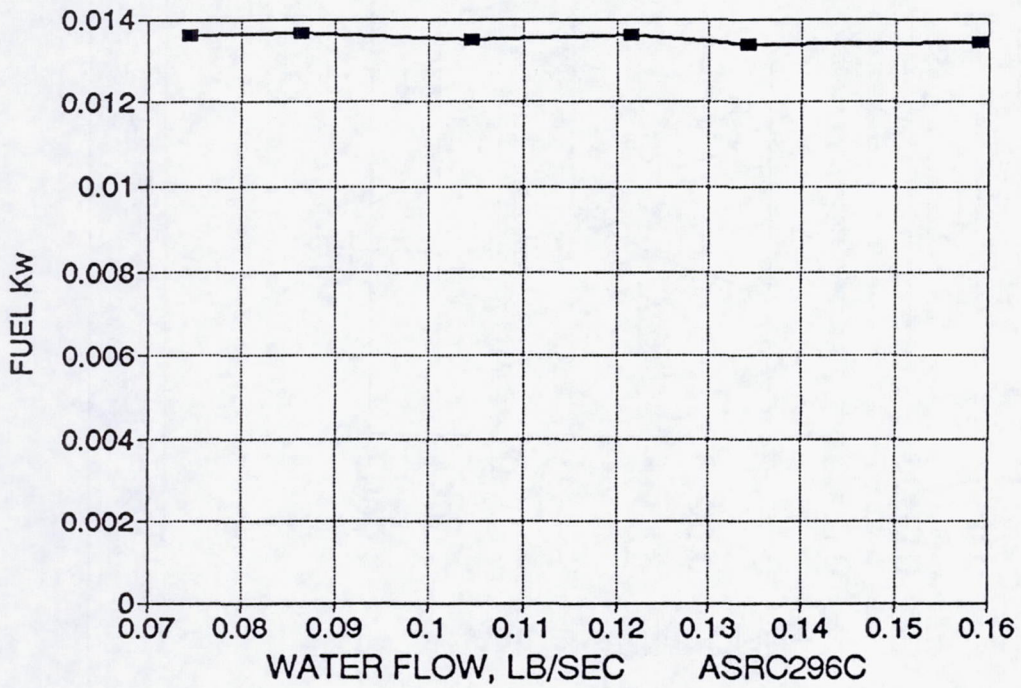


Figure 6.2-10. 100 lb SN 5 in. Kw vs Water Flow

Injector TSN-03.1-1 Rows 6 and 7

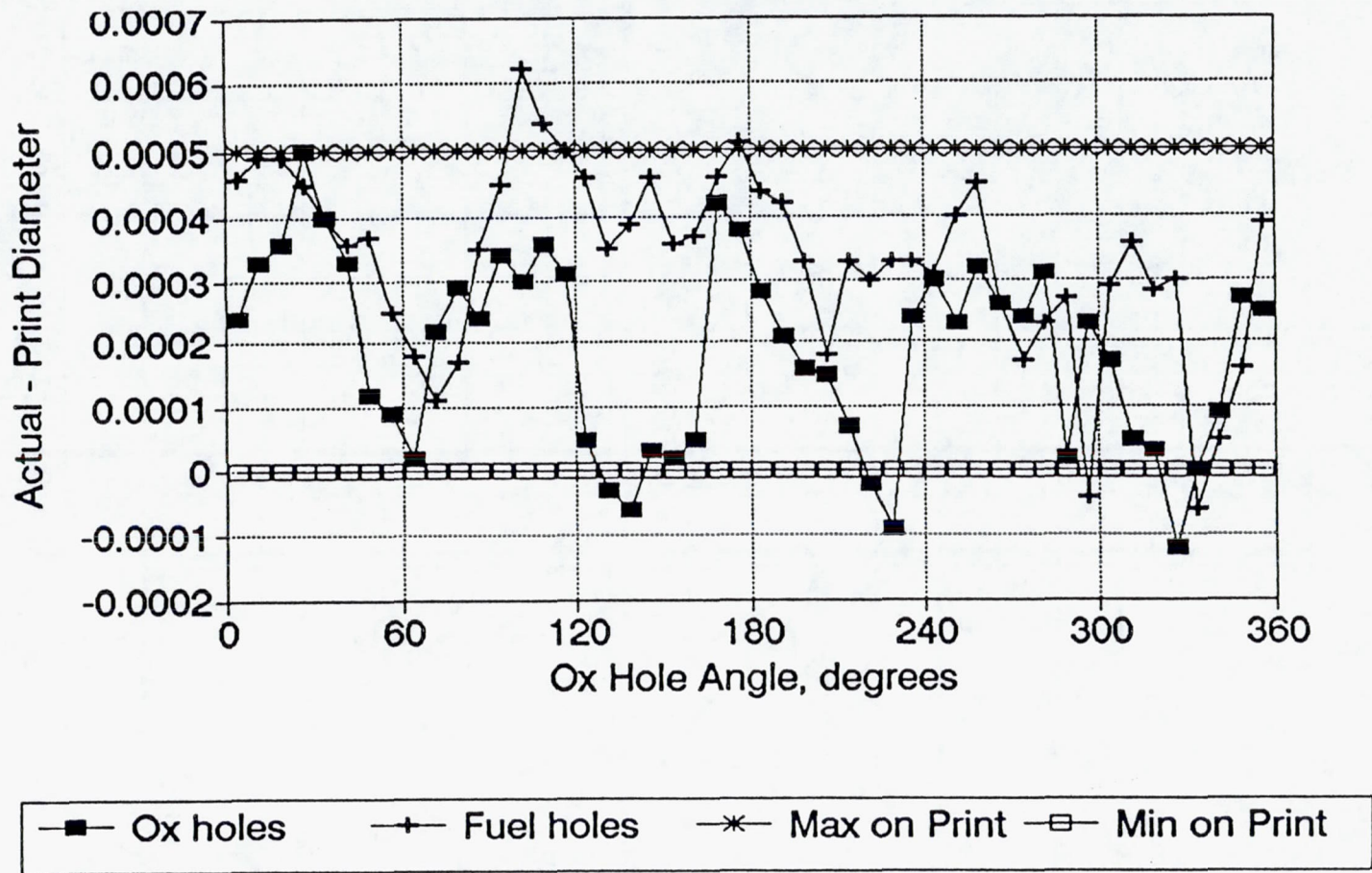
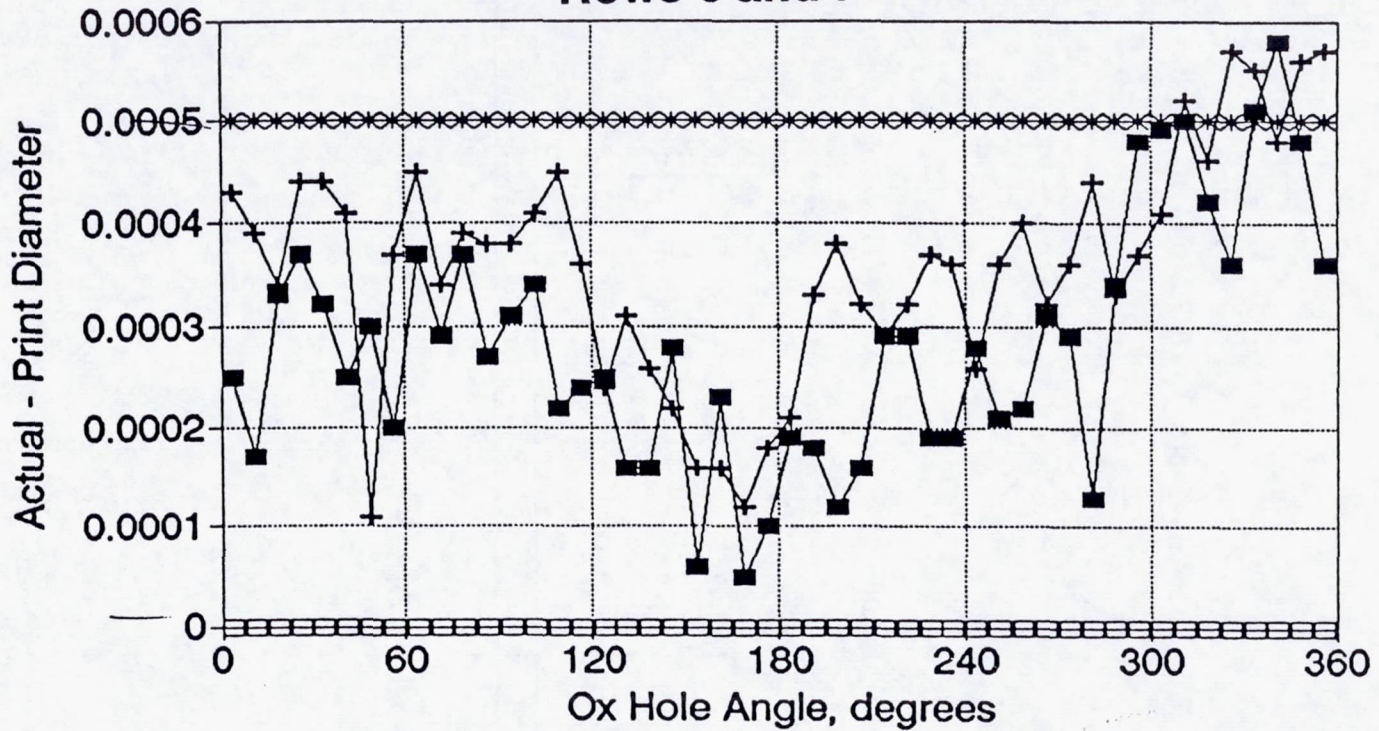


Figure 6.2-11. Mod B SN 4 Injector Orifice Dimensions

+ .0005
.0078
- .0000

Injector TSN-7-2 Rows 6 and 7



■ Ox holes + Fuel holes * Max on Print □ Min on Print

Figure 6.2-12. Mod C SN 5 Injector Orifice Dimensions

Table 6.2-3. Injector SN 5 Platelet 3C Status

ASRC279

TSN-	UNIT	RANGE OF MIXTURE RATIO			DIA RANGE, 6,7 REL TO DES., MILS	RANK
		1,2,3	ROWS 4,5	6,7		
1	1	1.81--2.02	1.73--2.03	1.38--1.58	-1.5	7
2		1.81--2.56	1.69--2.05	1.41--1.55	-0.4	5
3		1.81--1.93	1.73--2.06	1.34--1.64	+1	6
4		1.85--2.07	1.74--2.02	1.36--1.65	-0.5	4
6	1	1.79--2.07	1.76--2.04	1.42--1.6	-0.3	3
7[1]	2	1.8--1.96	1.73--2.13	1.4--1.58	+1	1
8		1.82..1.99	1.77--1.98	1.38--1.56	+1.5	2

[1] USED IN ASSEMBLY OF S/N 5

6.2, Proof, Leak, and Water Flow Tests (cont.)

Figures 6.2-13 and 6.2-14 for SN 4 and SN 5, respectively. The maximum spreads, $\pm 9\%$ for SN 4 and $\pm 6\%$ for SN 5 are both acceptable. Uniformity of distribution promotes maximum specific impulse and long life.

Using a special collection fixture, outer and core flows were collected separately for the three injectors. Outer and core MR for SN-2, -4 and -5 are plotted in Figure 6.2-15; mass flow ratio, defined as outer flow/inner flow, is plotted in Figure 6.2-16.

SN 6-1 and SN 6-2 Injectors

Both injectors were flow tested with water to check their pattern and to determine Kw. The flow pattern for both circuits operating are shown in Figures 6.2-17 and 6.2-18. The apparent difference in fine mist visible with SN 6-2 is caused by the wind which was blowing when this unit was tested. Although not evident in these photos, slight leakage occurred at the film cooling plugs on SN 6-1. In addition, one small fuel leak occurred on SN 6-2, about 9 micrograms per second, or 0.013% of fuel flow. The SN 6-1 film cooling port plugs were subsequently welded closed and do not leak. Because the SN 6-2 leak is too small to effect operation repair was not required or attempted. Both injectors passed intermanifold leak checks with nitrogen.

Flow conditions for the two injectors are shown in Figure 6.2-19 for the oxidizer circuits and Figure 6.2-20 for the fuel circuits. The hydraulics of the two injectors are similar; the oxidizer Kw are within $\pm 0.24\%$, the fuel Kw are within $\pm 0.7\%$.

Flow distribution between the outer row and core was measured and is plotted in Figures 6.2-21 and 6.2-22. The injectors have essentially the same distribution. The outer and core mixture ratio for SN 6-1 and SN 6-2 are shown in Figure 6.2-23, along with the values for injectors SN 2, 4, and 5.

Subtask 1.4.1.4 – Cooled Chambers and Other Items

Fuel-Cooled Front End

The fuel-cooled chamber head ends, instrumented as shown in Figure 6.2-24, have been proof and leak tested using the setup shown in Figure 6.2-25. Rather than proof the regen

Injector TSN-03.1-1

Rows 6 and 7

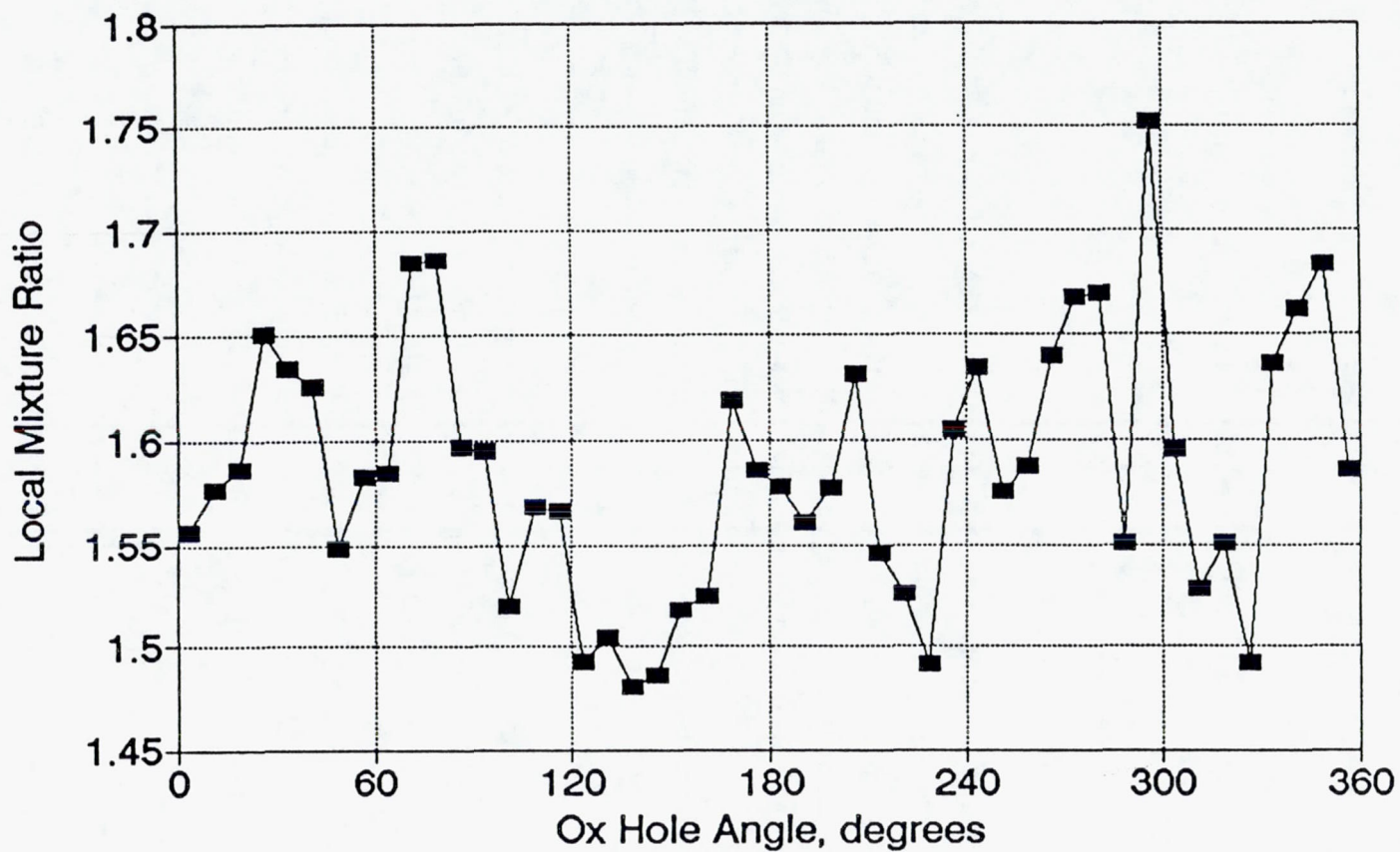


Figure 6.2-13. Mod B SN 4 Injector Local MR

Injector TSN-7-2

Rows 6 and 7

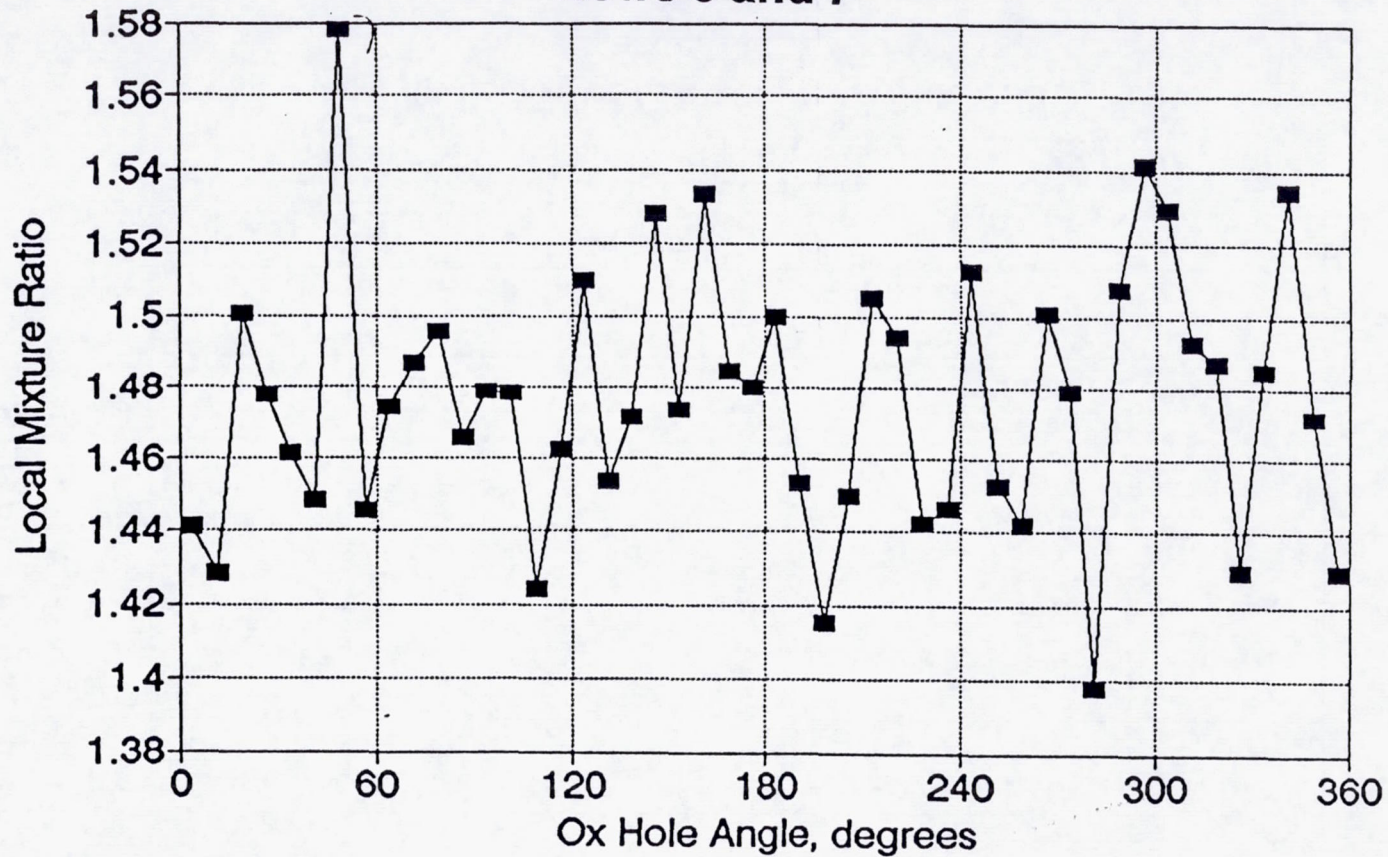


Figure 6.2-14. Mod C SN 5 Injector Local Mixture Ratio

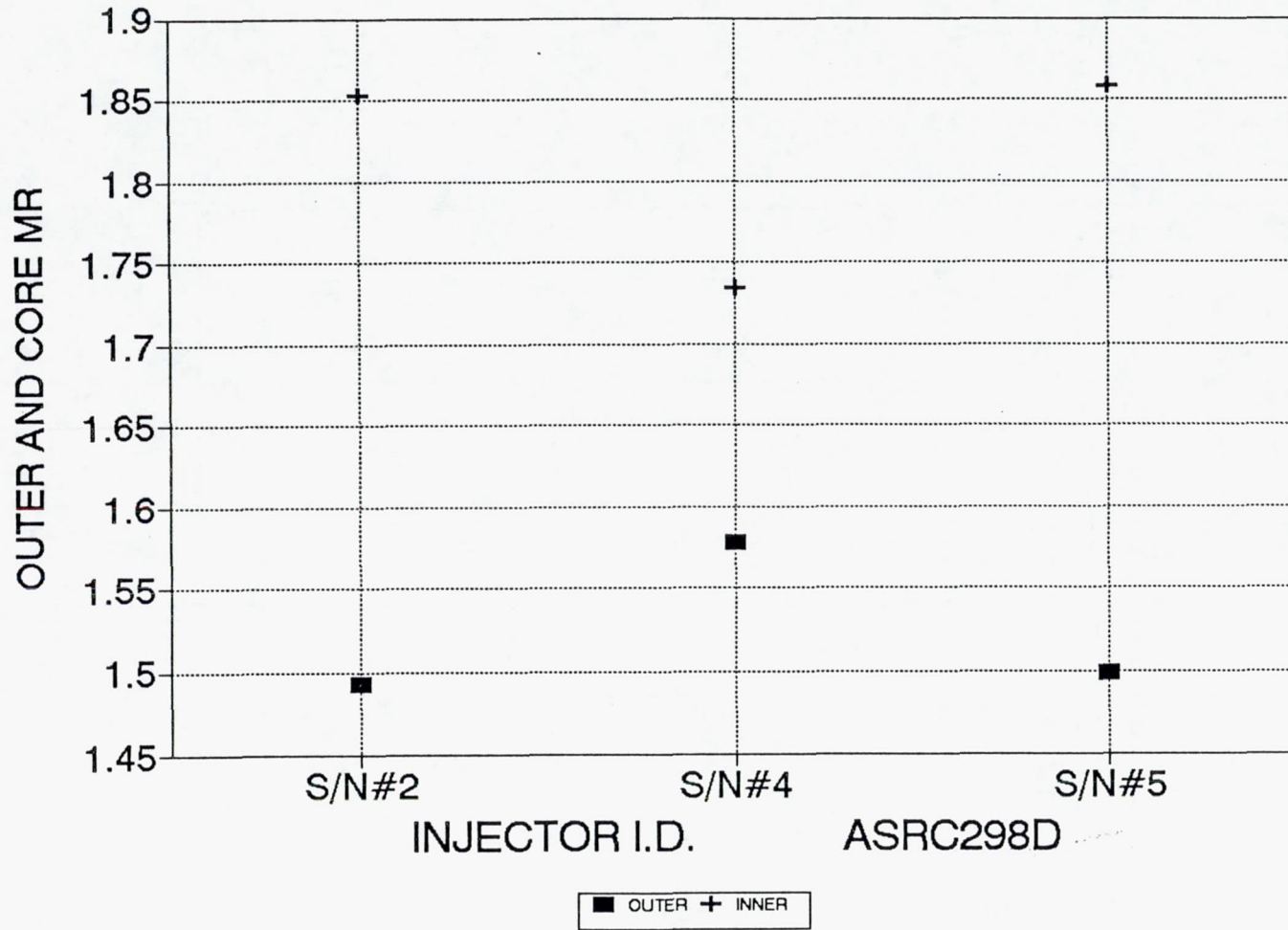


Figure 6.2-15. 100# Injector SN 2, 4, and 5 Inner and Outer MR

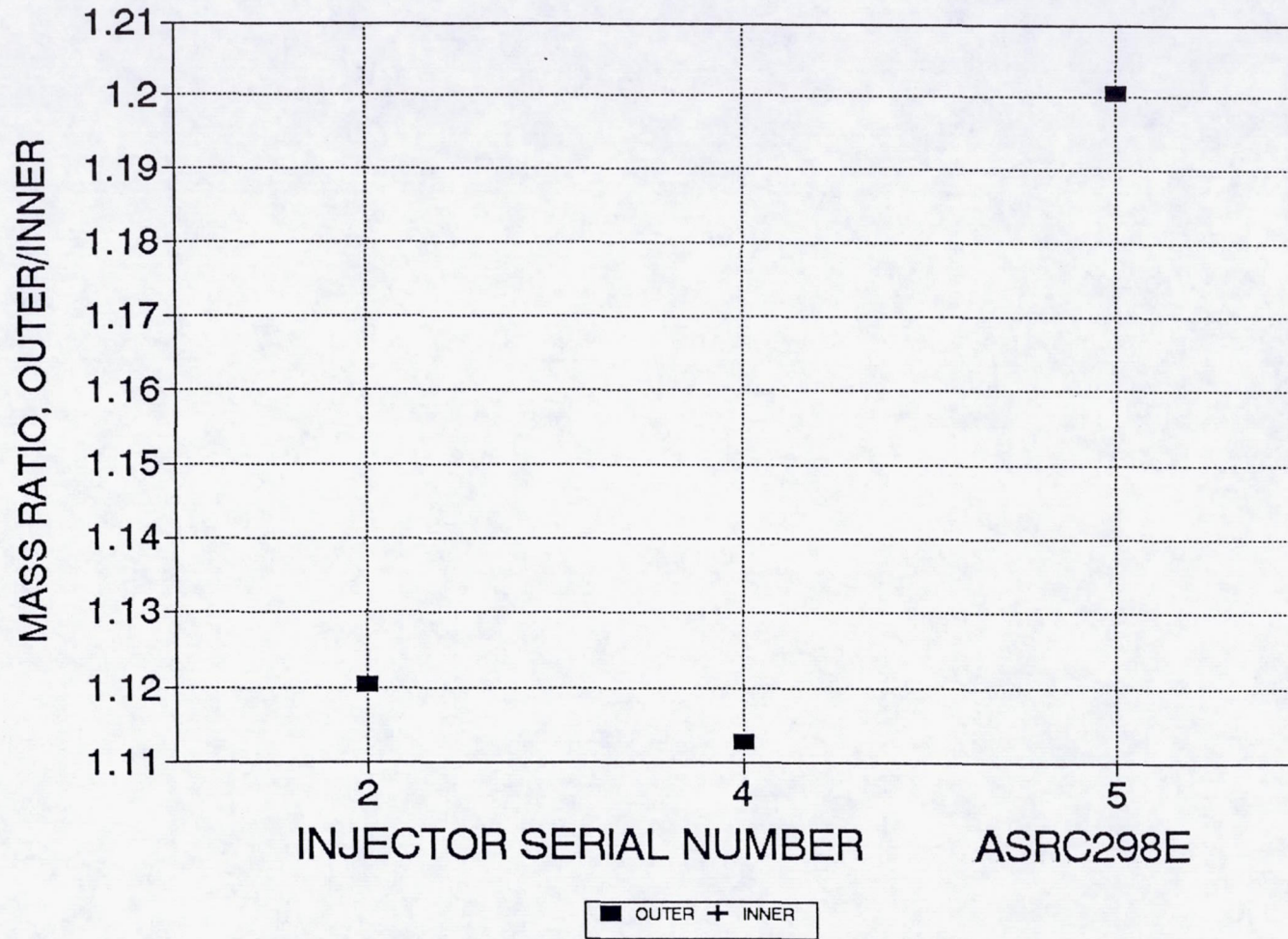


Figure 6.2-16. 100# Injector Mass Ratio = Outer/Inner

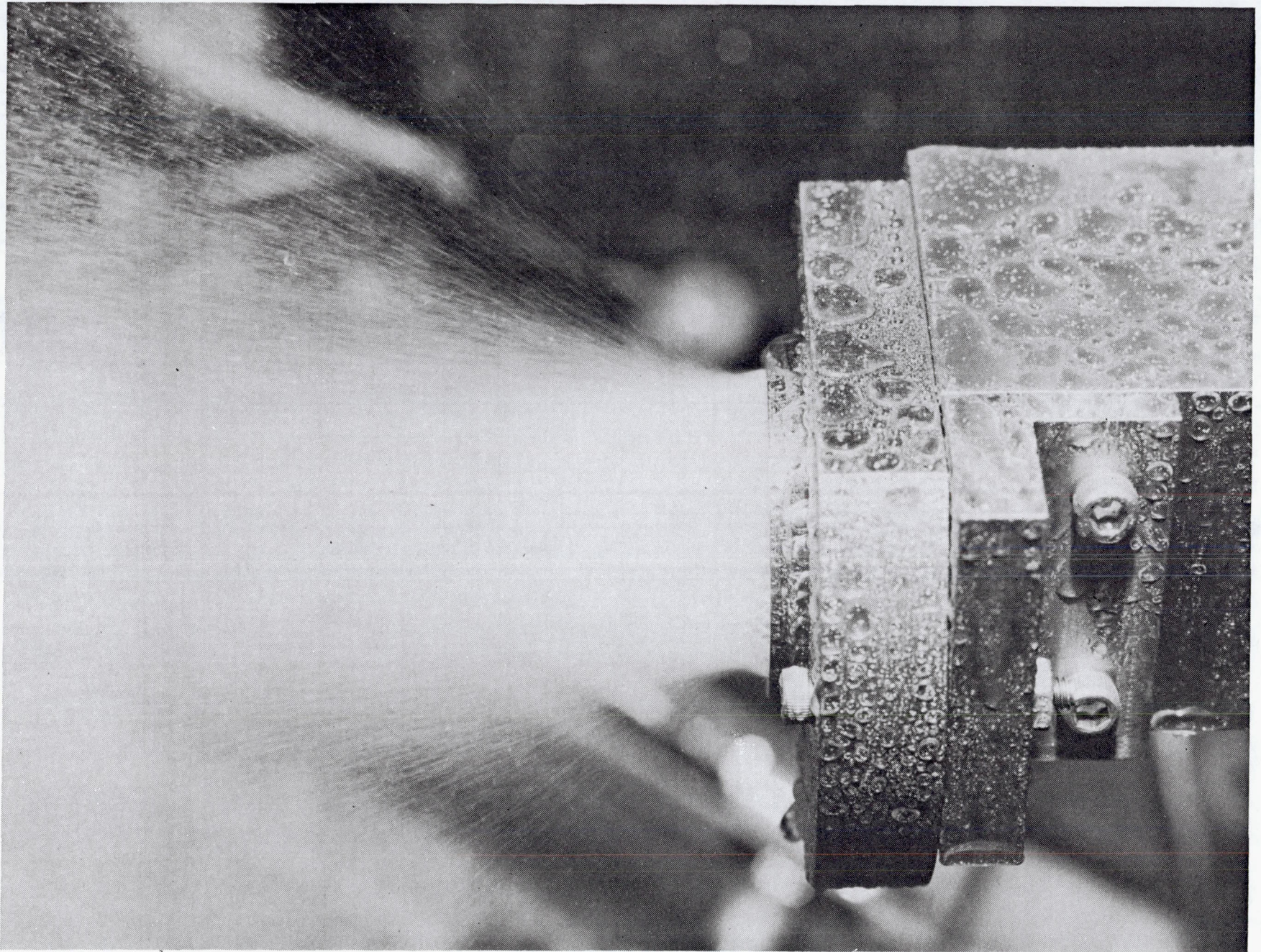


Figure 6.2-17. Water Flow Pattern Test – SN 6-1



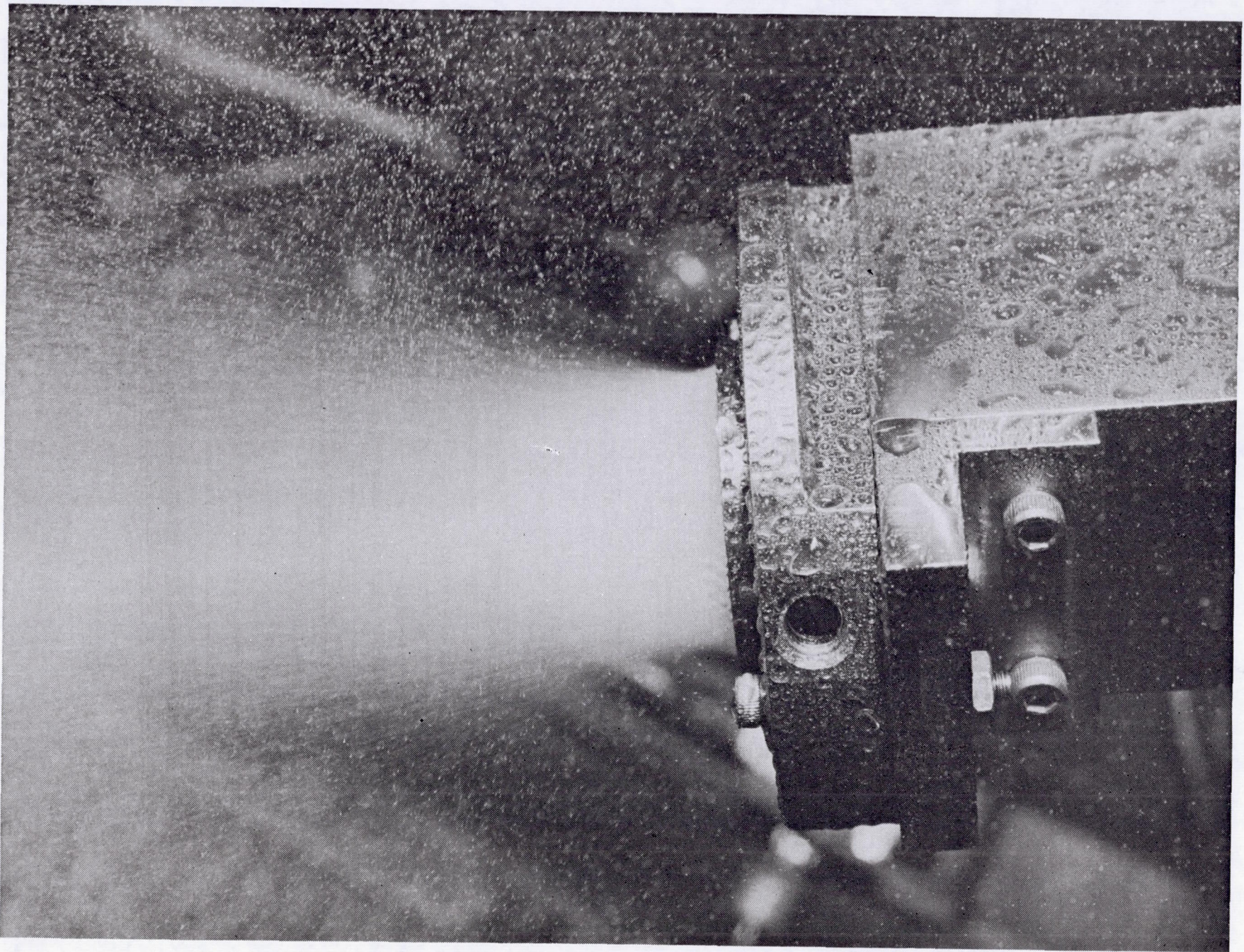


Figure 6.2-18. Water Flow Pattern Test – SN 6-2

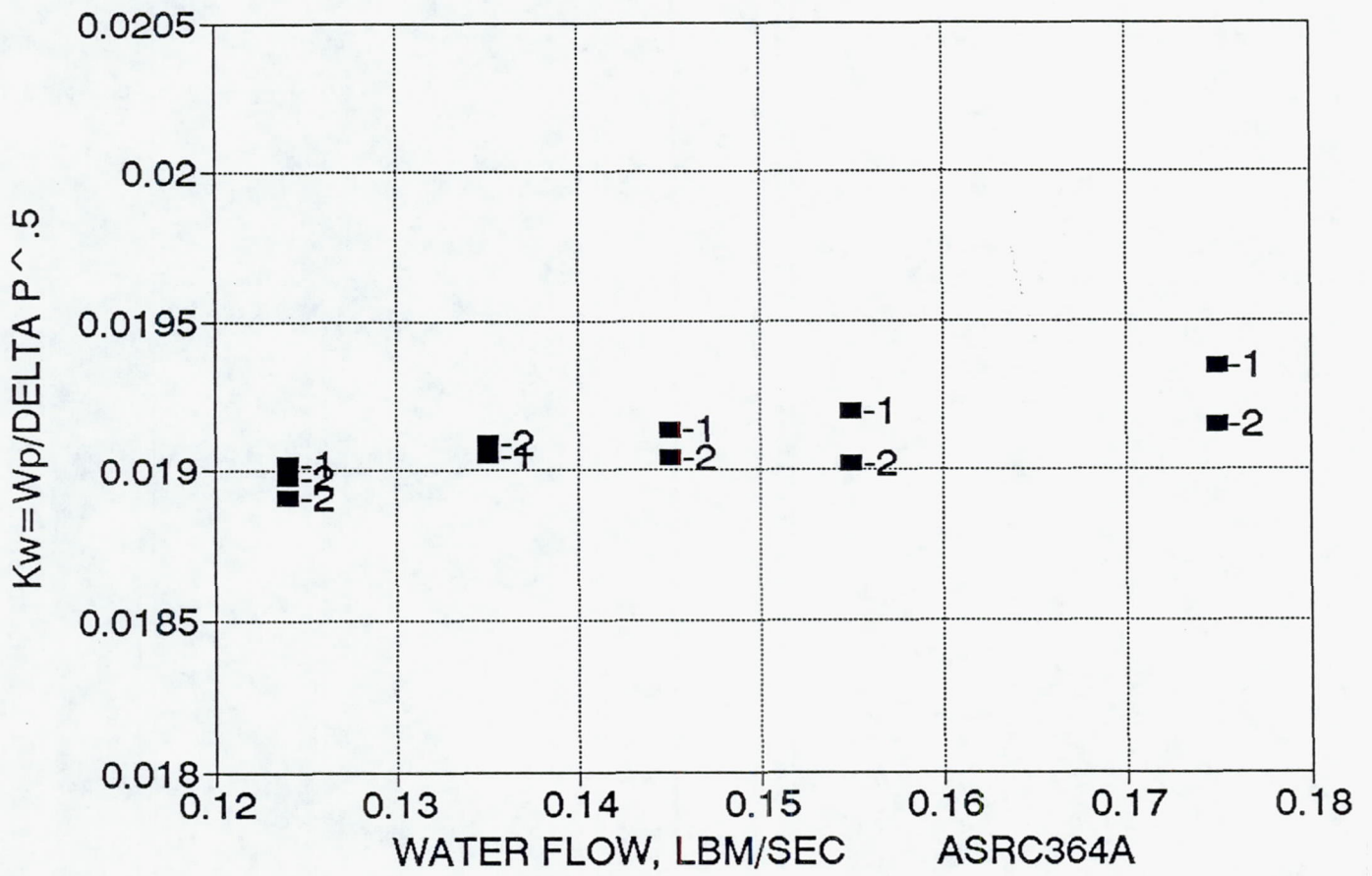


Figure 6.2-19. K_w vs Water Flow Rate SN 6-1 and 6-2 Oxidizer Circuit Water Flow 11-14-91

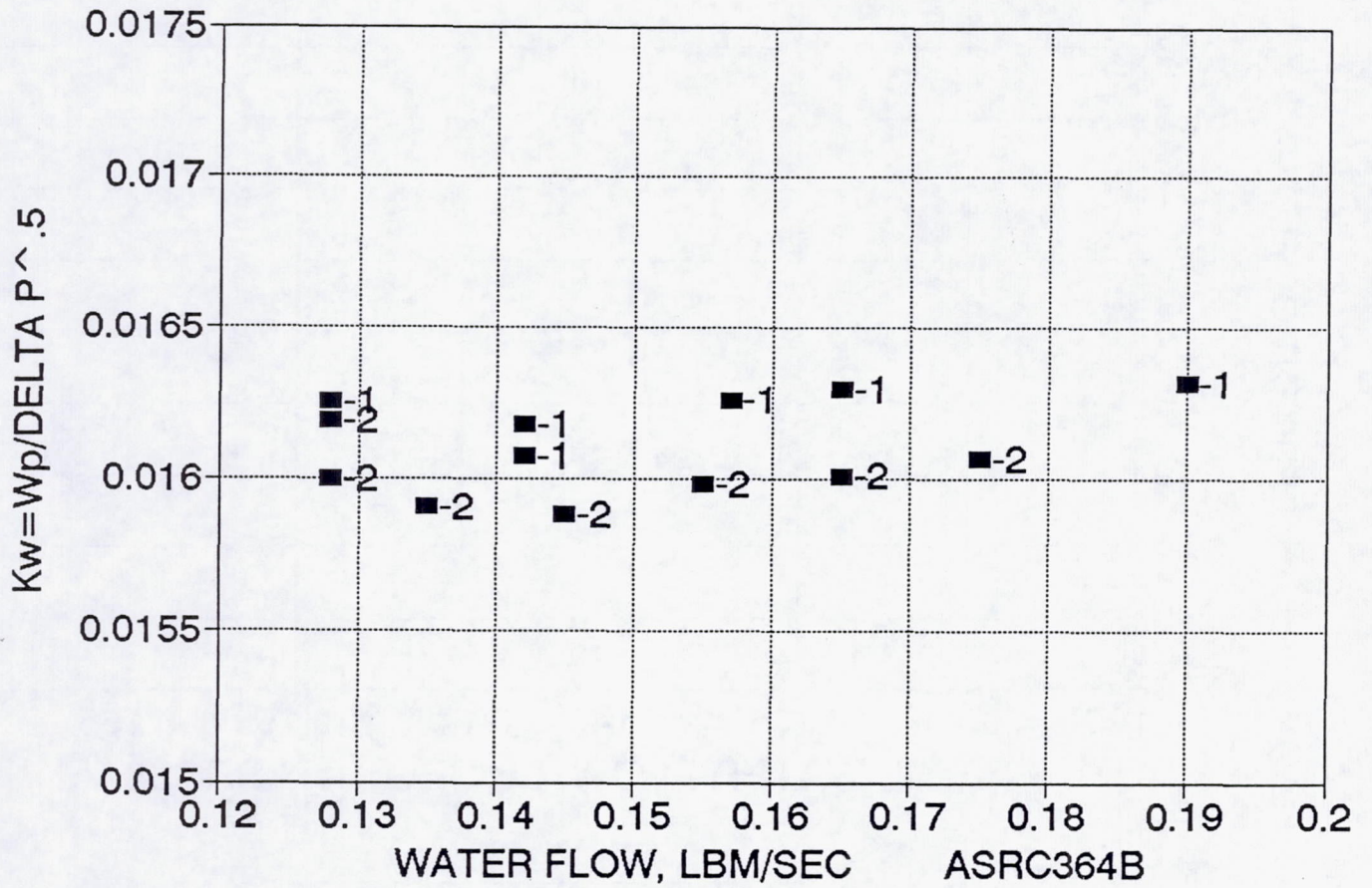


Figure 6.2-20. Kw vs. Water Flow Rate SN 6-1 and 6-2 Fuel Circuit Water Flow
11-14-92

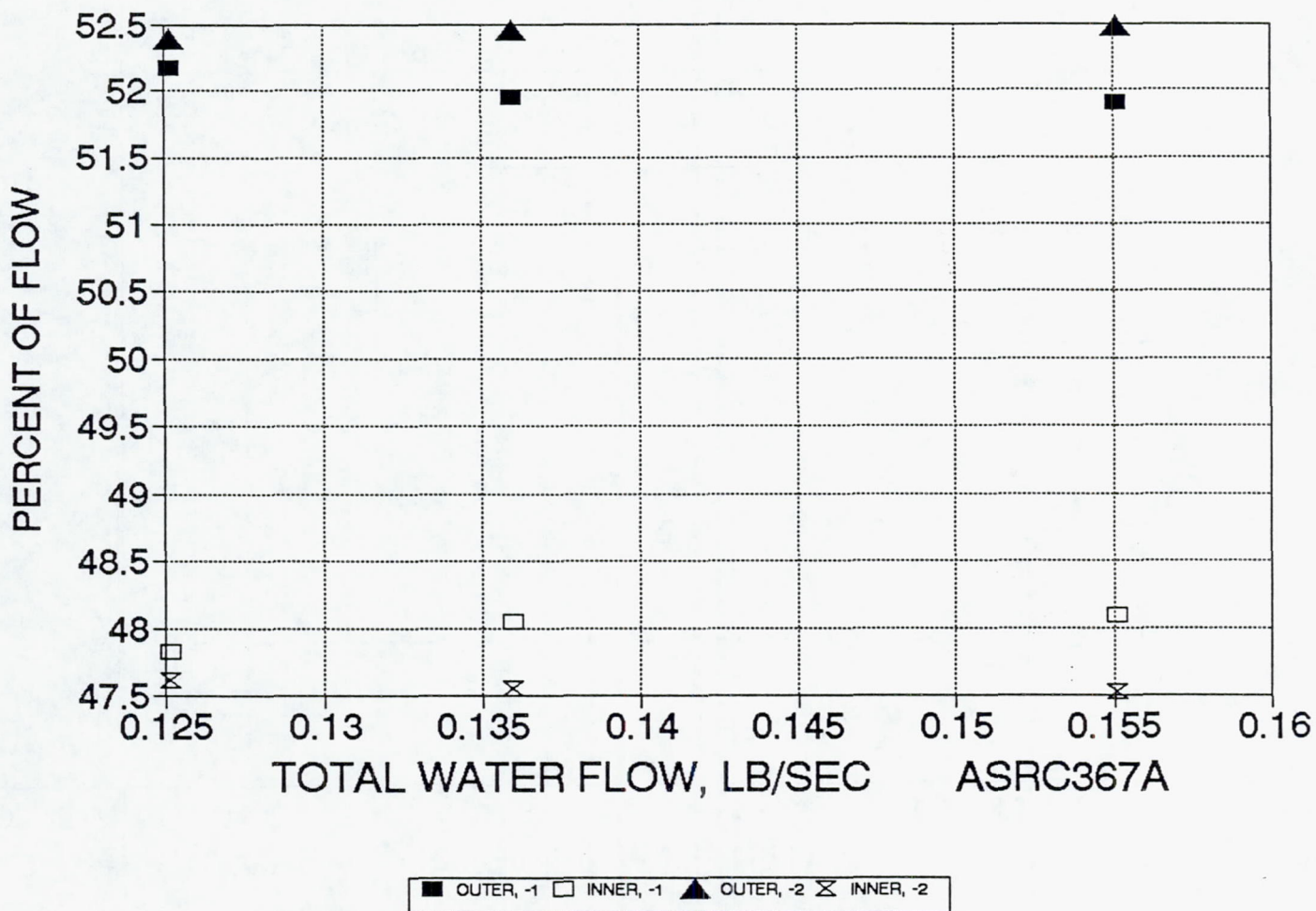


Figure 6.2-21. SN 6-1 and -2: % Inner and Outer Oxid Flow – Outer = Rows 6 and 7; Water

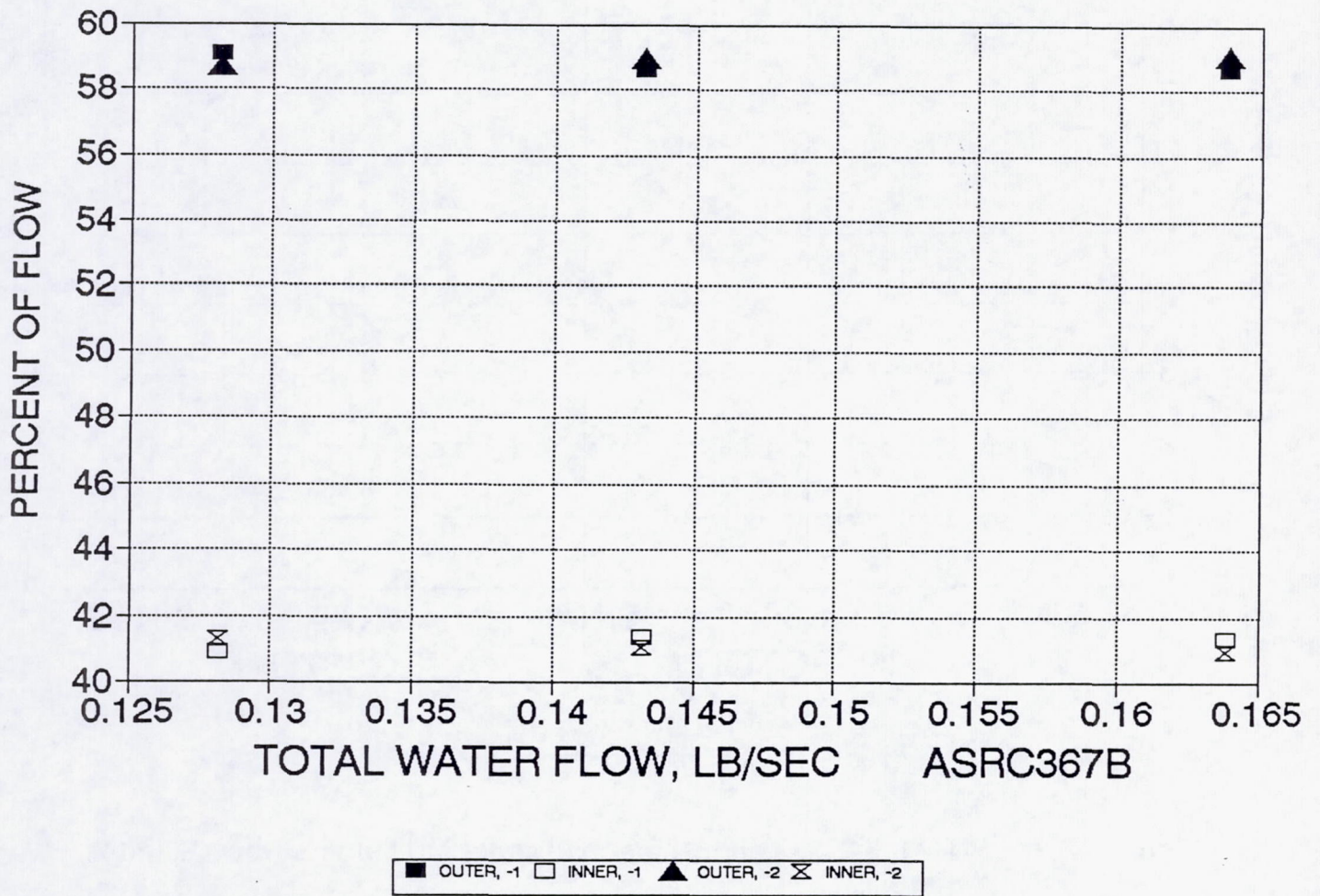


Figure 6.2-22. SN 6-1 and -2: % Inner and Outer Fuel Flow – Outer = Rows 6 and 7; Water

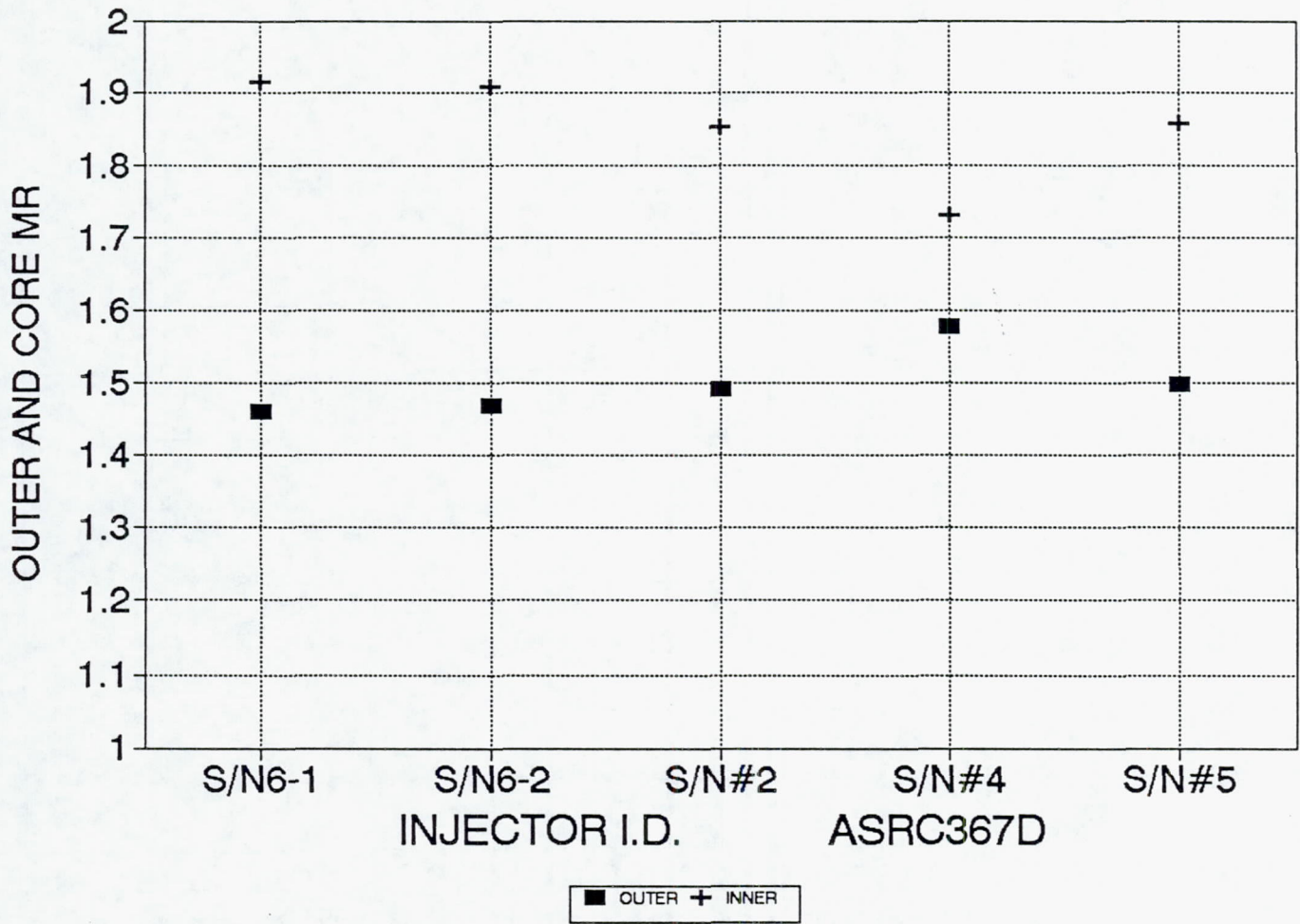
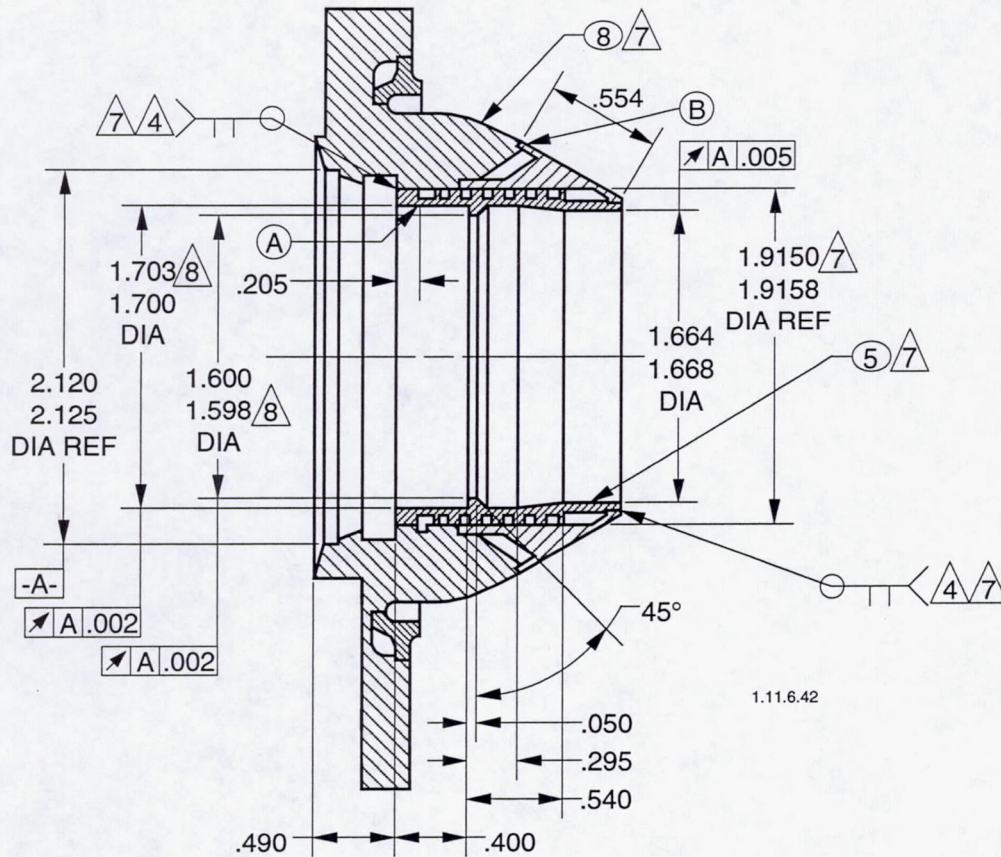


Figure 6.2-23. SN 6-1, 6-2, 2, 4 and 5 Inner and Outer MR Outer = Rows 6 and 7; Water Flow

1206354 Adapter, Chamber



Conduct Proof and Leak Tests of Two (2) Adapters

1. Install 2 biaxial strain gages equally spaced at (A) and at (B). Pressurize to 500 PSIG in 5 steps; record strain. (Anticipated strain is low, of the order of 0.05%).
2. Pressurize with GN₂ to 370 PSIG, perform bubble leak check.
3. Flow for K_w (.06 - .20 lb/sec fuel)
 ~.05 - .175 lb/sec H₂O

Figure 6.2-24. Proof, Leak and Flow Test Cooled Adapter Covered by U.S. Patents 4882904 and 4936091 and German Patent P39 23 948.9-13

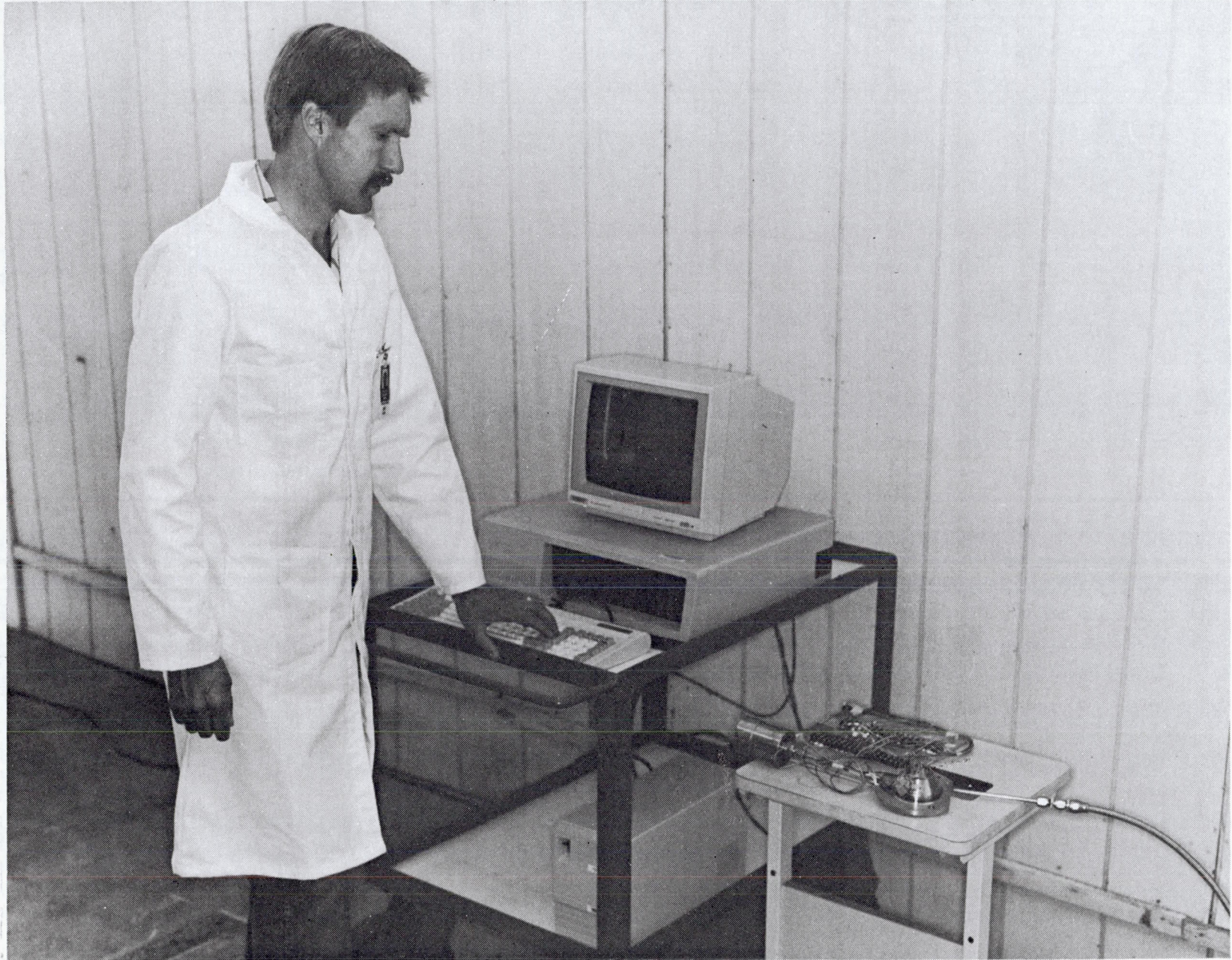


Figure 6.2-25. Test Setup for Leak Testing Fuel-Cooled Chamber Head Ends

6.2, Proof, Leak, and Water Flow Tests (cont.)

sections to 1320 psia (the flight requirement is 4 times working pressure) they were proofed to 500 psig (sufficient for ground test) while measuring the resulting strain. Figure 6.2-26 is a closeup of one of the instrumented cooled sections. The measured strain as a function of pressure is shown in Figures 6.2-27 through 6.2-30. At the worst location, the part has a margin of 11 on yield (0.2%) at maximum operating pressure.

The results of water flow tests of the two fuel-cooled front end sections are shown in Figure 6.2-31.

After assembly of the SN 1 welded flight engine, flight balance calculations were made from flow characteristics measured during hot fire. For the design inlet conditions of 230 psia, the engine would provide 484 newtons with no fuel balance orifice and a 14 psi orifice in the oxidizer circuit. Available pressure drop as a function of thrust level (i.e., required balance orifices to produce a desired thrust level) is shown in Figure 6.2-32. Operation of this engine at 490 N and $MR = 1.650$ would require 233.9 psia inlet pressure on the fuel side, instead of 230 psia.

Proof and Leak Checks

Component, subassembly, and engine assemblies were proof and leak checked at appropriate stages of manufacture, assembly and hot fire. These tests are summarized in Tables 6.2-7, -8 and -9.

The leakage noted was of two types. The chamber joint leak noted in Table 6.2-7 was the result of excessive EB weld power which vaporized some S.S. during the EB braze of the S.S. weld ring to the Re chamber. Welding at the proper conditions will eliminate this leak. Leaks were detected at the omni seals in the propellant circuits using GN_2 . Although no propellant leakage was ever detected here, and two of the three sets of seals would be eliminated in a flight-qualified design, one set must remain to permit replacement of the valve. Therefore, this questionable seal should be modified.

All leaks detected were minor and caused no hardware damage or performance degradation.

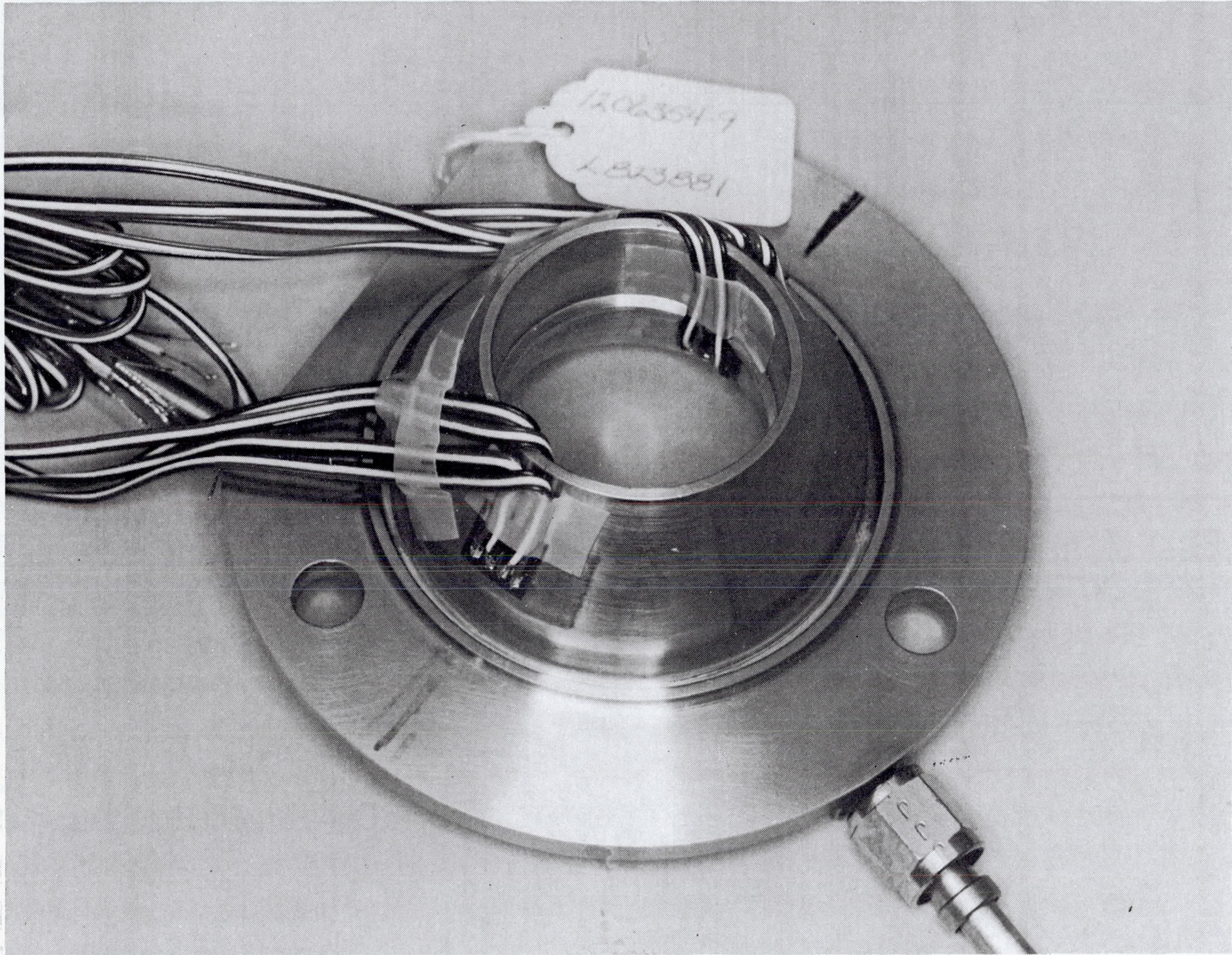


Figure 6.2-26. Fuel-Cooled Chamber Head End Showing Strain Gage Installation

(Strain Gage 0,1,2,3)

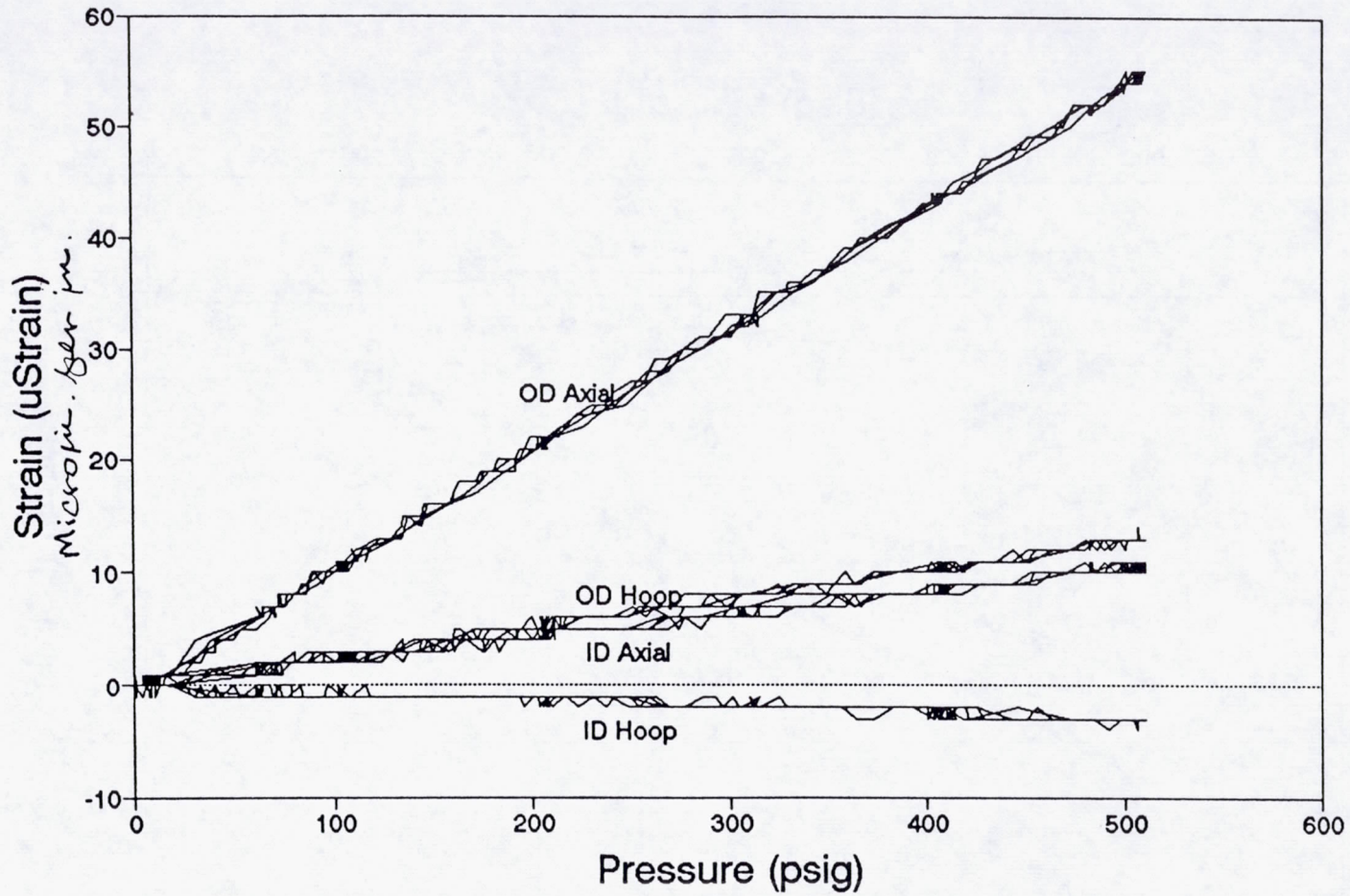


Figure 6.2-27. 100 lb Cooled Section SN 1 – Proof Test

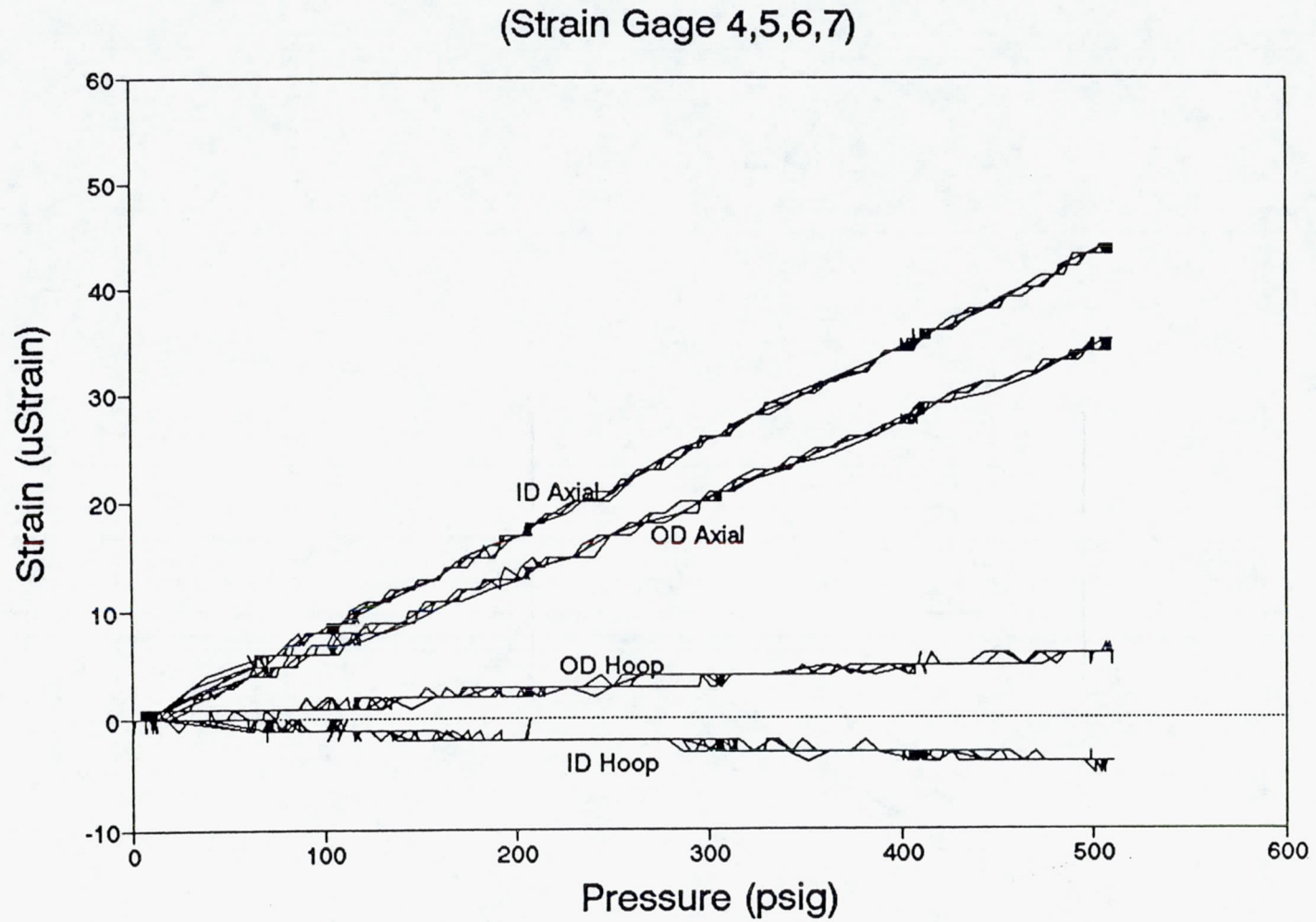


Figure 6.2-28. 100 lb Cooled Section SN 1 – Proof Test

(Strain Gage 0,1,2,3)

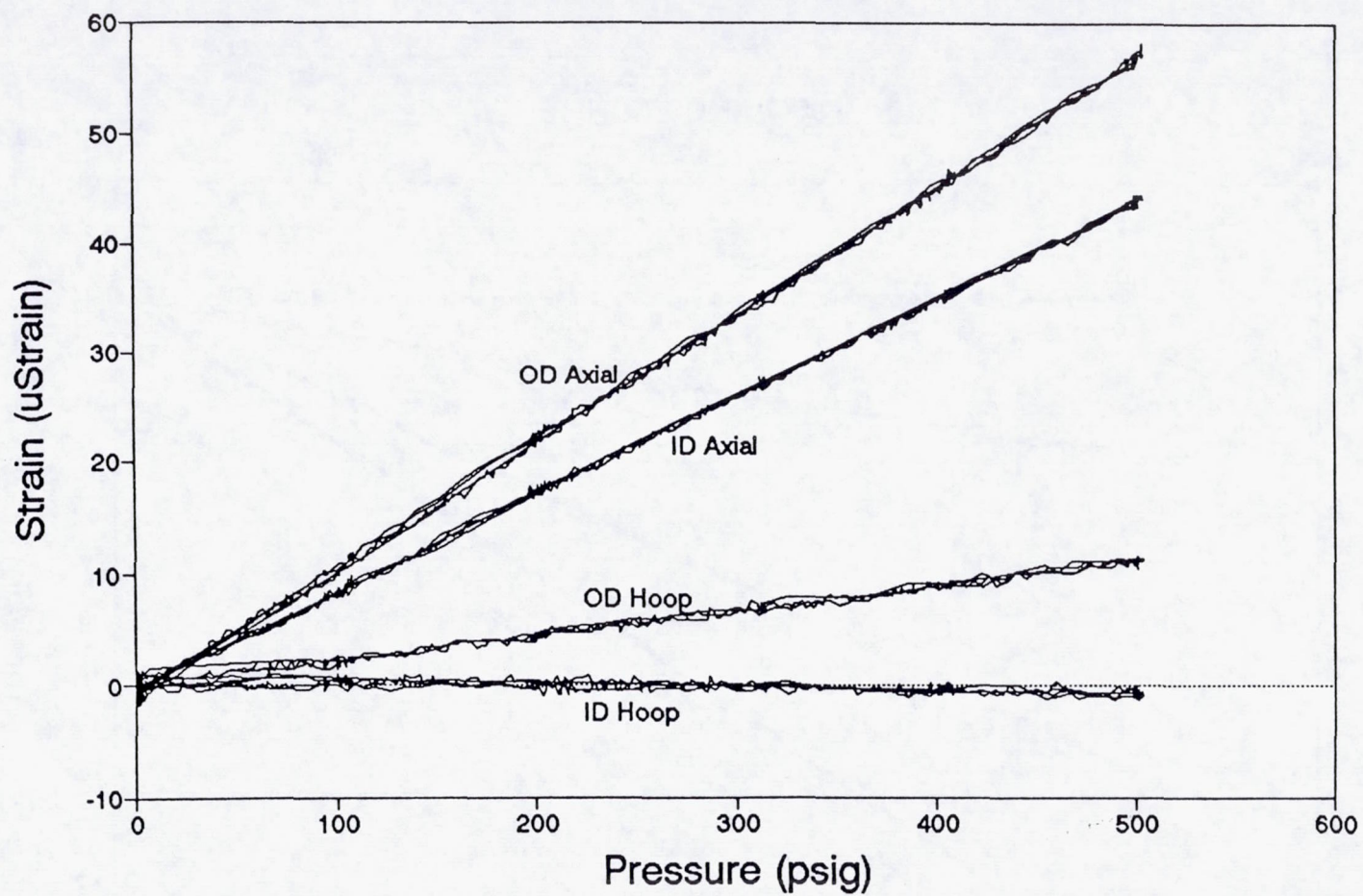


Figure 6.2-29. 100 lb Cooled Section SN 2 – Proof Test

(Strain Gage 4,5,6,7)

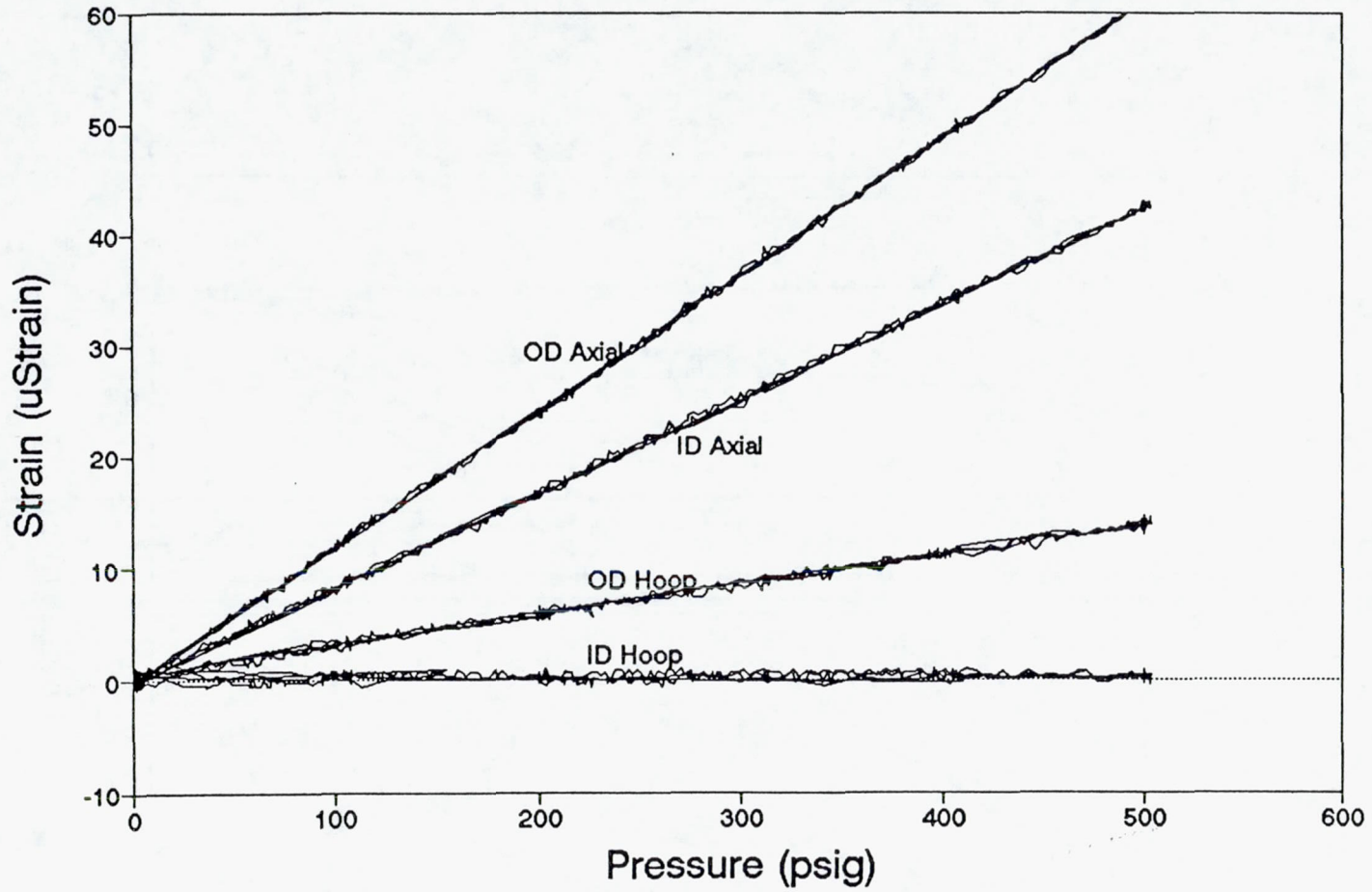


Figure 6.2-30. 100 lb Cooled Section SN 2 – Proof Test

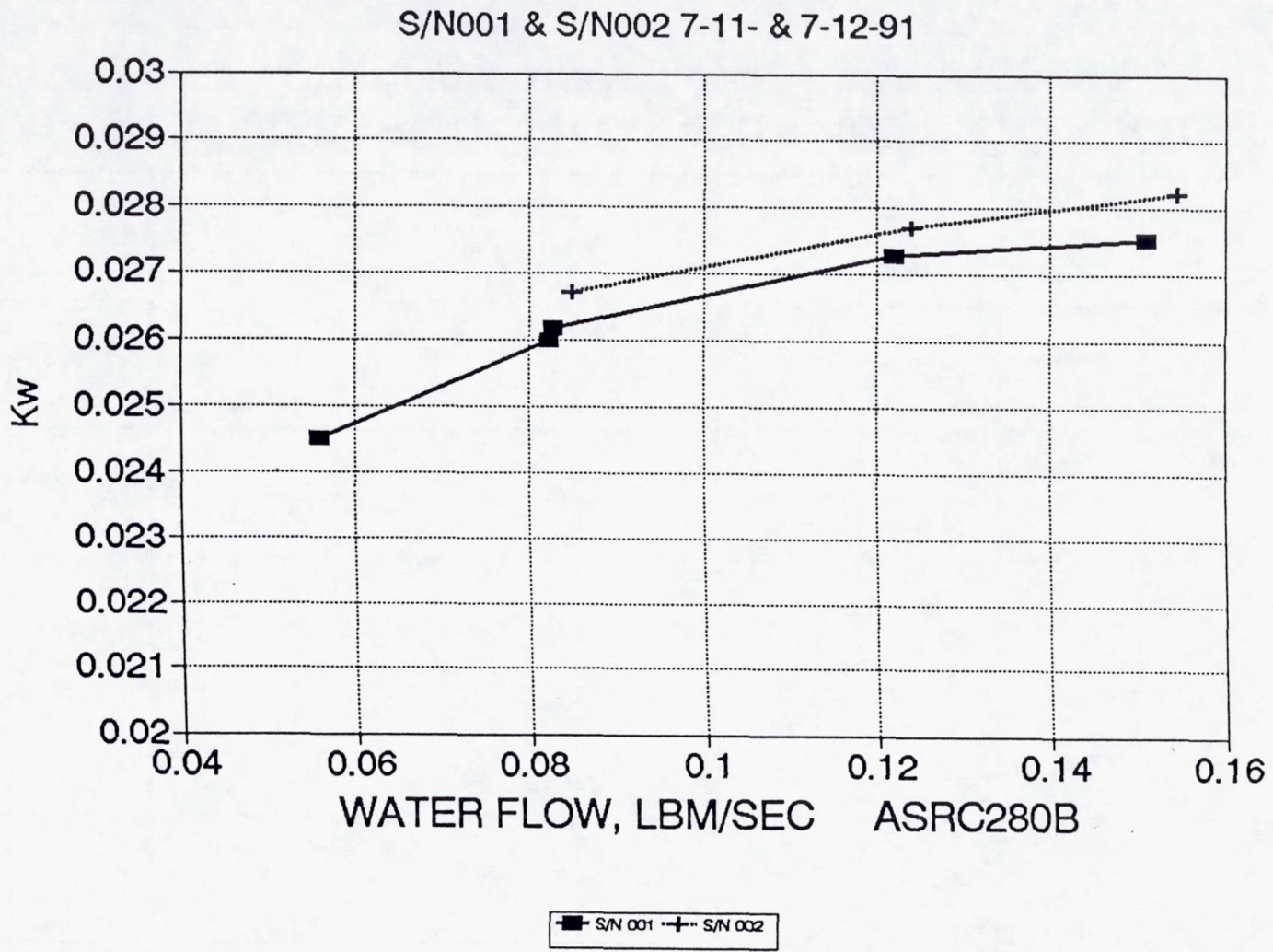


Figure 6.2-31. 100 lb Fuel-Cooled Adapter Kw vs Water Flow Rate

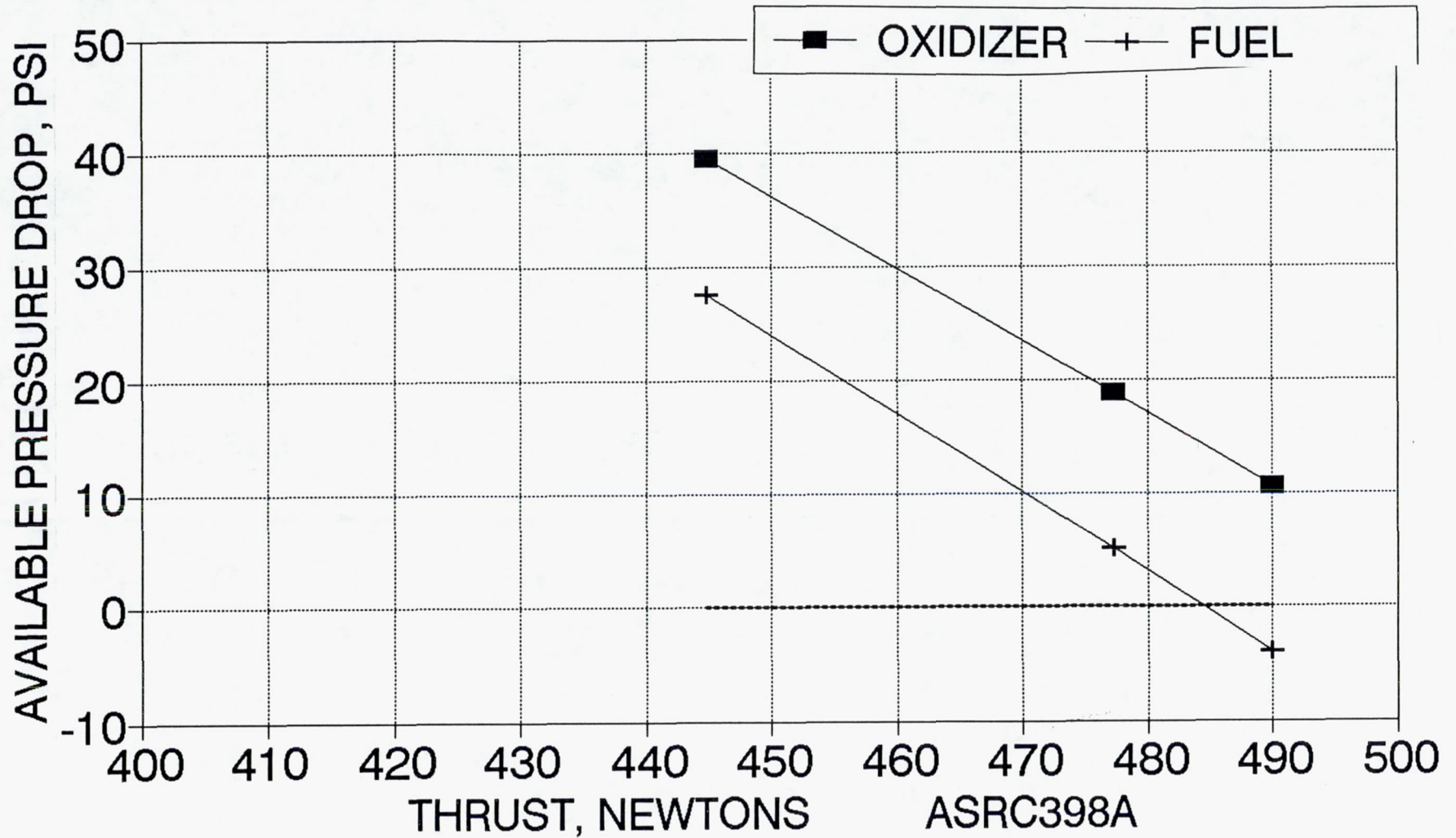


Figure 6.2-32. 490 Newton Flight Engine Balance - Available Pressure Drop vs. Thrust

Table 6.2-7. Summary of Leak and Proof Checks

<u>Date</u>	<u>Part</u>	<u>Pressure</u>	<u>Result</u>
8-22-91	1206383-9: S.S. Ring to Re Chamber	100 psi GN ₂	No leak
9-4-91	1206354 Adapter to 1206383-9 Chamber	Proof With GHe at 200 psig Leak Check at 75 psig	Pass Minor Leak
9-7-91	Chamber Assembly	Proof With GHe at 200 psig Leak Check at 75 psig	Pass Minor Leak at Seal Weld
5-18-92	See Table 6.2-8		
5-5-93	See Table 6.2-9		

Table 6.2-8. Leak Check 47:1 Thruster Assembly Prior to -279

<u>Pressure Location</u>	<u>Leak Check Location</u>	<u>Fluid</u>	<u>Pressure</u>	<u>Detection</u>	
				<u>Method</u>	<u>Results</u>
Valve, Ox Inlet	Between Valve and 1206397-1 Plate	GN ₂	50 psig	Snoop	No Leak
Valve, Fuel Inlet	Between Valve and 1206397-1 Plate	GN ₂	50 psig	Snoop	No Leak
Chamber (Throat Plug)	Between 1206397-1 Plate and Injector	GN ₂	50 psig	Snoop	No Leak
	1206354 Cooled Adapter Chamber Welds	GN ₂	50 psig	Snoop	No Leak
Nozzle/1206381-1 Plug	Re/Cb Weld Joint	GN ₂	50 psig	Snoop	No Leak
		GNS	15 psig	Snoop	No Leak

Table 6.2-9. Results of Post-Test Leak Test of AJ10-221 Engine Assembly at Development Operations Post-Test-351

ASFC585

3-23-93

UPDATE 5-6-93

<u>LOCATION</u>	<u>GAS</u>	<u>PRESSURE</u> <u>PSIG</u>	<u>DETECTION</u> <u>METHOD</u>	<u>RESULTS</u>	<u>COMMENT</u>
VALVE INLET BLOCK	GN2	300	SNOOP	LEAKS--OXID > 1E-4 CCS	LEAKAGE AT WITNESS PORTS FROM OMNI-SEALS
	GN2	300	SNOOP	LEAKS--FUEL > 1E-3 CCS	
VALVE EXTERNAL	GN2	275	SNOOP	NO LEAK, OXID OR FUEL	
VALVE INTERNAL	GN2	275	BUBBLE DETECTOR	NO LEAK, OXID OR FUEL	
VALVE/INJECTOR	GN2	275	BUBBLE DETECTOR	NO LEAK	
CHAMBER/ADAPTER WELD AT SPLIT RNG	GN2	50	SNOOP	LEAKS--> 1E-4 CCS	-(LEAKED AT THIS POINT AFTER ASSY, PRIOR TO TEST. NOT DETECTED HERE DURING TESTING. (PROBABLY WELD SCHEDULE PROBLEM
CHAMBER/ADAPTER WELD	GN2	50	SNOOP	NO LEAK	
COOLED ADAPTER--INTERNAL	GHe	100	BUBBLE DETECTOR	NO LEAK	
COOLED ADAPTER--EXTERNAL	GHe	100	MASS SPEC	2X10-8CC/SEC	APPEARS AT CHAMBER/ADAPTER WELD: NOT EXPECTED; VERY SMALL LEAK

6.2, Proof, Leak, and Water Flow Tests (cont.)

6.2.1 Results of Post Test Leak Checks

At the conclusion of hot fire testing, the engine was subjected to extensive leak tests. The results of these tests are shown in Table 6.2-9.

6.3 HOT FIRING (NTO/MMH)

Hot fire thruster testing was conducted throughout the program for design development, design verification and flight prototype engine demonstration, of a 110 lbf Ir-Re radiation cooled thruster using NTO/MMH propellant. A total of 248 tests with an accumulated duration of 7.27 hr was conducted on 14 different thruster configurations. The hot fire test program is summarized in Table 6.3-1.

The initial test hardware consisted of bolt-together engine configurations which permitted rapid evaluation of injector performance, compatibility and stability in 1.68:1 sea level testing (test groups A, B, and F). This was followed by testing using 44:1 bolt-together hardware in altitude testing, test groups C and E, which permitted longer duration testing and provided performance data which give more certain extrapolation to flight area ratios. Test group D was conducted with bolt-together hardware with a welded C-103 miniskirt to evaluate the Re/C-103 weld under hot fire conditions. The all-welded Ir-Re thruster which evolved from this testing, AJ10-221 SN 1, was then evaluated in altitude testing in test groups H, I and J. A short test series with NTO/AH was conducted in test group G.

6.3.1 Sea Level Tests

The first test series, test group A, had as its objective the evaluation of injector SN 4 as compared to the SN 2 reference injector from JPL Contact 957882 (Ref. 3). This testing is detailed in Table 6.3-2. This table shows test conditions, measured performance and hardware characteristics. Two chamber pressure locations are shown, PC2, which is in the cylindrical section of the chamber downstream of the trip, and PC1, which is in the injector resonator cavity. The column "INJ/TRIP" refers to the configuration tested: N/ is the injector serial number, /4 and /2 are identical ramped trips; /4RW is the /4 trip remachined to form an abrupt trip. The reported $I_{s_{vac}}$ is calculated from sea level thrust corrected to vacuum for the 1.68:1 area ratio nozzle. Characteristic exhaust velocity, C^* , is based on the cold throat dia (0.846 in.) and uncorrected PC2.

Table 6.3-1. Summary of 100 lbf Hot Fire Testing on Advanced Small Rocket Chamber Contract

ASRC310

TASK No.	TEST SERIES	TEST GROUP	HARDWARE		FUEL	TEST No.s	NUMBER OF TESTS	STATUS
			INJECTOR	CHAMBER				
13.3	SEA LEVEL PERFORMANCE/COMPAT.	A	S/N 2 & 4	HEATSINK 1.6:1, Re FOIL	MMH	-101-- -147	47	COMPLETE
13.3	BAY 2 CHECKOUT--SEA LEVEL/1.6:1	B	S/N 2 & 4	HEATSINK 1.6:1	MMH	-148-- -161	14	COMPLETE
13.3	INJECTOR SELECTION--ALT/44:1	C	S/N 2, 4, & 5	JPL Ir/Re/44:1 EXTENSION	MMH	-162-- -170 & -189-- -206	27	COMPLETE
13.3	SKIRT WELD THERMAL CYCLE	D	S/N 2	CUT-OFF JPL Ir-Re WITH WELDED C-103 MINISKIRT	MMH	-171-- -188	15 DEEP THER- MAL CYCLES	COMPLETE
13.3	INJECTOR PERFORMANCE--ALT/44:1	E	S/N 6-1 & 6-2	JPL Ir/Re/44:1 EXTENSION	MMH	-207-- -244	38	COMPLETE
13.3	COMPATABILITY--S.L. 1.6:1	F	S/N 6-1	HEATSINK 1.6:1, Re FOIL	MMH	-247-- -258	12	COMPLETE
13.3	HYDRAZINE PERF.--ALT/44:1	G	S/N 6-1	JPL Ir/Re/44:1 EXTENSION	AH	-245, -246	2	COMPLETE
15.2	PERFORMANCE--ALT/286:1	H	S/N 6-2	WELDED S/N 1 W/286:1 C-103 NOZZLE	MMH	-259 -- -278	20	COMPLETE
15.3	DURABILITY--ALT/47:1	I	S/N 6-2	WELDED S/N 1 MOD W/47:1 C-103 NOZZLE	MMH	-279 -- -347	69/ 3.64 HRS	COMPLETE
15.4	ENDURANCE (J-AREA)--ALT/47:1	J	S/N 6-2	WELDED S/N 1 MOD W/47:1 C-103 NOZZLE	MMH	-348 -- -351 [-101 to -103]	1-, 100-, 7,200-, and 1,200 sec	COMPLETE

Table 6.3-2. Summary of 100 lb Testing – Preliminary Data, Sheet 1 of 2

RUN NO.	INJ/ TRIP	FIRING TIME sec	PC2 pole	MR O/F	Isvac sec	C* R/sec	FOIL -	LOSS RATE, mil/HR	THRUST		PROPELLANT		DELTA/ Tregon of	Vjox R/sec	Vj R/sec	RUN
									S.L., lbf	VAC., lbf	WO lbf/sec	WF				
101	2/4	0.6	-	-	-	-	NO	-	-	-	-	-	-	-	-	101
102	2/4	1.0	84.1	1.484	224.8	5348	NO	-	80.7	83.9	0.1703	0.1140	8.8	77.8	108.3	102
103	2/4	1.0	91.4	1.678	228.8	5378	NO	-	86.6	88.8	0.1828	0.1180	11	88.1	110.0	103
104	2/4	7.0	97.8	1.852	238.8	5387	NO	-	84.6	77.7	0.2046	0.1298	78.8	94.3	121.8	104
105	2/4	1.0	108.8	1.808	228.8	5428	NO	-	88.3	81.4	0.2221	0.1338	18.1	102.2	138.8	105
106	2/4	1.0	108.4	1.867	227.4	5398	NO	-	70.2	83.4	0.2282	0.1378	18.1	104.7	132.4	106
107	2/4	7.0	110.0	1.853	234.3	5305	NO	-	74.7	87.9	0.2338	0.1414	78.9	108.0	138.2	107
108	2/4	1.0	115.6	2.030	228.8	5348	NO	-	78.4	88.6	0.2618	0.1288	18.8	120.7	124.6	108
109	2/4	7.0	113.8	2.011	231.2	5284	NO	-	78.9	80.1	0.2804	0.1288	80.8	120.4	138.0	109
110	2/4	7.0	113.3	1.989	231.5	5263	Re-002	-	77.1	80.3	0.2888	0.1305	80.2	120.8	130.4	110
111	2/4	7.0	112.8	2.018	232.1	5248	Re-002	-	77.1	80.2	0.2800	0.1288	84.7	121.0	128.3	111
112	2/4	7.0	112.8	1.988	232.6	5248	Re-002	41.8	77.2	80.3	0.2888	0.1302	84.6	120.6	130.3	112
113	2/4	7.0	87.8	2.028	238.2	5312	Re-003	-	87.6	70.6	0.2003	0.0888	105.4	82.8	88.3	113
114	2/4	4.3	87.9	2.040	234.2	5321	Re-003	XX	88.8	88.8	0.2004	0.0883	88.8	82.6	88.6	114
115	2/4	4.2	87.9	2.010	236.4	5328	Re-004	XX	87.0	70.2	0.1982	0.0881	101.7	81.8	88.2	115
116	2/4	7.0	118.7	2.020	231.8	5237	Re-001	37.7	78.6	82.7	0.2873	0.1323	88	128.4	132.7	116
117	4/2	1.0	105.0	1.881	223.7	5289	NO	-	87.4	80.8	0.2208	0.1388	18.8	98.2	121.1	117
118	4/2	7.0	108.1	1.888	229.0	5240	NO	-	70.7	83.9	0.2288	0.1373	84.8	101.4	123.0	118
119	4/2	7.0	111.8	2.001	227.4	5207	NO	-	74.8	88.0	0.2882	0.1280	104.2	114.8	117.0	119
120	4/2	7.0	88.4	1.185	223.1	5128	NO	-	84.8	88.0	0.1634	0.1418	88.4	71.8	134.3	120
121	4/2	7.0	123.2	1.970	227.8	5180	NO	-	84.7	87.8	0.2848	0.1448	88.4	128.8	130.3	121
122	4/2	7.0	112.0	1.854	228.6	5226	Re-006	15.8	75.4	88.6	0.2643	0.1312	88.7	114.0	118.7	122
123	4/2	2.2	102.7	1.878	228.8	5363	NO	-	88.3	78.6	0.2288	0.1204	48.3	100.8	108.7	123
124	4/2	7.0	131.8	1.884	228.0	5213	NO	-	80.8	104.0	0.2888	0.1883	71.8	133.6	143.3	124
125	4/2	7.0	135.3	1.882	227.0	5213	NO	-	83.4	108.6	0.2844	0.1780	81.1	132.6	188.8	125
126	4/2	7.0	108.1	1.882	229.4	5271	NO	-	71.8	85.1	0.2328	0.1383	78.8	104.6	124.8	126
127	4/2	7.0	82.1	1.810	228.7	5288	NO	-	81.2	84.4	0.1848	0.0888	108.7	82.8	108.8	127

Table 6.3-2. Summary of 100 lb Testing – Preliminary Data, Sheet 2 of 2

ASPC218																
RUN NO.	INJ/ TRIP	FIRING TIME sec	PC2 psi	MR C/F	Iavac sec	C* R/sec	FOIL -	LOSS RATE, ml/HR	THRUST		PROPELLANT		DELTA			RUN
									S.L., lbf	VAC., lbf	WO lbf/sec	WF	Trogen of	Vjox R/sec	Vj R/sec	
128	4/4FW	7.0	118.3	1.910	230.3	5271	NO		78.7	91.9	0.2618	0.1371	97.6	118.4	124.8	128
129	4/4FW	7.0	111.1	1.890	229.8	5289	NO		74.1	87.3	0.2371	0.1426	97	108.4	129.1	129
130	4/4FW	7.0	140.2	1.845	228.3	5247	NO		97.2	110.3	0.3008	0.1827	95.4	135.5	164.1	130
131	4/4FW	7.0	94.8	1.702	232.8	5337	NO		81.8	74.8	0.2024	0.1188	107.9	90.8	108.4	131
132	4/4FW	7.0	82.7	1.838	235.0	5367	NO		82.3	85.5	0.1731	0.1067	118.9	77.3	98.7	132
133	4/4FW	1.0					NO						0			133
134	4/4FW	7.0	78.3	1.818	232.8	5377	NO		48.5	58.7	0.1587	0.0890	128.68	71.1	88.9	134
135	2/4FW	1.1	104.8	1.747	229.3	5414	NO		67.1	80.3	0.2228	0.1274	11.4	103.4	122.4	135
136	2/4FW	7.0	103.8	1.839	234.4	5372	NO		88.7	81.9	0.2170	0.1324	95.3	102.0	132.5	136
137	2/4FW	7.0	105.8	1.810	234.8	5380	Re-008	16.8	70.2	83.3	0.2190	0.1380	90.7	103.0	136.0	137
138	2/4FW	7.0	133.3	1.898	232.5	5329	NO		82.0	105.2	0.2848	0.1678	88.4	134.2	167.7	138
139	2/4FW	7.0	98.9	1.827	238.8	5413	NO		85.5	88.7	0.1798	0.1108	101.3	83.8	111.1	139
140	2/4FW	7.0	133.4	1.974	231.8	5304	Re-007	9.9	82.2	105.3	0.3019	0.1530	78.5	143.3	153.7	140
141	2/4FW	5.0	88.2	2.048	234.0	5382	Re-008	216.8	54.8	67.7	0.1946	0.0890	112.3	90.8	95.8	141
142	2/4FW	7	104.8	1.853	235.0	5388	NO		88.5	82.6	0.2191	0.1328	85.4	103.2	133.0	142
143	2/4FW	1.1					NO			13.2			0			143
144	2/4FW	7	70.3	1.839	234.3	5382	NO		42.4	55.8	0.1473	0.0898	95.9	88.1	90.0	144
145	2/4FW	7	80.2	1.821	231.7	5289	NO		34.7	47.9	0.1277	0.0788	78.64	80.0	77.8	145
146	2/4FW	7	49.5	1.888	224.1	5088	NO		28.2	39.4	0.1089	0.0680	85.3	81.5	84.0	146
147	2/4FW	7	105.0	1.987	231.7	5385	RE-008	18.3	88.5	81.7	0.2345	0.1181	80.4	110.8	117.8	147

133

ORIGINAL PAGE IS
OF POOR QUALITY

6.3, Hot Fire Testing (cont.)

The hardware used in this testing consisted of platelet injectors, SN 2 and SN 4, a fuel-cooled trip/adaptor section, and a heat sink stainless steel chamber with an integral nozzle of 1.68:1 area ratio. This bolt together hardware is shown schematically in Figure 6.3.1-1.

The compatibility/performance chamber is shown in Figure 6.3.1-2 mounted on the sea level test stand in Bay 3. A section of the chamber is lined with 3 mil Re foil, thermally isolated with Grafoil, using the components illustrated in Figure 6.3.1-3. A close-up of one of the foils is shown in Figure 6.3.1-4 after test. The foil erosion rate based on mass loss is shown in Figure 6.3-5.

The Bay 3 test series demonstrated the compatibility and stability of the two injectors and their relative performance. No evidence of instability based on Kistler pressure measurements was seen. Compatibility based on measured erosion rates was satisfactory; however, systematic deviations in thrust and flow measurement were noted during the Bay 3 testing. Performance measurements made in this sea level test series are subject to a wide error band. However, injector SN 4 clearly had lower performance than SN 2. Injector SN 4 had design changes intended to increase its performance, while also improving fabricability. Therefore, a new injector was designed and built, SN 5. This injector was intended to duplicate the performance of SN 2. Accurate performance comparisons of the three injectors were obtained in the 44:1 altitude tests, to be described in Section 6.3.2.

Tests -101 through -109 were conducted for checkout and to obtain baseline performance data with injector SN 2. Tests -110 through -116 were conducted to obtain compatibility data. This test logic was then to be repeated with injector SN 4. However, during hardware changeover, a fuel leak was noted at a weld in the cooled adapter/trip assembly (identified as SN 4). While this unit was at the shop for weld repair, SN 4 injector was assembled with a second cooled adapter, SN 2, in test series -117 through -127. The reworked cooled adapter which, in addition to weld repair also had the trip recontoured (trip SN 4RW) was installed and the testing of SN 4 injector was continued as Tests -128 through -134. Injector SN 2 was then tested with the reworked trip in Tests -135 through -147.

The range of injector inlet pressure over which the engine was operated is shown in Figure 6.3-6 for the sea level Tests -101 through -161. The range of P_c and MR that

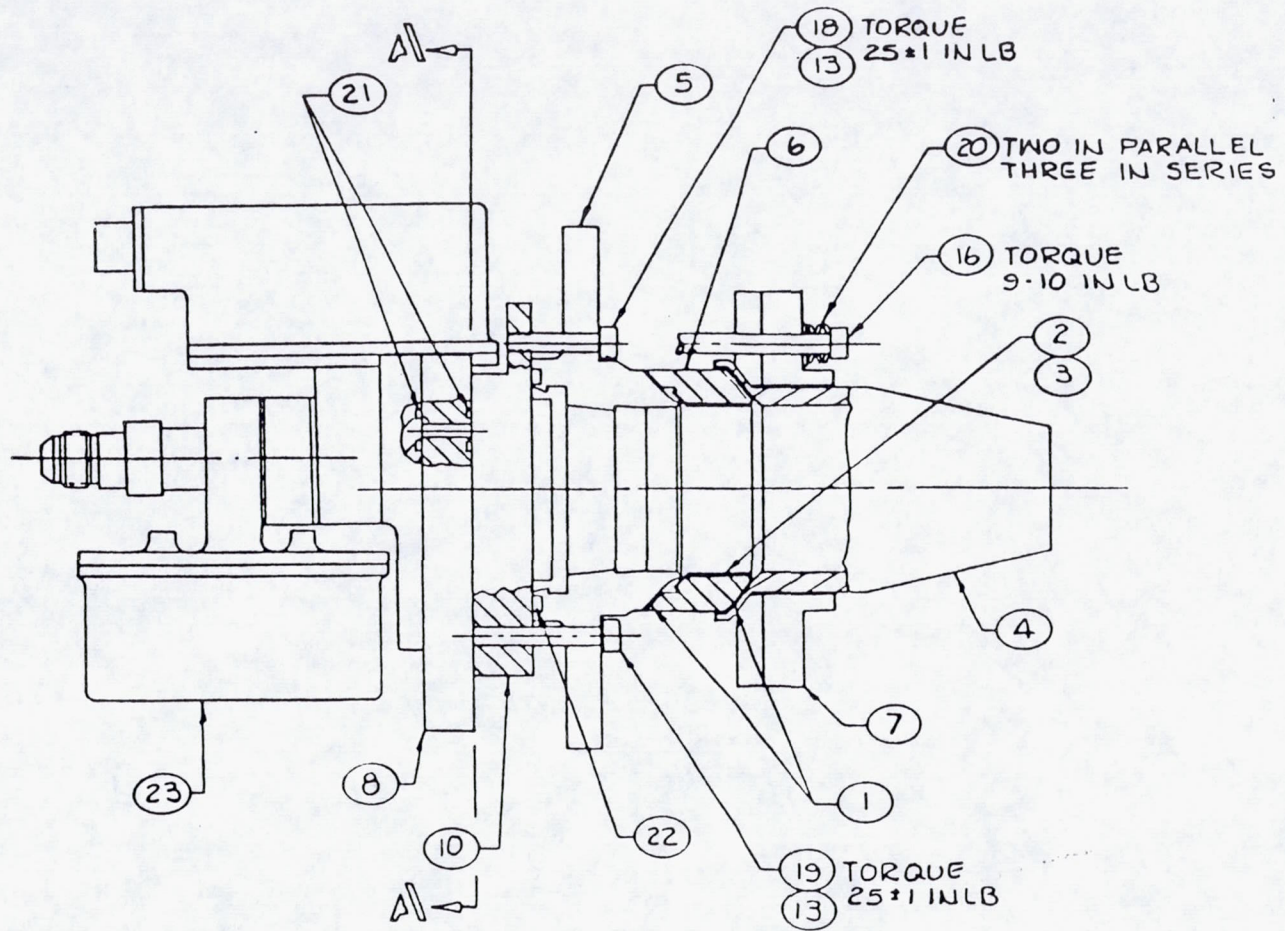


Figure 6.3.1-1. Drawing of Bolt-Up Sea Level Thruster Assembly

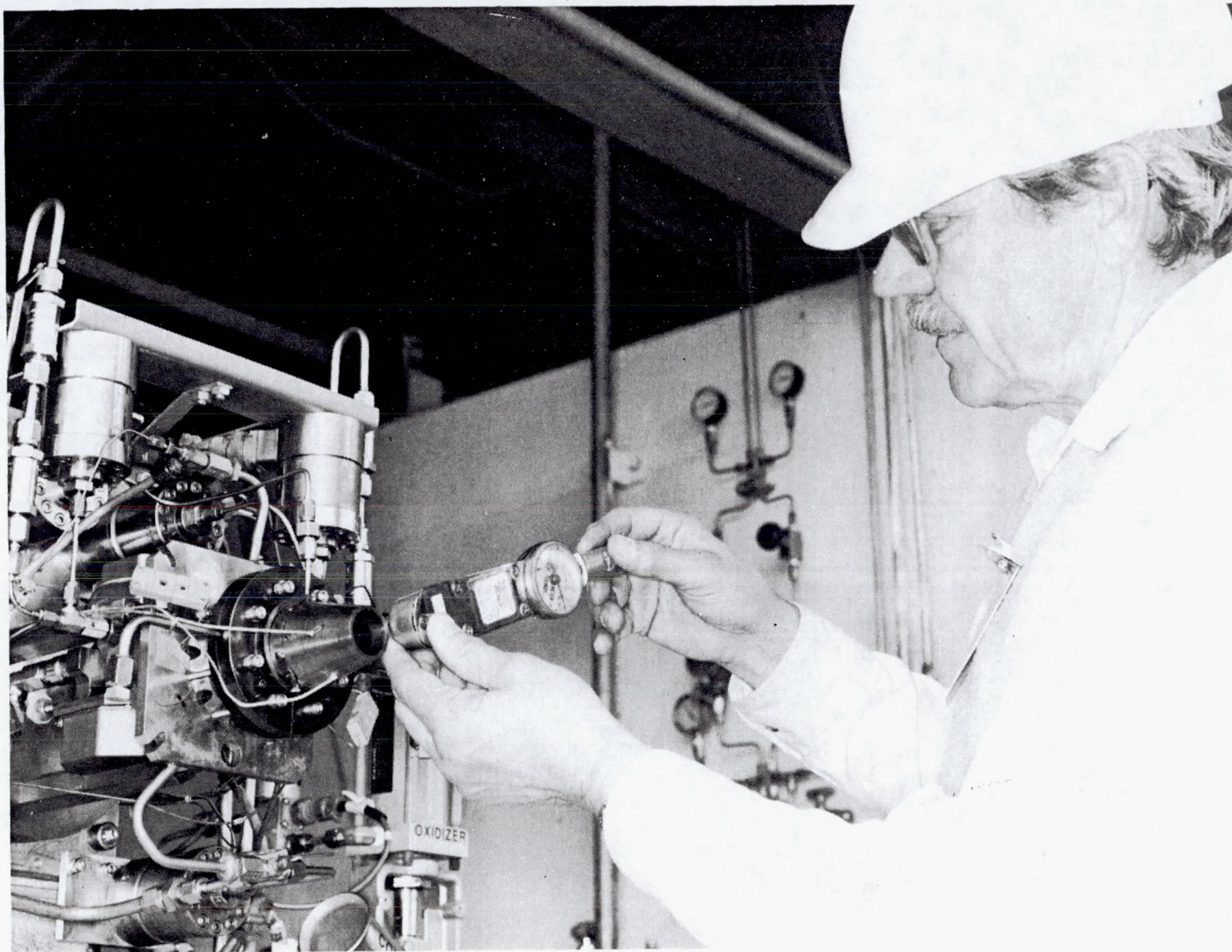


Figure 6.3.1-2. Compatibility/Performance Chamber



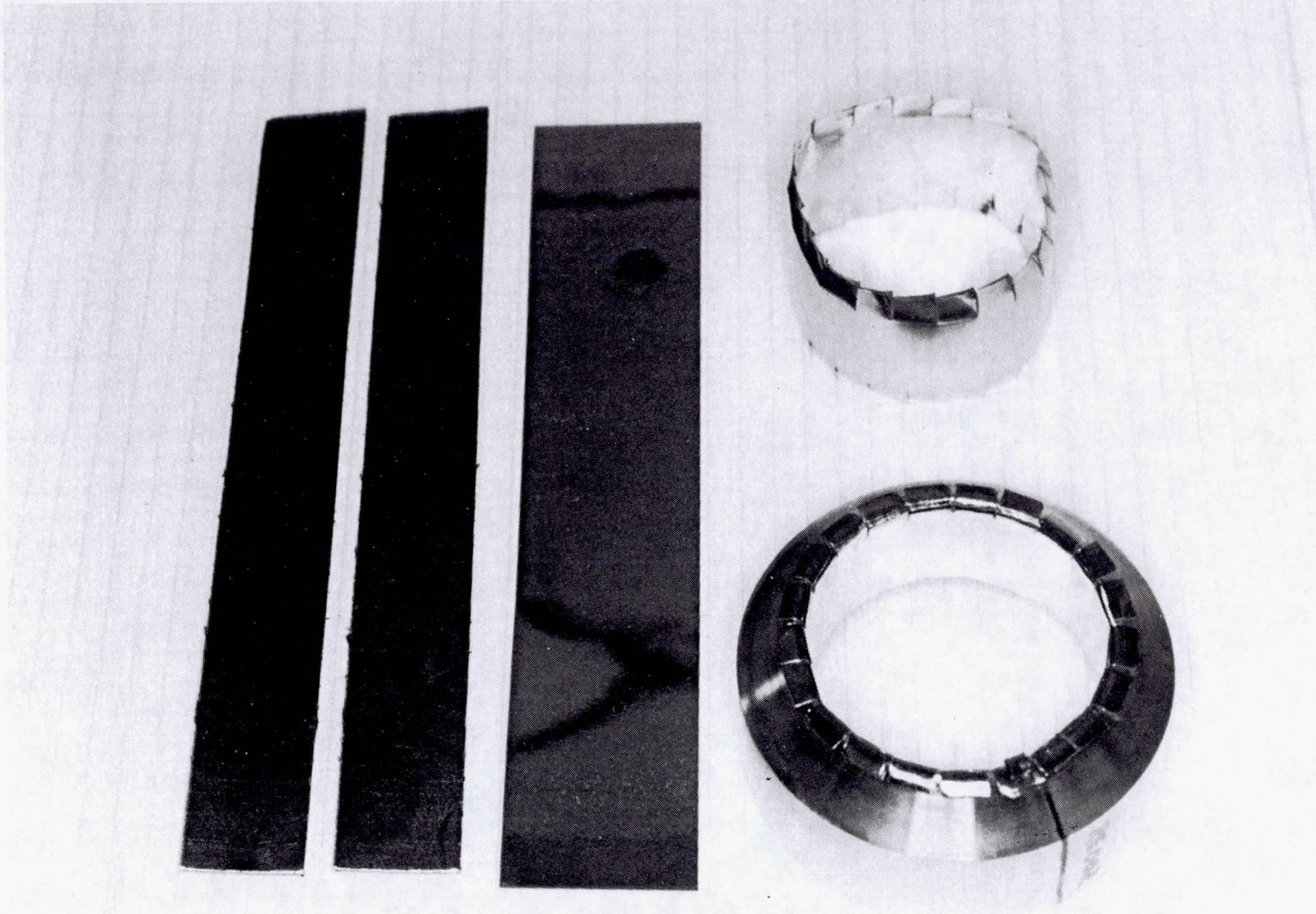


Figure 6.3.1-3. 100-lbf Compatibility Chamber Materials

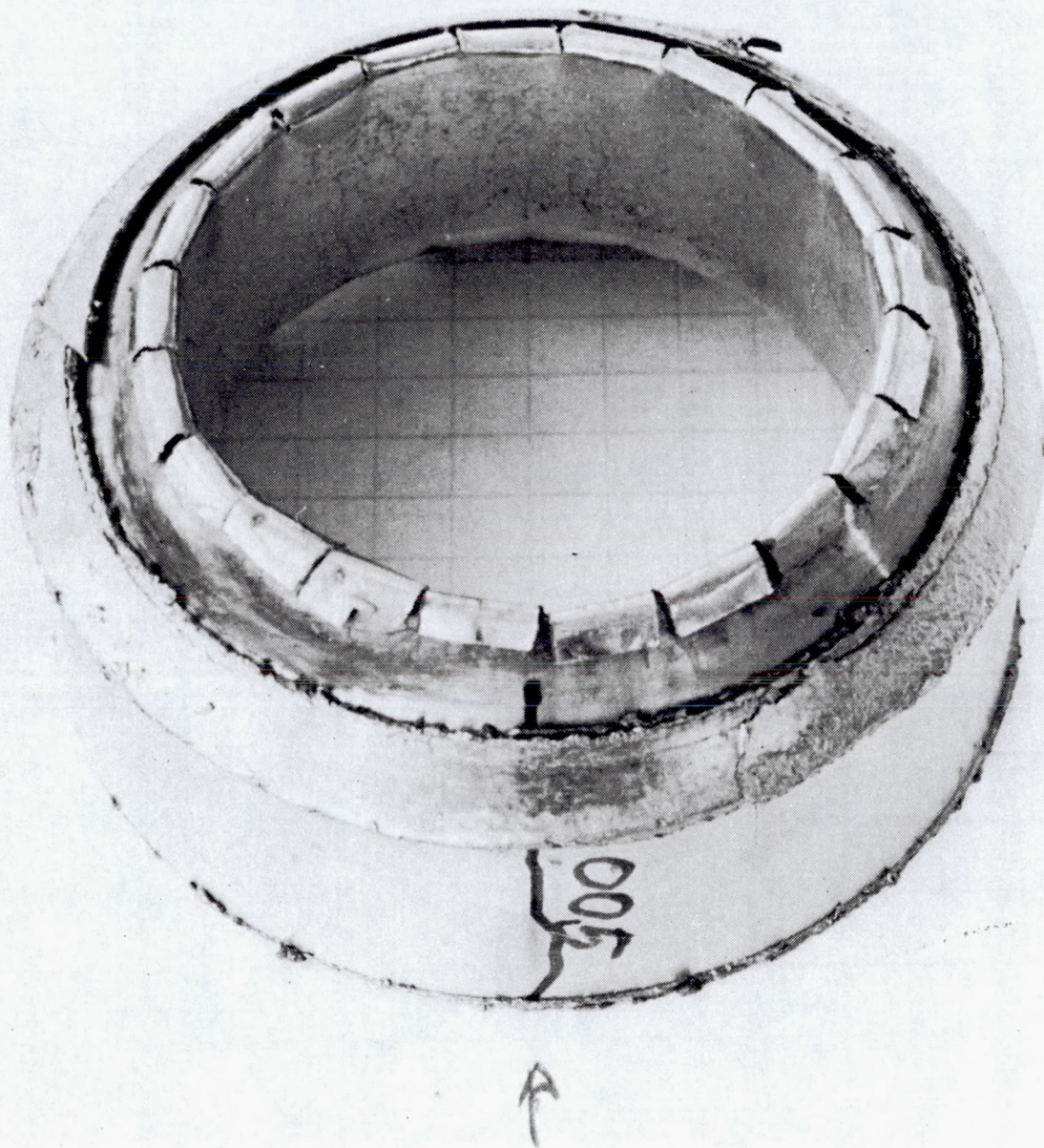


Figure 6.3.1-4. 100 lbf Ir-Re Thruster Injector Characterization Foil After Test



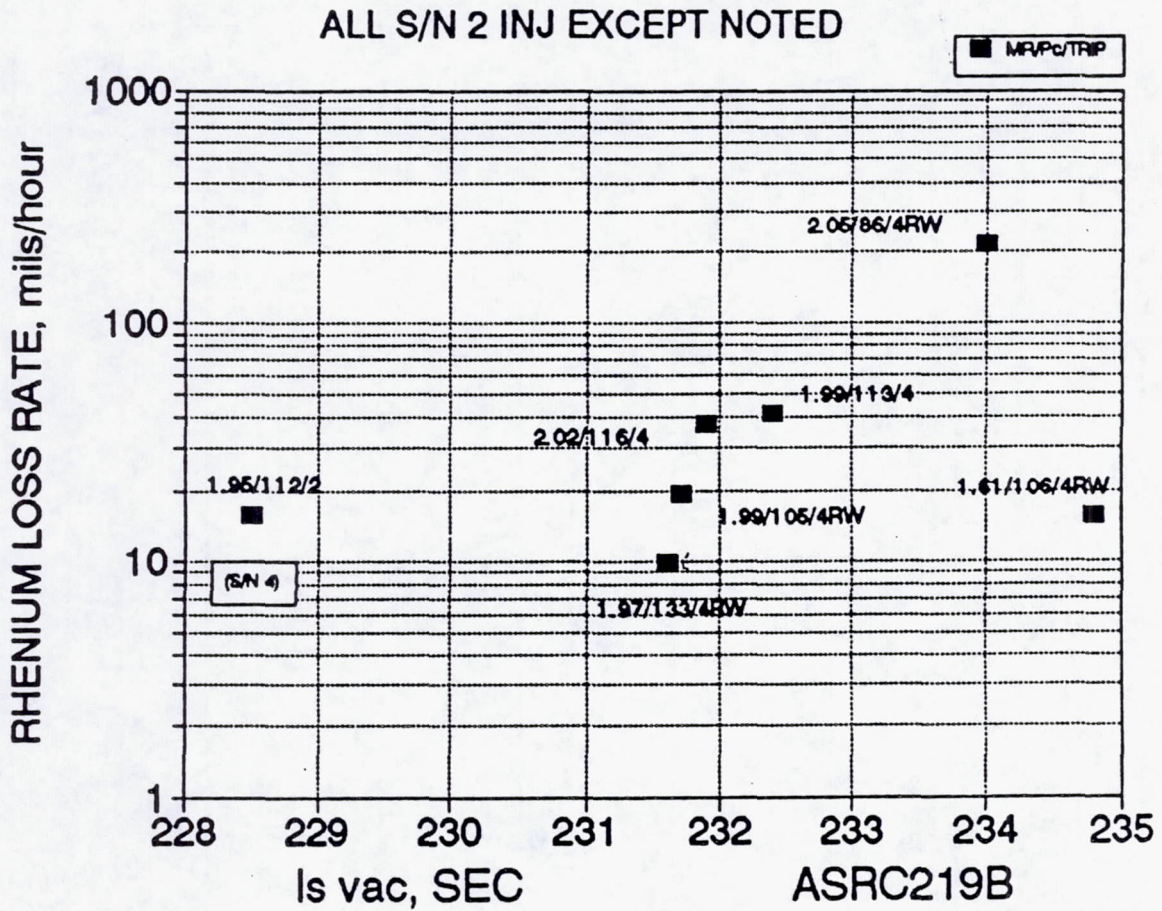


Figure 6.3-5. 100# Rhenium Loss Rate vs Isvac

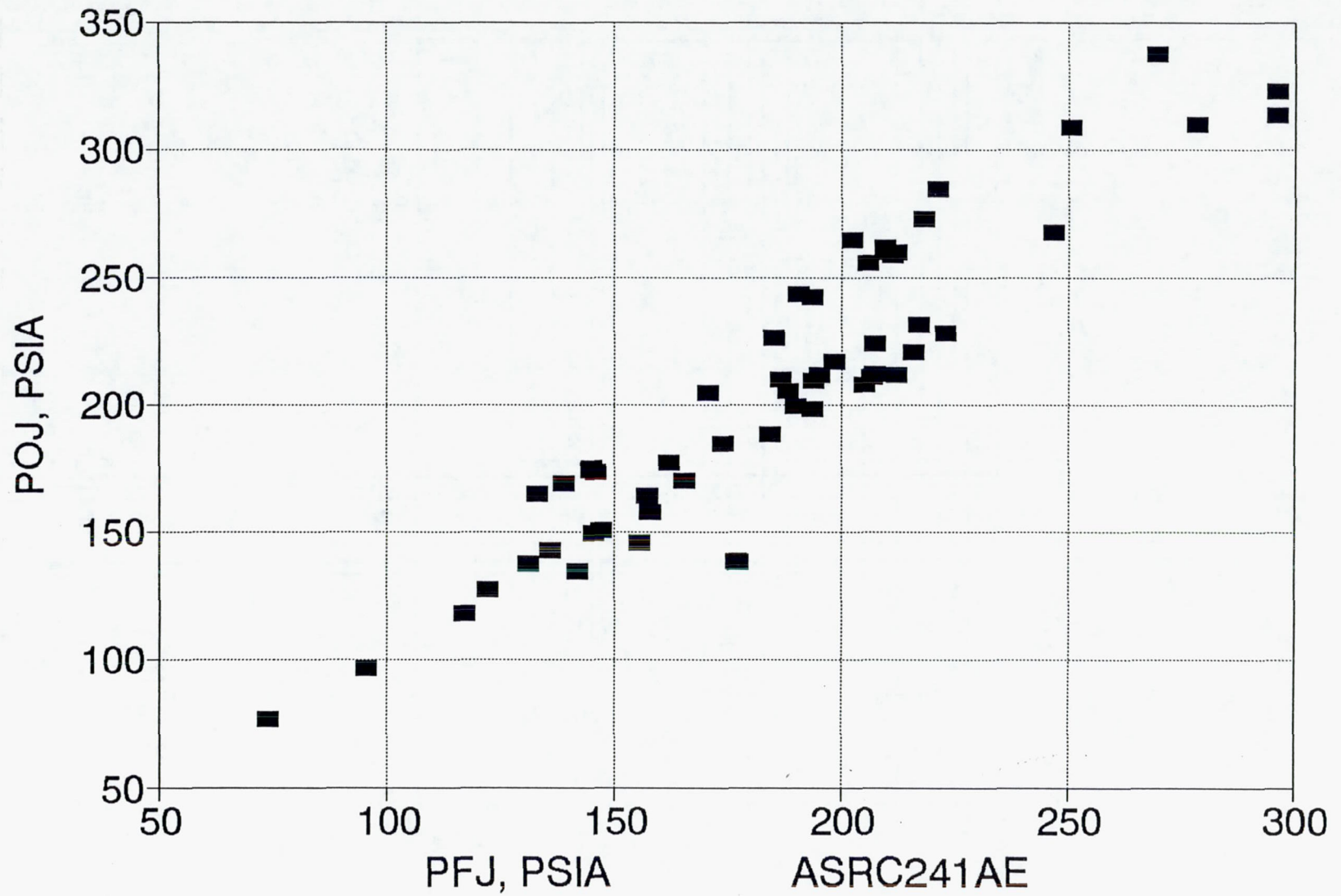


Figure 6.3-6. 100# Thruster POJ vs PFJ – Sea Level Tests -101 thru -161

6.3, Hot Fire Testing (cont.)

resulted is shown in Figure 6.3-7. The temperature rise in the fuel circuit is shown in Figure 6.3-8 for the various combinations of injector and trip. The ratio of Pc-1 to Pc-2, shown in Figure 6.3-9 was about 1.025 at nominal and increased slightly with decreasing Pc-2.

Absolute performance data have a wide error band for the Bay 3 tests because of unresolved flow and thrust errors. Since further tests were conducted in Bay 2, with a new stand and flow measuring system, it was not productive to resolve completely the measurement problem. Specific impulse versus chamber pressure is shown in Figures 6.3-10 through -13 for the different injector/trip configurations tested in Bay 3, all plotted to the same scales to aid comparison. It should be noted that many of these tests were run at high MR (1.9 to 2.0) and all are of short duration (max = 7 sec). The difference between the Bay 3 and Bay 2 test results can be seen by comparing Figure 6.3-13 with 6.3-14, the same configurations in Bay 3 and Bay 2, respectively. The Bay 3 data at nominal conditions show an I_s of 234.5, while the (more accurate) Bay 2 data show 231.5, a difference of 1.3% and clearly significant in attempting to choose between configurations. For this reason, final performance choice was based on the 44:1 altitude tests in Bay 2.

However, at this time it was clear that SN 4 was lower performing relative to SN 2, as a comparison of 6.3-12 and -13 shows, about 231 versus 234.5 or about 1.5% lower.

Fabrication of an injector to duplicate SN 2 was therefore initiated, for altitude testing in Bay 2.

Bay 2 Testing

Prior to 44:1 tests in the altitude facility, Bay 2, a group of sea level tests was conducted with injector SN 2 to checkout the thrust and force measurement of the new setup.

The Bay 2 test facility setup for sea level checkout is shown in Figures 6.3-15 through -18. Figure 6.3-15 is a view of the aft end of the test cell showing the thruster on the stand and the 32 in. flange to which the diffuser mounts. Figure 6.3-16 is a nozzle exit view of the thruster on the stand. The thrust stand is shown in Figure 6.3-17; one of the four support flexures and the calibration load cell are visible. The heat sink 1.68:1 thrust chamber is shown mounted on the test stand in Figure 6.3-18.

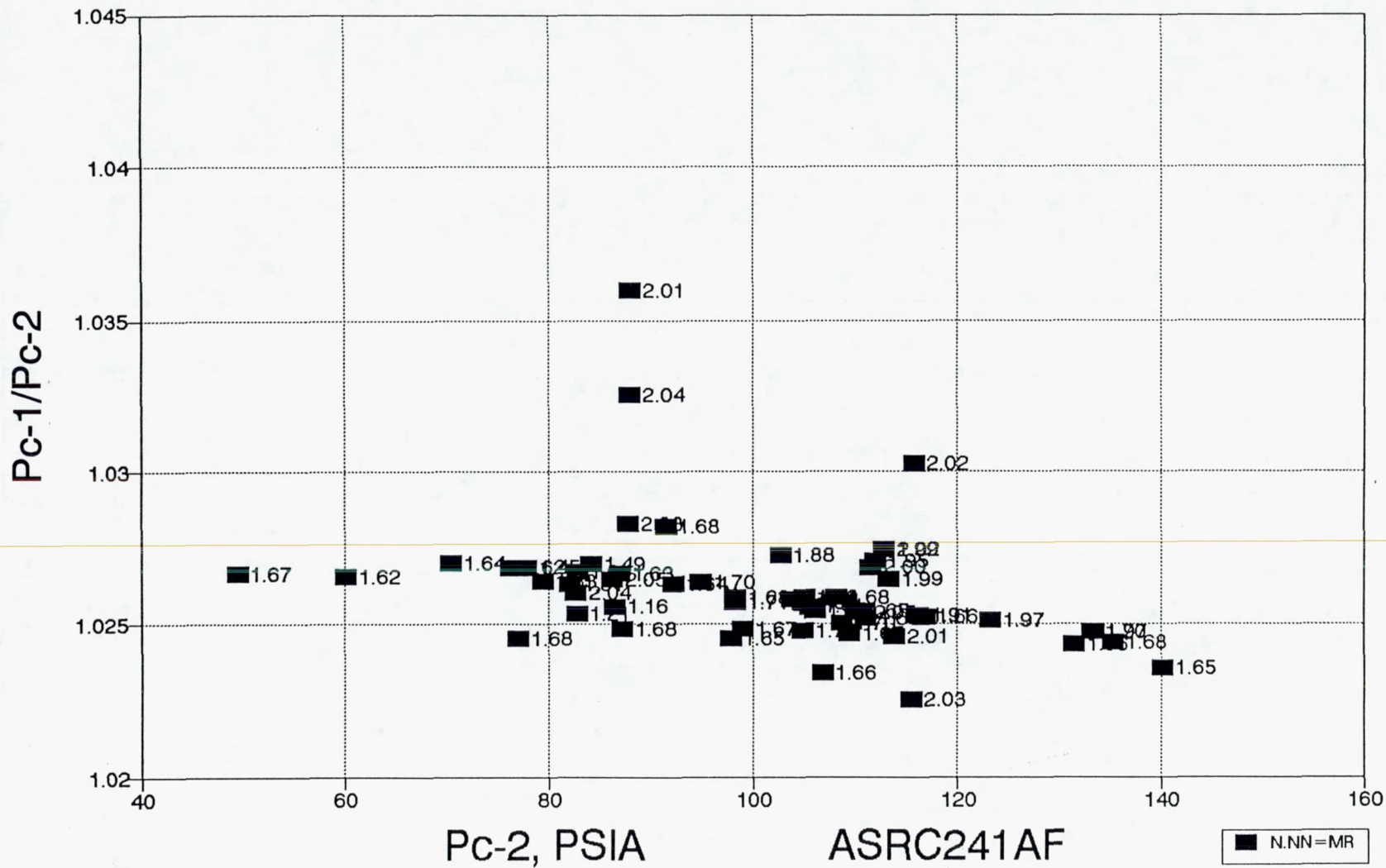


Figure 6.3-9. 100# Thruster Pc-1/Pc-2 vs Pc-2 – Sea Level Tests -101 thru -161

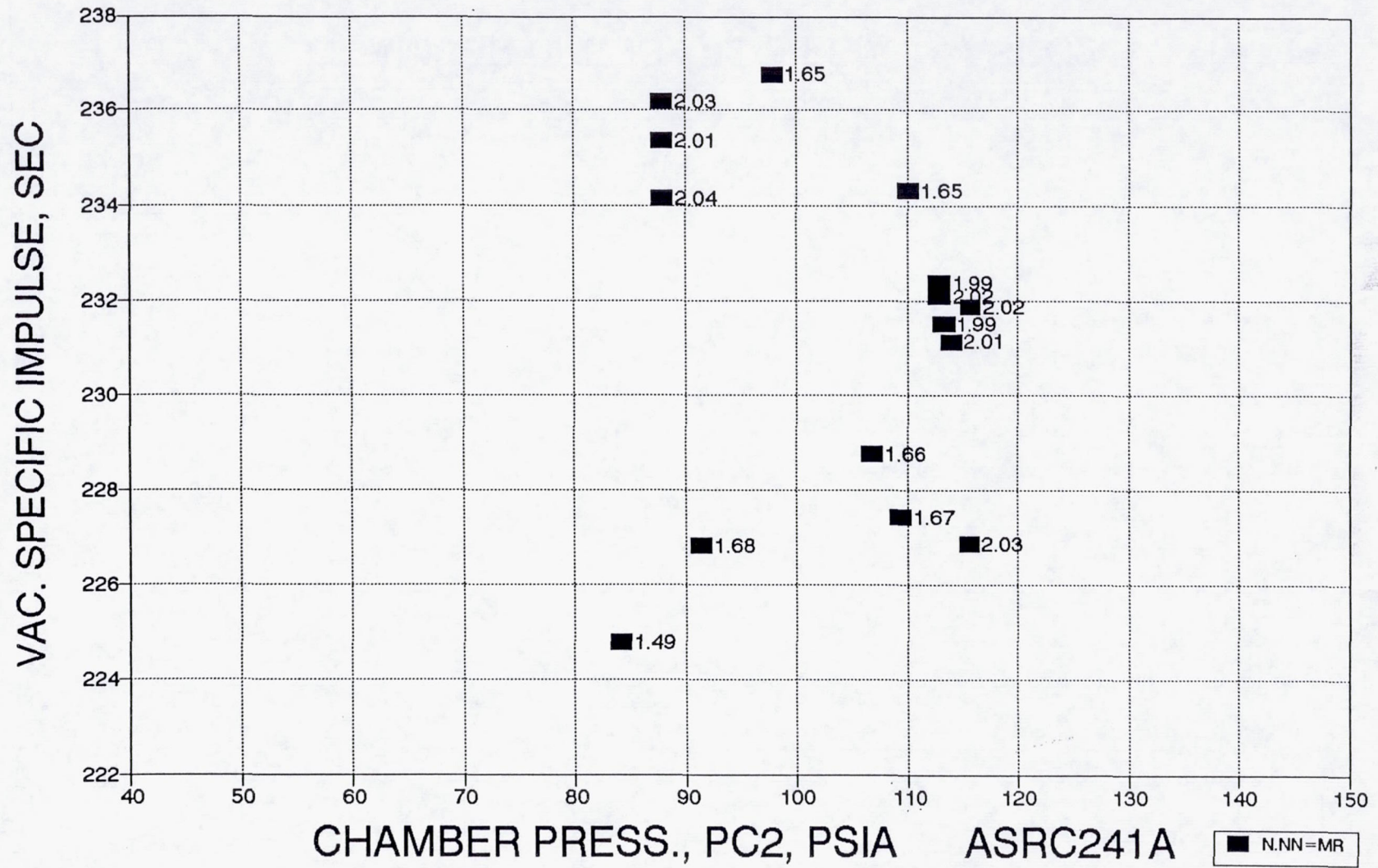


Figure 6.3-10. 100# Isvac Versus Pc-2 – Injector #2, Trip #4 (101-116) Bay 3

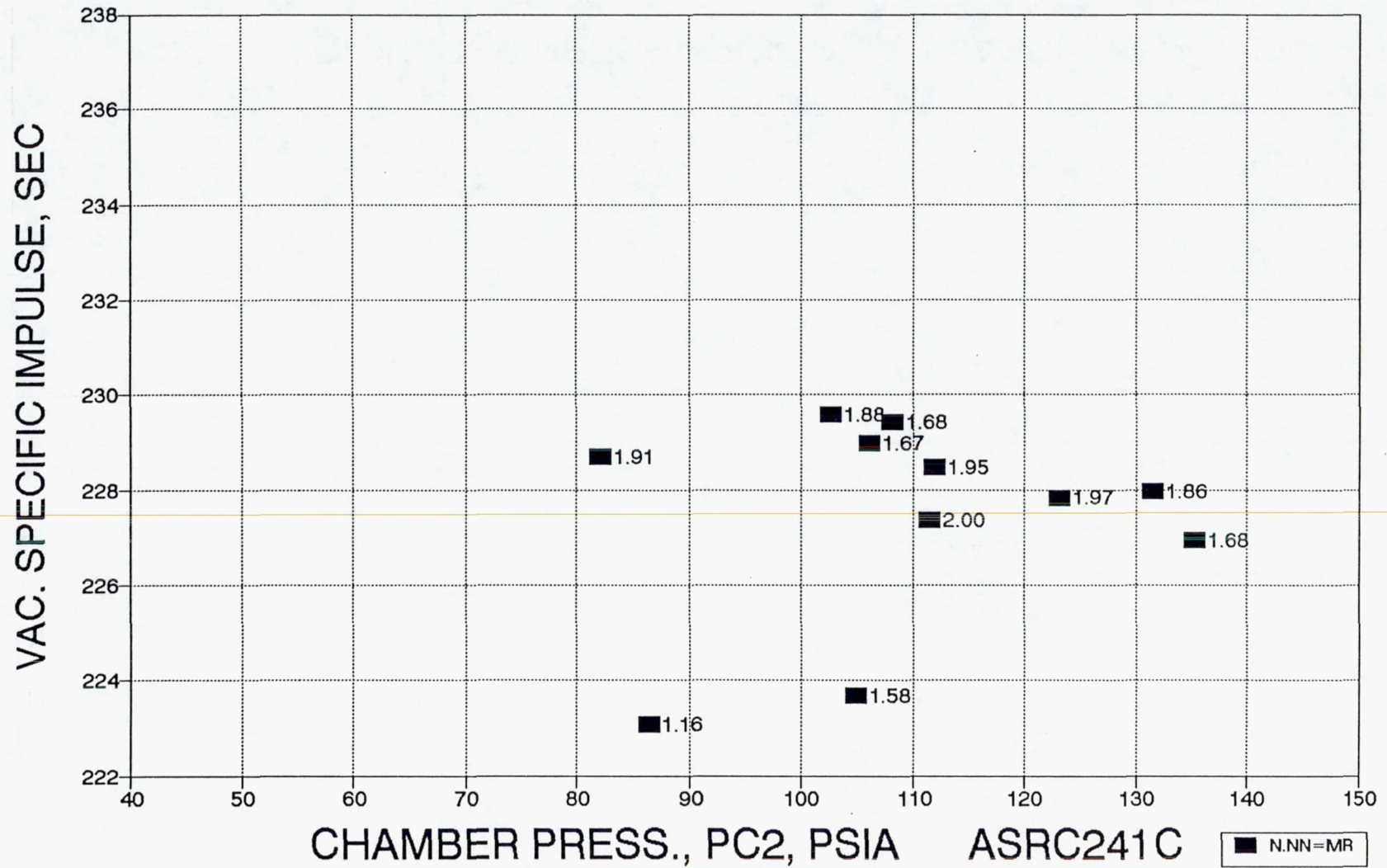


Figure 6.3-11. 100# Isvac Versus Pc-2 – Injector #4, Trip #2 (117-127) Bay 3

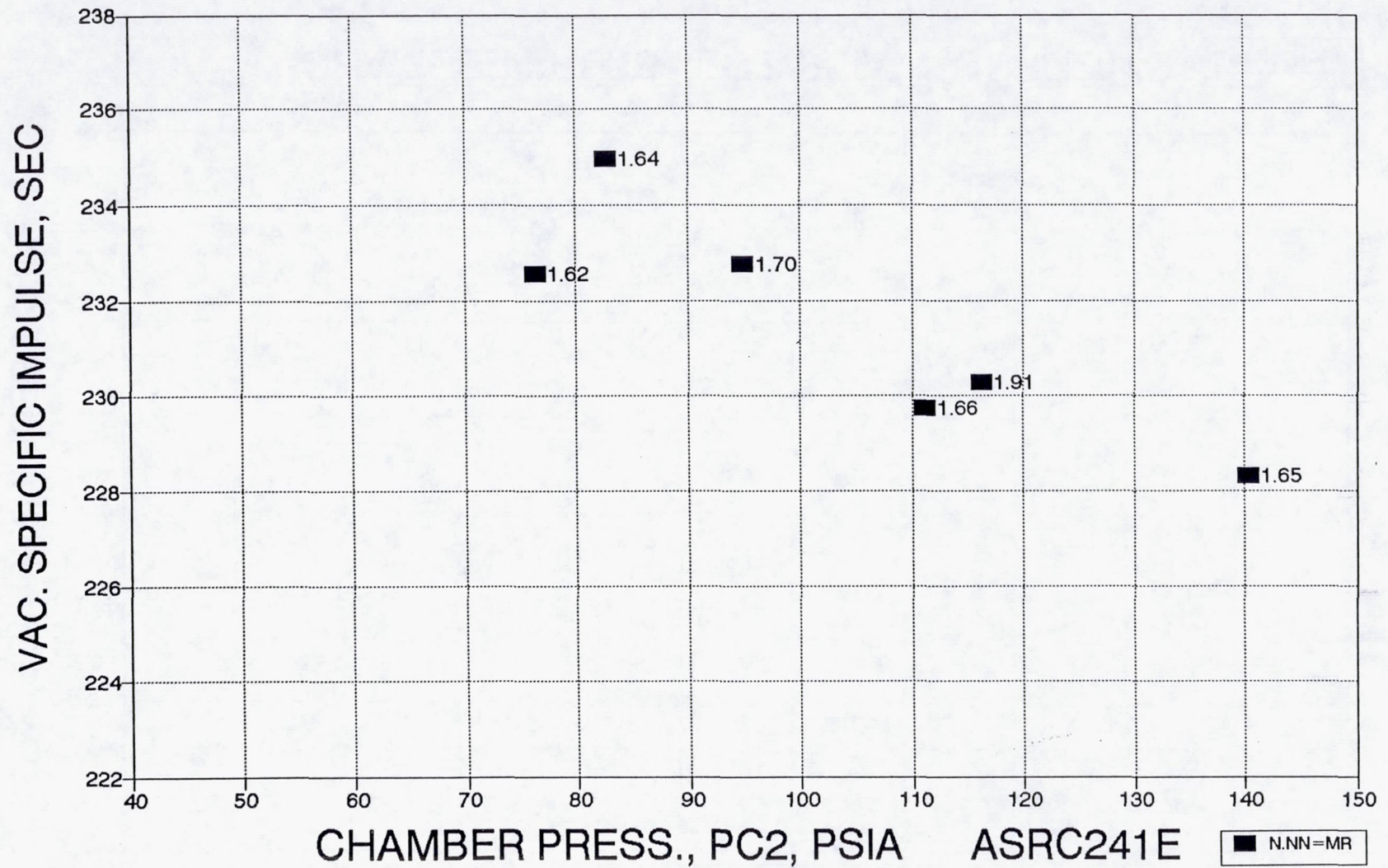


Figure 6.3-12. 100# Isvac Versus Pc-2 – Injector #4, Trip #4RW (128-134) Bay 3

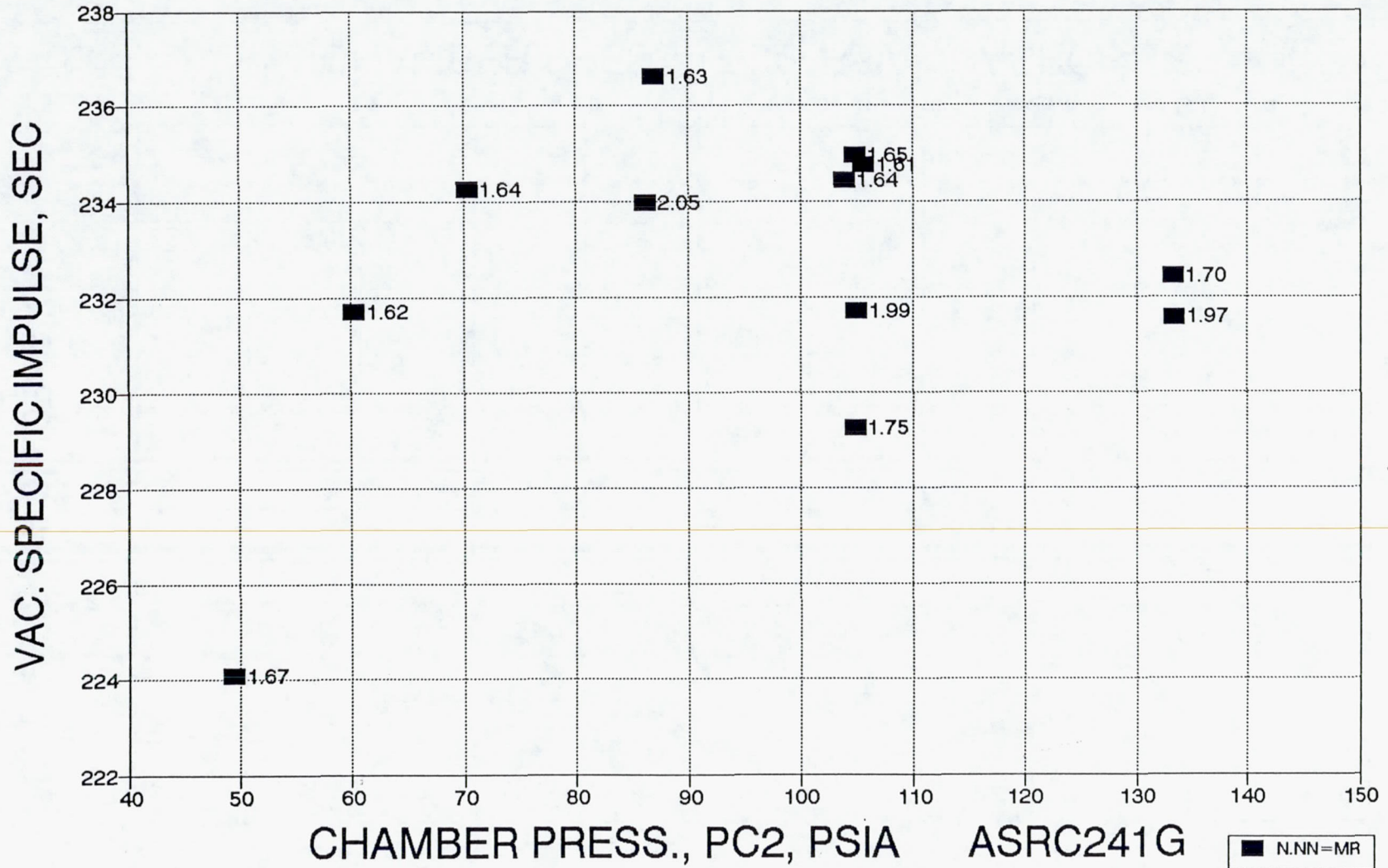


Figure 6.3-13. 100# Isvac Versus Pc-2 – Injector #2, Trip #4RW (135-147) Bay 3

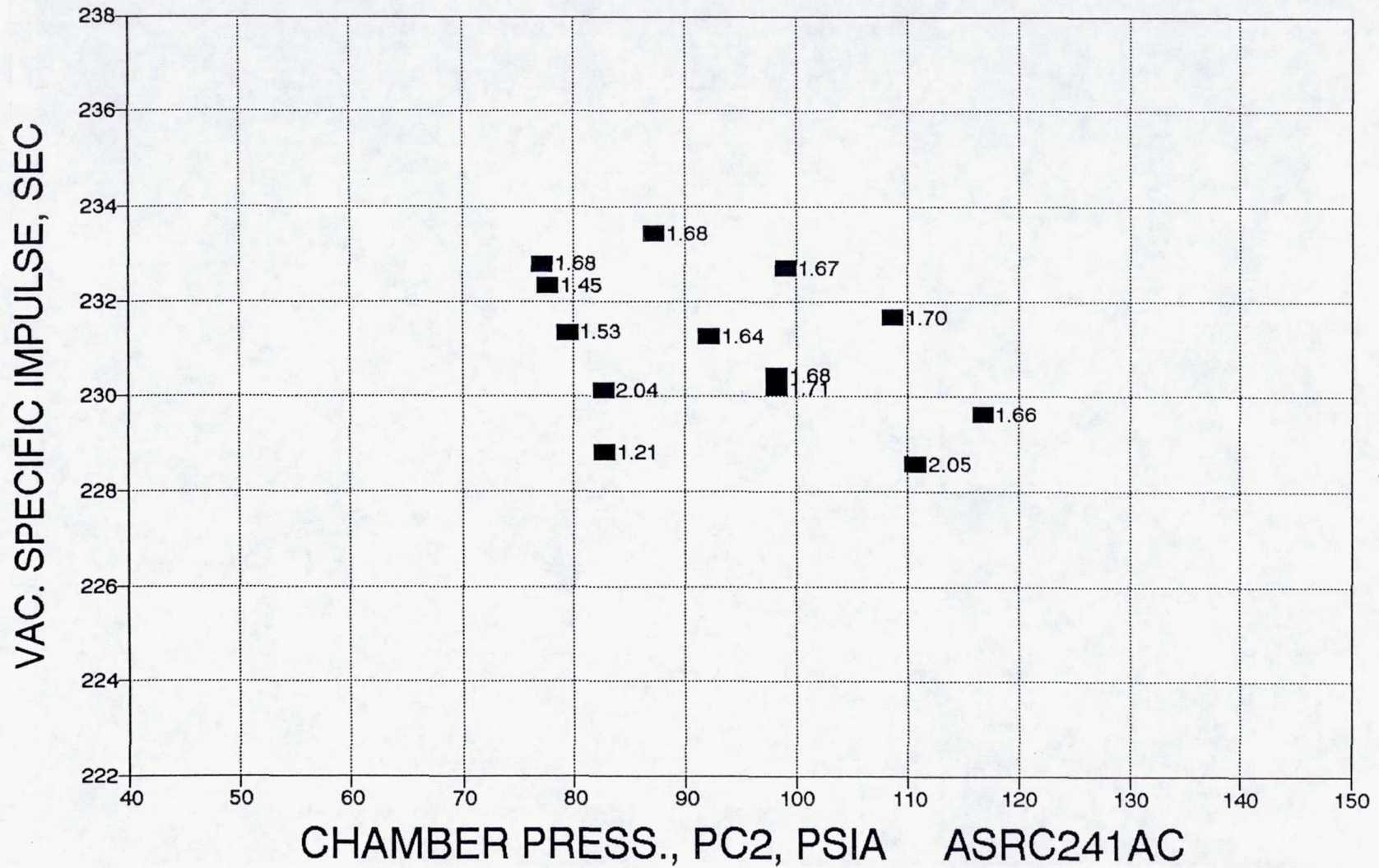


Figure 6.3-14. 100# I_{svac} Versus Pc-2 – Injector SN 2, Trip #4RW (-148-161) Bay 2

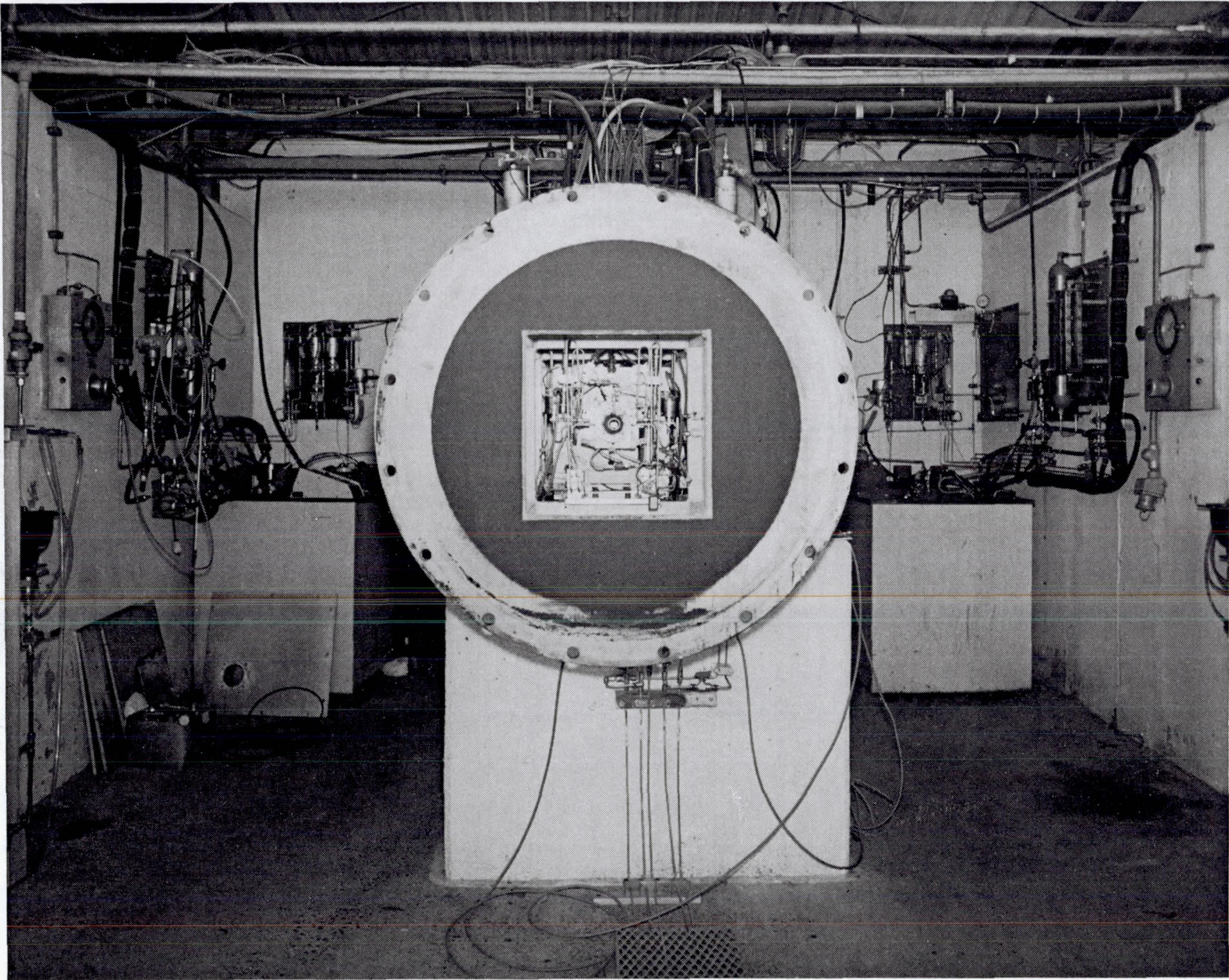


Figure 6.3-15. View of Bay 2 Test Cell



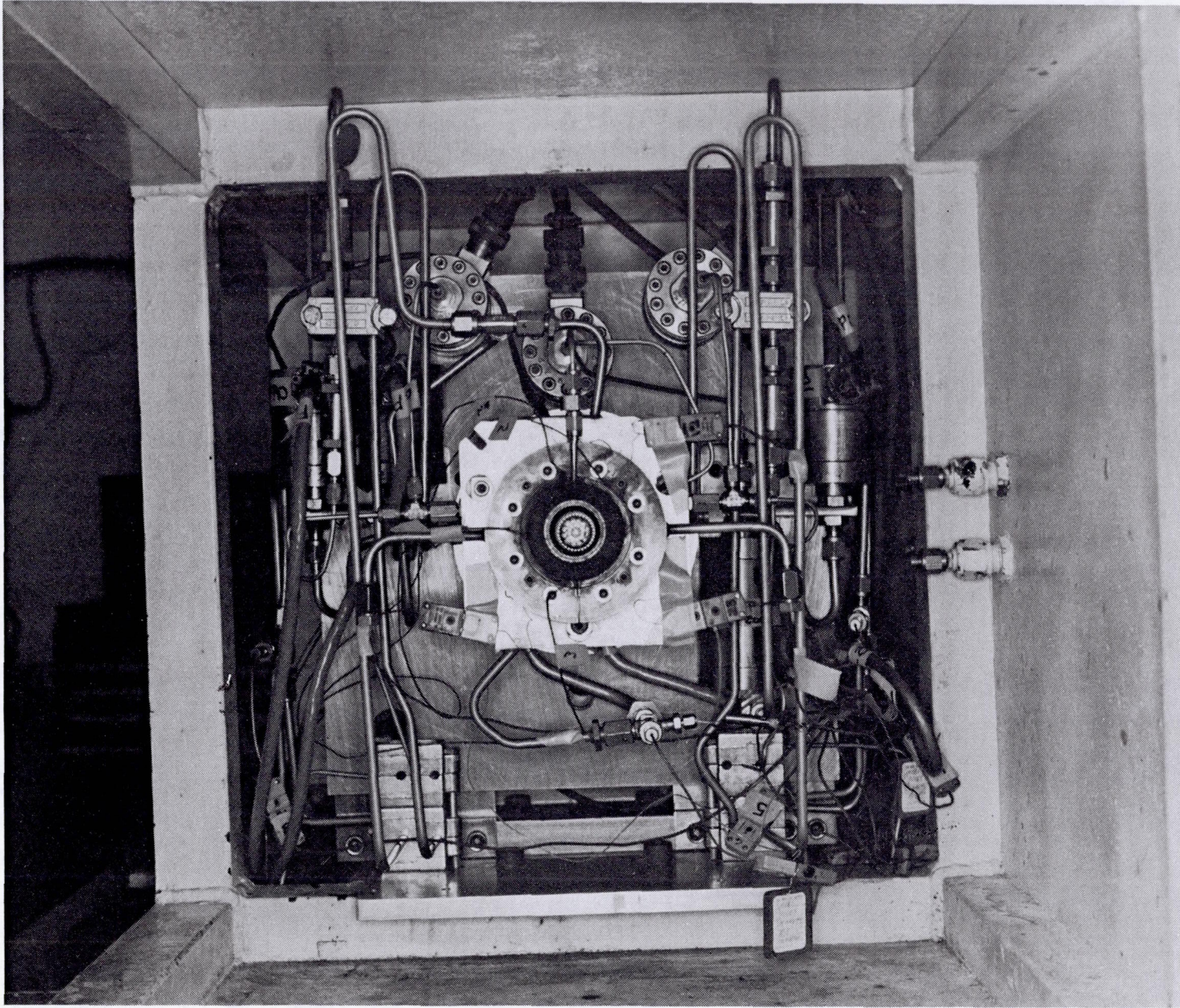


Figure 6.3-16. View of Nozzle Exit and Aft End of Bay 2 Stand

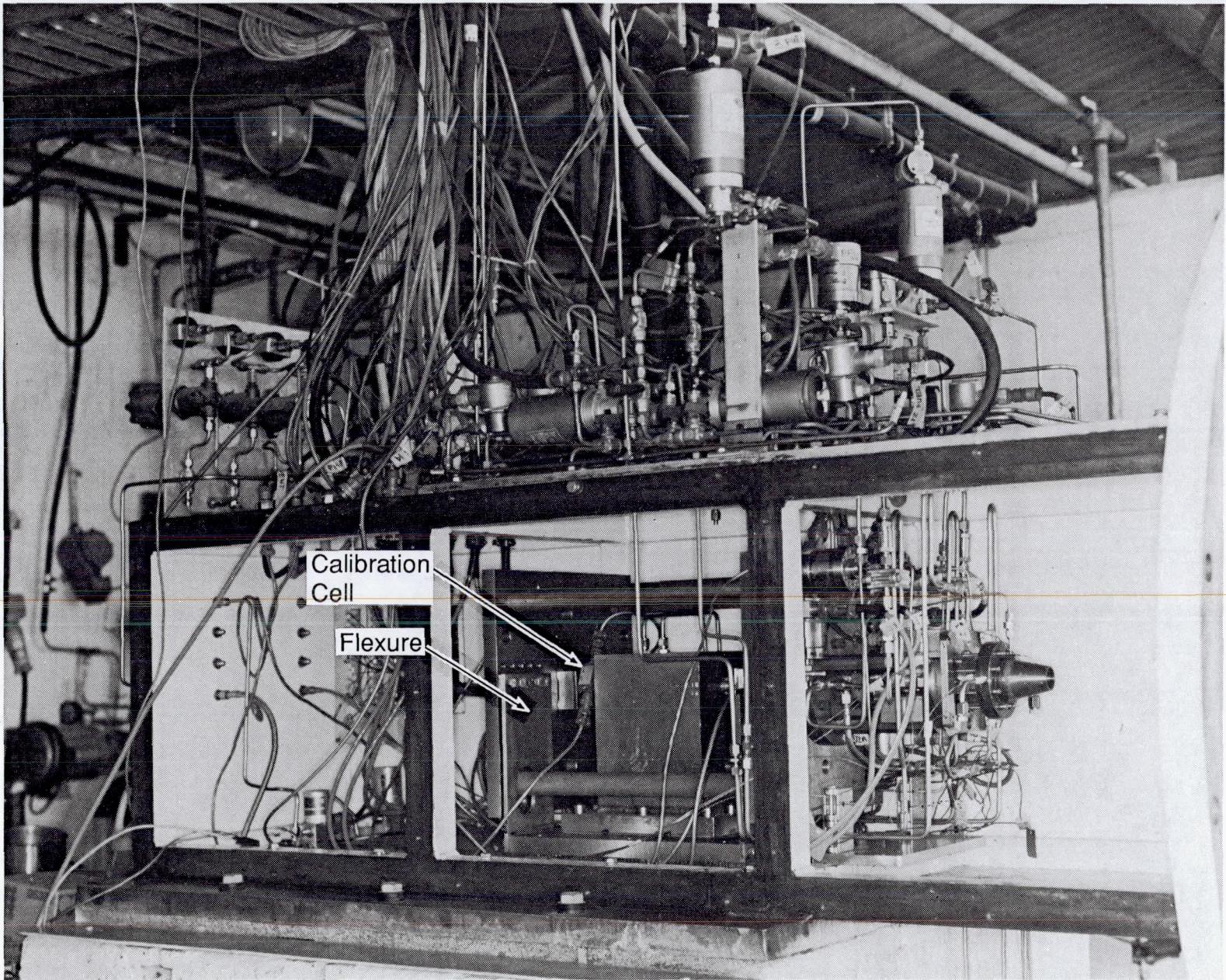


Figure 6.3-17. Side View of Bay 2 Thrust Stand

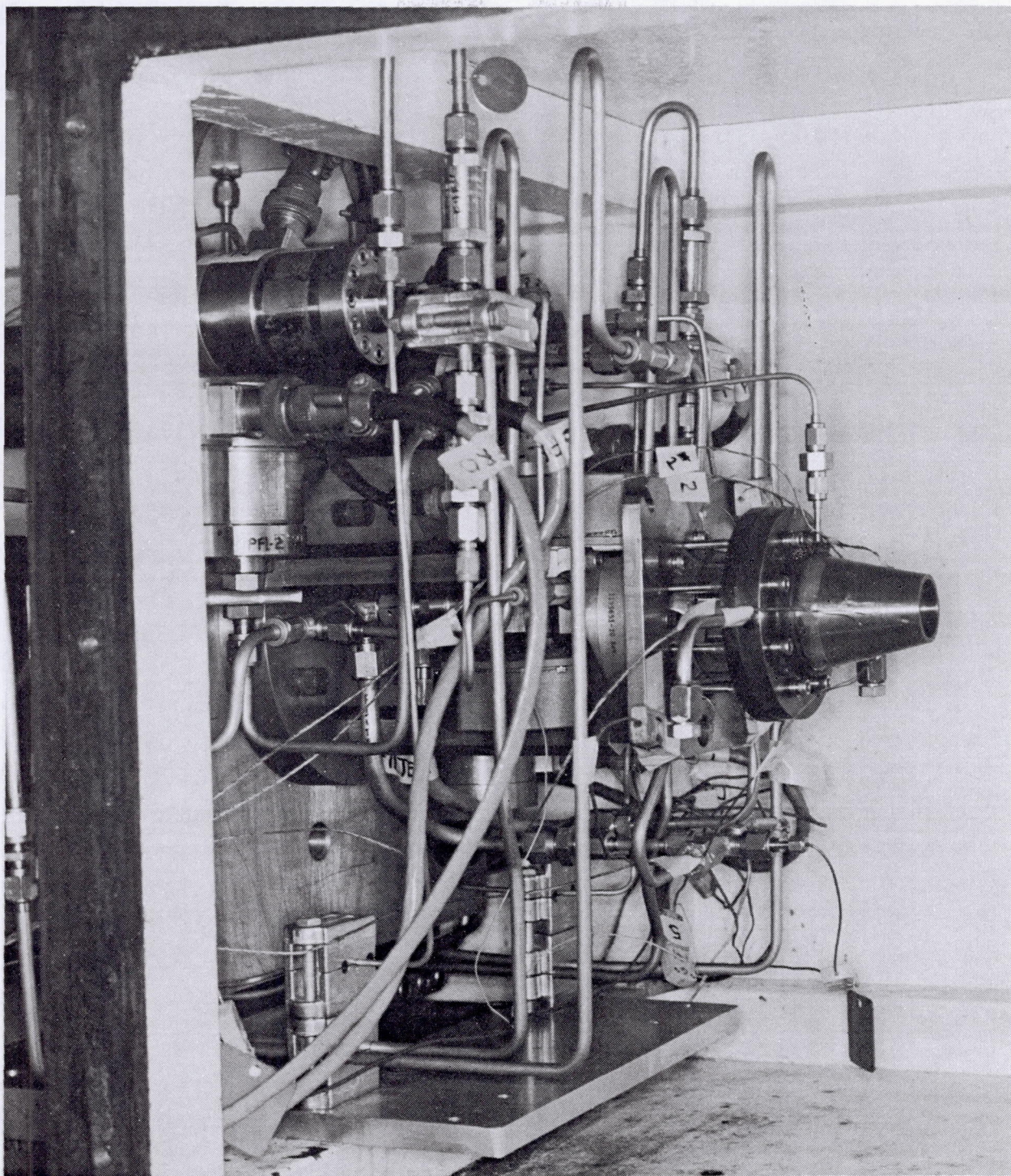


Figure 6.3-18. Heat Sink 1.6:1 Chamber in Bay 2 Stand

6.3, Hot Fire Testing (cont.)

Figure 6.3-19 is a portion of a series of sequence photos during Test -160 showing pre FS-1, FS-1 + 120 ms and FS-1 + 820 ms.

Sea level checkout tests of the Bay 2 test stand are presented in Table 6.3-3. The thrust stand is repeatable, with a very low thrust bias. The measured bias is plotted in Figure 6.3-20; the values are within $\pm 0.05\%$ of the average over the thrust range of 60 to 90 lbf.

Results for the sea level tests are summarized in Table 6.3-3. Table 6.3-4 is the instrumentation list for these tests.

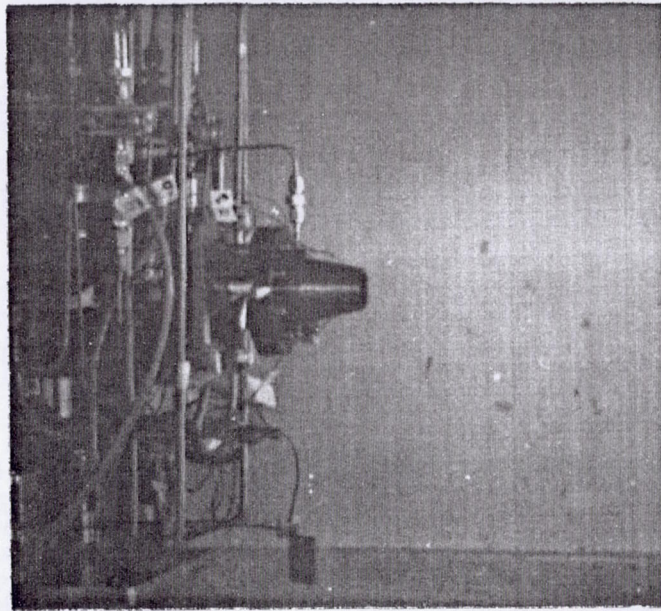
Specific impulse versus mixture ratio for injector SN 2 at 1.68:1 is plotted in Figure 6.3-21; fuel coolant ΔT is shown in Figure 6.3-22. Maximum measured temperature for the downstream end of the cooled adapter is plotted in Figure 6.3-23 as a function of chamber pressure. Component flow coefficients as a function of oxidizer and fuel flow rates are shown in Figures 6.3-24 and -25.

Injector SN 6-1 Sea Level Tests

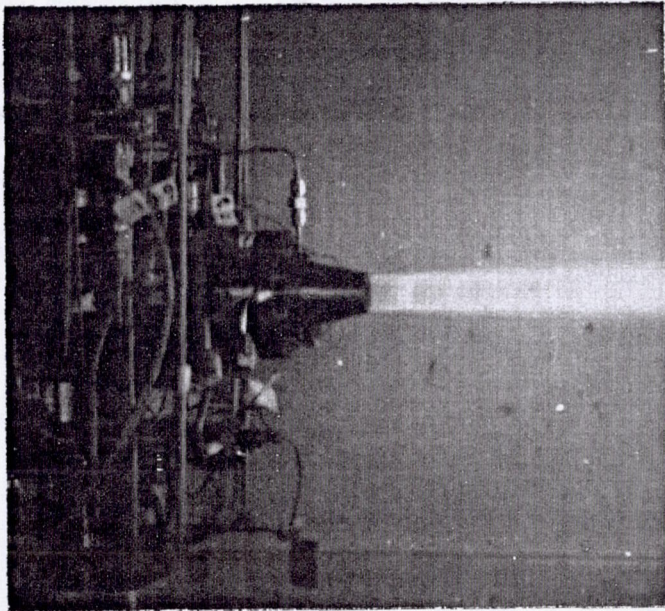
A final series of sea level compatibility tests was run, group F, with injector SN 6-1, Tests 247 through -258. The performance results for these tests are summarized in Table 6.3-5; the measured erosion rate data are shown in Figure 6.3-26. This injector showed erosion rates similar to those measured for injector SN 2. Since the latter injector was operated for over 5 hours without chamber damage in Ref. 3, these tests indicated that the SN 6 injectors should be as long lived as the SN 2 injector with similar low erosion rates.

The data for injectors SN 2 and SN 6-1 show a definite correlation of mass loss, directly with MR and inversely with P_c , over the MR range of ~ 1.6 to 2.0 and P_c ranges of ~ 85 to 115 psia. The approximate trends are as follows:

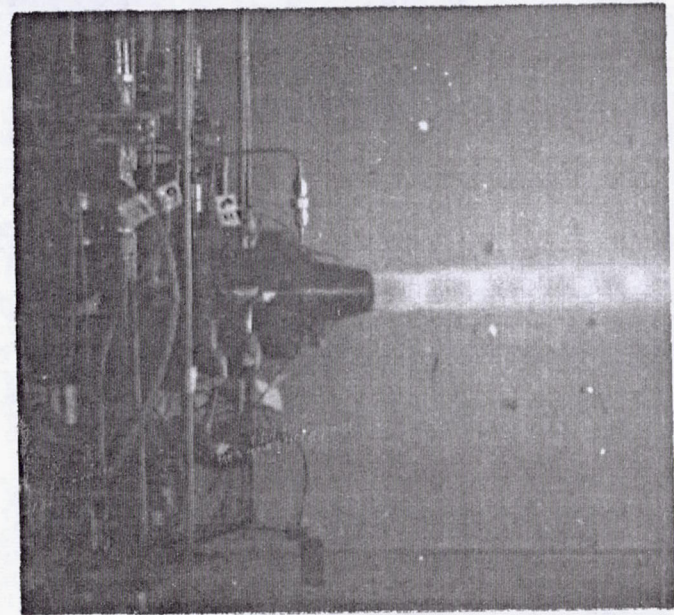
- P_c - Increasing P_c from 90 to 110 psia decreases mass loss rate by about an order of magnitude
- MR - Increasing MR from nominal to 1.80 increases mass loss rate by a factor of 3.
- Injector - The limited data set indicates that the SN 6-1 injector may have a somewhat higher erosion rate than SN 2 and the same loss rate as SN 4.
- Uniformity - The SN 6-1 erosion appears to be uniform.



Pre FS-1



Ignition Transient



Steady State

Figure 6.3-19. Frames From Sequence Camera Coverage of Bay 2
Sea Level Checkout Test With SN 2 Injector

Table 6.3-3. 100 lb Thruster – Bay 2 Sea Level Tests (1.68:1 Area Ratio)

1.6:1/SEA LEVEL/INJ SN 2/TRIP 4RW 6-21 THRU 6-25-91

RUN NO.	FIRING TIME	PC2	MR	Isvac	C*	STAND	PROPELLANT*		TTR	TC	DELTA	STAND	STAND	REGEN	(INCLUDES FILTER)		INJECTOR	INJECTOR
							WO	WF							MAX	MAX		
	sec	psia	O/F	sec	ft/sec	BIAS	lbm/sec		oF	oF	oF	KWOX	KWFU	KWFRE	KWOXV	KWFV	KWOJ	KWFJ
148	1	77.7	1.45	232.4	5411	1.0059	0.1638	0.1059	876	130	38.1	0.01483	0.01430	0.02490	0.03346	0.02993	0.01738	0.01456
149	1	SHUTDOWN ON FAULTY TTR-3 THERMOCOUPLE; NOT REDUCED																
150	7	79.4	1.53	231.4	5341	1.0061	0.1627	0.1061	1648	548	105.0	0.01487	0.01426	0.02579	0.03335	0.03062	0.01652	0.01469
151	7	98.3	1.71	230.2	5317	1.0062	0.2111	0.1231	1651	444	105.7	0.01544	0.01446	0.02576	0.03365	0.03216	0.01680	0.01465
152	7	98.2	1.68	230.4	5321	1.0069	0.2090	0.1247	1624	445	105.9	0.01544	0.01446	0.02613	0.03383	0.03134	0.01695	0.01468
153	7	92.2	1.64	231.3	5329	1.0066	0.1943	0.1186	1627	461	110.3	0.01537	0.01441	0.02616	0.03359	0.03118	0.01699	0.01470
154	7	116.8	1.66	229.6	5293	1.0059	0.2491	0.1501	1488	479	86.9	0.01555	0.01477	0.02633	0.03362	0.03168	0.01701	0.01458
155	7	110.7	2.05	228.6	5263	1.0063	0.2554	0.1248	1651	546	109.8	0.01558	0.01451	0.02632	0.03394	0.03142	0.01726	0.01461
156	7	82.6	2.04	230.1	5309	1.0067	0.1890	0.0924	1642	564	123.7	0.01524	0.01411	0.02580	0.03294	0.03005	0.01758	0.01474
157	7	82.8	1.21	228.8	5273	1.0064	0.1553	0.1287	1305	451	85.2	0.01500	0.01455	0.02639	0.03259	0.03146	0.01766	0.01466
158	7	108.7	1.70	231.7	5335	1.0060	0.2318	0.1367	1500	516	96.3	0.01548	0.01466	0.02650	0.03374	0.03182	0.01756	0.01460
159	7	87.3	1.68	233.4	5390	1.0061	0.1833	0.1094	1641	505	111.4	0.01521	0.01438	0.02627	0.03326	0.03097	0.01766	0.01470
160	7	77.1	1.68	232.8	5379	1.0062	0.1625	0.0966	1587	520	106.7	0.01505	0.01421	0.02617	0.03294	0.03023	0.01764	0.01476
161	7	99.0	1.67	232.7	5363	1.0064	0.2090	0.1248	1553	515	104.0	0.01537	0.01459	0.02650	0.03354	0.03141	0.01757	0.01463

*BASED ON AVERAGE OF PDFM CALIBRATION

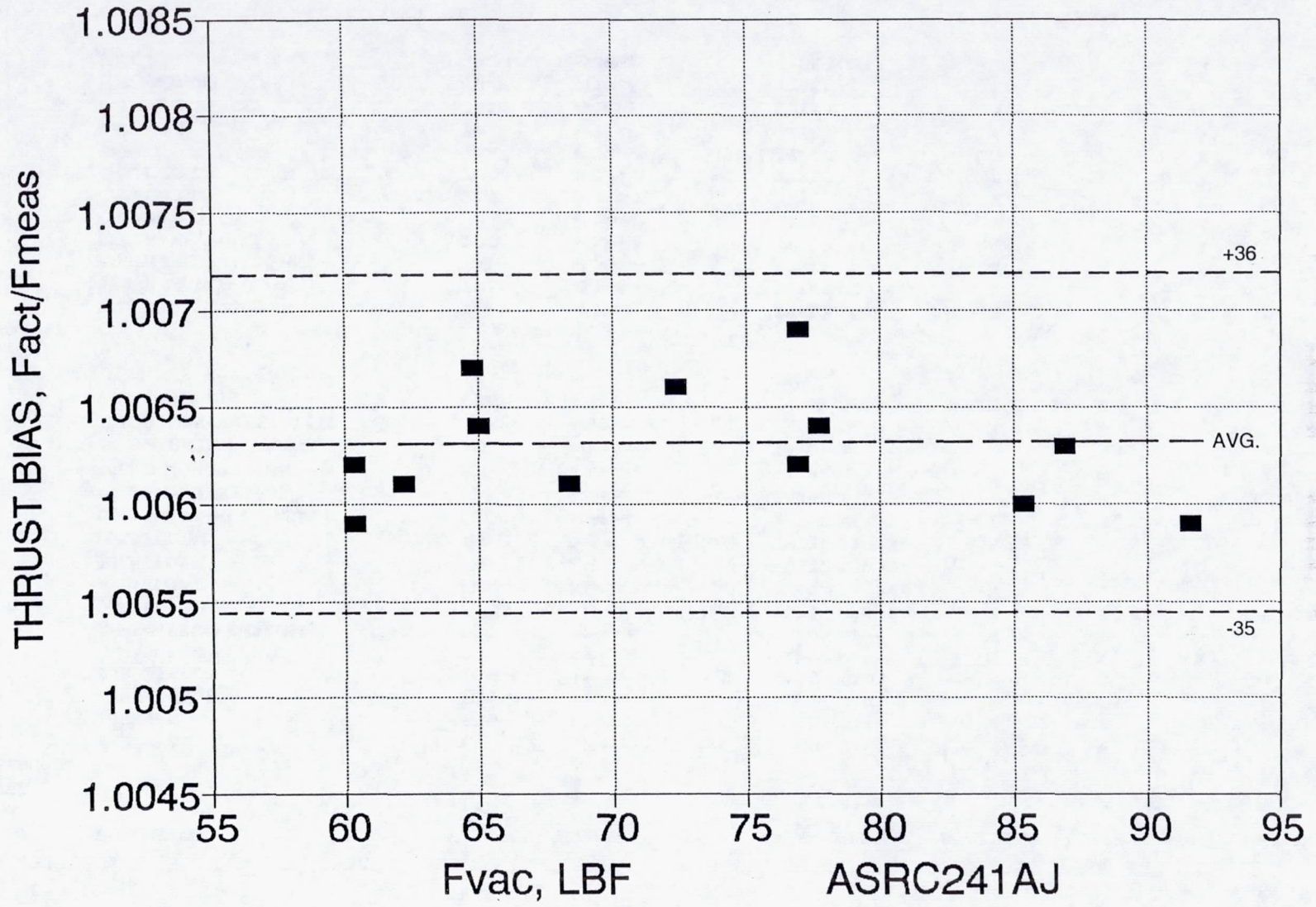


Figure 6.3-20. Thrust Bias vs Thrust

Table 6.3-4. 100 lb Bay 2 Checkout Instrumentation List - Heat Sink Chamber (at S.L.), Sheet 1 of 2

FUNCTION	PARAMETER	SYMBOL	RANGE	TRANSDUCER	DIGITAL	RECORDING		
						O-GRAPH	VISUAL	FM TAPE
THRUSTER PERFORMANCE								
	THRUST A	FA	0-200 lbf	STRAIN GAGE	X	X		X
	THRUST B	FB	0-200 lbf	STRAIN GAGE	X	X		
	THRUST CAL A	FCAL-A	0-200 lbf	STRAIN GAGE	X	X		
	THRUST CAL B	FCAL-B	0-200 lbf	STRAIN GAGE	X	X		
	CHAMB. PRESS 1 (INJ)	PC-1	0-200 psia	TABOR 206	X	X		X
	CHAMB. PRESS 2 (CHAMB)	PC-2	0-200 psia	TABOR 206	X	X		
	OXID FLOW 1	FMO-1	0.13-0.3 lbrn/sec (prop.)	TURBINE METER	X	X		
	OXID FLOW 2	FMO-2	0.13-0.3 lbrn/sec (prop.)	TURBINE METER	X	X		
	FUEL FLOW 1	FMF-1	0.08-0.3 lbrn/sec (prop.)	TURBINE METER	X	X		
	FUEL FLOW 2	FMF-2	0.08-0.3 lbrn/sec (prop.)	TURBINE METER	X	X		
	OXID. VALVE INLET PRESS.	POL-2	0-500 psia	TABOR 206	X	X		
	OXID INJ. INLET PRESS.	POJ	0-500 psia	TABOR 206	X	X		
	FUEL INJ. INLET PRESS.	PFJ	0-500 psia	TABOR 206	X	X		
	FUEL REGEN INLET PRESS.	PFL-2	0-500 psia	TABOR 206	X	X		
	FUEL REGEN OUTLET PRESS.	PFRO	0-500 psia	TABOR 206	X	X		
	VALVE VOLTAGE	VTVC	0-30 Vdc		X	X		
THRUSTER TEMPERATURE								
	VALVE BODY TEMP.	TVB	40-500°F	TYPE K	X			
	REGEN SECTION T1 (TRIP)	TTR-1	40-2000°F	TYPE K	X			X
	REGEN SECTION T2 (TRIP)	TTR-2	40-2000°F	TYPE K	X			X
	REGEN SECTION T3 (TRIP)	TTR-3	40-2000°F	TYPE K	X			X
	CHAMBER T1	TC-1	40-2000°F	TYPE K	X			X
	CHAMBER T2	TC-2	40-2000°F	TYPE K	X			X
	CHAMBER T3	TC-3	40-2000°F	TYPE K	X			X
	CHAMBER T4	TC-4	40-2000°F	TYPE K	X			X
	OXID INLET TEMP	TOJ	40-1000°F	TYPE K	X			
	FUEL REGEN INLET	TR-IN	40-1000°F	TYPE K	X			X
	FUEL REGEN OUTLET	TR-OUT	40-2000°F	TYPE K	X			
	FUEL REGEN INTERIOR	TR-PROP	40-5000°F	TYPE K(.010")	X			X
OPTICAL	OPTICAL MULTICHANNEL ANALYSER (OMA)				RECORDED SEPARATELY			
STABILITY	CHAMBER HIGH FREQ	PHF	500-15000Hz	KISTLER 601		X		X

Table 6.3-4. 100 lb Bay 2 Checkout Instrumentation List - Heat Sink Chamber (at S.L.), Sheet 2 of 2

FUNCTION	PARAMETER	SYMBOL	RANGE	TRANSDUCER	DIGITAL	RECORDING		
						O-GRAPH	VISUAL	FM TAPE
FACILITY PRESSURES	OXID TANK	POTS	0-500 psia	TABOR 206	X			X
	FUEL TANK	PFTS	0-500 psia	TABOR 206	X			X
	OXID LINE	POL-1	0-500 psia	TABOR 206	X			X
	FUEL LINE	PFL-1	0-500 psia	TABOR 206	X			X
FACILITY TEMPERATURES	OXID LINE	TOL	40-1000F	TYPE K	X			X
	FUEL LINE	TFL	40-1000F	TYPE K	X			X
	TEST CELL	TCELL	0-2500F	TYPE K	X			X

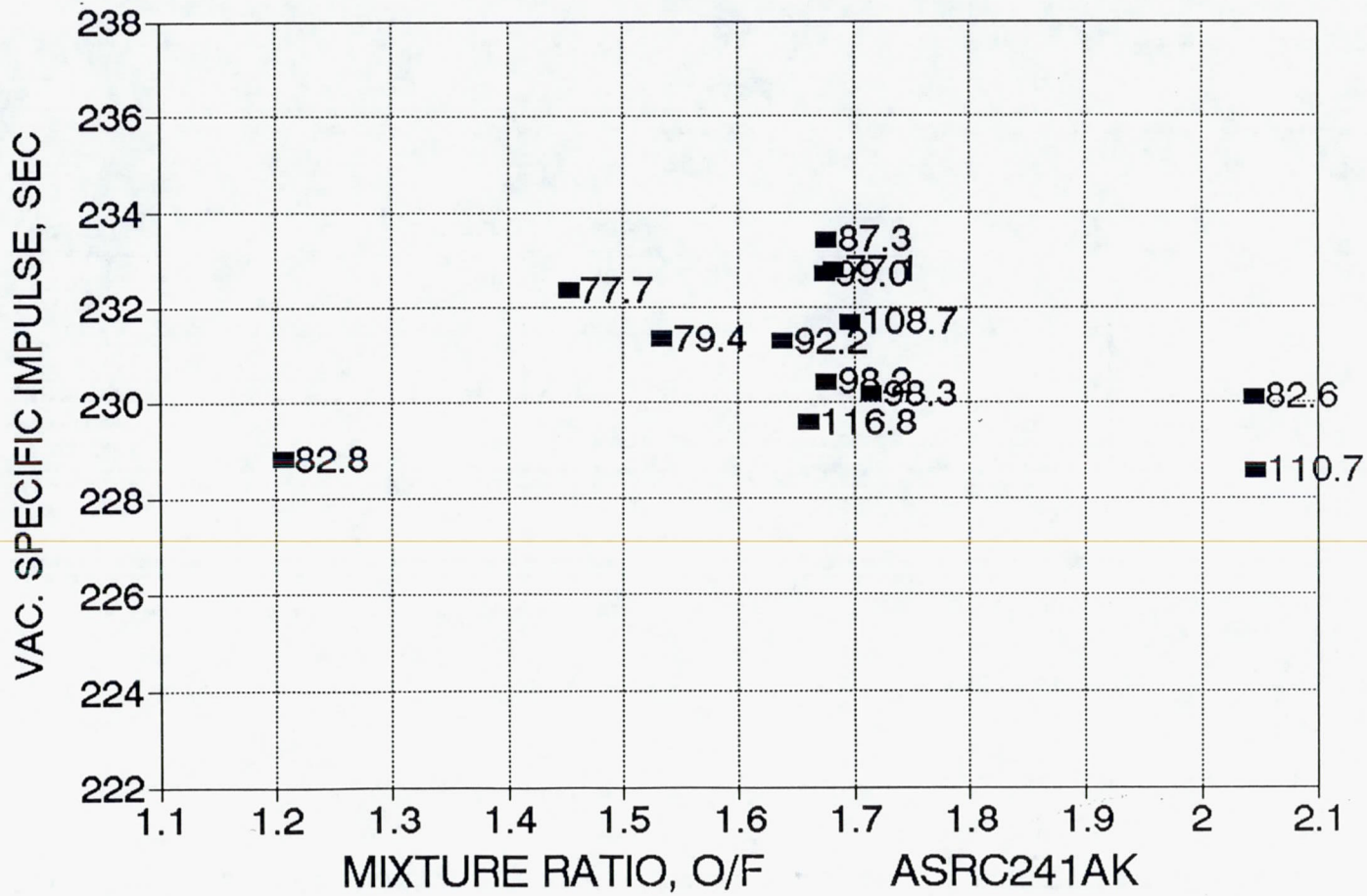


Figure 6.3-21. 100# I_{svac} Versus MR – Bay #2 – Injector #2, Trip #4RW (148-161)

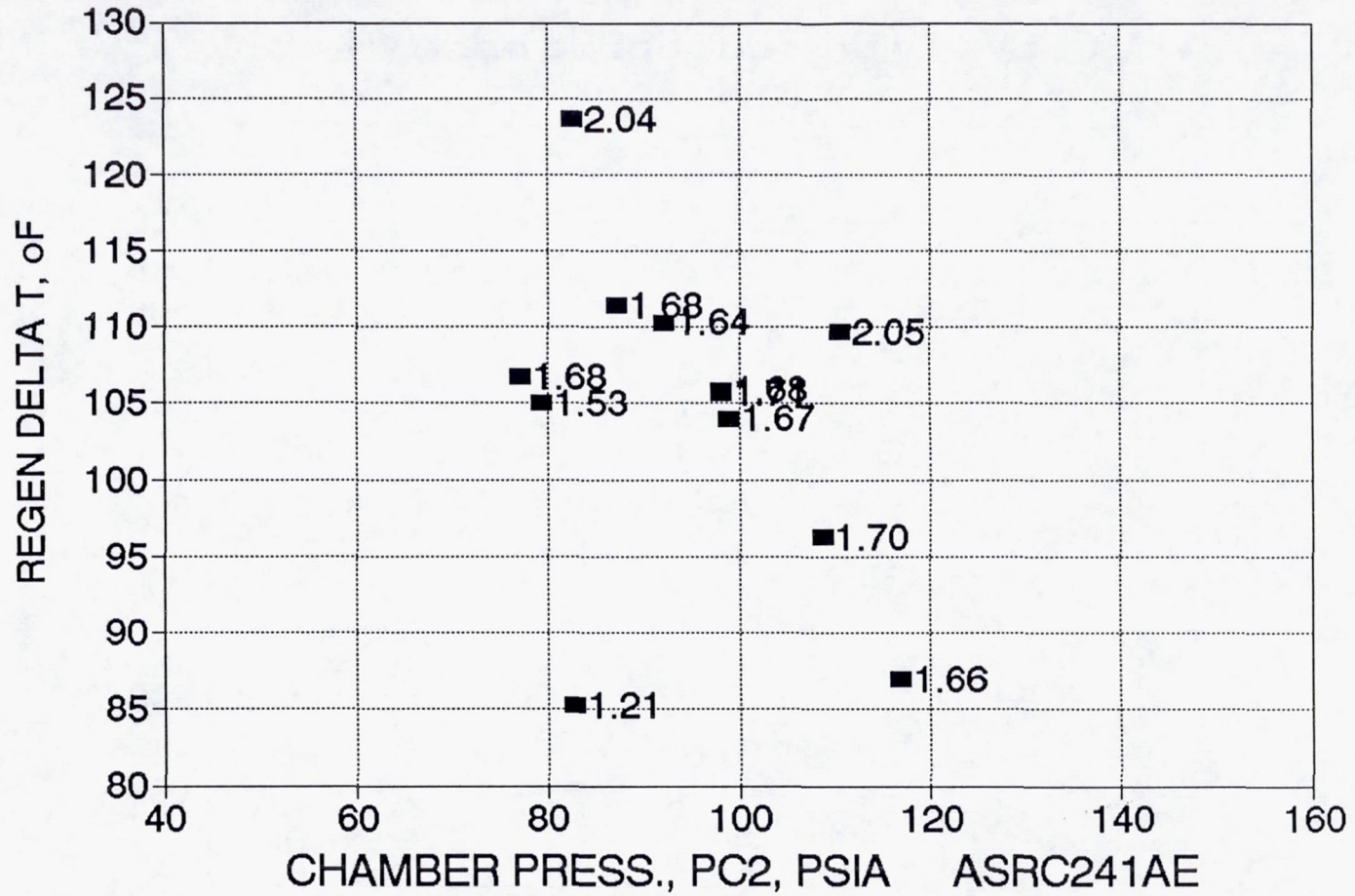


Figure 6.3-22. 100# Delta T Regen Versus Pc-2 – Bay #2 – Injector #2, Trip #4RW (148-161)

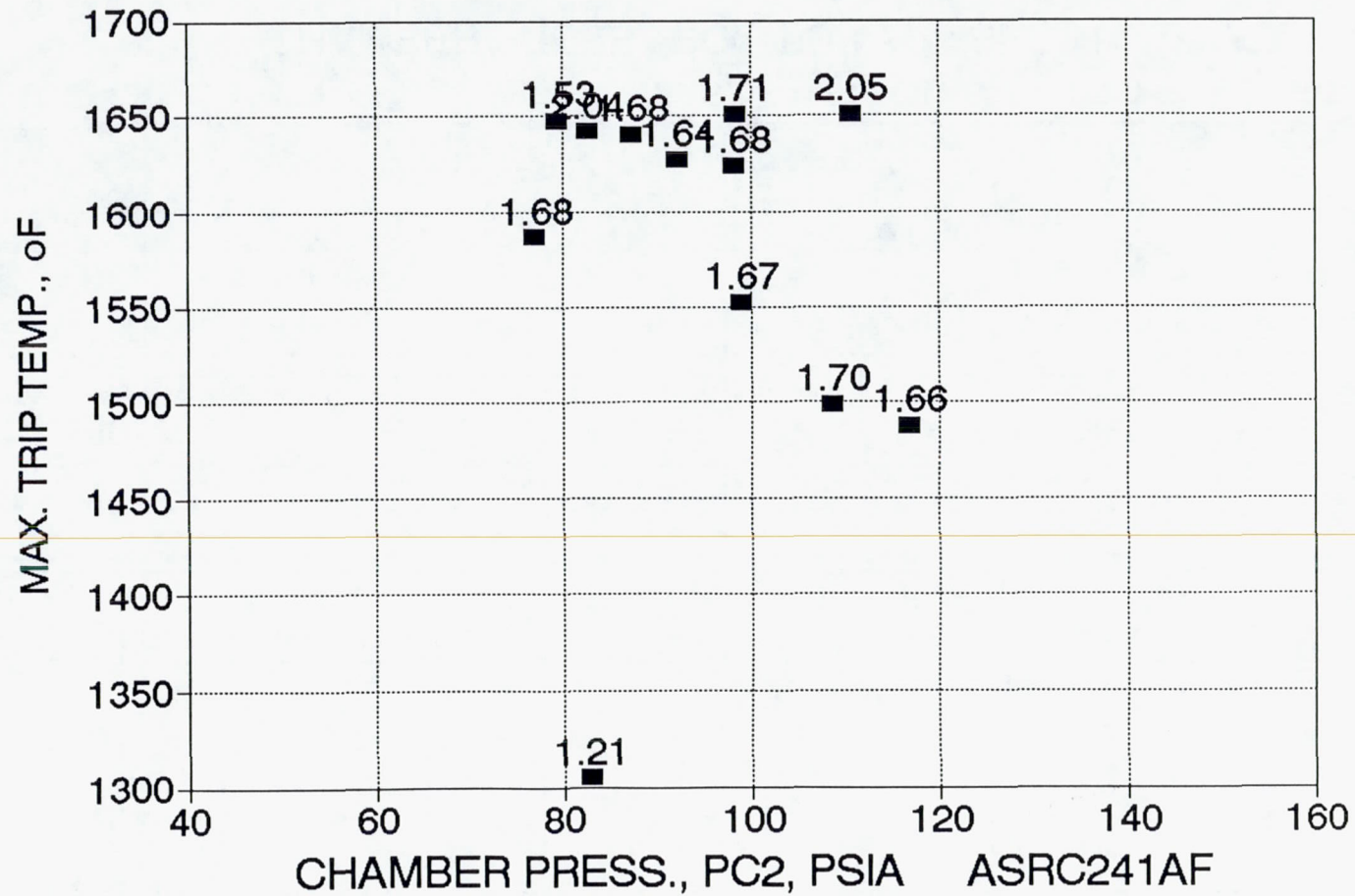


Figure 6.3-23. 100# Max Trip Temp Versus Pc-2 – Bay #2 – Injector #2, Trip #4RW (148-161)

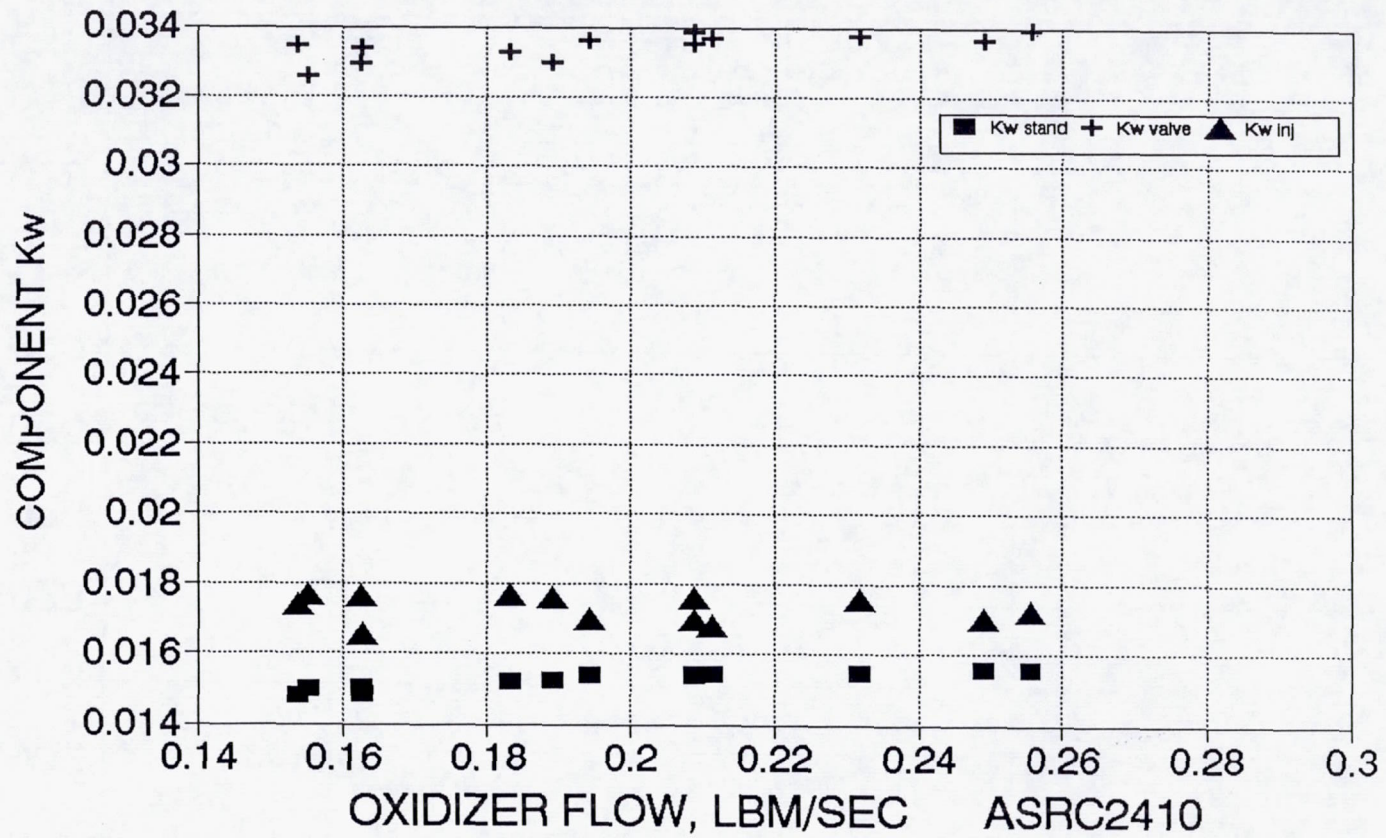


Figure 6.3-24. Oxid Kw vs Oxid Mass Flow – Injector #2, Tests -148 – -161

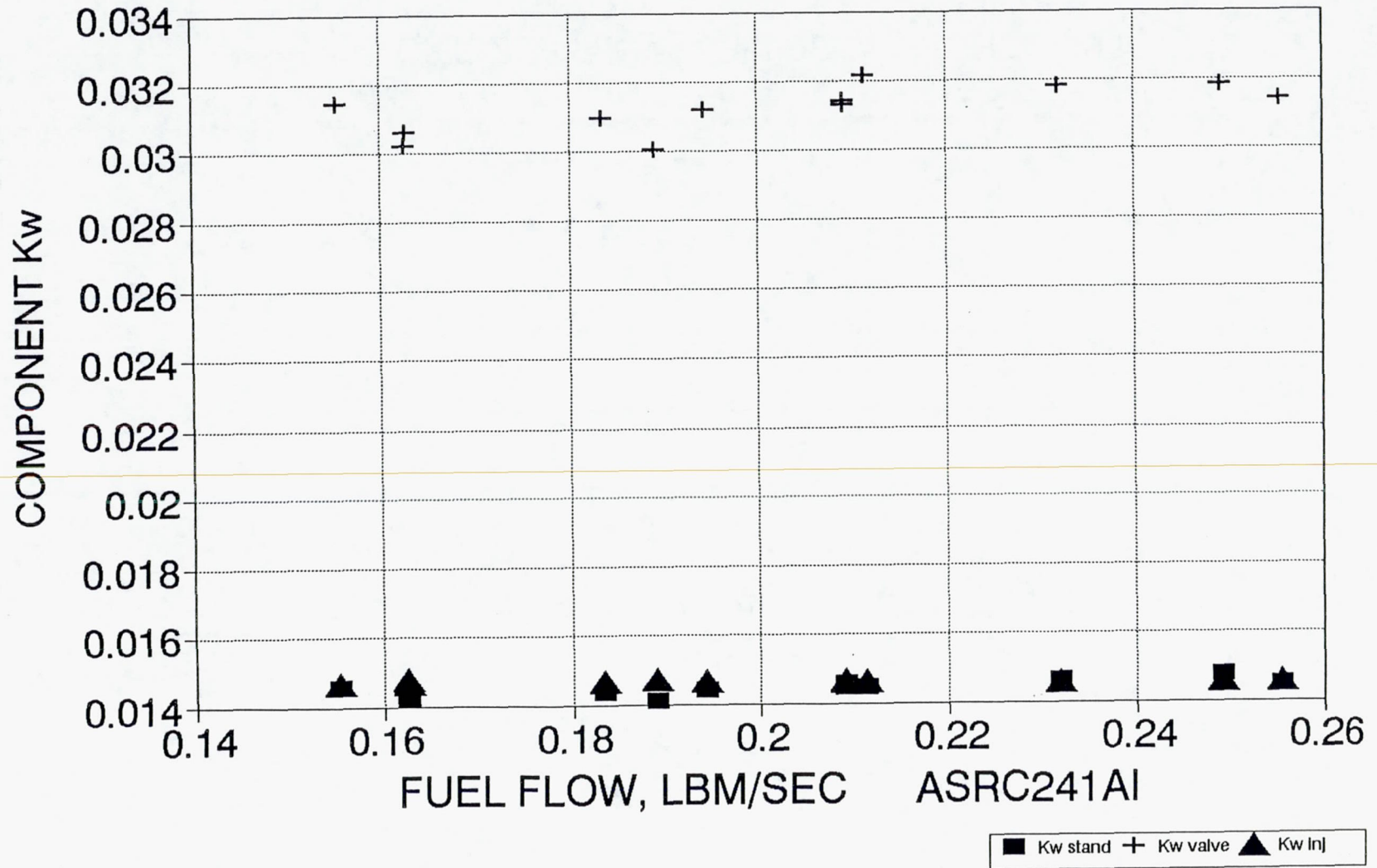


Figure 6.3-25. Fuel Kw vs Fuel Mass Flow – Injector #2, Tests -148 – -161

Table 6.3-5. Results of Compatibility Testing

SEA LEVEL, 1.6:1 Re FOIL TESTS

RUN NO.	DATE	INJECTOR	FIRING TIME, sec	DATA TIME sec	Pc psia	PDFM MR O/F	FOIL	W1 gm	W2 gm	DELTA W, gm	LOSS RATE, gm/HR
247	1-29-92	S/N6-1		Valve input shorted			NONE	--	--	--	--
248	1-29-92	S/N6-1	1	0.755	113.8	1.679	NONE	--	--	--	--
249	1-29-92	S/N6-1	1	0.754	109.6	1.650	NONE	--	--	--	--
250	1-29-92	S/N6-1	1	0.752	88.9	2.160	NONE	--	--	--	--
251	1-29-92	S/N6-1	7	6.51	107.6	1.627	NONE	--	--	--	--
252	1-29-92	S/N6-1	7.00	6.51	104.1	1.637	Re-10	6.8250	6.7828	0.0422	21.70
253	1-29-92	S/N6-1	7.00	6.50	85.8	2.114	Re-11	6.9119	4.6489	2.2630	[1163] *
254	1-29-92	S/N6-1	7.00	6.51	108.9	1.818	Re-12	6.8814	6.8008	0.0806	41.45
255	1-29-92	S/N6-1	4.18	3.50	89.4	1.858	Re-13	6.8116	3.5796	3.2320	[2783] *
256	1-29-92	S/N6-1	7.00	6.51	90.0	1.811	Re-14	6.8088	6.2366	0.5722	294.27
257	1-31-92	S/N6-1	7.00	6.51	115.9	1.800	Re-15	6.2081	6.1374	0.0707	36.36
258	1-31-92	S/N6-1	7.00	6.51	87.0	1.672	Re-16	6.8336	6.5136	0.3200	164.57

* Foil damaged during test.

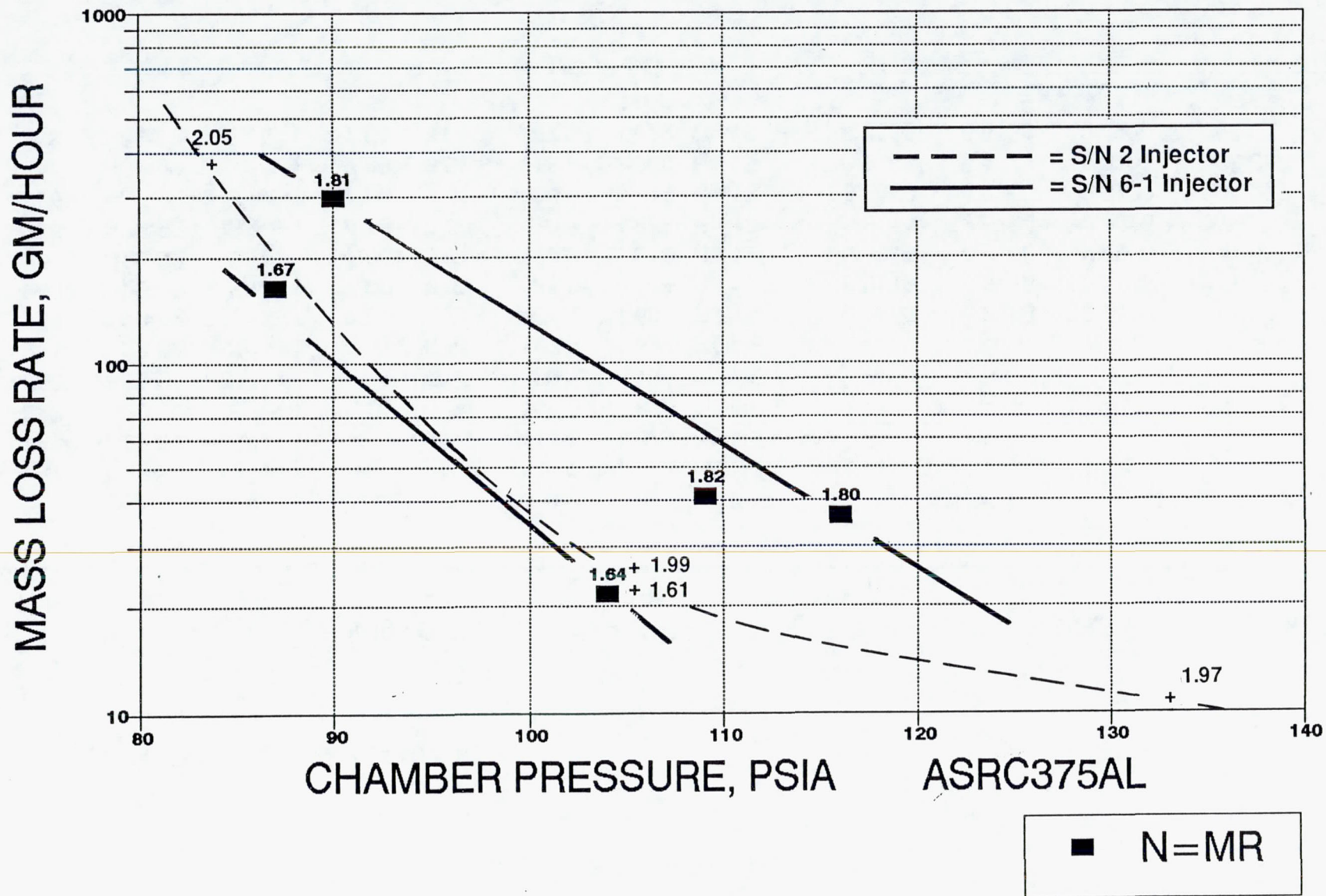


Figure 6.3-26. Mass Loss Rate, GM/HR, Runs -253 to -258, SN 6-1

6.3, Hot Fire Testing (cont.)

Vacuum specific impulse for the 1.68:1 nozzle based on the sea level thrust measurements is shown in Figure 6.3-27.

6.3.2 44:1 Tests

The primary purpose of the 44:1 area ratio tests was to compare injector performance by providing accurate measured thrust data which can be scaled to the full area ratio (286:1) with confidence. As shown in Figure 6.3-28 there is a significant difference between attitude performance and measured performance at 1.68:1 (about 36%), but only a small increment in performance extrapolating from 44:1 to 286:1 (about 4%). In addition, the 44:1 bolt-up hardware utilizes Ir-Re chambers, so test duration is limited by the test facility, not the thruster.

The 44:1 hardware as configured for these tests is shown in Figure 6.3-29. All 44:1 tests used the hydrogen shroud ring with a flow rate of 0.0001842 lbm/sec to protect the exterior of the chamber from oxidation. The Ir-Re chamber, which ends at an area ratio of 16:1, was extended by a stainless steel skirt which continued to 44:1. This skirt was held in place with four tie bolts. A more complete description of this hardware is given in Ref. 3. Figure 6.3-30 is a photograph of the 44:1 hardware setup in Bay 2.

The measurements made in these test groups are shown in Table 6.3-6. Three different flow measurement systems were used in series on each propellant circuit, positive displacement flow meters (PDFM), a pair of redundant turbine flow meters, and micromotion mass flow meters. The propellant delivery system is shown in Figure 6.3-31.

The test facility was modified so that the six-inch diffuser used in these tests could be interchanged with the 14 in. diffuser to be used in 286:1 tests, as shown in Figures 6.3-32 and -33.

6.3.2.1 Injector Design Selection

The first series of 44:1 testing was designated test group C; this testing, summarized in Table 6.3-7, included tests 162 through 170 and 189 through 206.

To make the final injector design selection the three candidate injectors, SN 2, SN 4, and SN 5, were tested at altitude with a 44:1 Ir-Re chamber. This reduced the uncertainty in extrapolation of the performance data to the 286:1 nozzle, relative to using the sea level

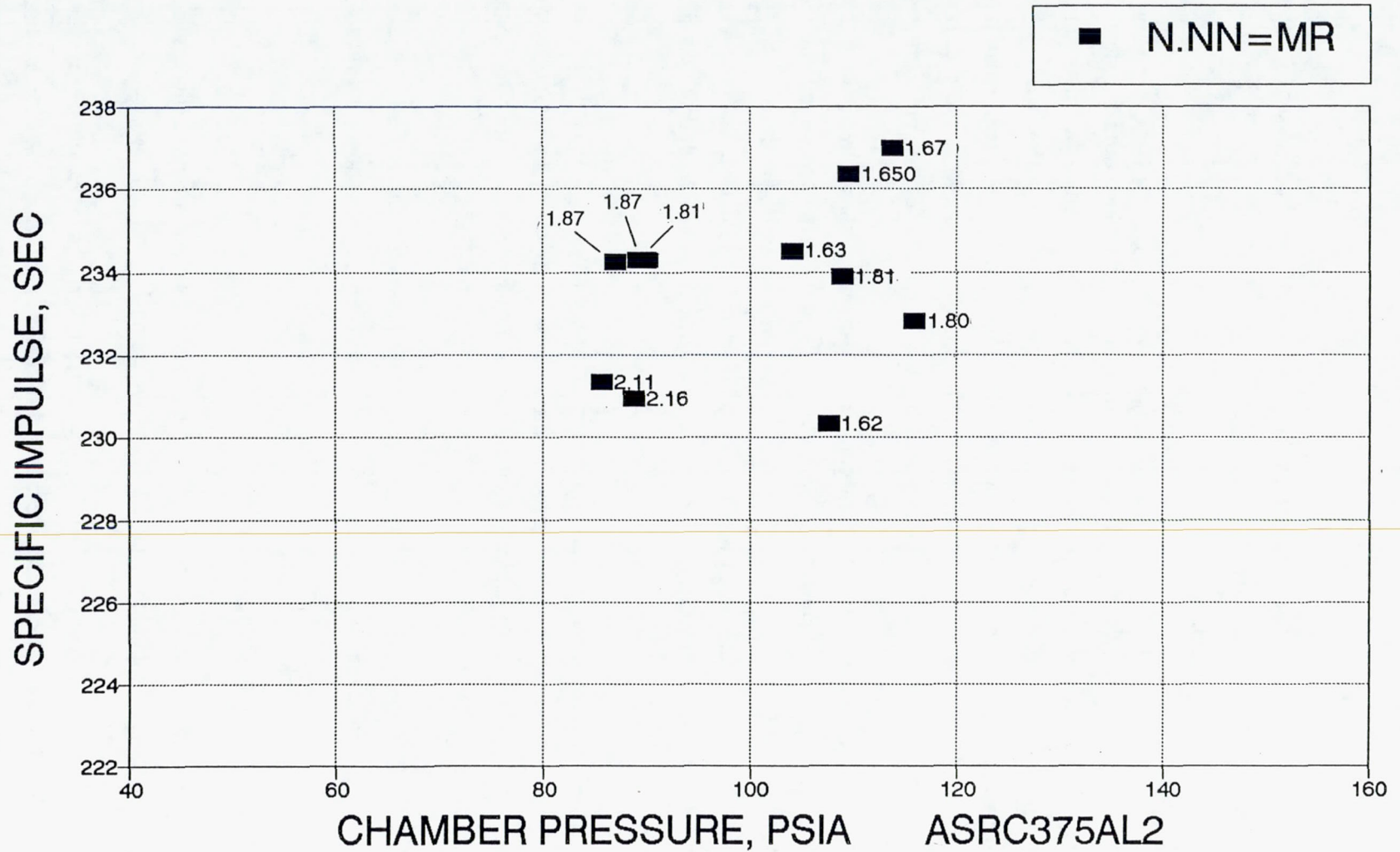


Figure 6.3-27. Isvac vs Chamber Pressure – Runs -247 to -248, Injector SN 6-1, 1.68:1

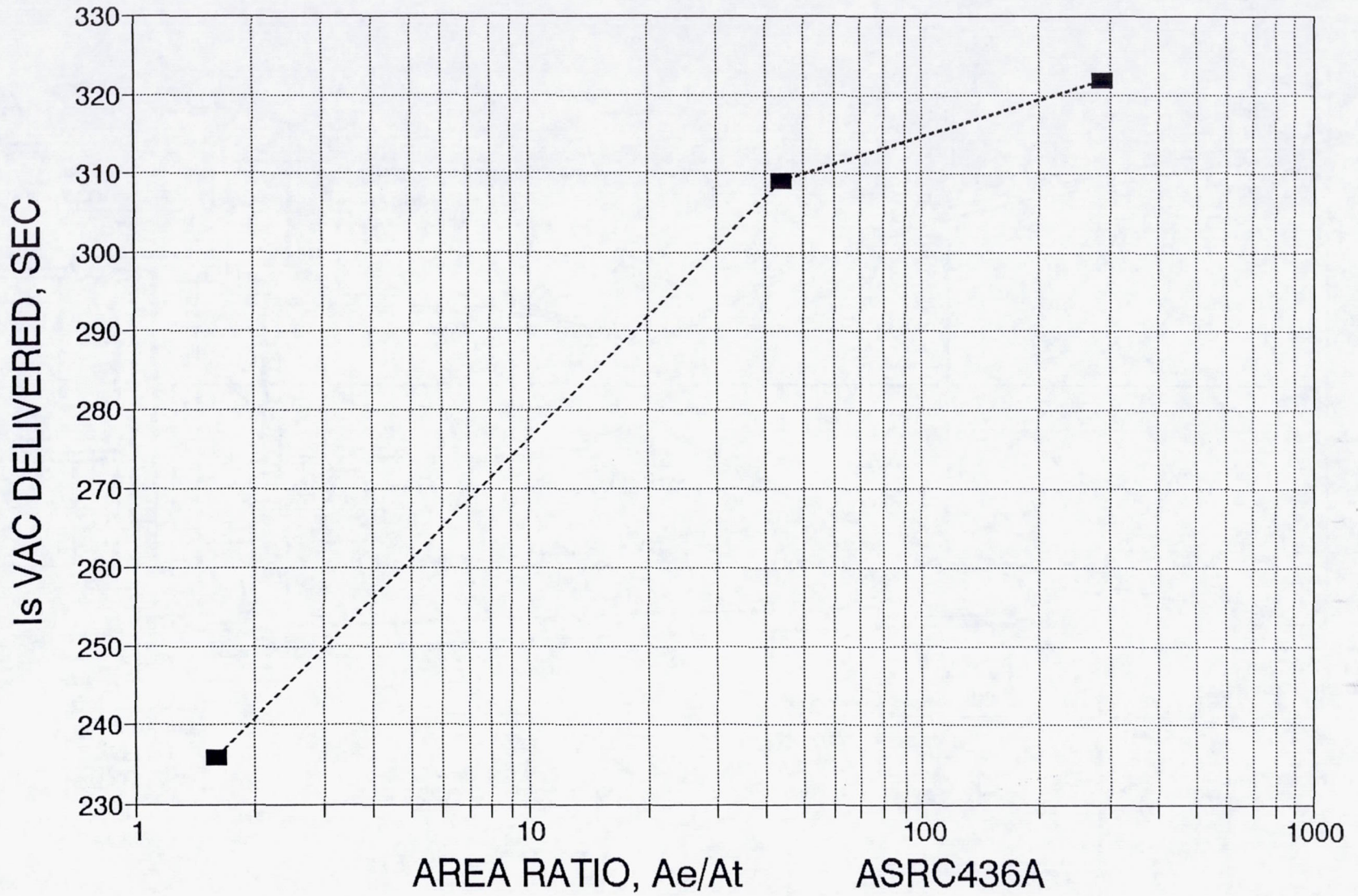


Figure 6.3-28. Measured I_{svac} vs Area Ratio – Ir-Re Thruster, NTO/MMH, MR = 1.65

170

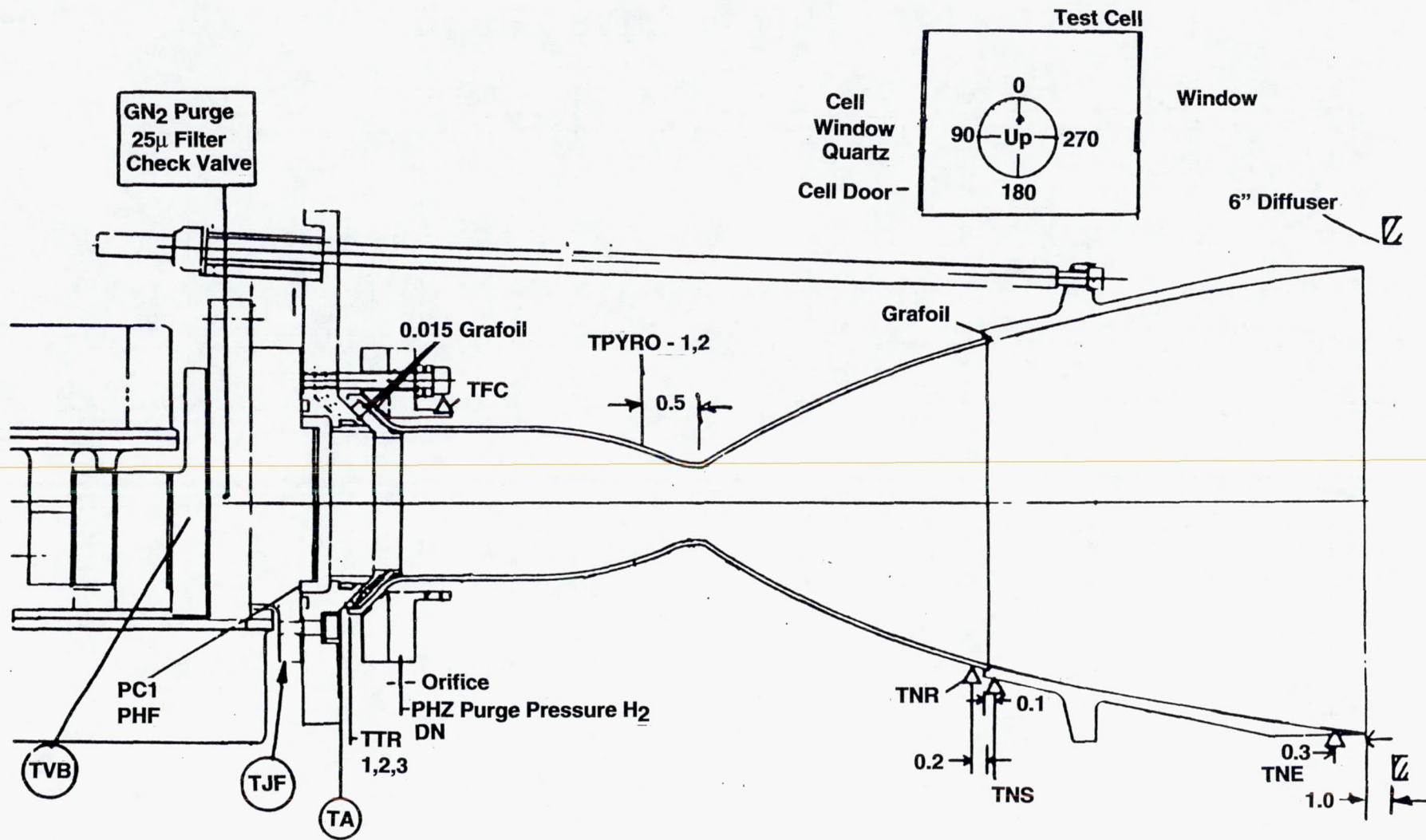


Figure 6.3-29. 100 lb 44:1 Bolt-Up Thruster Assembly

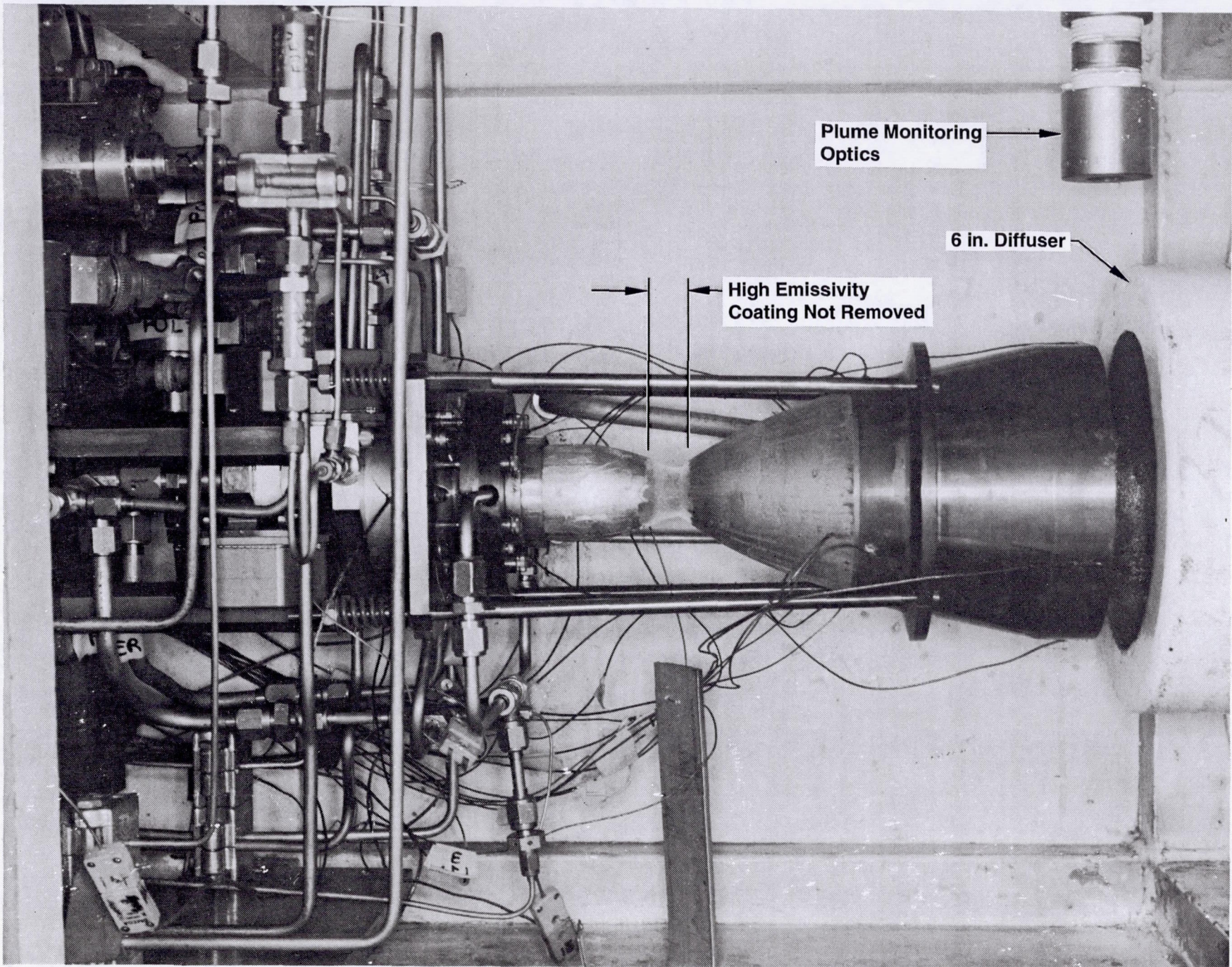


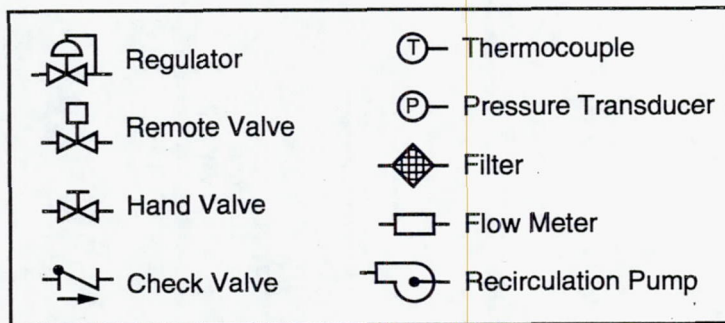
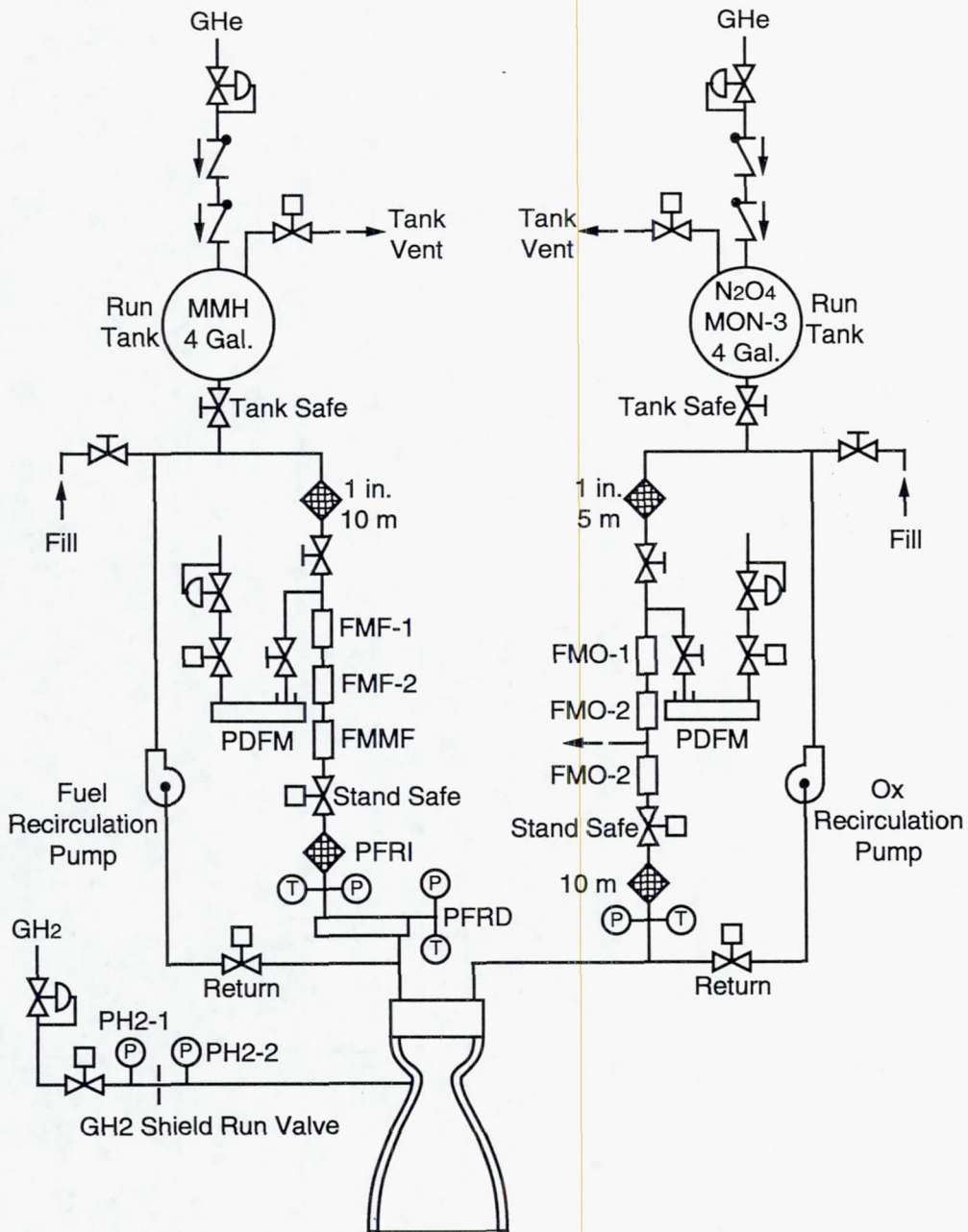
Figure 6.3-30. JPL 44:1 Ir-Re Chamber in Altitude Facility for Injector Performance Comparison Tests

Table 6.3-6. 100 lb Bay 2 Checkout Instrumentation List Altitude Tests of 44:1 JPL Ir-Re/SS Skirt (Sheet 1 of 2)

FUNCTION	PARAMETER	SYMBOL	RANGE	TRANSDUCER	DIGITAL	RECORDING			
						O-GRAPH	VISUAL	FM TAPE	
THRUSTER PERFORMANCE	THRUST A	FA	0-200 lbf	STRAIN GAGE	X	X	X		
	THRUST B	FB	0-200 lbf	STRAIN GAGE	X	X			
	THRUST CAL A	FCAL-A	0-200 lbf	STRAIN GAGE	X	X			
	THRUST CAL B	FCAL-B	0-200 lbf	STRAIN GAGE	X	X			
	CHAMB. PRESS 1 (INJ)	PC-1	0-200 psia	TABOR 206	X	X		X	
	OXID FLOW 1	FMO-1	0.13-0.3 lbm/sec (prop.)	TURBINE METER	X	X			
	OXID FLOW 2	FMO-2	0.13-0.3 lbm/sec (prop.)	TURBINE METER	X	X			
	FUEL FLOW 1	FMF-1	0.08-0.3 lbm/sec (prop.)	TURBINE METER	X	X			
	FUEL FLOW 2	FMF-2	0.08-0.3 lbm/sec (prop.)	TURBINE METER	X	X			
	OXID. VALVE INLET PRESS.	POL-2	0-500 psia	TABOR 206	X	X			
	OXID INJ. INLET PRESS.	POJ	0-500 psia	TABOR 206	X	X			
	FUEL INJ. INLET PRESS.	PFJ	0-500 psia	TABOR 206	X	X			
	FUEL REGEN INLET PRESS.	PFL-2	0-500 psia	TABOR 206	X	X			
	FUEL REGEN OUTLET PRESS.	PFR0	0-500 psia	TABOR 206	X	X			
	EXIT AMBIENT-1	PVAC-1	0-1 psia	BARATRON	X	X		X	
	EXIT AMBIENT-2	PVAC-2	0-1 psia	BARATRON	X	X		X	
	VALVE VOLTAGE	VTVC	0-30 Vdc		X	X			
	TEMPERATURE THRUSTER	OXID INLET TEMP	TOJ	40-1000F	TYPE K	X			
		FUEL REGEN INLET	TR-IN	40-1000F	TYPE K	X			X
FUEL REGEN OUTLET		TR-OUT	40-2000F	TYPE K	X				
INJ. FLANGE		TJF-1,-2,-3	40-5000F	TYPE K	X				
VALVE BODY TEMP.		TVB	40-5000F	TYPE K	X				
REGEN SECTION (TRIP)		TTR-1,-2,-3	40-20000F	TYPE K	X			X	
CHAMBER ADAPTOR FLANGE		TCF-1,-2,-3	40-20000F	TYPE K	X			X	
NOZZLE/EXT. JOINT (Re)		TNR-1,-2,-3	40-20000F	TYPE K	X				
NOZZLE/EXT. JOINT (S.S.)		TNS-1,-2,-3	40-20000F	TYPE K	X				
NOZZLE EXIT		TNE-1,-2,-3	40-20000F	TYPE K	X				
REGEN. INTERNAL		TRI	40-5000F	TYPE K; .010 dia	X				
H2 FILM COOLING SKIRT		TFC	40-20000F	TYPE K	X				
CHAMBER HOT SPOT		TPYRO-1	2600-4000F +	IRCON HIGH RANGE	X	X		X	
CHAMBER HOT SPOT		TPYRO-2	1500-4000F	MIKRON	X	X		X	
STABILITY		CHAMBER HIGH FREQ	PHF	500-15000Hz	KISTLER 601		X		X
OPTICAL	OPTICAL MULTICHANNEL ANALYSER (OMA)				RECORDED SEPARATELY				

Table 6.3-6. 100 lb Bay 2 Checkout Instrumentation List Altitude Tests of 44:1 JPL Ir-Re/SS Skirt (Sheet 2 of 2)

FUNCTION	PARAMETER	SYMBOL	RANGE	TRANSDUCER	DIGITAL	O-GRAPH	VISUAL	FM TAPE
FACILITY PRESSURES	OXID TANK	POTS	0-500 psia	TABOR 206	X		X	
	FUEL TANK	PFTS	0-500 psia	TABOR 206	X		X	
	OXID LINE	POL-1	0-500 psia	TABOR 206	X		X	
	FUEL LINE	PFL-1	0-500 psia	TABOR 206	X		X	
	H2 ORIFICE UP	PH2UP	0-100 psia	TABOR 206	X		X	
	H2 ORIFICE DOWN	PH2DN	0-50 psia	TABOR 206	X		X	
	ALTITUDE TANK (@ DIFF. EXIT)	PDX	0-5 psia	TABOR 206	X		X	
	DIFFUSER WATER	PDW	0-100 psia	TABOR 206	X		X	
FACILITY TEMPERATURES	OXID LINE	TOL	40-1000F	TYPE K	X		X	
	FUEL LINE	TFL	40-1000F	TYPE K	X		X	
	TEST CELL	TCELL	0-2500F	TYPE K	X		X	
	VACUUM TANK	TVT	0-2500F	TYPE K	X			
	VACUUM PUMP INLET	TVP	0-2500F	TYPE K	X			
	DUCT ELBOW	TDUCT	0-2500F	TYPE K	X			



1.12.5.24

Figure 6.3-31. Test Bay A-2 Propellant Feed System

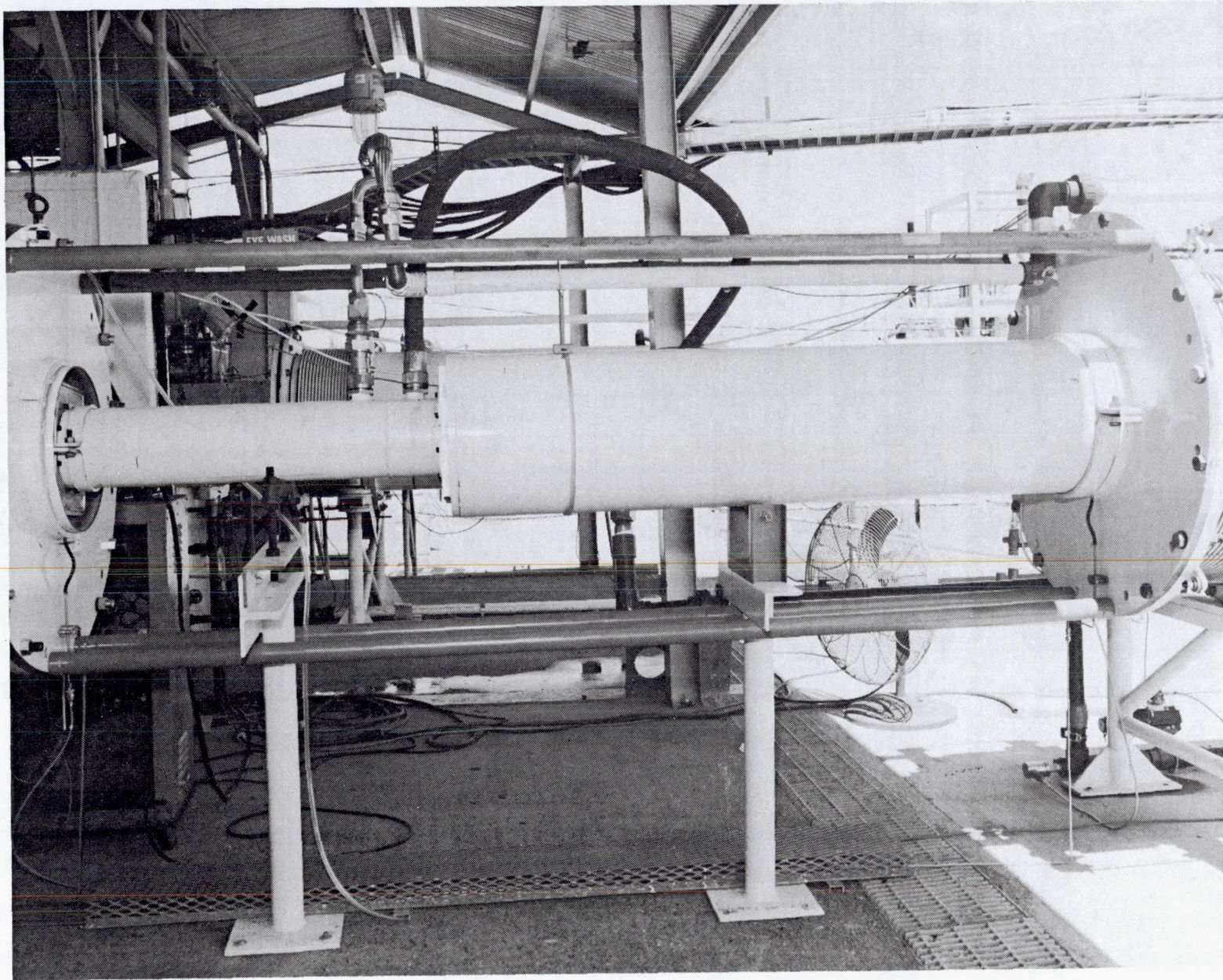


Figure 6.3-33. 6 in. Diffuser Set Up for 44:1 Injector Performance Screening Tests

Table 6.3-7. Final Performance Data for SN-2, -4, and -5 Injectors

RUN No.	DATE	INJ. S/N	FIRING TIME, sec	DATA TIME, sec	13	25	26	30	69	72	105	106	108	110	111	112	113	DELTT	INJECTOR	REGEN	Q,
					PC1	TOL	TFL	TROUT	PVAC1	PYROHI	WOX	WF	MR	FVAC	ISVAC	C*	CF	REGEN	Kwaj	Kwtj	BTU/SEC
					psia	°F	°F	°F	PSIA	°F	lbm/sec	lbm/sec	O/F	LBF	SEC	FT/SEC		°F			
166	7-26-91	2	90	87.5	103.7	80	80	191	0.198	3696	0.2113	0.1283	1.648	105.07	309.4	5518	1.803	111	0.01781	0.01455	10.3
167	7-26-91	2	90	87.5	103.4	81	82	193	0.193	3783	0.2103	0.1280	1.644	104.85	309.9	5519	1.806	111	0.01776	0.01454	10.3
168	7-26-91	2	90	87.5	104.2	80	82	195	0.184	3772	0.2136	0.1278	1.672	105.49	309.0	5515	1.803	114	0.01757	0.01454	10.5
169	7-26-91	2	90	87.5	91.1	81	84	219	0.184	4021	0.1879	0.1102	1.705	91.85	308.1	5519	1.795	136	0.01756	0.01459	10.9
170	7-26-91	2	90	87.5	114.6	81	83	186	0.224	3504	0.2347	0.1416	1.657	116.02	308.3	5499	1.802	103	0.01766	0.01451	10.5
193	8-15-91	4	90	87.5	95.5	72	72	199	0.164	3314	0.1928	0.1221	1.579	96.08	305.1	5479	1.790	126	0.01884	0.01637	11.2
194	8-15-91	4	90	87.5	108.0	72	73	186	0.182	3253	0.2213	0.1366	1.620	109.04	304.7	5450	1.797	114	0.01891	0.01630	11.2
195	8-15-91	4	90	87.5	85.8	73	75	225	0.149	3467	0.1751	0.1068	1.639	86.17	305.6	5494	1.789	151	0.01857	0.01642	11.8
196	8-15-91	4	90	87.5	97.2	73	75	185	0.164	3160	0.1907	0.1309	1.457	97.7	303.8	5460	1.789	110	0.01880	0.01633	10.4
197	8-15-91	4	90	87.5	96.8	74	77	225	0.167	3373	0.2042	0.1159	1.762	98	306.2	5465	1.802	149	0.01872	0.01634	12.6
198	8-15-91	4	90	87.5	94.4	73	76	209	0.161	3293	0.1924	0.1187	1.621	95.13	305.8	5480	1.794	133	0.01871	0.01634	11.5
200	8-17-91	5	90	87.5	93.4	69	69	154	0.179	3100	0.1885	0.1204	1.566	93.9	304.0	5463	1.790	85	0.01673	0.01338	7.3
201	8-17-91	5	90	87.5	106.4	69	70	149	0.202	2974	0.2166	0.1374	1.576	107.58	303.9	5430	1.801	79	0.01665	0.01337	7.7
202	8-17-91	5	90	87.5	86.3	70	71	162	0.167	3196	0.1747	0.1098	1.591	86.59	304.4	5478	1.788	90	0.01676	0.01348	7.1
203	8-17-91	5	90	87.5	96.5	69	72	150	0.184	2976	0.1891	0.1306	1.448	96.84	302.9	5450	1.788	79	0.01675	0.01341	7.3
204	8-17-91	5	90	87.5	96.3	71	74	165	0.188	3225	0.2031	0.1160	1.751	97.49	305.5	5450	1.804	92	0.01671	0.01340	7.6
205	8-17-91	5	90	87.5	94.3	71	74	160	0.182	3127	0.1919	0.1196	1.605	94.91	304.7	5467	1.793	86	0.01673	0.01339	7.4
206	8-17-91	5	90	87.5	94.5	72	75	161	0.164	3128	0.1924	0.1198	1.606	95.1	304.6	5467	1.793	86	0.01671	0.01338	7.4

177
6-3

6.3, Hot Fire Testing (cont.)

1.68:1 steel chamber data for extrapolation. Initial test results showed significant propellant flow calibration discrepancies, of the order of 1 percent. These were the result of inadequate calibration duration available from the test stand positive displacement flowmeters (PDFM). New, larger PDFM's were installed in Bay 2 for use in recalibrating flowmeters for performance tests of the SN 1 286:1 welded flight thruster and for reprocessing previous test data.

Table 6.3-7 summarizes the test results for the three injectors. The vacuum specific impulse is shown in Figure 6.3-34 for injectors SN 2, 4, and 5 as a function of chamber pressure, for the 44:1 nozzle. The difference in performance between injector SN 2 and the others (4 and 5) is significant, about 5 sec or 1.6%. There is a slight and not significant difference of about 1 sec between SN 4 and SN 5. Over the range of chamber pressure tested in the performance tests (85 to 115 psia) their I_{sp} varies by only 1 to 2 sec. The effect of mixture ratio on I_s for the 3 injectors is shown in Figure 6.3-35. Corresponding plots of cold throat C^* for the three injectors are shown in Figures 6.3-36 and 6.3-37 as a function of P_c and MR, respectively.

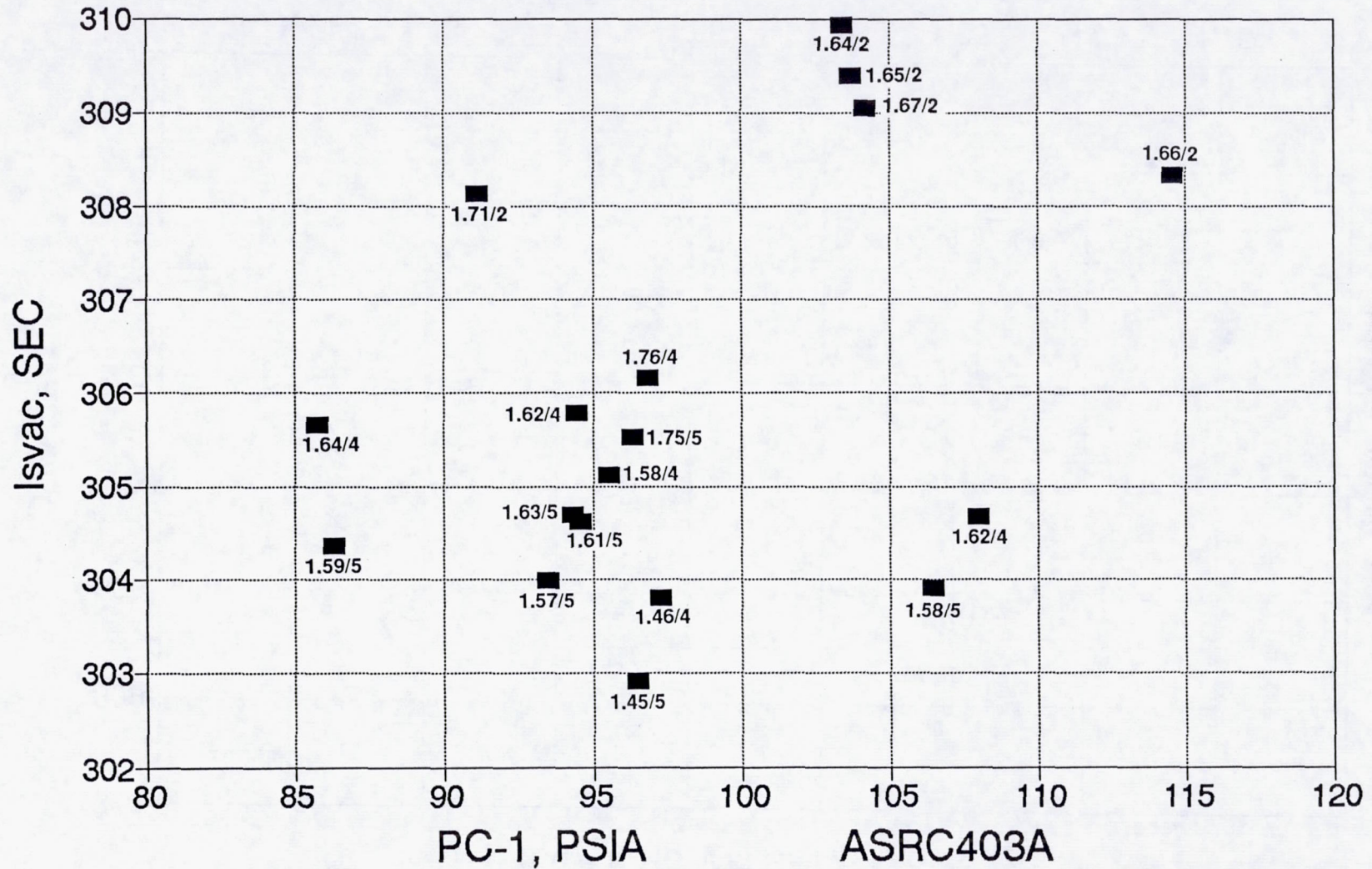
Significant thermal differences between the injectors are apparent. The most marked is chamber temperature as measured with an optical pyrometer targeted on the Re chamber at a point on the chamber contraction region about 0.5 in. ahead of the throat. Figures 6.3-38 and -39 show that the SN 2 injector is significantly hotter than either 4 or 5 at nominal conditions (3850 F versus 3325 and 3025, respectively). The maximum temperature measured, 4020 F at $P_c = 91$ psia, is within the proven operating range of the Ir-Re system. The higher temperatures for SN 2 are consistent with its higher performance. It should be emphasized that the JPL 44:1 chamber used for these tests has its high emissivity coating removed over all its surface except immediately around the throat, as can be seen in Figure 6.3-30 which shows the JPL 44:1 chamber installed in the altitude facility. With the complete coating in place the chamber runs about 200°F cooler.

Since the propellants were not temperature conditioned during this test series, there were systematic changes between injectors, as ambient temperature varied. This is illustrated in Figures 6.3-40 and -41 which show oxidizer and fuel supply pressures as a function of run number for injectors SN 2, 4 and 5. The average oxidizer inlet temperatures were about 81, 73 and 70°F in the progression from SN 2 to SN 5.

A second thermal difference between the three injectors is illustrated in Figure 6.3-42, which shows heat transfer to the fuel-cooled chamber adapter section, based on

Is VAC @ 44:1 VS. PC-1--FINAL DATA

100# Ir-Re; INJ S/N 2, 4, 5

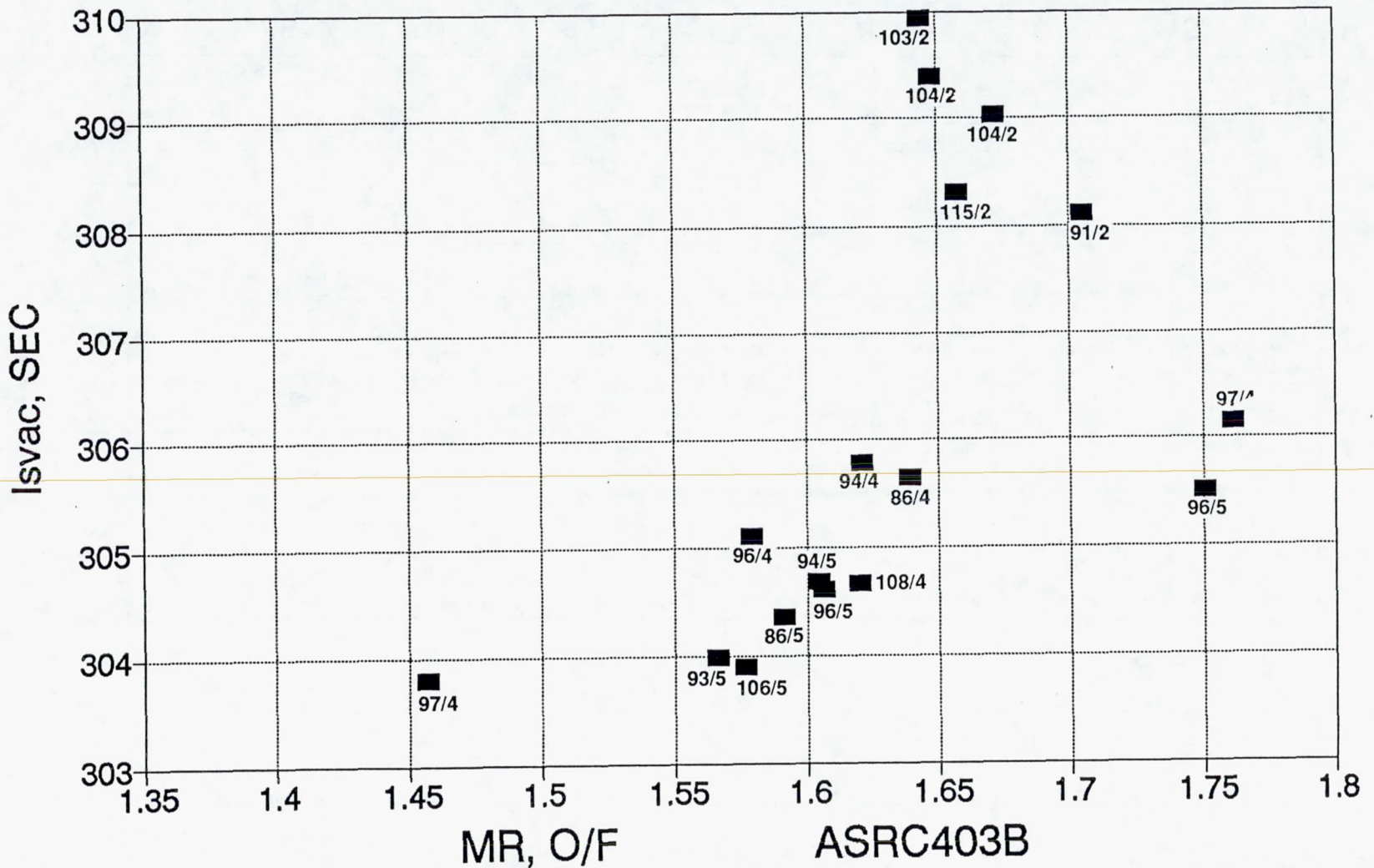


■ M/N=MR/INJ

Figure 6.3-34. Vacuum Specific Impulse at 44:1 for Injector SN -2, -4 and -5 Versus Chamber Pressure Over Fuel Test Range

Is VAC @ 44:1 VS. MR--FINAL DATA

100# Ir-Re; INJ S/N 2, 4, 5



■ M/N=PC/INJ#

Figure 6.3-35. Vacuum Specific Impulse at 44:1 for Injectors and SN -2, -4 and -5 Versus Mixture Ratio Over Fuel Test Range

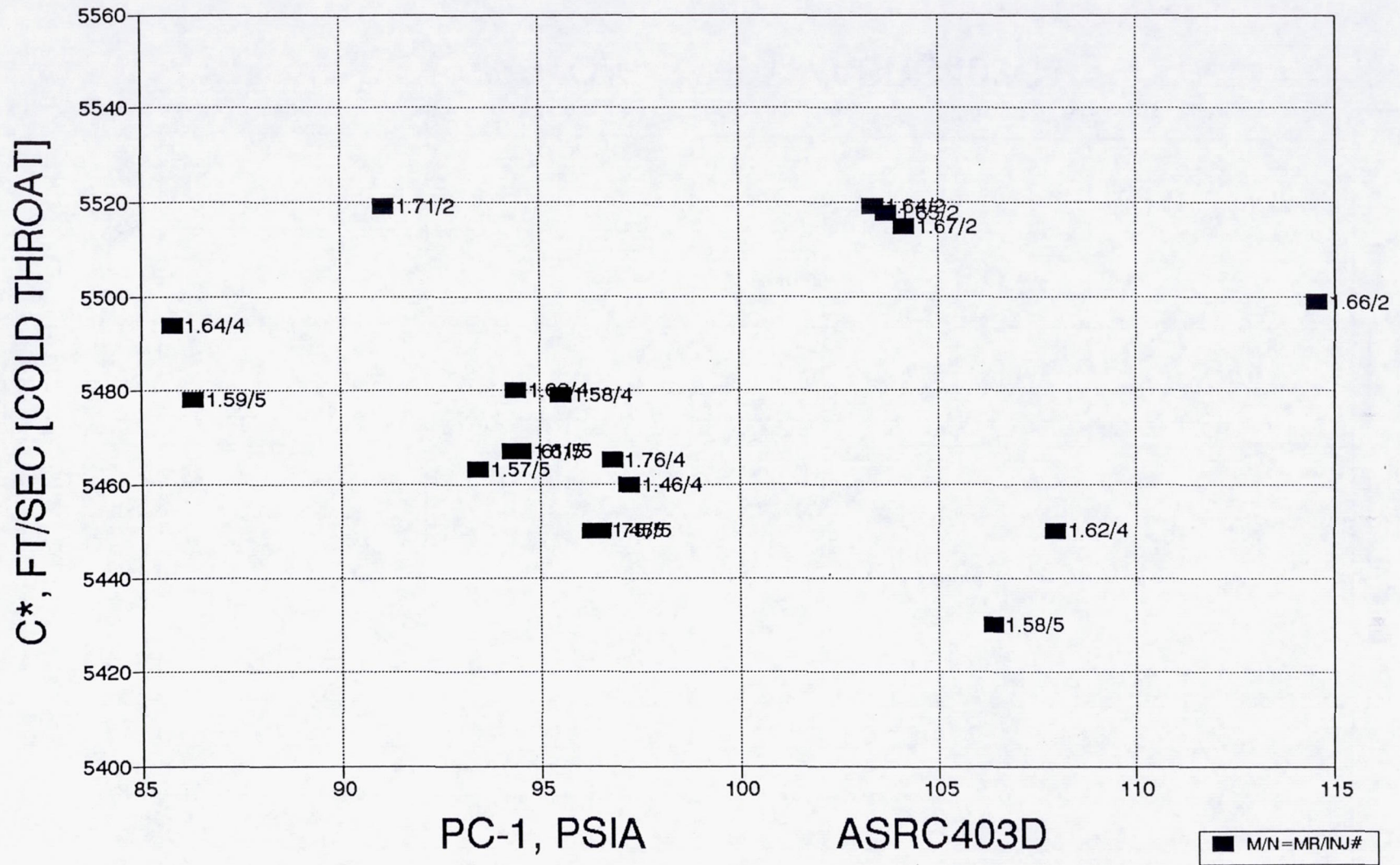


Figure 6.3-36. C* vs Pc-1 – Final Data (Cold Throat) – 100# Ir-Re; Injector SN 2, 4, 5

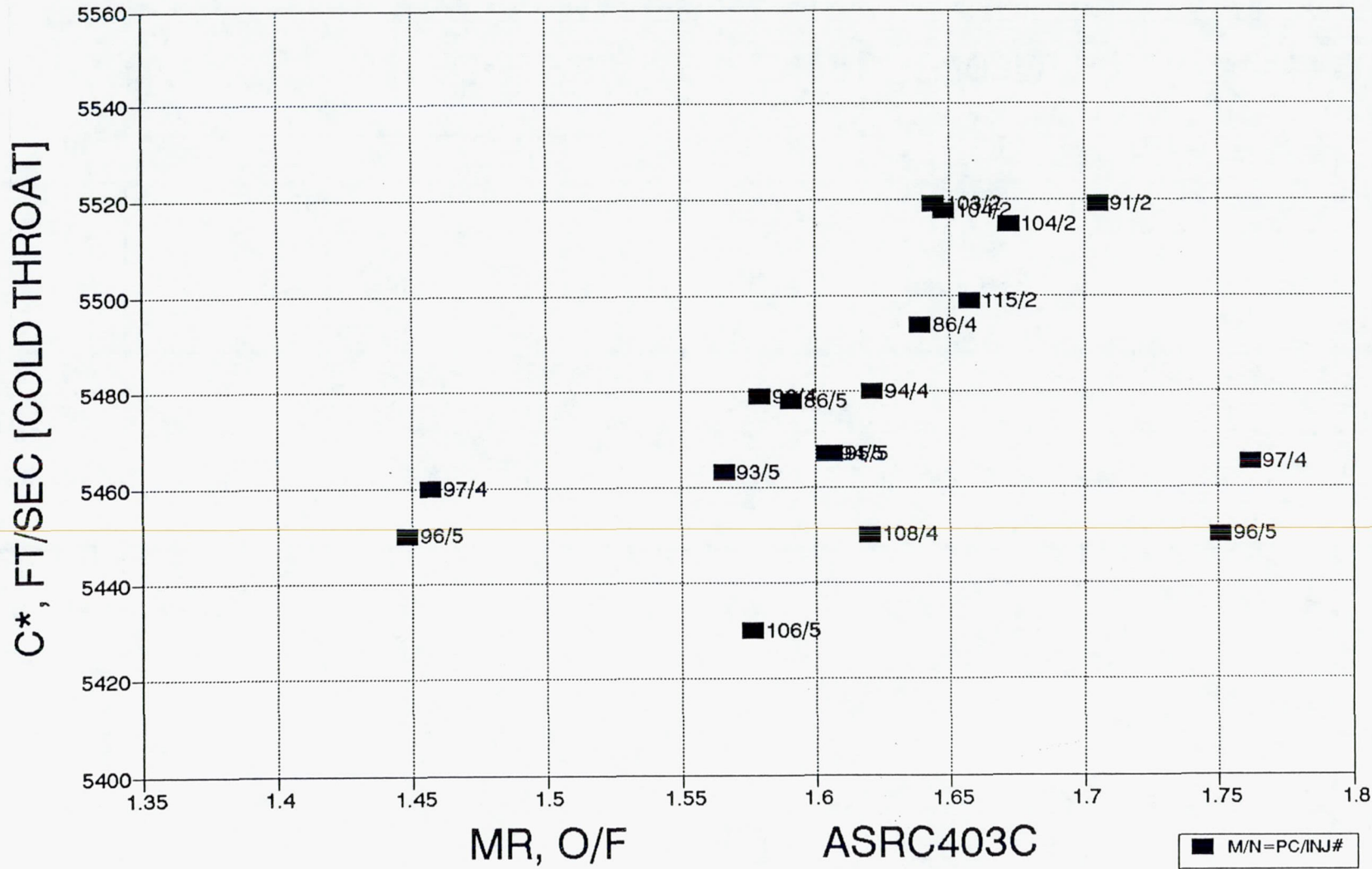


Figure 6.3-37. C* vs MR – Final Data (Cold Throat) – 100# Ir-Re; Injector SN 2, 4, 5

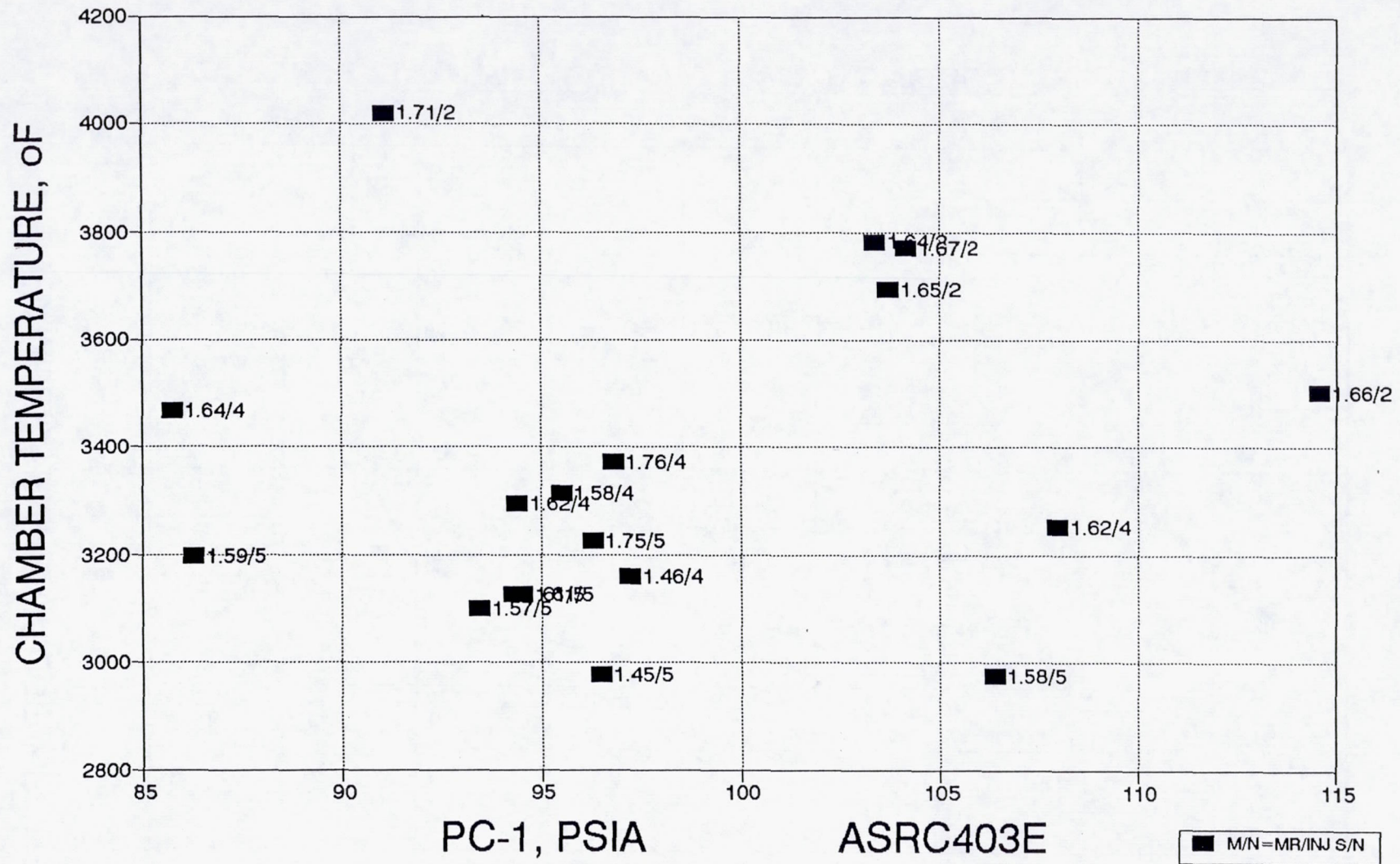


Figure 6.3-38. Chamber Temperature vs Pc-1 – Final Data – 100# Ir-Re; Injector 2, 4, 5

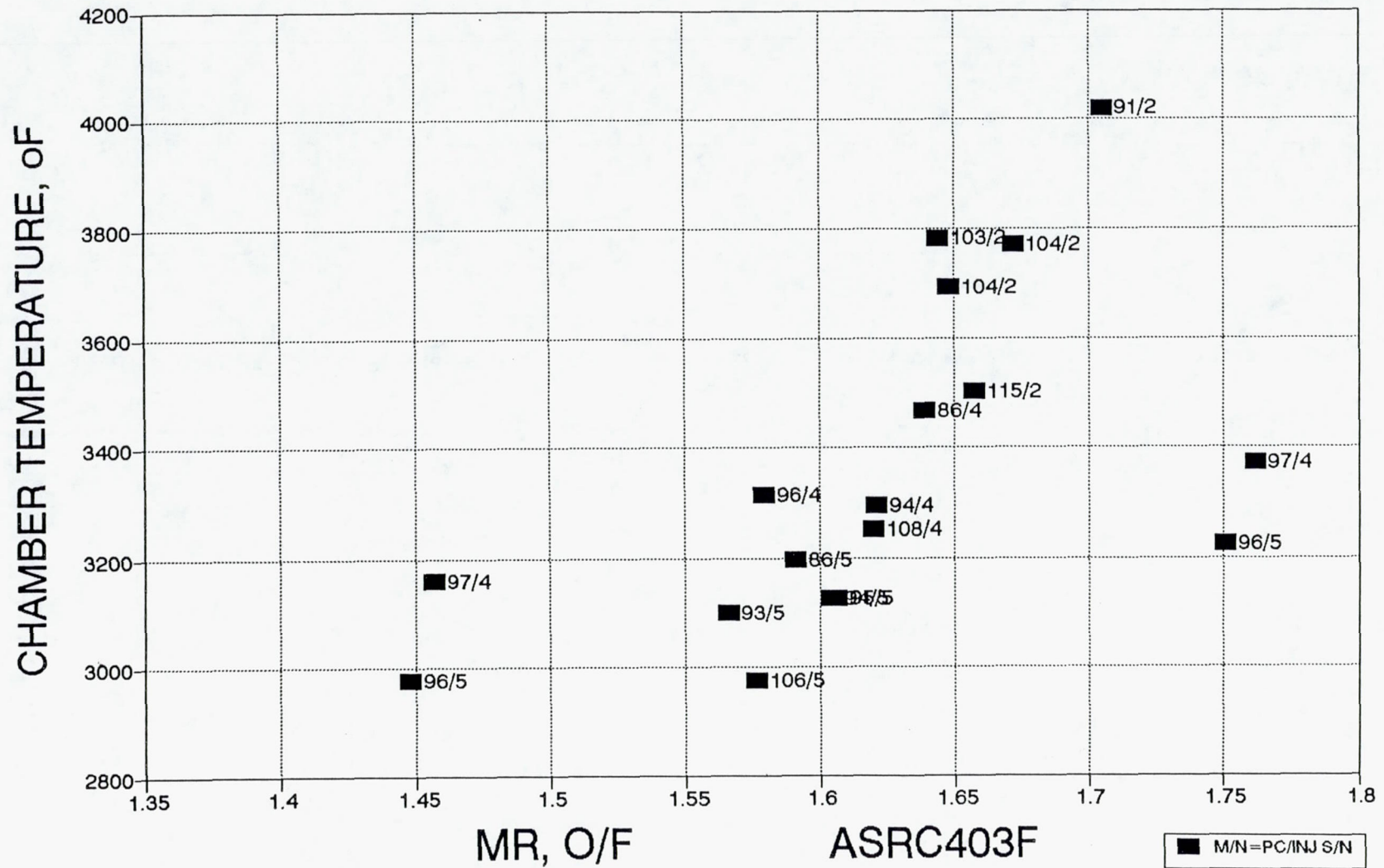


Figure 6.3-39. Chamber Temperature vs MR – Final Data – 100# Ir-Re; Injector SN 2, 4, 5

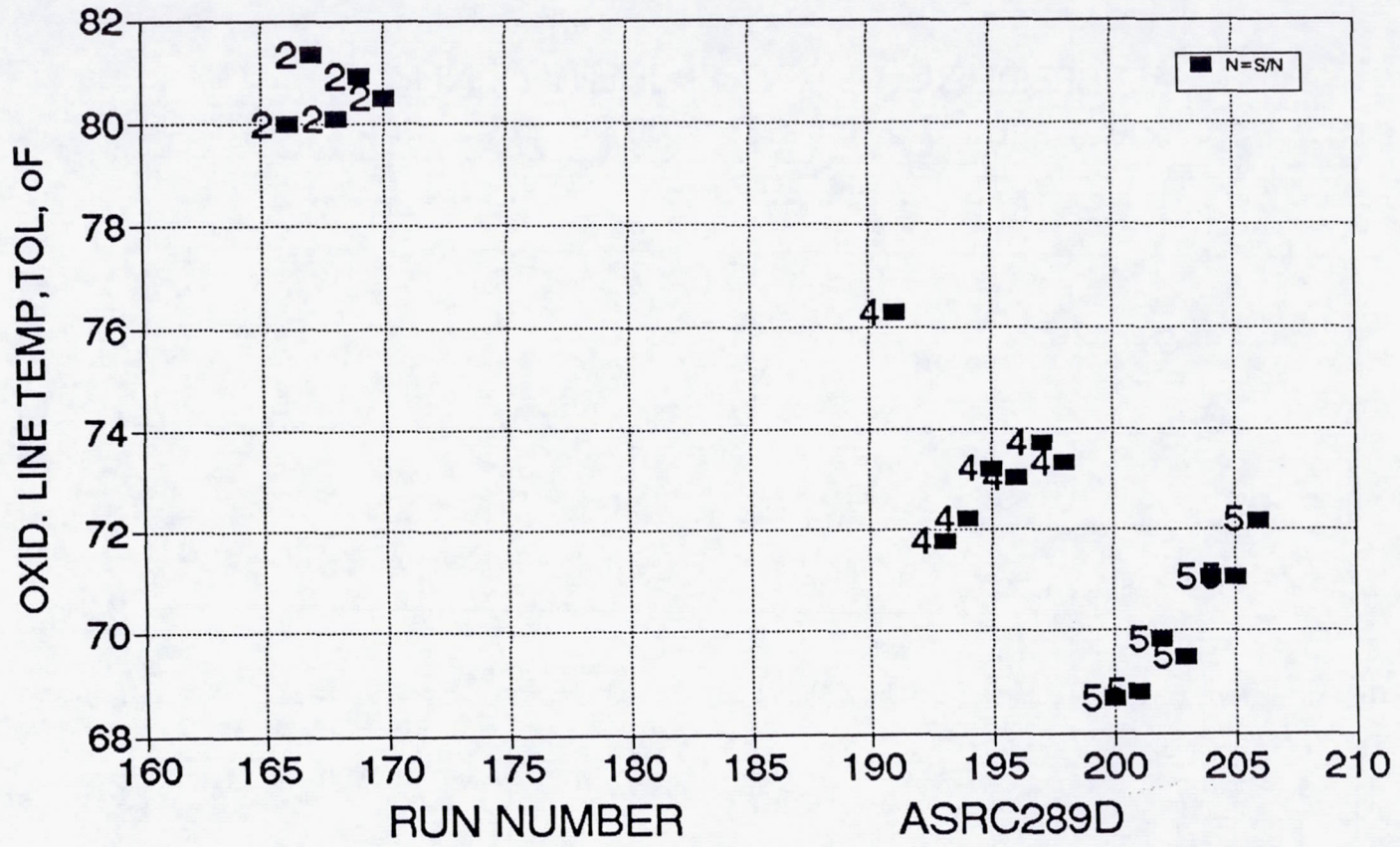


Figure 6.3-40. Oxid Line Temp vs Run Number – 100# Ir-Re, e = 44:1; Injector SN 2, 4, 5

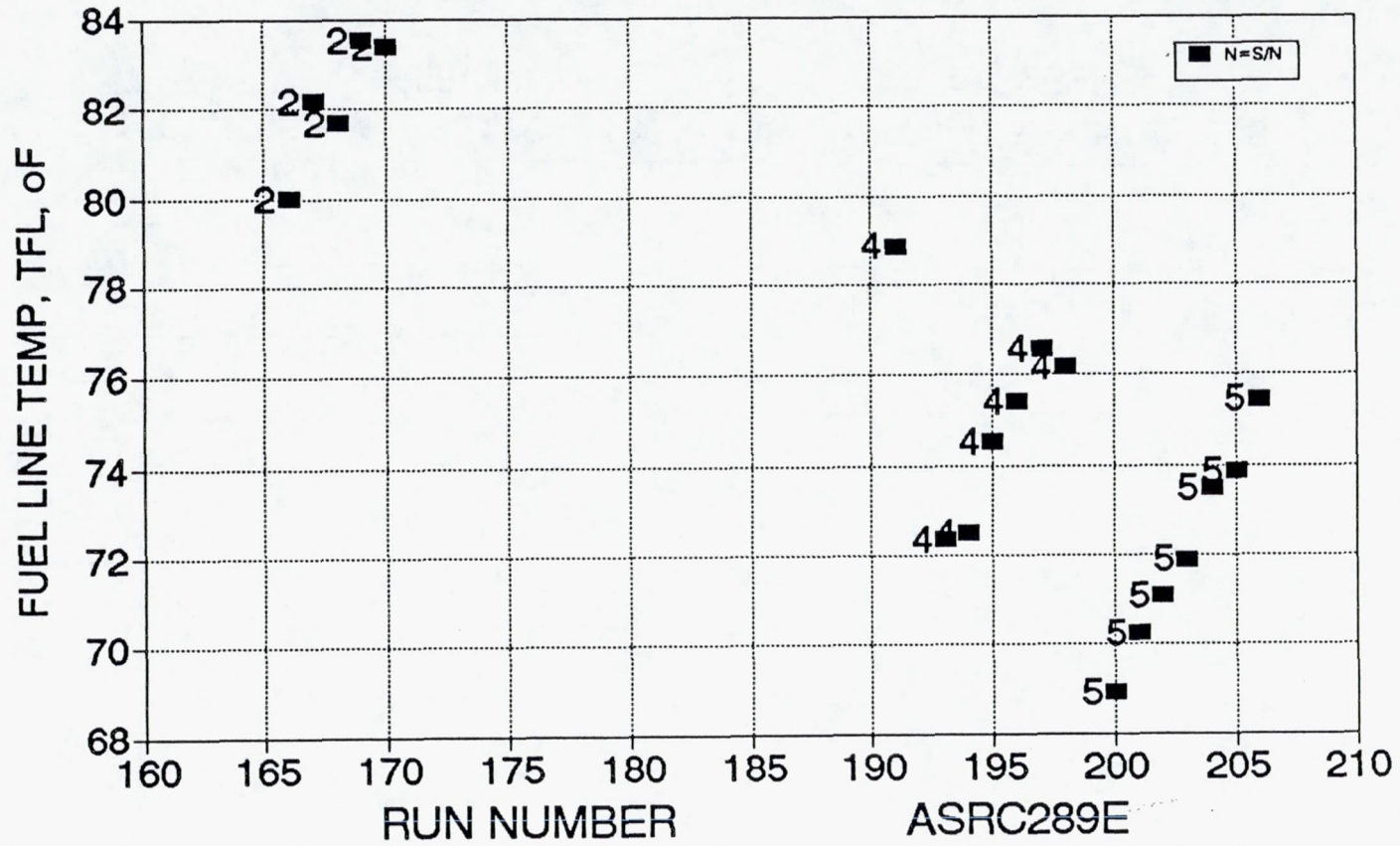


Figure 6.3-41. Fuel Line Temp vs Run Number – 100# Ir-Re, e = 44:1; Injector SN 2, 4, 5

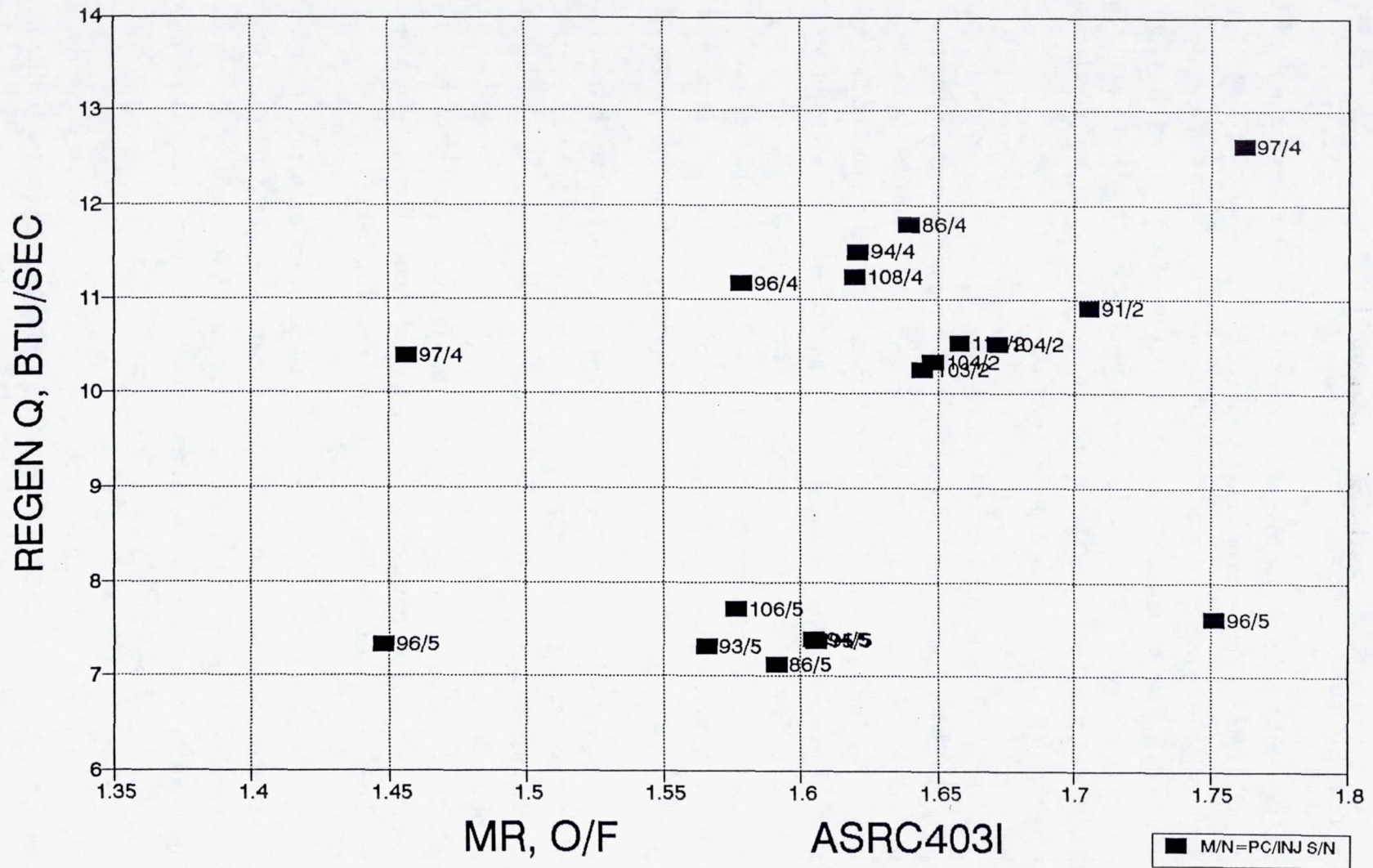


Figure 6.3-42. Regen Q vs MR – Final Data – 100# Ir-Re; Injector SN 2, 4, 5

6.3, Hot Fire Testing (cont.)

measured fuel flow rate and temperature rise as a function of MR. As can be seen the heat input for injector SN 5 is independent of mixture ratio, while the SN 2 and 4 injectors show an increase in heat flux with MR. Moreover, the thermal trend for 2 and 4 is reversed from the performance data. At the same MR, SN 4 has about 14% higher heat flux than SN 2. The heat flux for injector SN 5 is about 39% lower than for SN 2. Looking at heat flux as a function of chamber pressure, in Figure 6.3-43, SNs 2 and 4 heat flux can be seen to correlate slightly negatively with pressure, while that of 5 shows very slight positive correlation.

Thermal transient response of the cooled adapter for a hot restart, Test -170 is shown in Figure 6.3-44. Just prior to FS-1, the fuel cooled adapter internal temperature had reached 284 F. Eighty millisecond after ignition, the fuel temperature rose to 289°F, showing that the thermocouple was close to but not at the hottest location in the fuel circuit, and then fell to about 182°F in 1.5 sec. This is shown more clearly in Figure 6.3-45, which shows the first two seconds of the firing. The fuel temperature remained steady at FS-2 at 90 sec, when it made an initial rise to about 216°F, fell back and then rose gradually. At 150 sec it had reached 251°F, on its way back up to the maximum soak temperature. The initial rise at shutdown is caused by soak from the cooled adapter wall; the secondary rise is thermal soak from the Re chamber.

Optical emission measurements made on the 44:1 thruster normally showed no significant spectral features. Multiple spectral scans were made throughout a firing using an EG&G optical multispectral analyses (OMA) consisting of a 1024 diode array detector, a 1/4 M Jerrold Ash spectrometer, coupled to the exhaust plume with quartz fiber optics and a nitrogen purged quartz imaging lens. During altitude checkout tests improper operation of the temperature conditioning propellant recirculation system introduced helium bubbles into the propellant which were evident in propellant flow measurements and engine operation.

Figure 6.3-46 shows three of the multiple scans, the normal background, taken prior to the test, and two scans taken during the test at FS-1 + 20 and +40 sec, with the background subtracted. A strong peak at 589.6 is noted. The possible candidates are sodium and helium. Since sodium has not been seen with these propellants and since helium bubbles were known to be present, they are a likely source of the emission .

The design intent for injectors SN 2 and 5 was to be fuel rich at the wall and oxidizer-rich in the core, while SN 4 was designed to have a nearly flat MR profile with a

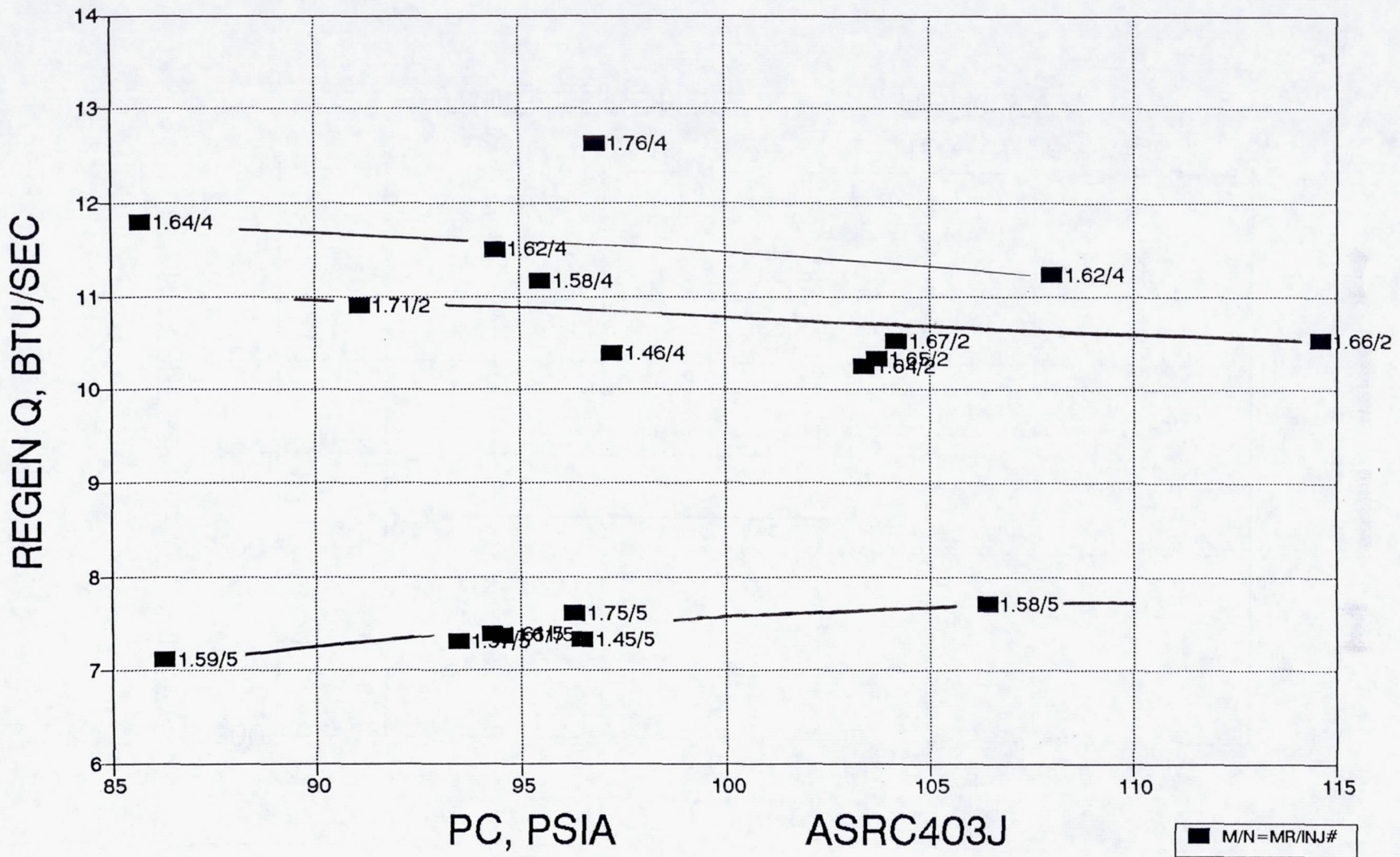


Figure 6.3-43. Regen Q vs Pc – Final Data – 100# Ir-Re; Injector SN 2, 4, 5

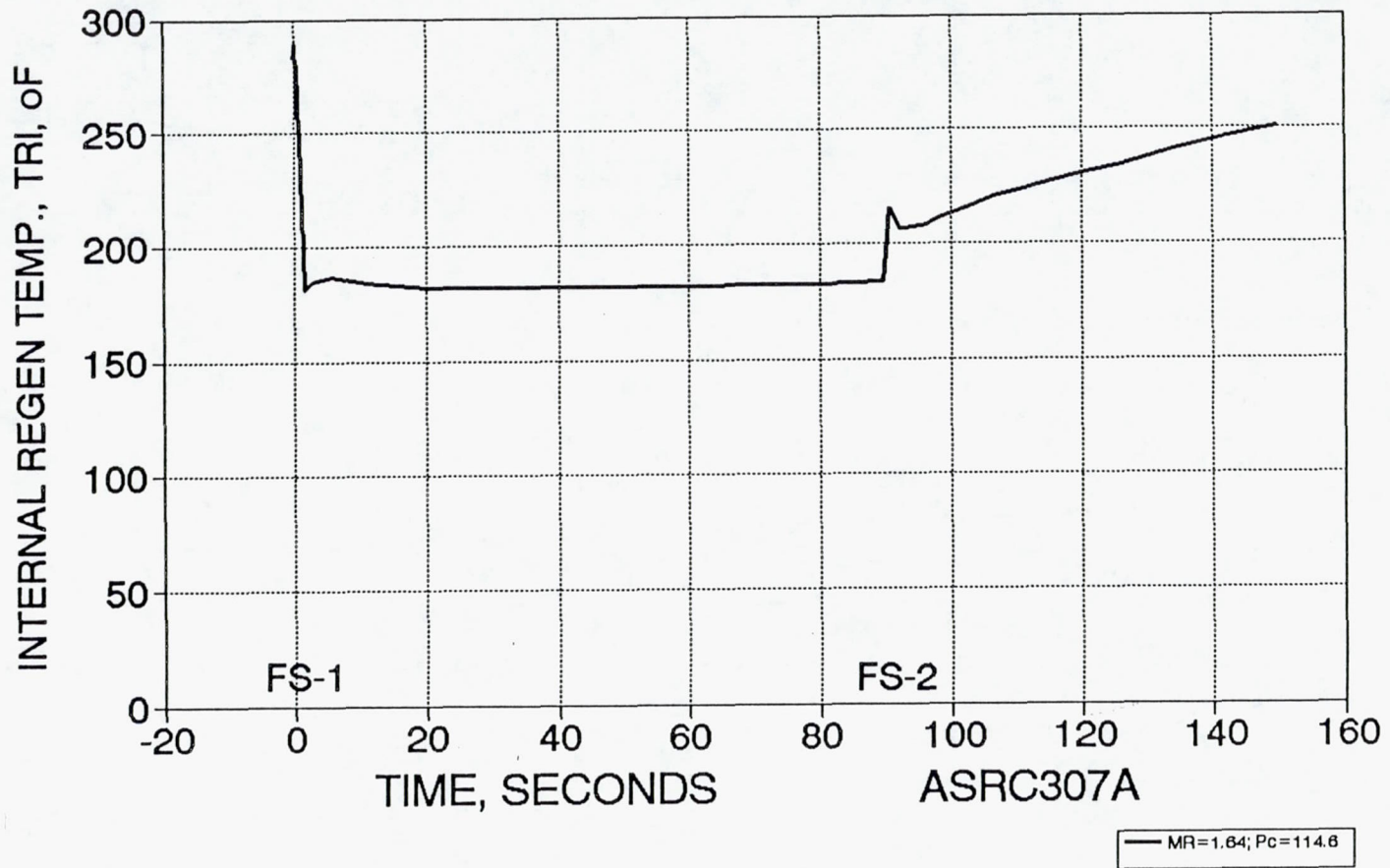


Figure 6.3-44. 100 lb Thruster Internal Regen Temp - Run -170, Hot Start Test

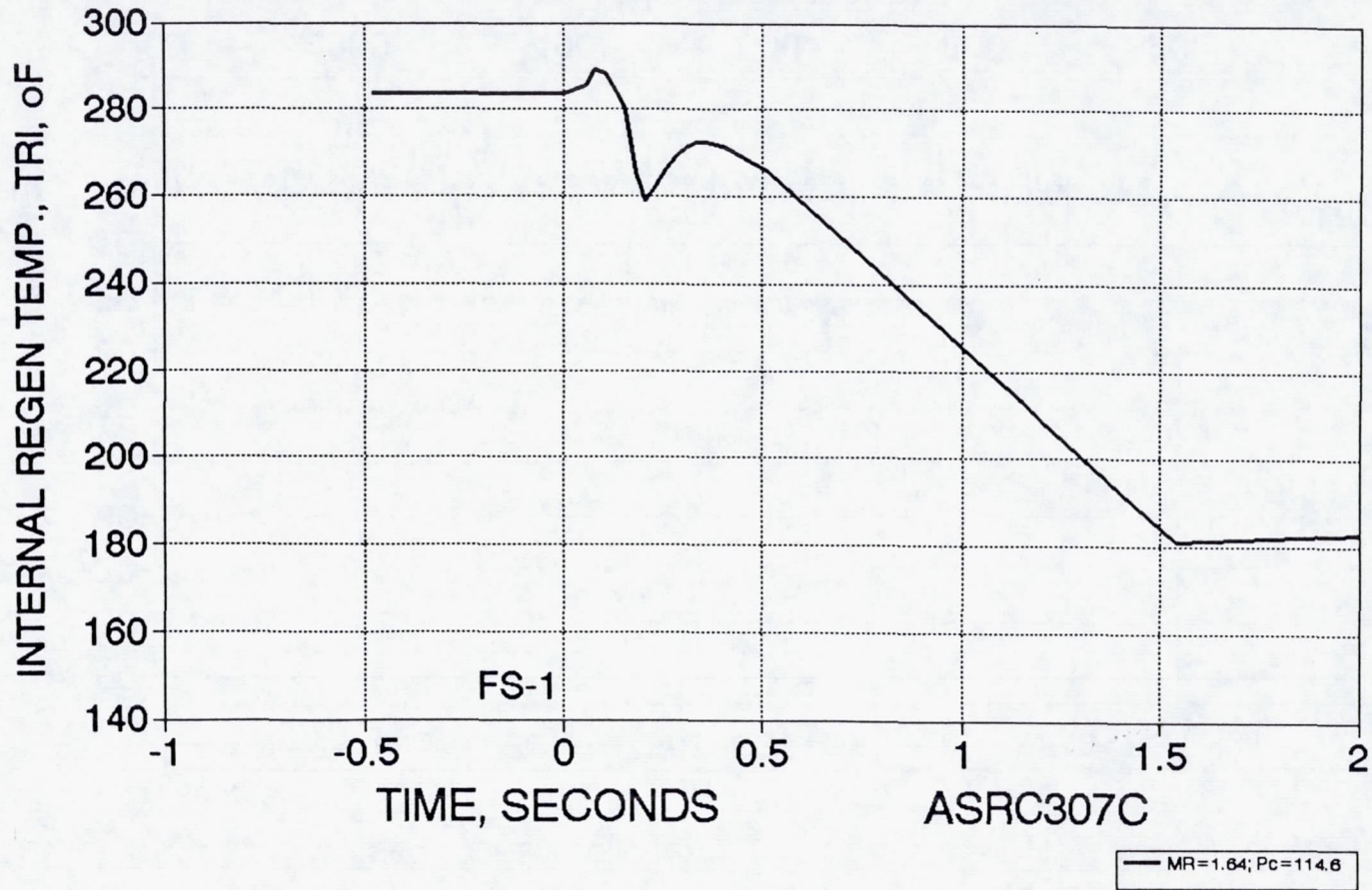
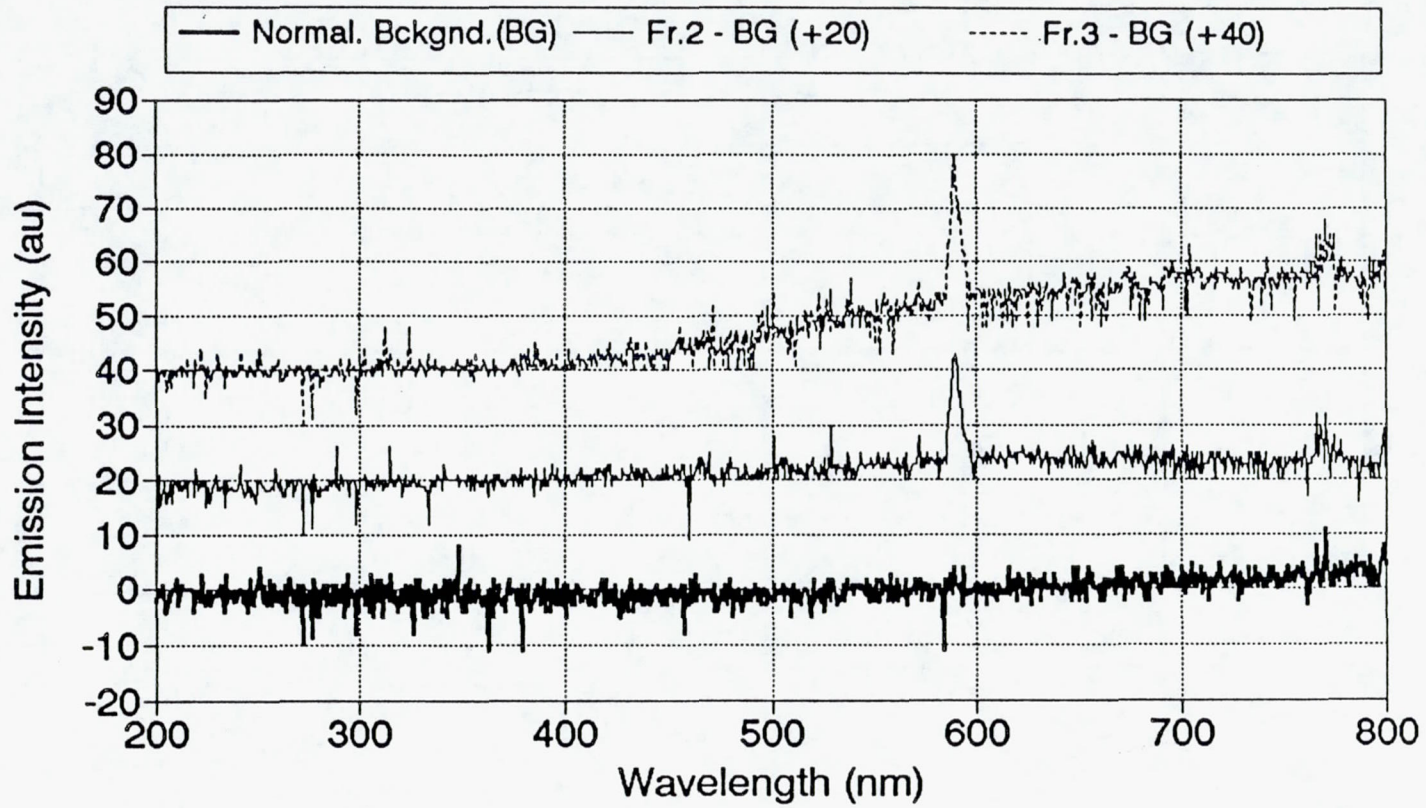


Figure 6.3-45. 100 lb Thruster Internal Regen Temp - Run -170, Initial Transient



KGH64001.DAT

Figure 6.3-46. 100# Thruster Plume Spectral Emission – Test -164 With Helium Ingestion

6.3, Hot Fire Testing (cont.)

slight low-MR bias near the wall to account for manufacturing tolerances. Flow collection tests made on the three injectors indicate that the design mixture ratio profiles were obtained in each case, as was shown in Figure 6.2-15. However, the intended duplication of mass flow distribution between the outer and inner zones of SN 2 and SN 5 was not achieved, as shown in Figure 6.2-16.

The appearance of injector SN 5 after firing, which is typical for these injectors, is shown in Figure 6.3-47.

6.3.2.2 Duplication of Injector SN 2

To demonstrate that the high performance and compatibility of SN 2 injector could be duplicated using current manufacturing procedures (SN 2 was built in 1987), two new injectors, SN 6-1 and 6-2 were built with patterns identical to SN 2. As previously shown, in Section 6.2, their hydraulic characteristics are similar to SN 2 and to each other (Figures 6.2-19 through 6.2-23). The SN 6 injectors were tested in the 44:1 bolt up hardware to compare their performance to SN 2 and to each other.

The SN 6-1 and SN 6-2 injectors hot fire comparison in thrust, flow, performance and thermal measurements testing using the 44:1 Ir-Re chamber showed no statistical differences in the test results for these two injectors. Testing began on 12-11-91 with Run -207 and was completed on 12-19-91 with Run -244.

Initial tests, -207 through -224, conducted with SN 6-2 injector showed erratic performance results with an apparent scatter of as much as $\pm 1\%$ accompanied by erratic Kw data and a lower than expected Is. This problem was traced to the effects of propellant recirculation which was being done to condition the propellants thermally. This apparently caused stable helium bubble formation in the propellant. Both the PDFM's and turbine flow meters, therefore, gave higher than actual propellant flow indications as they are essentially volume measuring devices. The Micromotion meters, which should be insensitive to bubbles, gave good agreement with the other meters which is unexpected and not explained.

Eliminating the propellant recirculation and assuring that the propellant delivery systems were free of bubbles before testing gave very consistent test data in Runs -225 through -244. The data for these tests are given in Table 6.3-10.

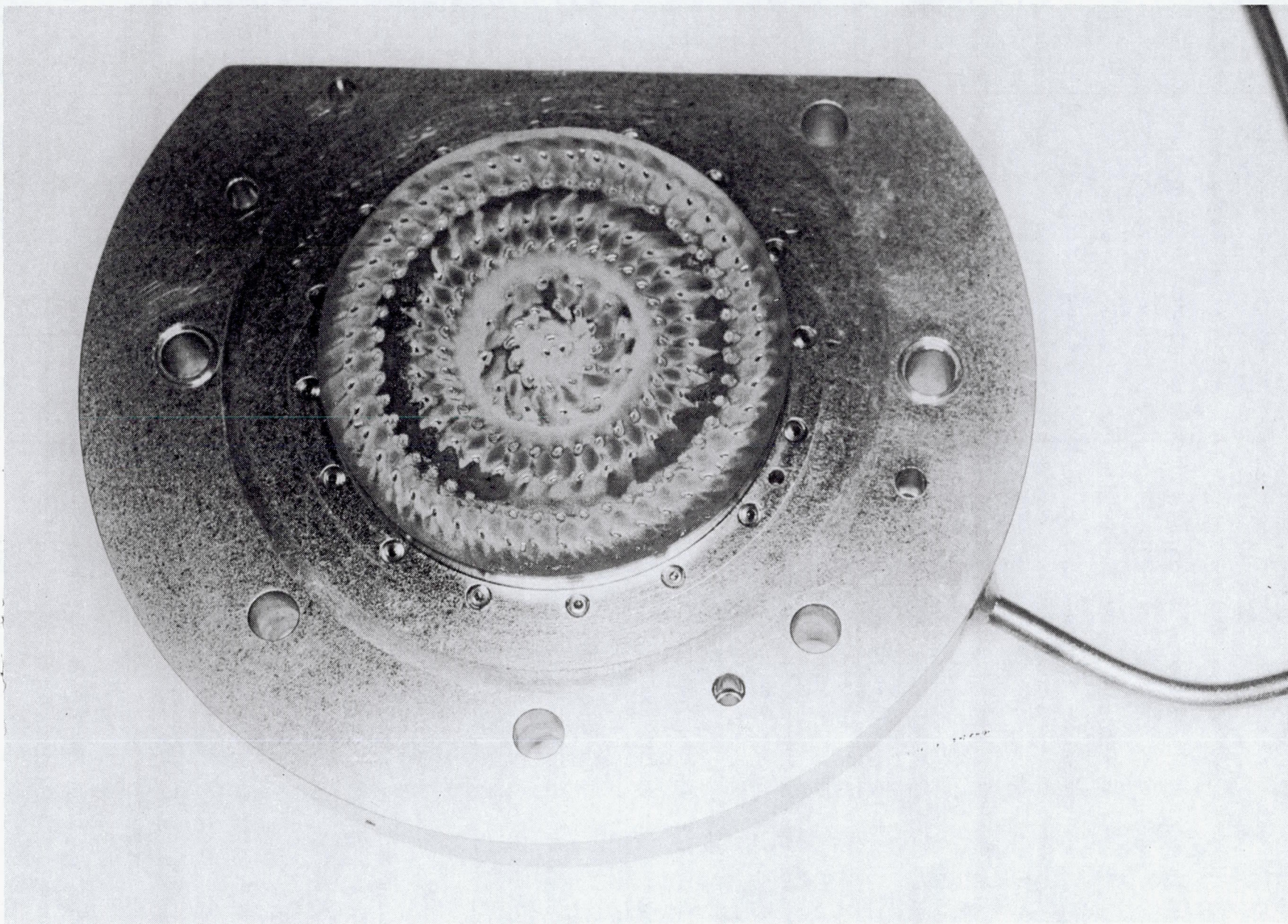


Figure 6.3-47. SN 5 Injector After Performance Tests

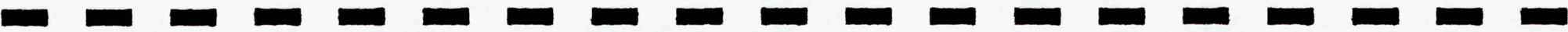


Table 6.3-10. Comparison of SN6-1 and -2 at 44:1

RUN NO.	INJECTOR	FIRING TIME, (sec)	Pc (psia)	MR O/F	Fvac (lbf)	Is vac (sec) @44:1	C* (ft/sec, @ Dt=0.846 in)	Cf --	REGEN. OUTLET (F)	REGEN. DELTA T, (F)	CHAMB. TEMP., (F)
225	S/N6-2	27.0	100.5	1.516	101.3	308.1	5489	1.805	166	116	3514
226	S/N6-2	25.0	100.2	1.662	101.4	309.6	5489	1.814	181	132	3638
227	S/N6-2	25.0	100.2	1.675	101.5	309.7	5489	1.815	184	136	3635
228	S/N6-2	25.0	99.5	1.648	100.7	309.6	5490	1.814	180	133	3631
229	S/N6-2	25.0	110.2	1.620	111.7	308.8	5474	1.815	163	116	3438
230	S/N6-2	25.0	90.5	1.632	91.5	309.7	5498	1.812	193	147	3824
231	S/N6-2	25.0	100.8	1.505	101.5	308.0	5489	1.805	166	120	3487
232	S/N6-2	25.0	100.6	1.788	102.3	310.3	5477	1.822	192	146	3719
233	S/N6-2	25.0	100.5	1.637	101.7	309.8	5489	1.814	176	131	3621
234	S/N6-1	25.0	101.4	1.716	102.8	310.0	5486	1.817	188	138	--
235	S/N6-1	25.0	101.2	1.620	102.3	309.6	5493	1.812	180	131	3704
236	S/N6-1	25.0	100.5	1.647	101.7	309.8	5491	1.814	184	135	3734
237	S/N6-1	25.0	97.4	1.530	98.2	308.6	5491	1.807	175	127	3669
238	S/N6-1	10.8	108.6	1.571	109.6	308.4	5485	1.807	159	111	3204
239	S/N6-1	25.0	107.6	1.576	108.7	308.8	5485	1.810	170	122	3546
240	S/N6-1	25.0	89.6	1.553	90.2	308.6	5500	1.803	193	146	3862
241	S/N6-1	25.0	98.7	1.413	99.1	306.4	5480	1.798	163	116	3510
242	S/N6-1	25.0	98.6	1.720	100.1	310.4	5492	1.819	194	147	3844
243	S/N6-1	10.0	95.8	1.467	96.1	307.0	5492	1.797	167	120	3333
244	S/N6-1	90.0	101.0	1.614	102.2	309.6	5494	1.812	179	131	3665

6.3, Hot Fire Testing (cont.)

Specific impulse is shown in Figure 6.3-48 plotted versus mixture ratio for the two injectors. The significant information from this plot is the overlay of the SN 6-1 and SN 6-2 injector's performance data over the range of mixture ratio (1.42 to 1.8) and Pc (90 to 110 psia). A data range of one percent is indicated on the figure; the whole range of Isp data including mixture ratio and Pc effects is contained within $\pm 0.7\%$. The average specific impulse for all twenty points over the operating range is 308.5. The nominal operating condition (MR = 1.65, Pc = 100 psia) is shown in Figure 6.3-49. The specific impulse for these eight tests is 309.6 sec measured at an area ratio of 44:1.

Figures 6.3-50 and -51 show the I_s trends as a function of chamber pressure. Here it is evident that I_s is very flat over the Pc range varying $\pm 0.6\%$ from MR = 1.6 to 2.0 and is the same for both injectors.

Comparison of perfect injector predicted performance, based on two-dimensional kinetics (TDK), with actual measured performance for the SN 6 injectors is shown in Figure 6.3-52. This curve shows that the SN 6 measured performance is above 99% over the MR range of 1.5 to 1.8. The factors which determine the difference between theoretical and measured thruster performance will be discussed more fully in Section 6.3.4.

C^* measured for the -1 and -2 injectors is plotted in Figure 6.3-53 for the full range of MR tested, 1.4 to 1.8, and in Figure 6.3-54 for the MR range around nominal, 1.61 to 1.68. It should be noted that this C^* is not corrected for throat expansion during firing or for Pc corrected to total pressure. It is used only for engine rebalance calculations. The measured C^* as a function of Pc is plotted in Figure 6.3-55. Within the data accuracy there is no real trend in C^* with MR and a slight negative correlation with Pc.

Measured injector Kw for the SN 6-1 and -2 oxidizer circuits are shown, on a highly expanded scale, in Figure 6.3-56; they are within $\pm 0.2\%$ of each other over the full flow range. The fuel Kw is plotted in Figure 6.3-57; they agree within $\pm 1\%$.

Typical variation in fuel Kw is shown in Figure 6.3-58. This variation is due in part to real changes in flow condition, in the cooled adapter during the thermal transient (flow passage area, wall boundary layer conditions) and in part is an artifact of the uncertainty in fuel density, which changes throughout the cooled adapter. These calculations are based on an average using inlet and outlet temperature. The total variation of fuel Kw is about ± 0.25 around the steady state value.

S/N 6-1 AND 6-2 INJECTORS I_s vac VS MR FINAL PERFORMANCE DATA AT 44:1

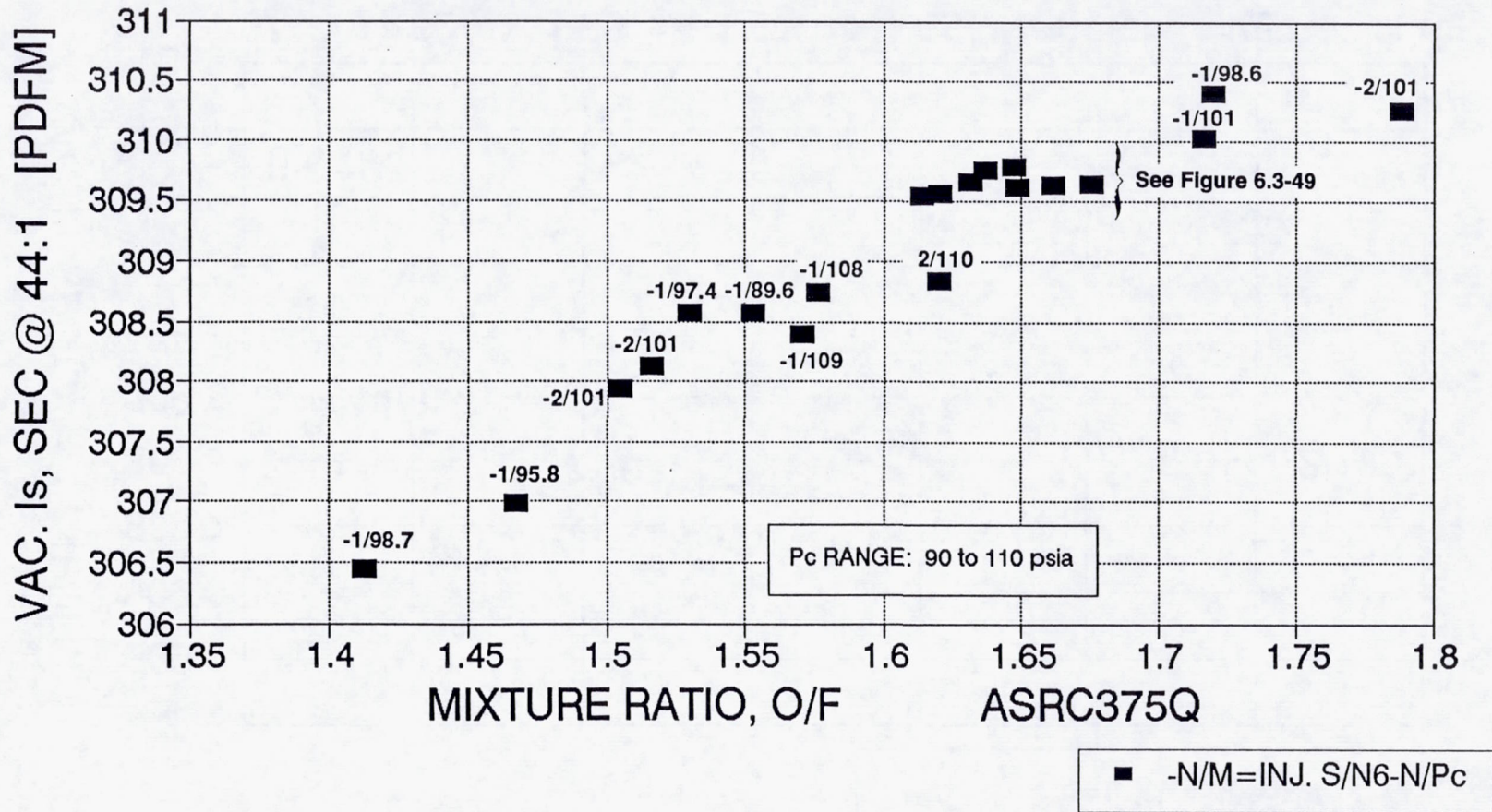


Figure 6.3-48. Vacuum Specific Impulse at 44:1 for Injectors SN 6-1 and SN 6-2 Versus Mixture Ratio Over Full Test Range

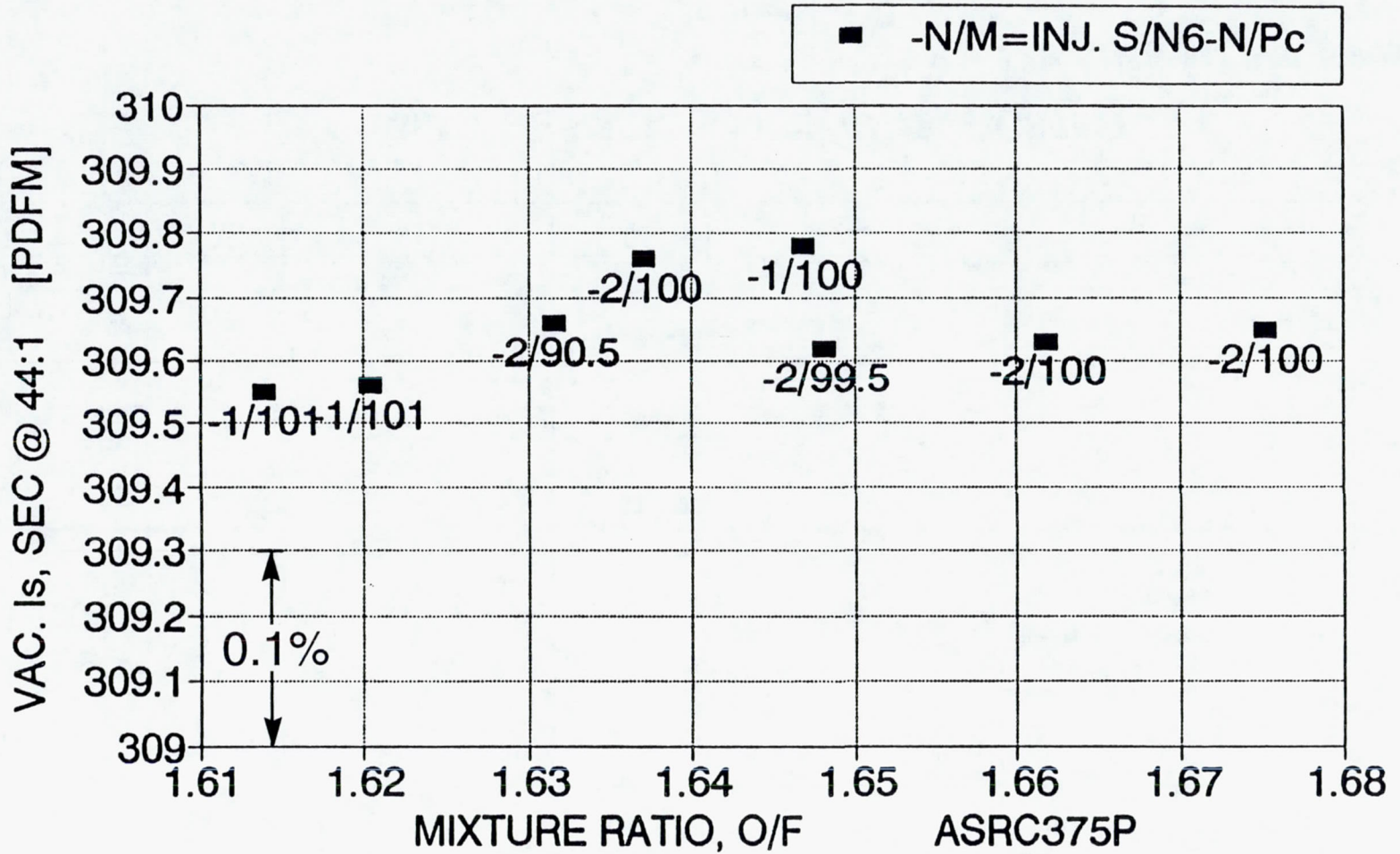


Figure 6.3-49. Vacuum Specific Impulse at 44:1 for Injectors SN 6-1 and SN 6-2 Versus Mixture Ratio at Nominal Conditions

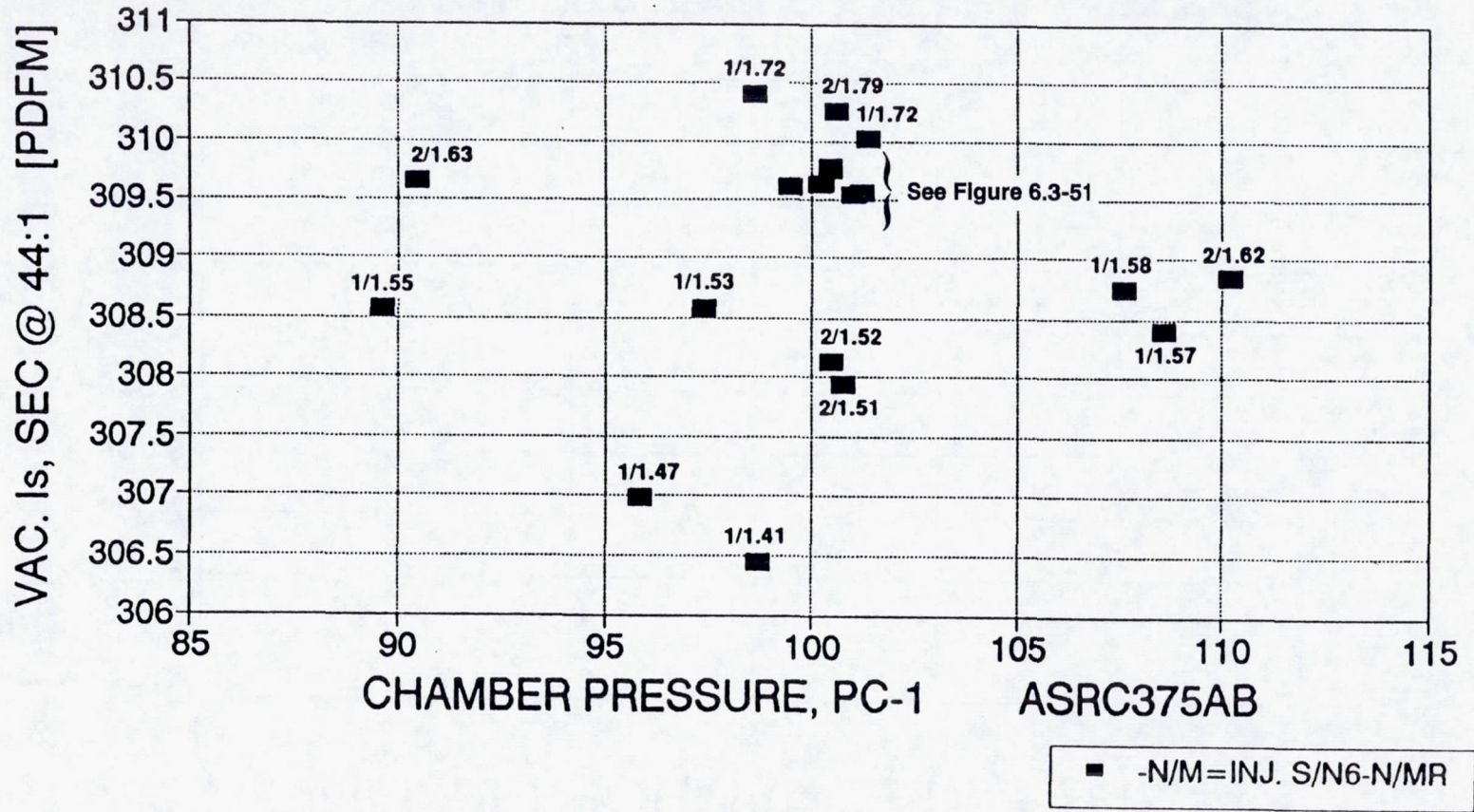


Figure 6.3-50. Vacuum Specific Impulse at 44:1 for Injectors SN 6-1 and SN 6-2 Versus Chamber Pressure Over Full Test Range

S/N 6-1 AND 6-2 INJECTORS I_s vac VS PC FINAL PERFORMANCE DATA AT 44:1

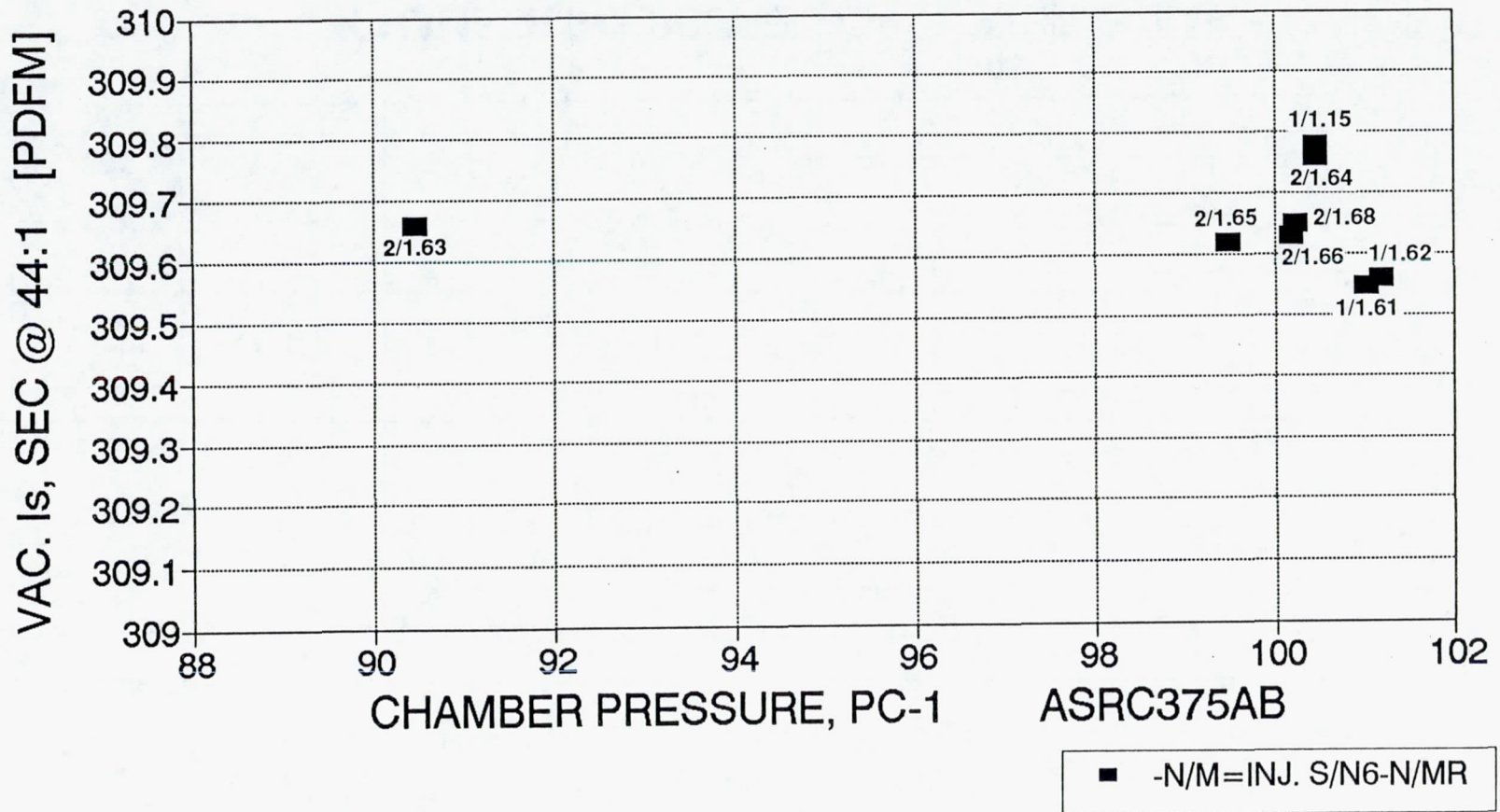


Figure 6.3-51. Vacuum Specific Impulse at 44:1 for Injectors SN 6-1 and SN 6-2 Versus Chamber Pressure at Nominal Conditions

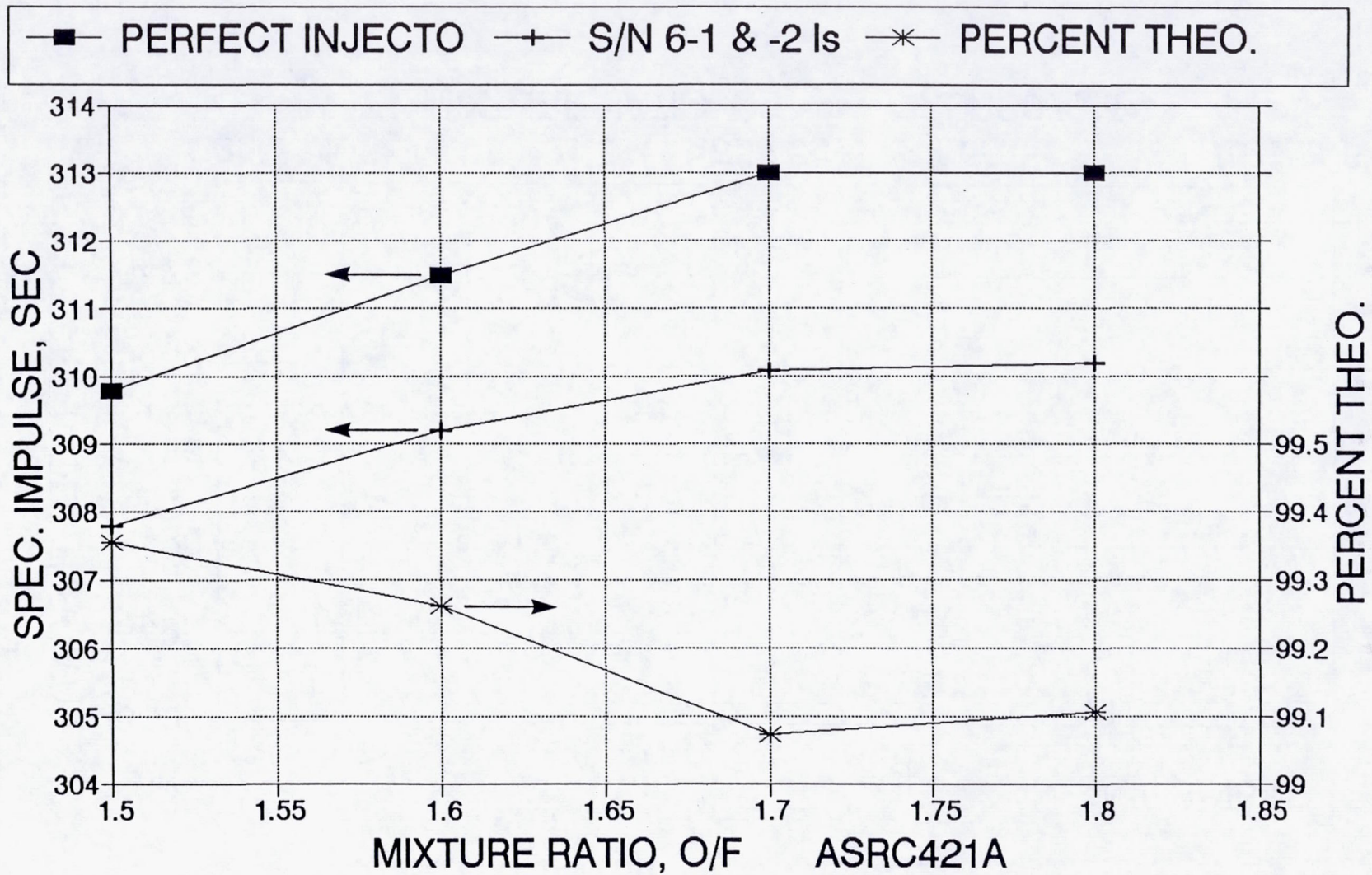


Figure 6.3-52. Specific Impulse and Percent vs MR Theoretical SN-6 at $\epsilon = 44:1$

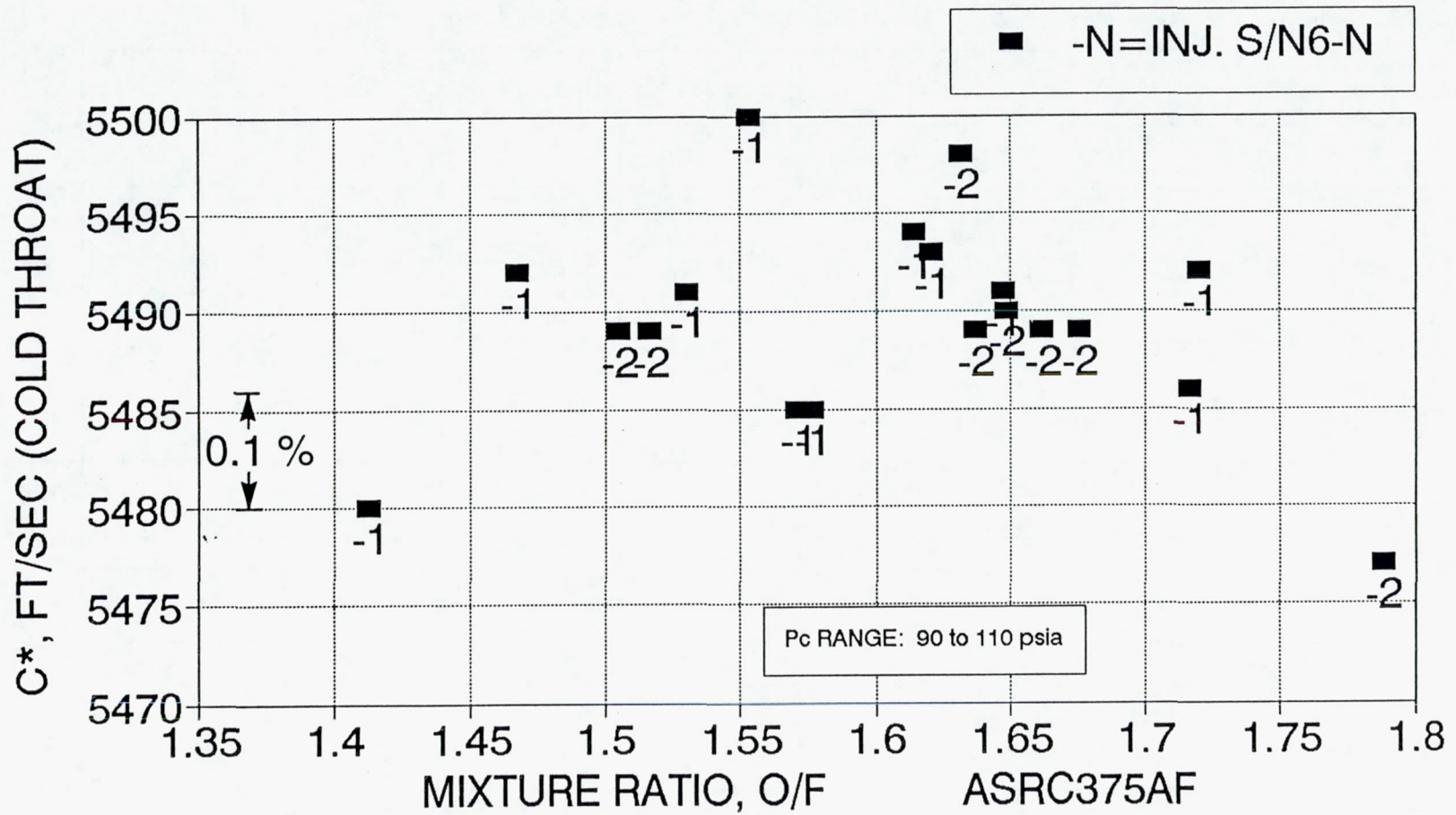


Figure 6.3-53. SN-6-1 and SN-6-2 Injector C* vs MR at 44:1, Full Test Range

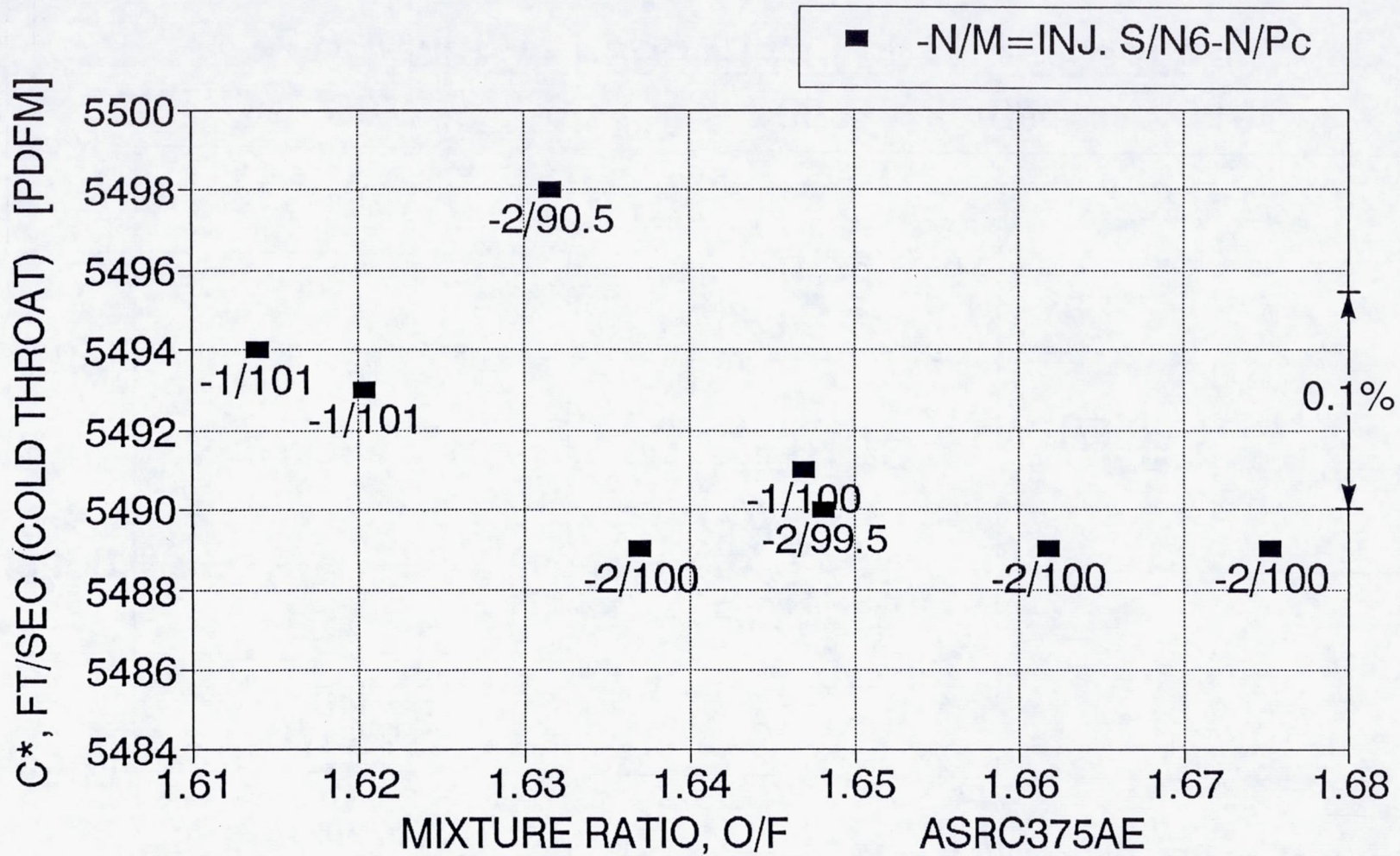


Figure 6.3-54. SN-6-1 and SN-6-2 Injector C* vs MR at 44:1, at Nominal

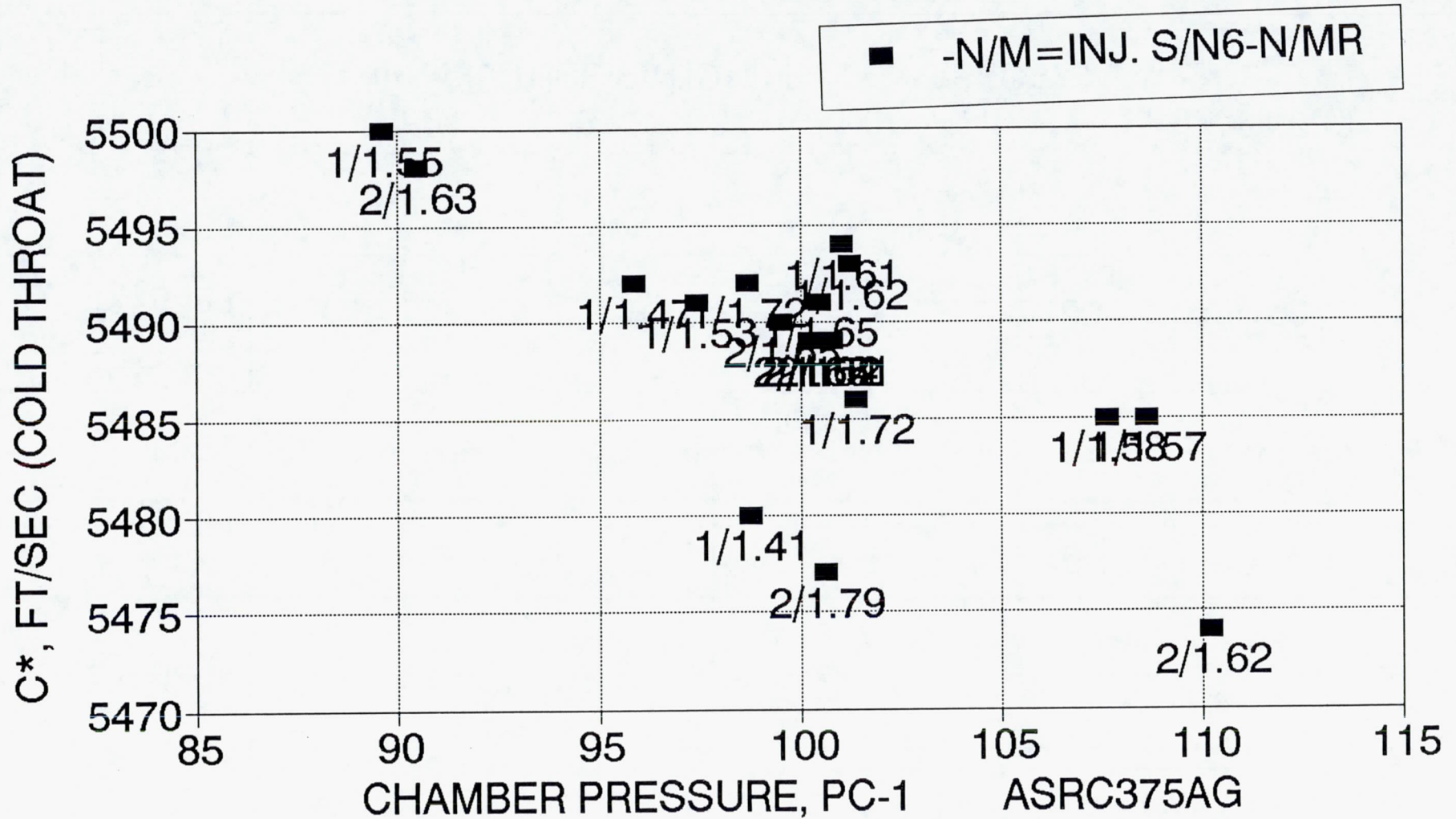


Figure 6.3-55. SN 6-1 and 6-2 Injectors C* vs PC – Final Performance Data at 44:1

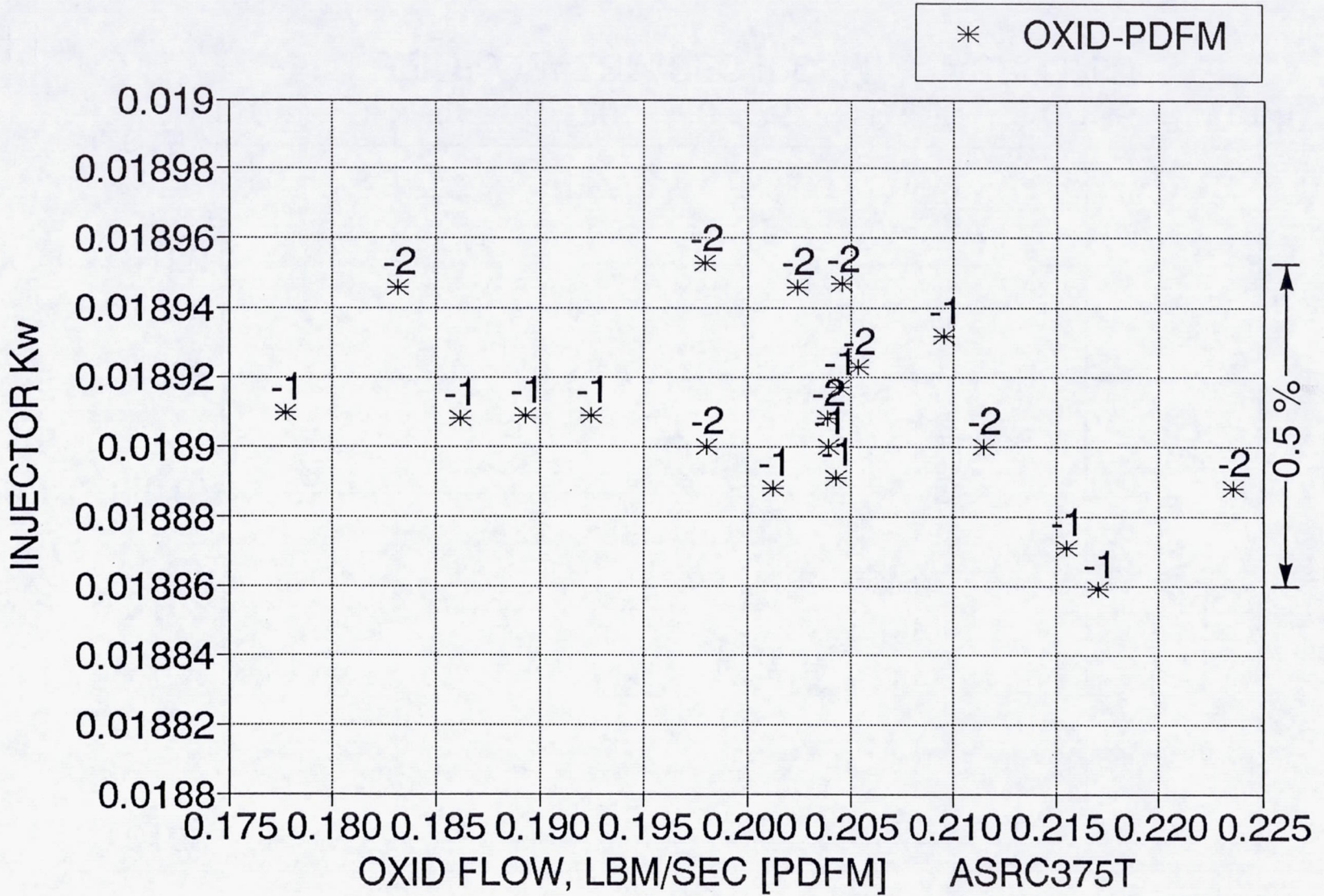


Figure 6.3-56. SN 6 Injector Oxid Kw vs Flow Rate

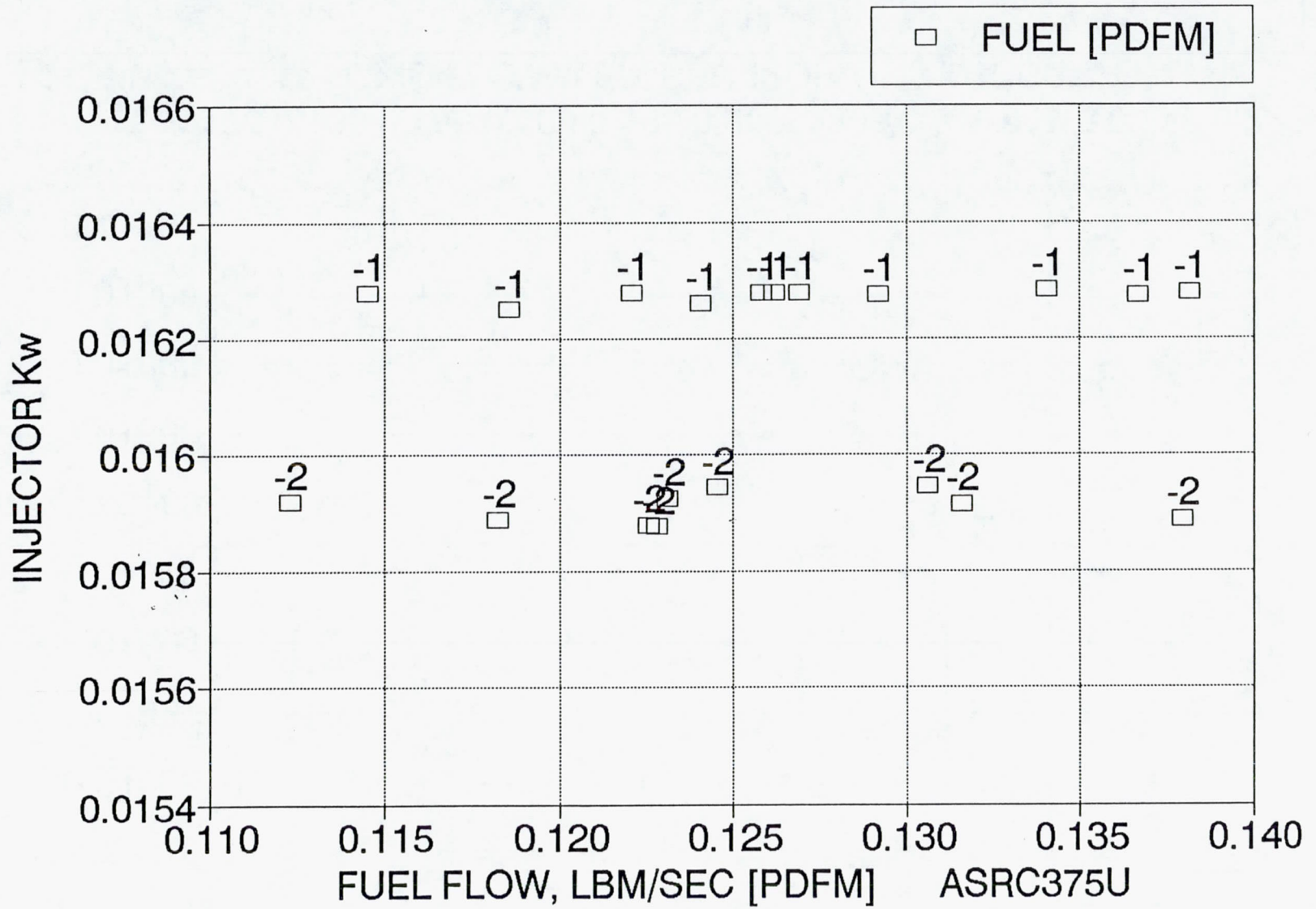


Figure 6.3-57. SN 6 Injector Fuel Kw vs Flow Rate

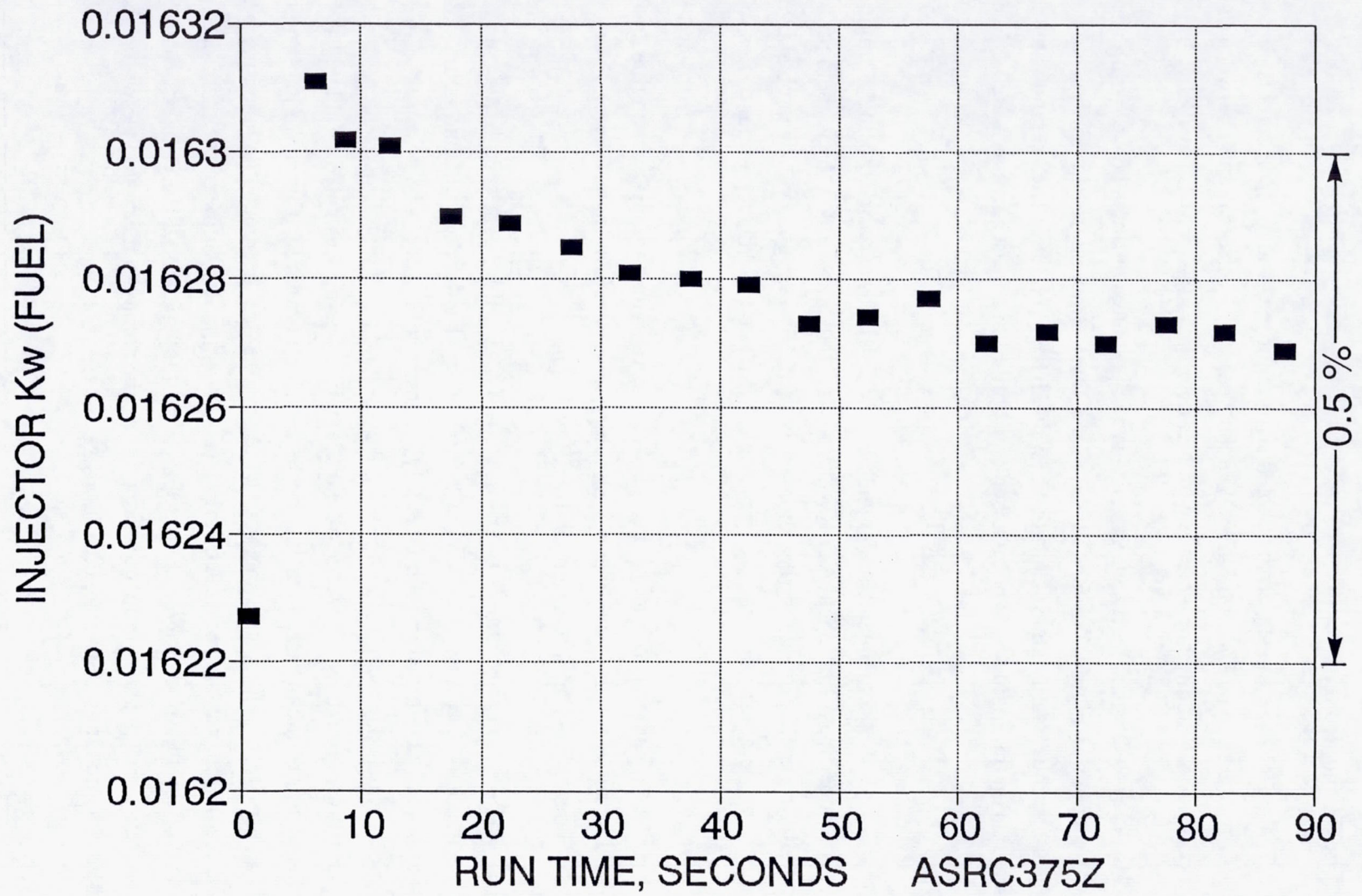


Figure 6.3-58. SN 6-1 Injector Fuel Kw vs Time Test -244

6.3, Hot Fire Testing (cont.)

Heat transfer to the cooled adapter for the -1 and -2 injectors is shown as a function of mixture ratio in Figure 6.3-59. Note that there is no differentiation between the injectors; both show a significant increase with MR over the range from 1.4 to 1.8.

Typical hardware and facility temperatures during a 90-sec firing and post test coast are shown in Figures 6.3-60 and -61. Since these temperatures are for bolt-up hardware they are not necessarily significant for the welded, flight engine. They do indicate that many locations on the engine have not reached equilibrium in a 90-sec firing or a 20-min coast.

6.3.3 Weld Thermal Cycle Test

A special chamber shown in Figure 5-10 was assembled using a previously fired Ir-Re chamber from Ref. 3 and a C-103 "miniskirt" that was welded to the rhenium with the PN 1206384-9 trimetallic transition ring shown schematically in Figure 5-7. The objective of this chamber was demonstration that the joint could be subjected to deep thermal cycles without failure.

The joint was located at a lower area ratio than in the flight engine design, so that it would be subjected to 150 F higher peak temperature at steady state. Figure 6.3-62 shows the chamber components prior to assembly by EB welding.

Leak check of the miniskirt Re-to-C103 weld joint assembly indicated an extremely small leak, probably at the CVD Cb-C103 joint. Evidence of disbond in the CVD Cb deposit was noted. The miniskirt joint assembly is shown in Figure 6.3-63 prior to thermal cycle test. The joint was leak checked after 15 thermal cycles; no change in the extremely small pretest leakage was noted. No evidence of leakage during testing was noted. Table 6.3-11 summarizes the results of the miniskirt thermal cycle tests, Test Group D. Figure 6.3-64 is a photograph of the weld test joint after testing; residue of spot welded thermocouple junctions are clearly visible on the uncoated portion of the C103 and on the Re. Some of the thermocouples were broken off by the shock wave which occurs at shutdown due to diffuser backflow. Figure 2.2-16 is a frame from a photo sequence taken during the complete thermal cycle which shows the miniskirt chamber at steady-state conditions.

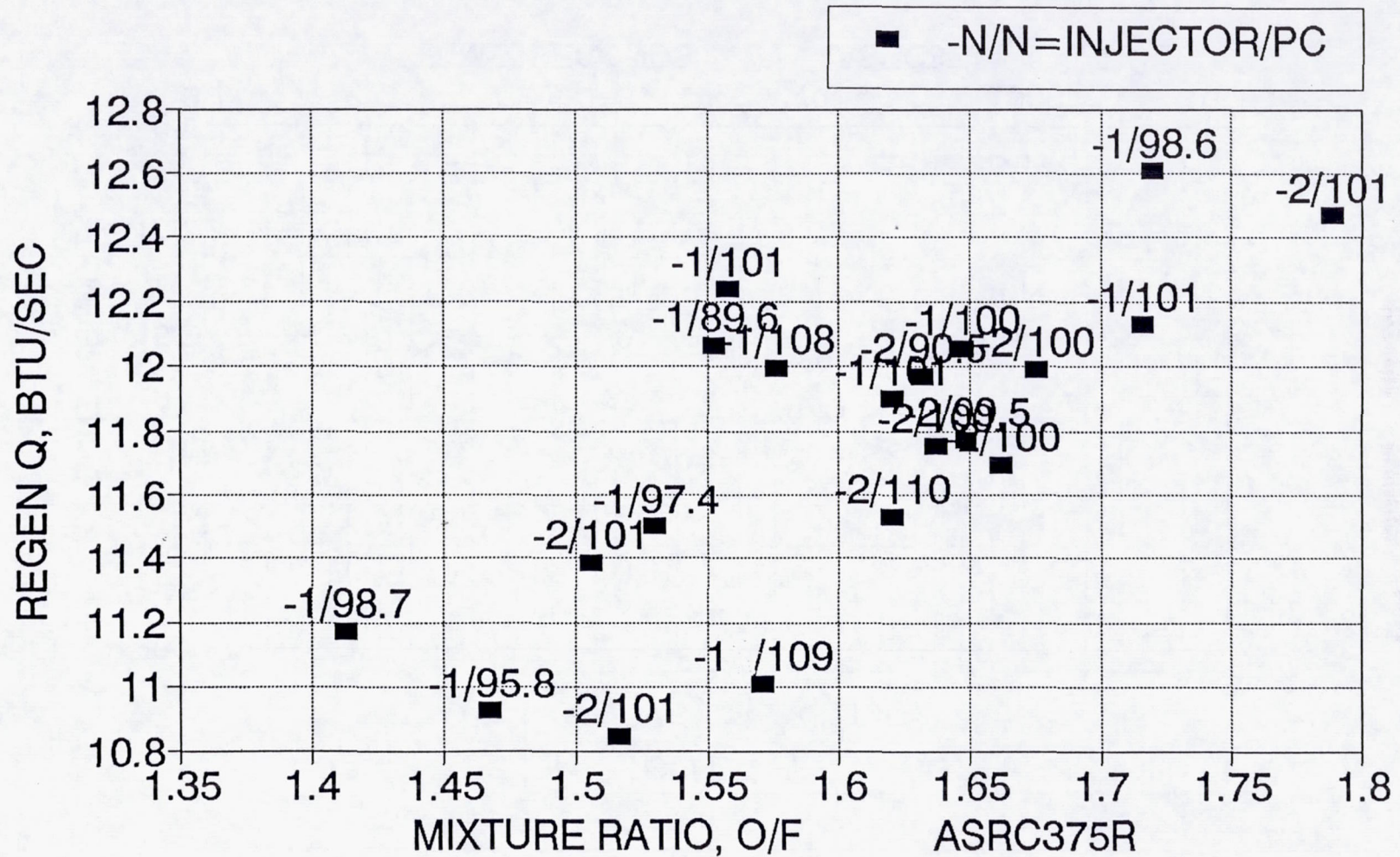


Figure 6.3-59. SN 6-1 and 6-2 Injectors Regen Q vs MR Final Performance Data at 44:1

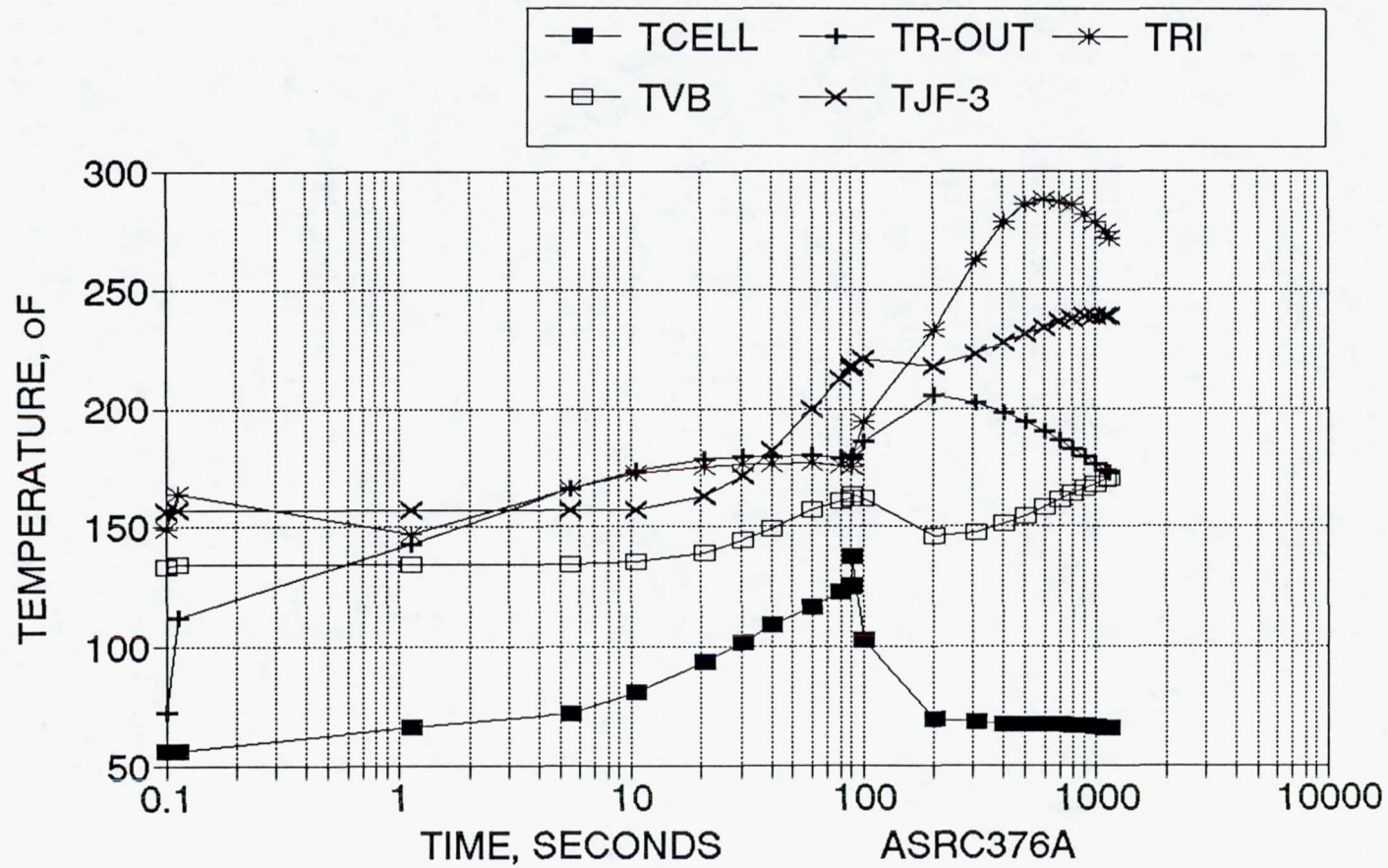


Figure 6.3-60. 100# Ir-Re SN 6-1 Temperature vs Time – Test -244, 90 Seconds

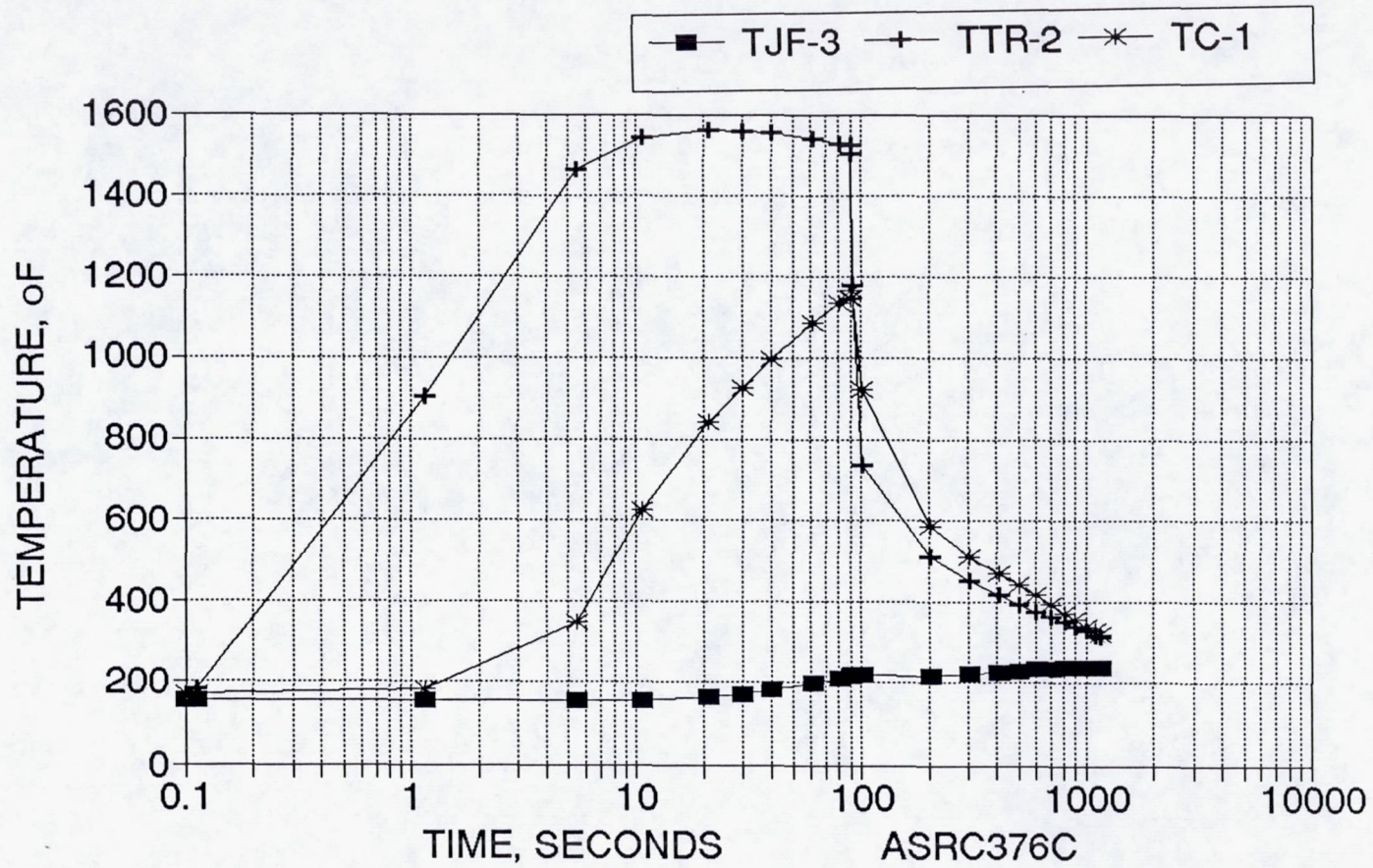
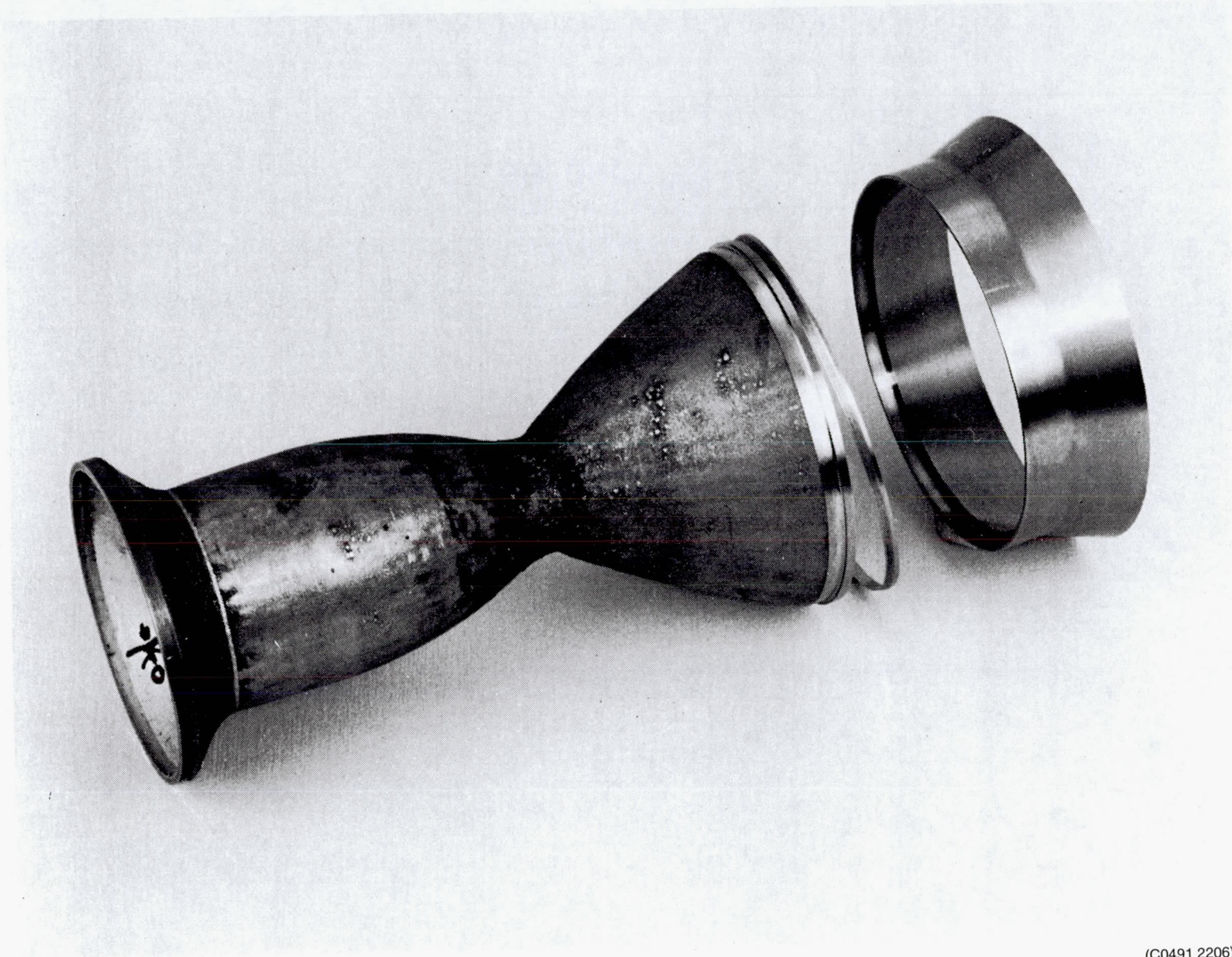


Figure 6.3-61. 100# Ir-Re SN 6-1 Temperature vs Time – Test -244, 90 Seconds



(C0491 2206)

Figure 6.3-62. Miniskirt Chamber Prior to Assembly





Figure 6.3-63. Miniskirt Weld Joint Thermal Cycle Chamber Prior to Test

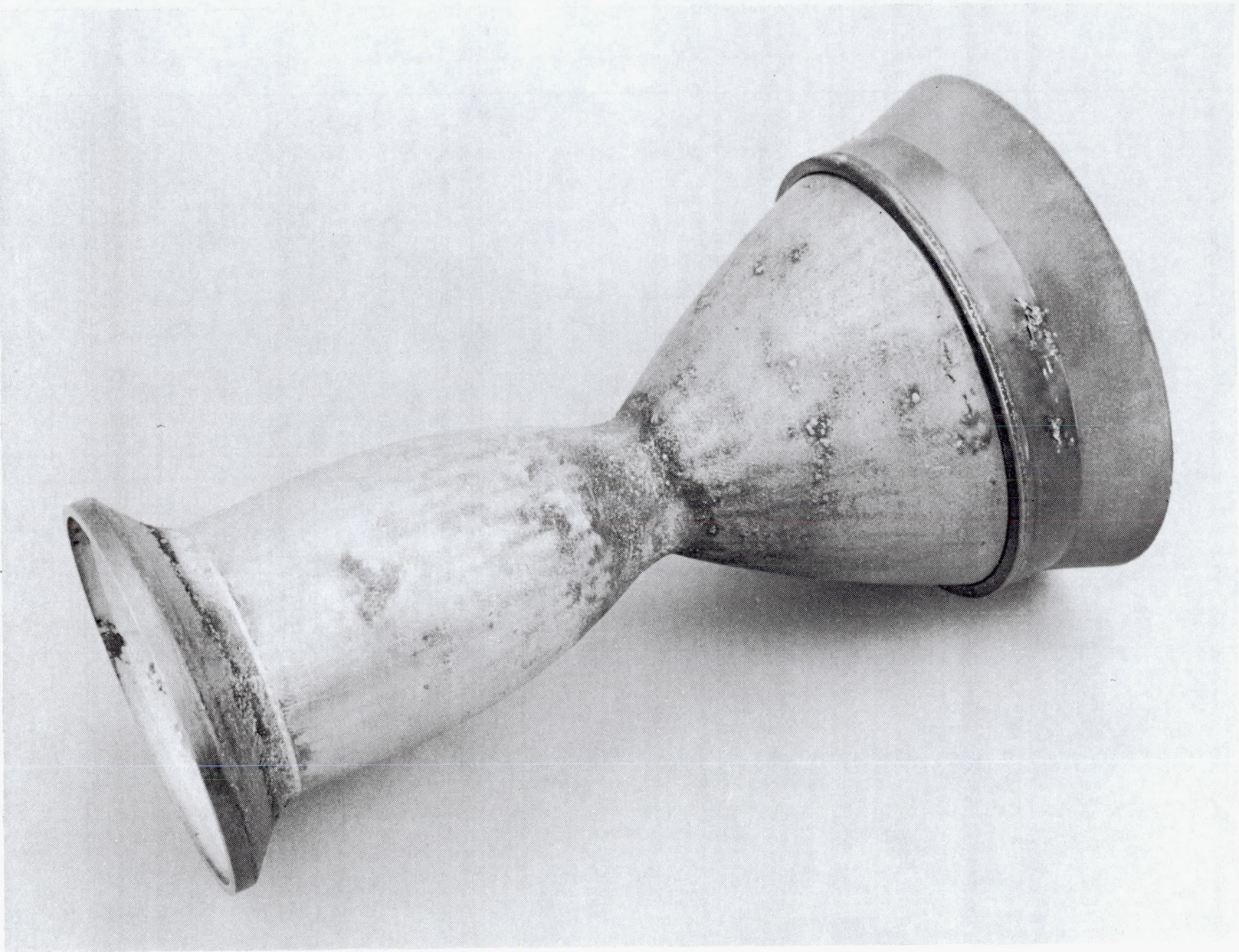


Figure 6.3-64. Miniskirt Weld Joint Thermal Cycle Chamber After 15 Cycles

6.3, Hot Fire Testing (cont.)

Table 6.3-11. The Miniskirt Test Series Thermally Cycled the Nozzle Weld Joint in Hot-Fire Tests

Test No.	Time, sec	Mixture Ratio, O/F	Pc, psia	Joint Temperature at Equilibrium, °F
171	90.0	1.68	107.2	2148
172	30.0	1.69	107.8	2144
173	18.8	4.78	115.0	2160
175	30.0	1.62	110.7	2014
176	4.0		95.0	<pyro limit
177	30.0	1.65	107.5	2192
178	30.0	1.64	106.5	2173
179	30.0	1.65	105.9	2174
180	30.0	1.63	106.3	2141
181	1.0		118.0	<pyro limit
182	30.0	1.64	104.9	2124
183	30.0	1.65	105.2	2135
184	30.0	1.63	106.0	2119
185	30.0	1.64	106.0	2123
186	30.0	1.65	106.5	2123
187	30.0	1.63	106.3	2106
188	30.0	1.64	106.0	2120
Total = 15 Deep Thermal Cycles No Degradation of Welded Re-C103 Nozzle Joint				

No degradation of the rhenium-to-C-103 nozzle joint was noted on completion of this testing. Following these tests, the full area ratio, flighttype engine was assembled using injector SN 6-2 as discussed in Section 5.7.

6.3.4 286:1 Performance Tests

The objective of the performance tests, Group H, was to measure directly thruster performance at altitude with the 286:1 flight nozzle. Since the thrust is measured directly and since the correction term, $P_a \cdot A_e$, to convert measured altitude thrust to vacuum thrust is small (about 2%, or 6 sec of I_s increase), there is high confidence in the resulting vacuum specific impulse reported.

The accuracy of the measurement is dependent on well-defined quantities: propellant flow rate, measured altitude thrust, nozzle exit pressure and cell ambient pressure. The propagation of error analysis for the specific impulse is described in Appendix G. The measured vacuum specific impulse for the 286:1 engine at MR = 1.65 and $F = 490$ N (110.2 lbf) is 321.8 ± 0.7 (1 σ).

The engine completed the performance test series without incident, while accumulating 986 sec of firing time. The engine assembly after test is shown in Figure 6.3-64.

6.3, Hot Fire Testing (cont.)

6.3.4.1 Facility

The test instrumentation list is shown in Table 6.3-12; it contains minor modifications from the 44:1 testing. Figure 6.3-66 documents the instrumentation location on the engine.

The test cell was modified by replacing the 6 in. diffuser with the 14 in. second throat diffuser, shown in Figure 6.3-33. At the planned maximum firing time of 120 sec, the diffuser exit pressure was predicted to be about 1 psia. At shutdown the nozzle is subjected to a sudden overpressure from the shock wave which travels up the diffuser. To eliminate any potential for damage of the high area ratio skirt by asymmetric overpressurization, the nozzle was surrounded by a "bumper" mounted from the diffuser inlet and designed to pick up any nozzle side loads if nozzle deflection exceeded 0.050 in.

Figures 6.3-67 and 6.3-68 show the engine pretest during installation in the altitude cell. The latter figure shows the pretest appearance of the nozzle exit. The outward step at the C103 skirt weld is accentuated in the photo because of glare; the measured value of the step is 0.010 to 0.020 in. which is incorporated in the design to avoid the occurrence of an inward step through tolerance buildup.

6.3.4.2 Testing

The complete performance test series included Runs -259 through -278, as shown in Table 6.3-13. The performance measurements shown in this data summary are final values based on data using the turbine flowmeters calibrated in propellant with the PDFMs.

Runs -259 and -260, of 1 and 5 sec duration, respectively, were conducted for facility checkout. Runs -261 through -264, of 10 sec duration, were used to determine PDFM pressure set points for the range of vacuum thrust to be investigated. Tests -265 through -269, of 25 sec duration, were run to provide propellant calibration of the turbine flowmeters against the PDFMs over the thrust and MR range planned for the long duration tests. The duration of these tests was set by the PDFM capacity, as shown in Figures 6.3-69 and 6.3-70. In 25 sec, the engine is close to thermal equilibrium but specific impulse is still rising slightly as the nozzle heats to its final value.

Test -270, of 5 sec duration, was a balance test to set propellant tank pressures for the long duration tests. Tests -271 and -272 explored longer firing times of 60 and 100 sec, respectively, primarily to determine the effect of the increased diffuser unload pressure on

Table 6.3-12. 100 lb Bay 2 Instrumentation List - Altitude Test at 286:1 (Sheet 1 of 3)

PAGE 1

UPDATE 2-8-92

@ = MODS FROM 44:1 LIST

@@ = MODS FROM INITIAL 286:1 LIST

RECORDING

FUNCTION	PARAMETER	SYMBOL	KILL	RANGE	TRANSDUCER	DIGITAL	RECORDING		
			LOW/HIGH				O-GRAPH	VISUAL	FM TAPE
THRUSTER	THRUST A	FA	--	0-200 lbf	STRAIN GAGE	X	X	X	
PERFORMANCE	THRUST B	FB	[NOT INSTAL.]	0-200 lbf	STRAIN GAGE	X	X		
	THRUST CAL A	FCAL-A	--	0-200 lbf	STRAIN GAGE	X	X		
	THRUST CAL B	FCAL-B	--	0-200 lbf	STRAIN GAGE	X	X		
	CHAMB. PRESS 1 (INJ)	PC-1	50/150	0-200 psia	TABOR 206	X	X	X	
	OXID FLOW 1	FMO-1	--	0.13-0.3 lbfm/sec (prop.)	TURBINE METER	X	X		
	OXID FLOW 2	FMO-2	--	0.13-0.3 lbfm/sec (prop.)	TURBINE METER	X	X		
	FUEL FLOW 1	FMF-1	--	0.08-0.3 lbfm/sec (prop.)	TURBINE METER	X	X		
	FUEL FLOW 2	FMF-2	--	0.08-0.3 lbfm/sec (prop.)	TURBINE METER	X	X		
	OXID. VALVE INLET PRESS.	POVI	--	0-500 psia	TABOR 206	X	X		
	FUEL VALVE INLET PRESS.	PFVI	--	0-500 psia	TABOR 206	X	X		
	OXID INJ. INLET PRESS.	@ POJ	--	0-500 psia	TABOR 206	X	X		
	FUEL INJ. INLET PRESS.	@ PFJ	--	0-500 psia	TABOR 206	X	X		
	FUEL REGEN INLET PRESS.	PFRI	--	0-500 psia	TABOR 206	X	X		
	FUEL REGEN OUTLET PRESS.	PFRO	--	0-500 psia	TABOR 206	X	X		
	EXIT AMBIENT-1, -2	PEXIT-1, -2	-0.1/+0.2	0-1 psia	TABOR	X	X	X	
	EXIT AMBIENT-3, -4	PVAC-1, -2	--	0-10 Torr	BARATRON	X	X	X	
	VALVE VOLTAGE	VTVC	--	0-30 Vdc		X	X		

Table 6.3-12. 100 lb Bay 2 Instrumentation List - Altitude Test at 286:1 (Sheet 2 of 3)

FUNCTION	PARAMETER	SYMBOL	LOW/HIGH	RANGE	TRANSDUCER	RECORDING		
						DIGITAL	O-GRAPH VISUAL	FM TAPE
THRUSTER TEMPERATURE	OXID INLET TEMP	TOJ	--	40-100oF	TYPE K	X		
	FUEL REGEN INLET	TR-IN	--	40-100oF	TYPE K	X		X
	REGEN. INTERNAL	@ TRI	[NOT INSTAL.]	40-500oF	TYPE O P ; .010 dia	X		
	FUEL REGEN OUTLET	TR-OUT		250 40-200oF	TYPE K	X		
	INJ. BODY	@ TJB-1,-2,-3	0/250	40-500oF	TYPE K	X		
	VALVE BODY TEMP.	TVB	0/250	40-500oF	TYPE K	X		
	REGEN BODY	@ TRB-1,-2,-3	0/500	40-500oF	TYPE K	X		X
	VALVE/INJ ADAPTOR	@ TVJ-1,-2,-3	--	40-500oF	TYPE K	X		X
	NOZZLE/EXT. JOINT (Re)	@ TNR-1,-2,-3	--	40-2200oF	TYPE K	X		
	NOZZLE/EXT. JOINT (C-103)	@ TNC-1,-2,-3	-100/2000	40-2000oF	TYPE K	X		
	NOZZLE EXIT	@ TNE-1,-2,-3	[NOT INSTAL.]	40-2000oF	TYPE K	X		
	H2 FILM COOLING SKIRT	TFC		40-2000oF	TYPE K	X		
	CHAMBER HOT SPOT	PYRO-HI	/4100	2600-4000F+	IRCON HIGH RANGE	X	X	X
	NOZZLE TEMP.	PYRO-LO	/2200[NOT INSTAL.]	1500-2800F	IRCON LOW RANGE	X	X	X
	MOUNT, REGEN	@ TMR-1,-2,-3		40-500oF	TYPE K	X		
	MOUNT, STAND	@ TMS-1,-2,-3	[NOT INSTAL.]	40-500oF	TYPE K	X		
STABILITY	CHAMBER ACCELERATION	@ AC-1,-2,-3	[NOT INSTALLED]	100-15000Hz			X	X
OPTICAL	OPTICAL MULTICHANNEL ANALYSER (OMA)		[NOT INSTAL.]			RECORDED SEPARATELY		

Table 6.3-12. 100 lb Bay 2 Instrumentation List - Altitude Test at 286:1 (Sheet 3 of 3)

PAGE 3

UPDATE 2-8-92

FUNCTION	PARAMETER	SYMBOL	KILL		TRANSDUCER	DIGITAL	RECORDING		
			LOW/HIGH	RANGE			O-GRAPH	VISUAL	FM TAPE
FACILITY	MICROM. OXID FLOW	FMMO	--		MICROMOTION				
FLOWS	MICROM. FUEL FLOW	FMMF	--		MICROMOTION				
	OXID PDFM	WOPDFM	--			X	X	X	
	FUEL PDFM	WFPDFM	--			X	X	X	
FACILITY	OXID REGULATOR	POTR	--	0-500 psia	TABOR 206	X		X	
PRESSURES	FUEL REGULATOR	PFTR	--	0-500 psia	TABOR 206	X		X	
	OXID TANK	POTS	--	0-500 psia	TABOR 206	X		X	
	FUEL TANK	PFTS	--	0-500 psia	TABOR 206	X		X	
	OXID LINE	POL-1	--	0-500 psia	TABOR 206	X		X	
	FUEL LINE	PFL-1	--	0-500 psia	TABOR 206	X		X	
	H2 ORIFICE UP	PH2UP	15/100	0-100 psia	TABOR 206	X		X	
	H2 ORIFICE DOWN	PH2DN	--	0-50 psia	TABOR 206	X		X	
	ALTITUDE TANK (@ DIFF. EXIT)	PDX	/0.1*	0-5 psia	TABOR 206	X		X	
	DIFFUSER WATER	PDW	5/120	0-100 psia	TABOR 206	X		X	
	FACILITY	OXID LINE	TOL	--	40-100oF	TYPE K	X		X
TEMPERATURES	FUEL LINE	TFL	--	40-100oF	TYPE K	X		X	
	TEST CELL	TCELL	-100/300	0-250oF	TYPE K	X		X	
	VACUUM TANK	TVT	--	0-250oF	TYPE K	X			
	VACUUM PUMP INLET	TVP	--	0-250oF	TYPE K	X			
	DUCT ELBOW	TDUCT	--	0-250oF	TYPE K	X			
	LOAD CELL TEMP.	TF	--	0-250oF	TYPE K	X			
	CAL. CELL TEMP.	TFCAL	--	0-250oF	TYPE K	X			
	NOZZLE SUPPORT	@ VNS	/3.0 volt	0-5VDC	DC VOLT.	[not installed]		X	

-0-

*THIS KILL WILL BE INCREASED IN STEPS TO APPROX. 1.0 PSIA AS TESTING PROGRESSES.
 RUN OGRAPH AT LOW SPEED FOR 1 MIN. AFTER FS-2.

219

ORIGINAL PAGE IS
 OF POOR QUALITY

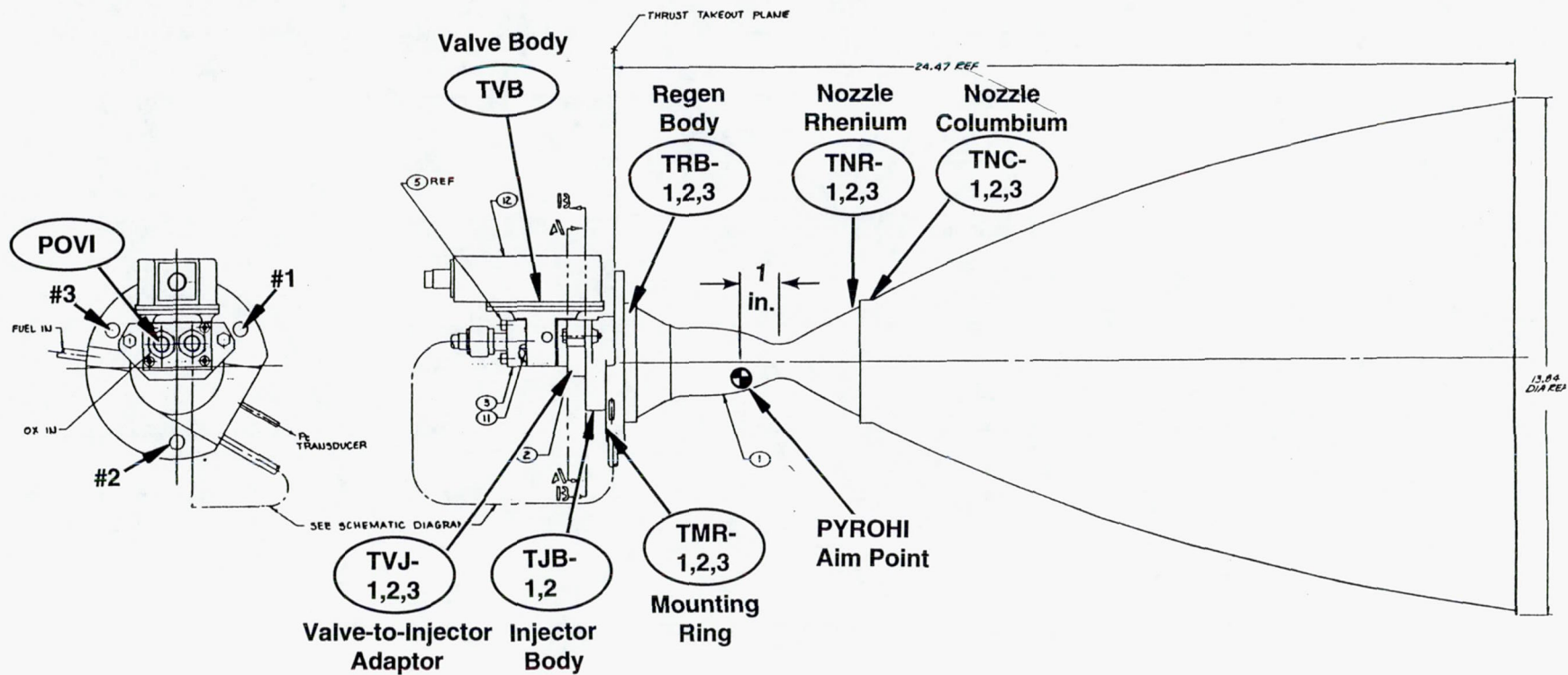
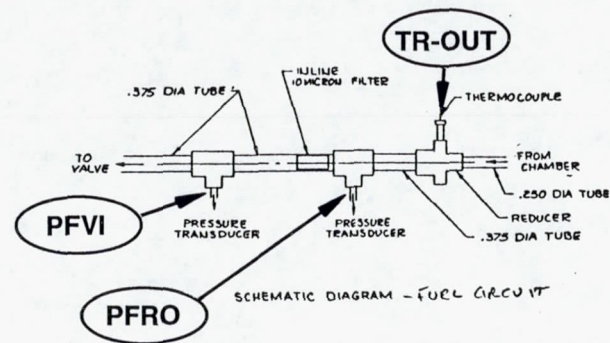


Figure 6.3-66. Instrumentation Locations on 286:1 Welded Thruster SN-1

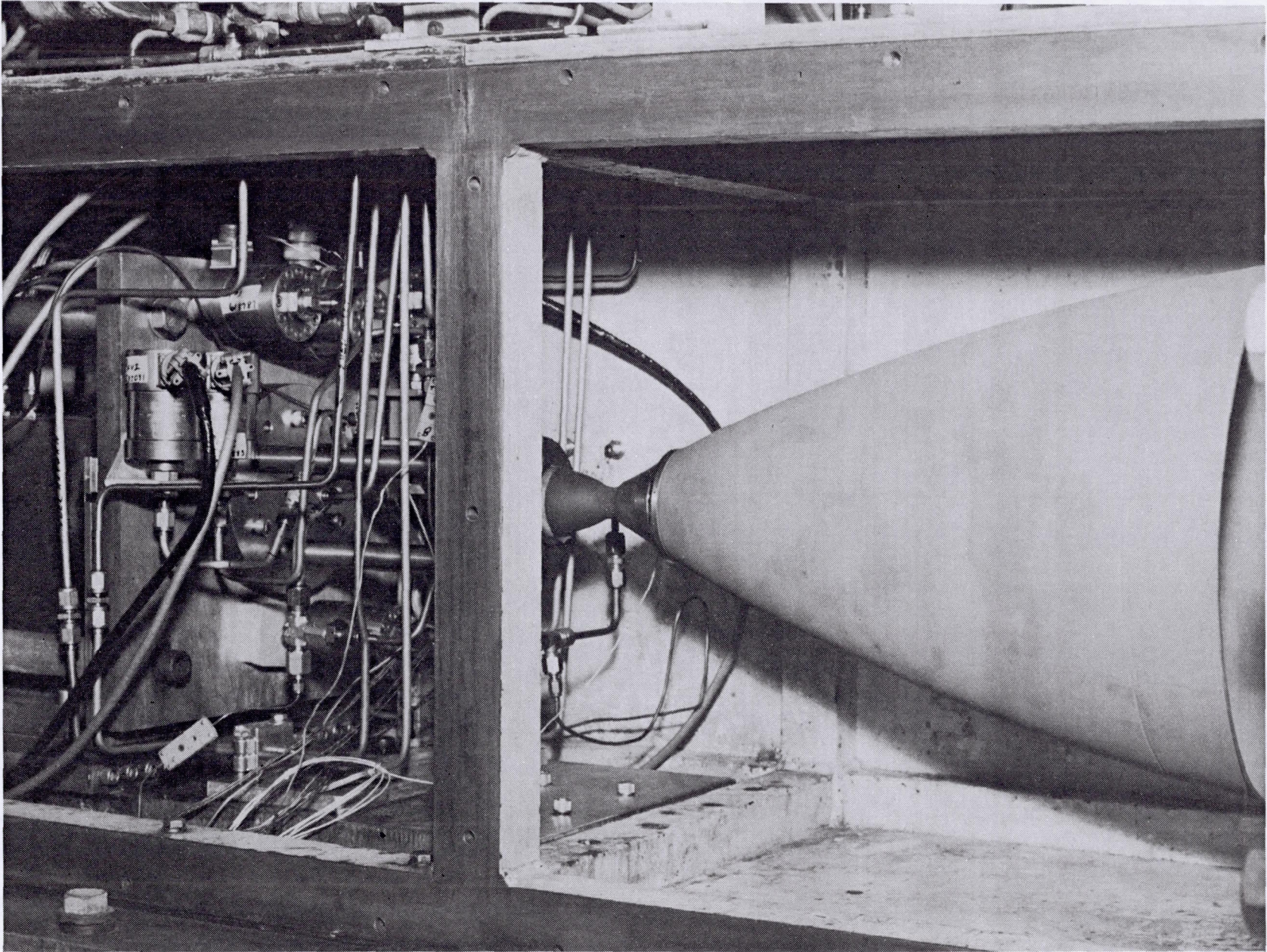


Figure 6.3-67. 286:1 Thruster Installed in Altitude Cell

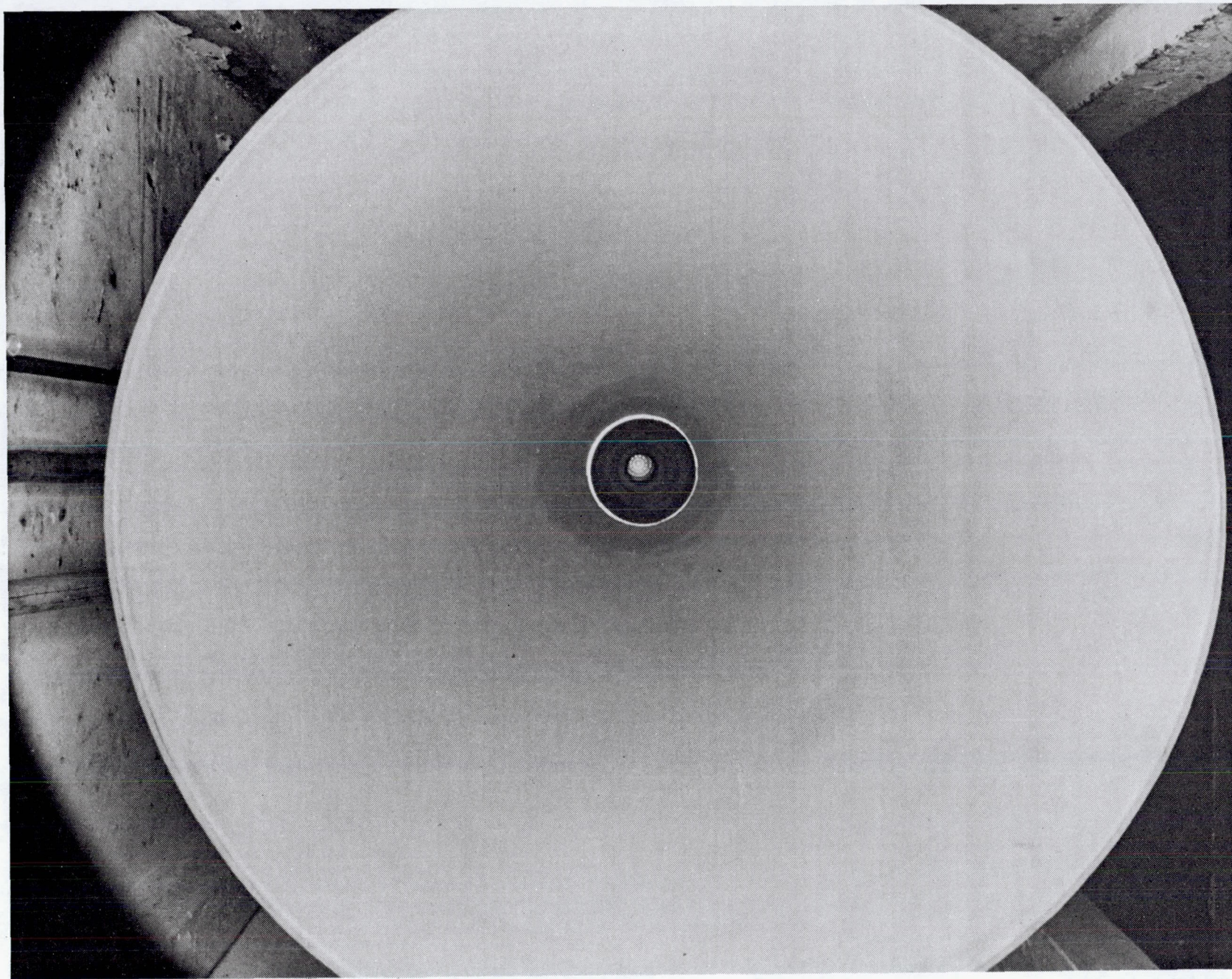


Figure 6.3-68. Pre-Test Appearance of 286:1 Nozzle Interior



Table 6.3-13 490N Liquid Apogee Engine Final Performance Data -
Welded Assembly with 286:1 Area Ratio

RUN No.	FIRING TIME, (sec)	Pc (psia)	MR O/F	Fvac (lbf)	Isp vac (sec)	C* (ft/sec)	Cf	REGEN. OUTLET (F)	REGEN. DELTA T, (F)	CHAMBER TEMP., (F)*
259	1.0	113.8	1.667	105.6	323.5	5574	1.867	119	59	
260	5.0	113.6	1.652	109.0	322.0	5489	1.887	179	120	
261	10.0	116.1	1.639	112.4	323.2	5478	1.898	183	124	2777
262	10.0	127.4	1.592	122.8	320.2	5449	1.891	168	108	2707
263	10.0	104.7	1.620	100.3	321.2	5497	1.880	200	142	2934
264	10.0	117.3	1.599	113.0	321.1	5467	1.890	175	117	3033
265	25.0	116.1	1.647	112.2	322.2	5472	1.895	193	134	
266	25.0	126.9	1.636	122.9	321.7	5449	1.900	178	119	3171
267	23.0	104.8	1.624	100.6	321.3	5494	1.882	210	151	3381
268	25.0	116.2	1.461	111.0	318.0	5462	1.873	176	118	3124
269	25.0	115.9	1.789	112.2	321.8	5456	1.897	207	149	3378
270	5.0	107.8	1.588	102.6	319.3	5484	1.873	178	120	2626
271	60.0	114.8	1.594	110.7	321.6	5469	1.891	193	133	3251
272	100.0	113.5	1.581	109.2	320.8	5471	1.885	194	135	3259
273	120.0	113.7	1.587	109.8	321.8	5471	1.891	195	136	3263
274	120.0	103.5	1.609	99.5	321.2	5482	1.884	217	157	3391
275	120.0	116.5	1.514	111.5	318.8	5461	1.877	183	124	3170
276	120.0	114.8	1.637	110.8	321.5	5469	1.886	200	139	3288
277**	51.7	114.9	1.800	111.2	321.6	5454	1.896	215	153	3391
278	120.0	127.6	1.672	123.8	321.6	5438	1.901	184	124	3199

Total= 985.7 Sec

Avg. Is= 321.2

*With high emissivity surface ($\epsilon = 1.0$)

**Premature shutdown caused by erroneous pyrometer signal

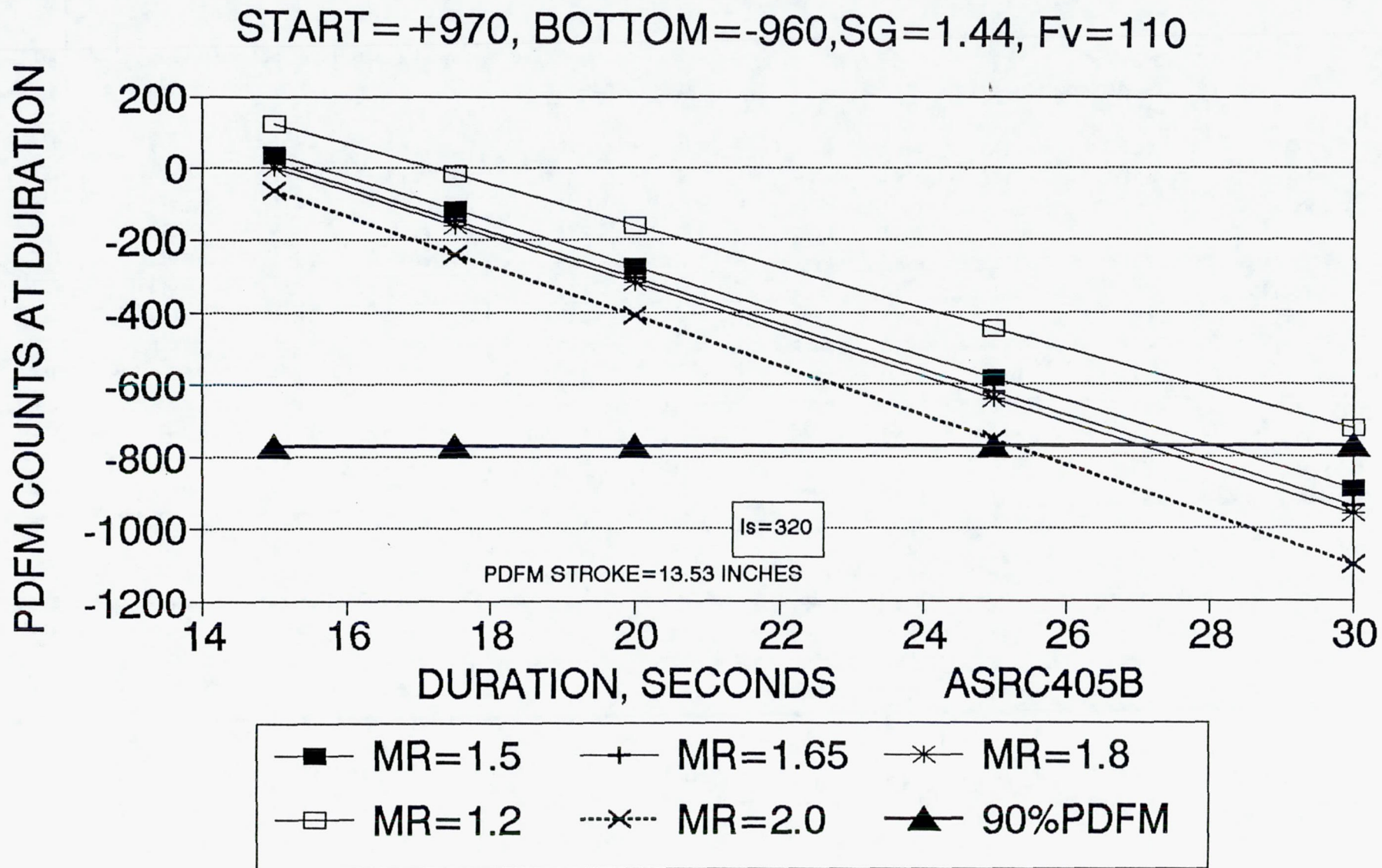


Figure 6.3-69. Capacity of Oxidizer PDFM

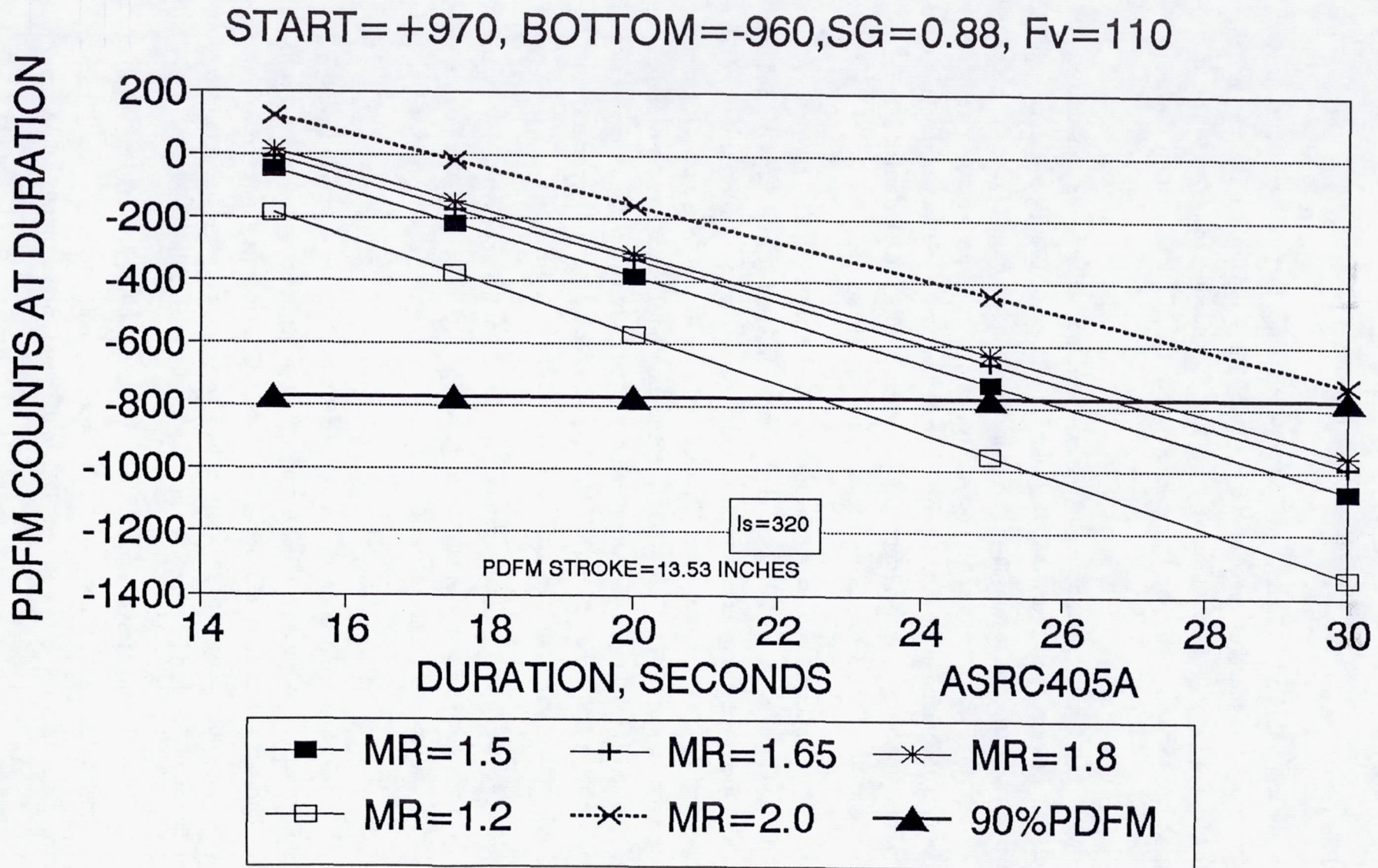


Figure 6.3-70. Capacity of Fuel PDFM

6.3, Hot Fire Testing (cont.)

the engine and test cell. Tests -273 through -278 provided engine performance data at steady thermal conditions over the thrust range of 100 to 124 lbf (P_c of 104 through 128 psia) and the MR range of 1.5 to 1.8. All of these tests were 120 sec long with the exception of -277; an erroneous signal from the low range optical pyrometer exceeded its kill limit, shutting down the firing.

Initially some difficulty was experienced in determining accurate cell pressure which was measured with 2 each 0-10,000 micron (0-0.2 psia) Baratron transducers backed up with two 0-1 psia strain gage transducers. Nominal cell pressure during firing was about 880 micron (0.017 psia). There was an initial uncertainty in the cell pressure which was resolved through post test calibration of the transducers. The effect of error in cell pressure on measured vacuum specific impulse is shown in Figure 6.3-71 for the 286:1 and 47:1 nozzles. The final performance data in Table 6.3-13 uses the corrected ambient pressures.

Specific impulse for the tests of 50 sec duration and longer (Runs 271 through 278) is plotted in Figures 6.3-72 and 6.3-73 versus MR and P_c , respectively. The data points are identified by test number so that the other test parameters can be obtained from Table 6.3-13. Specific impulse is very flat with MR, within ± 0.5 sec over the range from 1.8 to about 1.58, and then falls about 0.8% by MR = 1.5. The data show no effect of P_c on I_s over the range of 104 to 127 psia. The full range of performance data points is plotted in Figure 6.3-74 as a function of MR from 1.45 to 1.8; the gradual fall in I_s with decreasing MR is more evident. The full range of I_s vs P_c is plotted in Figure 6.3-75, I_s is flat from 104 to 127 psia.

Chamber wall temperature shows an increasing trend with mixture ratio (Figure 6.3-76 rising about 220 F over the MR range of 1.5 to 1.8. The trend with P_c is reversed (Figure 6.3-77) with chamber wall temperature dropping about 190 F in going from 104 to 127 psia.

Fuel temperature rise in the regeneratively cooled section is shown as a function of mixture ratio in Figure 6.3-78. A more extensive set of performance and thermal data for the 286:1 thruster tests is given in Appendices H and I. Data characterizing the instrumentation and test facility operation are given in Appendix J. A summary of maximum thruster temperatures at the end of firing and during coast soak out are given in Table 6.3-14.

The post test appearance of the thruster installed in the facility is shown in Figure 6.3-79, which shows the water-cooled 16 in. second throat diffuser in place. Figure 6.3-80 shows the thruster assembly post test -278, on the stand. Some bluing of the nozzle

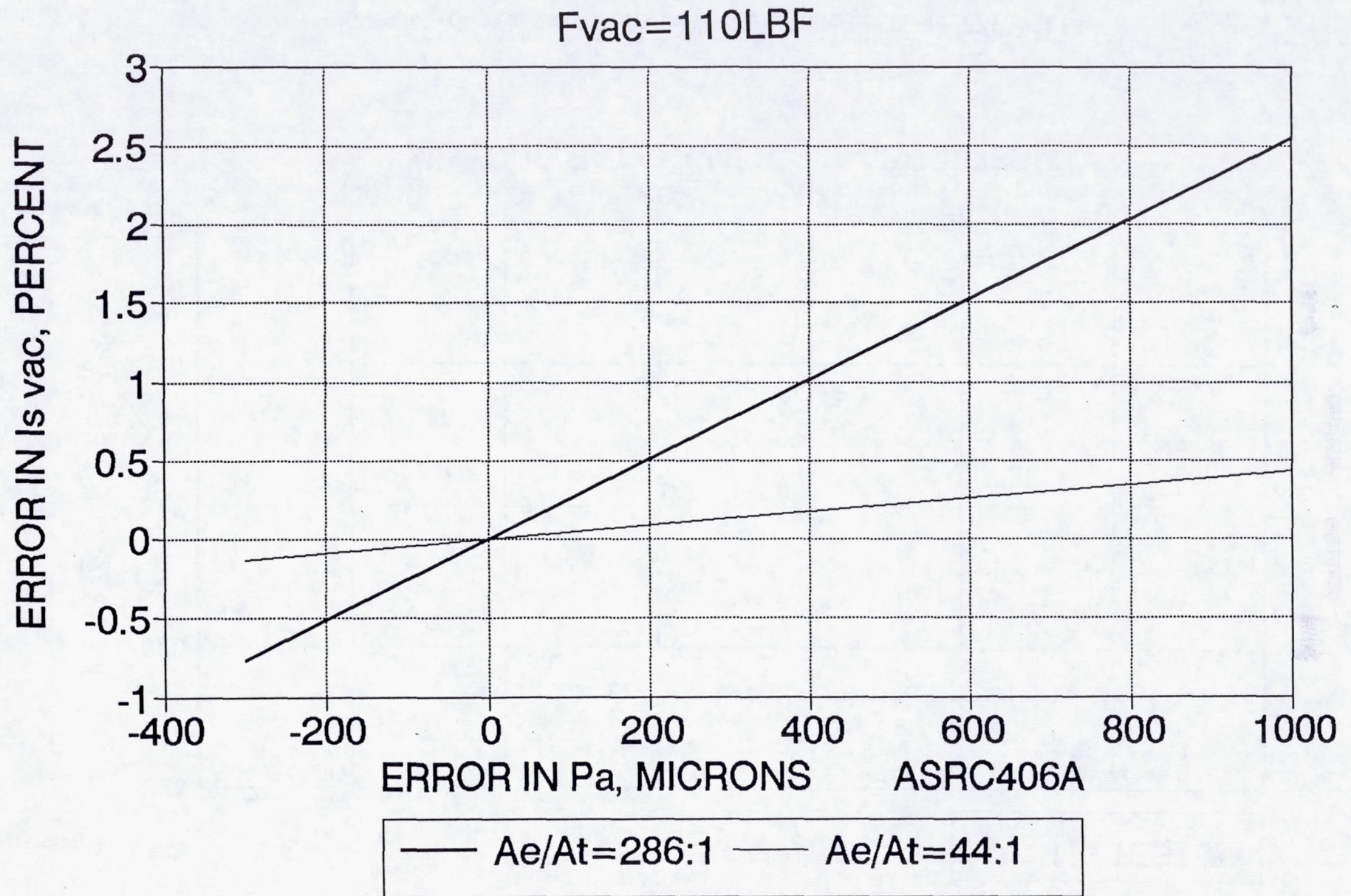


Figure 6.3-71. Specific Impulse Error vs Cell Pressure Error

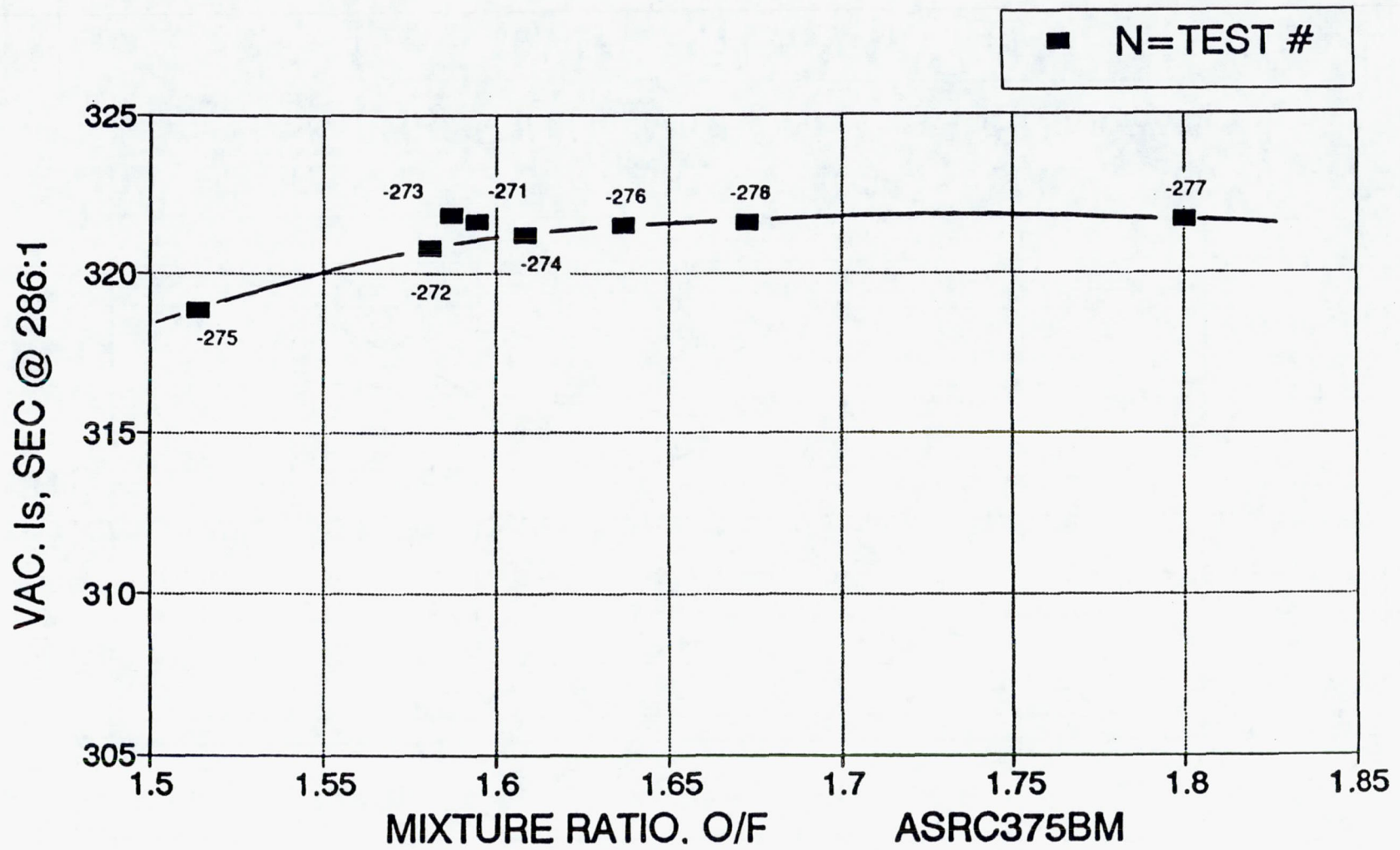


Figure 6.3-72. Vac Is at 286:1 vs Mixture Ratio for Tests -271 to -278

Ir-Re WELDED THRUSTER-- Is vac VS PC-1 FINAL DATA AT 286:1; -271 TO -278

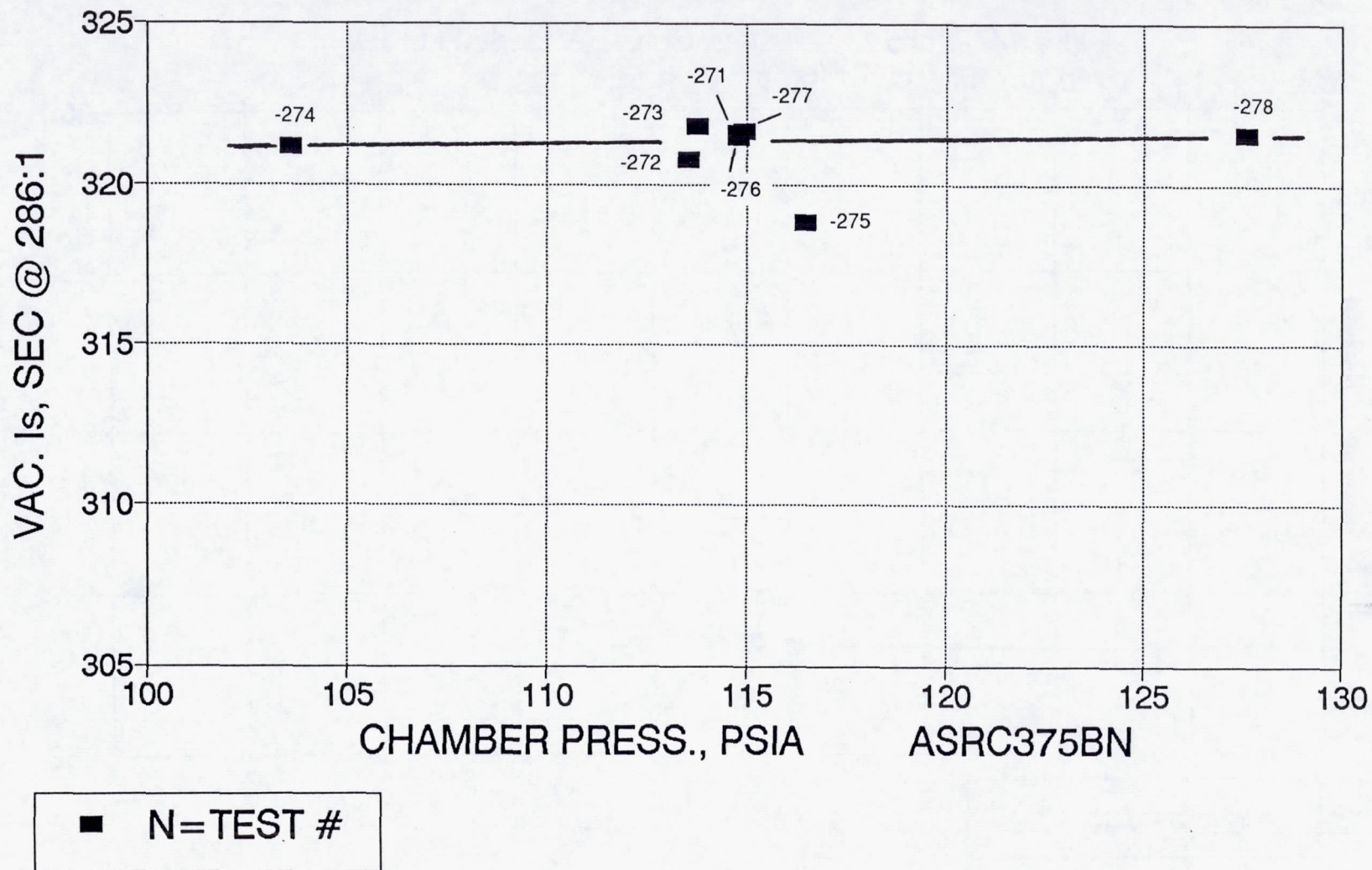


Figure 6.3-73. Vac Is at 286:1 Versus Pc for Tests -271 to -278

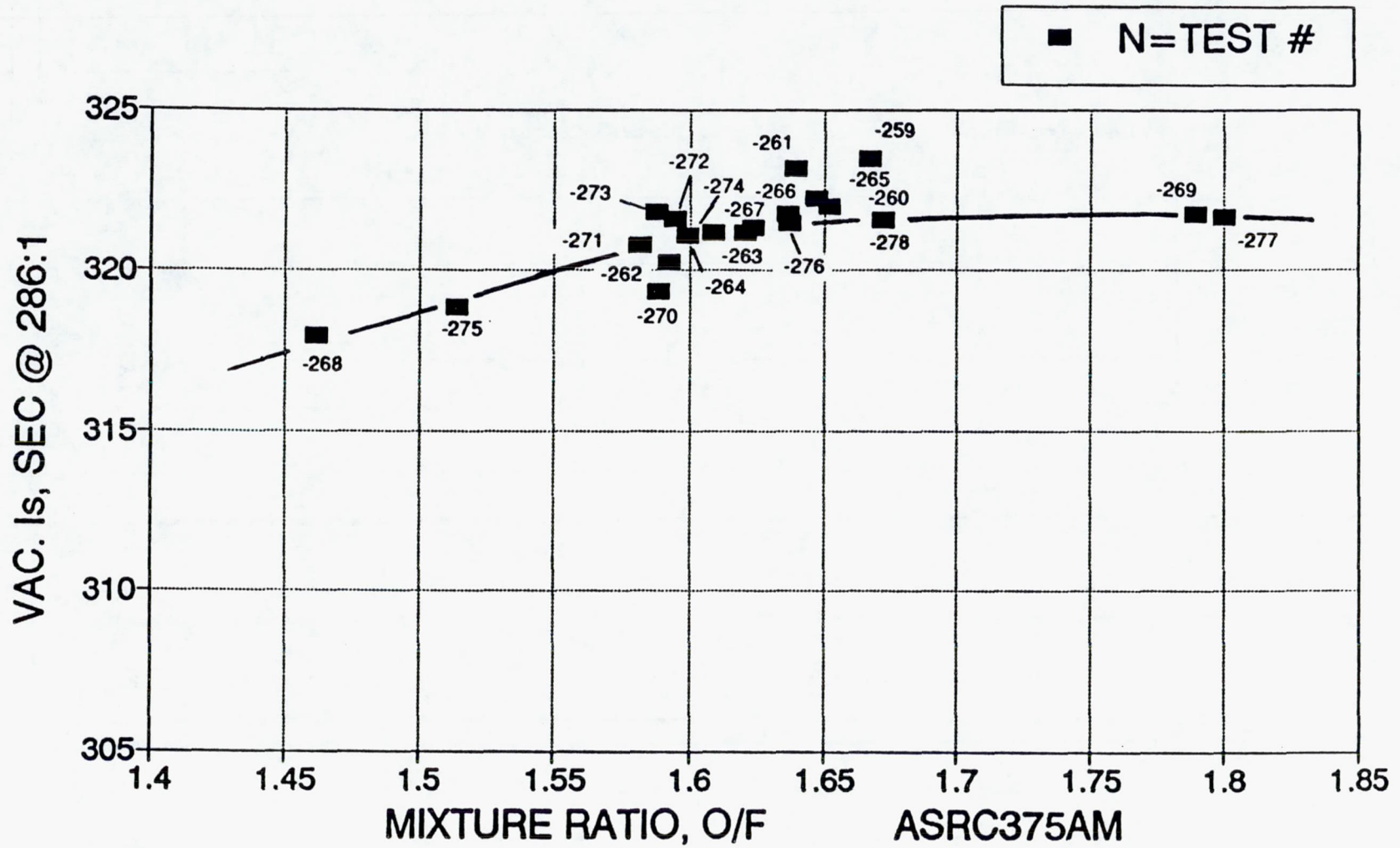


Figure 6.3-74. Vac Is at 286:1 Versus Mixture Ratio; All Tests

Ir-Re WELDED THRUSTER-- Is vac VS PC-1 FINAL DATA AT 286:1; ALL TESTS

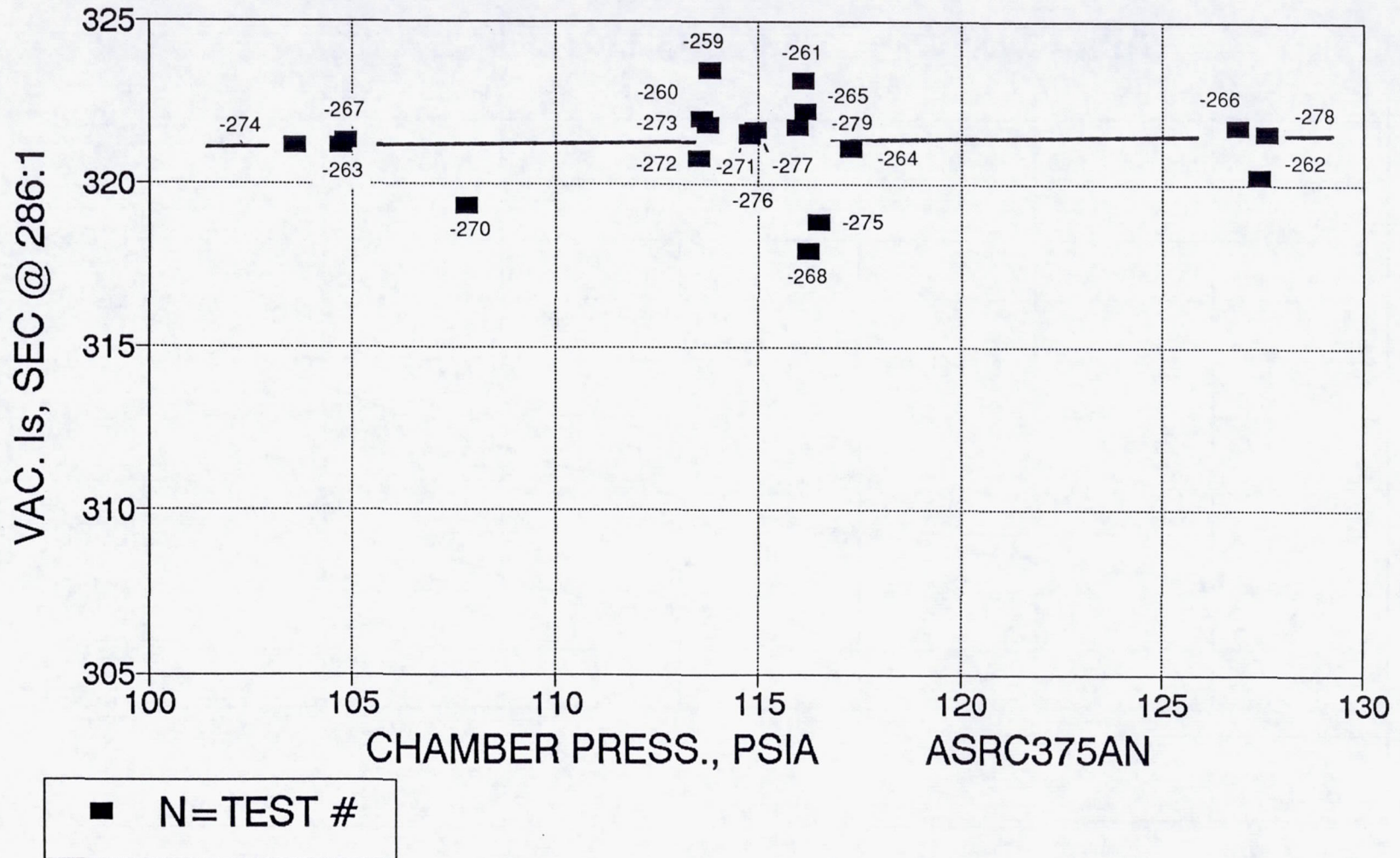


Figure 6.3-75. Vac Is at 286;1 Versus Pc; All Tests

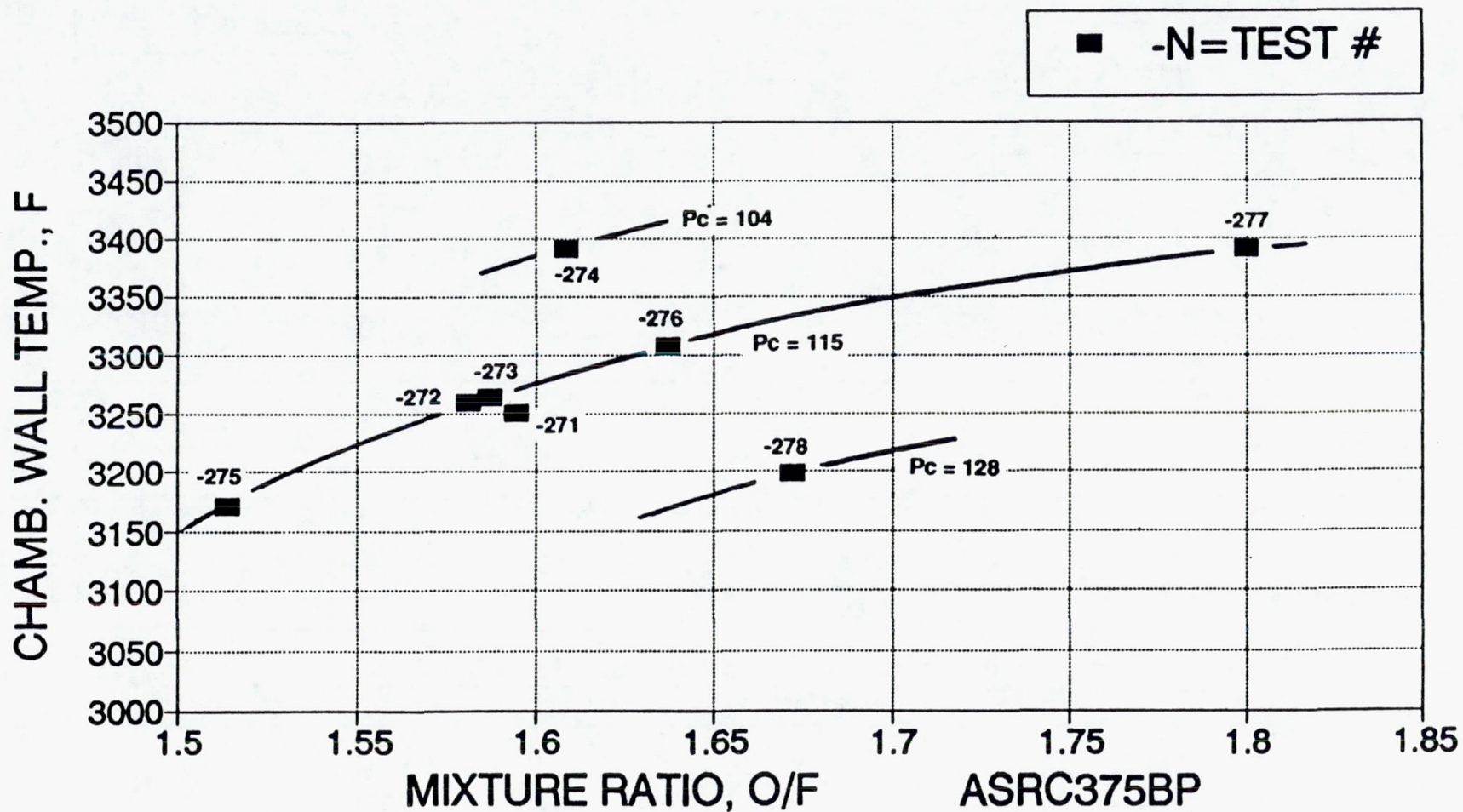


Figure 6.3-76. Chamber Wall Temperature Versus Mixture Ratio for Tests -271 to -278

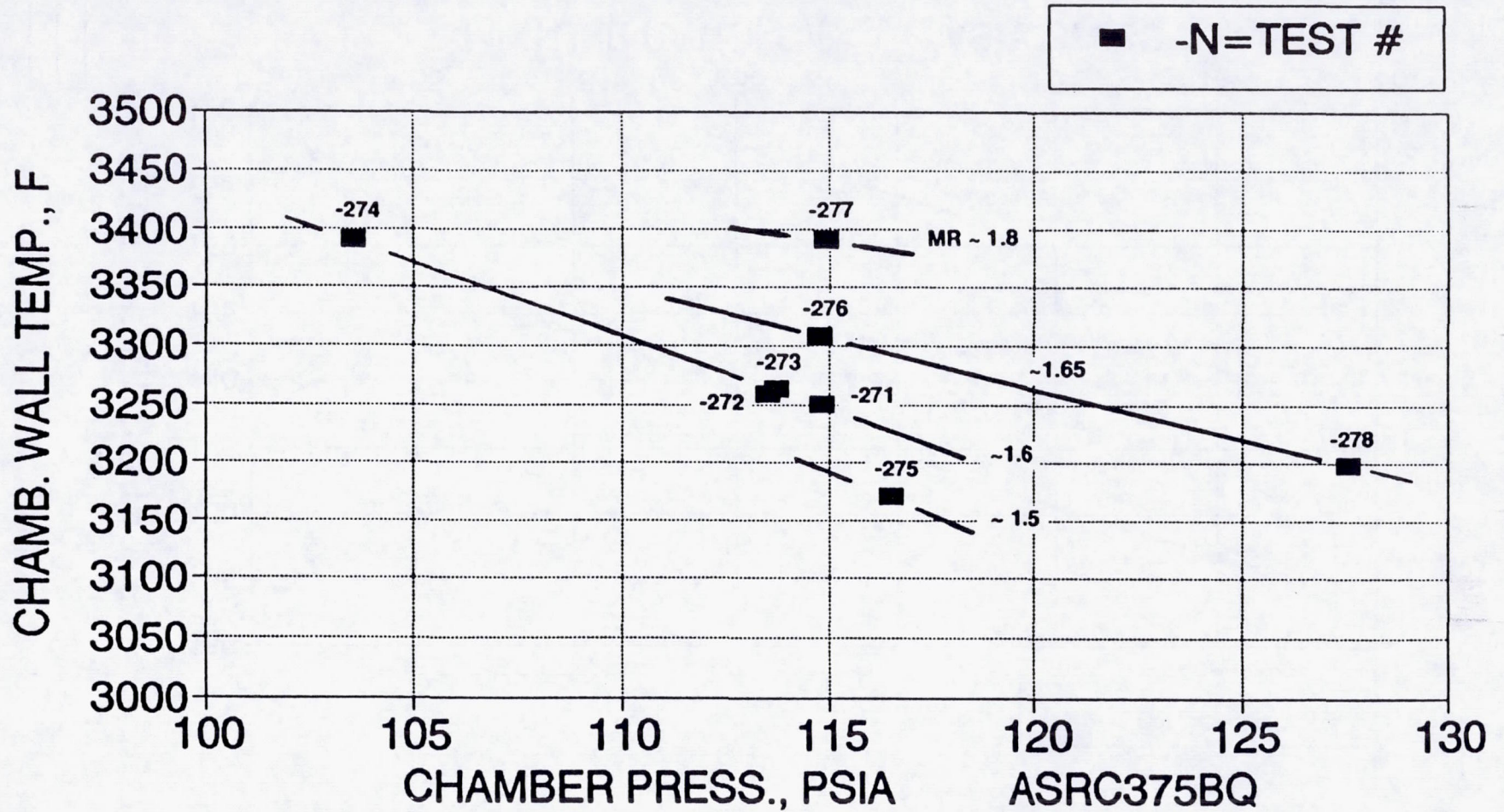


Figure 6.3-77. Chamber Wall Temperature Versus Pc for Tests -271 to -278

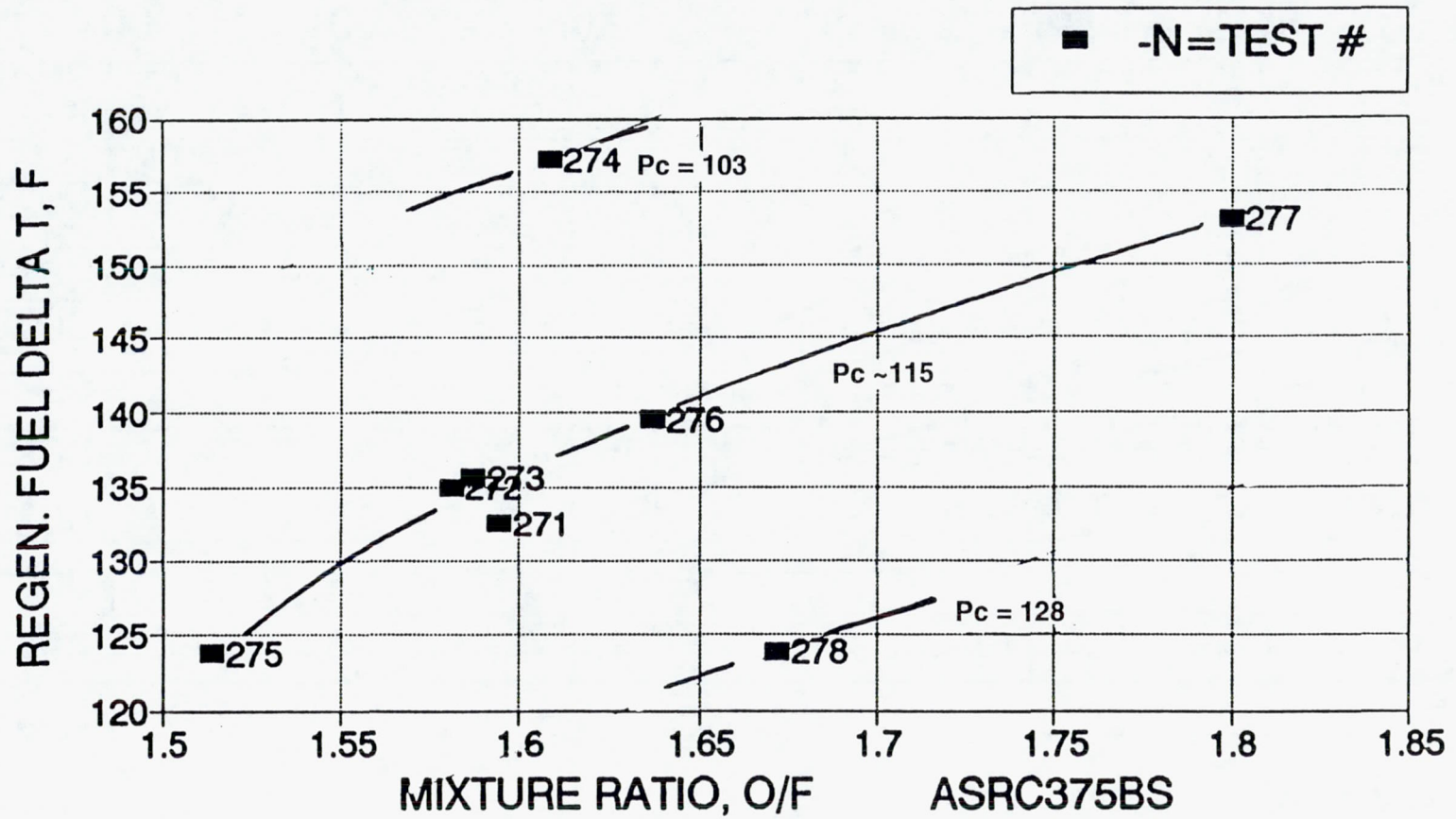


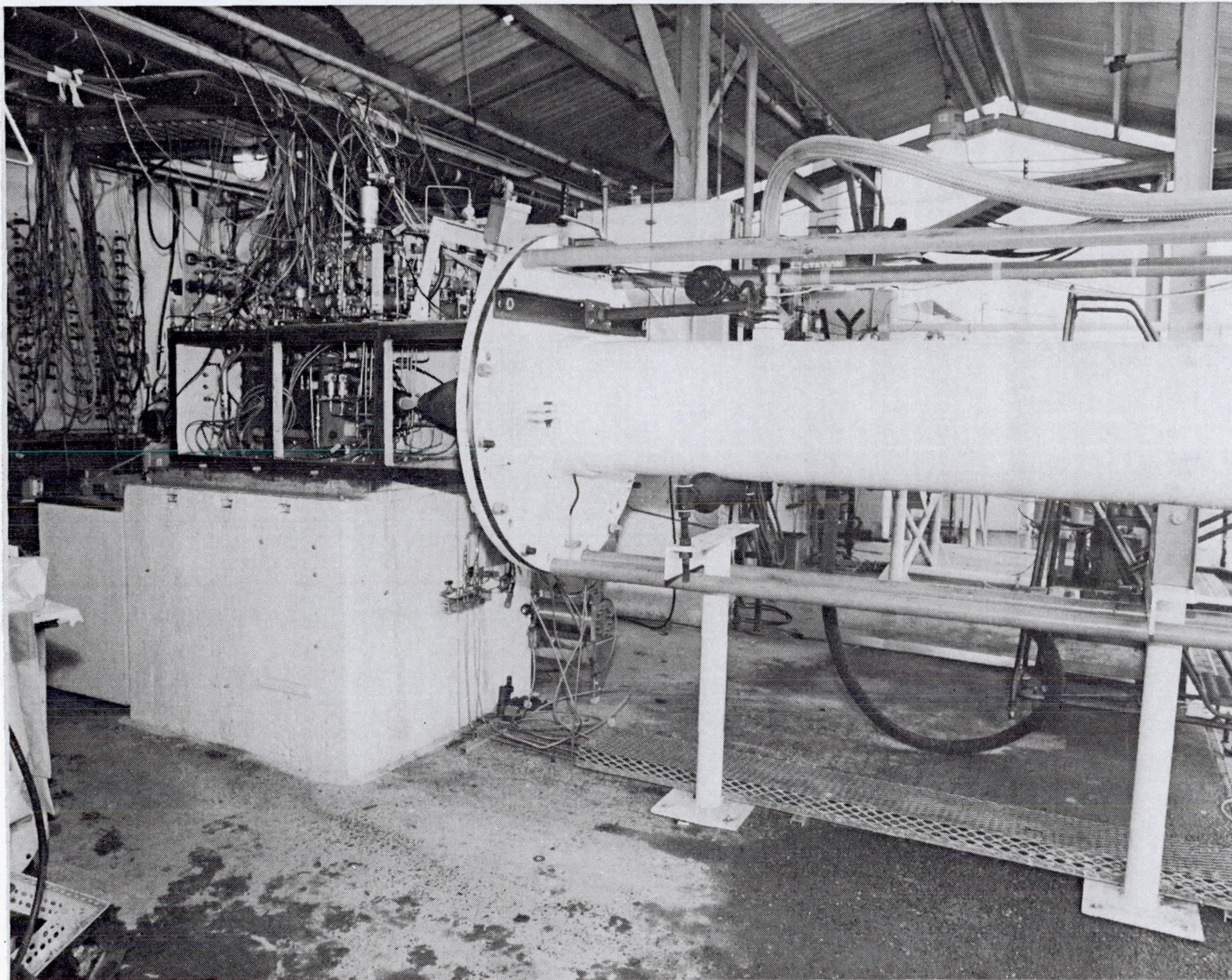
Figure 6.3-78. Regen Fuel ΔT Versus Mixture Ratio, Tests -271 to -278

Table 6.3-14. Maximum Operating Temperatures Ir-Re Welded 286:1 Thruster at Nominal Conditions

ASRC434

MR=1.65
 F=490 N
 θ =120 SEC

LOCATION	MAX. FIRING TEMP., F	MAX. COAST TEMP., F	TIME OF MAX. COAST TEMP., SEC
REGEN O.D.	280	340	150
THRUST MOUNT	122	252	454
REGEN INLET	60	~ 170	>650
REGEN OUTLET	200	201	161
VALVE BODY	179	~ 170	>650
INJECTOR BODY	181	201	402
Re NOZ. @ WELD	2111	<2111	120
C-103 NOZ. @ WELD	1859	<1859	120
CHAMBER WALL	3316	<3316	120



(CO292 0974)

Figure 6.3-79. Bay A-2 Altitude Test Facility and 286:1 Welded Ir Re Thruster,
Post Test -278

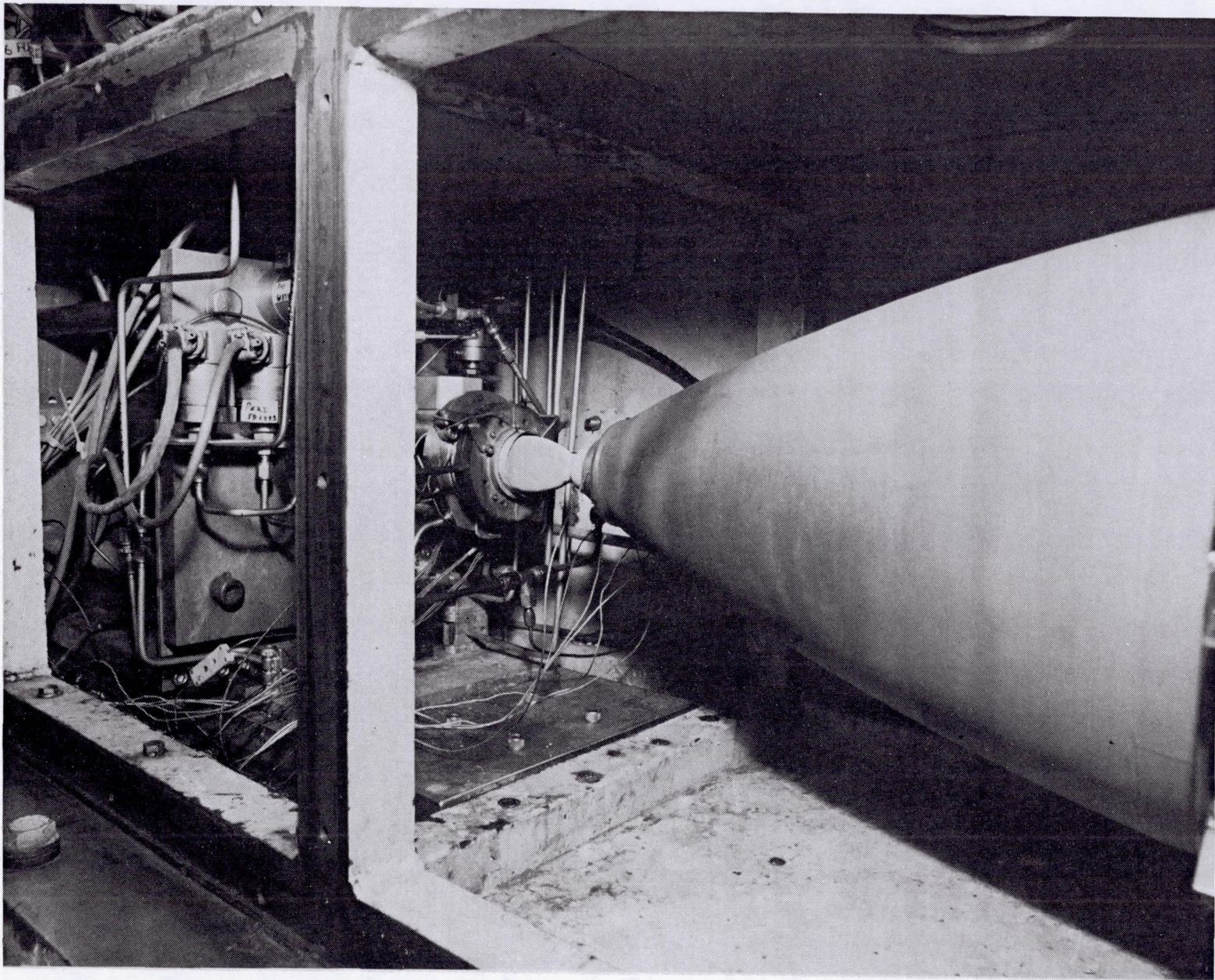


Figure 6.3-80. Welded 286:1 Ir-Re Thruster in Altitude Cell, Post Test -278 (C0292 0969)

6.3, Hot Fire Testing (cont.)

region aft of the nozzle weld on the top (0 degree) side of the nozzle is visible. This is believed to be a submicron thick layer which occurs through reaction of the hot nozzle with the O₂ in the cell gases after the protective H₂ shroud is turned off. There is no corresponding heating pattern on the inside of the nozzle, so the mechanisms must be strictly external. Figure 6.3-81 shows the overall 286:1 nozzle interior. The stain at the bottom of the nozzle (180 degree) is believed to be the result of residual liquid (primarily MMH) expelled during post test -278 purges to free the propellant lines from fuel and oxidizer prior to removal from the stand. Closer detail of the nozzle at and aft of the joint is shown in Figure 6.3-82. Note that no streaking is visible; only thermal heating coloration zones are evident. The throat and joint areas are shown in Figure 6.3-83. No evidence of erosion was seen or measured.

The nozzle "bumper" ring installed on the diffuser entrance to protect the exit cone against potential damaging deflection loads when the diffuser unloads at shutdown is shown in Figure 6.3-84. The bumper ring was spaced about 0.05 in. from the nozzle surface and would pick up any loads which otherwise would deflect the nozzle past this point. At shutdown a shockwave travels up the diffuser to pressurize the cell from the steady state running pressure (ca 0.0165 psia) to diffuser exit pressure (ca 0.9 psia). No evidence of contact of the nozzle with the bumper ring was noted in post test visual examination of the silicide coating.

The thruster assembly after removal from the stand is shown in Figure 6.3-85. Figures 6.3-86 and -87 are close ups of the valve/injector/regen section to show details of the thermocouple installation in these areas. Figures 6.3-88 and -89 show details of the chamber and hot section of the nozzle at 270 degree and 0 degree respectively. During the testing, a weld joint thermocouple spot weld junction broke, allowing the fiberglass insulation to touch the hot Re nozzle and melt, forming the glaze evident in Figure 6.3-89. This was removed from the surface by grinding before testing was resumed to preclude potential Re damage by silica diffusion into the metal during extended time at high temperature. Although not documented for Re, such a failure mode is known to occur with Pt and silica.

6.3.5 Durability Testing

The primary purpose of the durability test series was to extend the continuous and accumulated firing times. To extend the continuous firing time, which was limited by the capability of the Bay 2 vacuum system, the 286:1 nozzle was cut off at 47:1, to match the 6 in. diffuser. Figure 6.3-90 is a drawing of the thruster; Figures 6.3-91, -92 and -93 show the hardware after cutting back the skirt.

The testing, Group I, consisted of 69 tests with a maximum duration of 650 sec and an accumulated firing time of 3.64 hours. At the end of this test series the engine had an

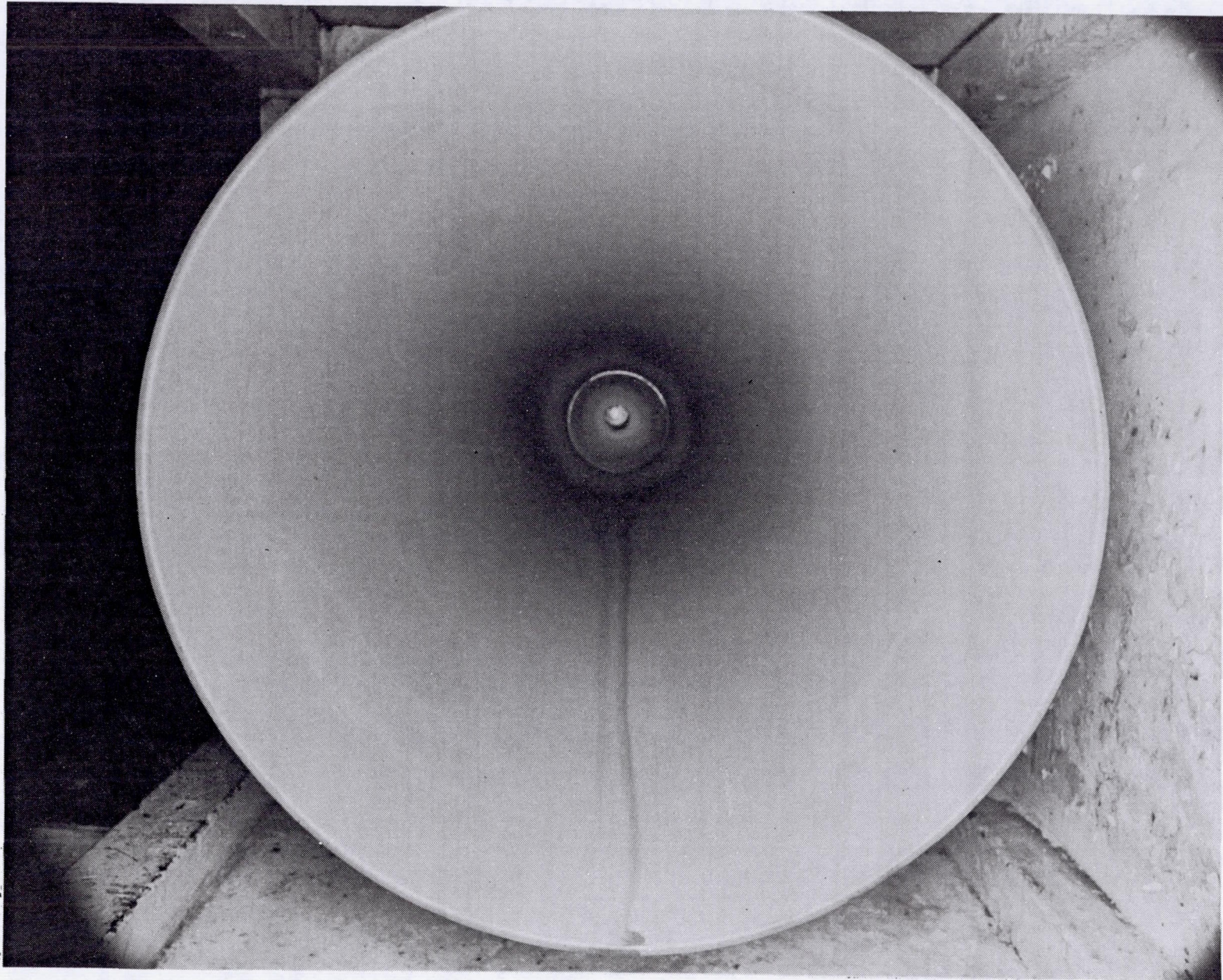


Figure 6.3-81. Welded 286:1 Ir-Re Thruster Overall nozzle Interior, post Test -278 (CO292 0977)

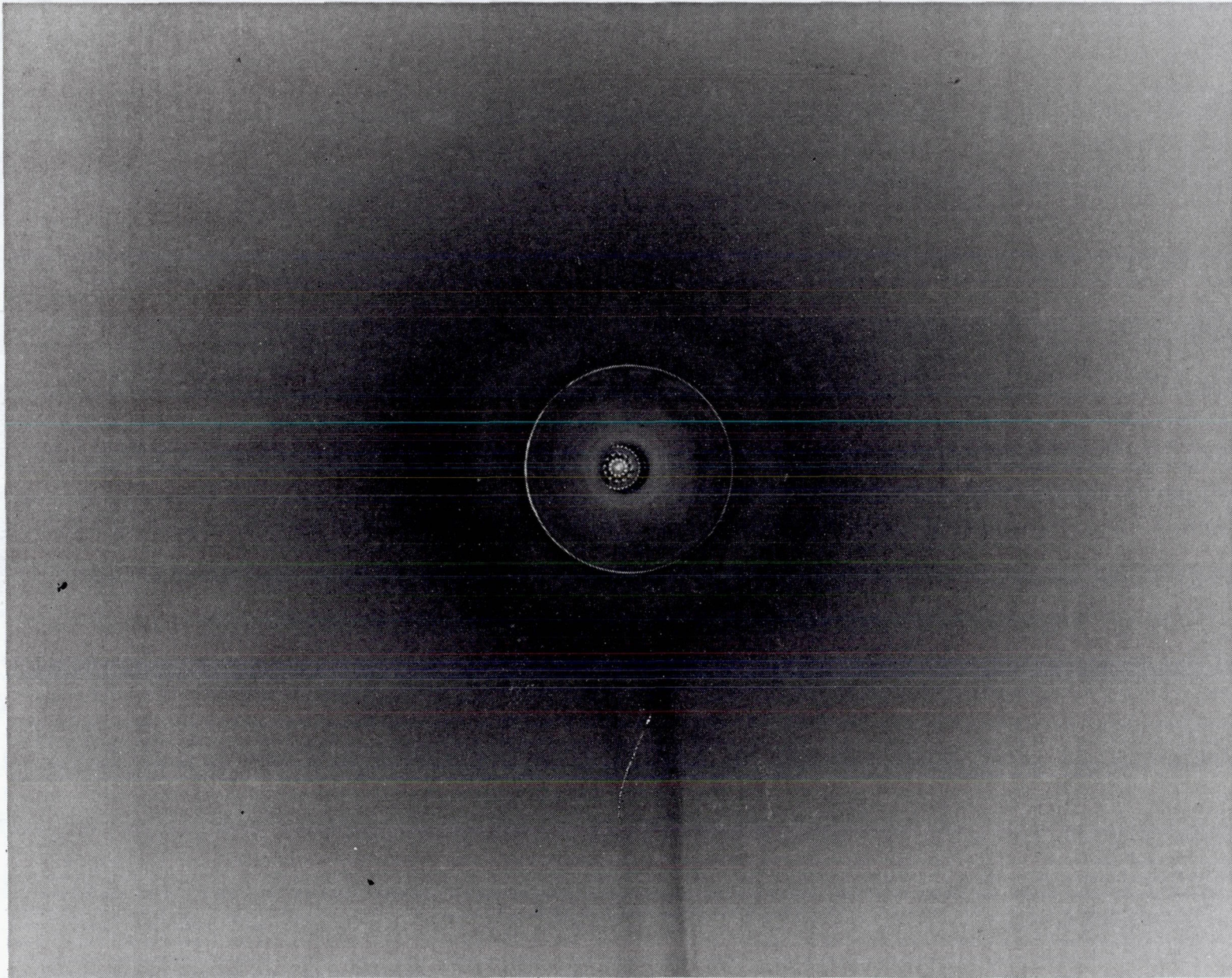


Figure 6.3-82. Welded 286:1 Ir-Re Thruster – Nozzle Interior Downstream of Weld, (C0292 0976)
Post Test -278; Note Injector in Background



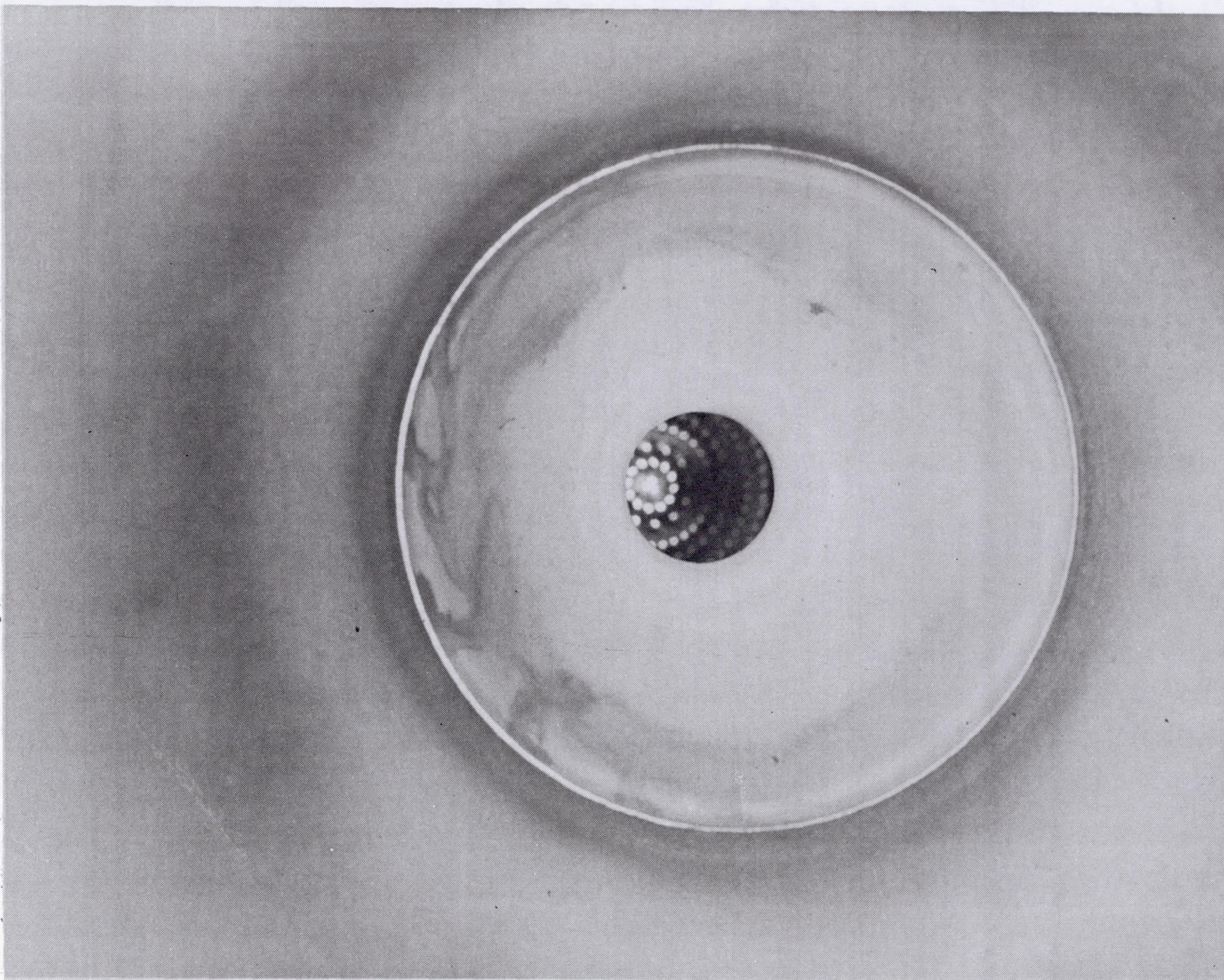


Figure 6.3-83. Welded 286:1 Ir-Re Thruster – Detail of Nozzle Interior From Throat to Weld, Post Test -278 (CO292 0967)

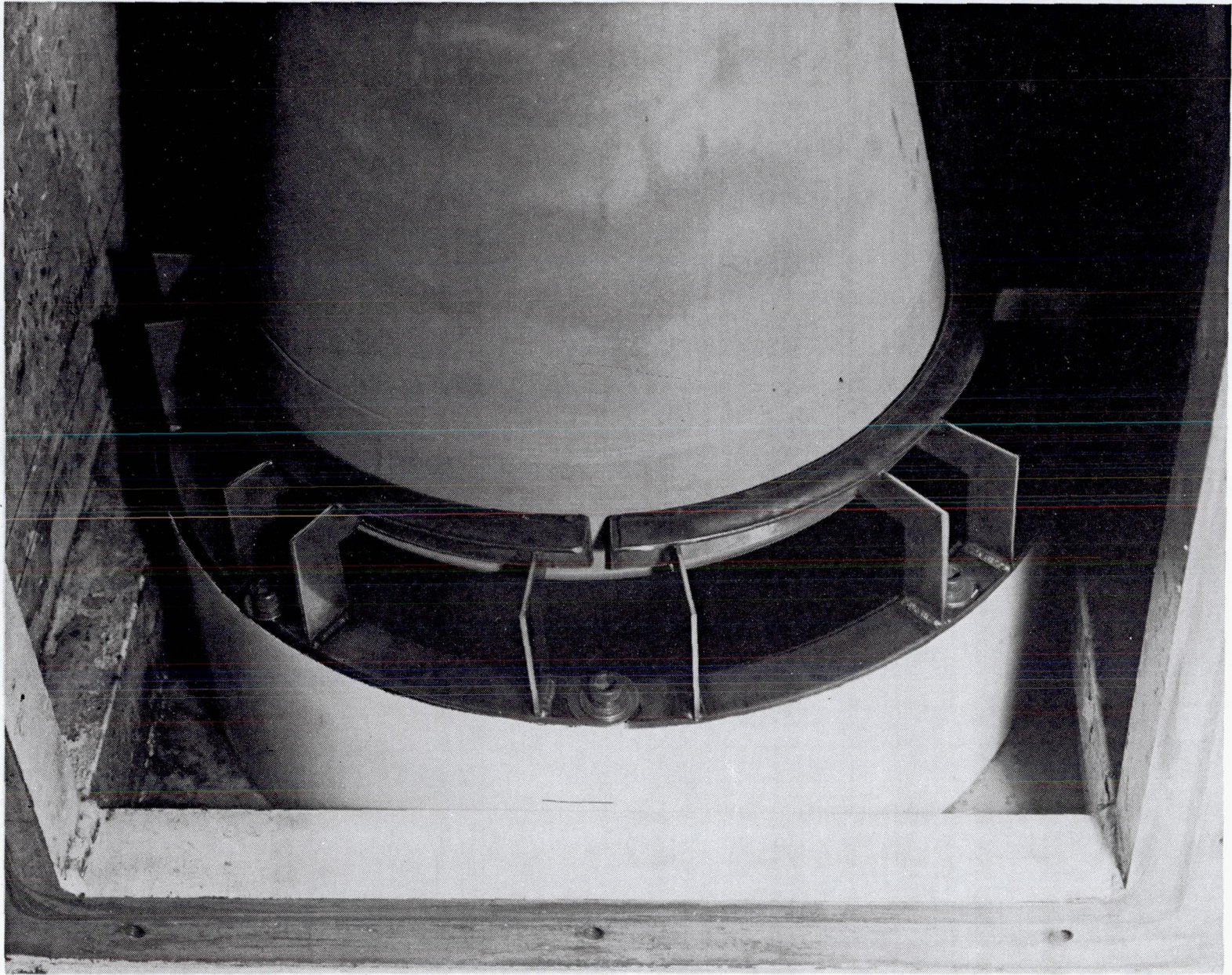
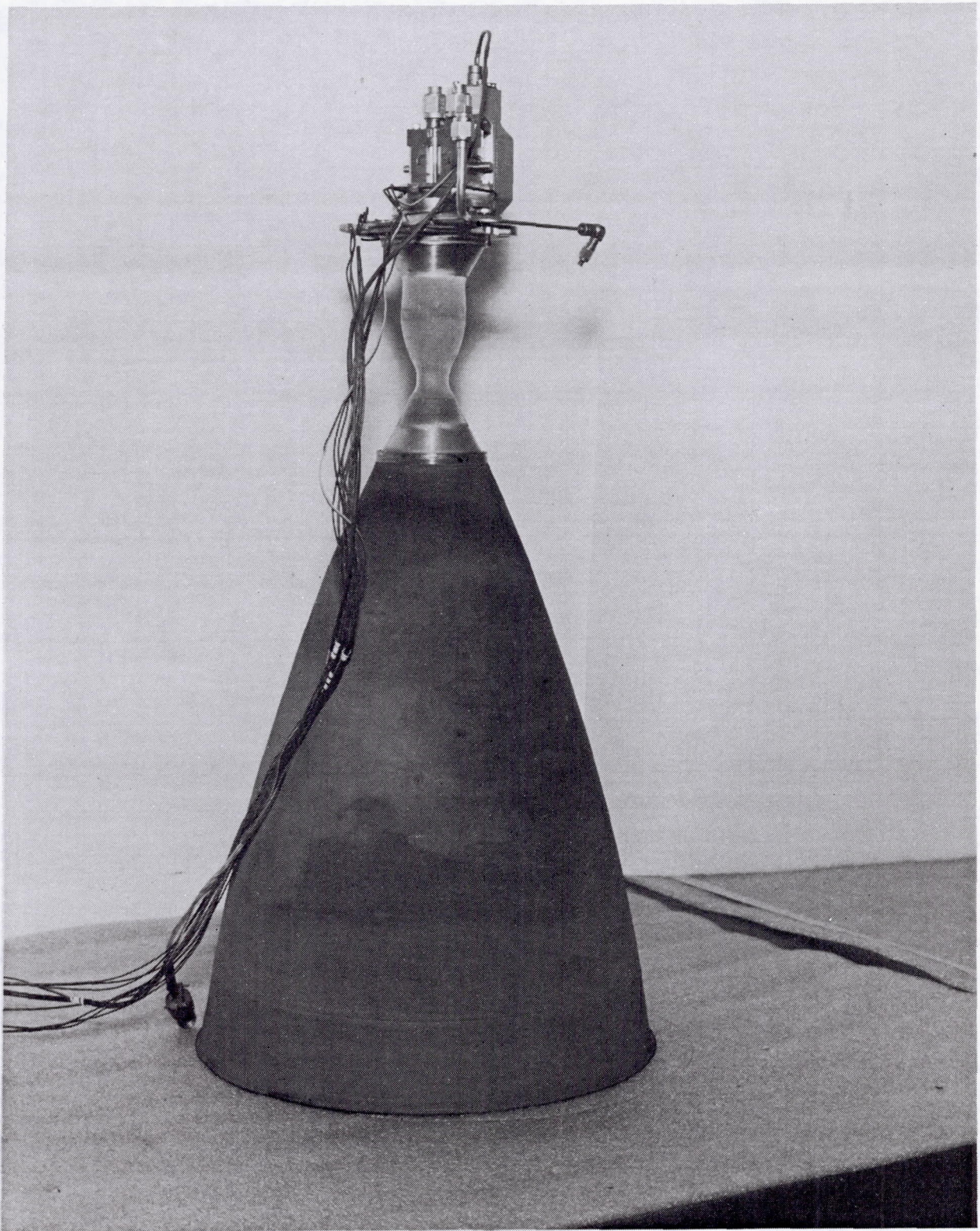


Figure 6.3-84. Detail of Nozzle "Bumper" Ring Installed to Prevent Nozzle
Damage When Diffuser Unloads

(C0292 0972)





(C0292 0965)

Figure 6.3-85. Welded 286:1 Ir-Re Thruster Assembly - Post Test -278

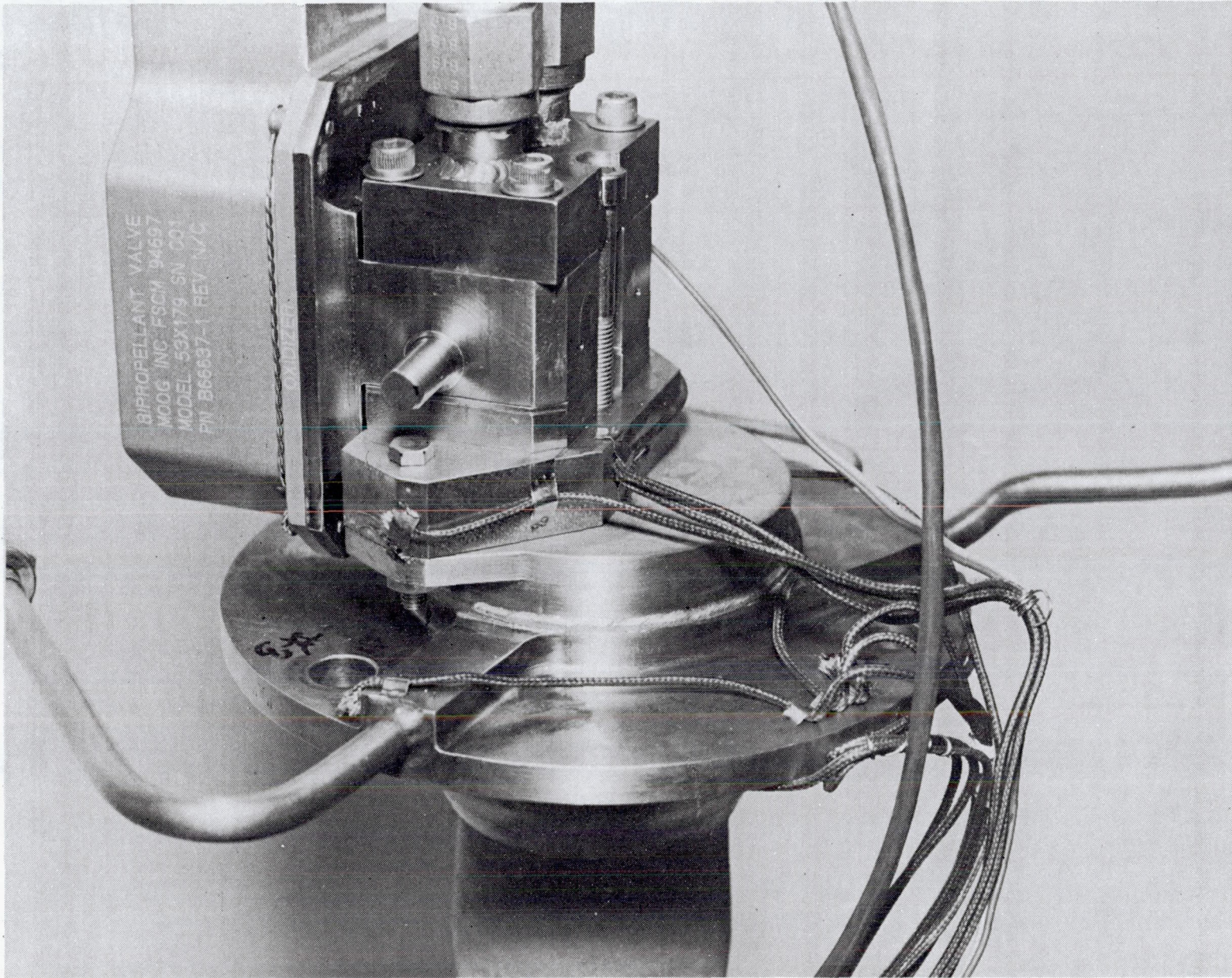


Figure 6.3-86. Welded 286:1 Ir-Re Thruster – Thermocouple Detail – Post Test
-278 at Approximately 330 Degrees



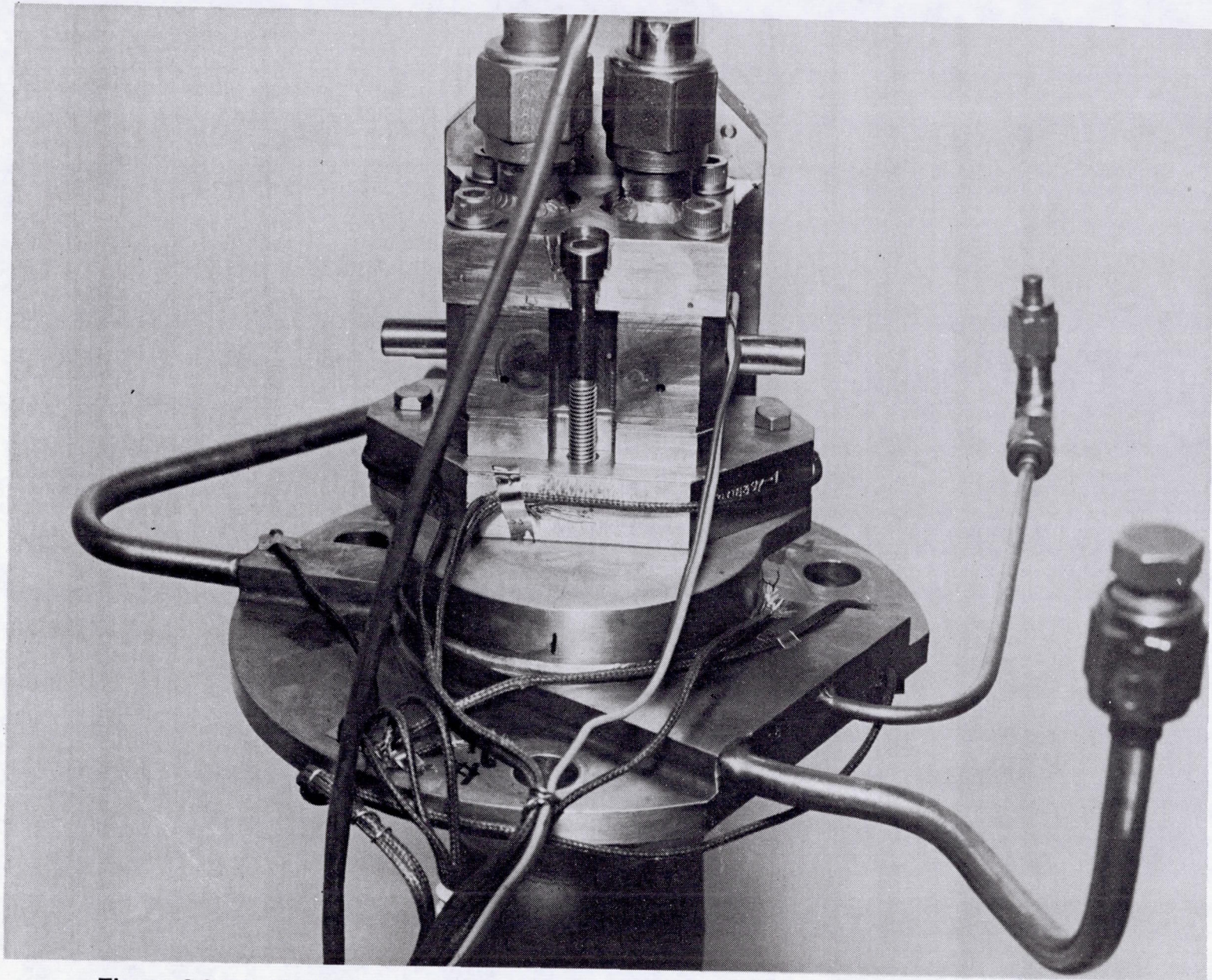


Figure 6.3-87. Welded 286:1 Ir-Re Thruster - Thermocouple Detail - Post Test -278 (C0392 1329)
at Approximately 120 Degrees



(C0392 1333)

Figure 6.3-88. Welded 286:1 Ir-Re Thruster – Post Test -278 Detail of Chamber and Nozzle Transition Weld



(C0392 1331)

Figure 6.3-89. Welded 286:1 Ir-Re Thruster – Post Test -278 Showing Glazed Area From Melted Thermocouple Insulation

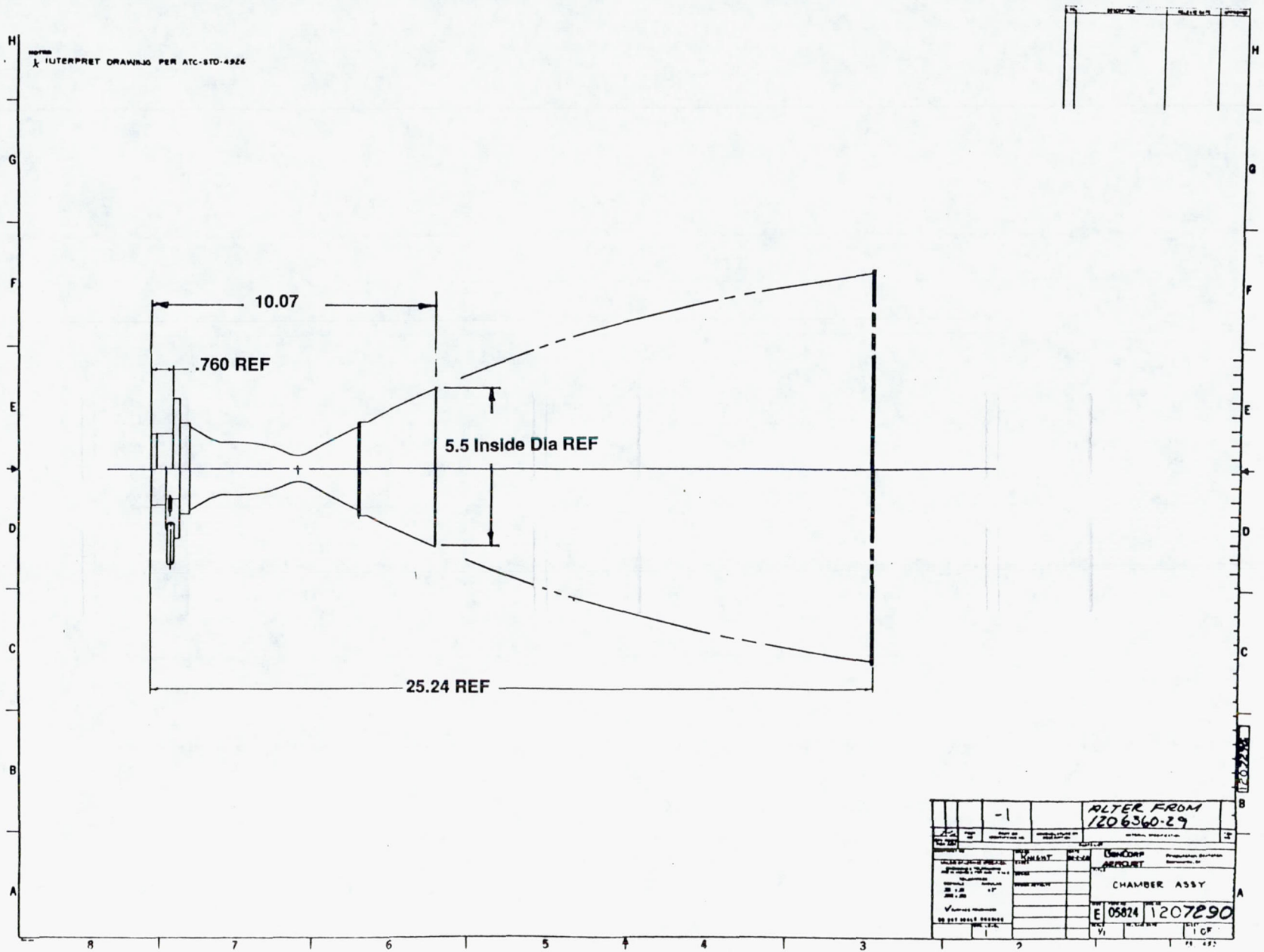
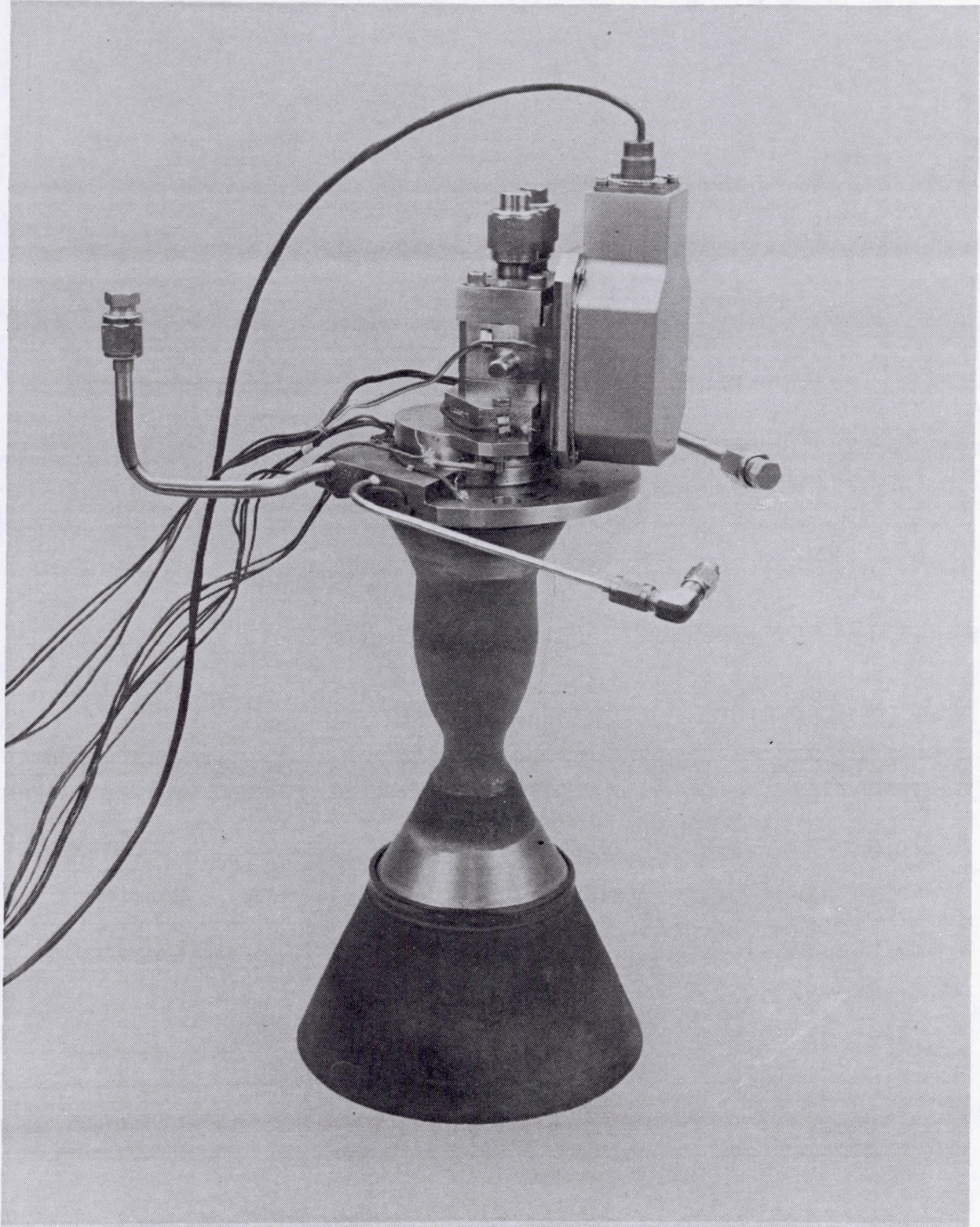


Figure 6.3-90. Drawing of 47:1 Mod 1 Welded Thruster Assembly



(CO492 2288)

Figure 6.3-91. Welded SN 1, Mod Thruster – 286:1 Cut Back to 47:1,
Overall Assembly

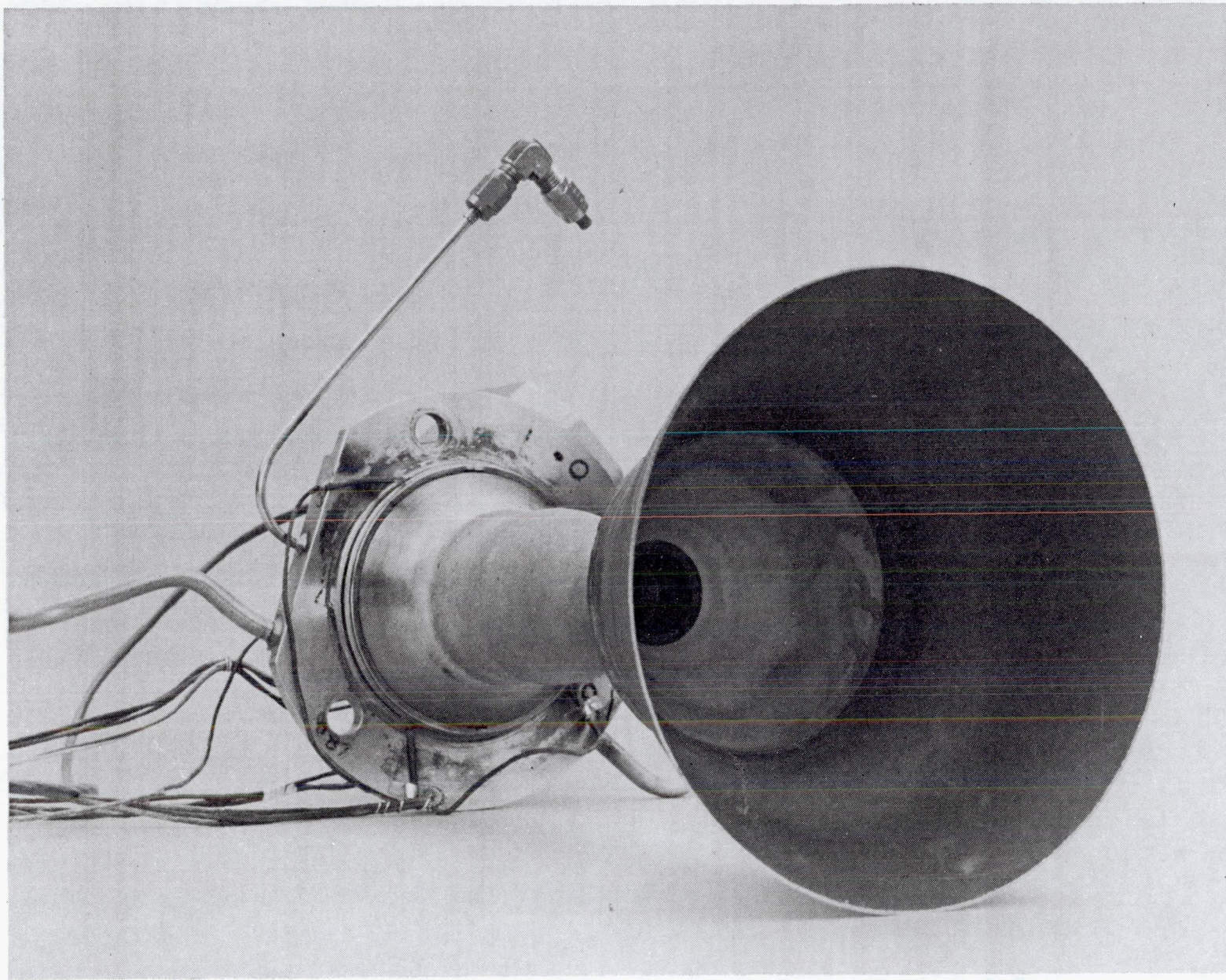


Figure 6.3-92. Welded SN-1, Mod Thruster – 286:1 Cut Back to 47:1, View of Chamber and Interior of Nozzle (Throat Plug In Place)

(CO492 2290)

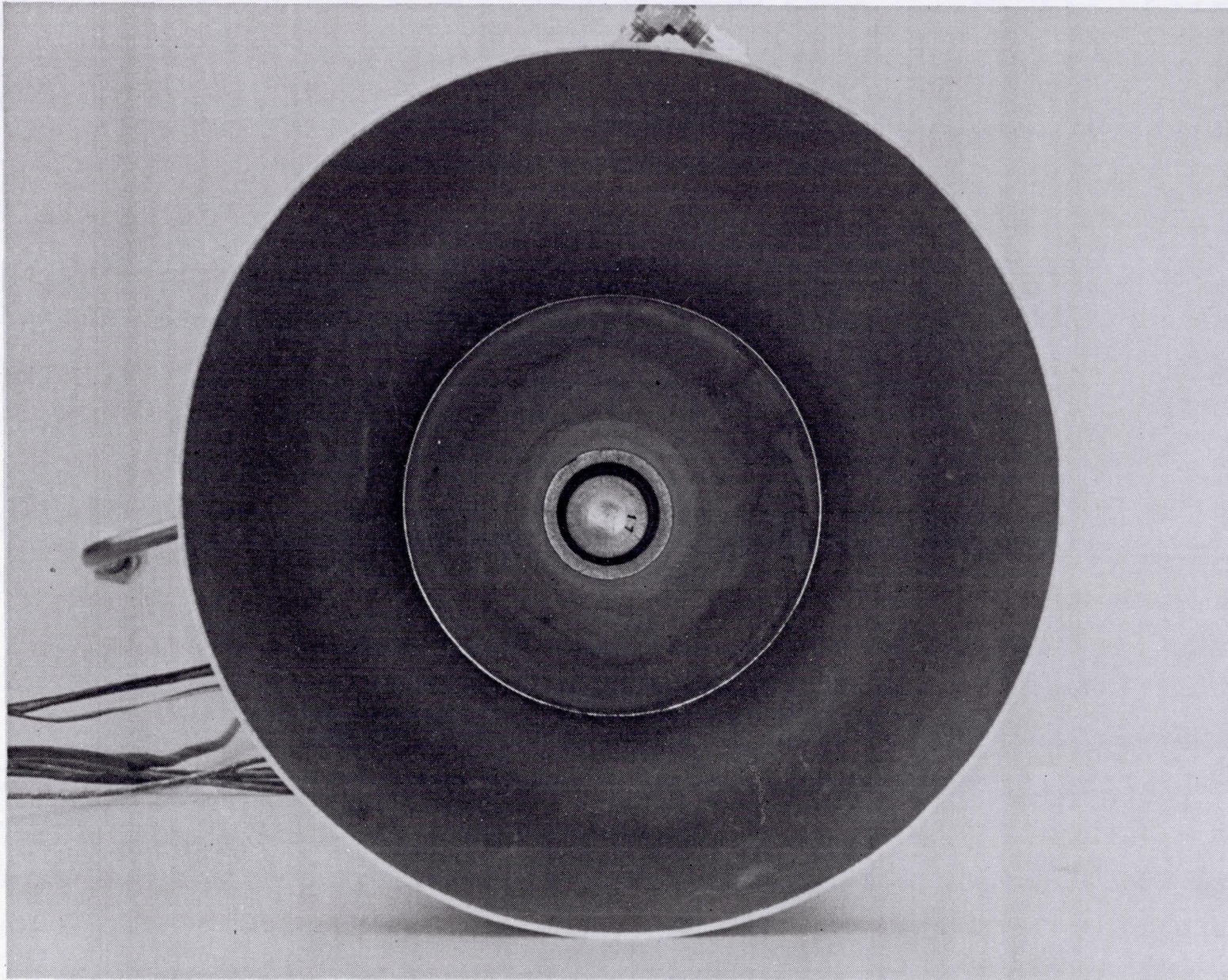


Figure 6.3-93. Welded SN-1 Mod Thruster – 286:1 Cut Back to 47:1, Closeup of (C0492 2291)
Nozzle Interior (Throat Plug In Place)

6.3, Hot Fire Testing (cont.)

accumulated firing time of 3.91 hours in 89 firings. The planned engine operation conditions for these tests are shown in Figure 6.3-94. The instrumentation locations for this testing are shown in Figure 6.3-95.

The durability test series was initiated on 5 June 1992. Test results are listed in Table 6.3-15. Initial tests showed that the existing 6 in. diffuser would not start. This is attributed to the high exit angle on the cut-off 47:1 area ratio coupled with the low ratio between diffuser inlet diameter and nozzle exit diameter which does not permit the flow to turn before impinging on the diffuser. A diffuser inlet adapter which converts the 6 in. straight pipe diffuser to a second throat diffuser was designed, fabricated, and installed for test number -287. The new diffuser (Figure 6.3-96) starts properly and provides a steady cell pressure of about 7300 micron (0.141 psia). Figure 6.3-97 shows the engine on the stand after Test -306.

The purpose of Tests -287 through -301 was to checkout the diffuser and to run 20 sec turbine flow meter calibration tests in combination with engine firings using the PDFM's. All tests were normal and no limiting operating conditions were encountered over the operating MR and Pc box.

The sensitivity of engine operating conditions to propellant inlet pressure is shown in Figures 6.3-98 and -99. These illustrate the need for tight control on propellant supply pressure to control MR and Pc. For example, if oxidizer pressure increases 2 psi while fuel pressure drops 4 psi, MR shifts from 1.62 to 1.66.

Test -302 was run for 10 sec duration to obtain system balance with the 40 gal tanks in preparation for long duration testing. Maximum duration of these tests is limited by the pressure in the large vacuum tank into which the diffuser exhausts. Diffuser unload occurs at a diffuser inlet-to-exit pressure ratio of about 3 psia. Therefore, maximum continuous firing time of 500 to 600 sec is set by the tank volume and the pumping capacity of the vacuum system. At fixed engine operating conditions, this is influenced by the extent to which the exhaust gas is cooled in the 12 ft dia x 100 ft long vacuum tank, which serves as a heat exchanger. The cooling is dependent on ambient temperature, which was in the range of 60 F to 100 F+ during this testing. Run duration (time to diffuser unload) is plotted versus gas temperature leaving the tank to show this correlation in Figure 6.3-100. Performance predictions made for the 286:1 nozzle cut off to 47:1 are shown in Figure 6.3-101.

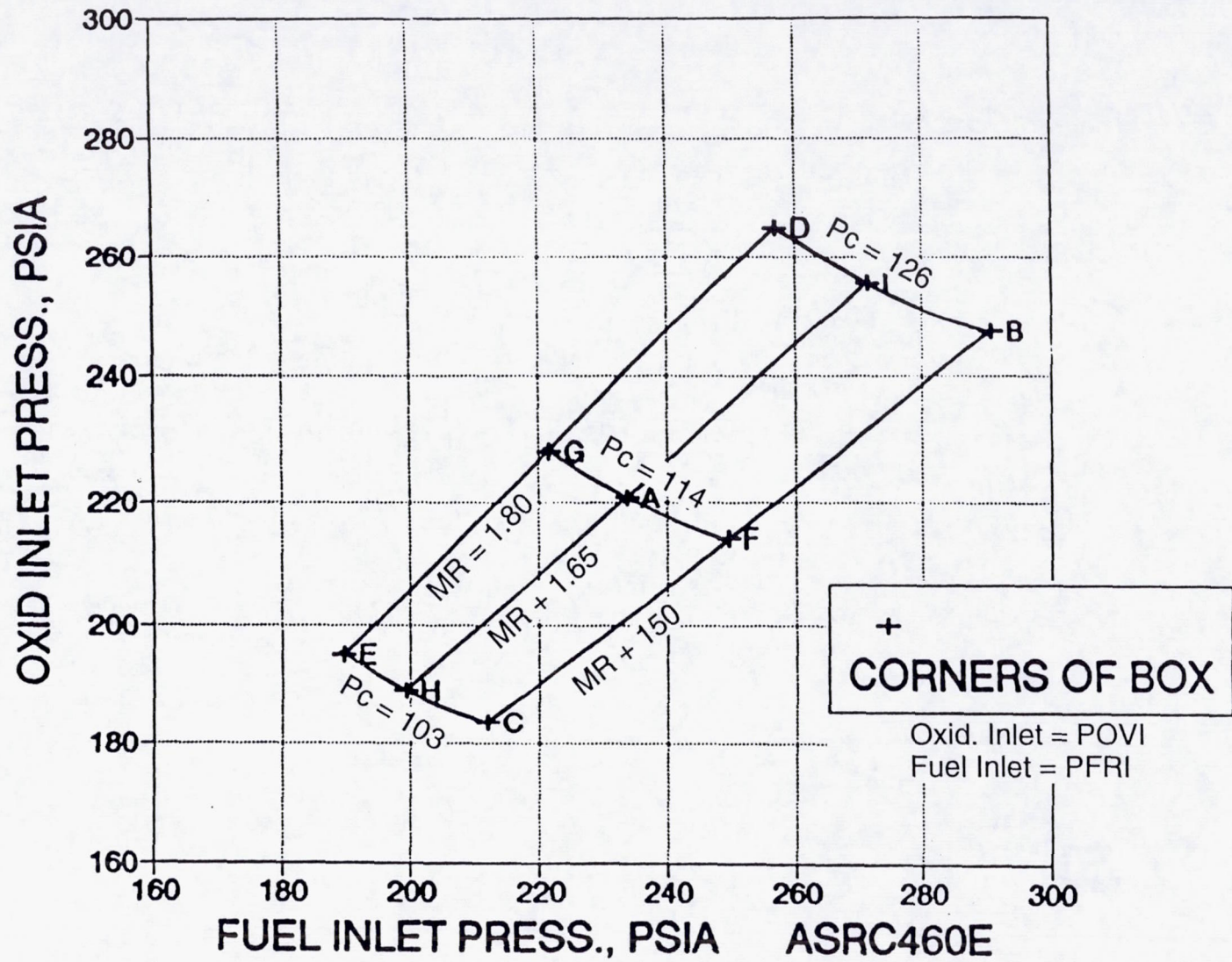


Figure 6.3-94. Oxid Inlet Pressure vs Fuel Inlet Pressure

254

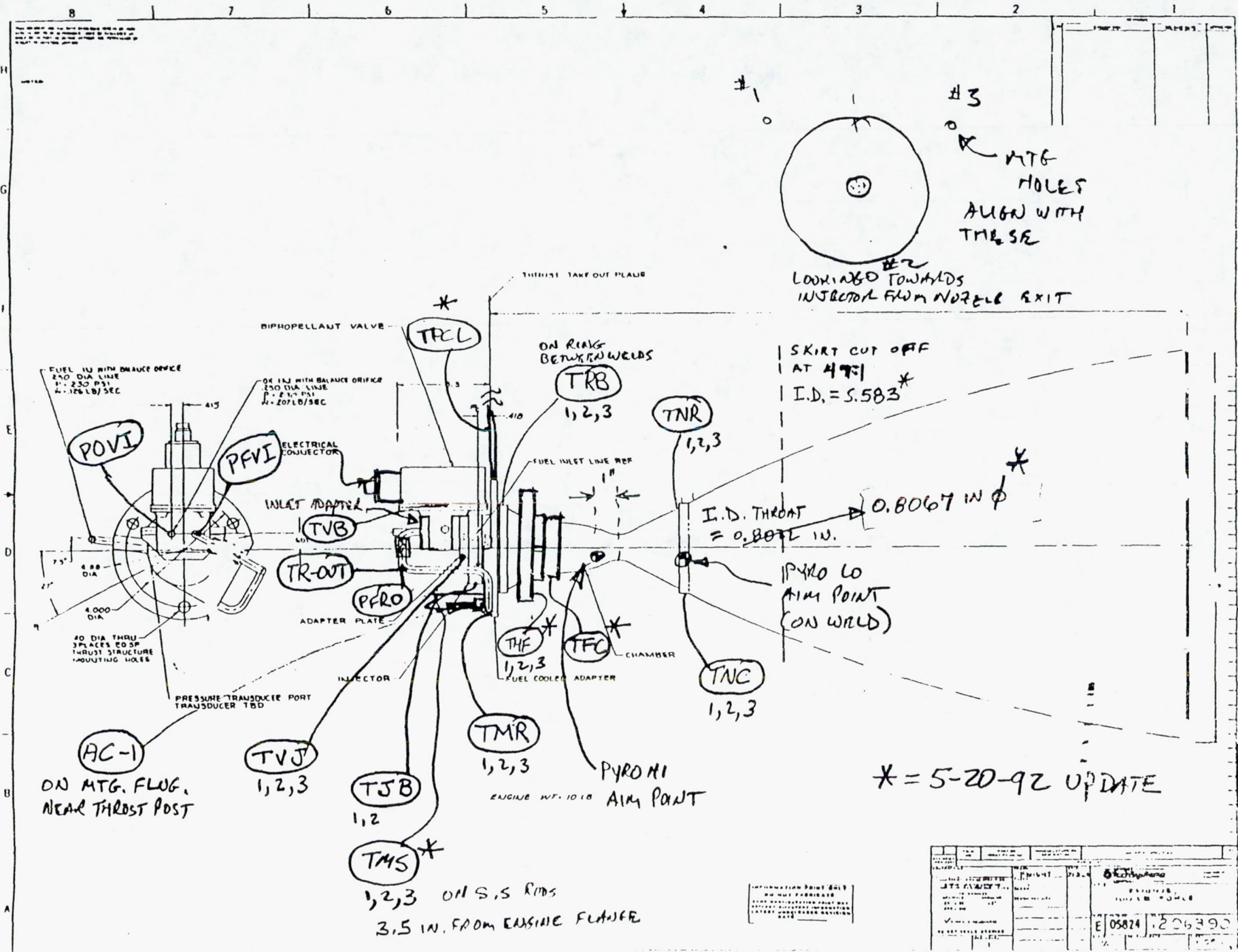


Figure 6.3-95. Instrumentation Locations for 47:1 490N Welded Thruster

REV	DATE	BY	CHKD	APP'D
1				
2				
3				
4				
5				
6				
7				
8				
9				
10				
11				
12				
13				
14				
15				
16				
17				
18				
19				
20				
21				
22				
23				
24				
25				
26				
27				
28				
29				
30				
31				
32				
33				
34				
35				
36				
37				
38				
39				
40				
41				
42				
43				
44				
45				
46				
47				
48				
49				
50				
51				
52				
53				
54				
55				
56				
57				
58				
59				
60				
61				
62				
63				
64				
65				
66				
67				
68				
69				
70				
71				
72				
73				
74				
75				
76				
77				
78				
79				
80				
81				
82				
83				
84				
85				
86				
87				
88				
89				
90				
91				
92				
93				
94				
95				
96				
97				
98				
99				
100				

Table 6.3-15. Durability Test Series Performance Data at 47:1, Sheet 1 of 3

UPDATE 7-26-92 Iridium-Rhenium Combustion Chamber

DURABILITY TEST SERIES											
RUN No.	DATE	FIRING TIME, (sec)	COMMENT	DATA TIME, (sec)	Pc (psia)	MR O/F	Fvac (lbf)	Isp vac (sec)	C* (ft/sec) [Cold throat]	CHAMBER TEMP., (F)*	NOZZLE WELD TEMP., (F)
280	6-5-92	0.51	KILL LOW GH2 FLOW		111.5	-					
281	6-5-92	1.00	OK		111.1	1.61					
282	6-5-92	1.86	KILL Pexit>.25		122.1	1.70					
283	6-5-92	2.21	KILL Pexit>.25		114.1	1.66					
284	6-5-92	2.81	KILL Pexit>.3		113.9	1.65					
285	6-8-92	5.15	PH2 ON @ 5; KILL Pexit>.3		114.4	1.62					
286	6-8-92	6.02	NOZ. I' INTO DIFF; PH2 ON @ 5; KILL Pexit>.3		115.3	1.64					
287	6-12-92	7.78	ERRONEOUS KILL ON PYRO-LO		115.3	1.90					
288	6-12-92	5.35	KILL ON TJB-2@250F		119	1.43					
289	6-12-92	10.00	MANUAL KILL ON TJB-2		117.2	1.49					
290	6-18-92	10.00	OK		121.3	1.73					
291	6-19-92	20.00	NOM PC/NOM MR	17.0	115.2	1.70	104.1	301.4	5418	3257	2153
292	6-19-92	0.53	KILL ON ERRONEOUS LOW FUEL FLOW								
293	6-19-92	16.08	KILL ON TJB-3>250F	7.5	126.7	1.49	113.7	296.9	5380	2666	1659
294	6-19-92	20.00	LOW PC/LOW MR	7.5	104.6	1.46	93.3	298.6	5437	2757	1626
295	6-19-92	20.00	HIGH PC/HIGH MR	7.5	125.5	1.83	113.9	300.1	5373	2845	1906
296	6-19-92	7.17	ERRONEOUS PYRO-LO;LO PC/HI MR	5.8	102.9	1.86	93.0	301.6	5426	2739	1427
297	6-19-92	20.00	NOM PC/LOW MR	17.0	115.4	1.52	103.9	299.7	5413	3119	2039
298	6-19-92	20.00	NOM PC/HIGH MR	17.0	114.7	1.85	104.1	300.8	5385	3353	2220
299	6-19-92	20.00	LOW PC/NOM MR	17.0	103.3	1.67	93.3	302.2	5440	3372	2199
300	6-19-92	20.00	HIGH PC/NOM MR	17.0	125.7	1.65	113.5	299.5	5387	3139	2074
301	6-19-92	20.00	NOM PC/ NOM MR	17.0	116.3	1.63	104.9	300.2	5408	3198	2089
302	6-24-92	10.00	OK; FROM MAIN TANKS; CALIBRATED FLOW METE	8.5	113.3	1.58	101.8	300.0	5429	2845	1427
303	6-24-92	47.35	KILL ON TJB-1>250F	41.1	114.2	1.66	103.1	300.6	5414	3228	2087
304	6-24-92	45.27	KILL ON TJB-3>350F	39.5	114.2	1.63	103.1	300.3	5407	3207	2064
305	6-24-92	120.00	OK	112.1	114.5	1.67	103.5	300.6	5401	3247	2092

Table 6.3-15. Durability Test Series Performance Data at 47:1, Sheet 2 of 3

UPDATE 7-26-92

Iridium-Rhenium Combustion Chamber

DURABILITY TEST SERIES											
RUN No.	DATE	FIRING TIME, (sec)	COMMENT	DATA TIME, (sec)	Pc (psia)	MR	Fvac (lbf)	Isp vac (sec)	C* (ft/sec) [Cold throat]	CHAMBER TEMP., (F)*	NOZZLE WELD TEMP., (F)
306	6-24-92	476.60	MANUAL KILL: BUBBLES IN OXID	440.1	114.5	1.67	103.9	301.3	5396	3255	2106
307	6-26-92	532.27	DIFFUSER UNLOAD	493.0	115.3	1.64	104.2	300.5	5403	3337	2188
308	6-29-92	650.09	TPC>750F/DIFFUSER UNLOAD	642.0	112.9	1.59	101.8	301.6	5437	3334	2100
309	7-1-92	400.46	MANUAL KILL; Tchamb DROPPING	352.0	114.3	1.65	103.4	301.1	5409	-	2380
310	7-1-92	241.91	KILL ON TVB>250F[ERRONEOUS READING]	223.0	114.8	1.66	104.0	301.2	5404	3505	2176
311	7-1-92	504.91	KILL ON PEXIT>0.3 PSIA	454.5	114.2	1.65	103.5	301.0	5397	3485	2097
312	7-2-92	485.42	KILL ON PEXIT>0.3 PSIA	444.5	108.0	1.42			5424	3296	1924
313	7-2-92	443.18	KILL ON PEXIT>0.3 PSIA	405.5	114.9	1.62			5400	3407	1967
314	7-2-92	463.92	KILL ON PEXIT>0.3 PSIA	432.6	114.3	1.66			5398	3439	1993
315	7-6-92	0.73	KILL ON OXID BUBBLE								
316	7-6-92	553.11	KILL ON PEXIT>0.3 PSIA	455.1	114.8	1.62			5406	3432	2073
317	7-6-92	466.39	KILL ON PEXIT>0.3 PSIA	435.0	114.6	1.66			5394		2084
318	7-6-92	471.98	KILL ON PEXIT>0.3 PSIA	437.5	114.3	1.67			5379		2094
319	7-7-92	4.26	KILL ON PEXIT>0.3 PSIA								
320	7-7-92	507.10	KILL ON PEXIT>0.3 PSIA	456.0	114.7	1.61			5418	3402	2134
321	7-7-92	502.74	KILL ON PEXIT>0.3 PSIA	453.0	114.2	1.63			5405	3415	2151
322	7-7-92	567.64	KILL ON PEXIT>0.3 PSIA	535.5	114.4	1.66			5425	3435	2168
323	7-8-92	590.40	KILL ON PEXIT>0.3 PSIA	547.1	115.5	1.60			5423	3390	2081
324	7-8-92	591.41	KILL ON PEXIT>0.3 PSIA	547.5	127.3	1.66			5387	3304	1932
325	7-8-92	0.73	FLOW LIMIT KILL								
326	7-8-92	514.46	KILL ON PEXIT>0.3 PSIA	471.7	127.9	1.51			5370	3162	1852
327	7-8-92	431.98	KILL ON LOW OXID FLOW [BUBBLE?]	387.6	102.6	1.49			5416	3441	1943
328	7-9-92	0.73	KILL ON LOW DIFFUSER WATER								
329	7-9-92	120.01	NOMINAL 40oF PROPELLANTS	113.5	109.3	1.61			5428	3542	2011
330	7-9-92	575.37	KILL ON PEXIT>0.3 PSIA	539.5	102.2	1.64			5437	3596	2067
331	7-9-92	600.06		552.1	114.9	1.79			5386	3548	2076
332	7-9-92	566.88	KILL ON PEXIT>0.3 PSIA	535.5	114.9	1.60			5389	3412	1970
333	7-9-92	600.06		552.1	114.3	1.66			5385	3492	2025

256

Table 6.3-15. Durability Test Series Performance Data at 47:1, Sheet 3 of 3

UPDATE 7-26-92

Iridium-Rhenium Combustion Chamber

257

DURABILITY TEST SERIES				DATA						CHAMBER	NOZZLE
RUN No.	DATE	FIRING TIME, (sec)	COMMENT	TIME, (sec)	Pc (psia)	MR O/F	Fvac (lbf)	isp vac (sec)	C* (ft/sec) [Cold throat]	TEMP., (F)*	WELD TEMP., (F)
334	7-10-92	20.001	CHECK PERFORMANCE	17.1	115.2	1.66			5400	3467	1956
335	7-10-92	20.001	CHECK PERFORMANCE	17.1	128.2	1.56			5370	3265	1875
336	7-10-92	20.001	CHECK PERFORMANCE	17.1	104.8	1.54			5426	3496	1971
337	7-10-92	20.001	CHECK PERFORMANCE	17.1	127.1	1.77			5364	3435	1990
338	7-10-92	20.001	CHECK PERFORMANCE	17.1	102.3	1.90			5401	3792	2142
339	7-10-92	20.001	CHECK PERFORMANCE	17.1	116.0	1.51			5396	3332	1907
340	7-10-92	20.001	CHECK PERFORMANCE	17.1	116.4	1.75			5384	3501	2020
341	7-10-92	20.001	CHECK PERFORMANCE	17.1	104.6	1.67			5418	3579	2044
342	7-10-92	20.001	CHECK PERFORMANCE	17.1	127.1	1.62			5370	3294	1919
343	7-13-92	120.011	HIGH TEMPERATURE PROPELLANTS	112.4	121.3	1.53	109.4	301.5	5430	3210	1927
344	7-13-92	120.011	HIGH TEMPERATURE PROPELLANTS	112.3	122.0	1.60	110.3	301.8	5425	3260	1961
345	7-13-92	120.011	HIGH TEMPERATURE PROPELLANTS	112.3	115.1	1.42	103.4	301.8	5459	3174	1896
346	7-13-92	120.011	HIGH TEMPERATURE PROPELLANTS	112.4	114.9	1.58	103.8	302.0	5432	3310	1973
347	7-13-92	120.011	HIGH TEMPERATURE PROPELLANTS	112.4	115.3	1.61	104.3		5498	3344	1995
TOTAL=		13104.44	SEC								
FIRINGS=		69									
DURABILITY		3.64	HR								
286:1 TESTS		0.27	HR								
WELDED TOT.		3.91	HR IN 89 FIRINGS								

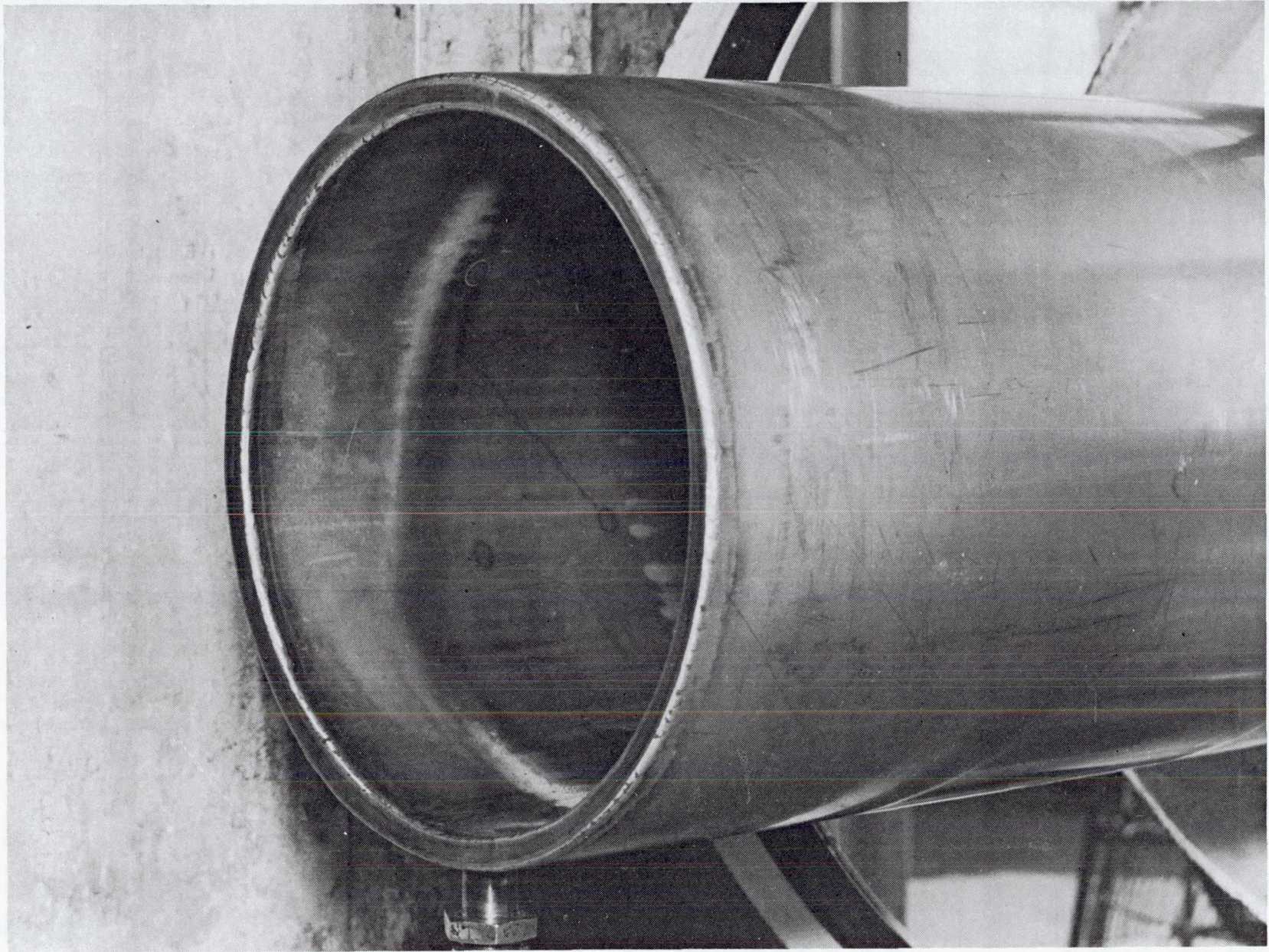


Figure 6.3-96. New Diffuser Inlet Section



oxidizer
+
fuel

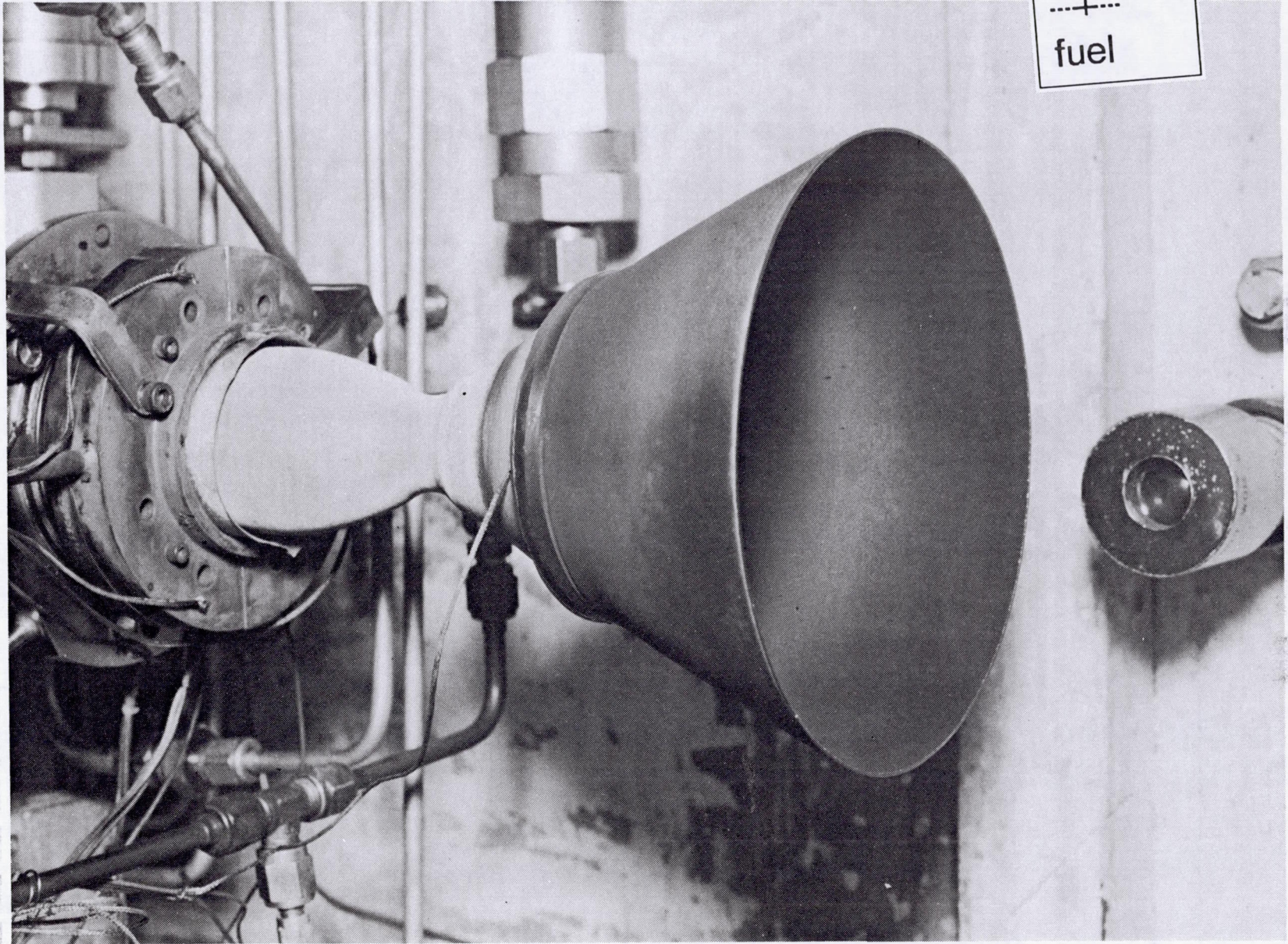


Figure 6.3-97. 47:1 Welded Ir-Re Thruster on Stand Post Test -306

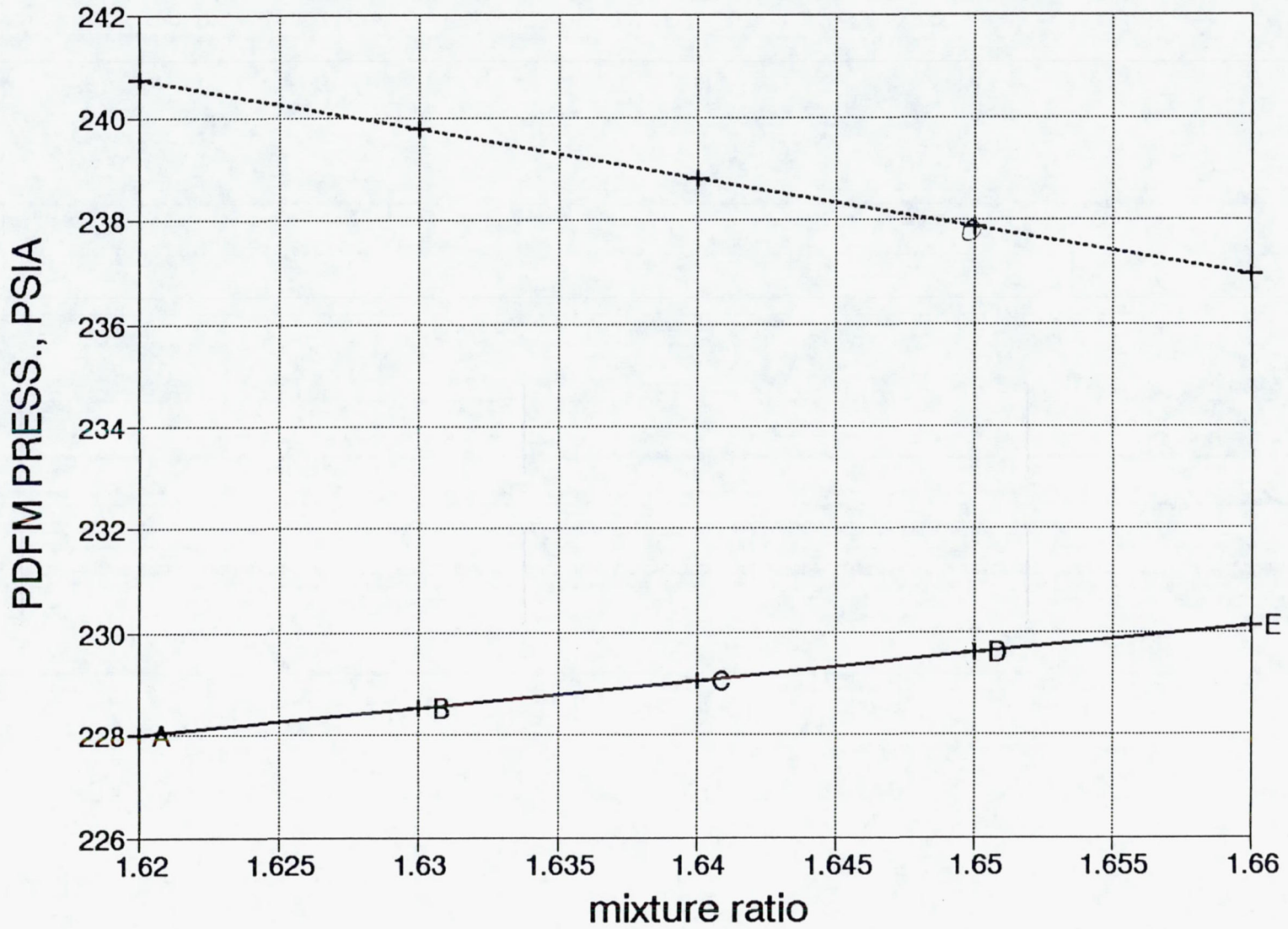


Figure 6.3-98. System Sensitivity to Small Pressure Changes

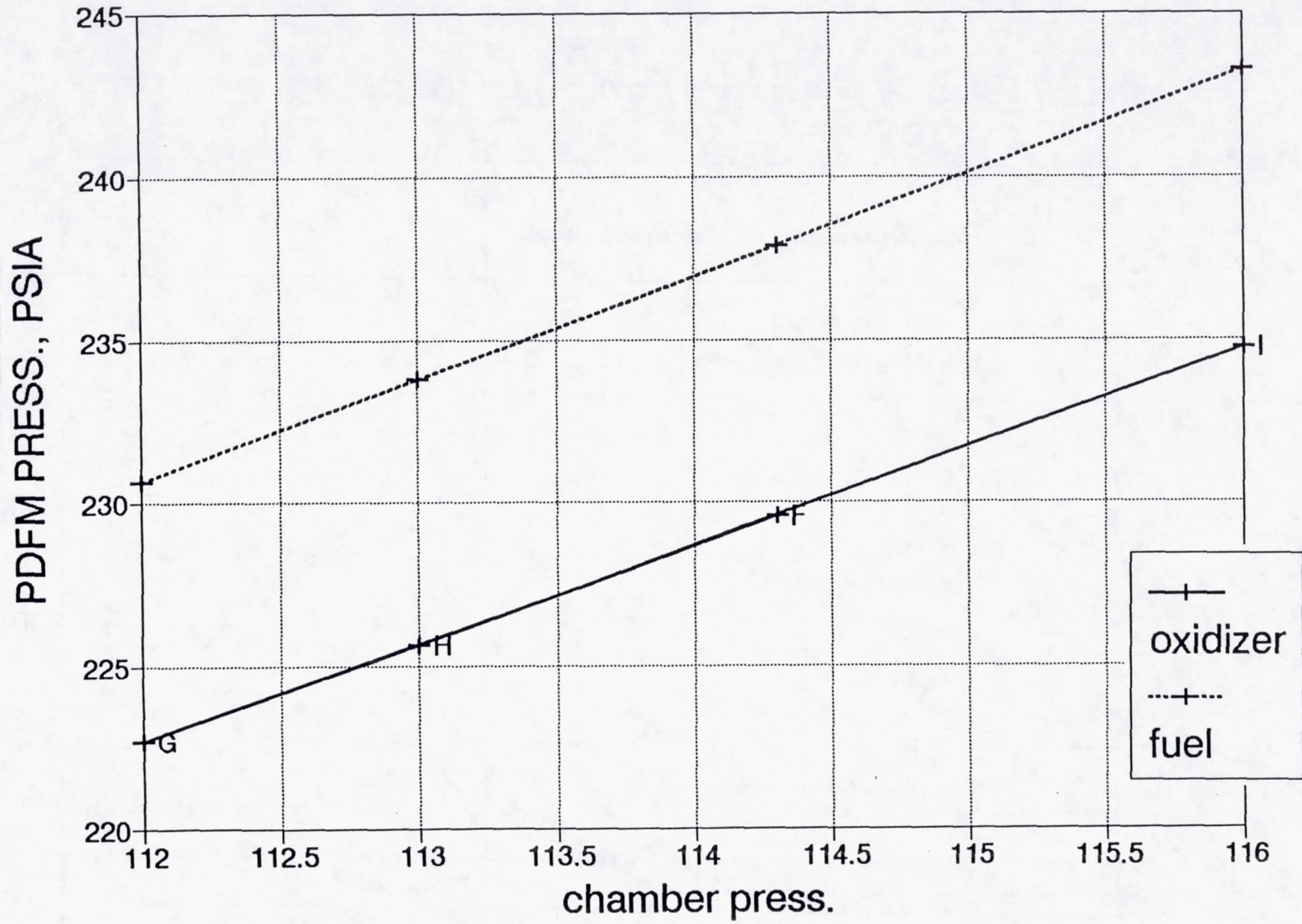


Figure 6.3-99. System Sensitivity to Small Pressure Changes

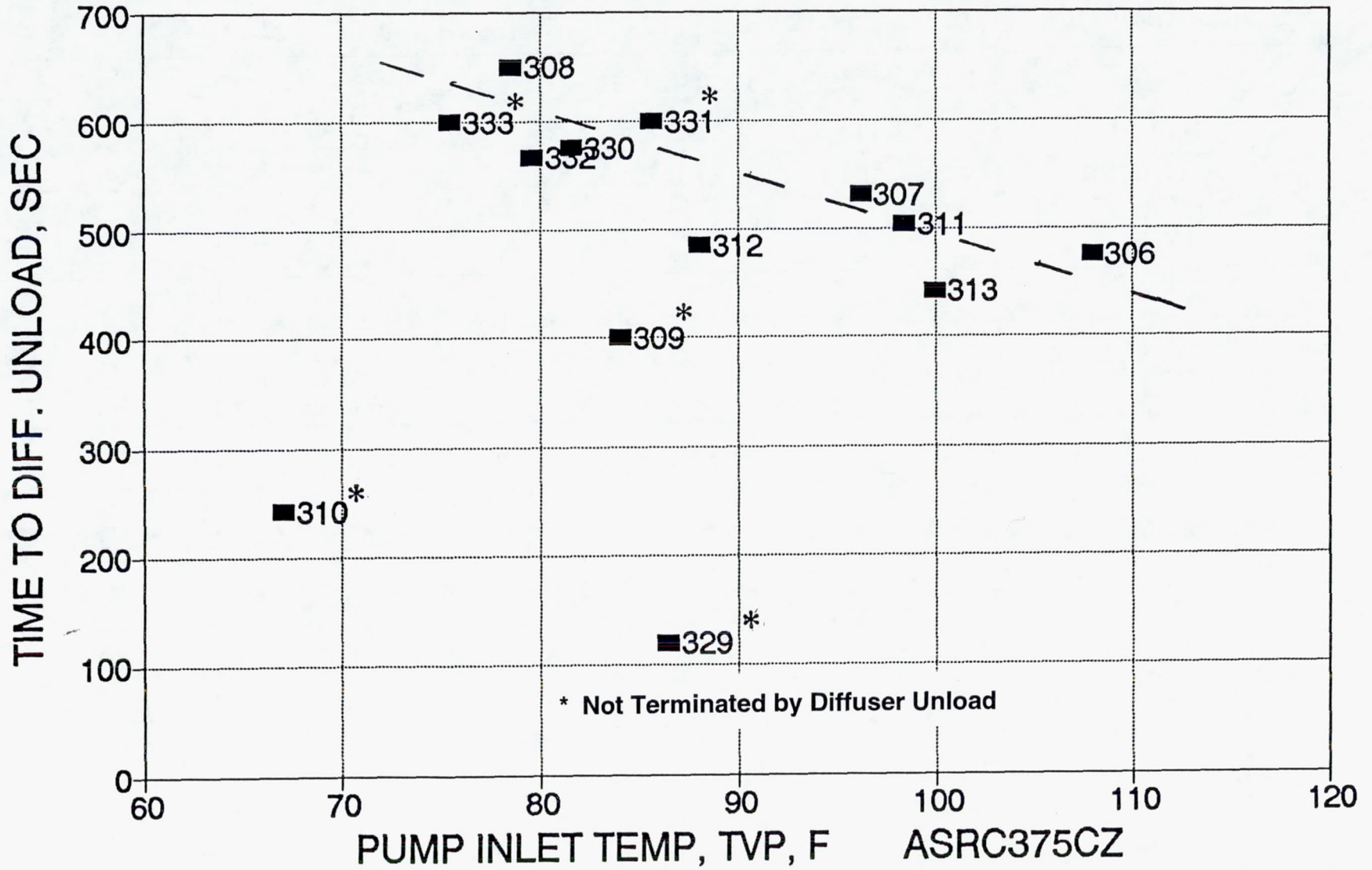


Figure 6.3-100. Ir-Re Welded Thruster – Duration vs TVP Durability Tests; 47:1

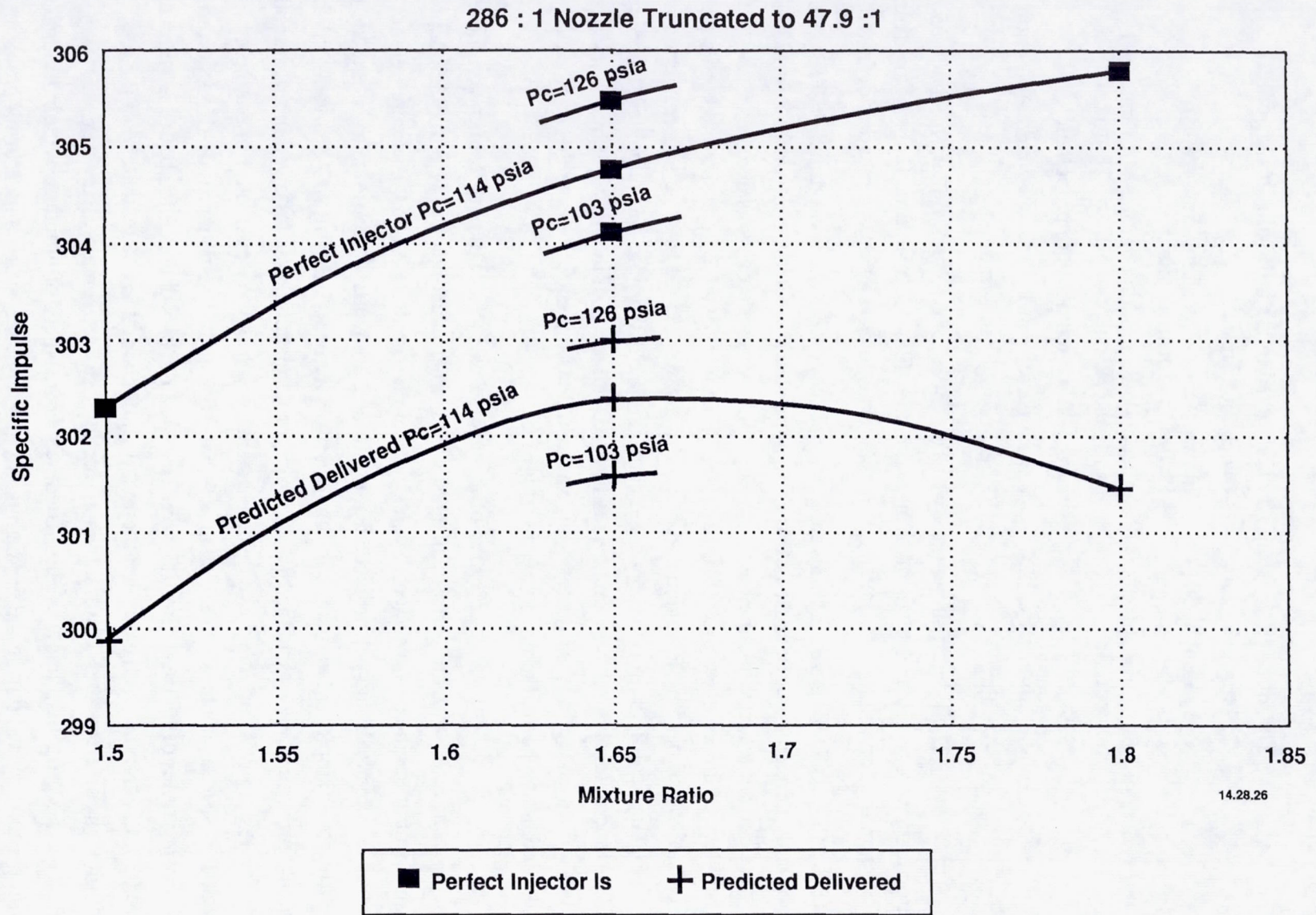


Figure 6.3-101. Isp Predictions for 100 lbf Engine

6.3, Hot Fire Testing (cont.)

This durability testing was conducted in the following groups of tests:

-279 through -290	Checkout diffuser
-291 through -301	Flowmeter on-line calibration against PDFM; performance map
-302 through -333 (except -329)	Accumulate duration over the MR range of 1.4 to 1.8 and Pc range of 102 to 128 psia
-329	Effect of low temperature propellant
-334 through -342	Repeat performance map/flowmeter calibration
-343 through -347	Effect of high temperature propellant

The longest single burn was Test -308, for 650 sec. Generally, the long duration tests were terminated by diffuser unload in the 400 to 600 sec time range. No adverse engine operating conditions were noted during the series; there was no overheating or instability.

During early testing an apparent high temperature was noted on TJB-2, an injector body temperature. Because of this the engine was inspected closely after Test -289 and high pressure leak tested with a new leak check fixture. A small leak was detected at the interface between the injector and the coolant adapter. This was found to be at the injector Pc port location which had been plug welded and machined away when the injector was converted from the bolt together configuration to the welded configuration. The plug was rewelded, stopping the leak. The anomalously high temperature reading was the result of incorrect thermocouple location; the T.C. intended for the injector body was installed on the area over the resonator cavity and was indicating normal temperatures for this area.

The primary objective of this testing was to accumulate test time on the engine, as contrasted with the performance test series, where the objective was to obtain a precise measurement of engine performance. Typically, accuracy goals of 0.1 to 0.2% were held for measurements made during performance testing; if measurements were known to be outside this range (by, for example, comparison of redundant measurements), testing was delayed until the measurement accuracy was satisfactory. A less rigorous standard was followed in the durability test series; testing was continued even when systematic errors were evident. For example, through Test -311, force bias was constant at about 0.5% and no stand thermal drift occurred, even at firing times of 650 sec. Starting with Test -312 the bias changed to about 1%, shown in Figure 6.3-102, and the stand exhibited thermal drift of about 2 to 3% by the end of the test. This condition was corrected after Test -342 when interference between a pressure transducer connector and a propellant line was eliminated. Other instances of problems with individual data measurements occurred during the test campaign; in many cases when a measuring problem

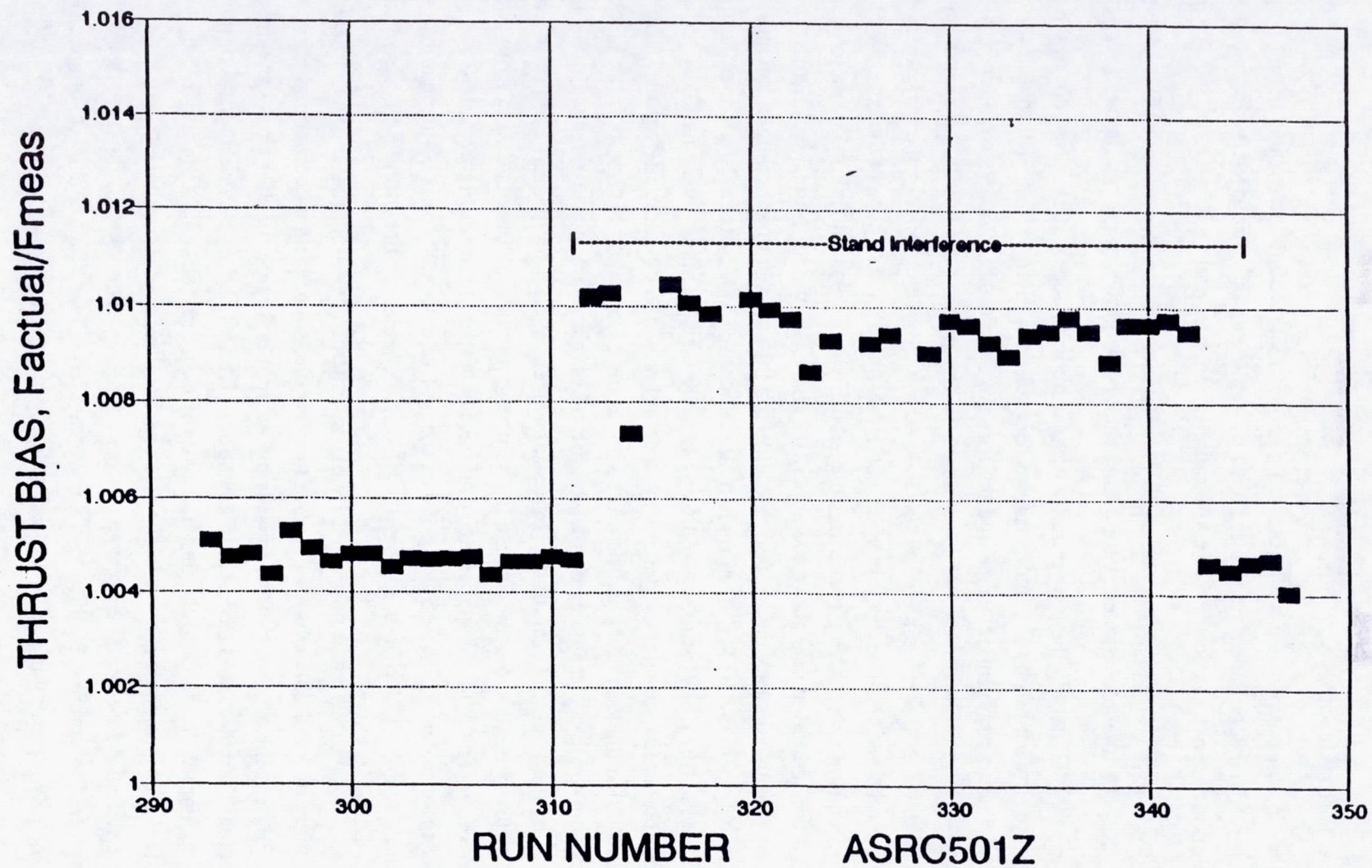


Figure 6.3-102. Thrust Bias vs Run Number for Durability Tests

6.3, Hot Fire Testing (cont.)

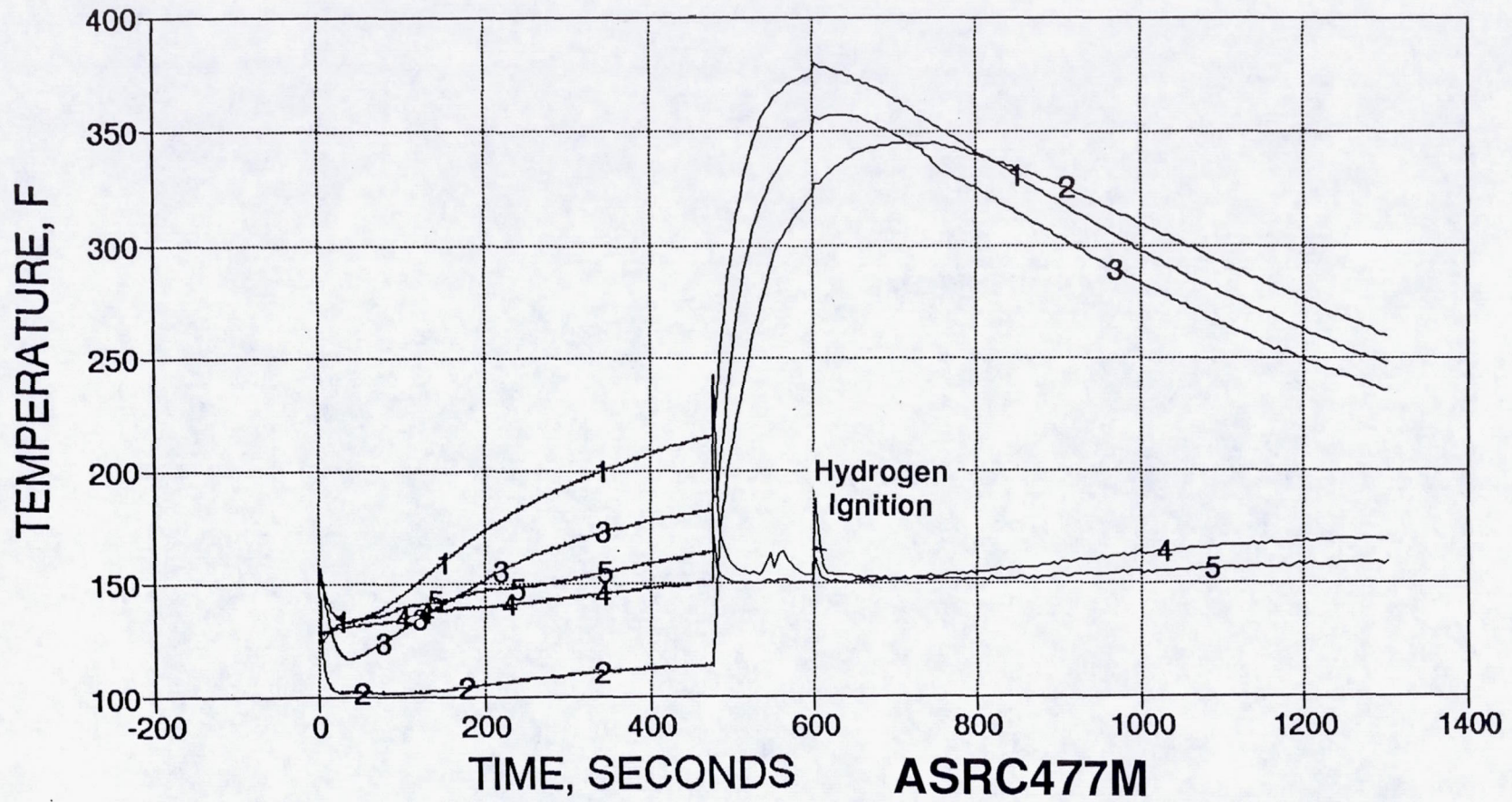
arose the decision was to proceed with life testing and correct the data later when testing would not be interrupted. It should be noted that at least 67 parameters are measured during a test and over 40 functions are calculated for the quick-look performance data.

Performance for each test is calculated at a time slice prior to FS-2. Measured and calculated performance parameters for a time slice near shutdown are tabulated in Appendix K.

Generally the long duration tests were followed by a 1000 sec coast, the time required for the slowest responding temperatures to reach maximum values. Thermal response data from the engine mounting interface and the forward stainless to stainless weld are plotted in Figure 6.3-103 for Test -306. Note the temperature spikes at about 2 min into the coast. These corresponded to a dim flame visible on video and were noted in a number of the early tests. They were the result of flashback of the hydrogen atmosphere used to protect the exterior of the Re chamber. During coast the hydrogen was turned off when the chamber cooled; up to this time the hydrogen concentration was above the upper flammable limit. As the residual hydrogen was diluted by background air leakage the concentration fell into the flammable range. Because of concern that the gas in the 10,000 ft³ altitude tank at about 0.2 to 0.3 atm might ignite, Test -309 was run with an argon -1% H₂ mixture replacing the 100% H₂. This test was manually terminated at 400 sec because of an indicated decay in chamber wall temperature (Pyro-hi). The argon mix provided inadequate oxidation protection to the exterior of the chamber; the black dentoid* coating oxidized, deposited on the window and affected the pyrometer reading. The chamber lost its high thermal emissivity. In the subsequent tests, with the 100% H₂ restored, the pyrometer measurements show an increase in chamber temperature of about 200 F, from about 3300 F to 3500 F. The external appearance of the Re chamber changed; Figure 6.3-104 shows the chamber prior to Test -279, i.e., at the end of the performance test series. The chamber without the dentoid coating is shown in Figure 6.3-105; the crystal structure of the Re is also visible.

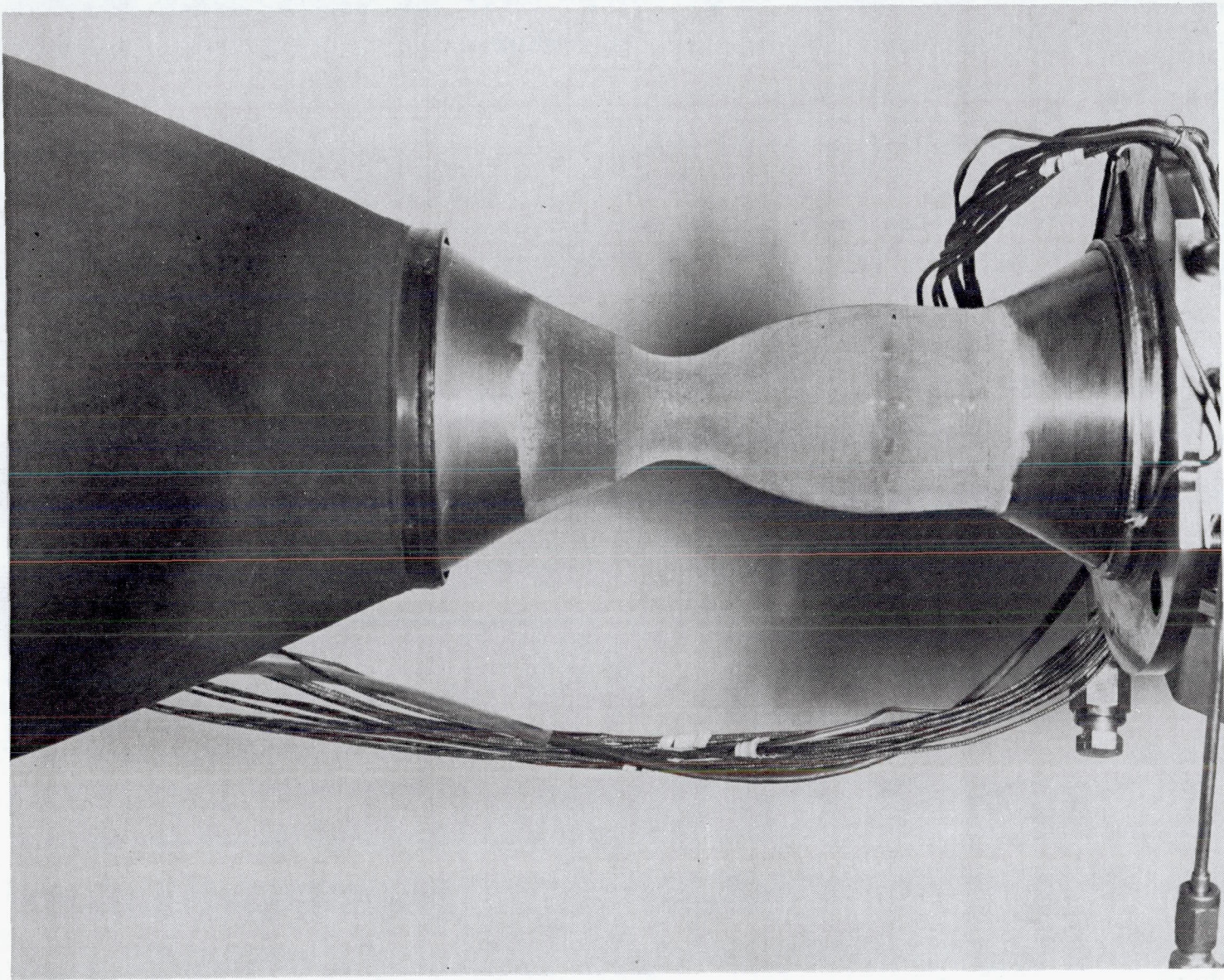
Pre -279 and post test -309 measurements of the external throat diameter show a decrease of 2 mil; however, because of the irregular shape with its compound curves this is probably beyond the accuracy of the measuring technique. Figure 6.3-106 shows the difference in external diameter measured at 5 axial stations (1.5, 2.0, 2.5, 3.0 - measured from the aft face of the mounting flange - and the throat) and three radial stations (60, 180, and 240 degree). The individual measurements show a wide variation, but their average indicates very little or no increase in external diameter. The average percent change in diameter as a function of axial location is plotted in Figure 6.3-107. Again, the measured values of about $\pm 1\%$ average close to zero and probably represent the error of the measuring technique.

*dentoid = tooth-like.



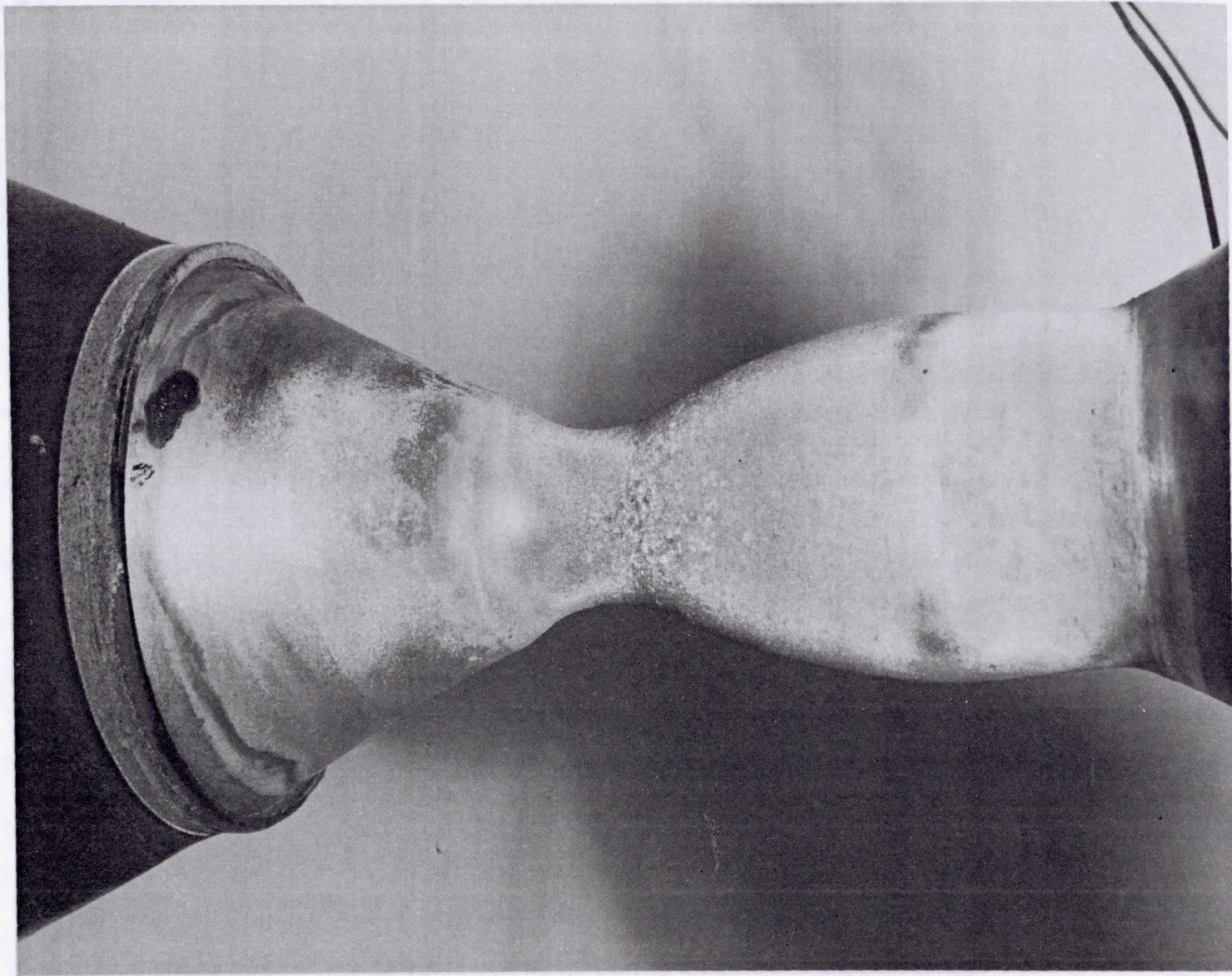
— 1=TMR-1	— 2=TMR-2	— 3=TMR-3
— 4=TMS-1	— 5=TMS-2	

Figure 6.3-103. Temperatures vs Time Test -306; 47:1 Durability



C0392 1333

Figure 6.3-104. Chamber Exterior at End of Performance Tests



C0792 4646

Figure 6.3-105. Chamber Exterior at End of Durability Tests

DIMENSION CHANGE, -347 - -279, INCH

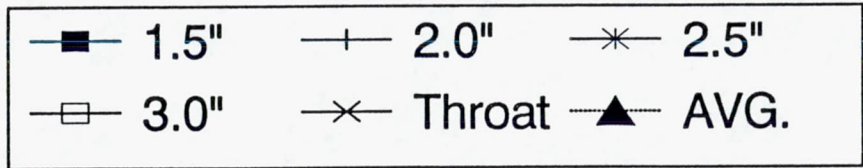
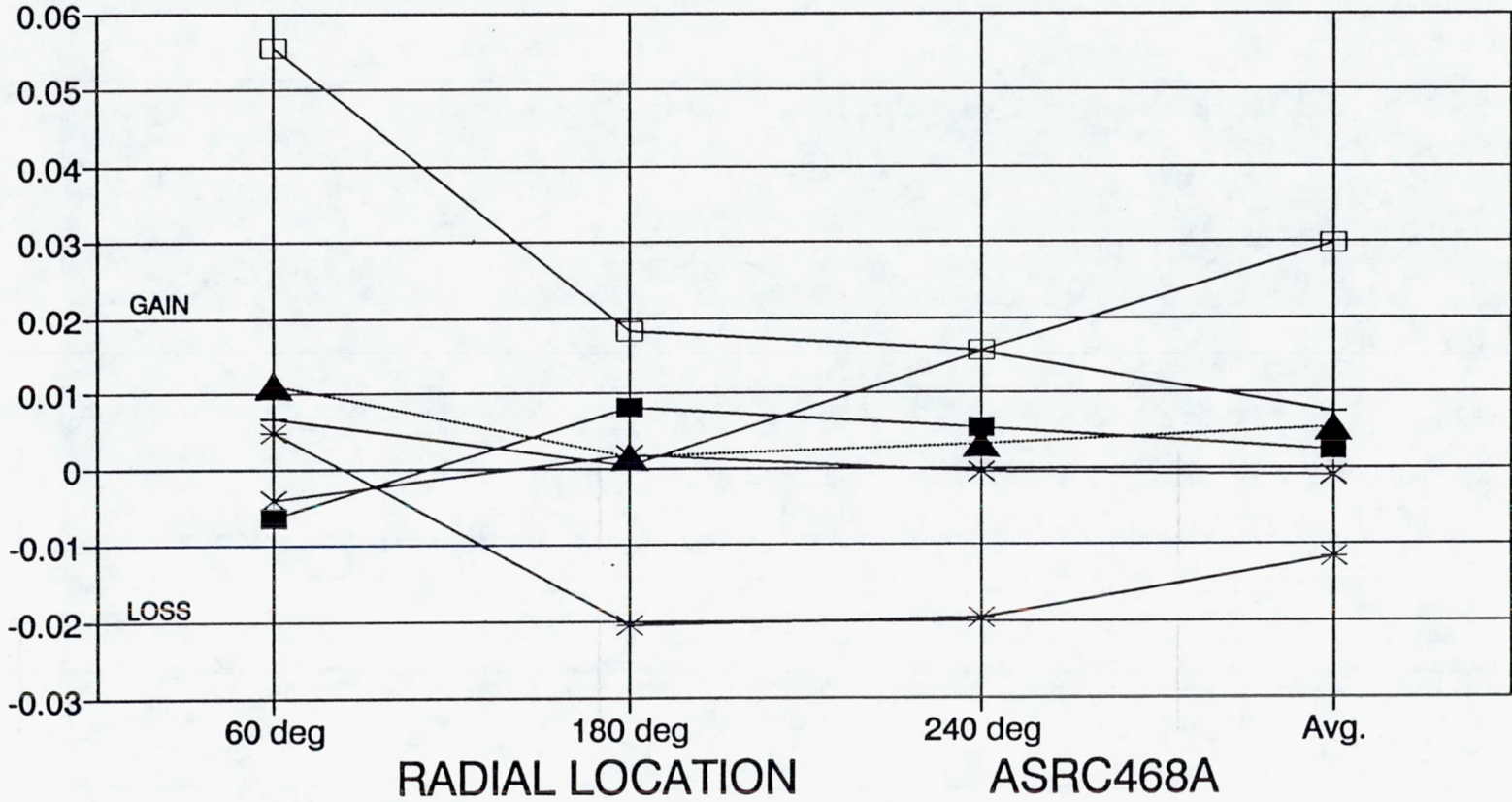


Figure 6.3-106. Change in External Dimensions; Durability Tests, -279 thru -347

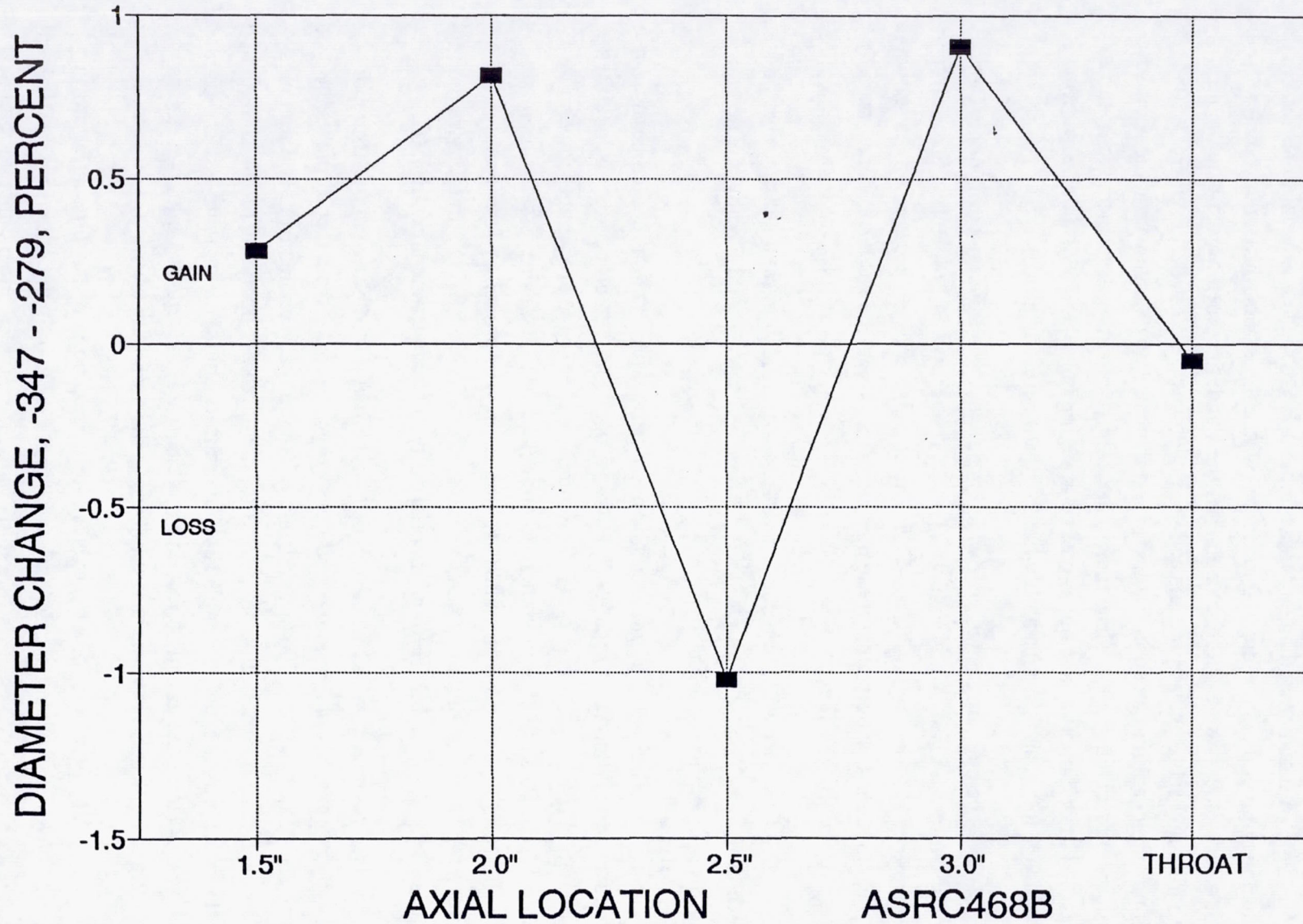


Figure 6.3-107. Change in External Dimensions, Percent; Durability Tests, -279 thru -347

6.3, Hot Fire Testing (cont.)

Throat internal diameter measurements were made at several times during the durability testing at several circumferential locations, with a three point throat micrometer. The first and last measurements were with the engine off the stand; the others were made on the stand. The individual sets of measurements and their averages are plotted in Figure 6.3-108. The variation from location to location and test to test indicated no change within the accuracy of the measurement technique. The difference in the average throat measurement from start to finish of the 3.64 hr of durability testing, as plotted in Figure 6.3-109, shows a decrease of 0.0004 in. which is less than the repeatability limit of the measurement.

The operating range over which the engine was tested in terms of chamber pressure and mixture ratio is shown in Figure 6.3-110. The thrust and I_s operating box as a function of inlet pressure is shown in Figure 6.3-111. The chamber wall temperature box is shown in Figure 6.3-112. It should be noted that these measurements are for 20 sec tests; steady-state temperatures are about 100 F higher.

Chamber wall temperature as a function of mixture ratio and chamber pressure is shown in Figure 6.3-113; the highest temperature measured is 400 F below the demonstrated long-life temperature of 4000 F.

The influence of mixture ratio and chamber pressure on fuel temperature rise in the cooled front end is shown in Figure 6.3-114; as propellant inlet temperature is increased the fuel temperature rise drops; this is shown in Figure 6.3-115 for the propellant temperature range of 40 to 120 F. The effect of mixture ratio on fuel ΔT and chamber pressure on outlet temperature are shown in Figures 6.3-116 and 6.3-117 for a range of propellant temperatures. The effect of inlet temperature on outlet temperature is shown in Figure 6.3-118. In all cases the fuel temperature is well below the MMH initial thermal decomposition temperature of 450 F.

A concern with fuel cooling is that the fuel not be heated above its vapor pressure for any required set of operating conditions. Figure 6.3-119 from Ref. 6 shows the vapor pressure of MMH as a function of temperature. The range of cooled front end fuel pressures as function of outlet temperature are plotted for the durability operating range, along with a plot of MMH vapor pressure, in Figure 6.3-120. Over this operating range there is a 150 psia margin on boiling. However, as can be seen in Figure 6.3-121, the required inlet pressure range for a typical flight application is wider than explored in the durability tests.

Temperatures for a typical test, -311, are plotted versus time in Figure 6.3-122, for the chamber wall and nozzle skirt weld, in 6.3-123, -124 and -125, for thruster locations and the test cell ambient. Heat transfer to the stand from the engine mount and total heat

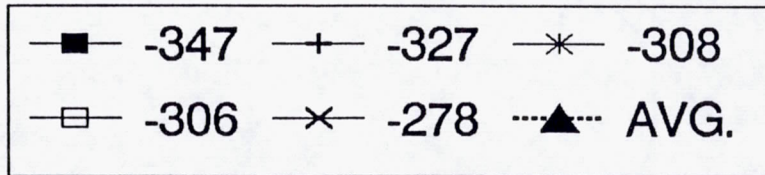
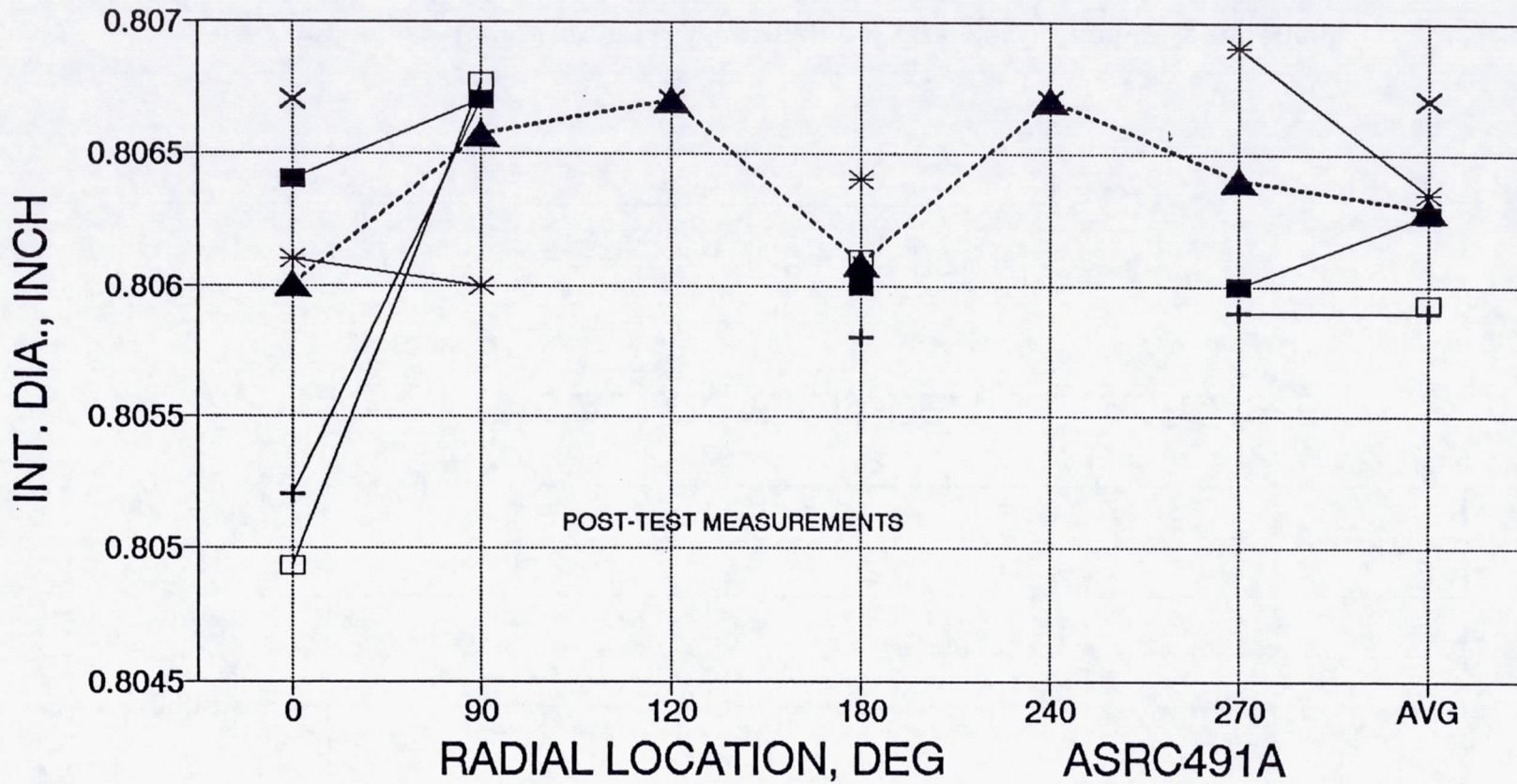


Figure 6.3-108. Throat ID Measurements; Durability Test Series

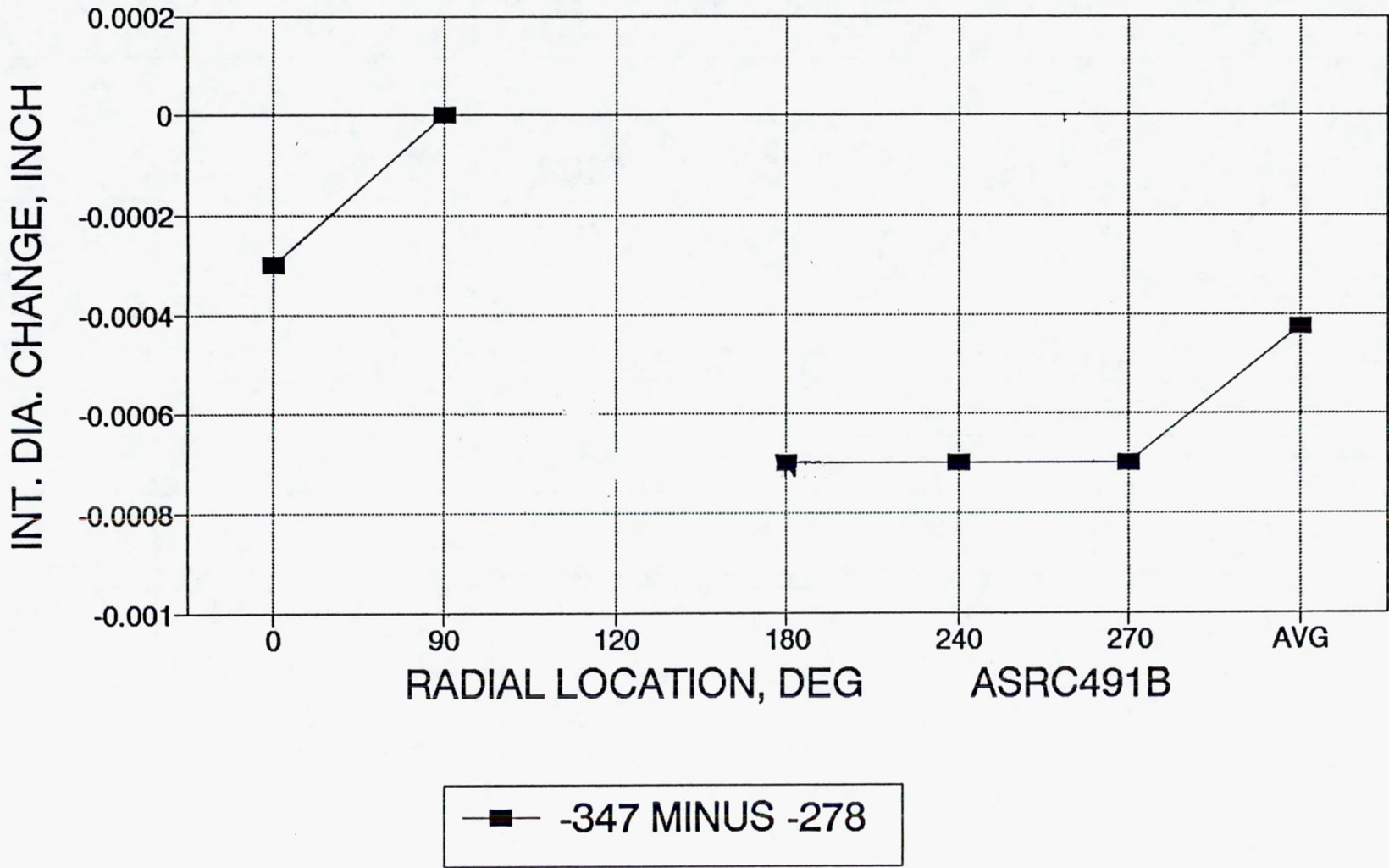


Figure 6.3-109. Throat I.D. Measurement Change; Durability Test Series

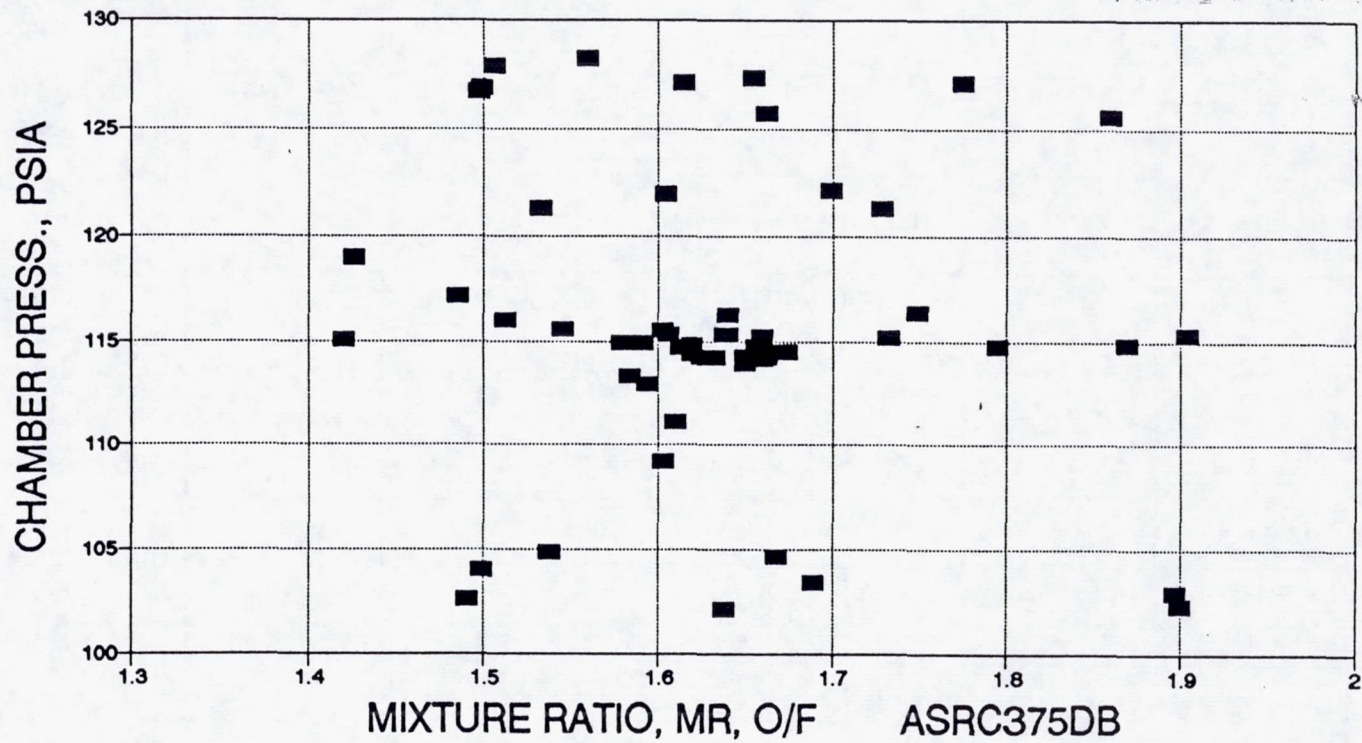


Figure 6.3-110. AJ10-221, High Performance LAE, the Minimum Chamber Pressure Was 102 psia at Mixture Ratio 1.64

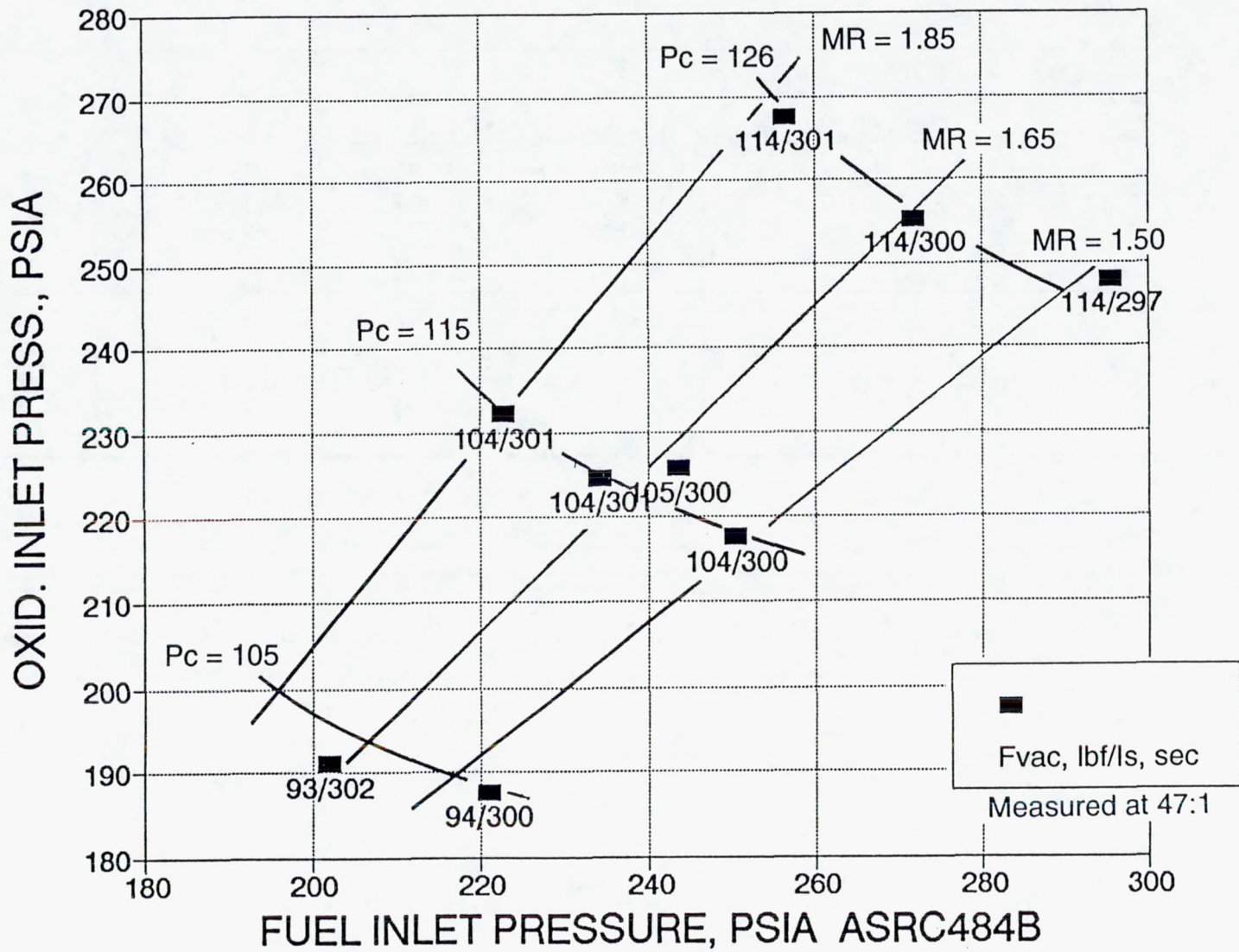


Figure 6.3-111. Ir-Re 490N Thruster-Nominal Box - 20 sec Flow Cals: -291 thru -301

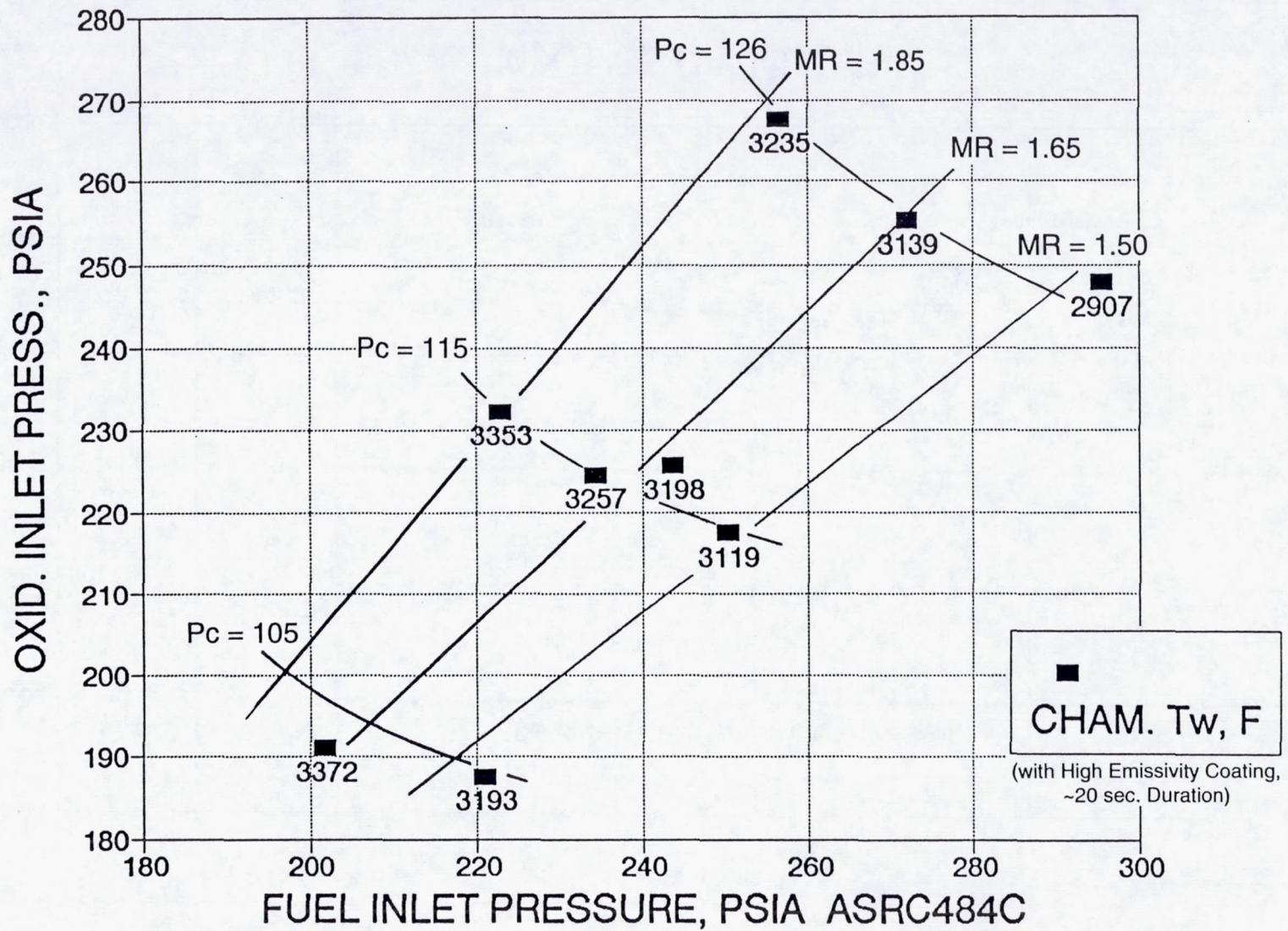


Figure 6.3-112. Ir-Re 490N Thruster-Nominal Box – 20 sec Flow Cals: -291 thru -301

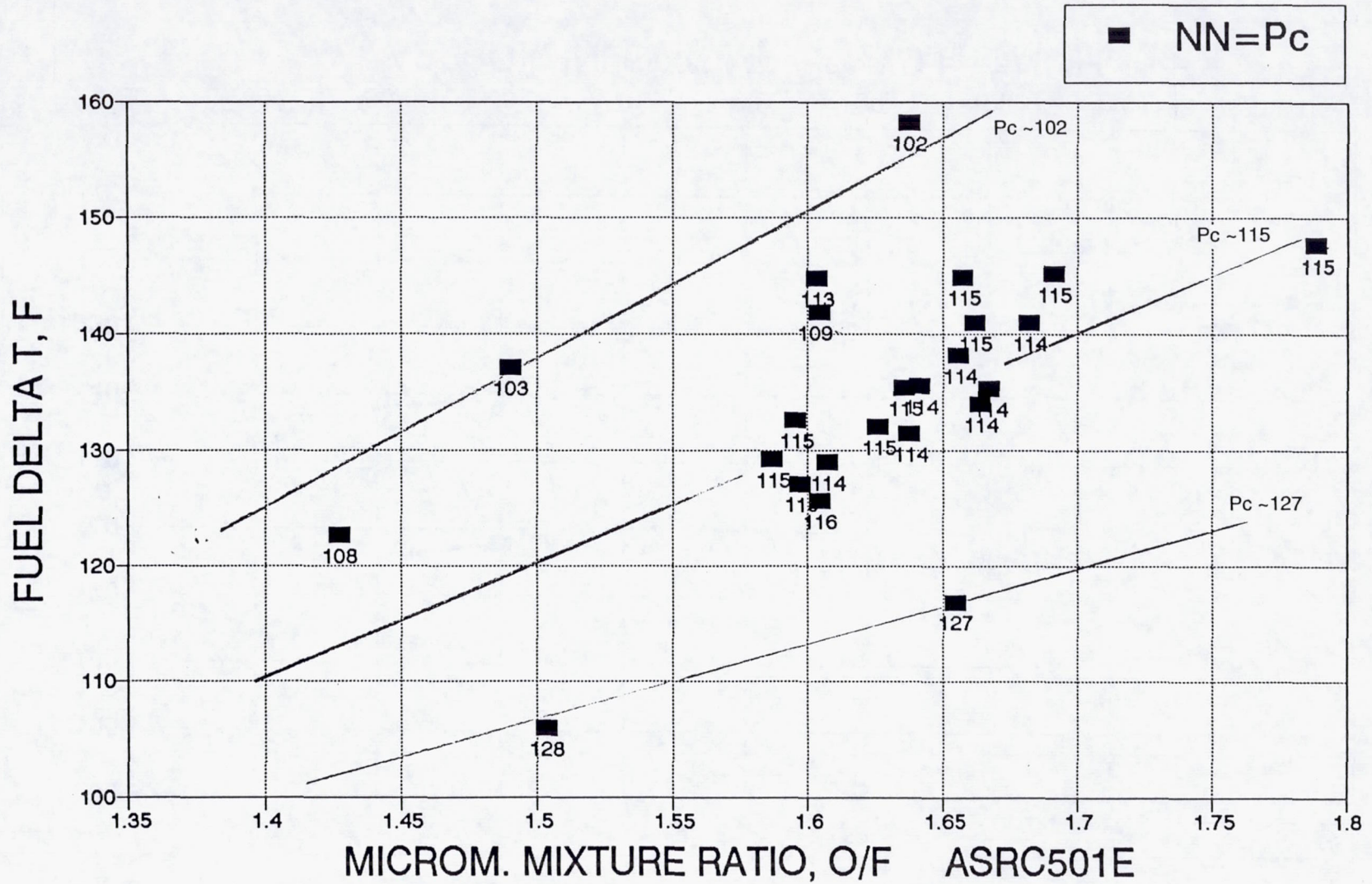


Figure 6.3-114. Fuel Regen Temp Rise vs MR and Pc – Durability Tests
W/Duration 7 = 120 sec

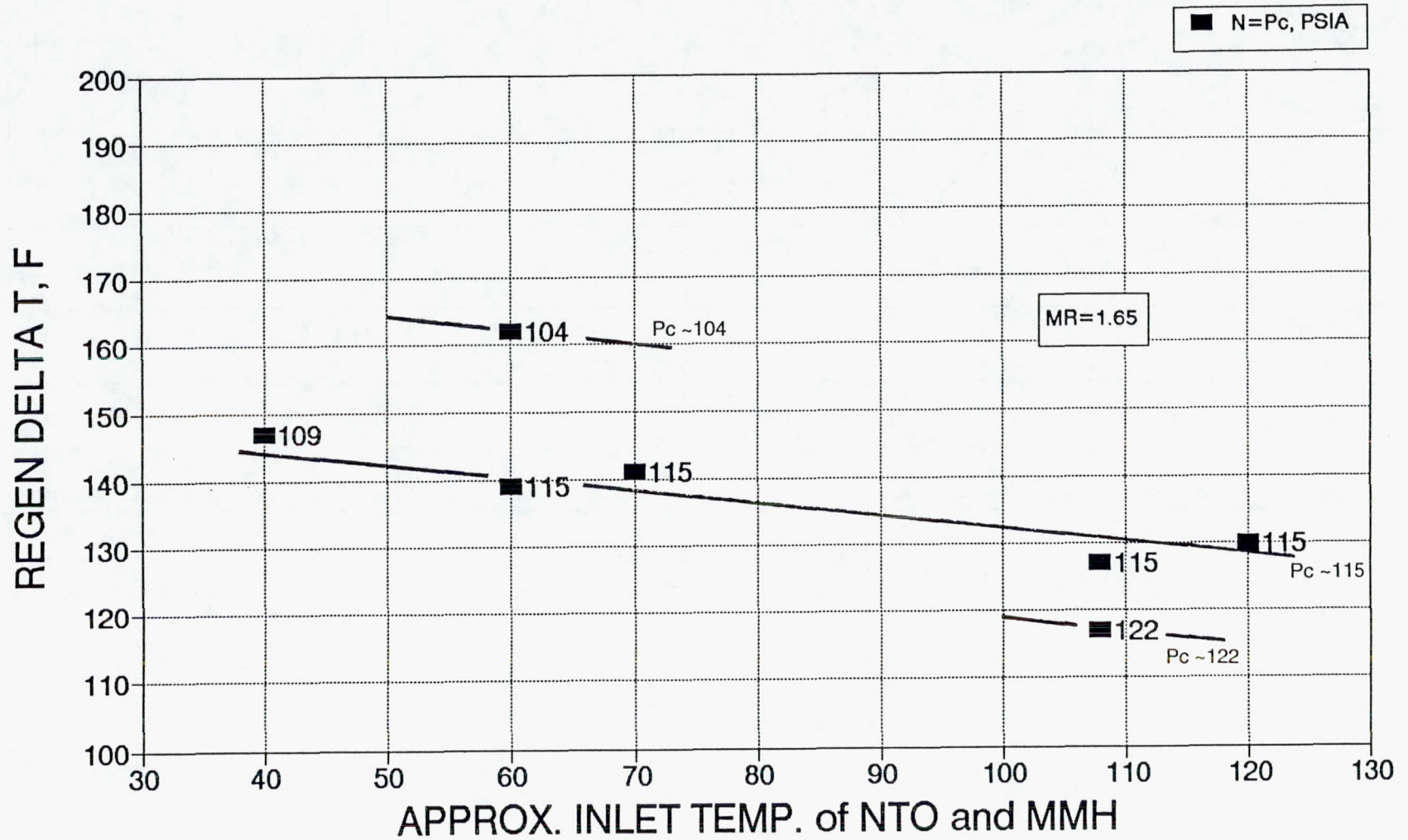


Figure 6.3-115. Ir-Re Welded Engine-Regen Delta T Effect of Propellant Inlet Temp

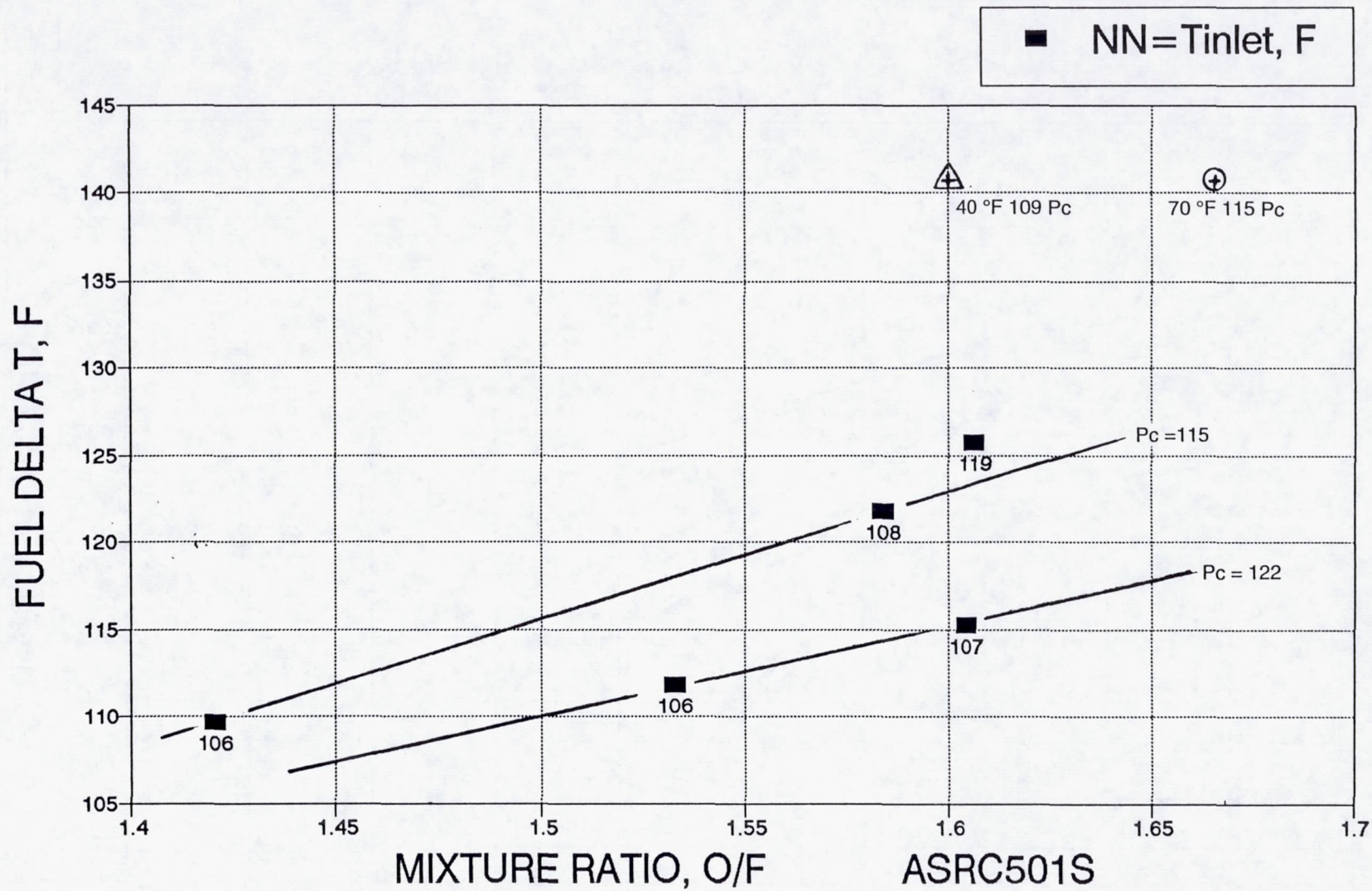


Figure 6.3-116. Fuel Regen Temp Rise vs MR and T_{prop} - Durability Tests - Effect of Propellant Temperature

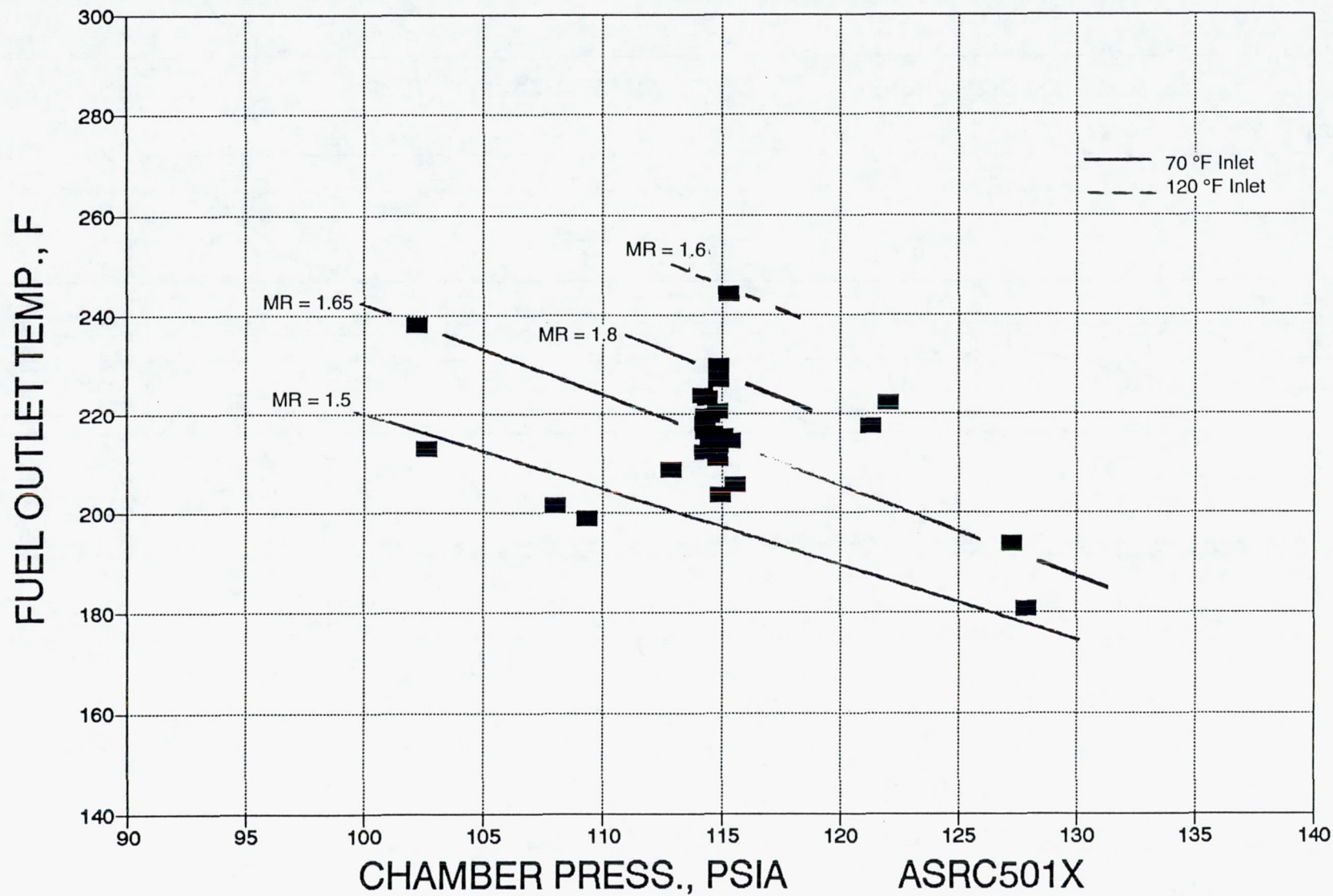


Figure 6.3-117. Fuel Regen Outlet Temp vs Pc and MR Durability Tests
W/Duration \geq 120 sec

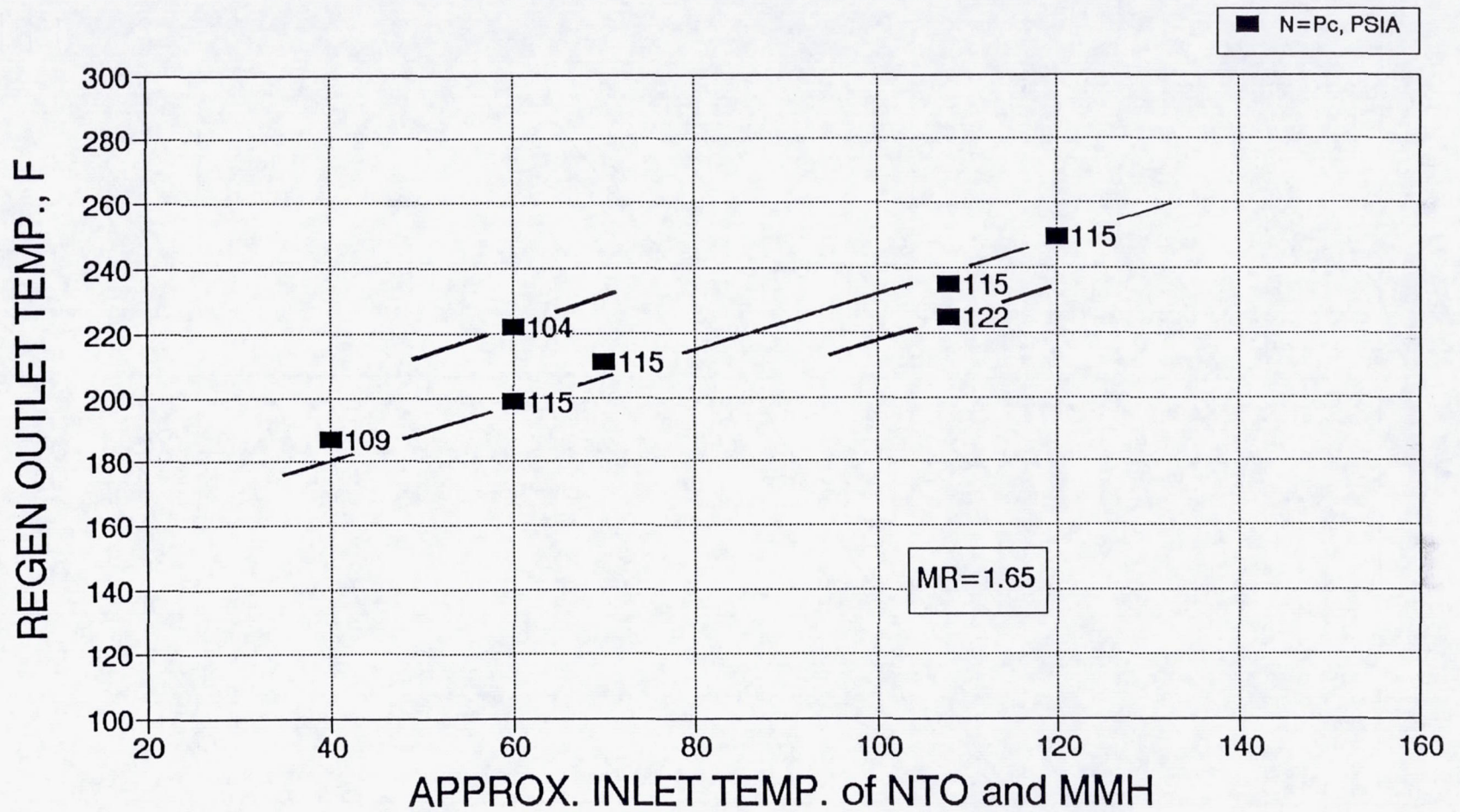


Figure 6.3-118. Ir-Re Welded Engine-Regen Outlet T Effect of Propellant Inlet Temperature

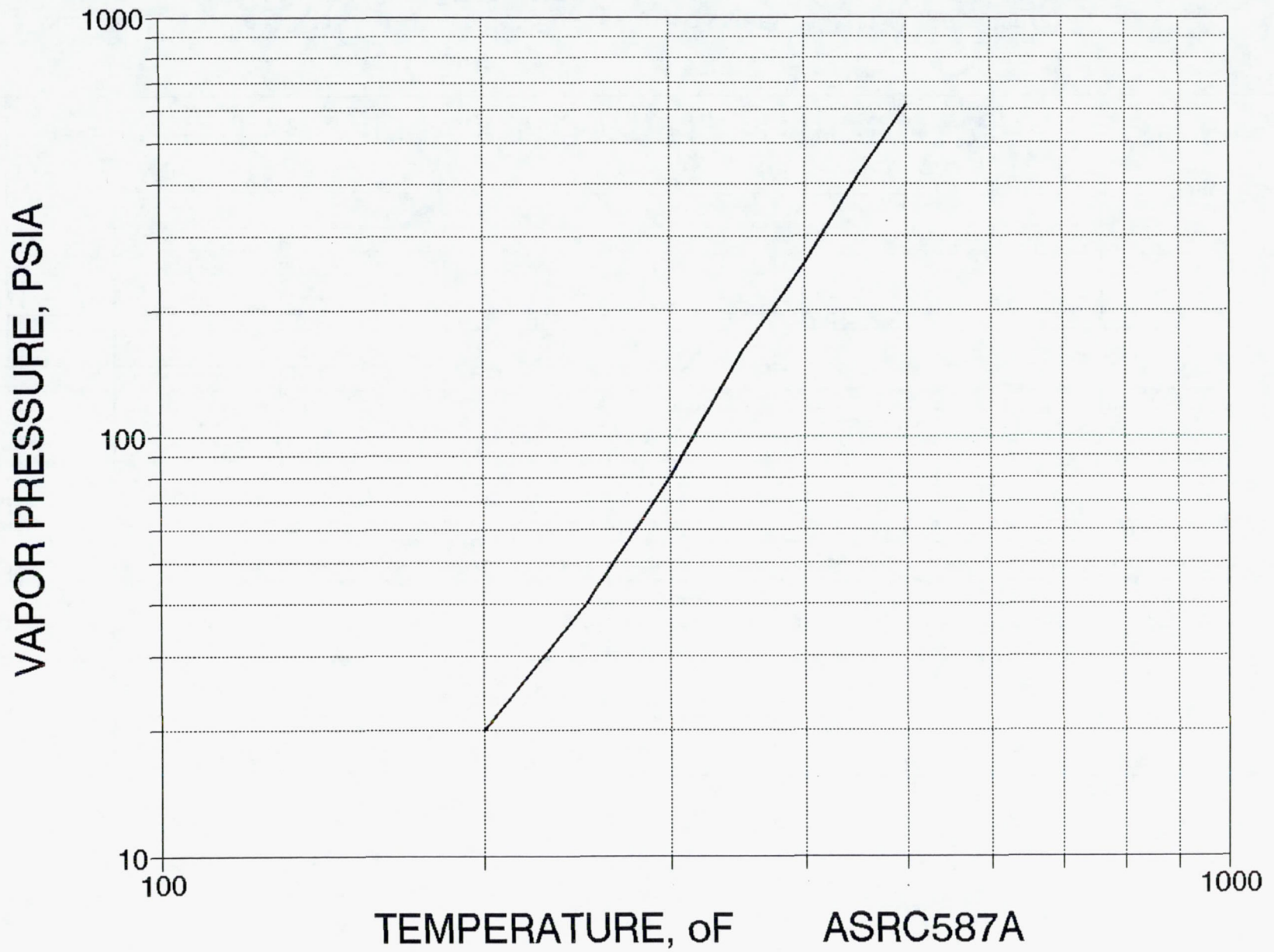


Figure 6.3-119. MMH V.P. vs Temperature – USAF Prop HDBK 3-70

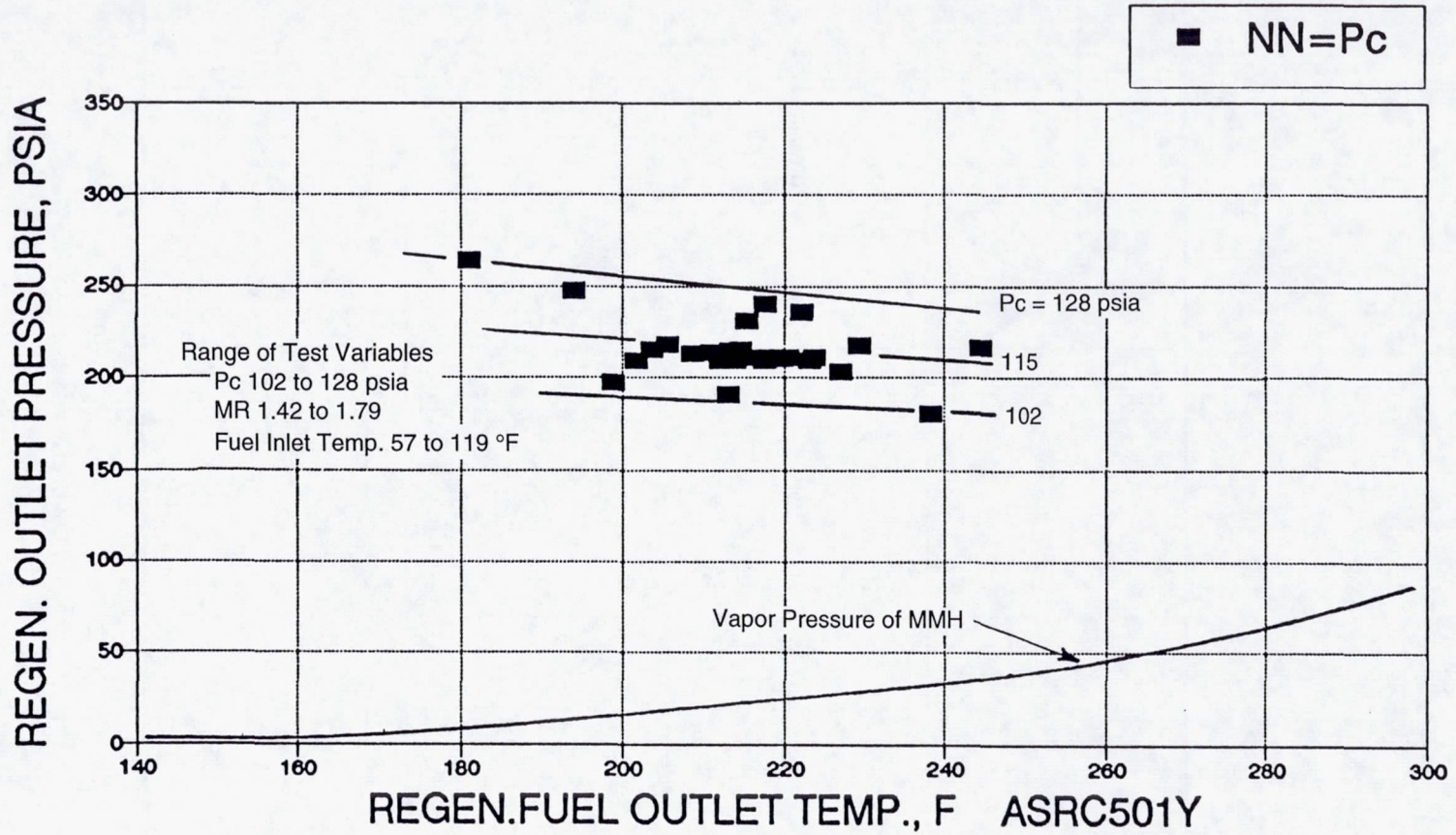


Figure 6.3-120. AJ10-221 High Performance – LAE Margin on Fuel Boiling Pressure is Greater Than 150 psi Over the Operating Range

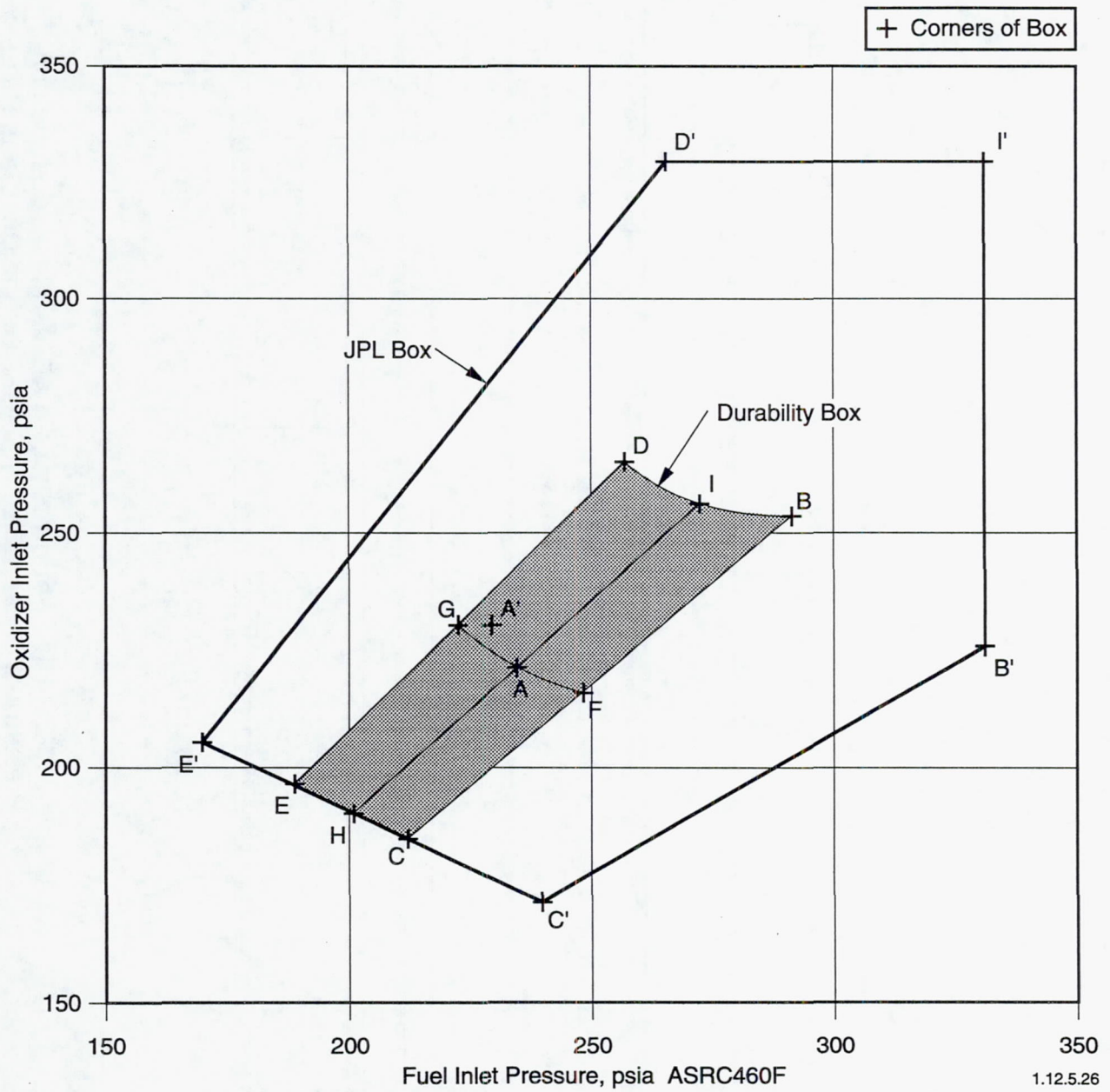


Figure 6.3-121. Oxid Inlet Pressure vs Fuel Inlet Pressure JPL Operating Box

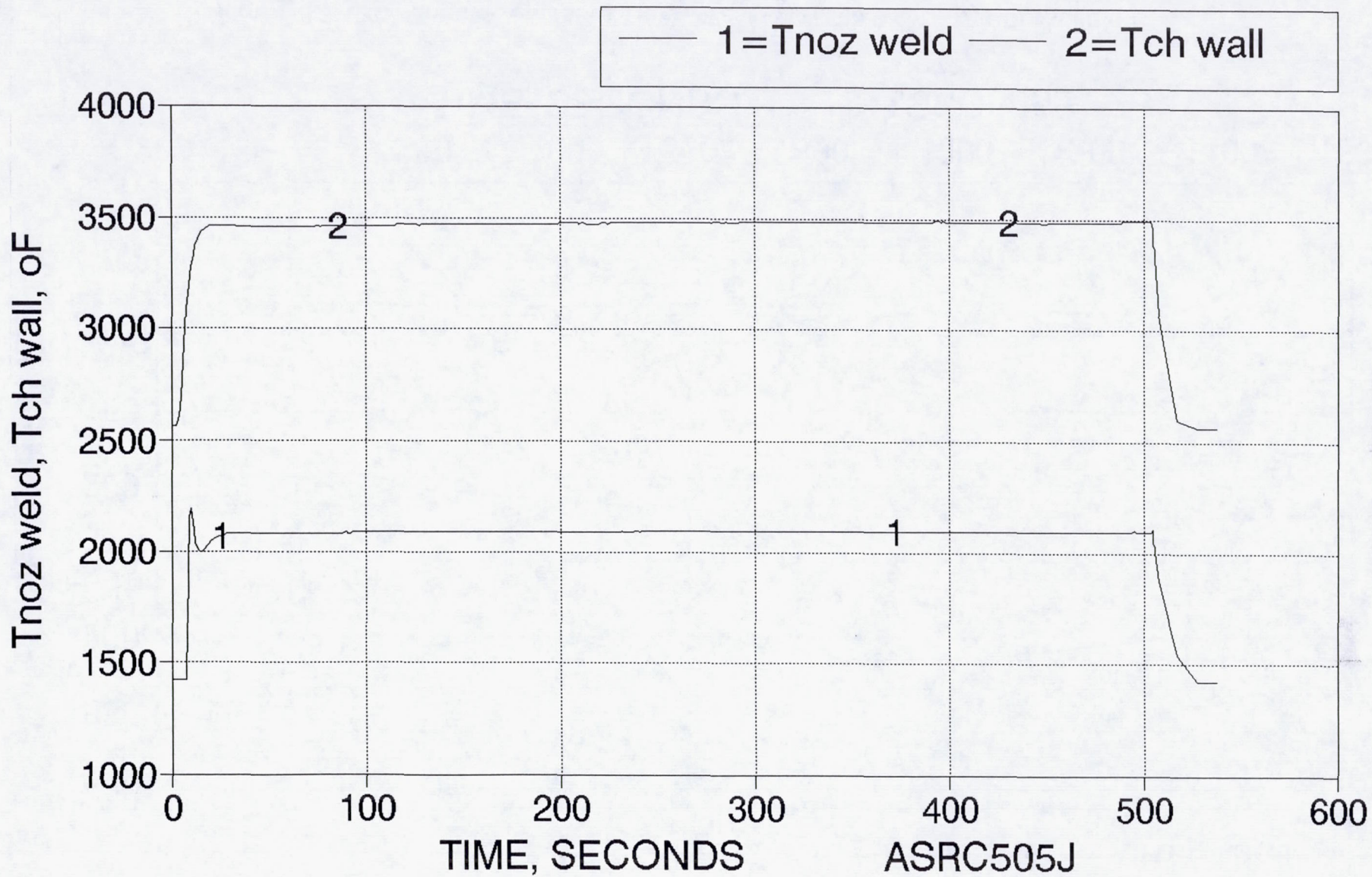


Figure 6.3-122. Nozzle Weld and Chamber Wall Temperature vs Time – Test -311, 504.9 sec; 47:1 Durability

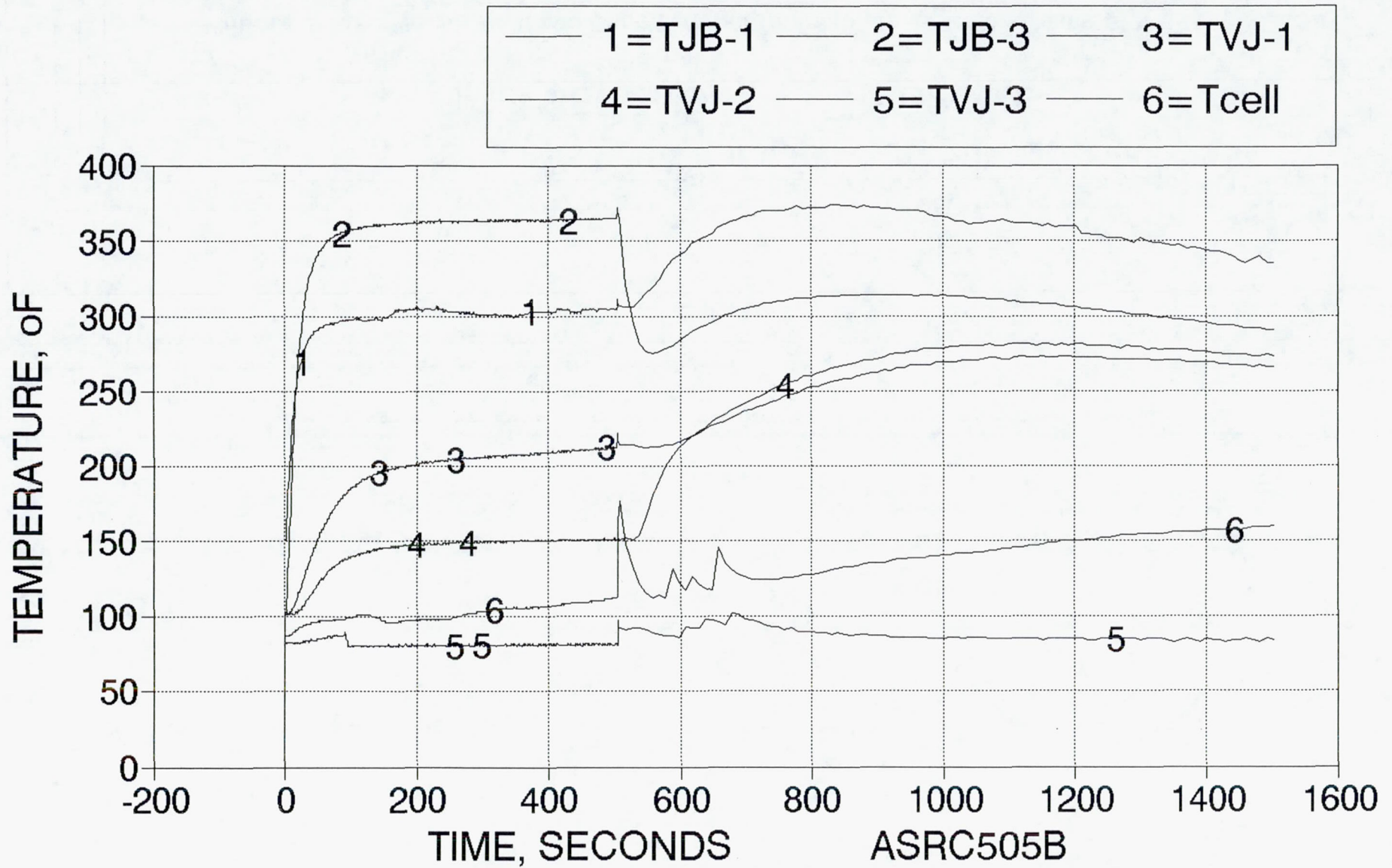


Figure 6.3-123. Engine Temps. vs Time – Test -311, 504.9 sec, 47:1 Durability

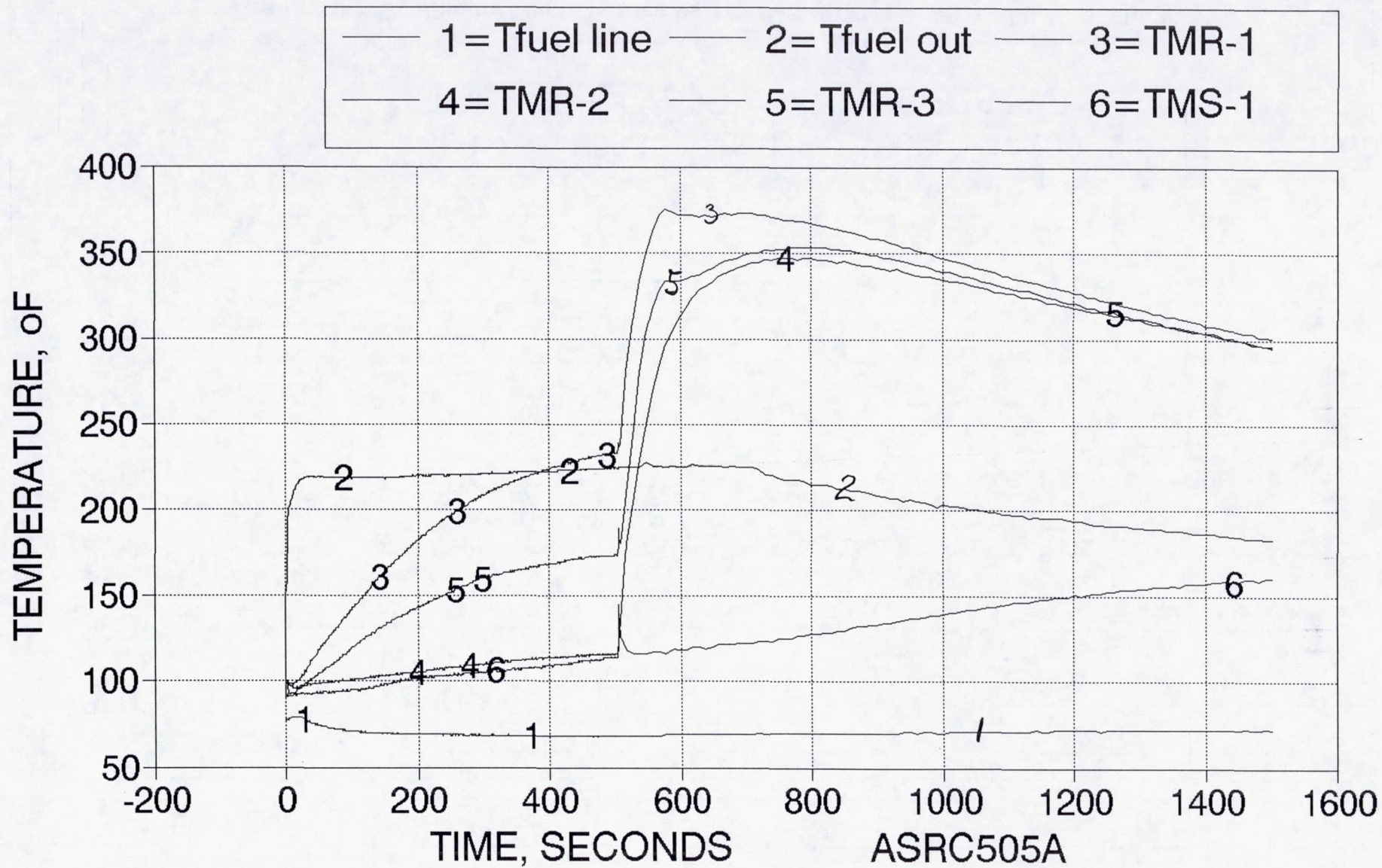


Figure 6.3-124. Fuel In, Out, Mounting Point Temperatures – Test -311; $\theta = 504.9$ sec

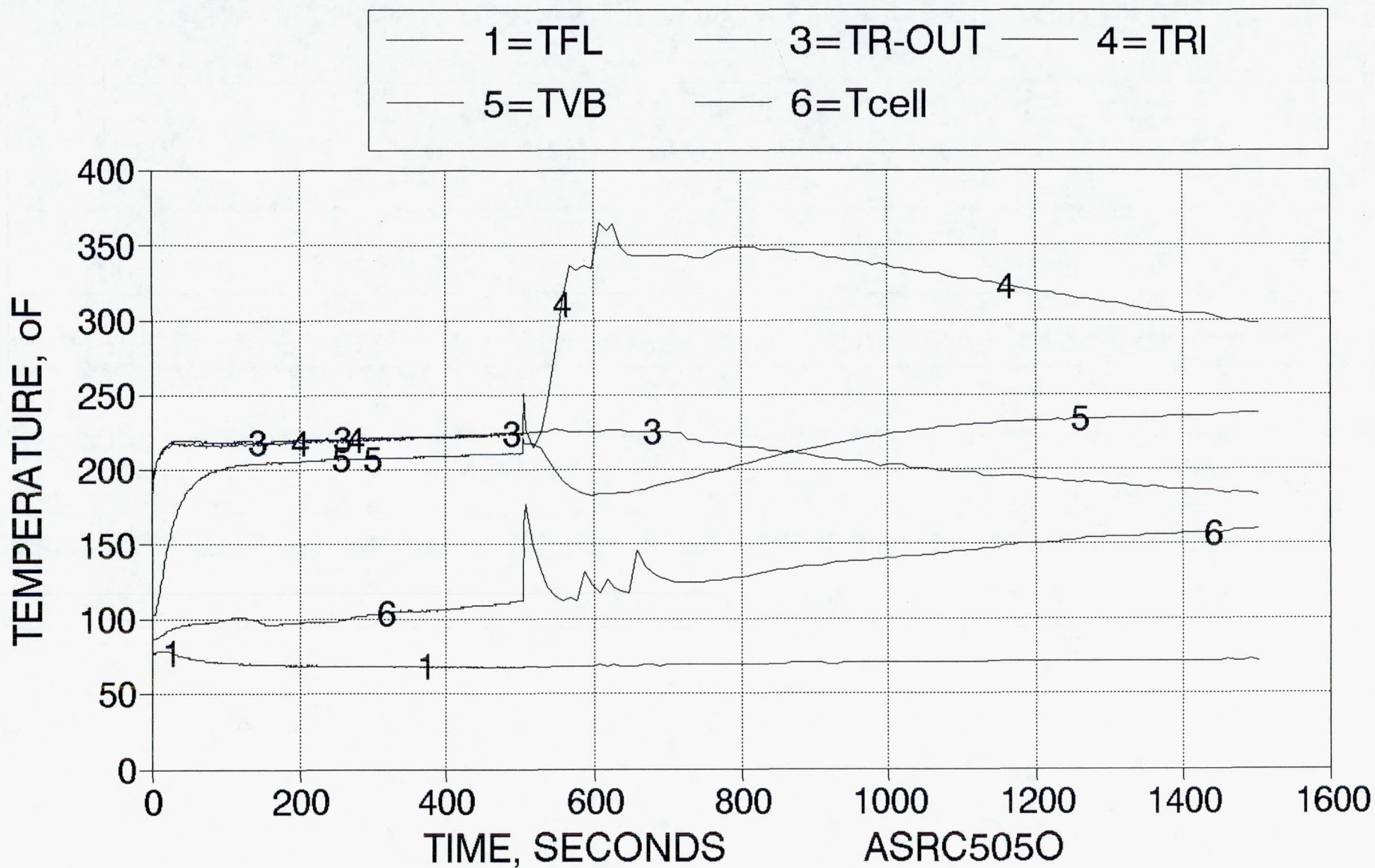


Figure 6.3-125. Engine Temperatures vs Time – Test -311 – MR = 1.65, Pc = 114.2; 504.9 sec; 47:1 Durability

6.3, Hot Fire Testing (cont.)

input during firing and soak is plotted in Figure 6.3-126. The maximum heat conduction rate to the stand is less than 0.035 BTU/sec.

Test facility temperatures, diffuser exit pressure and vacuum tank pressure are shown in Figure 6.3-127. Spikes in cell temperature are clearly visible. The first rise from about 115 to 175 F is the result of diffuser unload at shutdown and the hot 3 psia gas which pressurizes the cell. The other spikes during coast are the result of ignition of residual hydrogen in the cell.

Fuel delta T, outlet temperature and heat transferred to the fuel are shown in Figure 6.3-128 for Test -308.

Propellant system pressures versus time are shown in Figure 6.3-129; water hammer at ignition and shutdown is evident. As can be seen in Figure 6.3-130 cell pressure rapidly reaches a steady value and stays constant until diffuser unload.

Tests were conducted with increasing initial hardware temperature by varying the coast time between firings. Figure 6.3-131 shows front end temperature for these tests ordered by increasing hardware temperature. Tests were conducted with hardware temperatures at up to 200 F at ignition; no adverse effects were noted.

6.3.5.1 Stability

Engine operation was monitored for evidence of instability. Chamber pressure and thrust were examined for signs of high frequency resonances; none were found. Variations seen in chamber pressure and thrust are small, of very low frequency, and reflect the response of the regulators which control tank pressures. Figure 6.3-132 shows a highly magnified chamber pressure trace for Test -311, a 504 sec firing. Pressure fluctuations are less than ± 0.25 psi above the mean, which for this test drops about 1 psi throughout the 504 sec firing. Thrust, shown on a highly magnified scale in Figure 6.3-133, shows long term (several second) maximum variations of ± 0.5 lbf. To show the conventional appearance of the Pc and thrust traces, they are plotted with normal scales in Figure 6.3-134.

Since these measurements have limited frequency response, and since it was not practical to mount Kistler pressure or force transducers on the flight engine, a 3-axis accelerometer was mounted on the back of the injector body. In this way, combustion instability could be detected by its effect on the engine structure. No indication of structural response to instability was seen in these measurements.

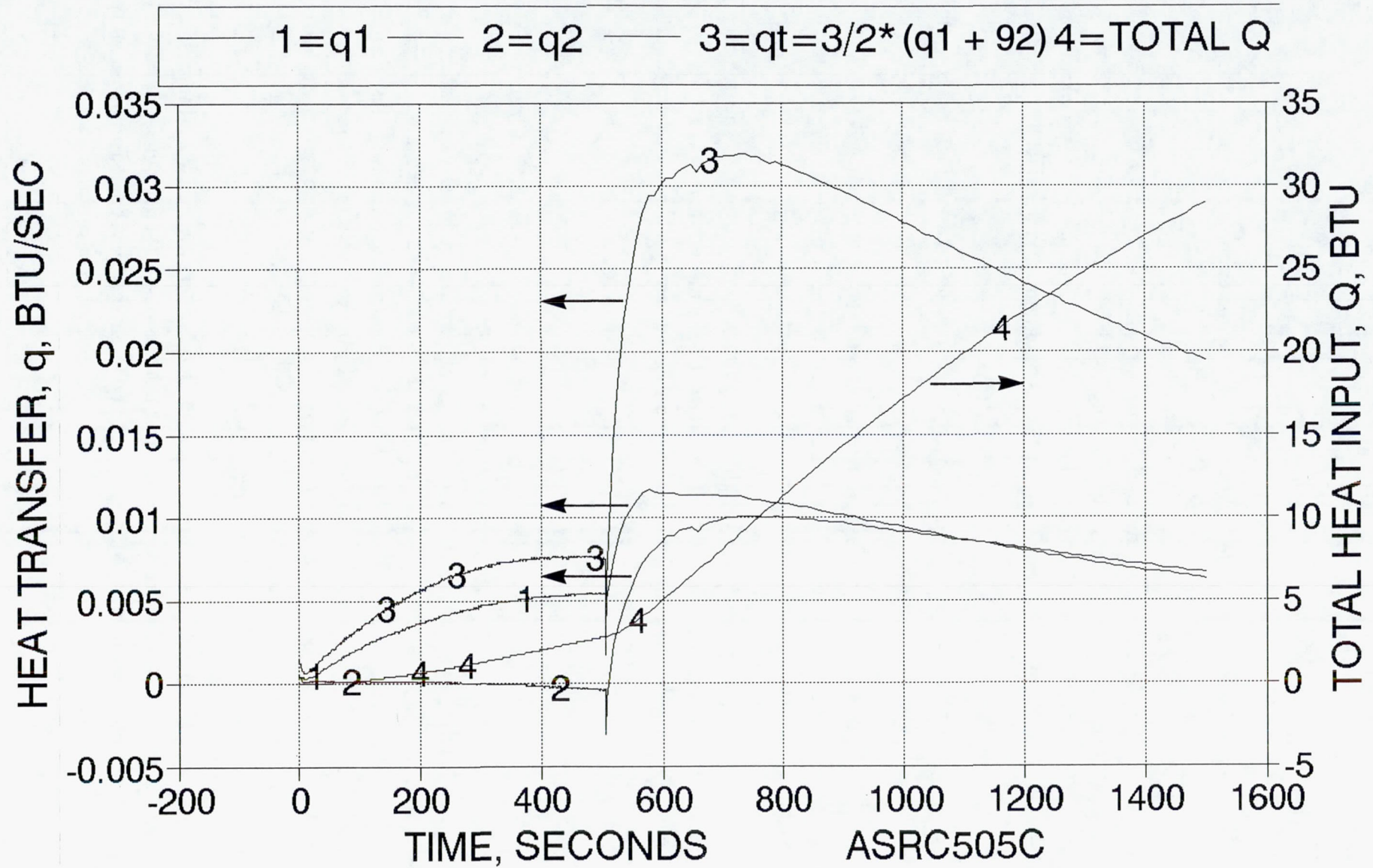


Figure 6.3-126. Heat Transfer Thru Engine Mount – Test -311, 504.9 sec; 47:1 Durability

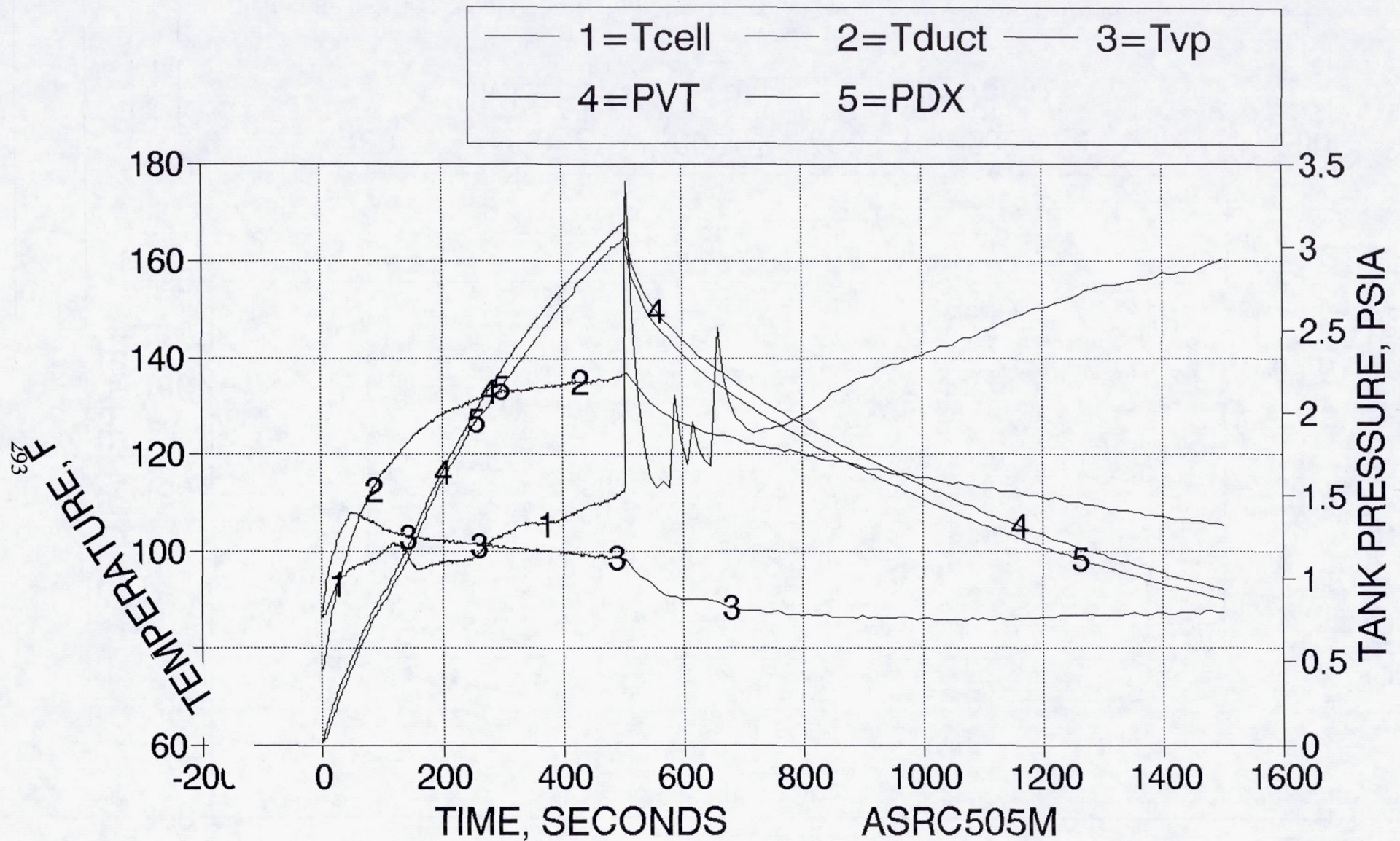


Figure 6.3-127. Facility Temperature and Pressure vs Time – Test -311, 504.9 sec; 47:1 Durability

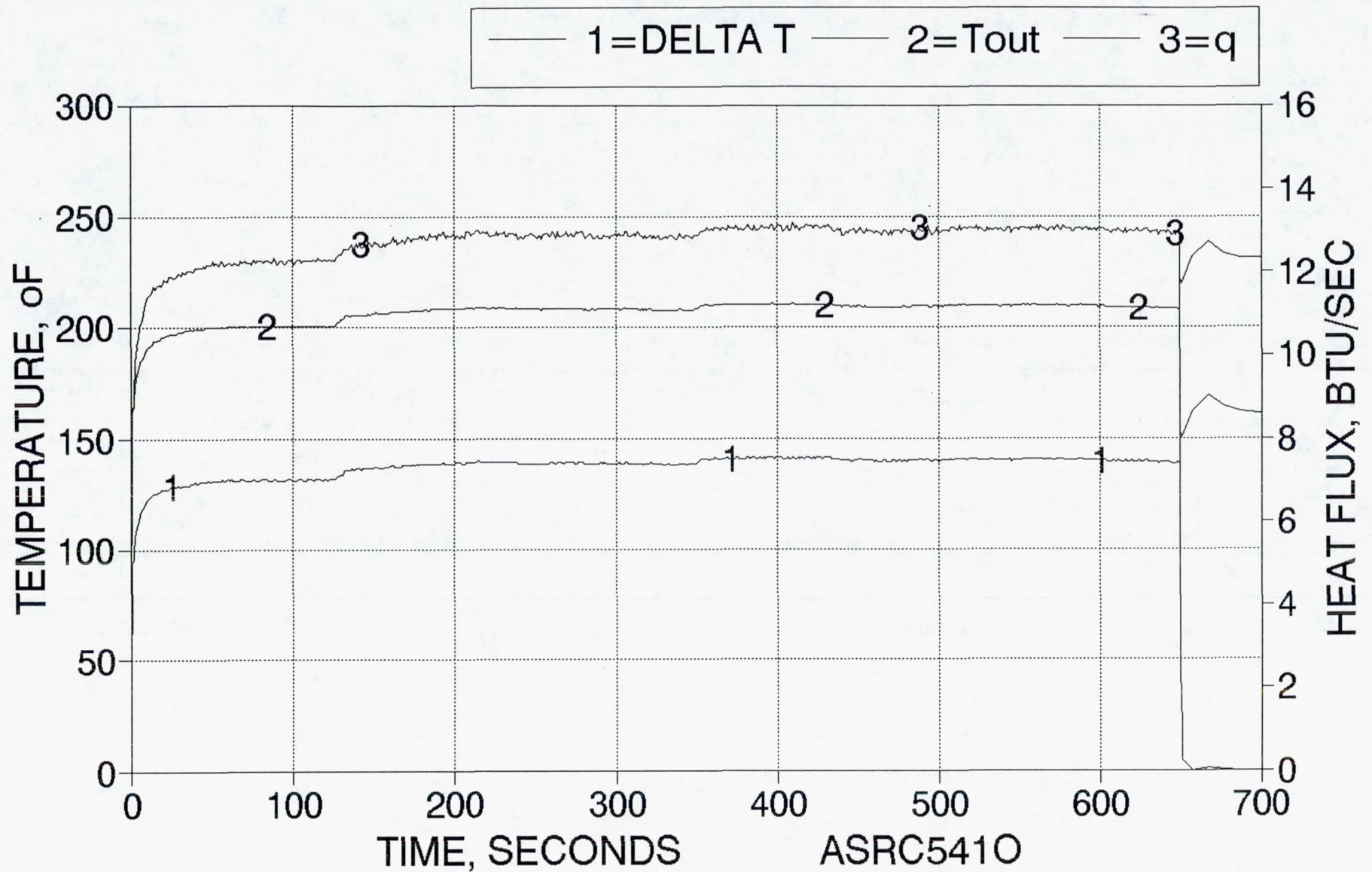


Figure 6.3-128. Fuel Delta T, T_{out}, Heat Flux Test -308; 650.1 sec, 47:1 Durability

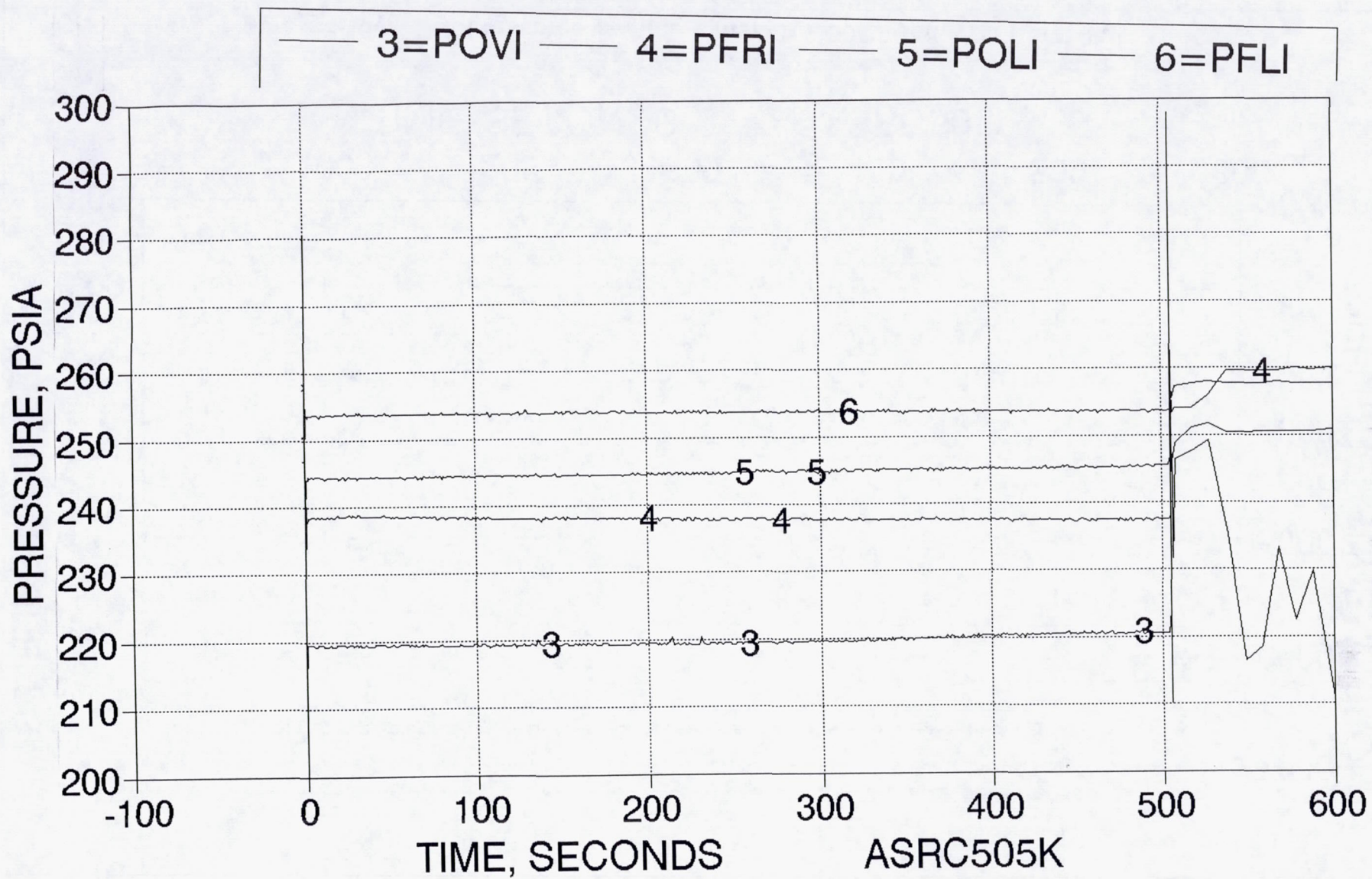


Figure 6.3-129. Line and Inlet Pressures vs Time – Test -311, 504.9 sec; 47:1 Durability

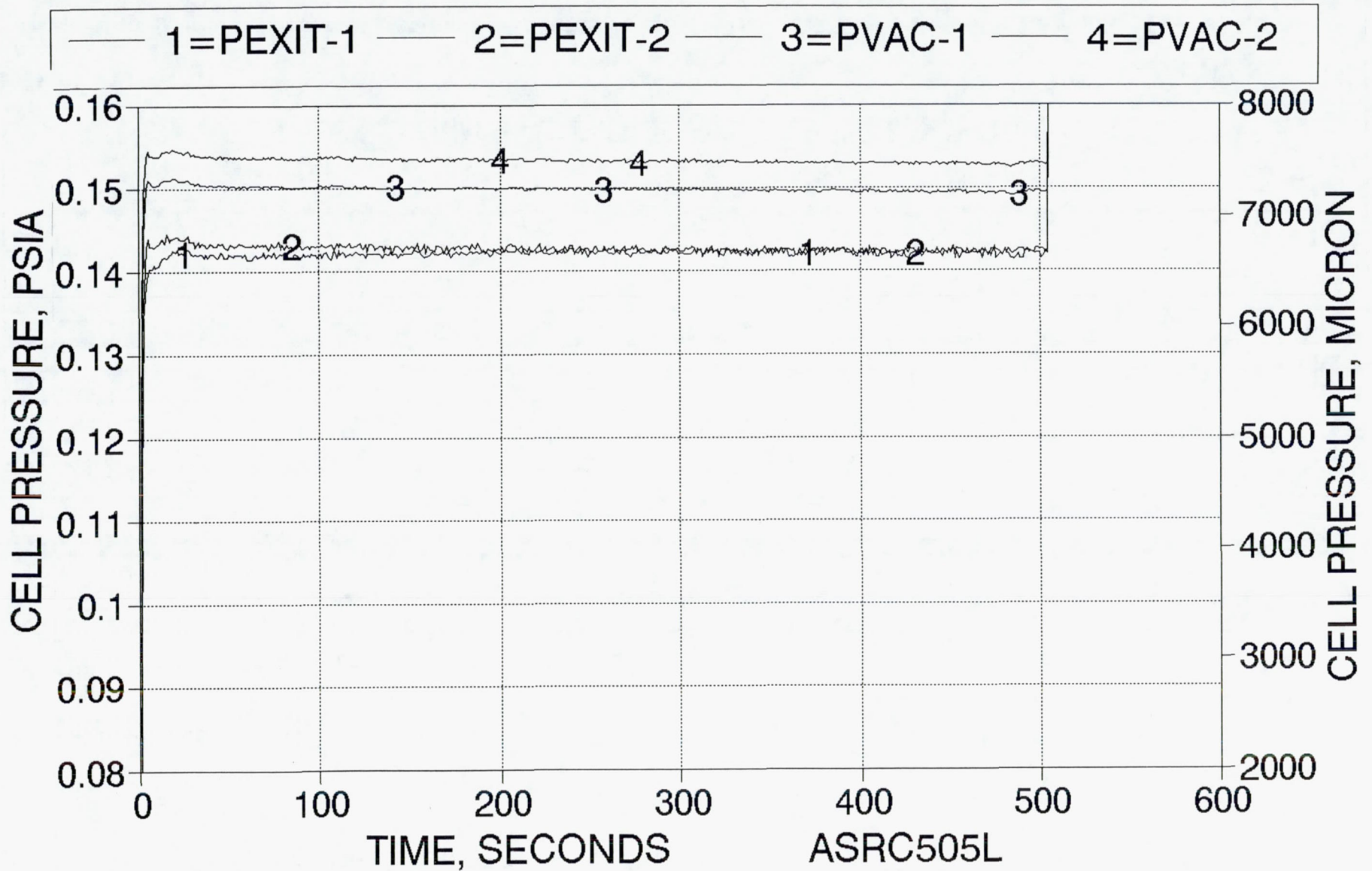


Figure 6.3-130. Cell Pressures vs Time – Test -311, 504.9 sec; 47:1 Durability

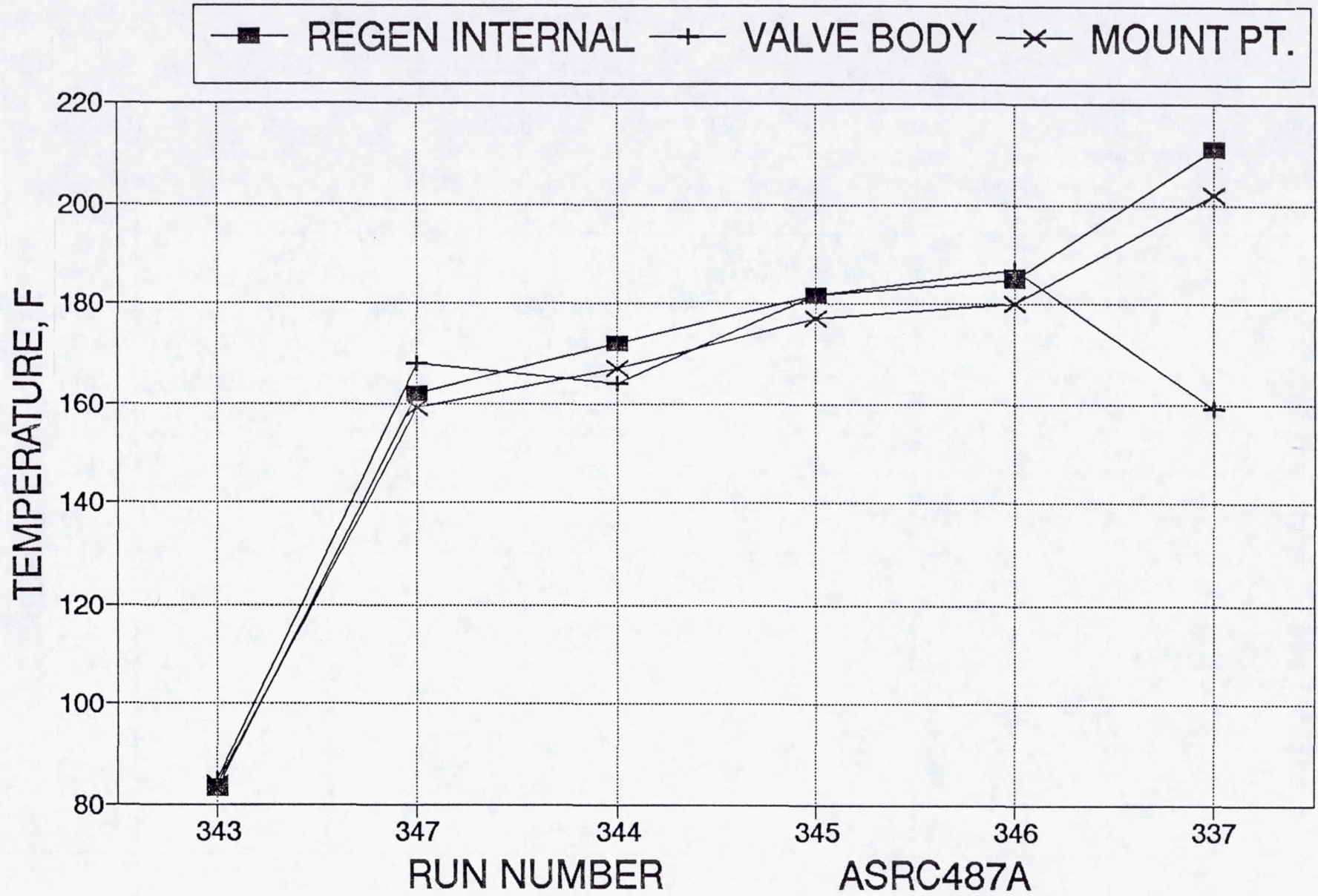


Figure 6.3-131. Hot Restart Temperatures – Pre-Fire, After Heat Soak

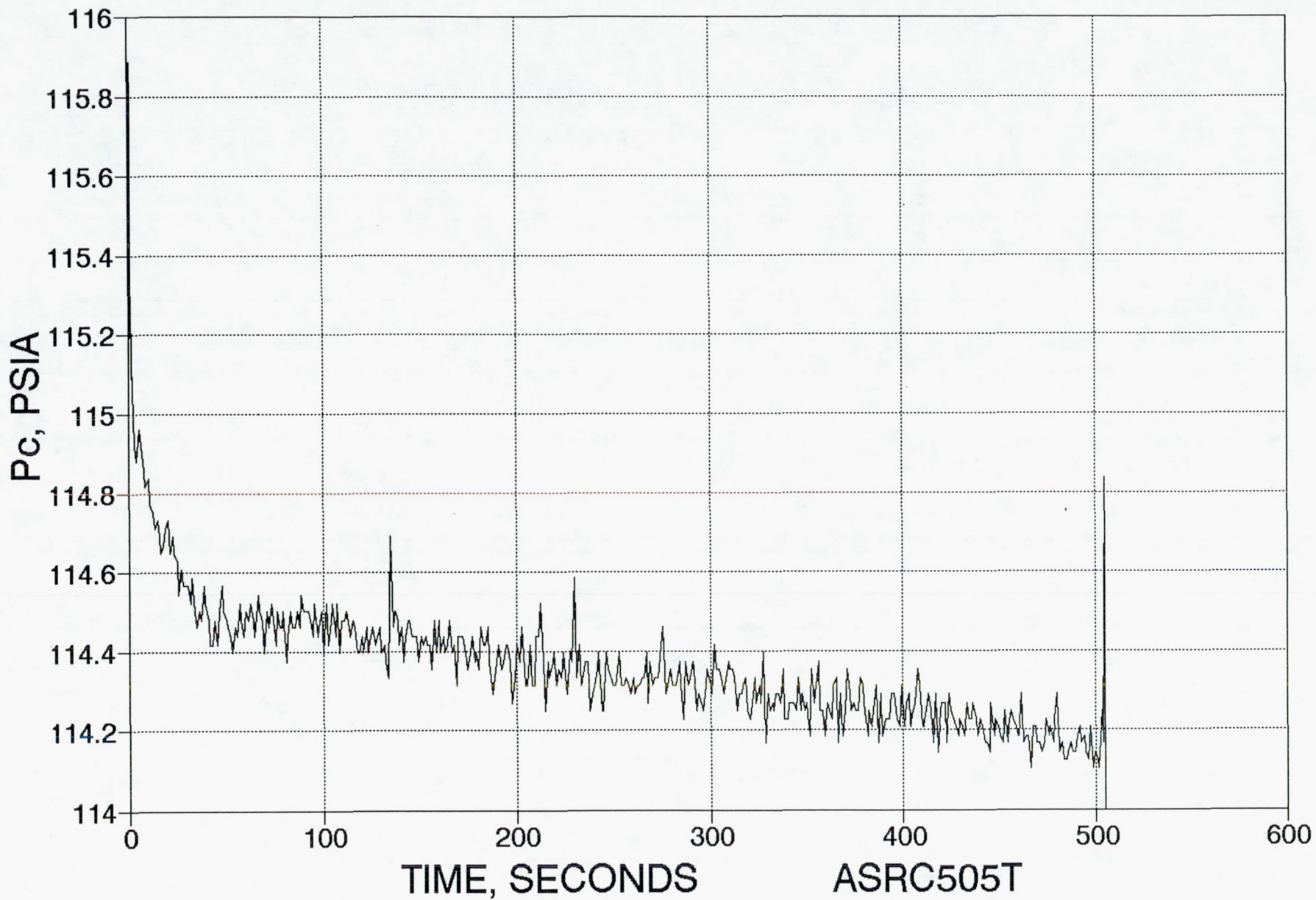


Figure 6.3-132. Pc vs Time – Test -311; 47:1 Durability: Firing

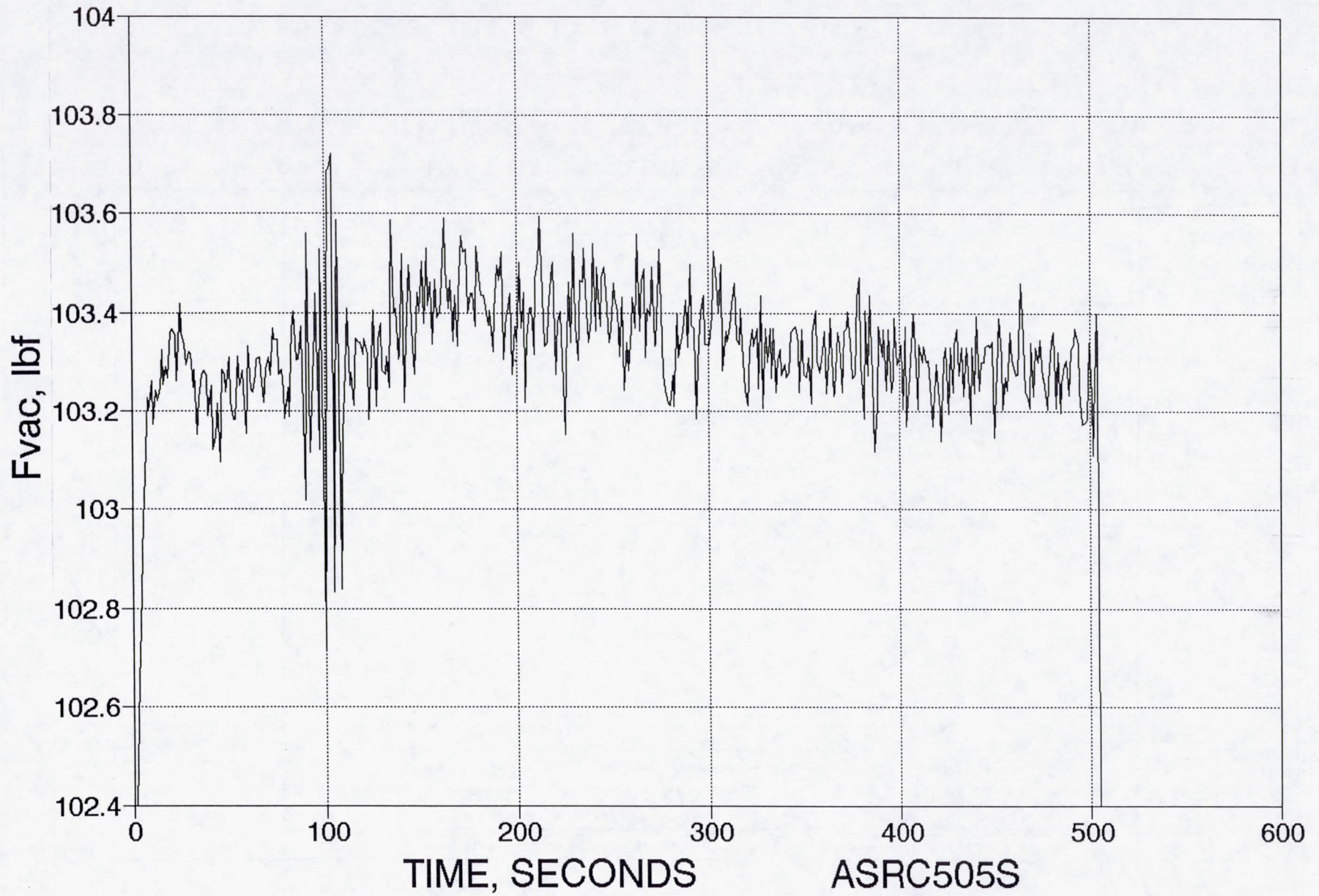


Figure 6.3-133. Vac Thrust vs Time – Test -311; 47:1 Durability: Firing

300

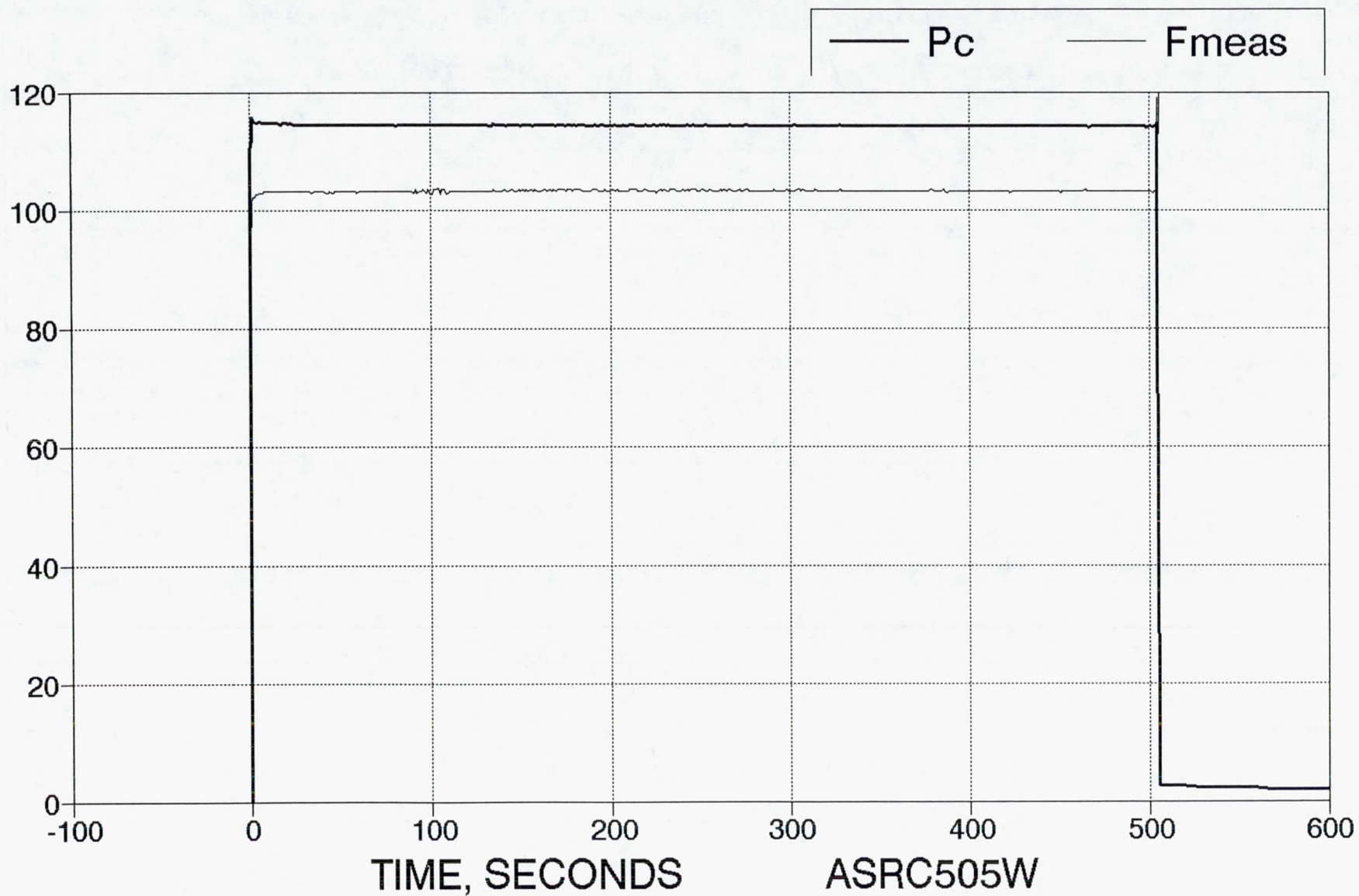


Figure 6.3-134. P_c , Vac Thrust vs Time – Test -311; 47:1 Durability

6.3, Hot Fire Testing (cont.)

Accelerometer data for Test -308, a 650-sec test, are shown in Figures 6.3-135 through -141. The first three figures are background spectral density plots taken prior to FS-1 for zero reference. The next three plots are the X-, Y-, and Z-axis spectral density plots for the time period from 5.33 to 10.66 sec. Careful comparison of the background and firing plots shows very little change. The most significant effects are an increase in power density at about 150 Hz to a peak of $1 \times 10^{-5} \text{ G}_2/\text{Hz}$ on the X-axis, in Figure 6.3-142. There are no significant changes on the Y-axis. The Z-axis (Figure 6.3-143) shows some low frequency components at 2.5 Hz ($1.5 \times 10^{-5} \text{ G}_2/\text{Hz}$), 5.0 Hz (8×10^{-5}), 18 Hz (3×10^{-5}), 22 Hz (2×10^{-5}), and 25 Hz (1×10^{-4}). For reference, the launch random vibration levels at 20 Hz are expected to be $1.3 \times 10^{-2} \text{ G}_2/\text{Hz}$, or over one hundred times higher than the levels measured during firing.

The final three plots show the X-, Y-, and Z-axis acceleration in G's for the first 46 ms of the firing, during the ignition transient. A delay of about 31 ms is evident in the traces which represents the time for the Moog torque motor valve seats to initiate lift off. For the next three ms there is evidence of accelerations due to valve operation, and propellant flow initiation. These levels fall back to close to the prefire background levels by 46 ms.

6.3.6 Endurance Testing

Objective

The objective of the endurance test program was to demonstrate long duration continuous operation of the Ir-Re 110 lbf thruster. A continuous burn of two hours was chosen as a compromise between flight system requirements for this class of thruster and the not insignificant propellant costs (approximately \$4 to \$5 per sec of firing time). The engine was successfully tested in four firings of about 1-, 100-, 7200- and 1200-sec. At the conclusion of this test series the engine has a total of 22,590 sec (6.3 hr) accumulated firing time.

Facility

The facility in which the tests were conducted can provide over four hours of testing in its present configuration, based on steam capacity for vacuum pumping; it has propellant capacity for over 20 hrs of testing. Figure 6.3-144 shows a drawing of the J-4 altitude cell and internal test cabin.

Figure 6.3-145 is an overall view of the J-4 area showing the outer test cell, exhaust system and part of the steam ejector system. Figures 6.3-146 and -147 show the internal test cabin and the thruster installation prior to testing. The layout of the inner test cabin, in

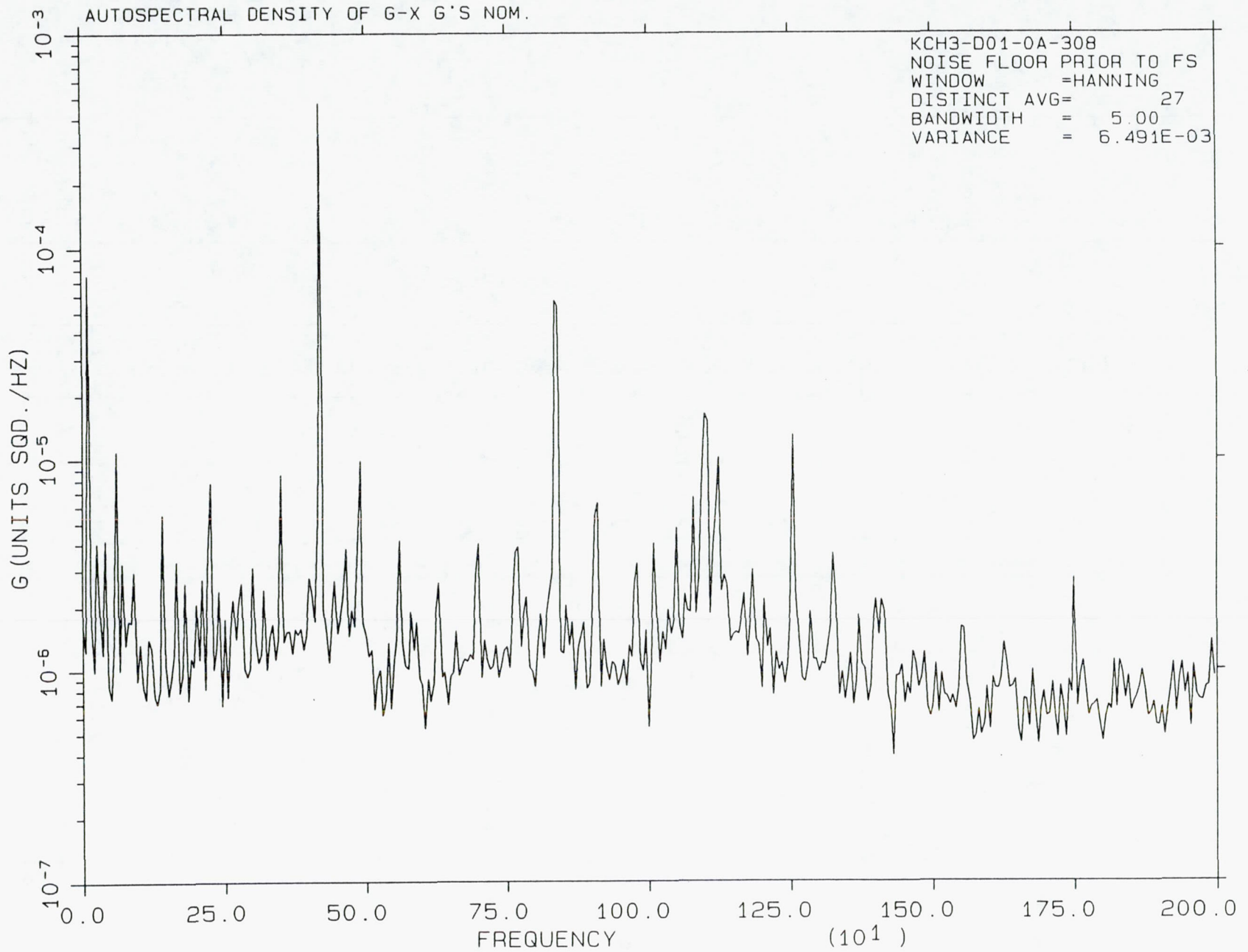


Figure 6.3-135. Accelerometer Data for Test -308 – 650-sec Test

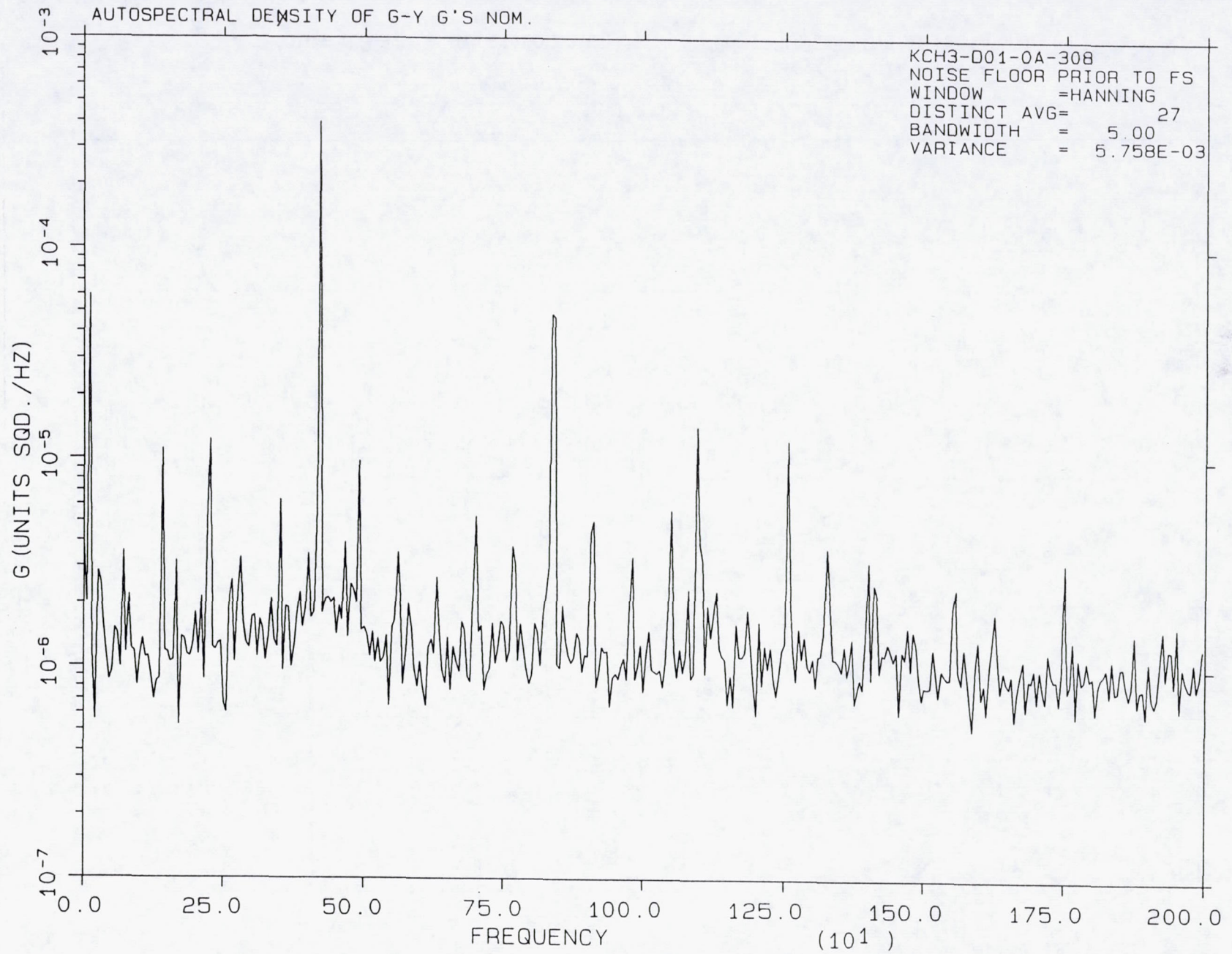


Figure 6.3-136 Accelerometer Data for Test -308 - 650-sec Test

304

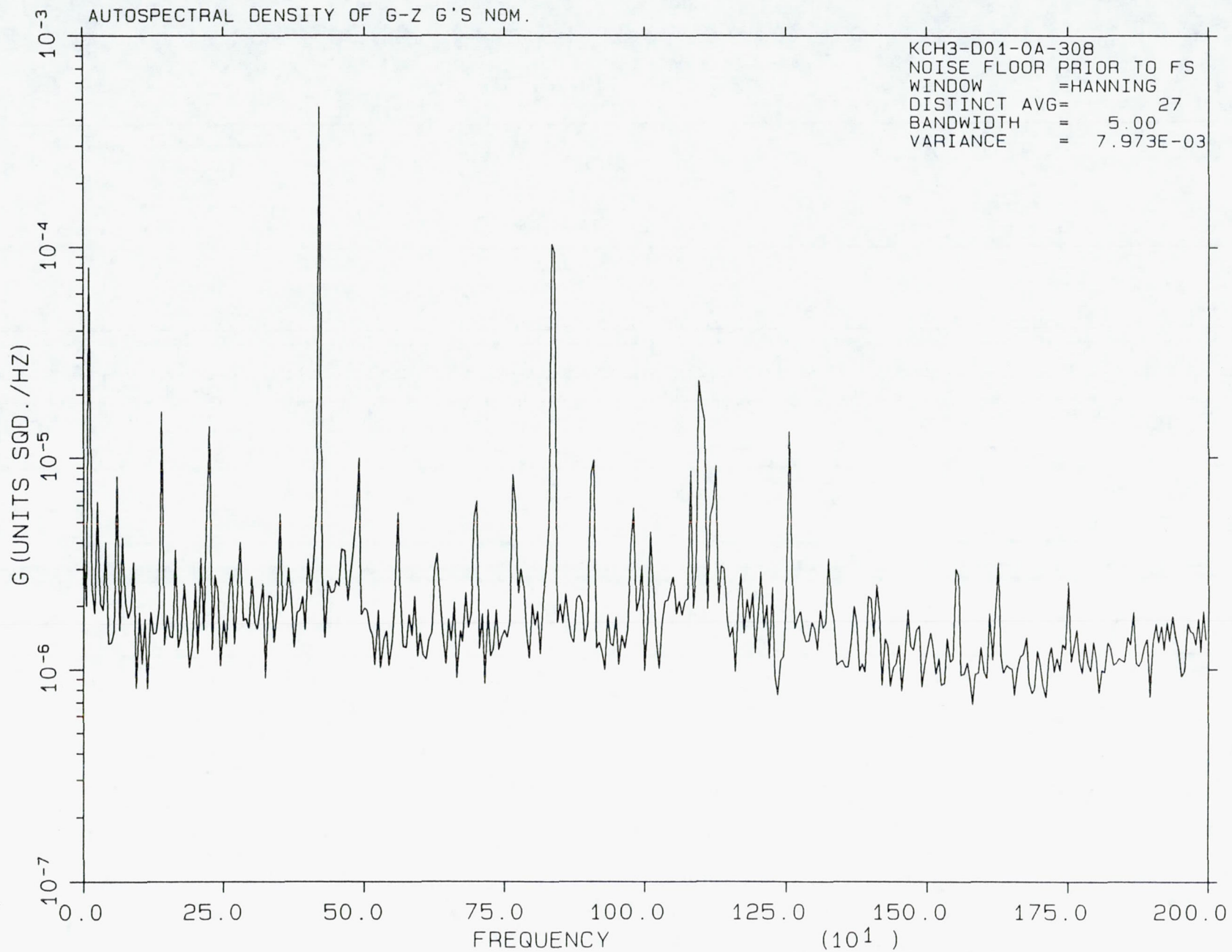


Figure 6.3-137. Accelerometer Data for Test -308 - 650-sec Test

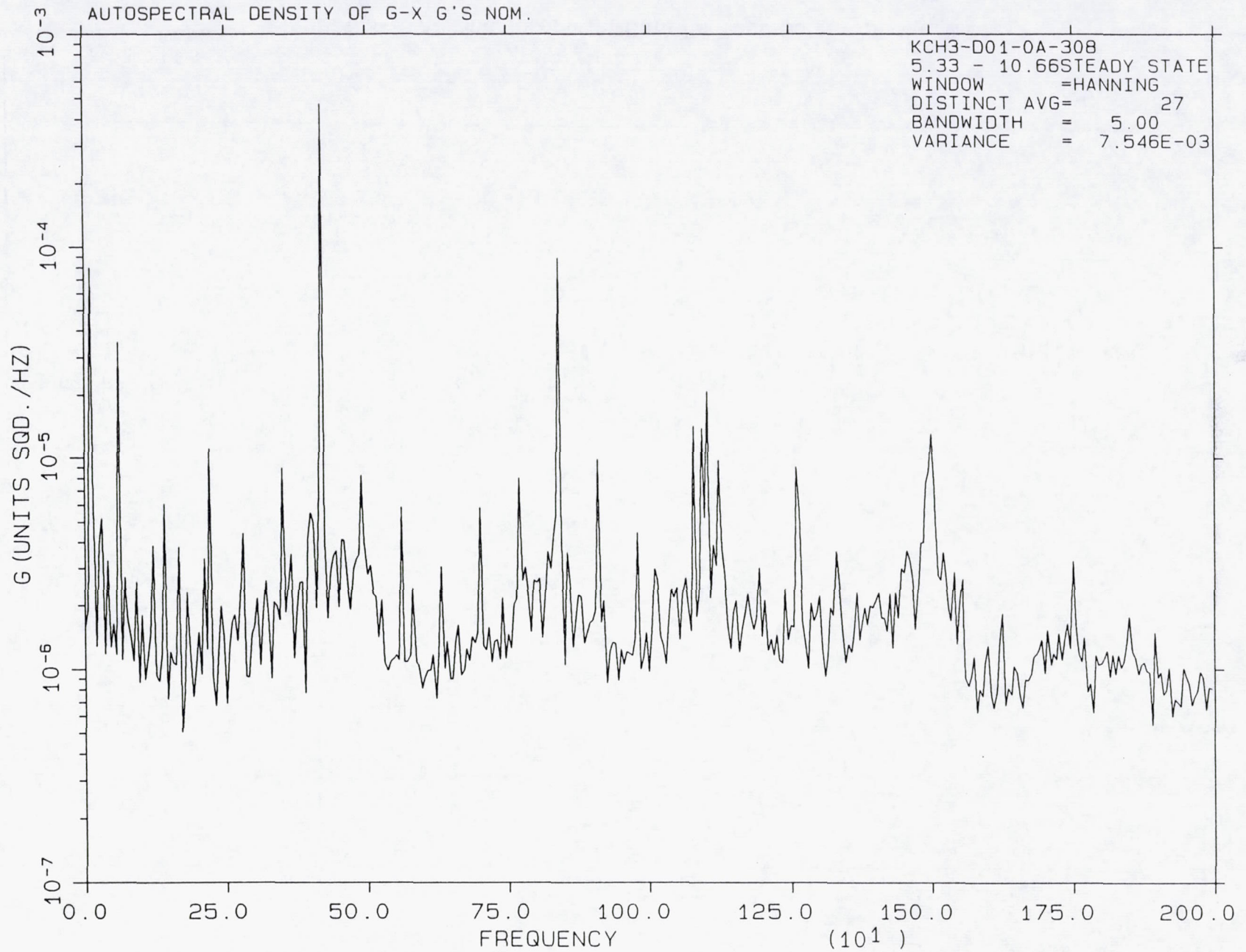


Figure 6.3-138. Accelerometer Data for Test -308 - 650-sec Test

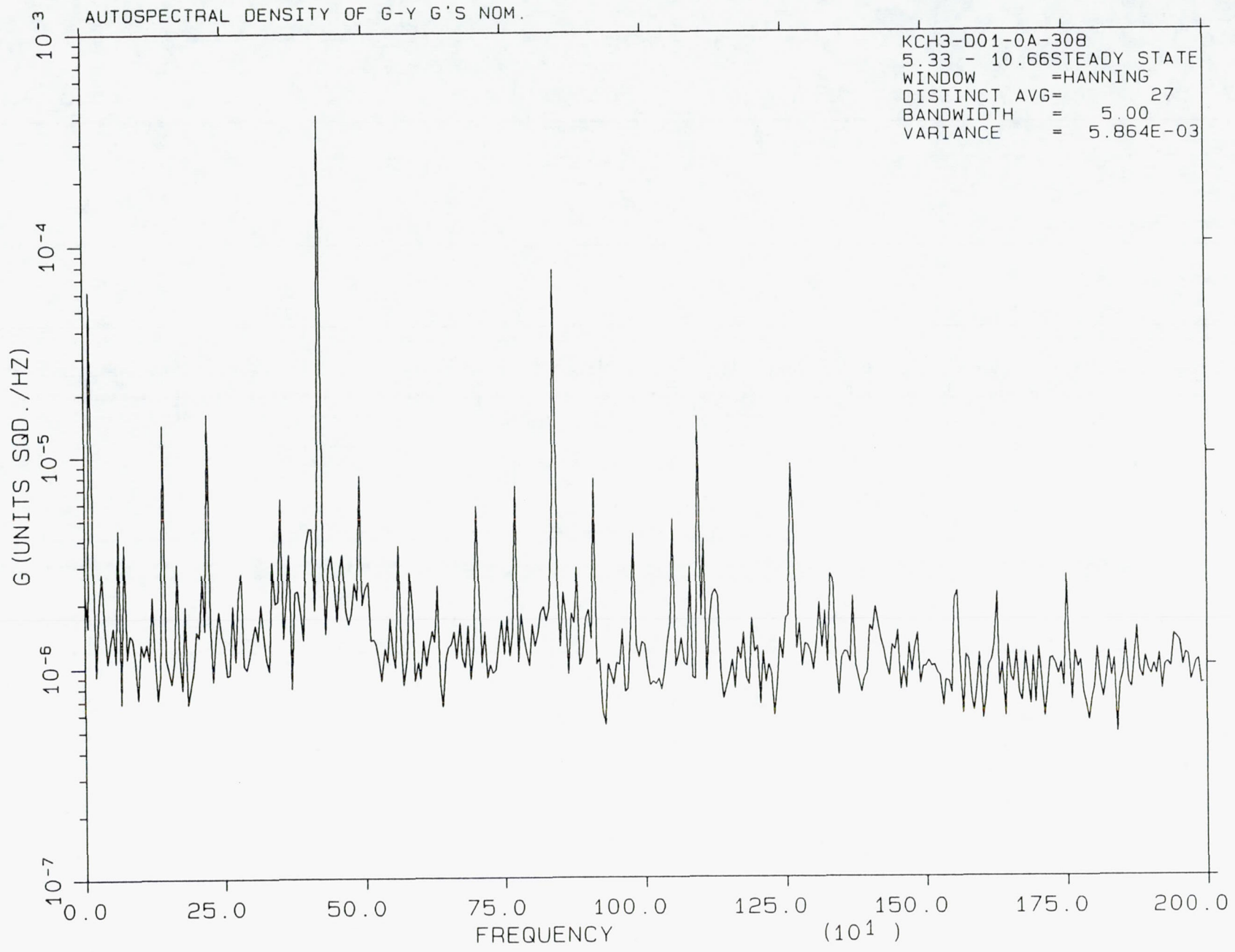


Figure 6.3-139. Accelerometer Data for Test -308 - 650-sec Test

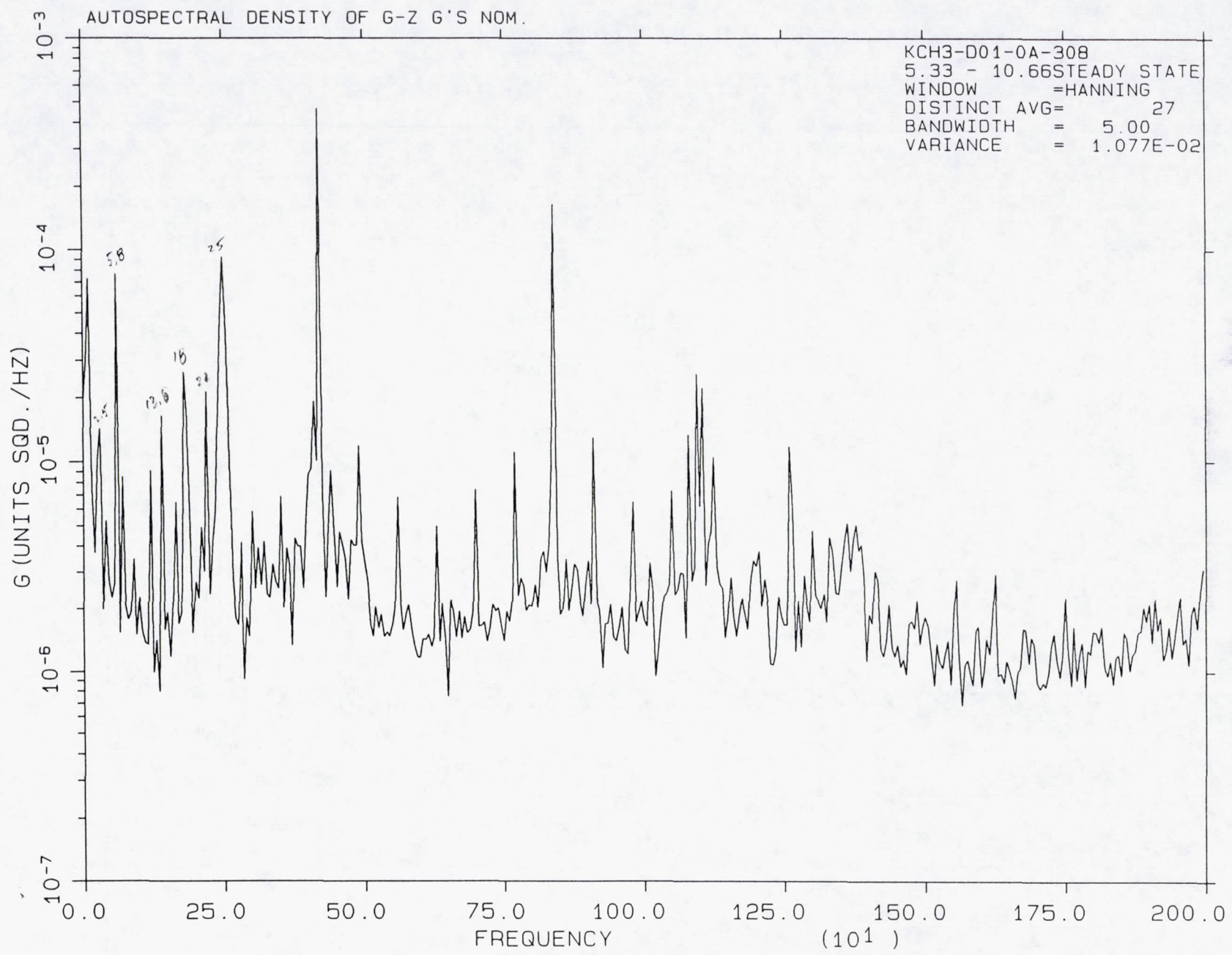


Figure 6.3-140. Accelerometer Data for Test -308 - 650-sec Test

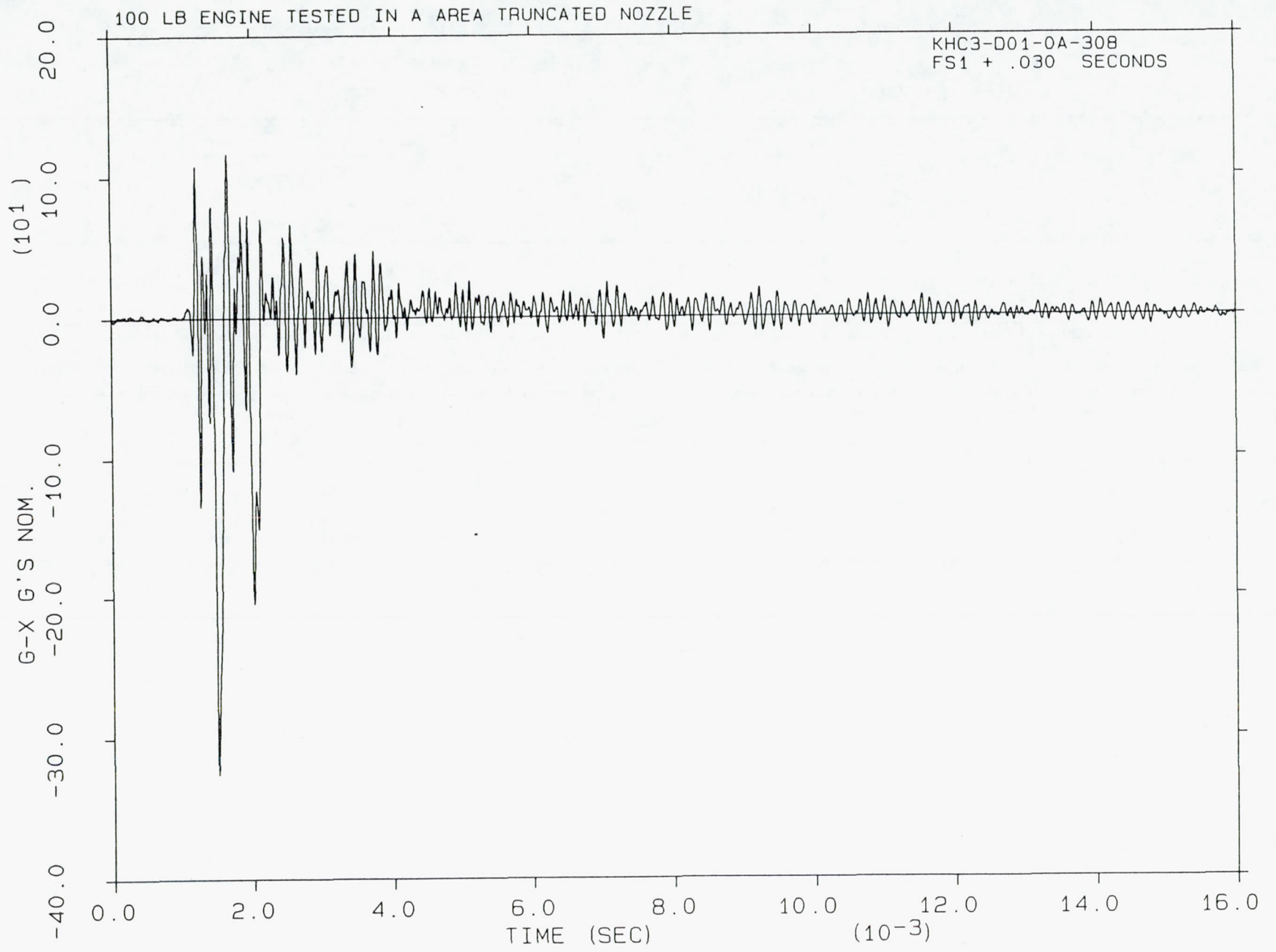


Figure 6.3-141. Accelerometer Data for Test -308 - 650-sec Test

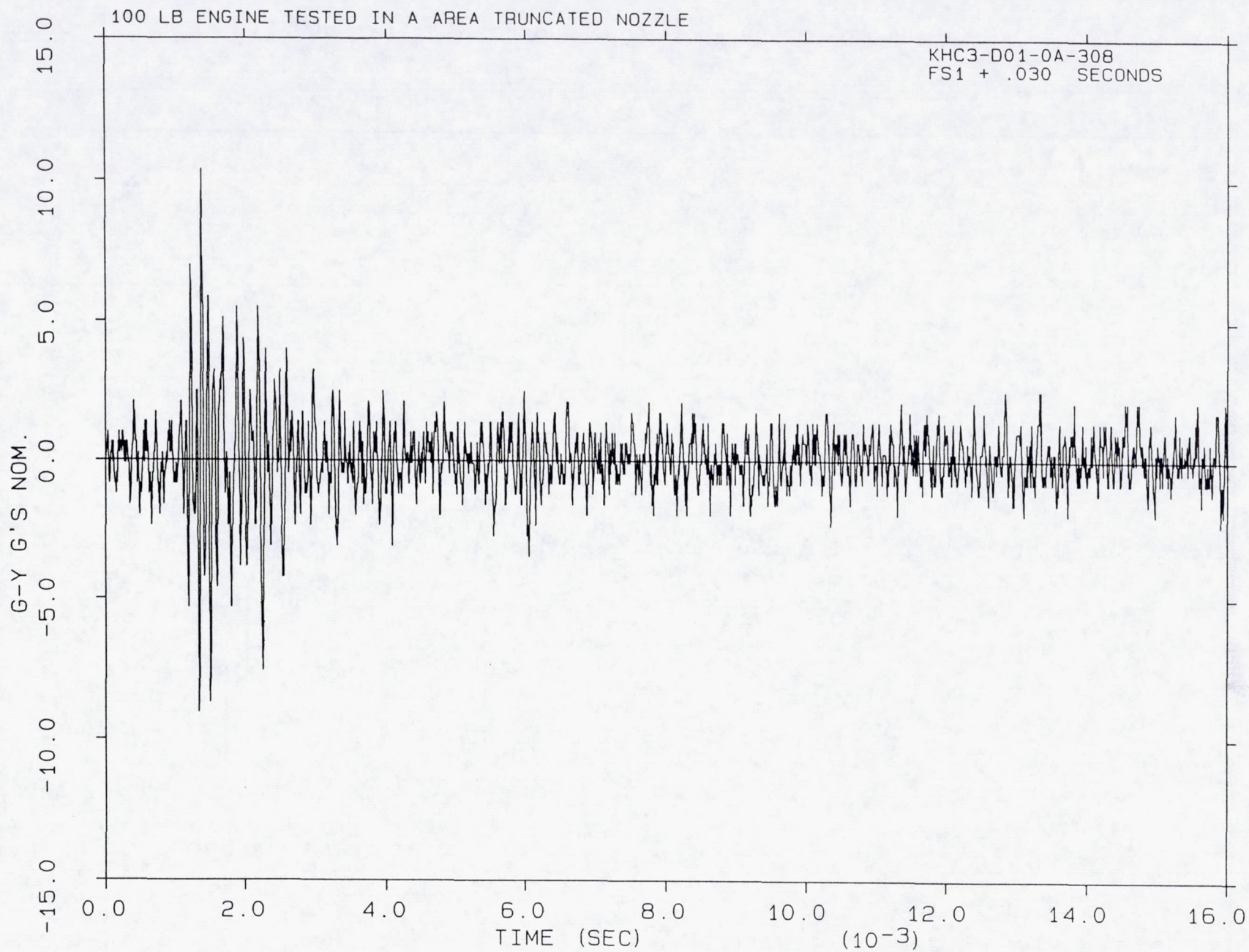


Figure 6.3-142. Accelerometer Data for Test -308 – 650-sec Test

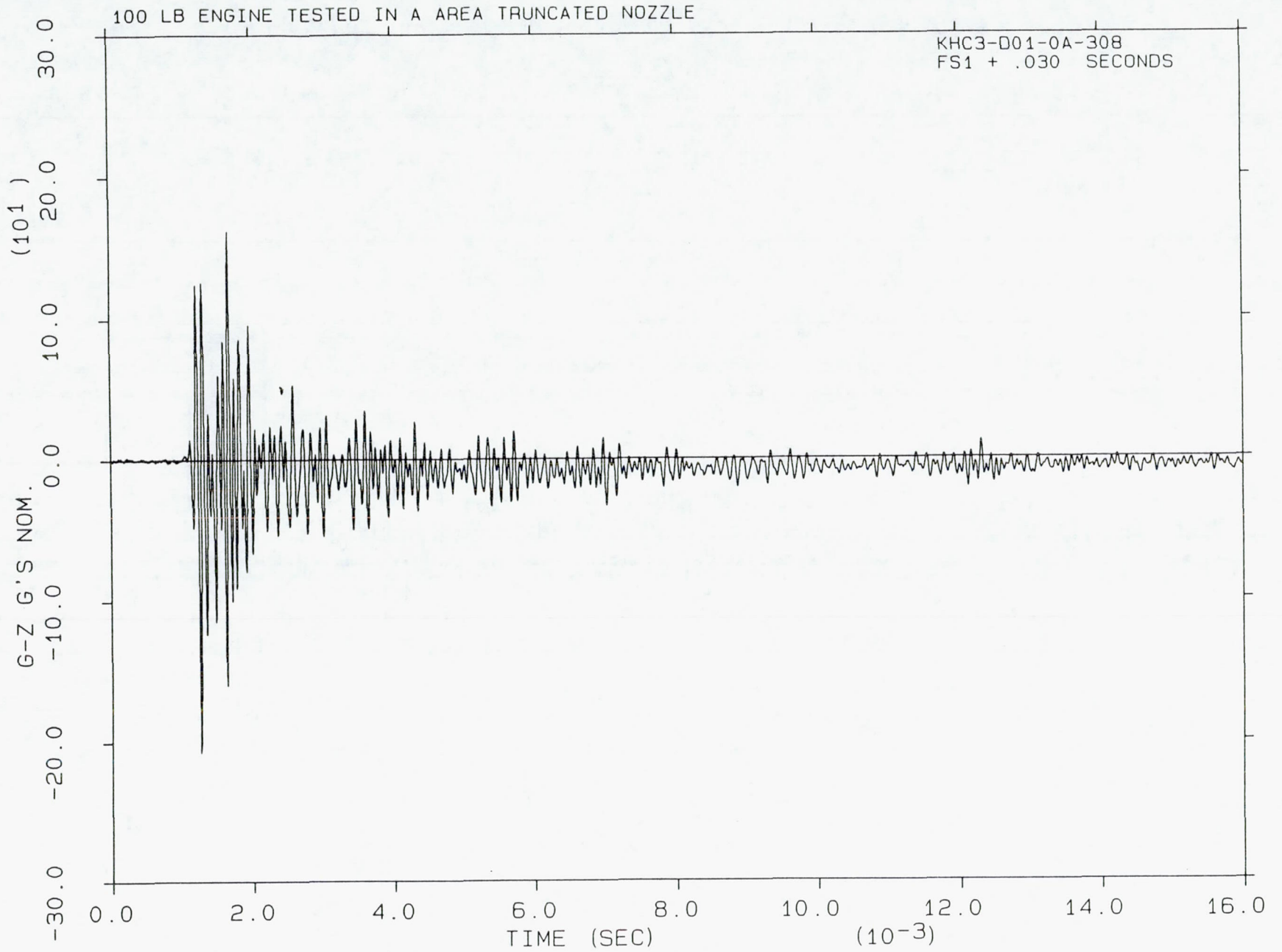


Figure 6.3-143. Accelerometer Data for Test -308 - 650-sec Test

**ENDURANCE TEST OF THE HIGH PERFORMANCE
Ir-Re ALL WELDED 490 NEWTON ENGINE
CRITICAL EXPERIMENT REVIEW NUMBER 10189**

311

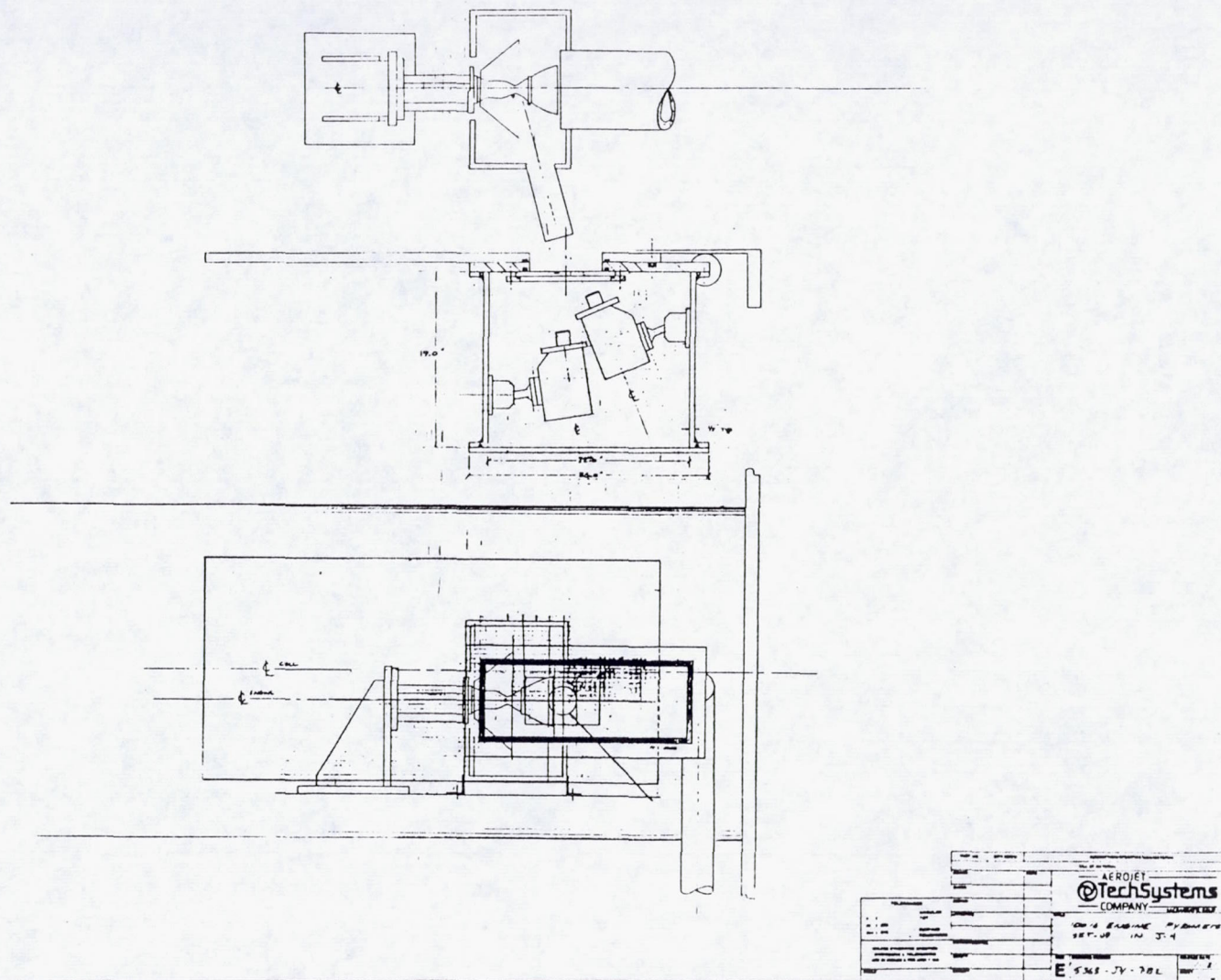
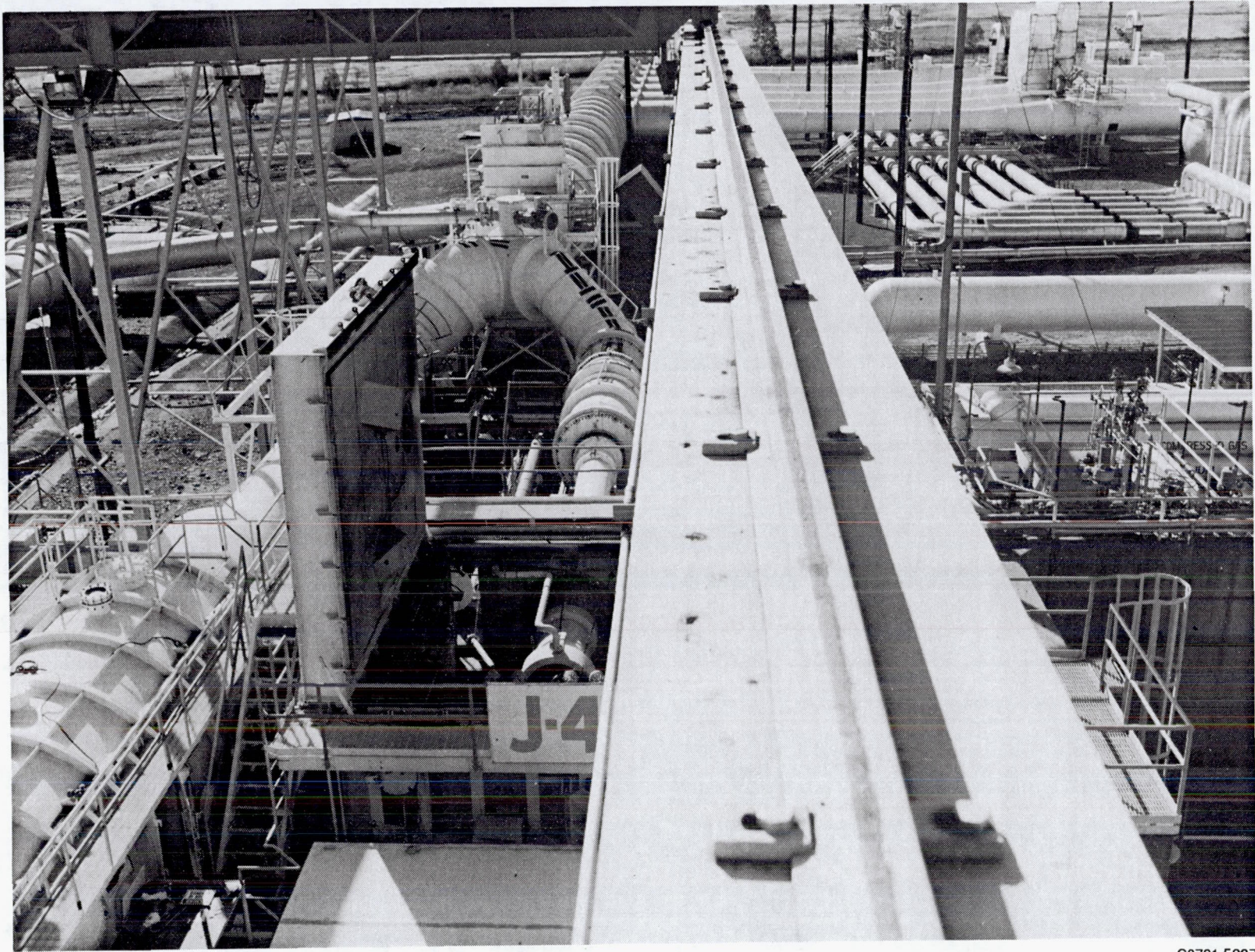
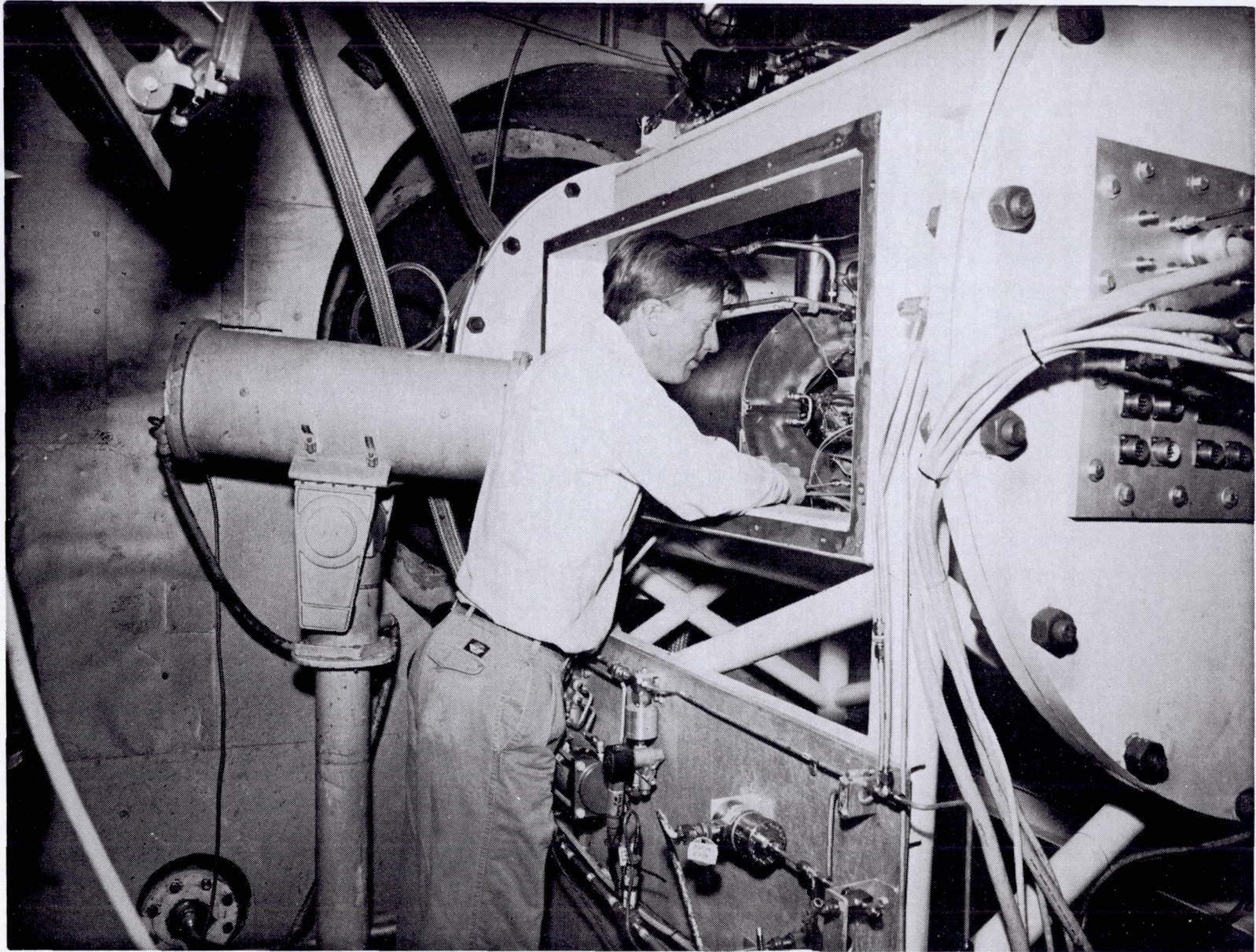


Figure 6.3-144. Cross Section of J-4 Altitude Cell and Internal Test Cabin



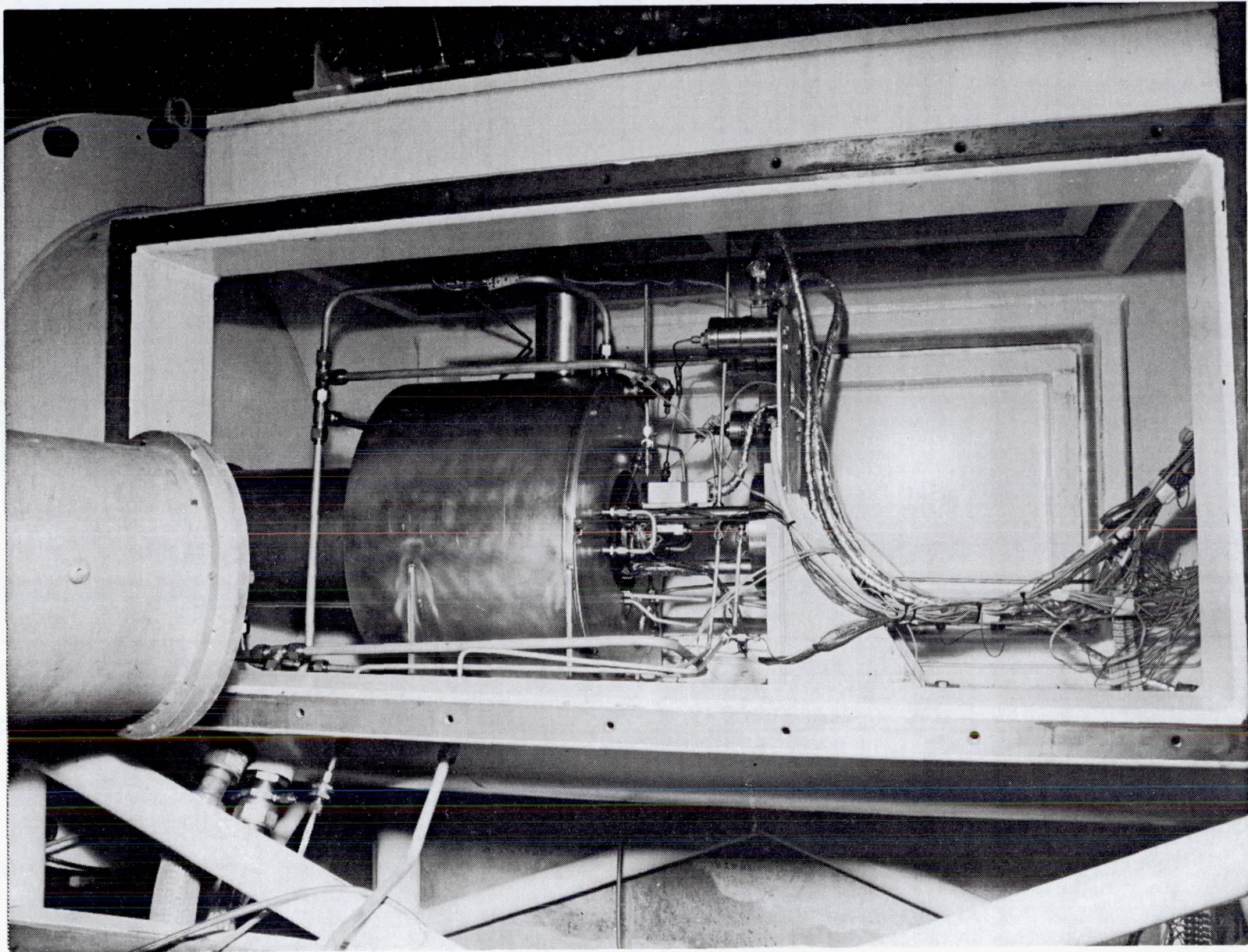
C0791 5207

Figure 6.3-145. Overall View of J-4 Outer Test Cell and Pumping System



C0293 1066

Figure 6.3-146. Test Cabin Inside J-4 Altitude Cell



C0293 1064

Figure 6.3-147. Internal Test Cabin

6.3, Hot Fire Testing (cont.)

which the engine is mounted, is shown in Figure 6.3-148 with the water cooled facility shields in place.

Facility vacuum is maintained by a steam ejector system, operated with steam from accumulators, which pumps the facility to about 0.6 psia prior to firing. The thruster exhausts into an 8 inch second throat diffuser which pumps the interior cabin down to operating pressure, about 0.12 psia at 47:1 area ratio.

Instrumentation

Thruster instrumentation locations are shown in the drawing of Figure 6.3-149, and defined in detail in Table 6.3-17. All data measurements, data measuring system, and expected steady state values are shown in Table 6.3-18. Because previous test experience has shown the Ir-Re engine is more reliable than the instrumentation, nearly all automatic kills were removed; those that were retained (Pc and cabin pressure) were set to a very wide range. Reliance was placed on human review of the on-line data and its assessment so that a test would not be terminated by an erroneous reading. This approach was considered feasible since experience has shown that the engine is robust, can withstand off-design operation, and has no failure modes that require rapid response other than diffuser unload/cabin pressure increase (facility problem, high P-ALT kill) or chamber burn through (low Pc kill). Post-test comment to facilitate data interpretation, are given in Table 6.3-19.

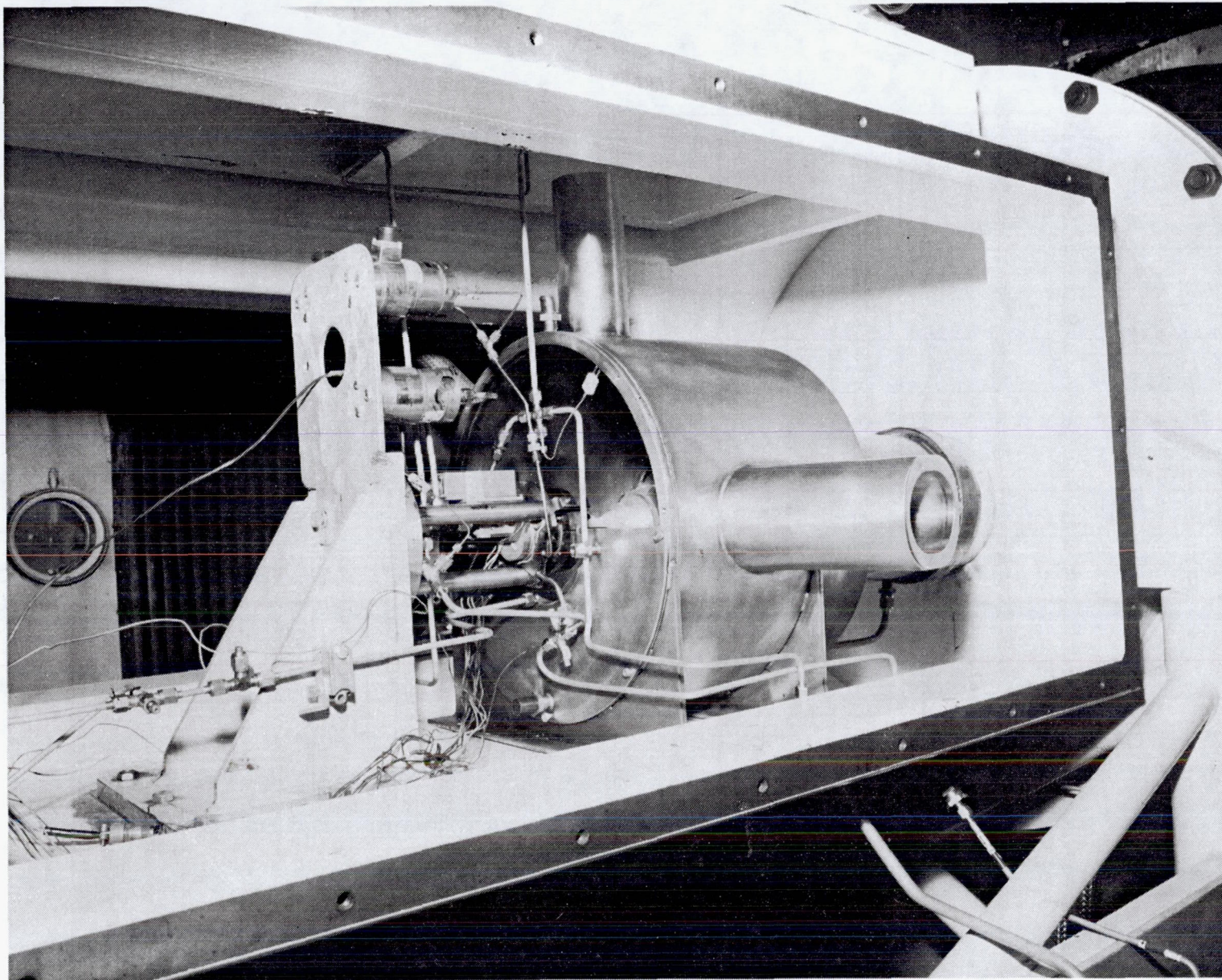
Engine Configuration

The engine configuration tested in the endurance test series was the same as that fired for the durability tests, the AJ10-221 SN 1 with the 286:1 nozzle truncated at 47:1.

The pressures used to calculate Kw through the thruster and test facility are shown in Table 6.3-20.

Table 6.3-20 Flight Thruster Component Resistance

<u>Component</u>	<u>Inlet Press.</u>	<u>Outlet Press.</u>
Facility – Tank to Flow Section	POTR PFTR	POL1 PFL1
Facility – Flow Sect. to Cell	POL1 PFL1	POTSS PFTSS
Facility – Drop-in Filters	POTSS PFTSS	POVI PFRI
Flight Inlet Conditions	POVI, PFRI	
Fuel Regen	PFRI	PFRO
Valve + Injector	POVI PFRO	PC1 PC1



C0193 0119

Figure 6.3-148. Layout of Inner Test Cabin



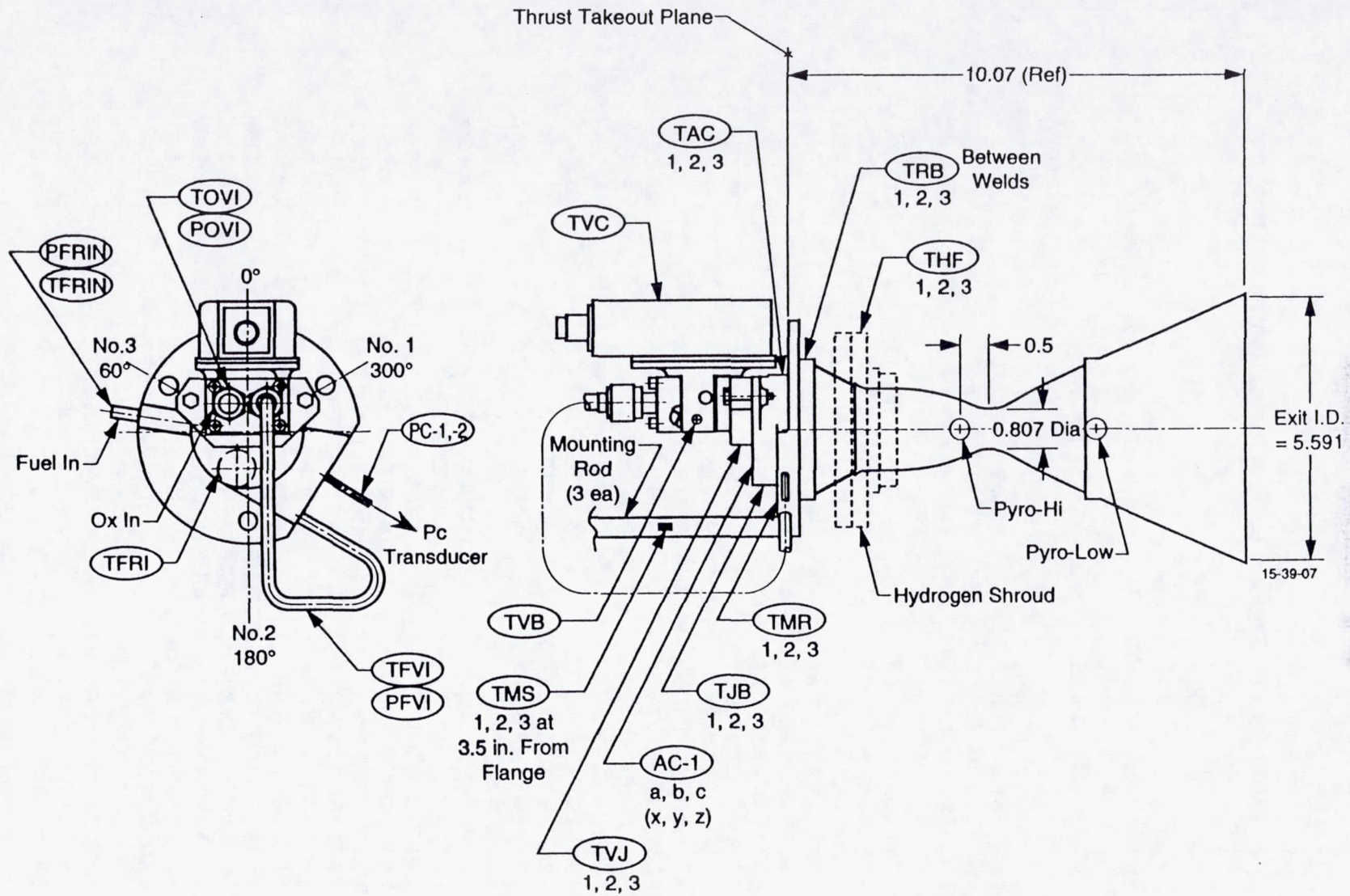


Figure 6.3-149. Endurance Test Instrumentation Locations

Table 6.3-17. Endurance Test Instrumentation Locations

ASRC563

2-8-93

[DEG LOOKING FROM NOZZLE; UP=0 DEG, BOLT#1=300, #2= 180, #3=60]

UPDATE 2-10-93

IDEN.	MEASURES	LOCATION		OTHER
		AXIAL	ROTATIONAL	
TOVI	OXID TEMP VALVE INLET	PROPELLANT LINE		VEHICLE INTERFACE
POVI	OXID PRESS VALVE INLET	PROPELLANT LINE		VEHICLE INTERFACE
TFVI	FUEL TEMP VALVE INLET	PROPELLANT LINE		
PFVI	FUEL PRESS VALVE INLET	PROPELLANT LINE		
TVB	VALVE BODY TEMP	CENTER VALVE BODY	270 DEG	
TVC	VALVE COIL [CAN] TEMP	CENTER COIL CAN	0 DEG	
TPCL	Pc LINE TEMP	INBOARD OF UNION	~ 240 DEG	
TAC-1	ACOUSTIC CAV. [EXT. WALL] TEMP.	CENTER, O.D.	300 DEG	
TAC-2	ACOUSTIC CAV. [EXT. WALL] TEMP.	CENTER, O.D.	180 DEG	
TAC-3	ACOUSTIC CAV. [EXT. WALL] TEMP.	CENTER, O.D.	60 DEG	
TRB-1	REGEN. O.D. TEMP [BETWN WELDS]	BETWEEN S.S. WELDS	300 DEG	
TRB-2	REGEN. O.D. TEMP [BETWN WELDS]	BETWEEN S.S. WELDS	180 DEG	
TRB-3	REGEN. O.D. TEMP [BETWN WELDS]	BETWEEN S.S. WELDS	60 DEG	
TFRI	REGEN INTERNAL TEMP	REGEN OUTLET MANIFOLD	~ 225 DEG	
TFRIN	REGEN INLET TEMP	PROPELLANT LINE	~ 90 DEG	VEHICLE INTERFACE
PFRIN	REGEN INLET PRESS	PROPELLANT LINE	~ 90 DEG	VEHICLE INTERFACE
TVJ-1	ADAPTER, VALVE/INJ, TEMP	ADAPTER PLATE O.D.	300 DEG	
TVJ-2	ADAPTER, VALVE/INJ, TEMP	ADAPTER PLATE O.D.	180 DEG	
TVJ-3	ADAPTER, VALVE/INJ, TEMP	ADAPTER PLATE O.D.	60 DEG	
TJB-1	INJ. BODY O.D. TEMP	MANIFOLD O.D.	300 DEG	
TJB-2	INJ. BODY O.D. TEMP	MANIFOLD O.D.	180 DEG	
TJB-3	INJ. BODY O.D. TEMP	MANIFOLD O.D.	60 DEG	
TMR-1	MTG FLNG TEMP	NEAR BOLT HOLE #1	300 DEG	
TMR-2	MTG FLNG TEMP	NEAR BOLT HOLE #2	180 DEG	
TMR-3	MTG FLNG TEMP	NEAR BOLT HOLE #3	60 DEG	
TMS-1	STEEL MTG ROD TEMP	3.5 IN FROM FLNG, #1	300 DEG	
TMS-2	STEEL MTG ROD TEMP	3.5 IN FROM FLNG, #2	180 DEG	
TMS-3	STEEL MTG ROD TEMP	3.5 IN FROM FLNG, #3	60 DEG	
THF-1	HYDROGEN SHROUD FLANGE TEMP	AFT HALF OF FLANGE	300 DEG	
THF-2	HYDROGEN SHROUD FLANGE TEMP	AFT HALF OF FLANGE	180 DEG	
THF-3	HYDROGEN SHROUD FLANGE TEMP	AFT HALF OF FLANGE	60 DEG	
TFC	H2 SHROUD RHENIUM FOIL TEMP	ON 3 MIL FOIL	~ 60 DEG	
PYRO-HI	CHAMBER WALL TEMP	~ 1/2 IN AHEAD OF THROAT	270 DEG	
PYRO-LO	RHENIUM/C-103 WELD TEMP	ON WELD	270 DEG	
AC-1a	ENGINE ACCEL-X-AXIS	BACK OF INJECTOR	~ 200 DEG	
AC-1b	ENGINE ACCEL-Y-AXIS	BACK OF INJECTOR	~ 200 DEG	
AC-1c	ENGINE ACCEL-Z-AXIS	BACK OF INJECTOR	~ 200 DEG	

Table 6.3-18. Endurance Test Data Display Locations (Sheet 1 of 4)

ASRC564

2-9-93

UPDATE 2-10-93

IDEN. MEASURES

EXPEC
VALUE

HALL DIG. FM OSC-
TV MONITOR PRINT DATA TAPE GRPH
DISPLAY
1 2 3 4 5 6 7 8

TEST DATA

IDEN.	MEASURES	EXPEC VALUE	1	2	3	4	5	6	7	8	HALL	DIG.	FM	OSC-	
FS/TC	FIRE SWITCH/TIME CODE													X	X
LIMIT CHECK-1	[scroll out of limits parameters]		1												
LIMIT CHECK-2	[scroll out of limit value]		1												
AC-1a	ENGINE ACCEL--X-AXIS													X	X
AC-1b	ENGINE ACCEL--Y-AXIS													X	X
AC-1c	ENGINE ACCEL--Z-AXIS													X	X
ETCV	VALVE VOLTAGE	9.7												X	X
ITCV	VALVE CURRENT	0.26					5							X	
FMF-1	FUEL FLOW METER #1[WATER]	0.148	2							X	X			X	X
FMF-2	FUEL FLOW METER #2[WATER]	0.148	2							X	X			X	X
FMO-1	OXID FLOW METER #1[WATER]	0.148	1							X	X			X	X
FMO-2	OXID FLOW METER #2[WATER]	0.148	1							X	X			X	X
PALT-1A	CABIN PRESSURE #1	0.14							8	X	X			X	
PALT-1D	CABIN PRESSURE #2	0.14							8	X	X				
PALT-1E	CABIN PRESSURE #3	0.14							8	X	X				
PC-1	CHAMBER PRESS (WALL STATIC)	114.5				4				X	X			X	X
PC-2	Pc [REDUNDANT XDUCER ONLY]	114.5				4				X	X			X	X
PFRI	REGEN INLET PRESS	237	2							X	X			X	X
PFVI	FUEL PRESS VALVE INLET	212	2							X	X			X	X
PH2DN	H2 ORIF DOWN PRESS	12				4				X	X				
PH2UP	H2 ORIFICE UP PRESS	50				4				X	X				
POVI	OXID PRESS VALVE INLET	221	1							X	X			X	X
PYRO-HI	CHAMBER WALL TEMP	3490				3				X	X			X	X
PYRO-LO	RHENIUM/C-103 WELD TEMP	2100				3				X	X			X	X
TAC-1	ACOUSTIC CAV.[EXT. WALL]TEMP.					3				X	X				
TAC-2	ACOUSTIC CAV.[EXT. WALL]TEMP.					3				X	X				
TAC-3	ACOUSTIC CAV.[EXT. WALL]TEMP	560				3				X	X				
TCELL	CELL TEMP	115						6		X	X				
TFC	H2 SHROUD RHENIUM FOIL TEM	2200												X	
TFRI	REGEN INTERNAL TEMP	215	2							X	X				
TFRIN	REGEN INLET TEMP	55	2							X	X				
TFVI	FUEL TEMP VALVE INLET	215	2							X	X				

Table 6.3-18. Endurance Test Data Display Locations (Sheet 2 of 4)

UPDATE 2-10-93		TV MONITOR								HALL	DIG.	FM	OSC-	
		EXPECTD	DISPLAY								PRINT	DATA	TAPE	GRPH
		VALUE	1	2	3	4	5	6	7	8				
THS-1	LORAL SHIELD TEMP[INNER]					4					X	X		
THS-2	LORAL SHIELD TEMP[INNER]					4					X	X		
THS-3	LORAL SHIELD TEMP[INNER]					4					X	X		
THS-4	LORAL SHIELD TEMP[INNER]					4					X	X		
THS-5	LORAL SHIELD TEMP										X	X		
THS-6	LORAL SHIELD TEMP										X	X		
THS-7	LORAL SHIELD TEMP										X	X		
THS-8	LORAL SHIELD TEMP										X	X		
THS-9	LORAL SHIELD TEMP										X	X		
THS-10	LORAL SHIELD TEMP										X	X		
THS-11	LORAL SHIELD TEMP										X	X		
THS-12	LORAL SHIELD TEMP										X	X		
THF-1	HYDROGEN SHROUD FLANGE TE	1015						6			X	X		
THF-2	HYDROGEN SHROUD FLANGE TE	1340						6			X	X		
THF-3	HYDROGEN SHROUD FLANGE TE	1420						6			X	X		
TJB-1	INJ. BODY O.D. TEMP	305									X	X		
TJB-2	INJ. BODY O.D. TEMP										X	X		
TJB-3	INJ. BODY O.D. TEMP	365									X	X		
TMR-1	MTG FLNG TEMP	235										X		
TMR-2	MTG FLNG TEMP	115										X		
TMR-3	MTG FLNG TEMP	175										X		
TMS-1	STEEL MTG ROD TEMP	115										X		
TMS-2	STEEL MTG ROD TEMP	125										X		
TMS-3	STEEL MTG ROD TEMP											X		
TOVI	OXID TEMP VALVE INLET	55	1								X	X		
TPCL	Pc TAP LINE TEMP	750						5				X		
TRB-1	REGEN. O.D.TEMP [BETWN WELD	390			3						X	X		
TRB-2	REGEN. O.D.TEMP [BETWN WELD	200			3						X	X		
TRB-3	REGEN. O.D.TEMP [BETWN WELDS]				3						X	X		
TVB	VALVE BODY TEMP	210			3						X	X		
TVC	VALVE COIL[CAN]TEMP				3						X	X		
TVJ-1	ADAPTER, VALVE/INJ, TEMP	215										X	X	
TVJ-2	ADAPTER, VALVE/INJ, TEMP	150										X	X	
TVJ-3	ADAPTER, VALVE/INJ, TEMP											X	X	

Table 6.3-18. Endurance Test Data Display Locations (Sheet 3 of 4)

UPDATE 2-10-93

CALCULATED VALUES

[#]

HALL DIG. FM OSC-
TV MONITOR PRINT DATA TAPE GRPH
DISPLAY
1 2 3 4 5 6 7 8

#C*	CHAR. EXH. VEL [CALC]	5450	4						X
#KFRI	FUEL REGEN Kw [CALC]	0.0282		6					X
#KFVI	FUEL INJ+VALVE Kw [CALC]	0.0145		6					X
#KOVI	OXID Kw [CALC]	0.0166		6					X
#MR	MIXTURE RATIO [CALC]	1.65	4						X
#Wf-1	FUEL FLOW #1[PROP]	0.13							X
#Wf-2	FUEL FLOW #2[PROP]	0.13							X
#Wo-1	OXID FLOW #1[PROP]	0.214							X
#Wf-2	OXID FLOW #2[PROP]	0.214							X
##%D FMO	OXID FLOWMETER ERROR								X
##%D FMF	FUEL FLOWMETER ERROR								X
#DT REG	REGEN DELTA T	160							X

FACILITY PARAMETERS

[@]

@DPFF	FUEL FILTER PRESS DROP								X
@DPOF	OX FILTER PRESS DROP								X
@LFCV-6				7					X
@LSV									X
@PALT-1B	J-4 CELL PRESSURE	1.00			8				X
@PALT-6U					8				X
@PALT-J3					8				X
@PFFCT	FUEL CATCH TANK PRESS								-
@PFFM	FUEL FLOW METER PRESS		2				X		X
@PFGN2	GN2 PRESS (FUEL)			5					X
@PFRT	FUEL RUN TANK PRESS		2				X		X
@PFT	FUEL TANK PRESS		2						X
@PH2T	HYDROGEN TANK PRESS								X
@POCT	OXID CATCH TANK PRESS								-

Table 6.3-18. Endurance Test Data Display Locations (Sheet 4 of 4)

		TV MONITOR DISPLAY								HALL PRINT	DIG. DATA	FM TAPE	OSC-GRPH
		1	2	3	4	5	6	7	8				
UPDATE 2-10-93													
@POFM	OXID FLOW METER PRESS	1								X		X	
@POGN2	GN2 PRESS (OXID)					5						NL	
@PORT	OXID RUN TANK PRESS	1								X		X	
@POT	OXID TANK PRESS	1										X	
@PSA						5						X	
@PSL	STEAM EJECT INLET PRESS											X	
@PSTG1-J3												X	
@PW6DSPD								7				X	
@PWDCO-U								7				X	
@PWCM												X	
@PWDCO-D												X	
@PWOD-1								7				X	
@PWOD-2								7				X	
@PWOD-3								7				X	
@PWOD-4								7				NL	
@PWS								7				X	
@T18-1									8			X	
@T18-2									8			X	
@T18-3									8			X	
@TOFM	OXID FLOWMETER TEMP											X	
@TFFM	FUEL FLOWMETER TEMP											X	
@TRAD-1	FAC. SHLD CYL WATER TEMP OUT					5				X		X	
@TRAD-2	FAC. SHLD FRNT WATER TEMP OUT					5						NL	
@TW6D-1								7				X	
@TW6D-2								7				X	
@TW6D-3									8			X	
@TWOD-1						5						X	
@TWOD-2						5						X	
@TWOD-3						5						X	
@TWOD-4												X	

Table 6.3-19. Comments on Endurance Test Data Listings

A. PERFORMANCE SUMMARIES [J0014]

1. THESE ARE AVERAGES FOR THE TIME PERIOD INDICATED
2. #40, TPYRO-HI, READS ABOUT 350°F HIGH BECAUSE OF THE COMBINED EFFECT OF THE CELL WINDOWS AND FIRST SURFACE MIRROR.
3. TPYRO-LOW IS NOT READING [LOWER LIMIT ON TPYRO-LOW IS 1427°F; 2560°F ON TPYRO-HIGH].
4. TFRIN AND TFVI ARE INTERCHANGED; FOR TEST -103 USE TFFM INSTEAD OF TFRIN.
5. C* CALCULATION USES COLD THROAT AREA
6. TRUE ETVC IS INDICATED ETVC*1.114

B. ENGINEERING DATA LISTINGS [J0003]

1. THESE ARE READINGS AT THE TIME INDICATED
2. SAME COMMENTS AS 2 THROUGH 6 ABOVE

ASRC571

2-18-93

6.3, Hot Fire Testing (cont.)

Detailed measurements of the Re Chamber post-durability test (-347) and pre-endurance test were made to document the existing external contour of the chamber using Aerojet's CORDAX inspection machine. The measurement system is shown in Figure 6.3-150. It consists of the thruster mounting table, the x-, y-, z-traversing head, controls, and operator display/computer station. Figure 6.3-151 is a closeup showing the traversing probe and engine during measurement.

The external chamber contour was measured at four circumferential stations and then compared to the design (print) dimensions. Wall thickness is calculated from the CORDAX measurement and the design internal dimensions whose initial values are dependent on the molybdenum mandrel used for the CVD process. The CORDAX measurements at 0 and 180 degree, are shown in Figure 6.3-152.

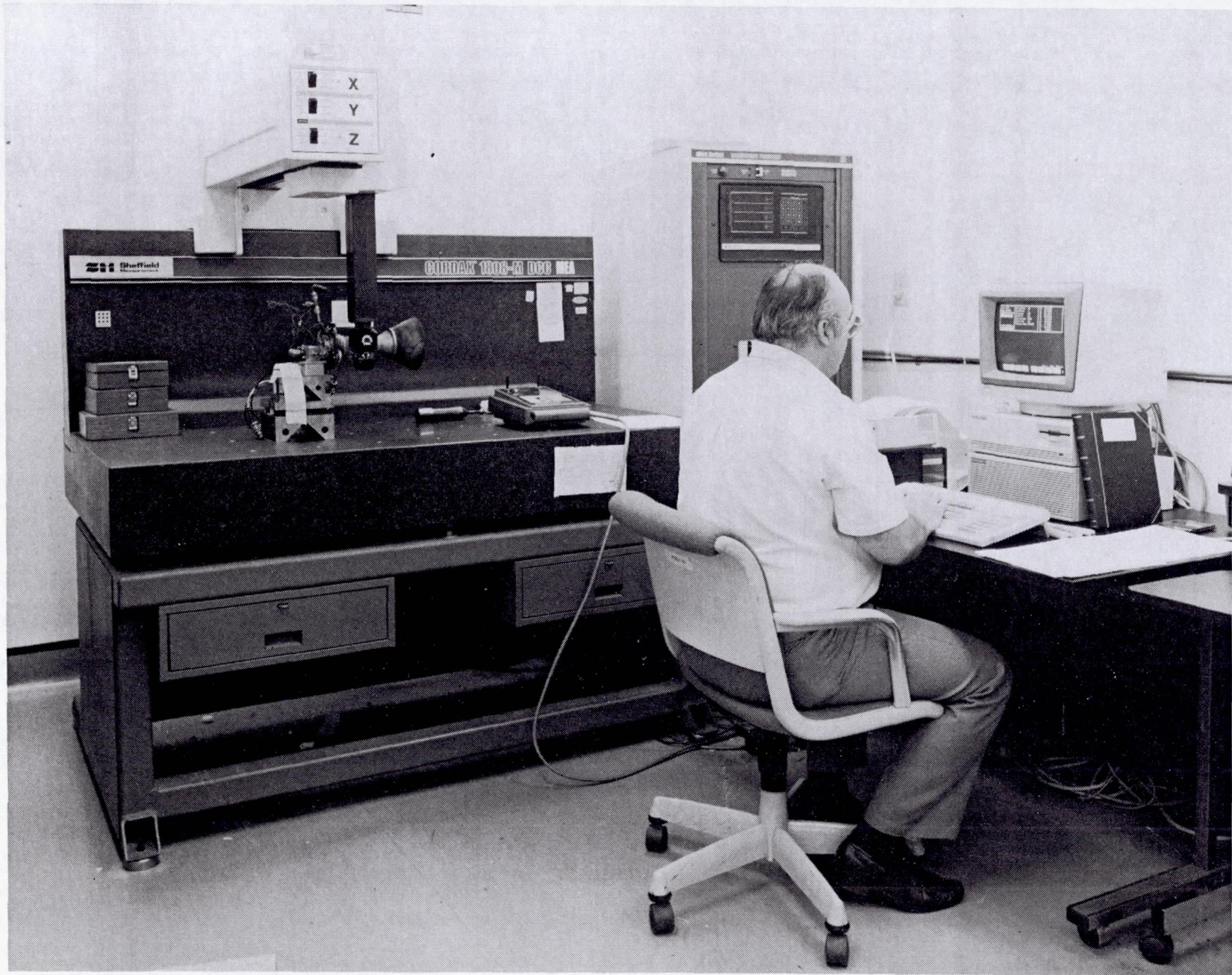
Prior to endurance testing the fuzz leak noted at the nozzle skirt joint was quantified by measuring with helium at 5 psig. The leakage rate was 6.5×10^{-3} scc/sec He.

Testing and Results

The results of the endurance testing, Series J, are summarized in Table 6.3-21. The series consisted of four tests, designated KGH3-DO1-OA-100 through -103 (-348 through -351 in the overall numbering system), of nominal 1-, 100-, 7200-, and 1200-sec duration, respectively. The first test, -100, was planned for 10-sec duration but was shutdown automatically at 1 sec when the control system first checked cabin pressure and found it to exceed the upper limit of 0.4 psia. This was caused by slower than anticipated pump down of the cabin.

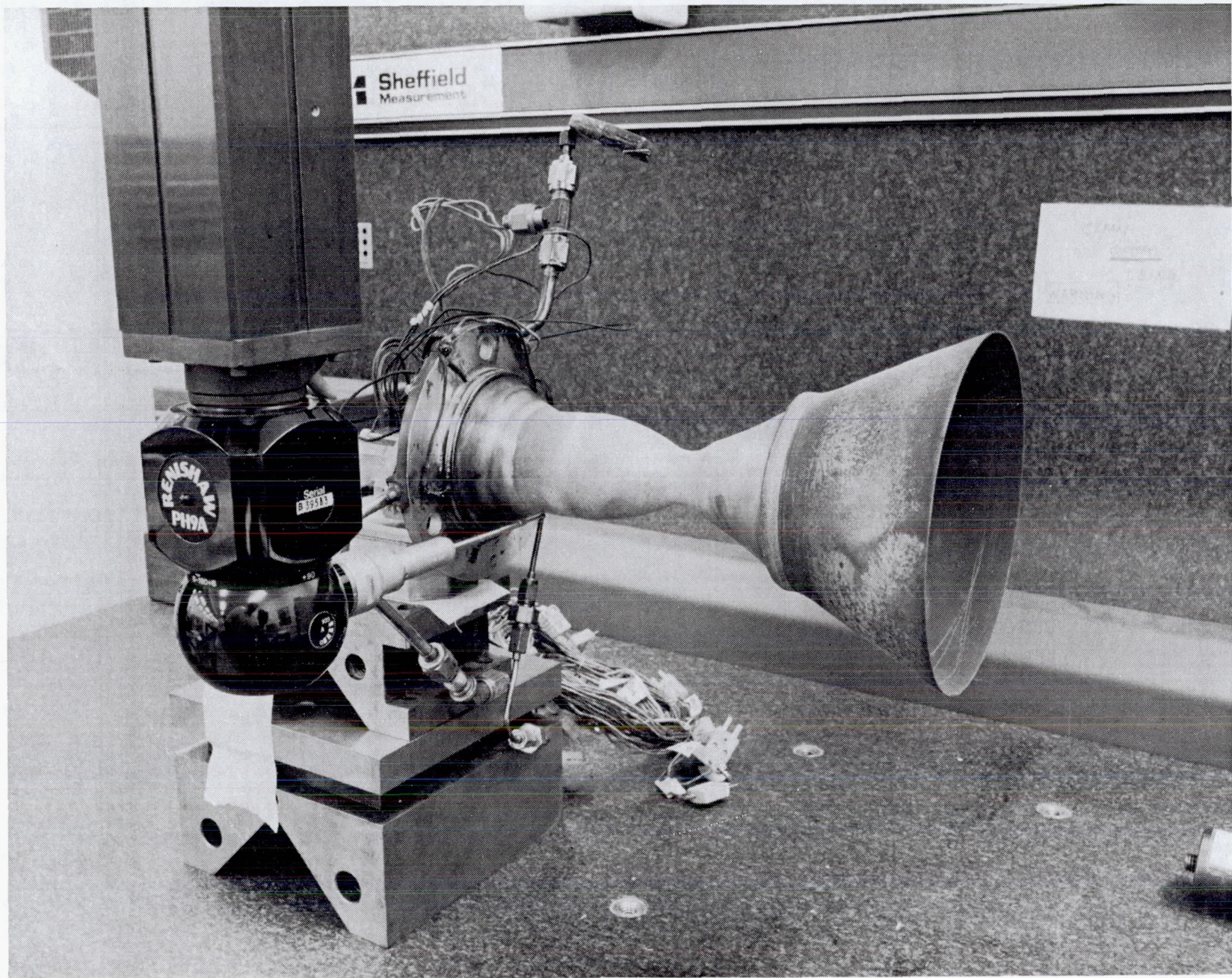
Plots of system pressures and flow rates are shown in Figure 6.3-153 for test -100. The rapid response of the engine, lack of Pc overshoot, and rapid stabilization of Pc are evident.

Since the system balance in the 1-sec test was within acceptable range for accurate correction, the 100-sec test was conducted next, with the check time on cell pressure increased to FS-1 + 10 sec and oxidizer tank pressure reduced to give the desired MR.



C1192 7147

Figure 6.3-150. CORDAX Measurement System



C1192 7149

Figure 6.3-151. AJ10-221 Engine Being Measured With CORDAX System

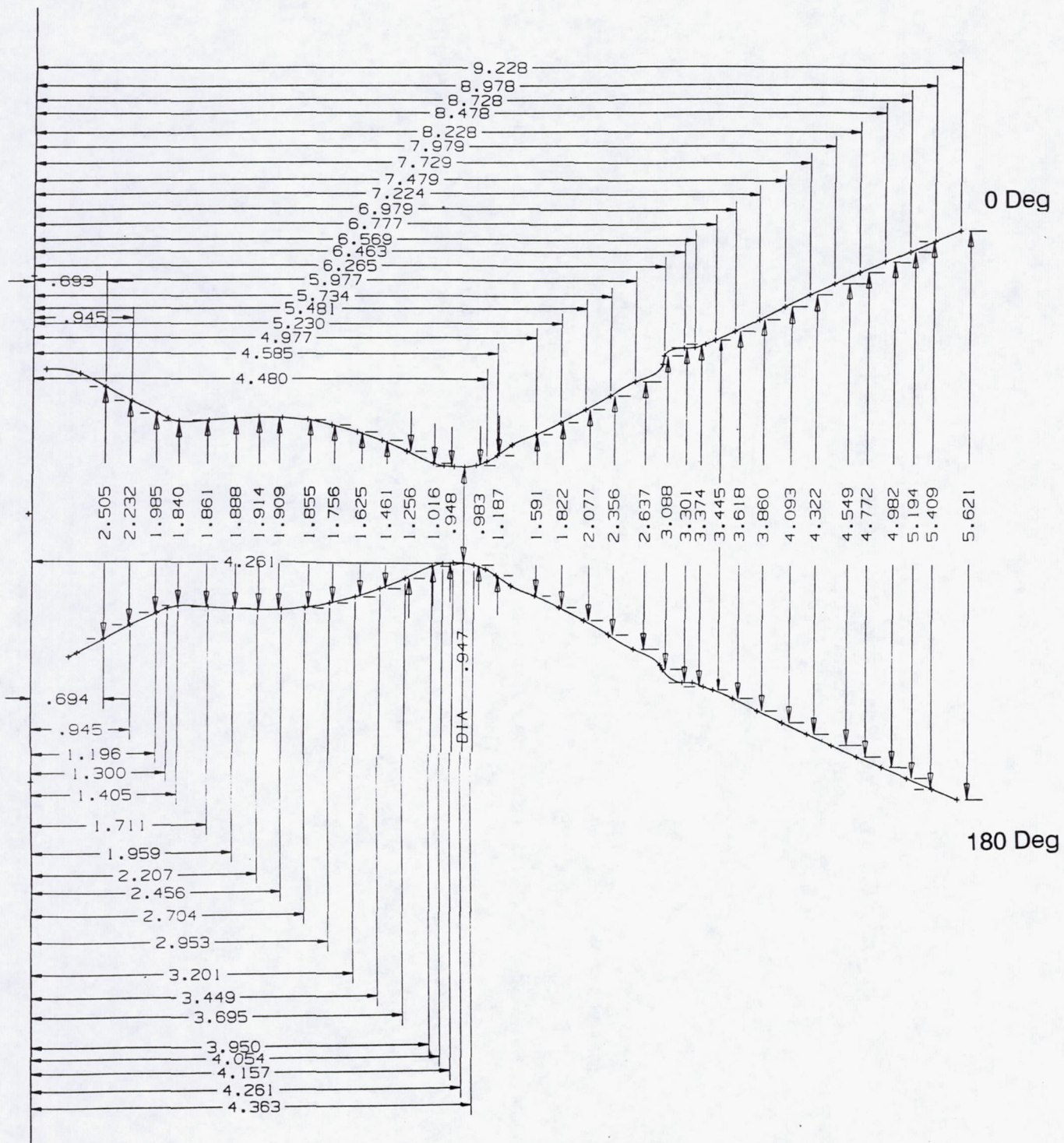


Figure 6.3-152. AJ10-221 CORDAX Measurements at 0 and 180 Degrees

Table 6.3-21. Test Results for 100 lbf Endurance Test Advanced Small Rocket Program

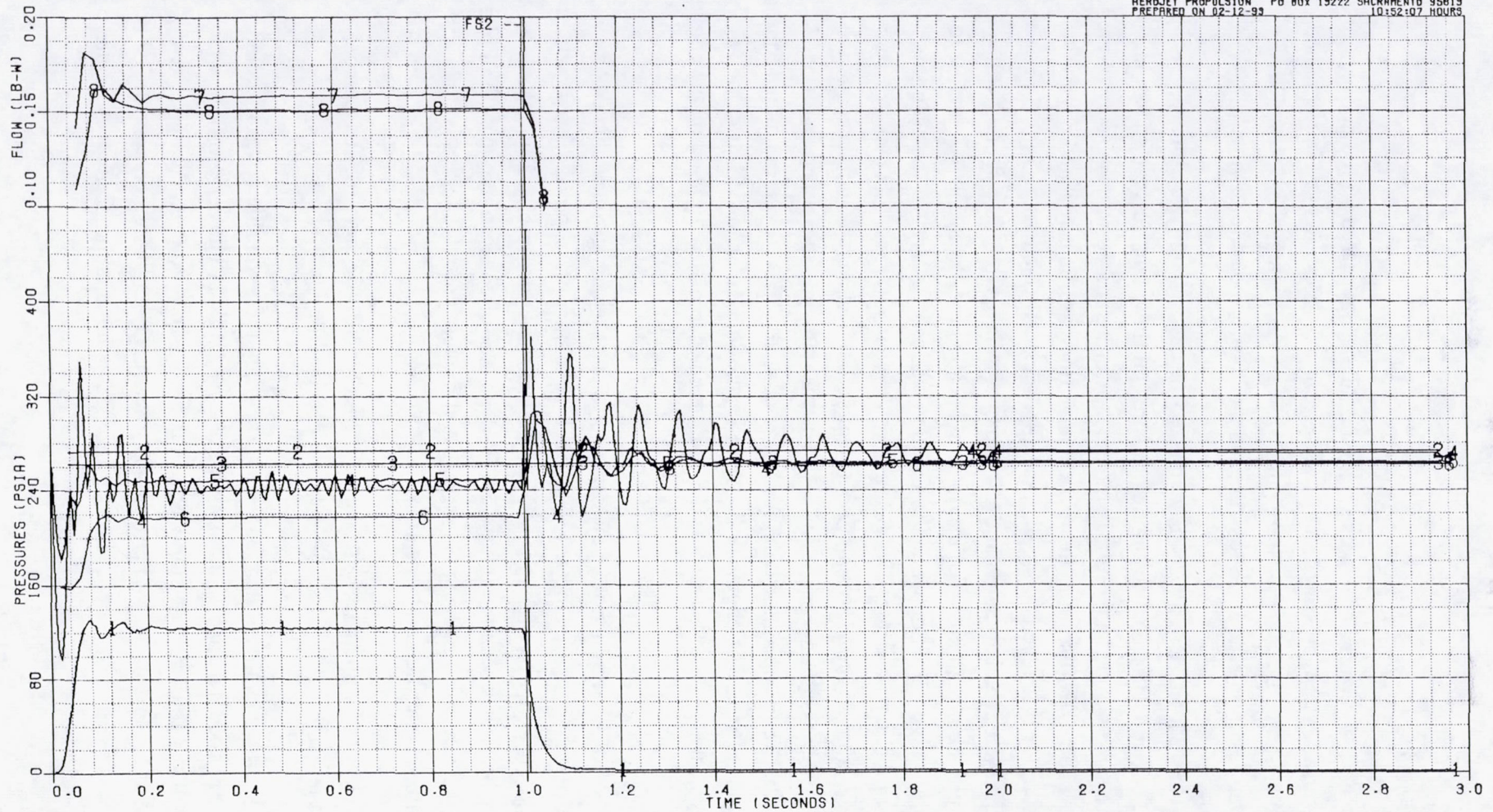
ASPC572

2-22-83

TEST	CONFIGURATION	TEST TIME, sec	Pc, PSIA	MR, O/F	CHAMBER TEMP. oF	NOZZLE WELD TEMP. oF	C*, [COLD THROAT] FT/SEC	TEST OBJECTIVE
1	No Heatshield	1.0	123.2	1.74	--	--	--	SYSTEM CHECK, BALANCE
2	"	99.9	118.5	1.66	3530	2050	5489	BALANCE
3	"	7200.2	118.6	1.65	3550	2050	5521	ENDURANCE TEST
4	With Heatshield	1198.4	118.0	1.67	3680	--	5490	CHECK EFFECT OF FLIGHT HEAT SHIELD
TOTAL FIRING TIME=		8499.5	SEC					
		=(2.361	HR)				

328

329



- 1 PC-1 PSIA 8 FMF-1 LB-W
- 2 PORT PSIA
- 3 PFRT PSIA
- 4 POVI PSIA
- 5 PFRI PSIA
- 6 PFVI PSIA
- 7 FMO-1 LB-W

KGH3-DO1-OA-100 DATE 02-11-93
100 LB THRUSTER TS: J-4

PLOT 2

Figure 6.3-153. Engine Pressures and Flows for 1-sec Test

6.3, Hot Fire Testing (cont.)

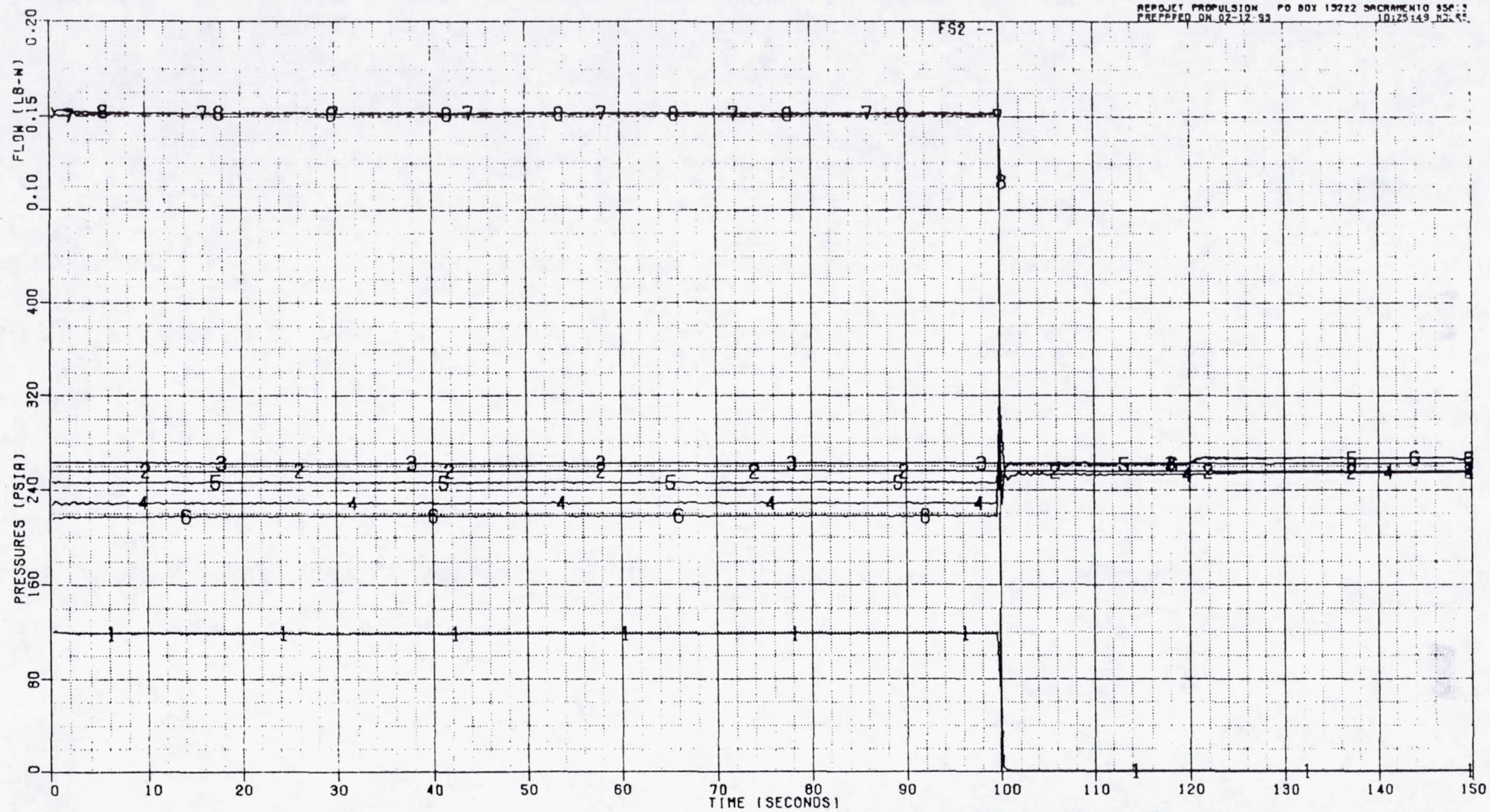
The 100-sec test, -101, was successful; all data appeared within normal limits. Figure 6.3-154 shows system pressures and flows; Figure 6.3-155 shows cell pressure and simulated altitude, illustrating the cabin pressure pump down rate. Figures 6.3-156 and -157 show engine temperatures during the 100-sec firing and the 300-sec coast following.

The 7200-sec test, -102 was conducted successfully on 12 February, beginning at about 11:15 am. The start up engine pressure and flow transients are shown in Figure 6.3-158; these same parameters for the complete 2-hr firing and 30-min coast are plotted in Figure 6.3-159. At about 4200-sec into the test a change (increase) in calculated Kw for the fuel-cooled adapter section was noted, along with the appearance of fluctuations in fuel pressure (1 to 2 psi). Since the system had no automatic kills except Pc (low kill = 50 psia, high kill = 150 psia, and cabin pressure (high kill = 0.4 psia), the plan called for increasing MR and Pc to move towards a more benign condition while the situation was assessed, rather than shutting down in the middle of the two hour test. For this reason, at about 4300 sec, fuel tank pressure was increased 16 psia, from 254 to 270 psia. Concurrent with this change, Kw returned to the previous value, and fuel pressures appeared normal. The fuel tank pressure was then dropped back to nearly the initial value; operation continued to be normal. The test was continued for the full 2-hrs with no other events. The engine is shown in Figures 6.3-160 and -161 after the two-hr test, with the facility heat shield moved aft. At this point the accumulated duration on the engine was 5.94 hr.

Post-test examination of the data shows that the change in calculated Kw was the result of an uncorrelated drop in indicated PFRI, fuel regen inlet pressure, of 4.7 psi, with no corresponding changes in either fuel flow rate, PFTR, fuel run tank pressure, or PFVI, fuel valve inlet pressure, as can be clearly seen in Figure 6.3-159. The lack of correlation makes the PFRI reading suspect. It is likely that the change in reading and fluctuations were indicative of a bad measurement, perhaps an intermittent connection.

Thruster temperatures are shown in Figures 6.3-162 and -163 for the complete firing and post test coast. All values were within expected limits.

With the facility shield moved aft, the flight radiation shield was installed. During the installation process it appears that side loads were applied to the nozzle skirt, which broke off cleanly at the Re to C-103 transition joint. Figure 6.3-164 shows an enlarged view of the skirt joint region after the 2-hr test and prior to the fracture. The joint region appearance is normal. The break was a brittle fracture, indicating inadequate material properties. A failure



1 PC-1 PSIA 8 FMF-1 LB-W
 2 PORT PSIA
 3 PFRT PSIA
 4 POVI PSIA
 5 PFRI PSIA
 6 PFVI PSIA
 7 FMO-1 LB-W

KGH3-DO1-DA-101 DATE 02-11-93
 100 LB THRUSTER TS: J-4 PLOT 2A

Figure 6.3-154. Engine Pressure and Flows for 100-sec Test

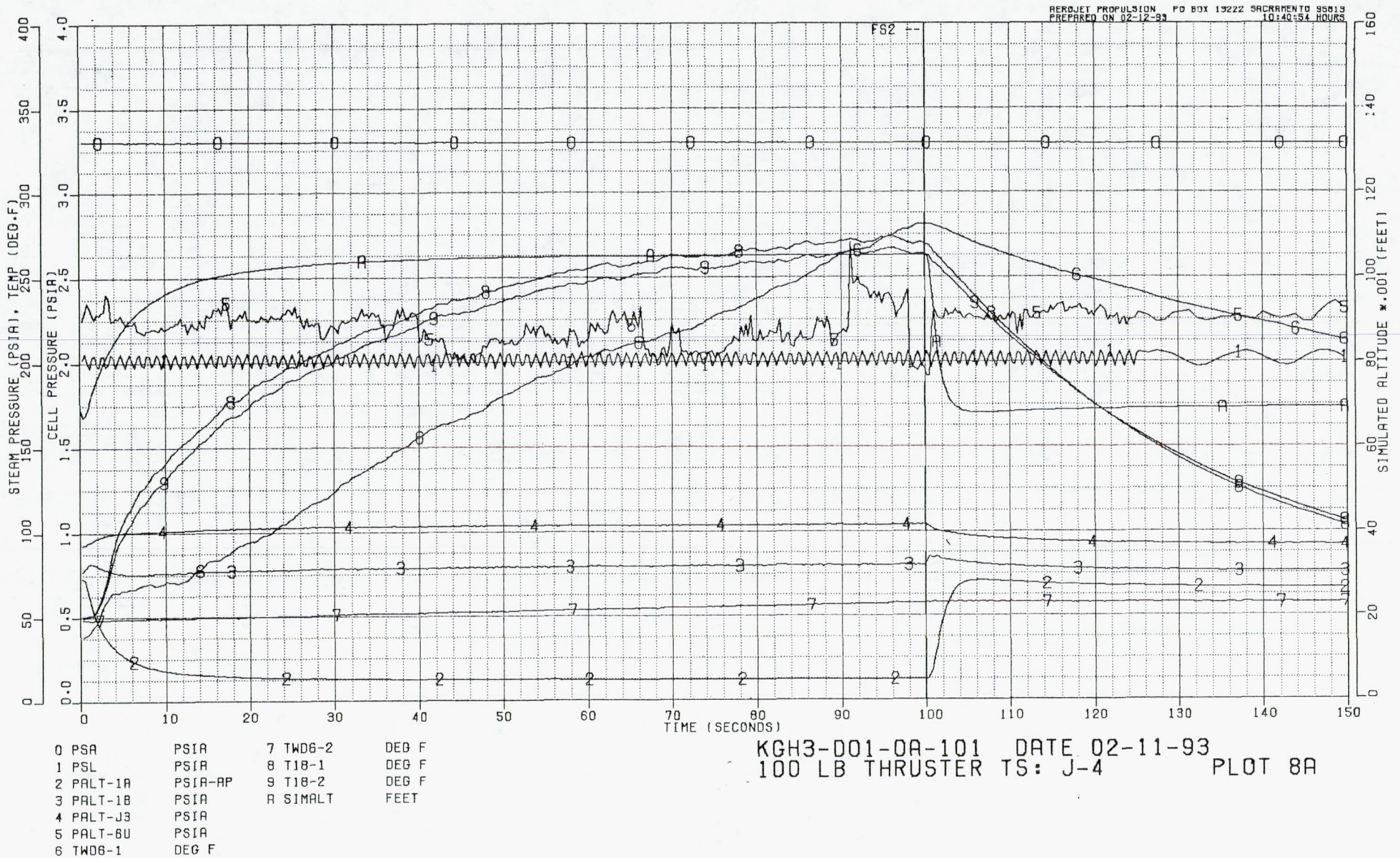
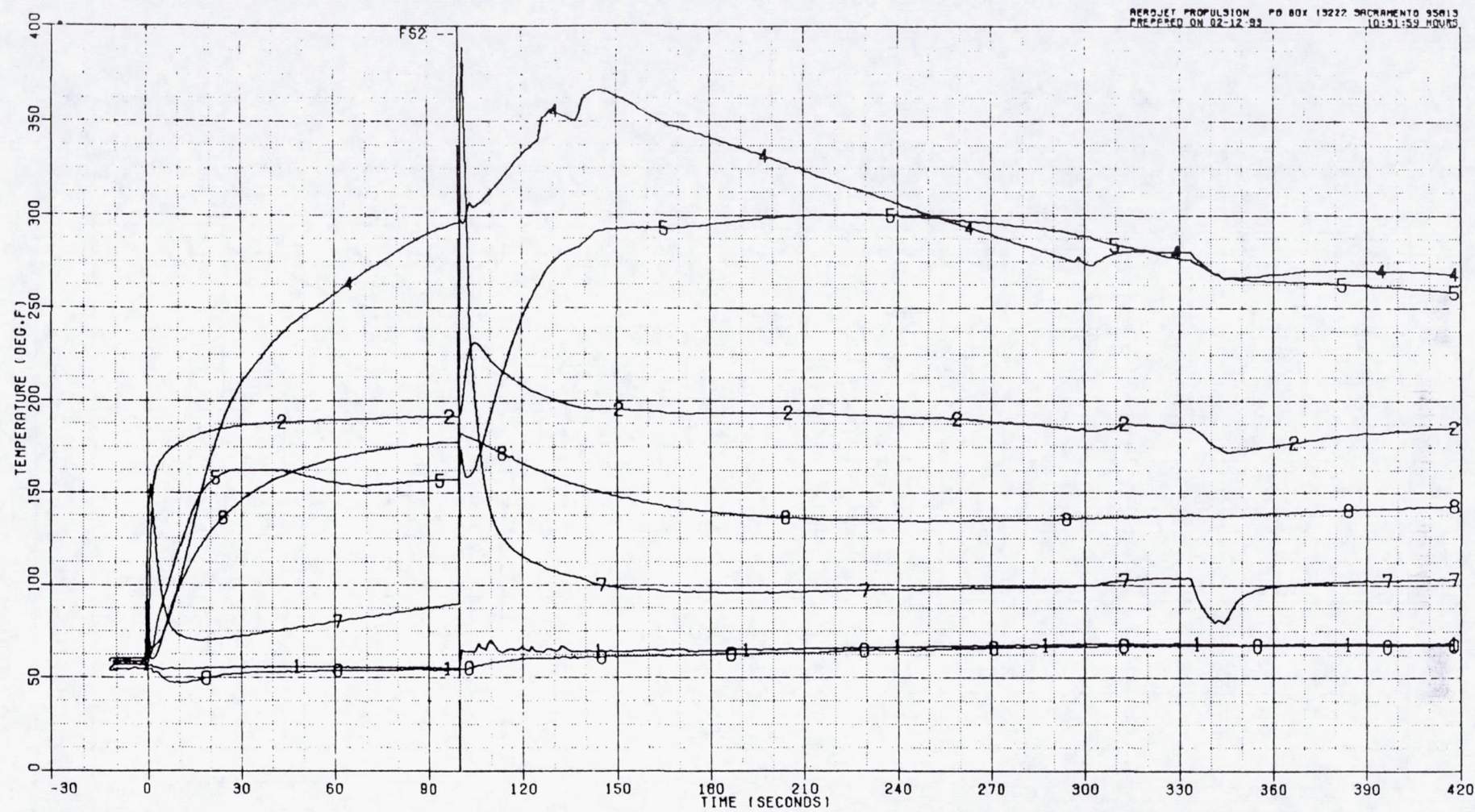


Figure 6.3-155. Cell Pressure and Simulated Altitude for 100-sec Test

333



KGH3-001-0A-101 DATE 02-11-93
100 LB THRUSTER TS: J-4 PLOT 4

Figure 6.3-156. Engine Temperatures, 100-sec Firing and Coast

334

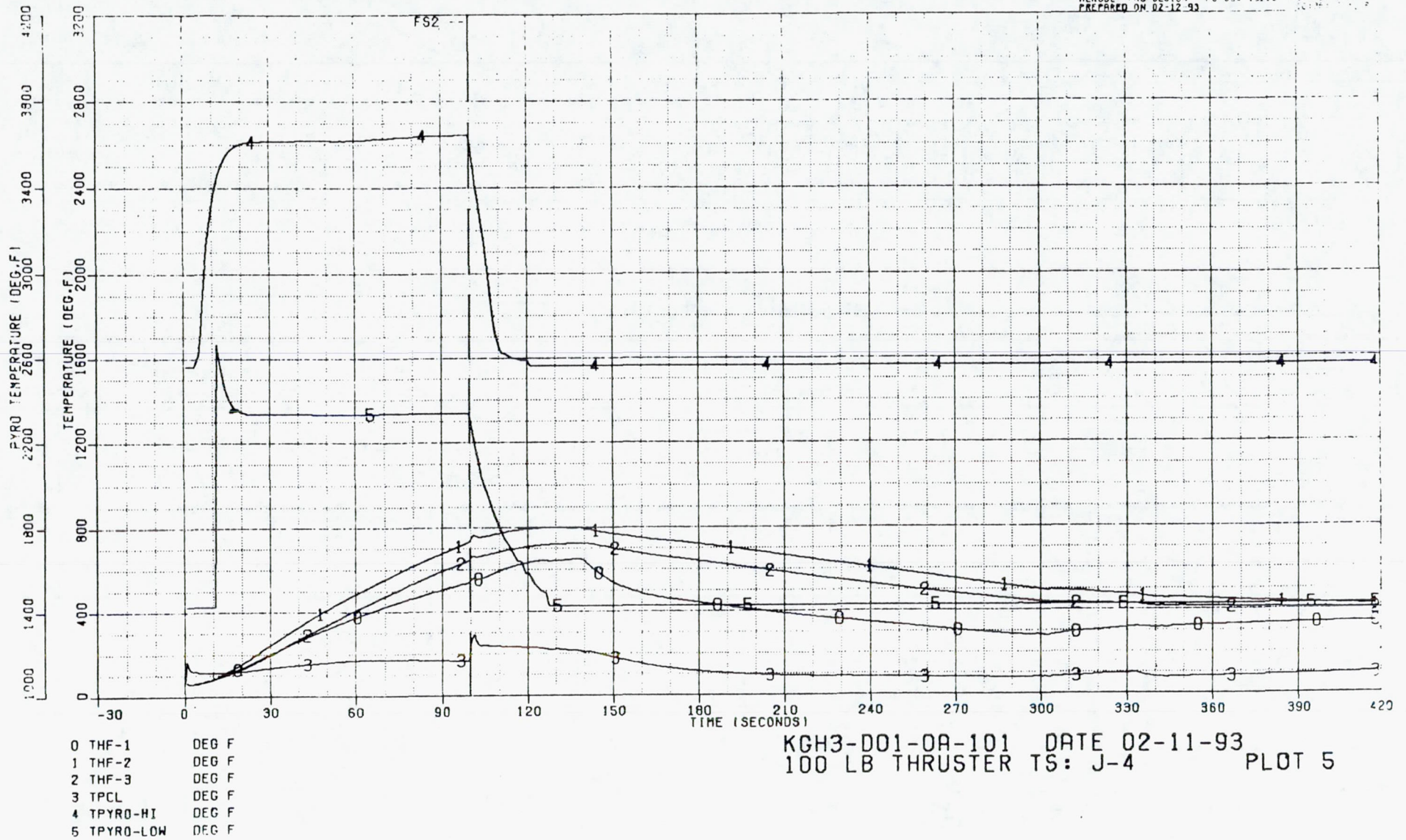


Figure 6.3-157. Engine Temperatures, 100-sec Firing and Coast

335

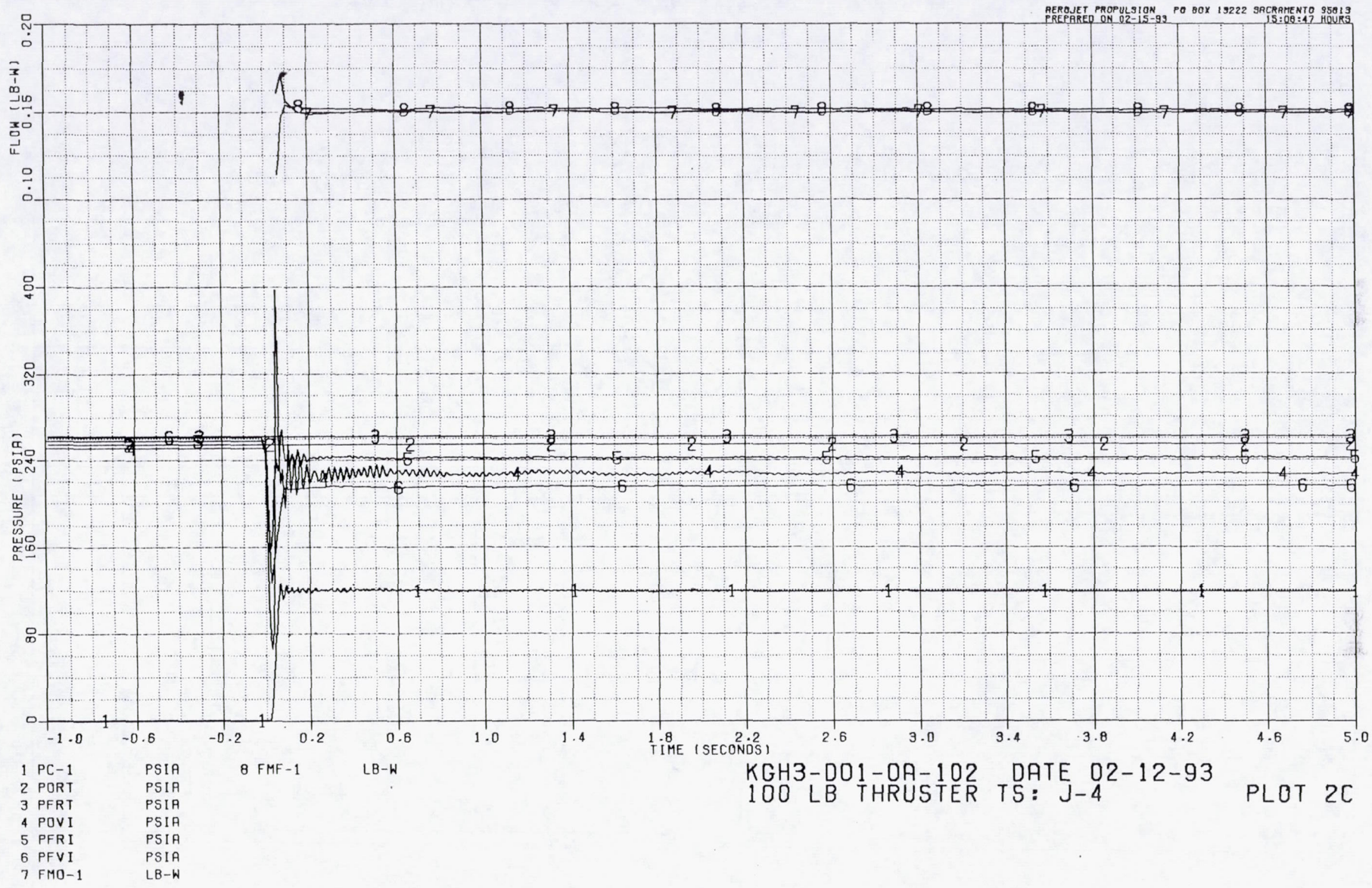


Figure 6.3-158. Engine Pressure and Flow Start Transient, 7200-sec Test

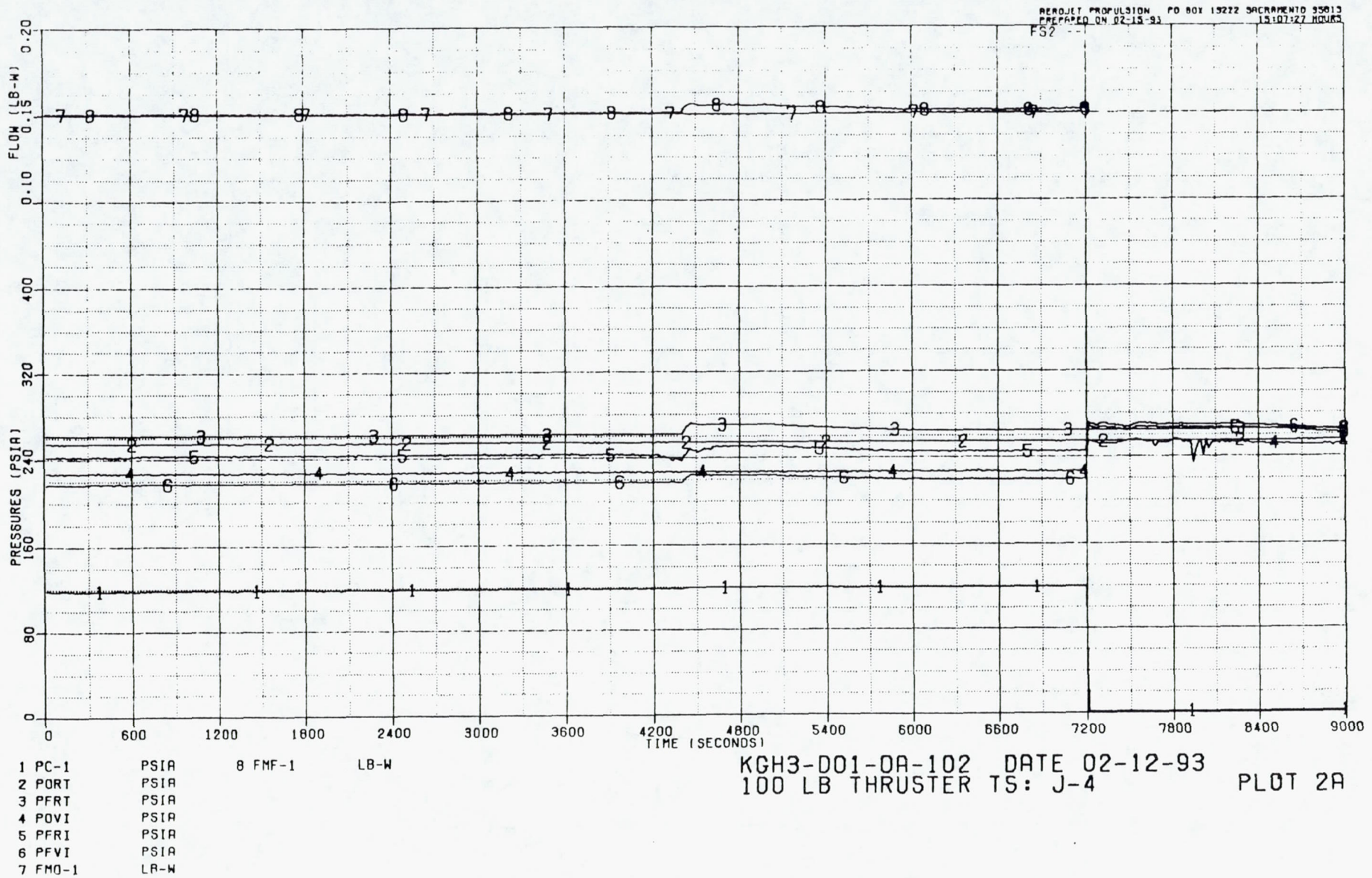


Figure 6.3-159. Engine Pressure and Flows, 7200-sec Test and 1800-sec Coast

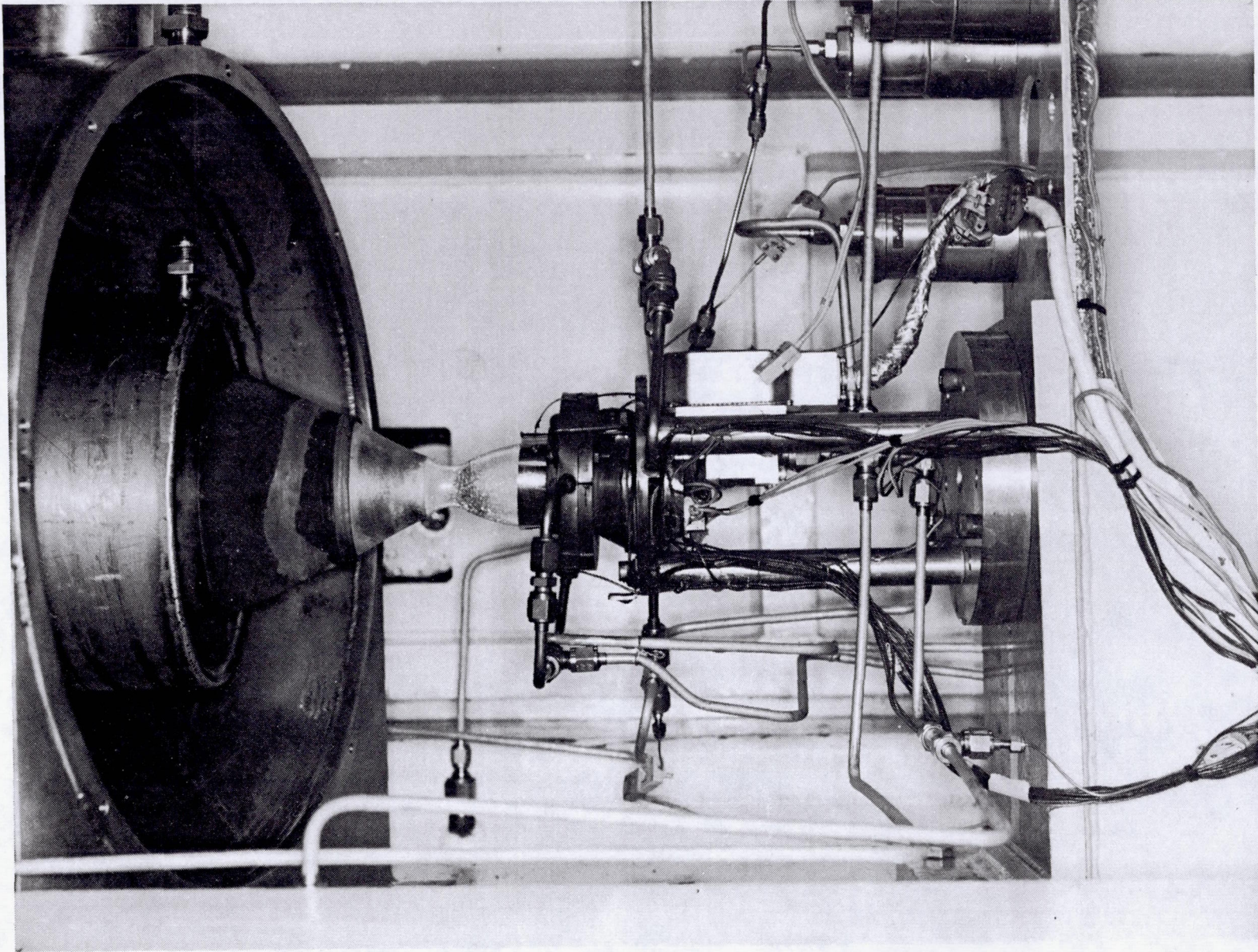
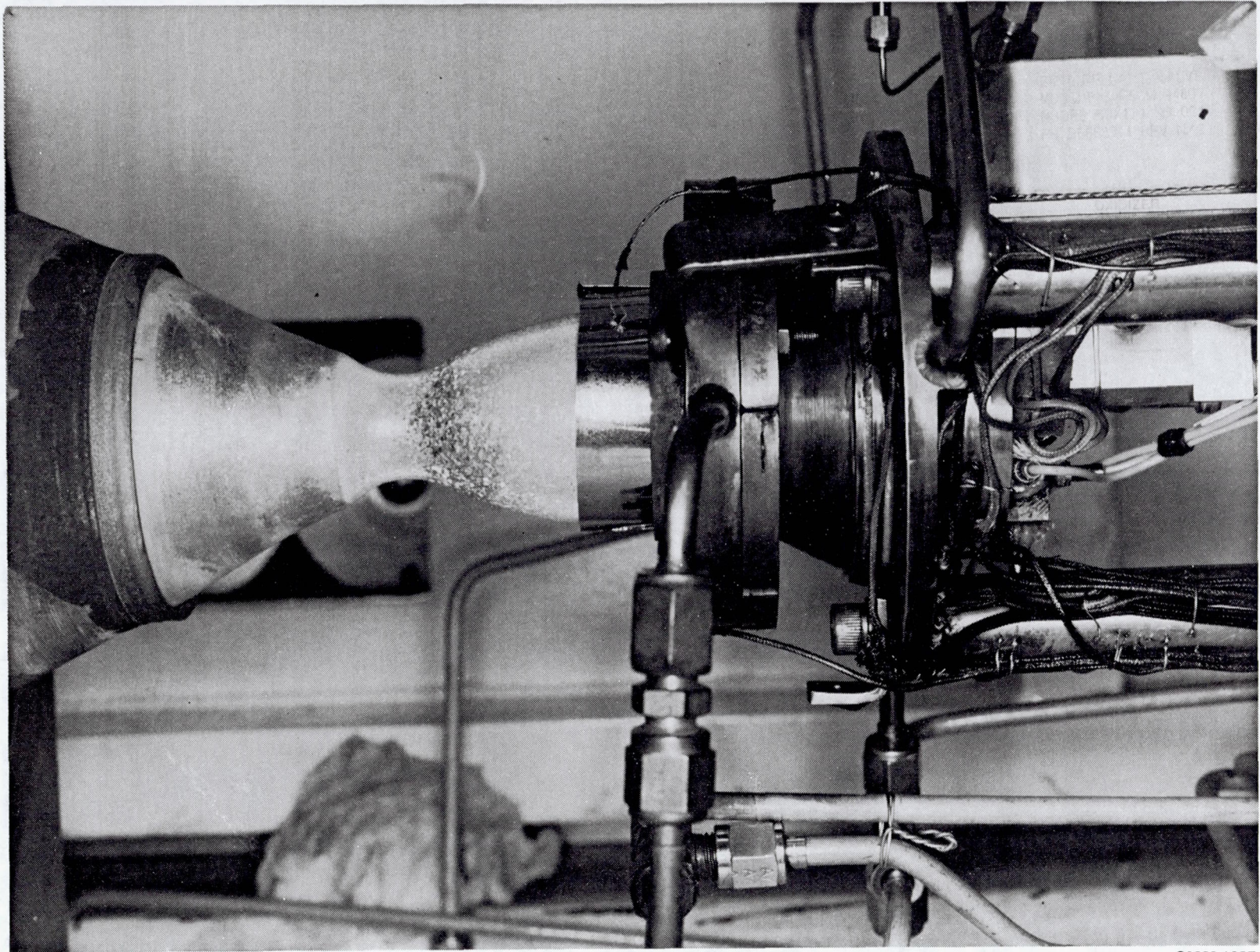


Figure 6.3-160. View of Engine Assembly on Test Stand After Successful Completion of 2-hr Endurance Test

C0293 1208



C0293 1207

Figure 6.3-161. Close-up of Engine Assembly After 2-hr Endurance Test

339

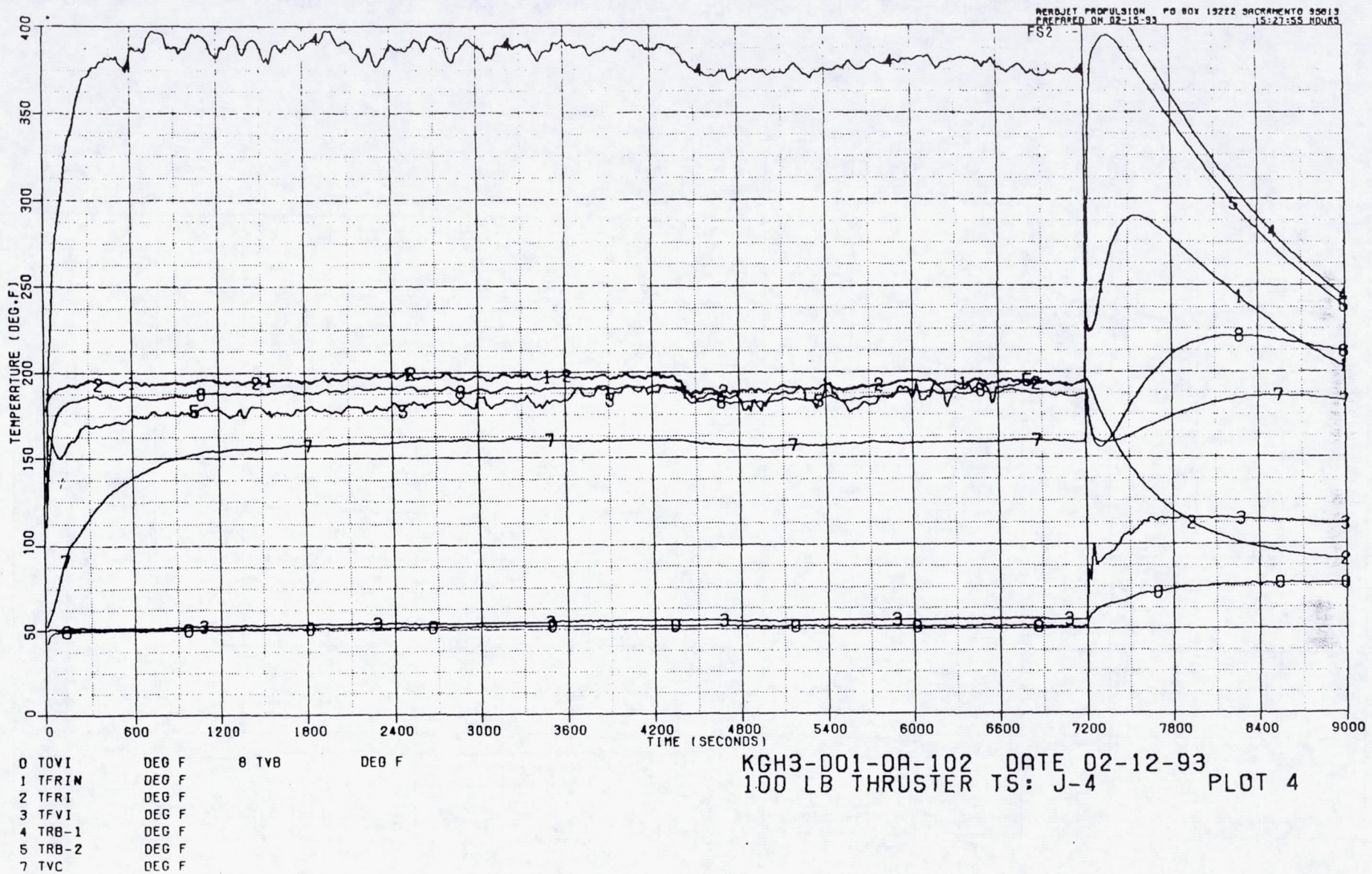


Figure 6.3-162. Engine Temperatures, 7200-sec Firing and 1800-sec Coast

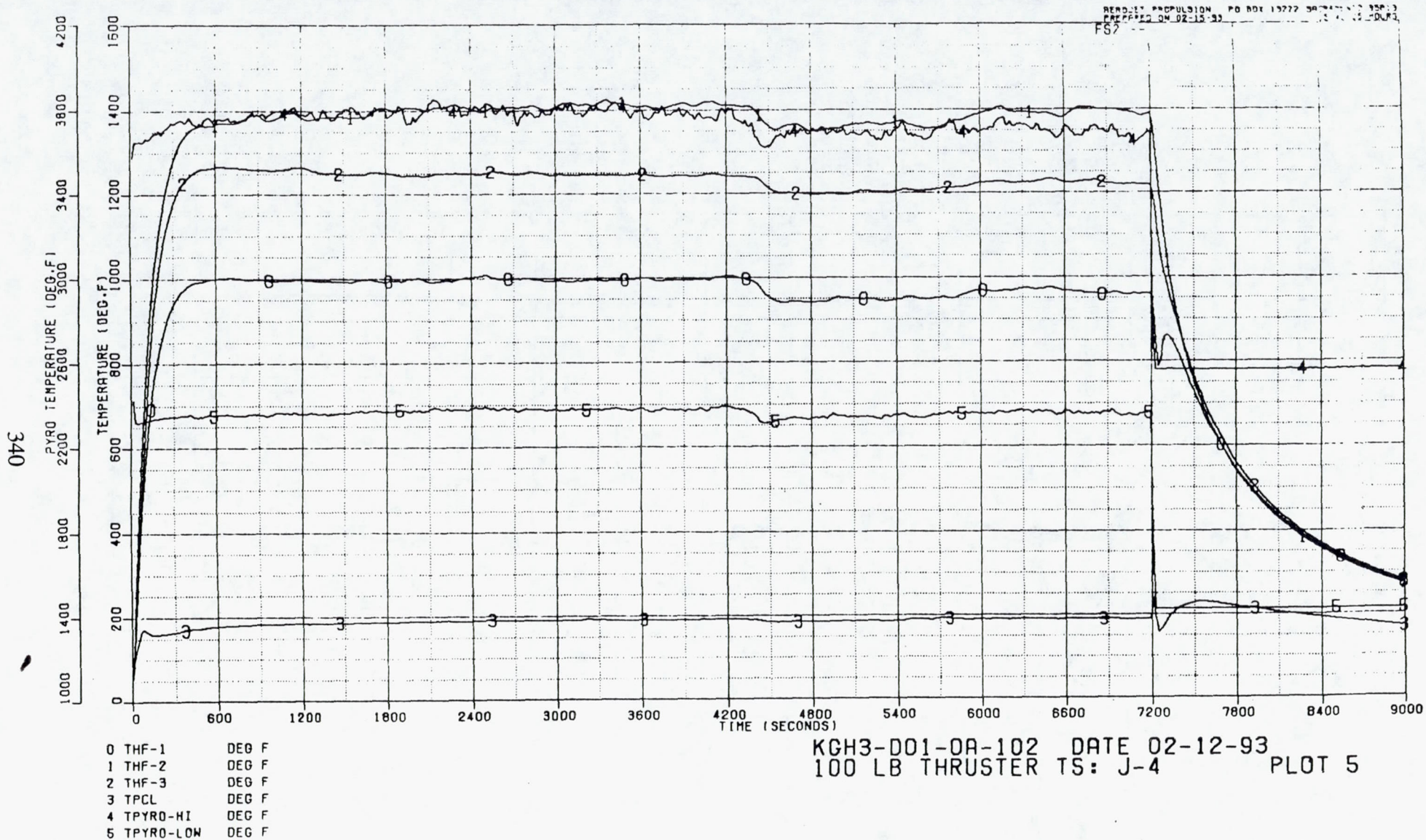
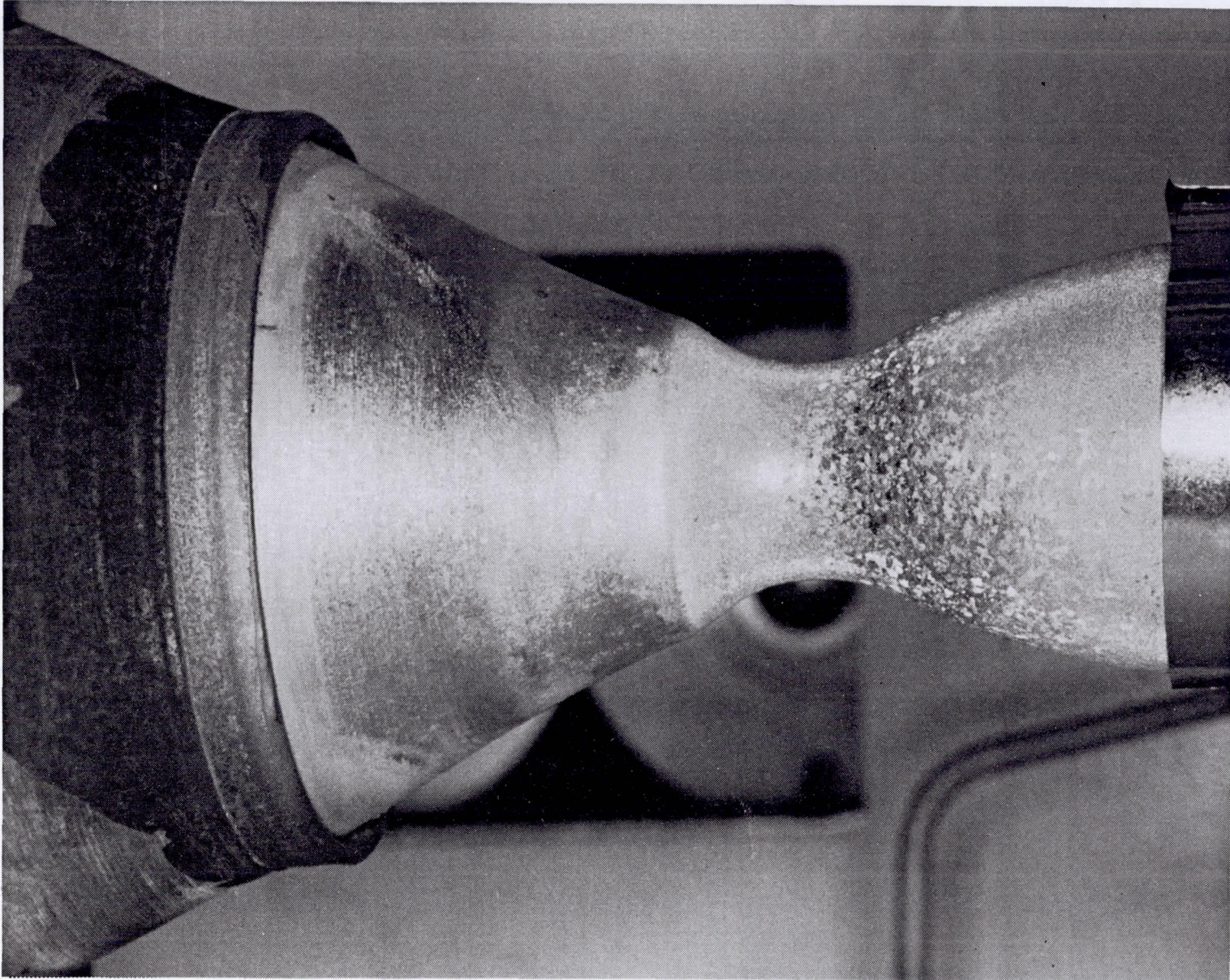


Figure 6.3-163. Engine Temperatures, 7200-sec Firing and 1800-sec Coast



C0293 1207

Figure 6.3-164. Detail of Skirt Joint After 2-hr Firing Looks Normal

6.3, Hot Fire Testing (cont.)

analysis was conducted and is described in Appendix L. The engine is shown in Figure 6.3-164 with the shield in place, after skirt separation, and in Figure 6.3-165 after removal of the skirt.

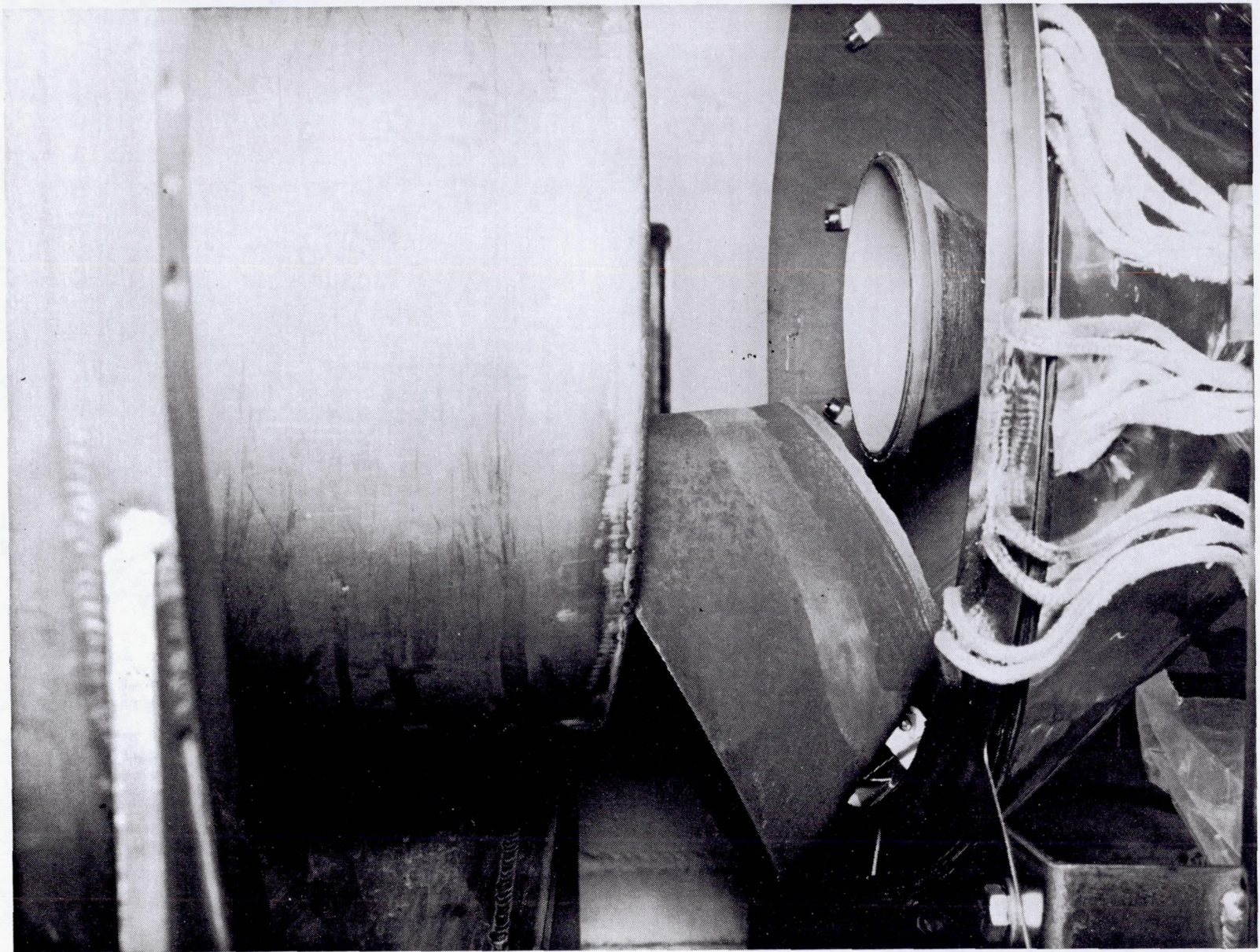
The final test, to check out the engine operation with a high temperature radiation shield shown in Figure 6.3-166, was then conducted, as test -103, for 1200-sec. The test was successful; engine and shield performed satisfactorily. Figure 6.3-167 shows engine pressures during firing and coast. The gradual (5 to 8 sec) fuel pressure rise after shutdown is the normal result of thermal soak back which is then relieved when a check valve in parallel with the stand safety, and with the flow direction back to the tank, cracks open.

Thruster temperatures are shown in Figures 6.3-168 and -169. PYRO-LO, nozzle joint pyrometer, was not active for this test. The indicated PYRO-HI, chamber wall pyrometer readings require correction in all tests because of window absorption and in this test because a first-surface mirror was required to view past the radiation shield. The initial heat up value, reached in about 100-sec, corresponds to the normal operating temperature for this engine, without high emissivity coating, of 3500 F. The subsequent heat up of the engine by the radiation shield adds another 180 F, giving a final temperature of about 3680 F, well below the long-life limit of 4000 F.

The appearance of the shield and thruster after the 1200-sec test is shown in Figure 6.3-170. Detailed examination of the engine hardware with boroscope and external photos show no problems other than the detached skirt. The throat, Ir coating, trip, cooled adapter, injector and valve look undamaged, except for a small chip in the Ir coating in the cool section of the nozzle exit. Extensive post-firing photos were taken of the engine. Some of these are included in Appendix M.

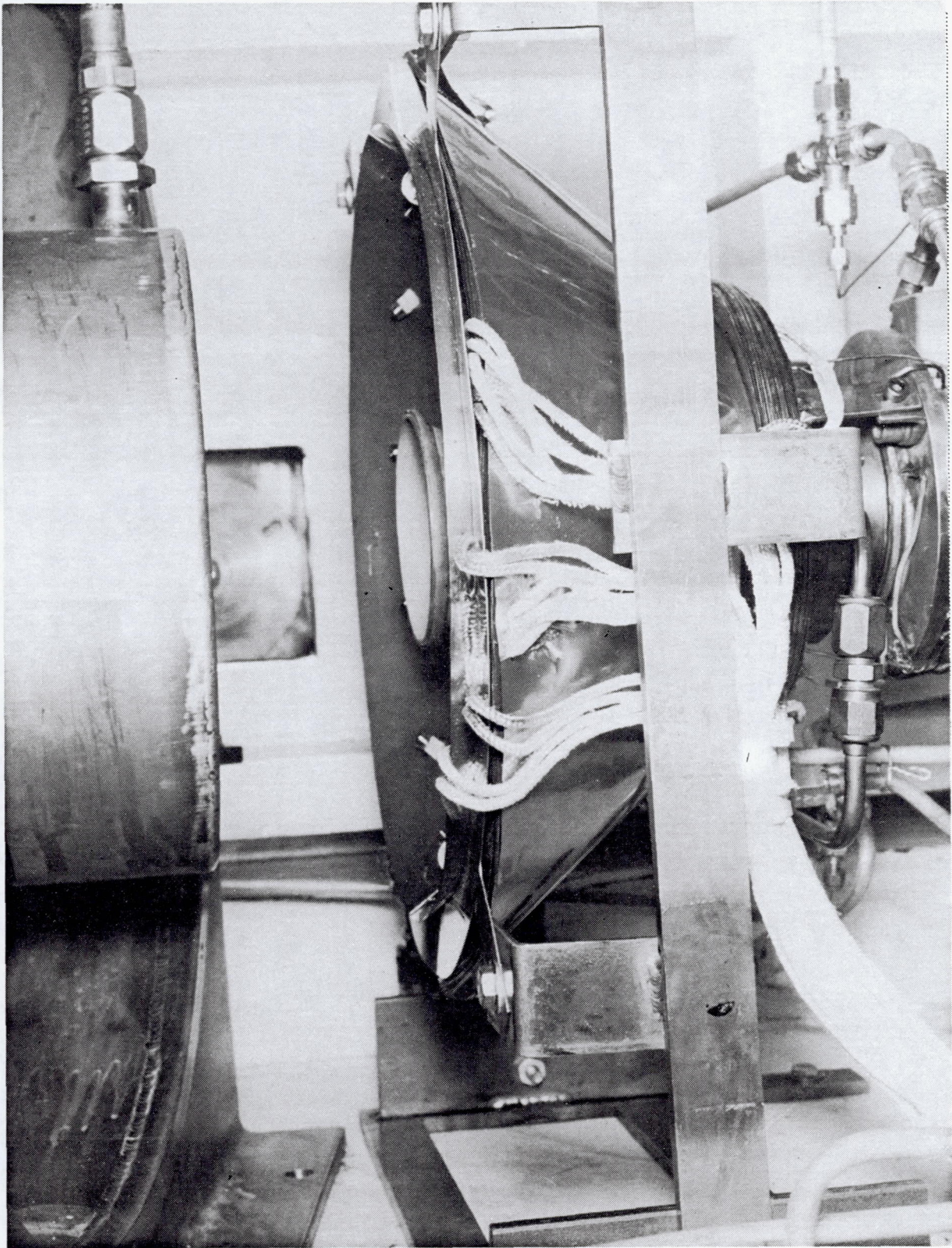
6.4 WORK HARDENING OF RHENIUM

During early stages of thruster design, it became apparent that uncertainty in the yield strength of annealed CVD Re was a major consideration. Data available for wrought Re (Refs. 6.4-1, -2) indicated values in the 40 Ksi to 50 Ksi range. However, the very limited data for CVD rhenium indicated values as low as 10 Ksi. Yield strength in the annealed condition controls the chamber headend and throat thickness required to avoid permanent deflection caused by launch random vibration since every engine will be acceptance hot fired and therefore annealed prior to launch. In addition, chamber yield in hoop stress is possible due to pressure spikes caused by gas bubbles in the propellant.



C0293 1212

Figure 6.3-165. Skirt Separated After Installation of Heat Shield



C0293 1214

Figure 6.3-166. Engine With Heat Shield in Place, Ready for Test

345

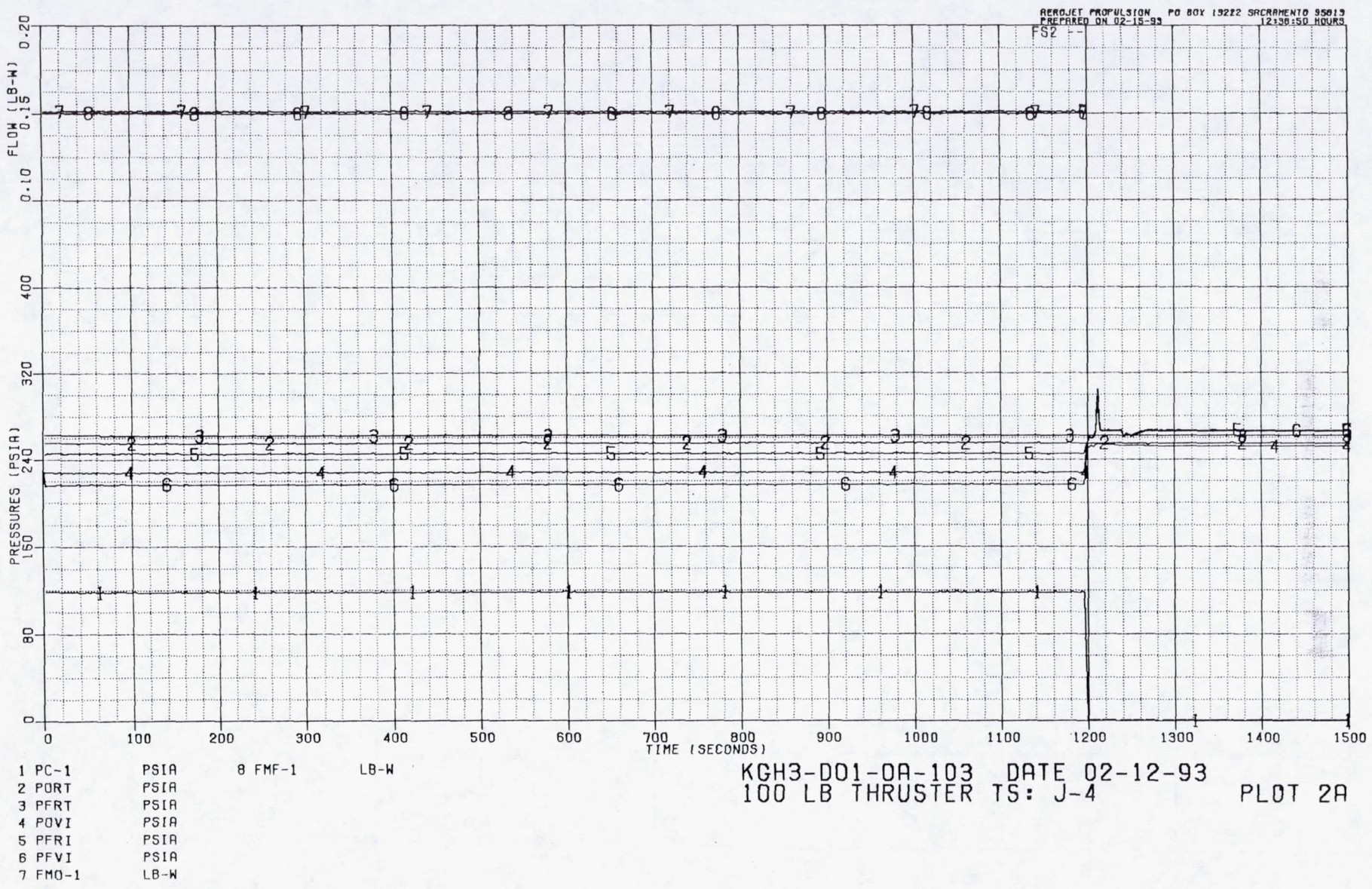


Figure 6.3-167. Engine Pressures and Flows During 1200-sec Test

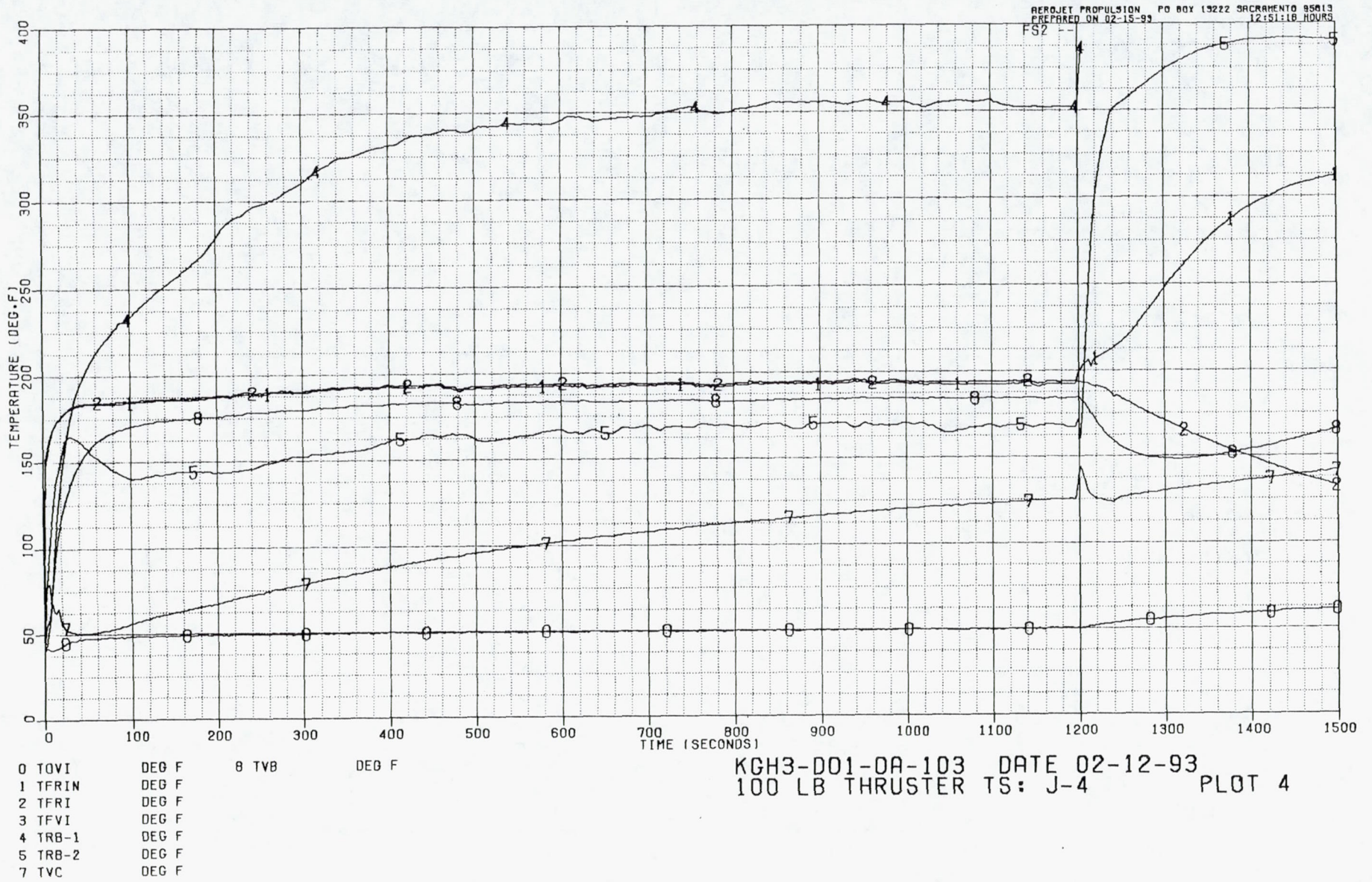


Figure 6.3-168. Engine Temperatures During 1200-sec Test

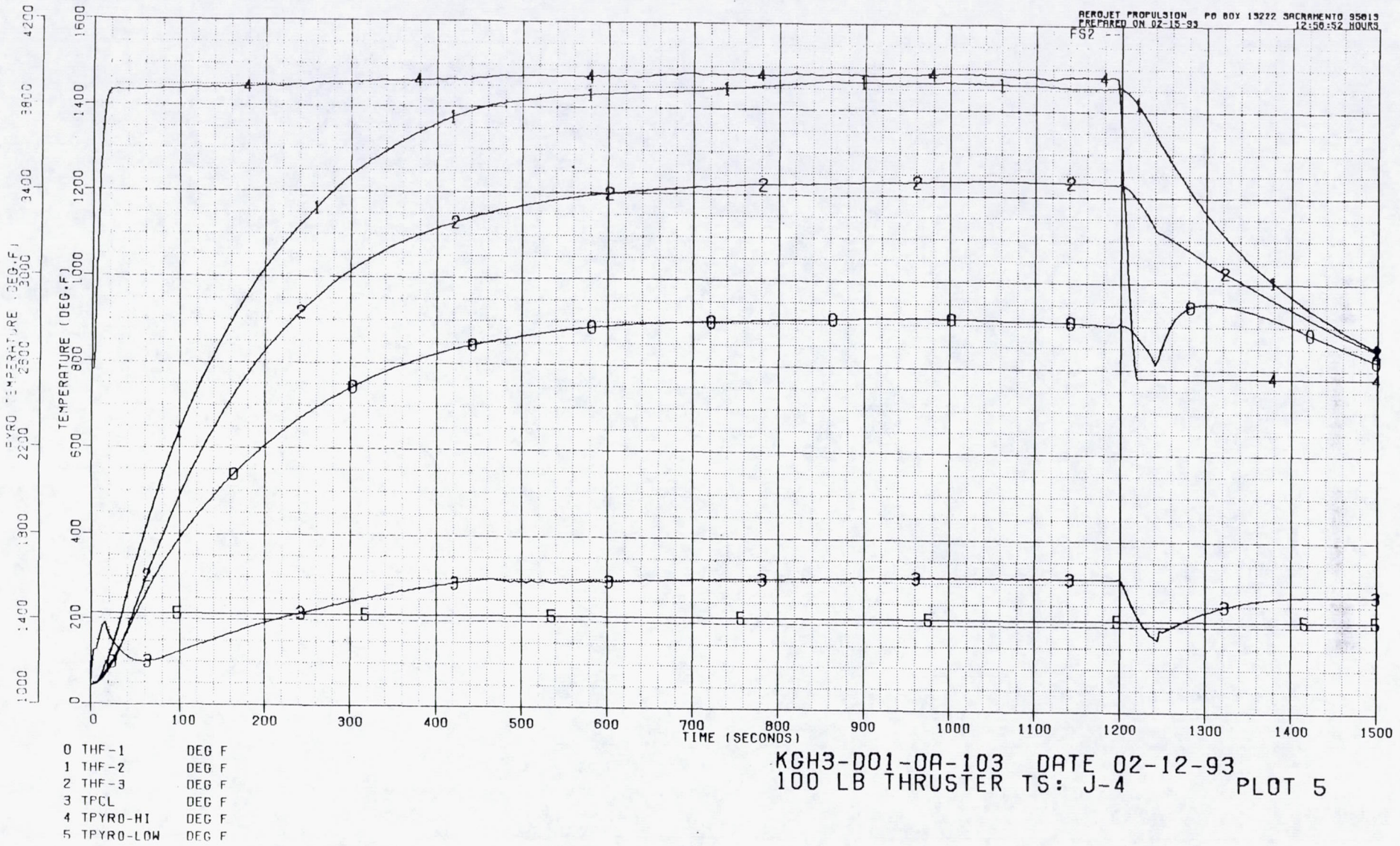
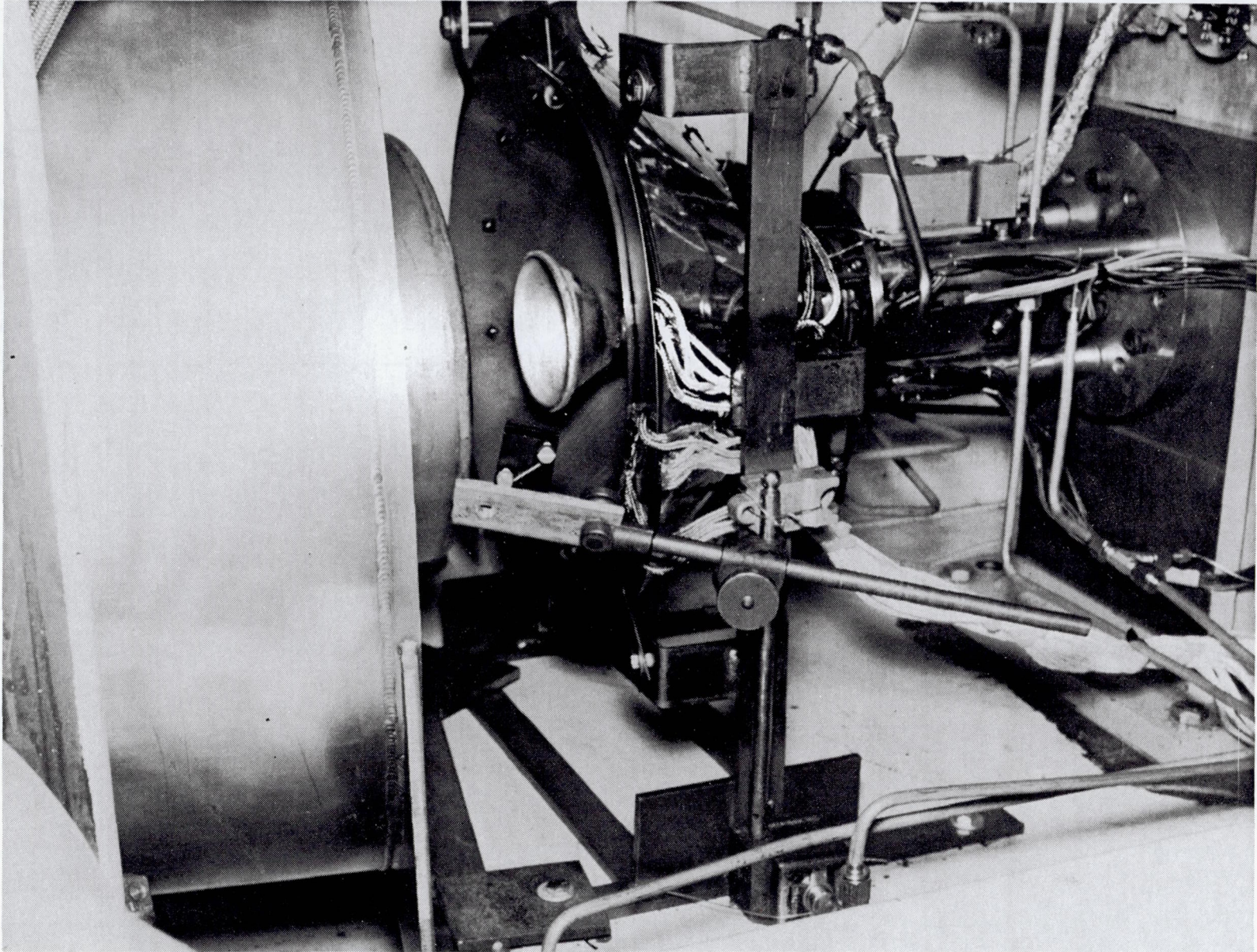


Figure 6.3-169. Engine Temperatures During 1200-sec Test



C0293 1205

Figure 6.3-170. Thruster and Heat Shield After 1200-sec Test

6.4, Work Hardening of Rhenium (cont.)

One method for increasing the yield strength of Re is by workhardening. Therefore, as part of Task 13.1, workhardening of Re was investigated.

Two annealed CVD rhenium specimens were strainhardened by cyclic strain in a tensile test irodine. The strain hardening resulted in an increase in yield strength from 9700 psi to 38,800 psi. The details of the strainhardening experiment are provided in Appendix N.

6.5 NTO/AH TESTS

Substitution of anhydrous hydrazine (AH) for monomethylhydrazine (MMH) in the 100 lbf Ir-Re thruster should increase delivered specific impulse by about 2 percent. This high temperature radiation cooled thruster does not require film cooling and, therefore, will have optimum performance with NTO/AH at an MR of 1.1 to 1.2, providing better volumetric efficiency than conventional highly film cooled NTO/AH thrusters which optimize at 0.9 to 1.0.

Design, fabrication, and test of a 100 lbf thruster specifically designed for NTO/AH was planned as part of this program. To obtain preliminary data for the design activity, tests were conducted with existing bolt-together hardware shown in Figure 6.3-30. The primary purpose of these tests was to determine optimum MR for NTO/AH.

6.5.1 Testing

The setup for the NTO/AH tests is shown in Figure 6.3-30. Hydrazine was delivered by a positive displacement flowmeter (PDFM) which was filled from a 4-gal tank.

The NTO/AH test series immediately followed the 44:1 performance testing of S/N 6-1 injector with NTO/MMH and used the identical hardware. The only change was the substitution of AH for MMH.

The objective of the testing was to determine (1) the optimum MR for the NTO/AH propellant system in the Ir-Re radiation cooled hardware and (2) the increase in performance in switching from MMH to AH.

The first test, -245, was a 1-sec firing for system checkout and determining hydraulic balance. The second test, -246, was intended to be a 10-sec checkout test. The test was normal until about 2.6 sec, at which time several pressure spikes occurred in PFJ and, to a lesser extent, in POJ and Pc. At about 3.0 sec, the first visual evidence of a problem was seen on

6.5, NTO/AH Tests (cont.)

the video display and at about 3.5 sec the bipropellant valve was signaled to close. Propellant flows reduced but did not stop, and further, lower spikes occurred in Pc, POJ and PFJ. This continued until 6 to 7 sec into the test, at which time the thruster slowly started to shift backwards and drop down. At about 8 sec, the thruster disappeared from the video image.

Upon opening the test cell, the chamber/nozzle assembly was found to be inserted into the diffuser. The injector was loosely mounted to the valve by the stubs of the bolts which held the valve/injector/chamber assembly together (Figure 6.5-1).

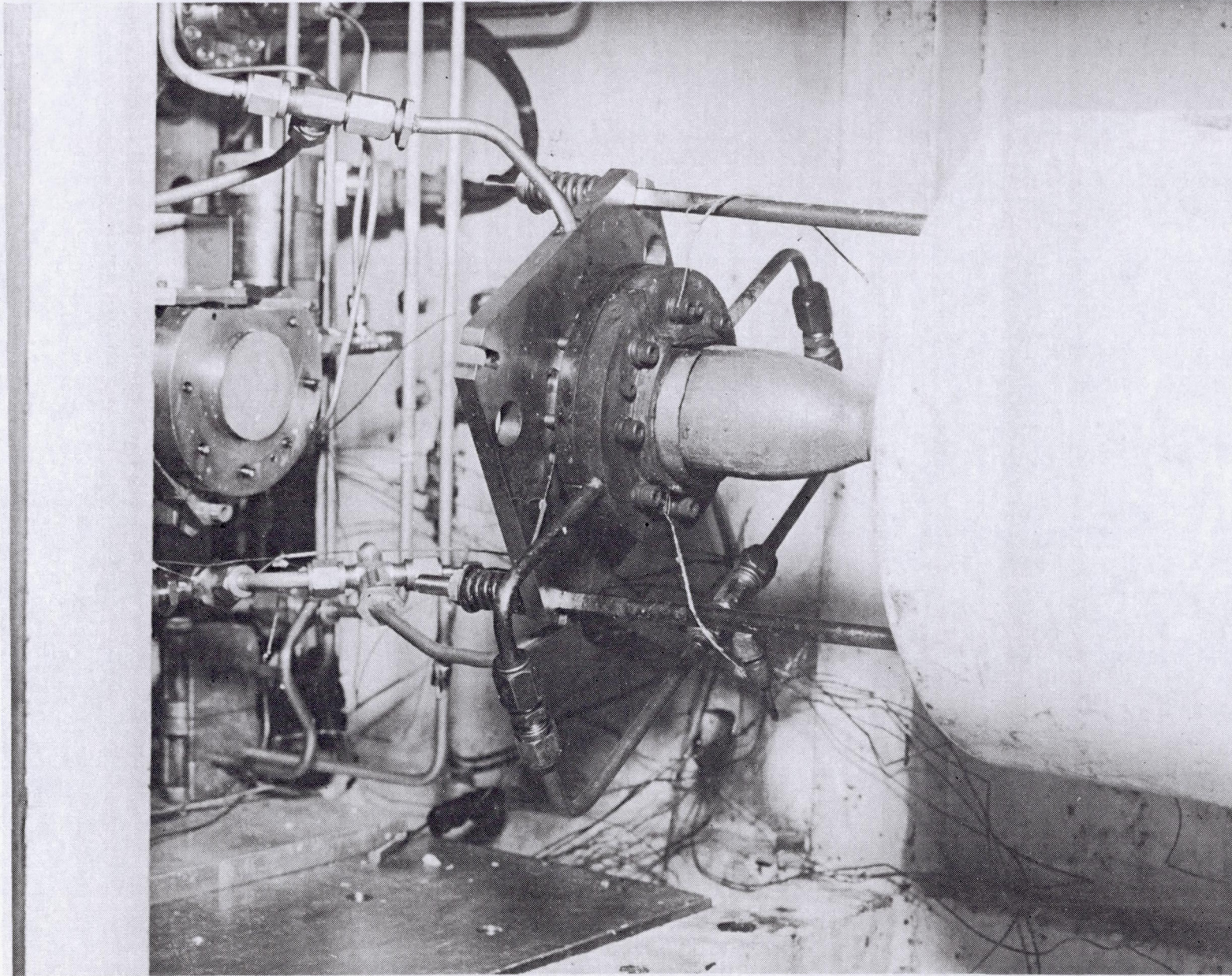
Test Data

Results for the two tests are summarized in Table 6.5-1. Even at the short firing time, specific impulse was running about 1.5% higher than in a comparable NTO-MMH test, as shown in Figure 6.5-2, where I_s for Tests -244 (NTO/MMH) and -246 are plotted versus time, along with the percent difference between them. Fuel temperature rise and fuel outlet temperature for Tests -246 (NTO/AH) and -276 (NTO/MMH) are compared in Figures 6.5-3 and 6.5-4. The temperatures for the AH case are lower, as would be expected at the higher fuel flow rate. Temperature of the tip of the cooled adapter is compared for tests with the two fuels in Figure 6.5-5. The temperature was slightly cooler for the AH case.

Heat transfer to the AH was smoothly increasing, as predicted, when the event occurred at 2.6+ sec, as shown in Figure 6.5-6. Propellant flows and mixture ratio were normal and steady when the event occurred, as shown in Figure 6.5-7. External thruster temperatures were normal until 3.3 sec, when they rose rapidly and became erratic, as shown in Figure 6.5-8.

Cell pressure was steady until 2.6+ sec, at which time it showed a very slight drop and some very slight roughness; at about 3.3 sec, it rose in about 1 sec to 10 times normal running pressure (about 2 psia was indicated; however, the transducer is 100% over range at this point). This continued until nearly 11 sec when the transducer went off scale; this is believed to be caused by thermally induced breakage of the cell windows, as indicated in Figure 6.5-9.

The timing of these events, as determined from digital data, FM tape, oscillograph and video tape is summarized in Table 6.5-2.



(C0192 0102)

Figure 6.5-1. View of Injector, Broken Bolts, and Chamber Assembly

Table 6.5-1. Test Results, Runs -245 and -246

ASRC375
NTO/AH Propellants

<u>Run No.</u>	<u>Date</u>	<u>Firing Time, sec</u>	<u>Data Time, sec</u>	<u>Pc, psia</u>	<u>MR O/F</u>	<u>F vac lbf</u>	<u>Is vac sec at 44:1</u>	<u>TFL F</u>	<u>Regen Outlet F</u>	<u>Regen Delta T, F</u>	<u>Heat Trans btu/sec</u>
245	1-6-92	1.0	0.75	103.0	0.899	99.9	306.4	52	114	62	7.98
246	1-6-92	2.6+	1.8	101	0.917	100.1	312.1	52	160	109	13.98

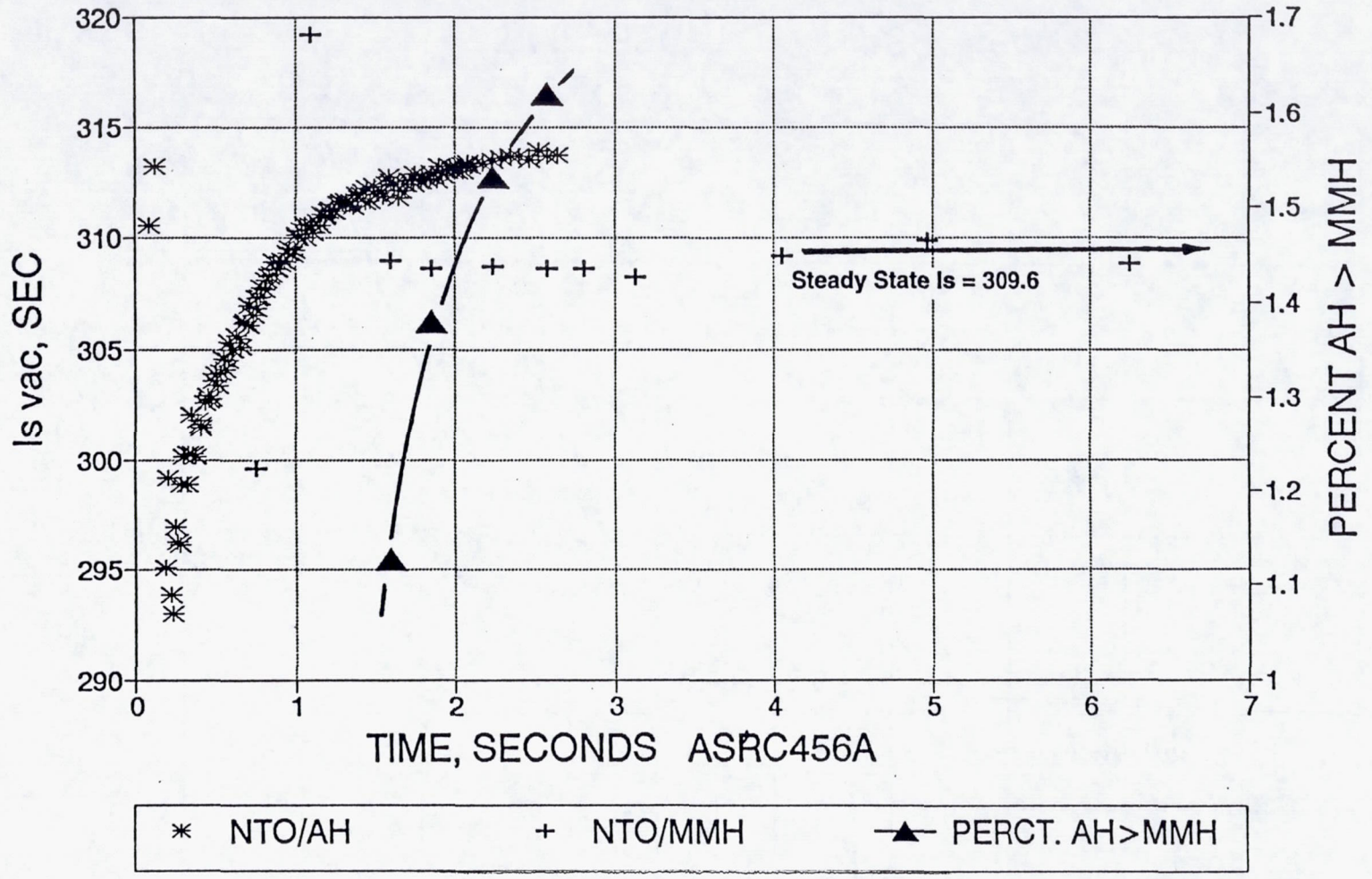


Figure 6.5-2. I_s Versus Time for NTO/MMH and NTO/AH

Bulk Rise is Lower for AH Because of Lower MR

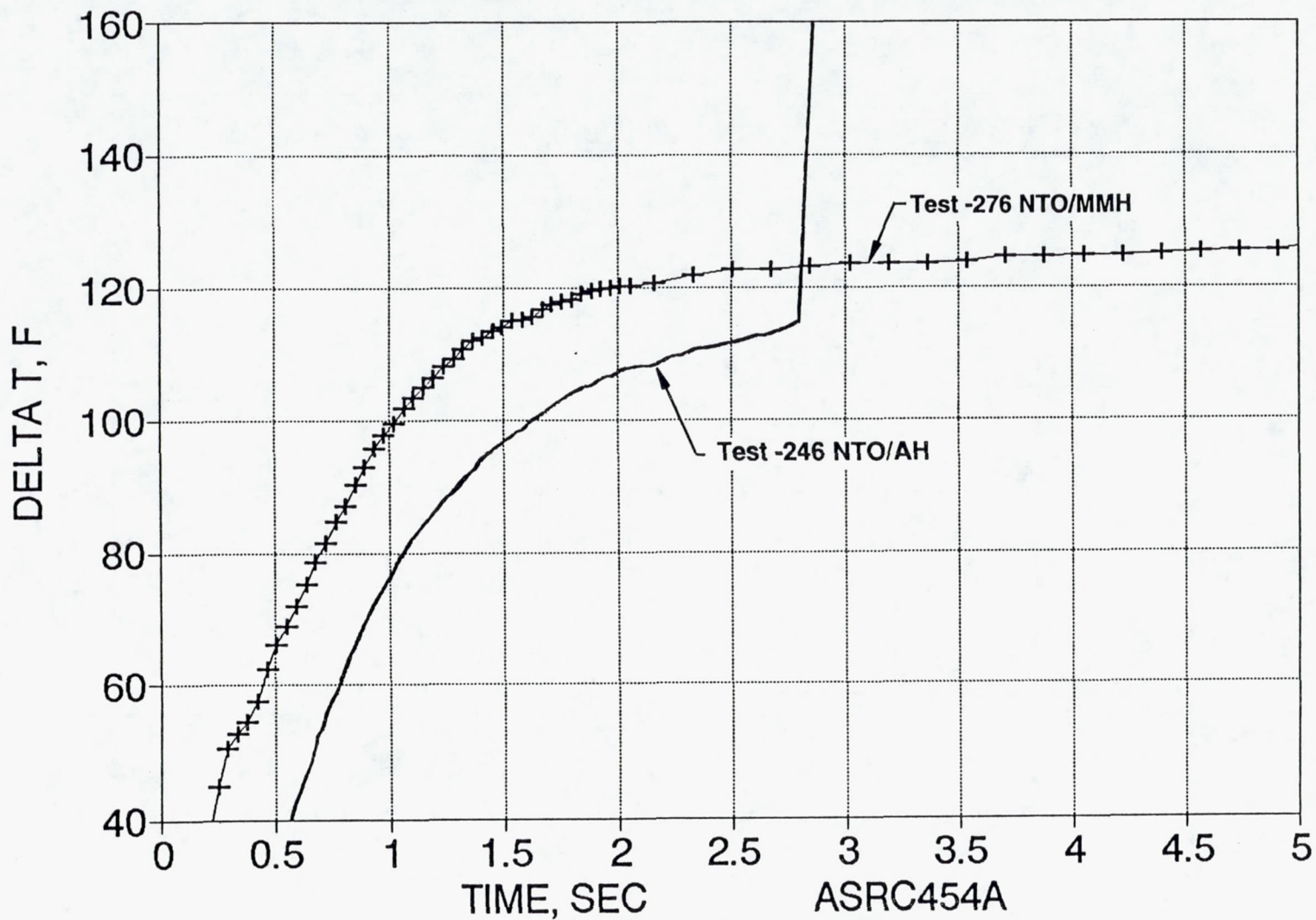


Figure 6.5-3. Fuel Temperature Rise, NTO/MMH and NTO/AH

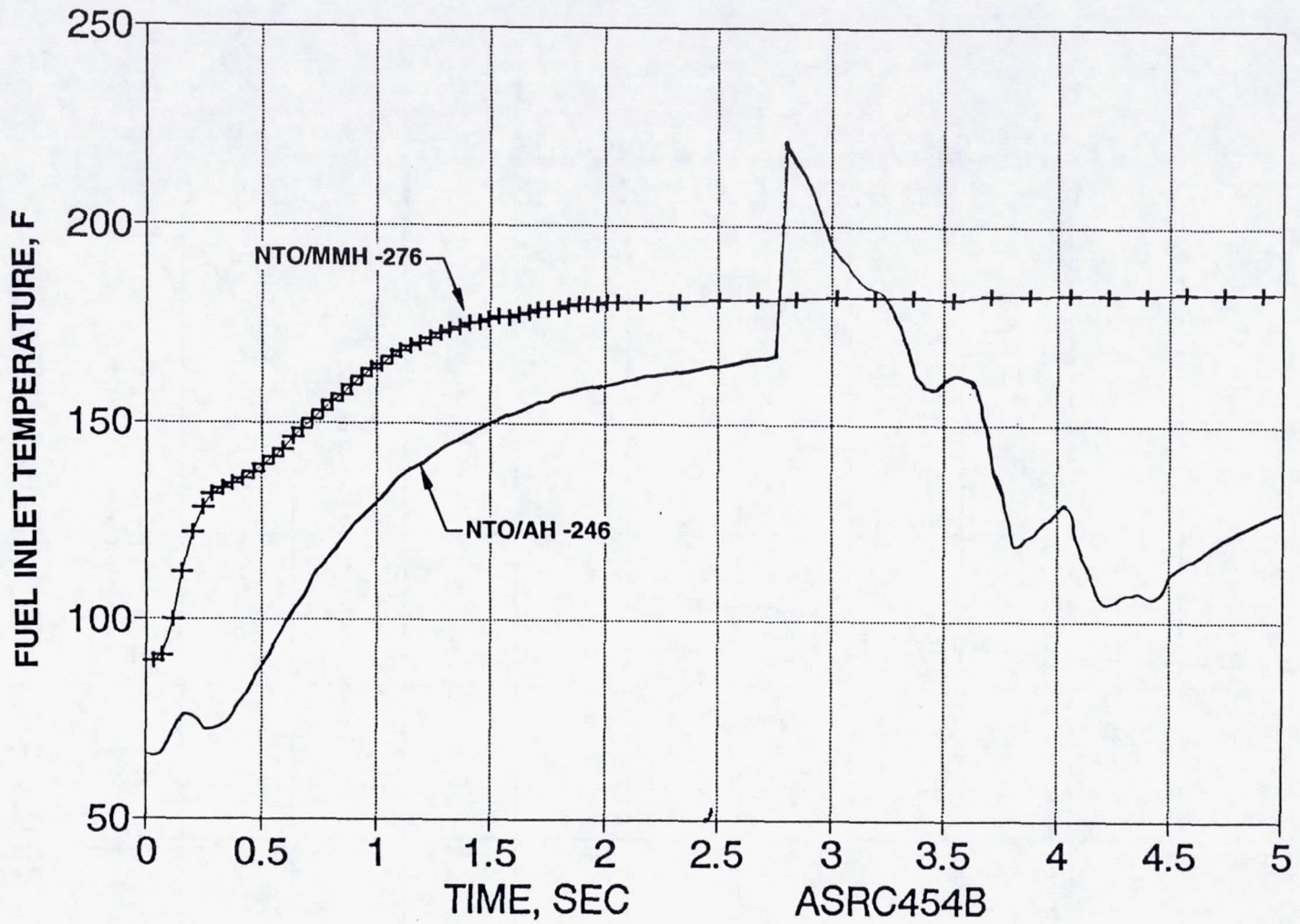


Figure 6.5-4. Fuel Outlet Temperature, NTO/MMH and NTO/AH

355

ASRC454B

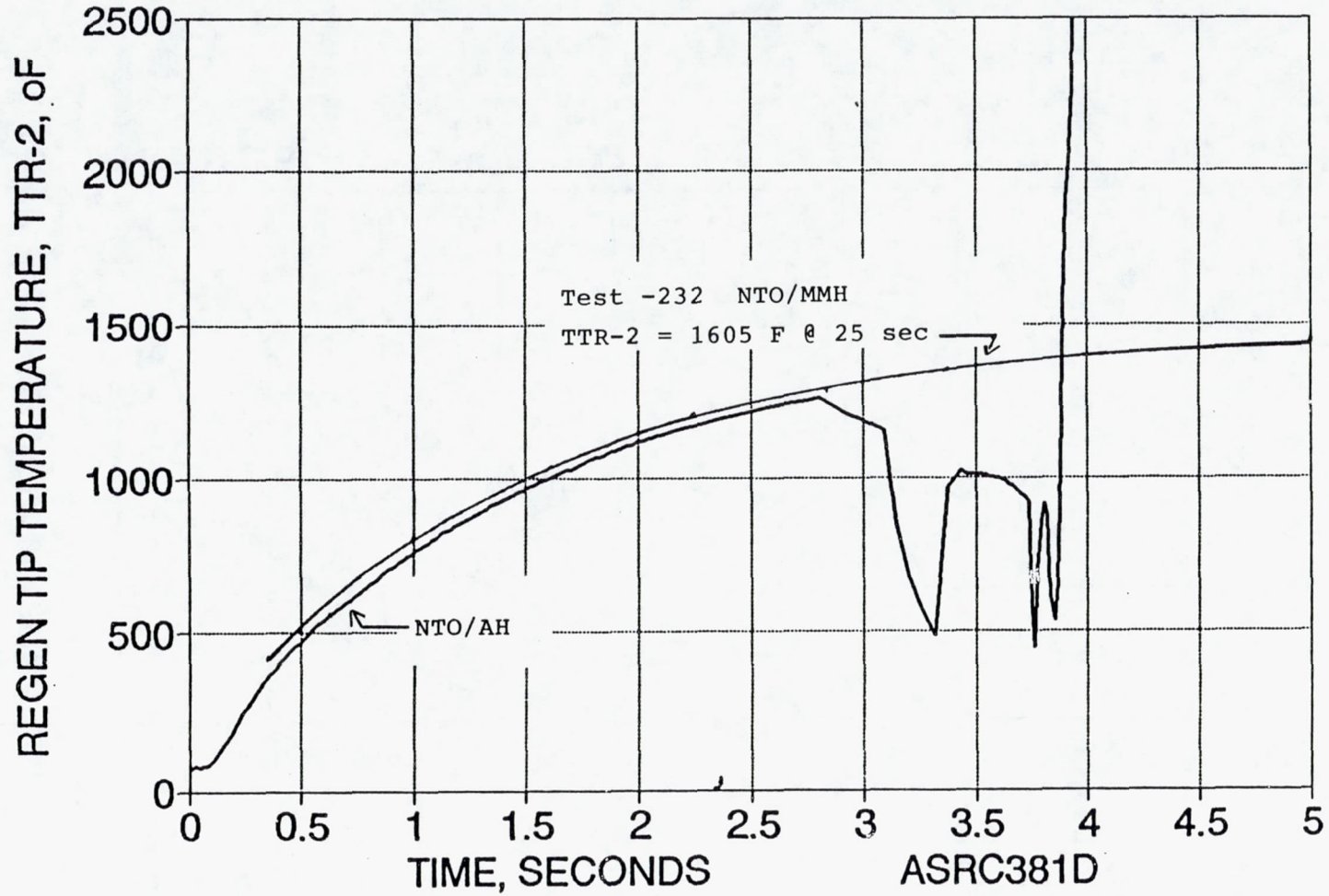


Figure 6.5-5. Regen Tip Temperature, NTO/MMH and NTO/AH

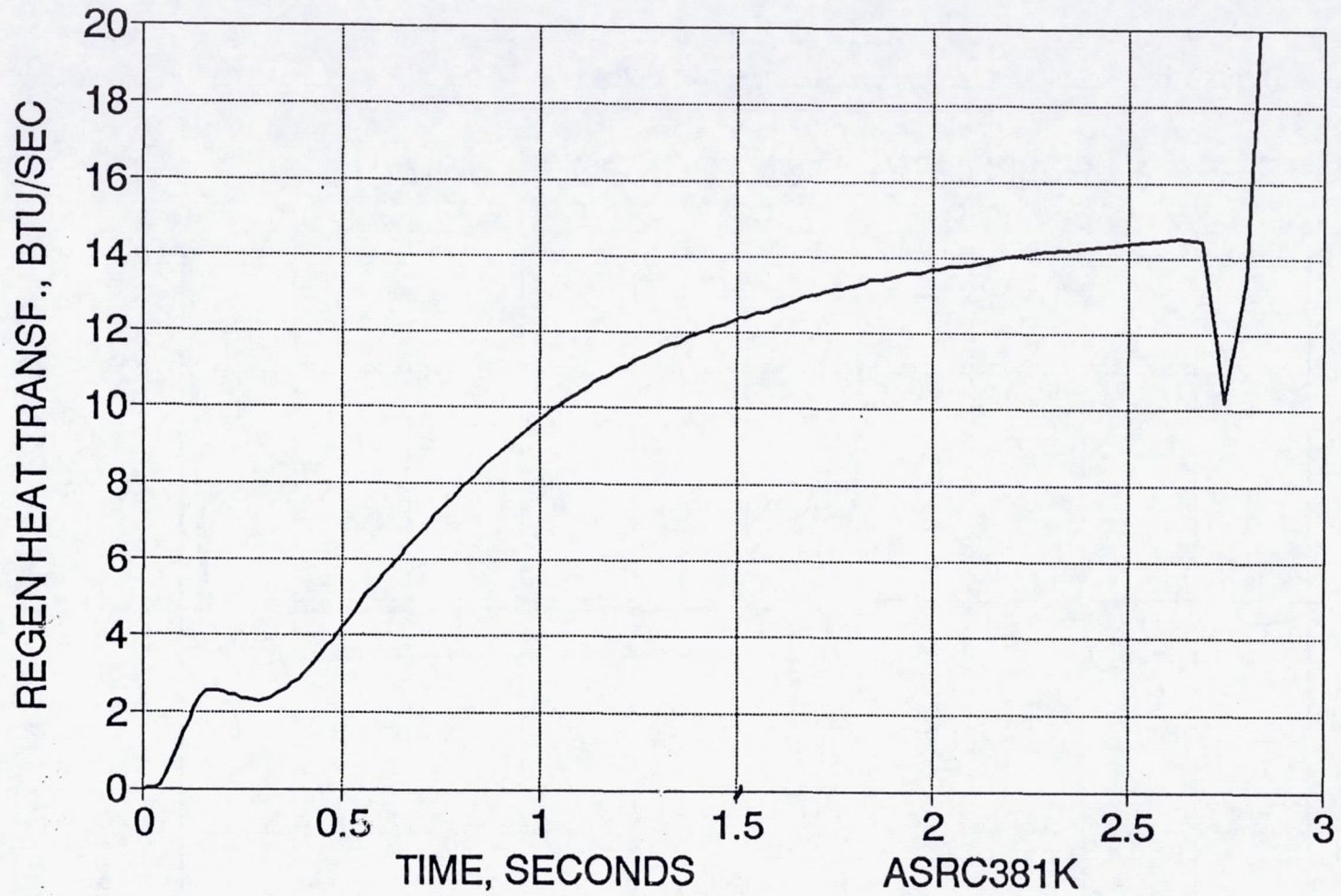


Figure 6.5-6. Heat Transfer to Fuel, Test -246

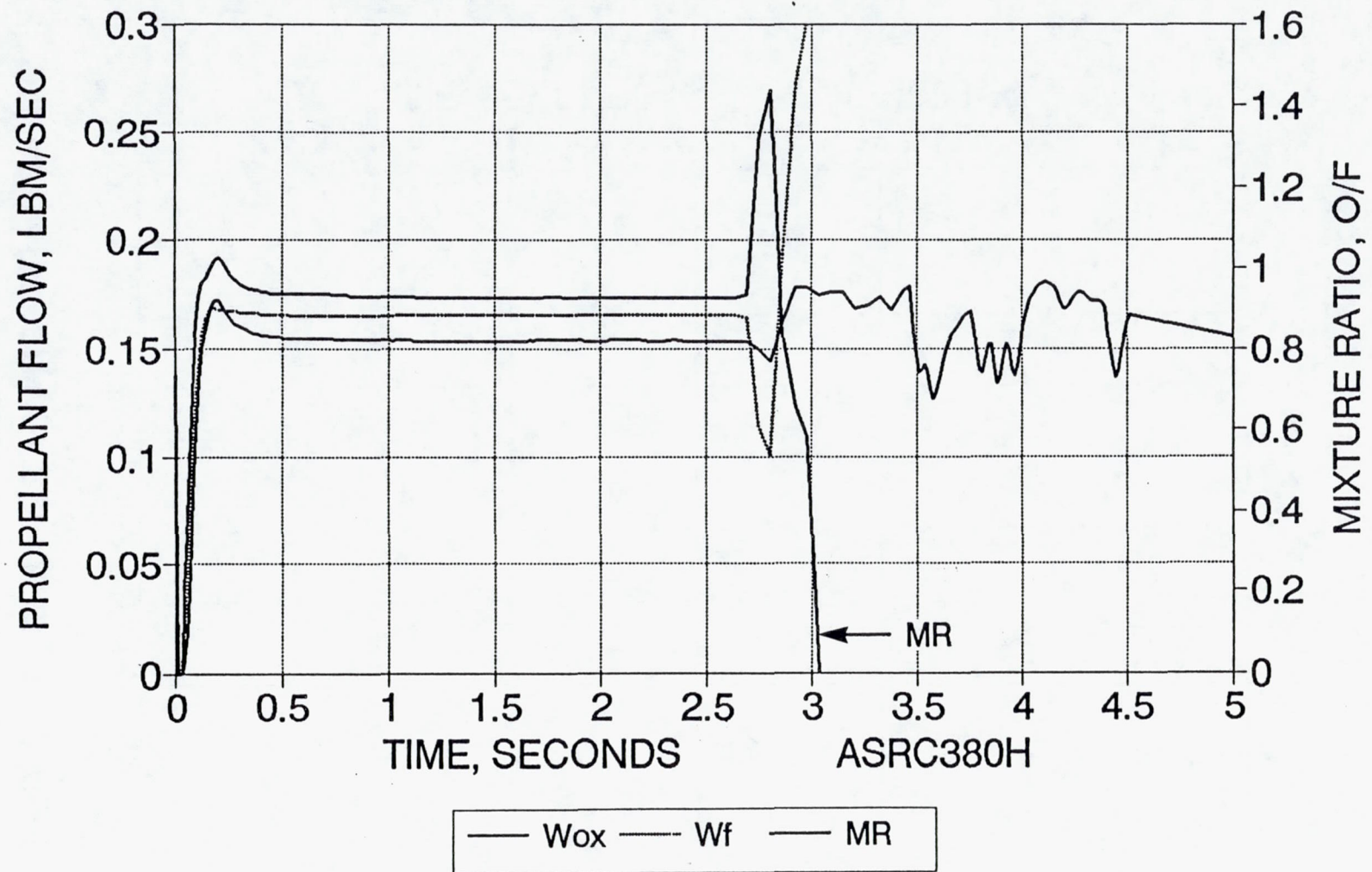


Figure 6.5-7. Propellant Flow Rate and Mixture Ratio, Test -246

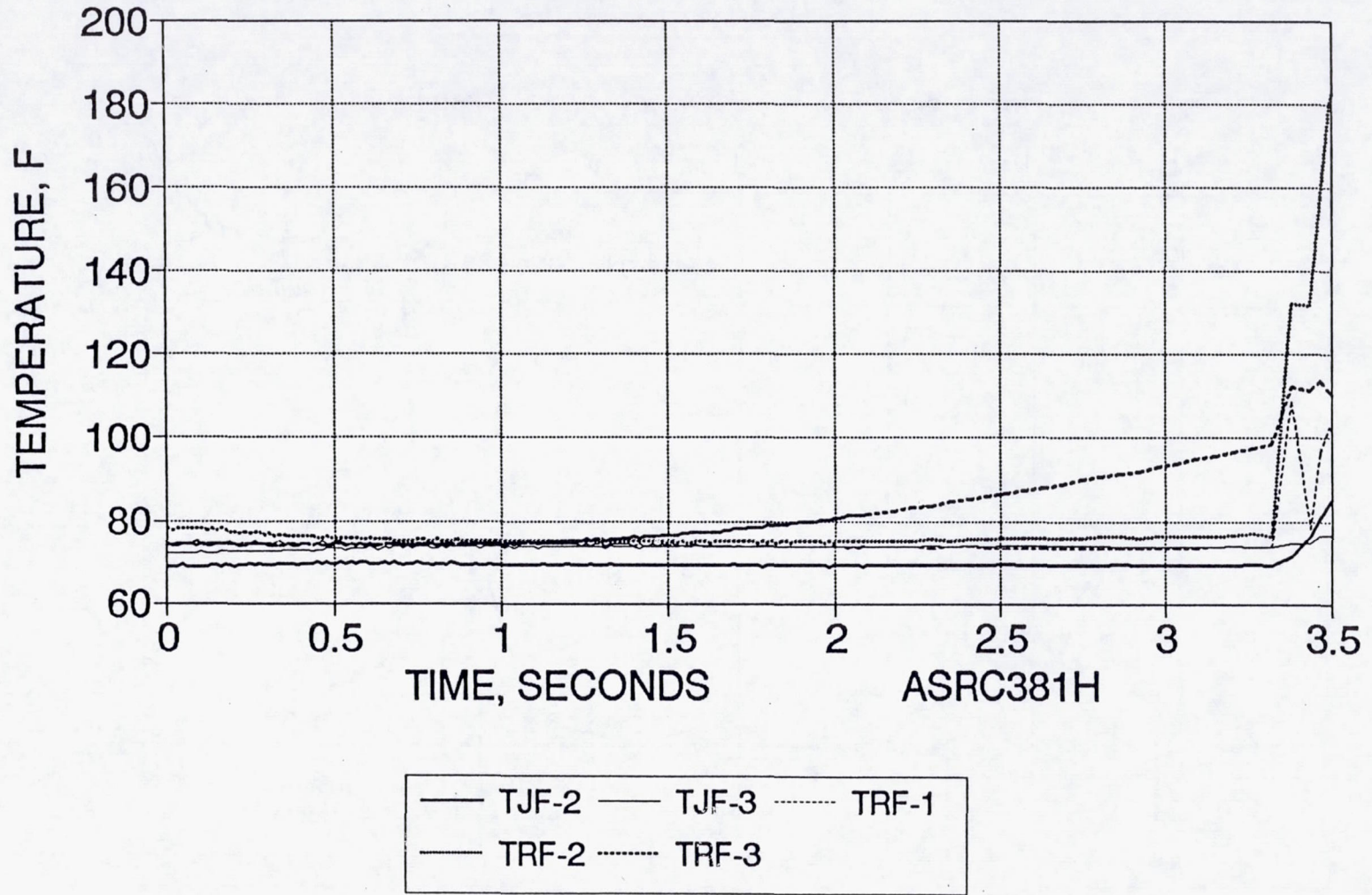


Figure 6.5-8. External Temperature, Test -246

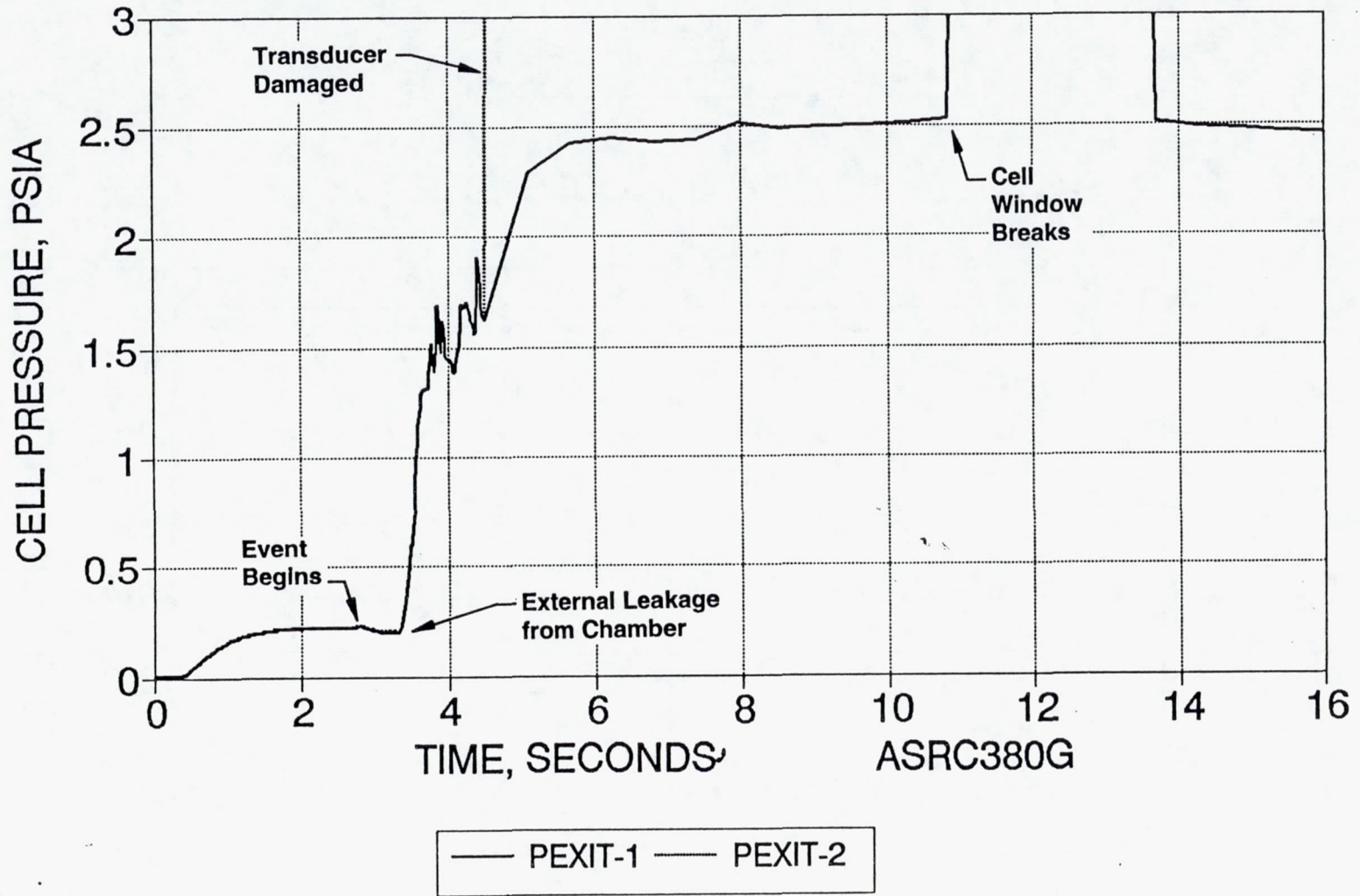


Figure 6.5-9. Cell Pressure Versus Time, Test -246

Table 6.5-2. Sequence of Events for Test -246

<u>Time</u>	<u>Event</u>	<u>Data Source</u>	<u>Time Basis</u>	<u>Description</u>
0.0	Ignition	Digital Ograph FM Tape Video	Time Code Time Code Time Code TC Wire Motion	Data From Digital Printout Data From Oscillograph Record Data From FM Tape Data From VHS Video of Test
2.6325	Last Normal Data	Digital	Time Code	Last Digital Sample With Normal Data
2.6898	First Anomalous Data	Digital	Time Code	1% Drop in Fuel Flow, 2.5 psi Rise in POTSS, 4.4 in POVI, 34.5 in PFTSS, 52.7 in PFRI, 5.4 in PC1, 52.5 in PFVI, 5.4 in POJ, 43 in PFJ
2.65	First Anomalous Data	FM Tape	Time Code	Rise in PFJ, POJ, PC1
2.78	Large Spike	FM Tape	Time Code	Large Peak in PFJ, POJ, PC1
2.81	Drop in PC1	FM Tape	Time Code	Continues to Spike Along With Other Pressures, but at Lower Level
3.1	First Anomalous Data	Video	Stopwatch	Flash
3.4712	FS-2 Signal	Digital	Time Code	Signal to Valve to Shut Down; Flows Reduce but Do Not Stop
6-7	Chamber Moves Aft	Video	Stopwatch	Chamber Gradually Rotates Down and Slowly Moves Aft
7.4	Chamber Releases	Video	Stopwatch	Chamber/Nozzle Assembly Disappears
10.4	Flare in Cell	Video	Stopwatch	Probable Time of Window Failure and Therefore Large Rush of Air Which Drags Chamber Into Diffuser

6.5, NTO/AH Tests (cont.)

Post Test Analysis

Initial appearance of the hardware suggested a large increase in chamber pressure, which broke the chamber bolts. However, review of the video record shows that the bolts actually failed slowly and progressively over a several-second-period. The data are consistent with the following:

- 2.69 seconds. Detonation occurs in cooled adapter causing a hydraulic pressure spike. The hydraulic pressure wave, followed by a hot gas pulse, damages the bipropellant valve. Over pressure spike breaks internal welds in cooled adapter allowing fuel to enter chamber directly.
- 2.6 – 3+ seconds. Pressure surges continue.
- 3+ seconds. Hot gas leak visible on the video. Leakage occurs because Pc spikes load the Belleville washers in the assembly bolts, unloading the Grafoil seal and allowing hot gas to flow by and erode the Grafoil gasket.
- 3.47 – 6 seconds. Valve signaled to close but is only partially functional. Propellants continue to flow, maintaining reduced chamber pressure and hot gas flow (primarily AH decomposition products at about 1800°F) which removes Grafoil seal and weakens bolts.
- 6-8 seconds. Weakened bolts progressively shear, allowing chamber to rotate down and move aft.
- 8 seconds. Hot decomposition products which have been impinging on test cell windows cause windows to break, permitting in rush of air which sweeps chamber and nozzle assembly into diffuser.

The post test status of the hardware is summarized in Table 6.5-3. The cooled adapter and dual shutoff bipropellant valve were damaged beyond economical repair. The rhenium chamber was inertially upset at the throat from the impact with the diffuser

Table 6.5-3. Post Test Hardware Status

<u>Item</u>	<u>Quantity</u>	<u>Name</u>	<u>P/N</u>	<u>S/N</u>	<u>Id No.</u>	<u>Owner</u>	<u>Contract</u>	<u>Condition</u>	<u>Disposition</u>
1	1	Adapter, Chamber	1201605-9	1		JPL	JPL 957882	Not Repairable	Scrap
2	1	Chamber	1199061			JPL	JPL 957882	Damaged; Possibly Usable	Test for Performance
3	1	Extension, Chamber	1199062			JPL	JPL 957882	Damaged; Repairable	Repair
4	1	Valve	A54077-1	001	Model 53E140	Aerojet	-	Damaged; Repair Cost Approximately Equal Replacement Cost	Return to Vendor; Repair Not Practical
5	1	Assembly, Injector	120653-9	006-1		NASA 3-25646	NAS 3-25646	Tested Satisfactorily	Test to Determine Status
6	4	Rod	1199063			JPL	NAS 3-25646	Not Repairable	Scrap

363

6.5, NTO/AH Tests (cont.)

(Figure 6.5-10). This reduced the throat dia from 0.843 to 0.802 in., caused an increase in throat expansion angle and probably damaged the Ir coating. The chamber is usable but not now representative for lifetime studies.

The injector, shown after the test in Figure 6.5-11, was studied in detail for damage; the results are summarized in Table 6.5-4. It was concluded that the injector was undamaged by its ordeal. It was subsequently fired with satisfactory results in Tests -247 through -258.

Cooled Adapter

The component that failed is P/N 1201605, adapter, chamber. This unit was built for the JPL test program described in Ref. 3, but was not fired in that program. It was first fired in the initial sea level compatibility tests of this program with injector S/N 2, Runs -101 through -116, on 3-25-91 through 3-27-91. During post test -116 inspection with nitrogen, leaks were noted on the ID of the part about 3/16 in. from the downstream edge. The adapter was sent to the shop for welding and concurrent machining of the trip contour, while tests with S/N 4 injector continued with the cooled adapter previously fired on the JPL program.

Because the 1201605 adapter material is 347 SS, it was TIG welded because EB welding of this alloy is often not satisfactory. The welded area overlapped the areas where leakage was noted but did not cover the full circumference of the part. It is evident from the damaged part that the reweld did not center on the old weld but barely overlapped the joint. It is also evident that the initial weld had grossly inadequate penetration. In the initial process of fabrication, the minimum wall thickness at the weld was 0.082 in. This was machined after welding to a design minimum of 0.053 in. which would have equaled the depth of a full penetration weld.

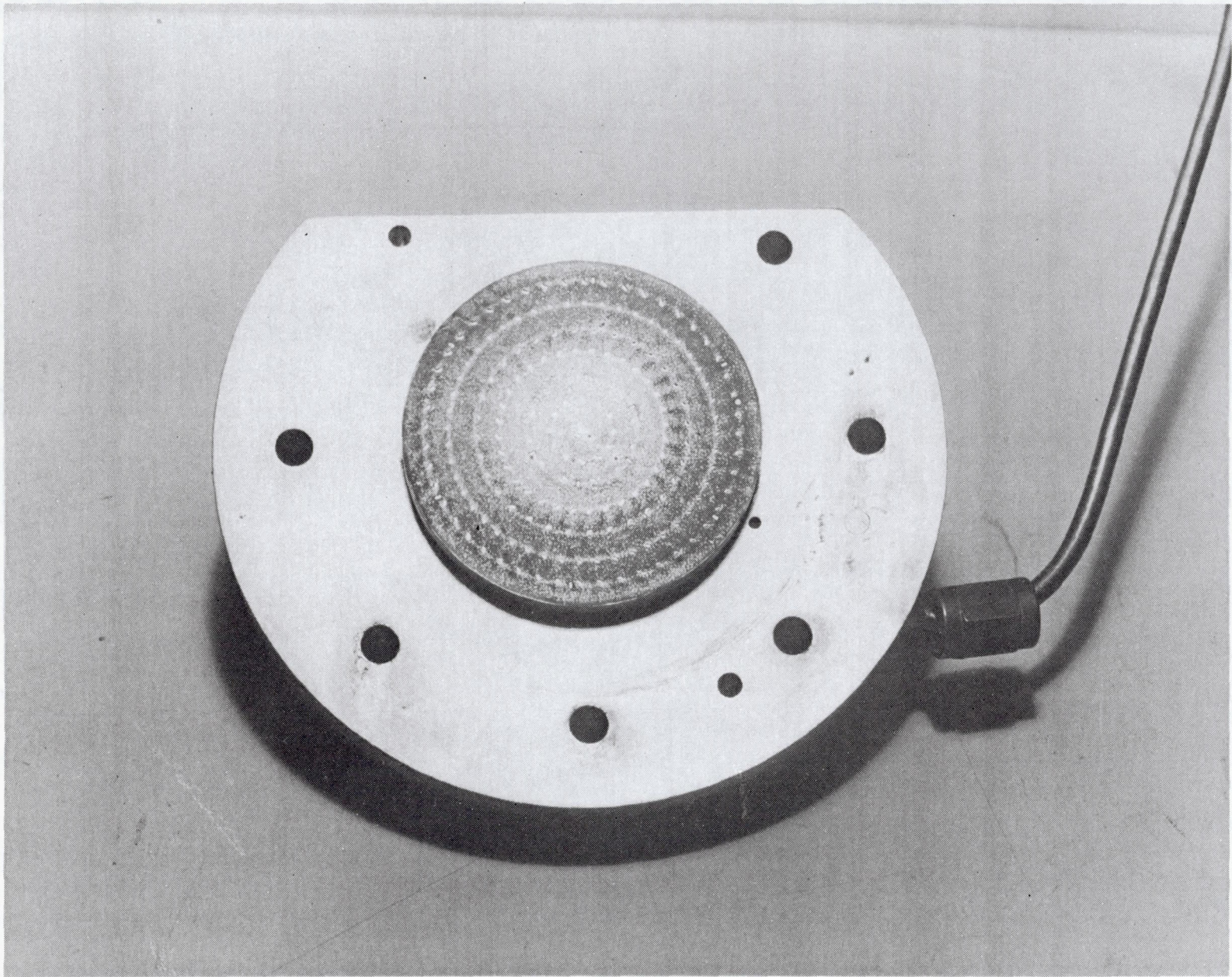
The welded section of the adapter is shown schematically in Figure 6.5-12. The inadequate weld had two consequences. It resulted in a narrow stagnant cavity on the fuel side about 0.045 in. deep which would be largely isolated from the main flow and in which fuel could heat to well above the bulk temperature. In addition, the wall temperature drop occurred over a thickness of about 1/6 design, resulting in a much higher liquid side wall temperature than design. In spite of this, the reworked cooled adapter operated satisfactorily in 117 tests (-128 through -244) with NTO/MMH over a very wide MR and Pc range for test durations of up to

365



(CO192 0123)

Figure 6.5-10. Ir-Re Chamber After Test -246



(CO192 0124)

Figure 6.5-11. Injector SN 6-1 After Test -246

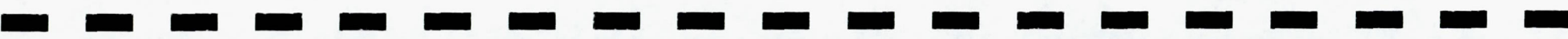
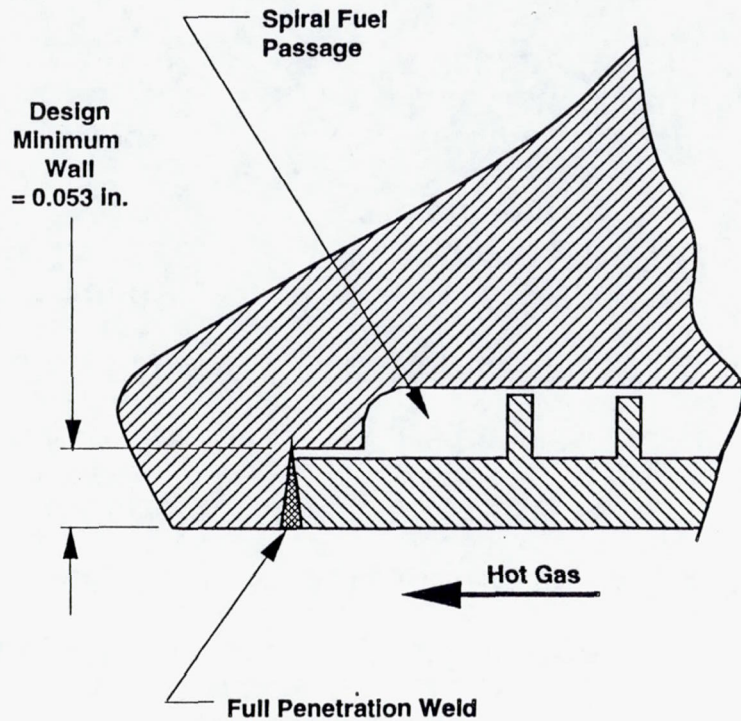


Table 6.5-4. Post Test Analysis of Injector SN 6-1

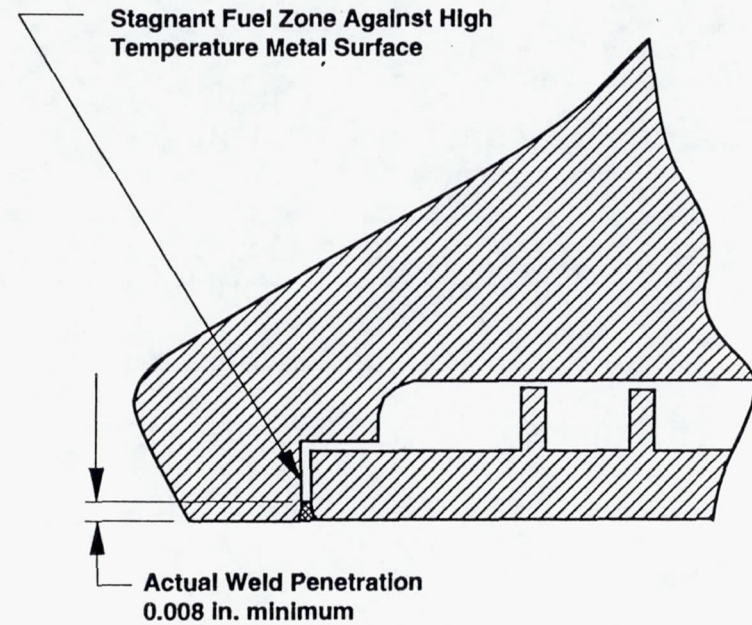
<u>Test</u>	<u>Result</u>	<u>Possible Interpretation</u>
Intermanifold Leak	No Leak at 50 psig GN ₂	Good Bond
Backflush Oxidizer	No Particles	No Contamination in Oxidizer Circuit
Backflush Fuel	1-2 Dozen Small Black Particles	Fuel Contamination From Valve Seat
Flow Oxidizer for Kw	3.4% Low	Screen Plugging or Cd Changed
Flow Fuel For Kw	4% Low	Screen Plugging or Cd Changed
Oxidizer Pattern	Normal	No Element Change
Fuel Pattern	Row 5/ ~ 225 Degree Has Higher Angle to Face Than Other Elements	Historical, Not Noticed or Particle Lodged in Cup
Appearance	Under Microscope No Sign of Face Deflection; Inner Surfaces Alligatored	No Internal Over Pressure; Surface Reaction

367

Actual Weld Penetration Was One-Sixth Design Value



Design Configuration



As-Built Configuration

Figure 6.5-12. Schematic of Cooled Adapter Weld

6.5, NTO/AH Tests (cont.)

90 sec. Given the geometry and heat transfer conditions, the MMH temperatures at the bottom of the slot must have been above the thermal decomposition temperature of about 450°F. However, any reaction which occurred was benign, perhaps resulting in gasification and charring in the slot, but certainly without explosive decomposition.

The AH, which is known to react more violently than MMH under similar thermal decomposition conditions, reacted violently.

Failure Mechanism

The predicted metal wall temperature at the liquid side is plotted in Figure 6.5-13 as a function of wall thickness for two levels of heat transfer to the part, 13 Btu/sec, corresponding to the results for NTO/MMH, and 15 Btu/sec corresponding to the results for NTO/AH. The predicted liquid side wall temperature for the design thickness are well under the fuel decomposition temperature of 450°F. However, at the measured wall thickness of 0.008 in. the corresponding fuel side temperatures are 630°F and 720°F, respectively, which are above the thermal decomposition temperature of the fuel.

Comparison to Flight Engine Cooled Adapters

The cooled adapters designed and built on this program do not have the weld in the high heat flux location. The weld was moved to the downstream lip; this is a more favorable location for EB welding which is now practical as the new part is made of 304 stainless. The old and new designs are compared in Figure 6.5-14.

If the original weld had been proper the original design would not have been influenced by the location of the weld. For example, weld preparation (V-groove) and use of filler rod rather than parent metal fusion would have produced a proper weld. A tradeoff exists in the designs, however. The original weld is more difficult to make but is easy to inspect by X-ray. The new weld is easy to make but difficult to inspect. The weld location must be carefully planned for a hydrazine-cooled adapter and a rigorous inspection plan must be developed.

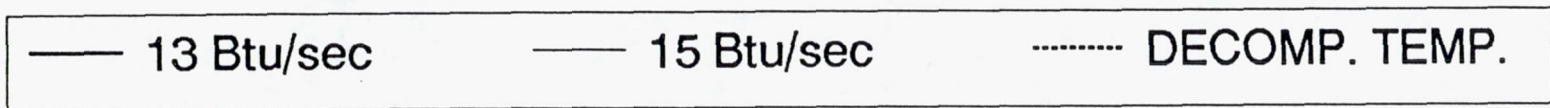
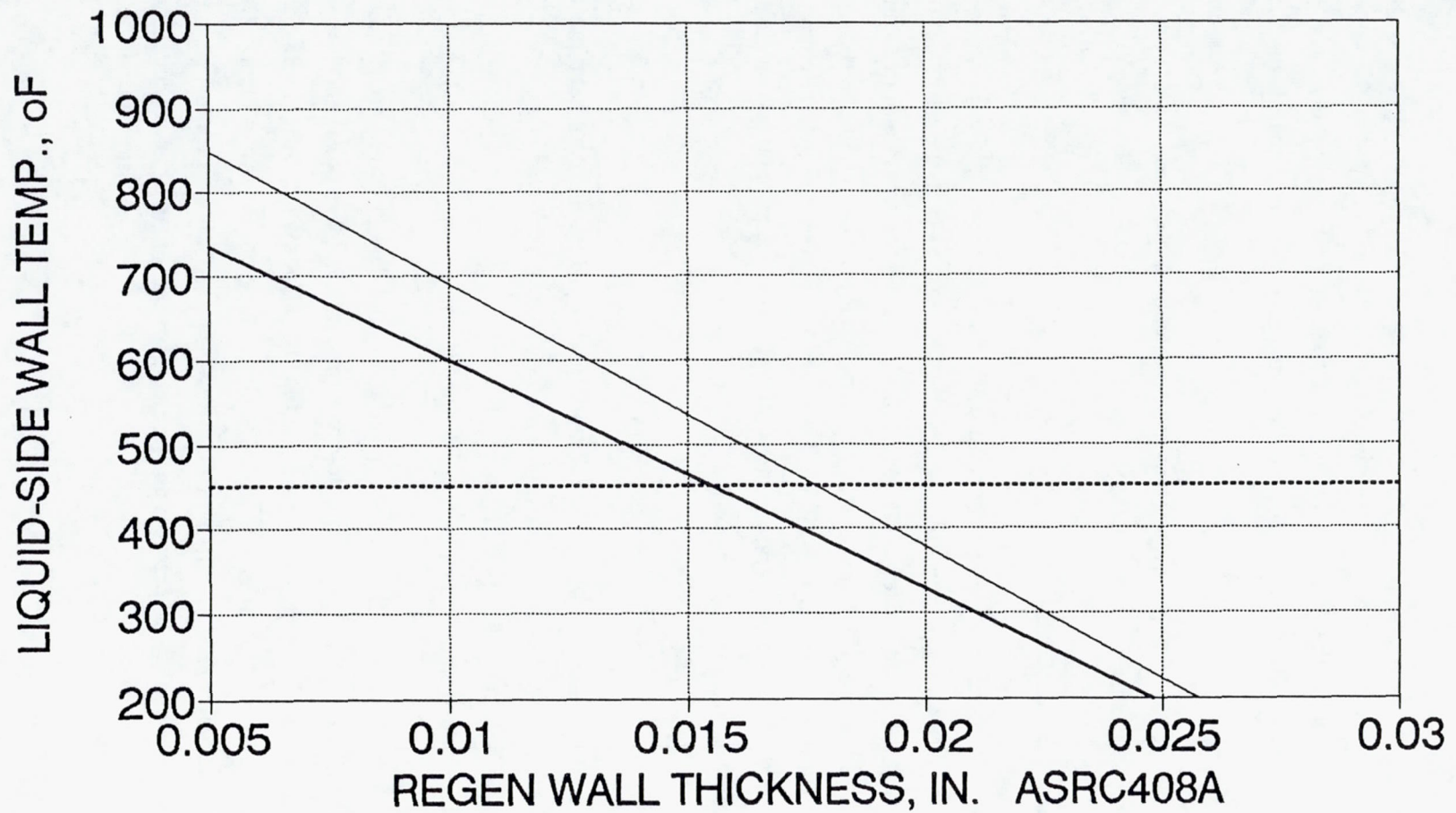
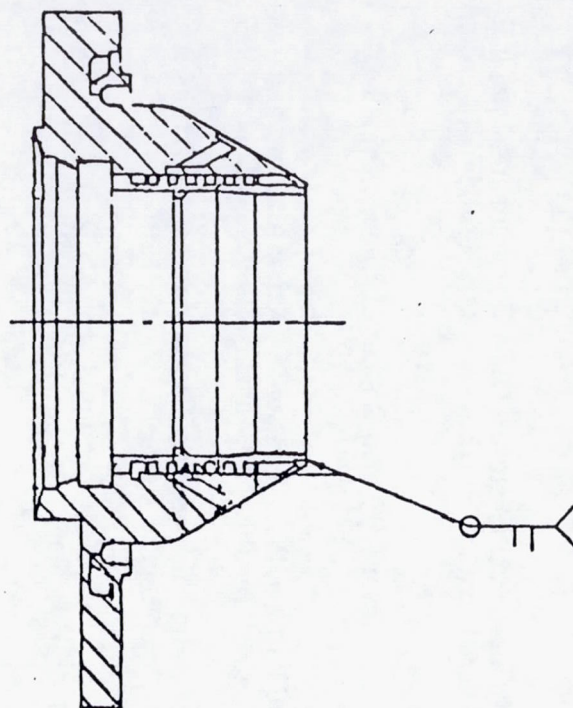
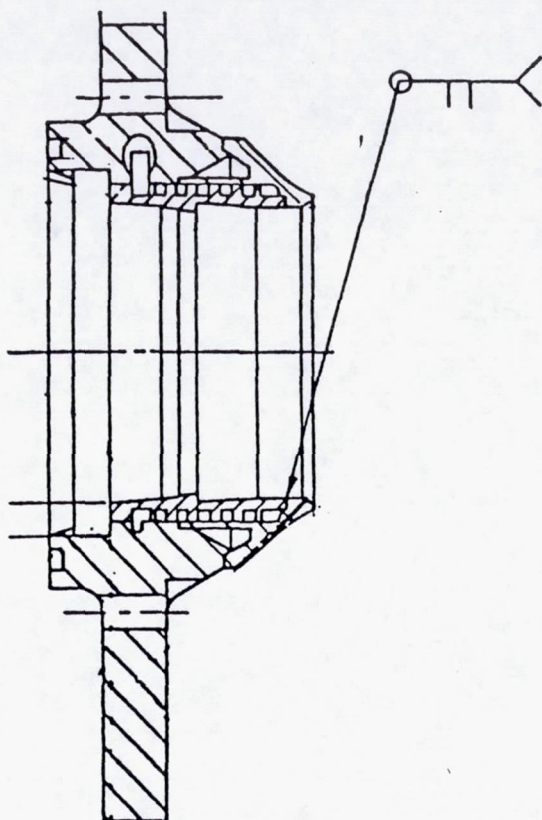


Figure 6.5-13. Predicted Cooled Adapter Liquid Side Wall Temperature



COMPONENT	COOLED ADAPTER
APPLICATION	R&D/BOLT-UP THRUSTER
P/N	1201605
SOURCE	JPL CONT 957882
DESIGN DATE	10-6-87
NTO/MMH EXPERIENCE	6.1 hr in 186 tests

COMPONENT	COOLED ADAPTER
APPLICATION	WELDED FLIGHT THRUSTER
P/N	1206354
SOURCE	NASA L&RC CONT NAS 3-25646
DESIGN DATE	12-7-90
NTO/MMH EXPERIENCE	0.27 hr in 20 tests

Figure 6.5-14. Comparison of Cooled Adapters

C-5
371

7.0 REFERENCES

1. Jassowski, D.M., "Advanced Small Rocket Chambers, Basic Program and Option II – Fundamental Processes and Material Evaluation," NASA-CR-195349, Final Report, September 1993.
2. Jassowski, D.M. and Gage, M.L., "Advanced Small Rocket Chambers, Option 1 – 14 lbf Ir-Re Rocket" NASA-CR-191014 Final Report, August 1992.
3. Schoenman, L., Franklin, J. and Lansaw, P.T., "Feasibility Demonstration of a High-Performance 100 lbf Rocket Engine," Final Report, January 1989, JPL Contract 957882.
4. Wooten, J.R., and Lansaw, P.T., "High Temperature Oxidation-Resistant Thruster Research," NASA CR-185233, Final Report, February 1990.
5. Svedberg, R.C., and Bowen, W.W., "High Temperature Creep and Tensile Properties of Chemically Vapor-Deposited Rhenium," DOE Report HEDL-SA-2695-FD, April 1982.
6. USAF Property Handbook 3-70.

REPORT DOCUMENTATION PAGE

Form Approved
OMB No. 0704-0188

Public reporting burden for this collection of information is estimated to average 1 hour per response, including the time for reviewing instructions, searching existing data sources, gathering and maintaining the data needed, and completing and reviewing the collection of information. Send comments regarding this burden estimate or any other aspect of this collection of information, including suggestions for reducing this burden, to Washington Headquarters Services, Directorate for Information Operations and Reports, 1215 Jefferson Davis Highway, Suite 1204, Arlington, VA 22202-4302, and to the Office of Management and Budget, Paperwork Reduction Project (0704-0188), Washington, DC 20503.

1. AGENCY USE ONLY (Leave blank)	2. REPORT DATE February 1995	3. REPORT TYPE AND DATES COVERED Final Contractor Report	
4. TITLE AND SUBTITLE Advanced Small Rocket Chambers Option 3-110 lbf Ir-Re Rocket Volume I and II		5. FUNDING NUMBERS WU-242-70-02 C-NAS3-25646	
6. AUTHOR(S) Donald M. Jassowski and Leonard Schoenman		8. PERFORMING ORGANIZATION REPORT NUMBER E-9457	
7. PERFORMING ORGANIZATION NAME(S) AND ADDRESS(ES) Gen Corp Aerojet Propulsion Division Sacramento, CA 95813		9. SPONSORING/MONITORING AGENCY NAME(S) AND ADDRESS(ES) National Aeronautics and Space Administration Lewis Research Center Cleveland, Ohio 44135-3191	
9. SPONSORING/MONITORING AGENCY NAME(S) AND ADDRESS(ES) National Aeronautics and Space Administration Lewis Research Center Cleveland, Ohio 44135-3191		10. SPONSORING/MONITORING AGENCY REPORT NUMBER NASA CR-195435	
11. SUPPLEMENTARY NOTES Project Manager, Steven J. Schneider, Space Propulsion Technology Division, NASA Lewis Research Center, organization code 5330, (216) 977-7484.			
12a. DISTRIBUTION/AVAILABILITY STATEMENT Unclassified - Unlimited Subject Category 20 This publication is available from the NASA Center for Aerospace Information, (301) 621-0390.		12b. DISTRIBUTION CODE	
13. ABSTRACT (Maximum 200 words) This report describes the AJ10-221, a high performance Iridium-coated Rhenium (Ir-Re) 110 lbf (490N) welded rocket chamber with 286:1 area ratio nozzle. This engine was designed, built, and hot fired for over 6 hours on this program. It demonstrated an I_s of 321.8 sec, which is 10 sec higher than conventional 110 lbf silicide coated Cb chambers now in use. The approach used in this portion of the program was to demonstrate the performance improvement that can be made by the elimination of fuel film cooling and the use of a high temperature (4000°F) (2200°C) Iridium-coated Rhenium (Ir-Re) rocket chamber. Detailed thermal, performance, mechanical, and dynamic design analyses of the full engine were conducted by Aerojet. Two Ir-Re chambers were built to the Aerojet design by Ultramet, using the chemical vapor deposition (CVD) process. Incorporation of a secondary mixing device or Boundary Layer Trip (BLT) within the combustion chamber (Aerojet Patents 4882904 and 4936091) results in improvement in flow uniformity, and a significant life and performance increase. The 110 lbf engine design was verified in bolt-up hardware tests at sea level and altitude. The effects of injector design on performance were studied. Two duplicate injectors were fabricated matching the preferred design and were demonstrated to be interchangeable in operation. One of these units were welded into a flight type thruster which was tested for an accumulated duration of 22,590 sec in 93 firings, one of which was a continuous burn of two hours. A design deficiency in the C-103 nozzle near the Re-Cb transition joint was discovered, studied and corrected design has been prepared. Workhardening studies have been conducted to investigate methods for increasing the low yield strength of the Re in the annealed conditions. An advanced 490N high performance engine has been demonstrated which, when proven to be capable of withstanding launch vibration, is ready for flight qualification.			
14. SUBJECT TERMS Rockets; Satellite propulsion; Rhenium thrusters; Iridium coatings; Chemical vapor deposition; Bipropellants; Radiation cooling; High performance; High temperature; Long life		15. NUMBER OF PAGES 678	
17. SECURITY CLASSIFICATION OF REPORT Unclassified		16. PRICE CODE A99	
17. SECURITY CLASSIFICATION OF REPORT Unclassified	18. SECURITY CLASSIFICATION OF THIS PAGE Unclassified	19. SECURITY CLASSIFICATION OF ABSTRACT Unclassified	20. LIMITATION OF ABSTRACT